EUROSAFE 2019

PROCEEDINGS

EUROSAFE **2019**

4 and 5 November
Cologne

Imprint

The Proceedings of the EUROSAFE 2019 are published on behalf of EUROSAFE and its partners by the

Gesellschaft für Anlagen- und Reaktorsicherheit (GRS) gGmbH
Schwertnergasse 1
50667 Cologne
Germany
http://www.grs.de/en

February 2020

ISBN 978-3-947685-51-6

www.eurosafe-forum.org

1 NUCLEAR SAFETY ASSESSMENT AND RESEARCH

Chairpersons: Karine Herviou (IRSN) & Michael Kund (GRS)

Chairpersons: Martina Adorni (Bel V) & Eija Karita Puska (VTT)

2

WASTE MANAGEMENT, DECOMMISSIONING & DISPOSAL

Chairpersons: Alexey Rodin (SEC NRS), Wilfried Pfingsten (PSI)

3 RADIATION PROTECTION, ENVIRONMENT & EPR

Chairpersons: Federico Rocchi (ENEA), Sigitas Rimkevicius (LEI)

ETSON AWARD SCIENCE SLAM

EUROSAFE 2019

1 NUCLEAR SAFETY ASSESSMENT AND RESEARCH

Actual issues of VVER reactor pressure vessel irradiation embrittlement assessment

Alexander Kryukov, Vladimir Lebedinsky

Scientific and Engineering Centre for Nuclear and Radiation Safety, Russia, Moscow, 107140, Malaya Krasnoselskaya st. 2/8, bld. 5

Abstract:

The possibility of extending the life of existing NPP is very attractive to utilities. An operational life of 60-80 years is being considered by many utilities in their plant life management programmes. The RPV is a key component of the NPP. The basic reason of RPV mechanical properties degradation is the neutron irradiation, resulting in embrittlement of steel, which the RPV is made of. In this paper the analysis of available data required for a precise prediction of radiation embrittlement of RPV materials after 60-80 years of operation has been performed. A number of RPVs may be reaching the generic screening criteria due to significant irradiation embrittlement. The thermal annealing can restore most of the original RPV steel toughness properties. This paper also devotes to the analysis of the effectiveness of relatively low temperature thermal annealing for the operated RPVs.

1 INTRODUCTION

The possibility of extending the life of existing Nuclear Power Plants (NPP) is very attractive to utilities, especially given the public opposition in several countries to construct new plants, while some governments see them as a way of limiting carbon emissions and power security and price stability. The long term operation of NPPs has already been accepted in many countries as a strategic objective to ensure adequate supplies of electricity over the coming decades. An operational life of 60 years, or even 80, is being considered seriously by many utilities in their plant life management programmes.

The Reactor Pressure Vessel (RPV) is a key component of the NPP. The integrity assessment of the RPV is one of the main issues for the safe and long term operation of NPPs.

The basic reason of RPV mechanical properties degradation is the neutron irradiation, resulting in hardening and embrittlement of the steel from which the RPV is made. The prediction of radiation embrittlement is performed usually in accordance with relevant codes and standards that are based on a large amount of information from surveillance and test irradiation programmes. Considerable data exists regarding the effect of neutron irradiation on pressure vessel steels both from mechanical properties and macrostructure features.

The analysis of all available data is required for a precise prediction of radiation embrittlement of RPV materials after 60-80 years of operation.

This paper presents the analysis of the experimental data from the International Database of RPV materials. The essential part of the analysis concerns the assessment of irradiation embrittlement of VVER steel irradiated with high neutron fluence.

So far a number of RPVs may reach the ductile-brittle transition temperature (T_k) limit due to significant irradiation embrittlement. Considering the NPP long term operation up to 60 years the mitigation of state-of-the-art or predictable embrittlement level is getting rather urgent.

The thermal annealing cycle at the temperature above the normal operating temperature can restore most of the original RPV steel toughness properties. This paper is also devoted to the analysis of the effectiveness of relatively low temperature thermal annealing for the operated RPVs.

2 INTERNATIONAL DATABASE ON RPV MATERIALS

Presently, a huge amount of RPV surveillance programme results exist all over the world. Moreover, there are a lot of data from experiments in test reactors which were carried out to support the power reactor surveillance programmes. In the framework of the International Atomic Energy Agency (IAEA) activities, the International Database on RPV materials (Database) was created in the nineties, [1]. Fourteen countries, including the USA, France, and Russia, supplied large amounts of surveillance results and data from national and international research programmes. The Database covers the major part of the operating and planned RPV steels (base metal and welds) of light water reactors (PWR and VVER), Table 1.

Table 1: The highest contents of impurities and fluence values both in the worldwide used RPV steels and in the IAEA Database.

Reactor type	Cu_{max}, wt %	P_{max}, wt %	Ni_{max}, wt %	Mn_{max}, wt %	$Fluence_{max}$, cm^{-2}	Remarks
PWR	0.42	0.025	1.2	2.1	3.7×10^{19}, E>1 MeV	PWR lifetime - 32 energy full power years
VVER	0.20	0.042	1.9	1.3	2.4×10^{20}, E>0.5 MeV	WWER-440 lifetime - 40 calendar years
Database surveillance	0.35	0.035	1.9	2.1	$\sim 2 \times 10^{21}$, E>0.5 MeV	Surveillance specimens
Database research	0.4	0.045	2.8	2.0	$\sim 2 \times 10^{21}$, E>0.5 MeV	Research programmes

Through a bilateral agreement, the Database and its maintenance have been transferred from the IAEA to the EC Joint Reseach Centre – Institute for Energy web-enabled Materials Database, which was developed for storing materials test data resulting from international research projects together with other documentation in a related Document Management database, providing fast access to confidential and public data sets.

3 IRRADIATION EMBRITTLEMENT OF VVER-440 RPV STEELS AT HIGH NEUTRON FLUENCE

The irradiated change in mechanical properties is a result of microstructural features resulting from high-energy neutrons impacting the RPV materials, [2,3]. There are the main embrittlement mechanisms that are manifested through fine-scale microstructural changes:

- matrix hardening resulting from irradiation-induced point defects inhibiting dislocation movement;
- hardening behaviour resulting from the clustering of key elements (such as copper, phosphorus, nickel, manganese, etc.) creating nanometer-size defects which also impede dislocation motion.

For some steels the non-hardening embrittlement occurring as elements (such as phosphorus) collect at grain boundaries resulting in intergranular fracture is also considered.

First-generation VVER NPP (VVER-440), which service life has so far exceeded 40 years established by the project, in accordance with current regulatory and technical documentation can be operated up to a maximum neutron fluence on the inner wall of the case of ~ 3 • 10^{20} cm^{-2}. Upon reaching this value, it is recommended to perform thermal annealing to extend safe operation.

The analysis of the surveillance test results of 15 VVER-440 RPV operated in Russia and overseas showed that if the metal has a low content of impurity elements (copper and phosphorus), the shift of the T_k after irradiation is low, namely less than 100-130°C for the fluence ~ 5 • 10^{20} cm^{-2}, Figure 1, [4,5,6]. As a result, the maximum allowable value of the neutron fluence for relatively "pure" ones (Cu < 0.13%, P < 0.017%) can be increased to ~ 5 • 10^{20} cm^{-2}. In this case, there is no need for annealing to extend the operational lifetime of VVER-440 up to 60-80 years.

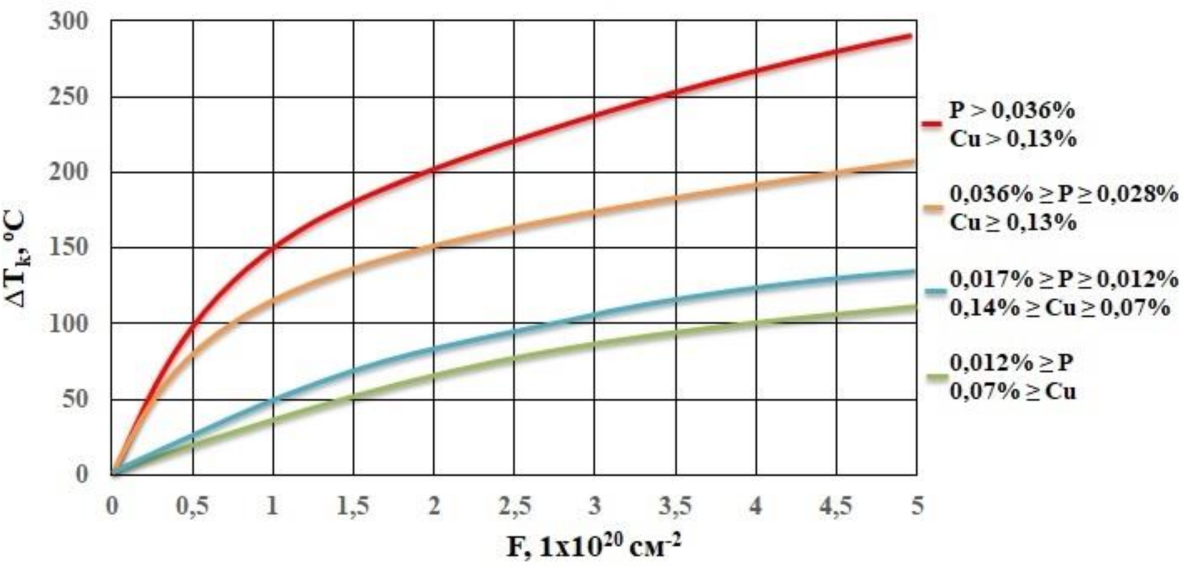

Figure 1: Irradiation embrittlement of VVER-440 steels at high neutron fluence.

4 LOW TEMPERATURE "WET" ANNEALING AS AN INSTRUMENT TO MITIGATE IRRADIATION EMBRITTLEMENT OF LOW COPPER RPV STEELS

4.1 Thermal annealing methods

There are several measures to prevent the reaching of T_k allowed value. The irradiation embrittlement can be mitigated, preferably in the early stages of NPP operation by reducing the neutron fluence (hence the fluence rate/flux) to the RPV wall:

1. The low-leakage fuel management is applied in most PWRs. Some or all of the peripheral fresh fuel assemblies are replaced by low reactivity fuel assemblies, i.e. those having spent one or three cycles in the reactor.

2. Some of peripheral fuel assemblies are replaced by dummy assemblies, which contain stainless steel. Typically 5-10% of the fuel assemblies need replacing to maintain the circumferential symmetry.

3. Installation of neutron absorbing materials on the core periphery. For instance, periphery control rods or burnable absorber rods placed at critical locations can be used to reduce the flux to RPV wall.

4. The fitting of the irradiation shields or reflectors between the outer fuel elements and the RPV.

In spite of the implementation of some of abovementioned measures, a number of RPVs may reach the generic screening criteria due to significant irradiation embrittlement. Considering the NPP long term operation up to 60 years the mitigation of state-of-the-art or predictable embrittlement level is getting rather urgent.

The thermal annealing cycle at the temperature well above the normal operating temperature can restore most of the original RPV steel toughness properties.

There are two basic types of RPV thermal annealing: “wet” and “dry”.

The “wet” anneal is performed at temperatures < 350°C. At that temperatures the reactor coolant water is generally heated by the reactor circulation pumps. The annealing is not as complicated from an engineering point because primary water temperature is controlled by pump heat up to the vessel design temperature of 343°C. The internals could be inside the reactor vessel.

The normal operating temperature of many commercial PWRs is approximately 288°C. The temperature difference between operation and “wet” annealing temperature 343°C seems to be not enough to obtain substantial mechanical property recovery. An approach for annealing that utilizes dry heat to soak the beltline region at a higher temperature can be applied. “Dry” anneals are performed at higher temperatures than “wet” anneals. The “dry” anneal requires removal of core internal structures and primary water so that a radiant heating source can be inserted near the vessel wall to locally heat the embrittled beltline region. Engineering difficulties are complex and need plant-specific evaluations to assure that other parts of plant (supports, primary coolant piping, pipe supports, adjacent concrete, insulation, etc.) are not harmed by high temperatures. Sixteen VVER-440 RPV have been annealed between 1987 and 2010 in Russia, Armenia, Eastern Germany, Czech and Slovak Republics, Bulgaria, Finland, Ukraine. The standard dry annealing regime for this RPV type was 460-490°C and 100-150 hours. The mechanical properties recovery was evaluated as 80-100% [2]. First “dry” annealing of VVER-1000 was performed in Russia in 2018 with temperature 565 ± 15°C and 100 hours.

The “dry” annealing certainly is more effective than the “wet” one though it more technically complex and much more expensive. The “dry” annealing was implemented in the late eighties for VVER-440 because their RPV welds irradiation embrittlement had already reached a critical value and needed to be mitigated very urgent and rather essentially.

In case of timely annealing application in combination with low-leakage management and other measures reducing the neutron flux the “wet” annealing could be an easy and inexpensive method to decrease the embrittlement and extend the NPP safe operation. The presumptive scheme of T_k shift mitigation for various options is shown in Figure 2. It should be mentioned that the specific PTS limit for VVER RPV component is determined by calculation, based on the scenario of the accident and the existing safety systems. It is seen that for the case considered in the Figure 2 the “wet” annealing ensures the sufficient RPV lifetime extension. However the predictable degree of the recovery and re-embrittlement rate after annealing should be entirely evaluated.

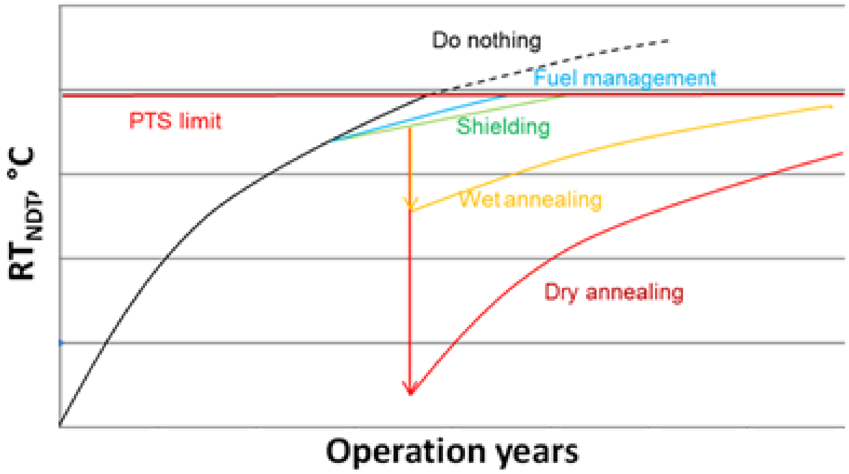

Figure 2: The presumptive scheme of T_k shift mitigation for various options.

4.2 Wet annealing recovery evaluation

In seventies – early eighties the "wet" annealing was seriously considered as a main instrument to mitigate the irradiation embrittlement of "old" RPVs with high Cu content. Because the older PWRs are usually constructed of hot-rolled plates, they also have axial welds in the entire reactor core area. To avoid thermal stresses in annealing, the annealing temperatures studied have been chosen to be as low as possible. A lot of mechanical test results came from 343°C annealing research [7-13]. Later in order to elaborate a model for irradiation embrittlement recovery due to annealing a big amount of PWR annealing results were gathered in [14]. The basic conclusion was done – the wet annealing was not effective enough for welds with high copper content.

In this paper we have evaluated the row data presented in [14] in respect to the dependency of residual after annealing T_k shift (ΔT_{res}) on copper content. The ΔT_{res} is important annealing efficiency index because it determines the starting point for embrittlement at post annealing irradiation.

The dependence of ΔT_{res} on copper content after annealing at 343°C is shown in Figure 3. The neutron fluence values vary from 1 to $6{\cdot}10^{19}$ (E>1 MeV) cm^{-2}. In spite of rather big scatter (due to different fluences) the tendency of ΔT_{res} reduction with Cu decrease is definitely seen. As to the point: ΔT_{res} = 47°C for Cu = 0.055%, it has to be noted, in this experiment the T_k shift is about 85°C and recovery is ~45%. The presented results reveal that annealing at 343°C could be rather effective for steels with low copper (less than 0.1%) content.

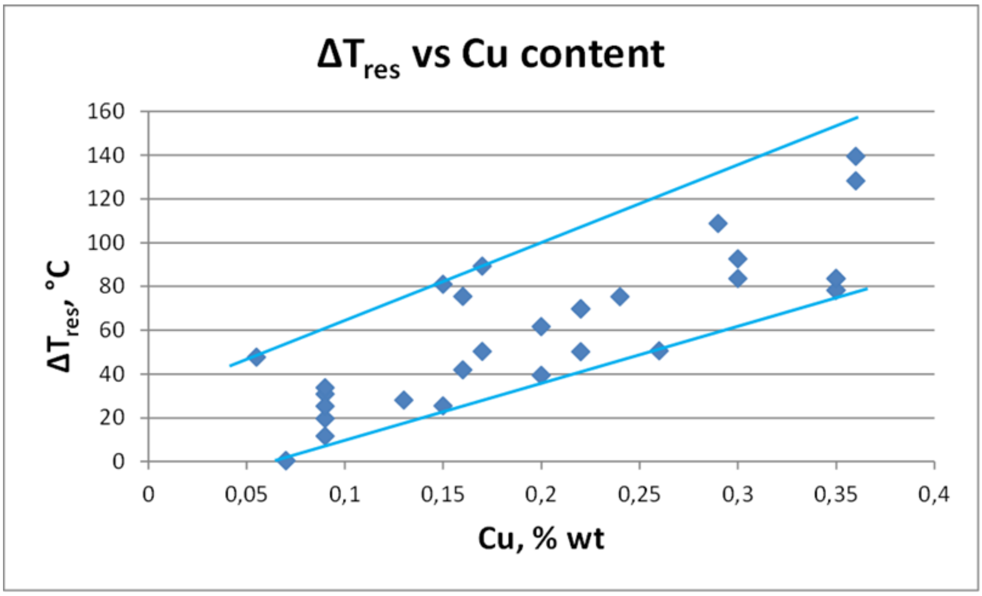

Figure 3: The dependence of ΔT_{res} on copper content after annealing at 343°C.

The microstructural examinations of irradiated and annealed VVER RPV steels were performed in [15-17]. Unfortunately, there are no microstructure results of VVER RPV steel irradiated and annealed at 343°C. Nevertheless some assumptions concerning the changes in steel microstructure due to "wet" annealing could be done. As it mentioned before, the main embrittlement mechanisms are matrix hardening from irradiation-induced point defects and dislocation loops and are also hardening from clustering of copper and other elements creating nanometer-size clusters and precipitates. Due to annealing, the elimination of radiation induced defects occurs. The nano-clusters eliminate at high annealing temperature 450°C and higher [15-17]. The activation energy of matrix defects is less than nano-clusters and at least part of them has to be eliminated at 343°C. The annealing of eventual phosphorus grain boundaries segregation is not considered because of the low phosphorus level in the modern PWR RPV steels.

The presumptive scheme of irradiation embrittlement mitigation by low temperature "wet" anneal is shown in Figure 4. It is seen in the Figure – the more neutron fluence, the more T_k shift recovery. In the event of low copper steel the Cu precipitate contribution in irradiation embrittlement is small or absent and recovery due to annealing is higher.

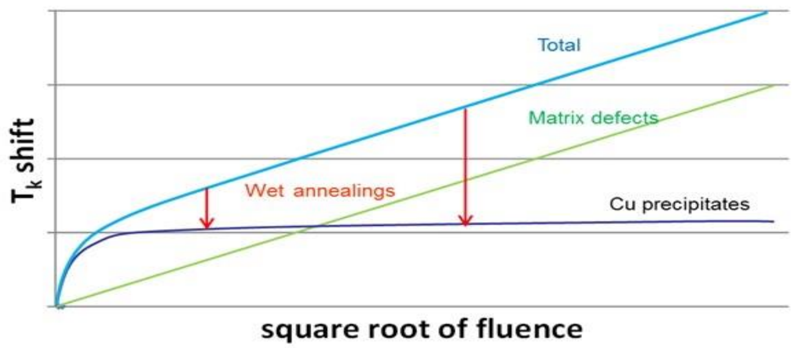

Figure 4: The presumptive scheme of irradiation embrittlement and mitigation by low temperature "wet" annealing.

The nickel content in steels, characterized in Figure 3, is not more than 1%. Thereupon the effectiveness of the annealing at 343°C for highly irradiated low copper high nickel steel has to be analyzed. The annealing at 400, 460 and 490°C of the highly irradiated low Cu high Ni VVER-1000 RPV weld is evaluated in this paper, see Figure 5. The experimental points presented in Figures 5-7 are the test results of specimens irradiated (including re-irradiation after annealing) in VVER surveillance channels. The presented results demonstrate almost full T_k shift recovery after thermal annealing at 400°C (ΔT_{res} not more than 20°C). It might be supposed that a such steel substantial recovery occurs after annealing at 343°C.

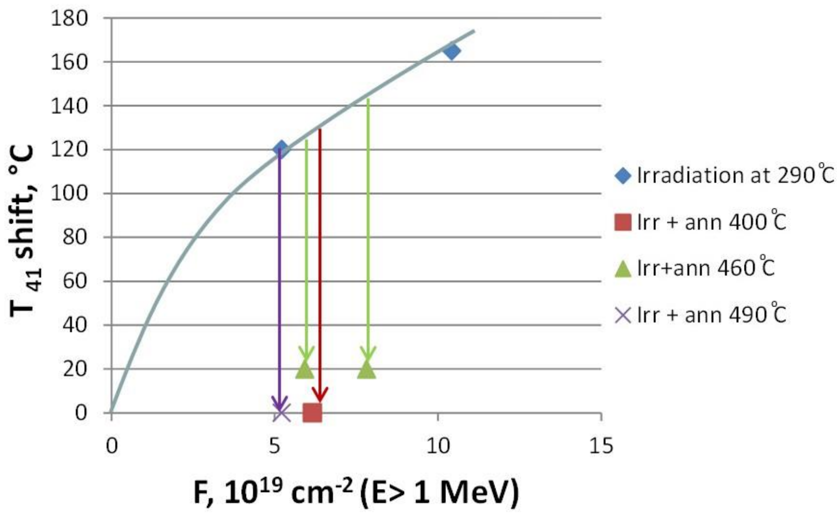

Figure 5: The VVER-1000 RPV weld (0,07% Cu, 1,68% Ni, 0,7% Mn, 0,008% P) irradiation and annealing.

At present, some RPV steels exhibit a considerable radiation embrittlement, even if the copper content is low [18]. The formation of so-called "Late Blooming Phases" (LBP) can occur in highly irradiated RPV steels. The LBPs are clusters/precipitates that contain nickel and manganese (and sometimes silicon) atoms and are part of a continuum of chemically complex irradiation induced features that evolve as the result of irradiation time and neutron fluence and were postulated by Odette as early as 1995 [19,20]. Significant research is ongoing in this area to include the development of thermodynamic-kinetic models. A recent atom probe analysis of low-Cu surveillance welds from the Ringhals Units 3 and 4 reactors have shown Ni-Mn-Si precipitates as the cause of T_k shifts over 160°C at 5 to $6x10^{19}$ cm^{-2} [18]. The copper contents in Ringhals units are 0.05 and 0.08%, the nickel contents are 1.58 and 1.66%. The activation energy of LBPs could be somewhat higher than those traditionally considered for Cu clusters/precipitates and they apparently do not eliminate unlike matrix defects due to annealing at 343°C.

4.3 Re- embrittlement after thermal annealing

The re-embrittlement rate after recovery anneal is usually smaller than that observed in the primary irradiation and depends on annealing temperature [7, 21-26]. The T_k recovery and re-embrittlement of low nickel VVER-440 steels three times irradiated and annealed at 340 and 460°C are presented in Figure 6 [7]. It is seen from Figure 6 that the embrittlement rate after annealing at 340°C is much less than primary irradiation and irradiation after the 460°C annealing. It might be supposed that due to annealing at 460°C and re-irradiation the elimination and re-formation both matrix defects and Cu precipitates occur. In the event of 340°C annealing the more stable Cu precipitates do not change. The reduction and increase of T_k shift are the results of matrix defects elimination and re-formation. As a result the re-embrittlement rate after low temperature annealing is substantially less than after high temperature annealing.

a)

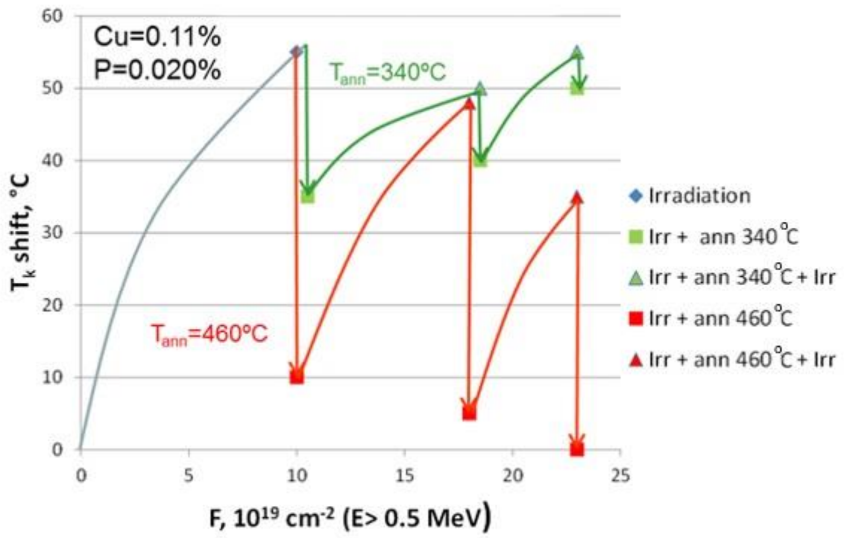

b)

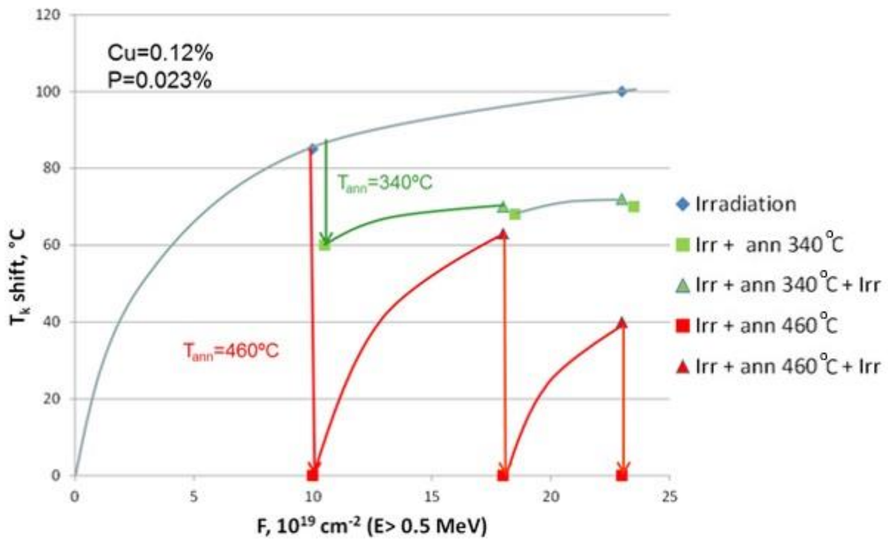

Figure 6: The T_k recovery and re-embrittlement of low nickel VVER-440 steels three times irradiated and annealed at 340 and 460°C, a) – base metal, b) – weld metal [7].

For the low copper RPV steels the Cu precipitates contribution is small and re-embrittlement rate should not depend much on annealing temperature. This is supported by the re-embrittlement of highly irradiated low Cu high Ni WWER-1000 weld annealed at 400°C and 490°C and re-irradiated at 290°C, see Figure 7. The re-embrittlement rate after full recovery is substantially less than primary embrittlement for both annealing temperatures. It might be supposed that the re-embrittlement is determined mainly by matrix defects. It is supposed that for low Cu high Ni steel the re-embrittlement rate after annealing at 343°C is to be substantially less than primary embrittlement. Undoubtedly, special experiments with specific PWR RPV steel have to be done particularly for eventual LBP formation.

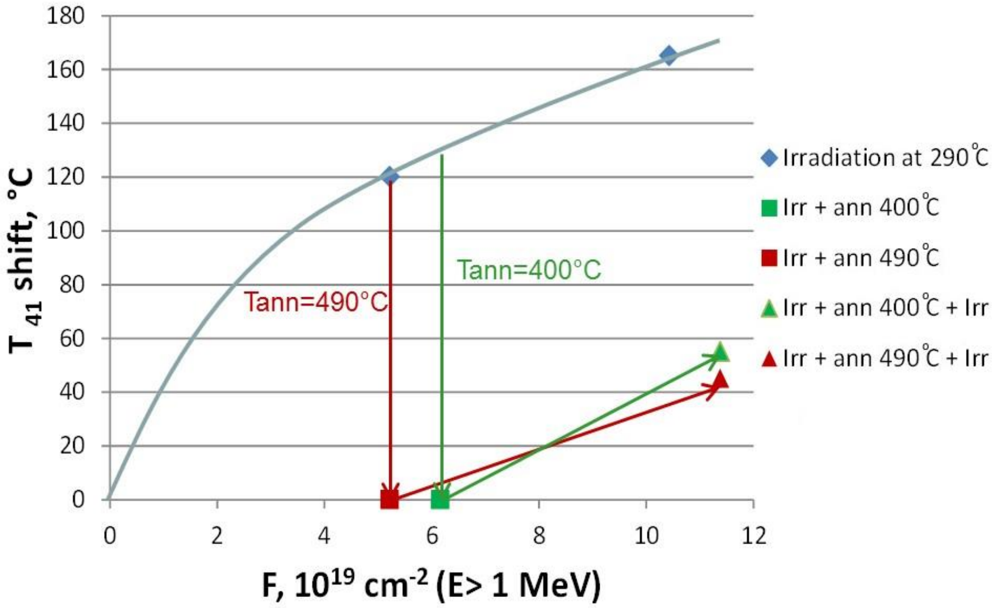

Figure 7: The recovery and re-embrittlement of VVER-1000 weld (0,07% Cu, 1,68% Ni, 0,7% Mn, 0,008% P) annealed at 400 and 490°C and re-irradiated at 290°C.

5 CONCLUSIONS

The analysis of the surveillance test results from IAEA Database showed that if the metal has a low content of impurity elements (copper and phosphorus), the shift of the T_k is low. Due to this the T_k maximum allowable value of the neutron fluence for relatively “pure” ones (Cu < 0.13%, P < 0.017%) can be increased from 3 10^{20} to ~ 5 • 10^{20} cm^{-2}.

The “wet” thermal annealing at ~340°C mitigates significantly the irradiation embrittlement of the irradiated RPV steels with relatively small copper content. The most part of irradiation induced matrix defects eliminate due to the annealing. This leads to the recovery of irradiated steel mechanical properties that is expressed in the reduction of T_k shift.

The residual after annealing T_k shift depends on Cu content and ΔT_{res} is to be less than 40°C for low Cu steel. It is supposed that the residual embrittlement results from radiation induced Cu precipitates, their activation energy is higher and they survive due to low temperature annealing.

The re-embrittlement rate after annealing at ~340°C is smaller than the observed in the primary irradiation. It is caused only by re-formation of matrix defects and it is not caused by Cu precipitation.

The “wet” anneal is performed at temperatures < 350°C. At that temperature the reactor coolant water is generally heated by the reactor circulation pumps. The annealing is not so complicated and internals could be inside the reactor vessel.

6 REFERENCES

1. A. Kryukov, A. Ballesteros, C. Bruynooghe, U. von Estorff, "International Database on Reactor Pressure Vessel Materials for Long Term Operation of NPPs", Journal of Nuclear Technology, vol.180, Dec. 2012, 443-449.
2. V. Slugen, A.Kryukov, “Microstructural study of WWER reactor pressure vessel steels”, Nuclear Engineering and Design, vol. 263, 2013, 308-312.
3. A.Kryukov, L.Debarberis, U. von Estorff, F.Gillemot, "The role of chemical composition in WWER RPV irradiation embrittlement", International Journal of Nuclear Knowledge Management, 4, 2010, 301-318.
4. A.Kryukov, D. Blagoeva, L. Debarberis, “Flux effect analysis in WWER-440 reactor pressure vessel steels”, Journal of Nuclear Materials, 443 (2013) 171-175.
5. A. Kryukov, L. Debarberis, U. von Estorff , F. Gillemot and F.Oszvald, "Irradiation Embrittlement of Reactor Pressure vessel Steel at Very High Neutron Fluence", Journal of Nuclear Materials, 422 (2012), 173-177.
6. A. Kryukov, L. Debarberis, P. Hähner, F. Gillemot, F. Oszvald, "Prediction of irradiation embrittlement of vanadium alloyed low nickel steel for future reactors", Journal of Nuclear Materials 419 (2011) 327-330.
7. Amaev, A., Kryukov, A., Sokolov, M, “Recovery of transition temperature of WWER vessel metal by Annealing”, ASTM STR 1170, 1993.
8. Hawthorne, J.R., NRL 8287, Naval Research Laboratory, February, 1979.
9. Hawthorne, J.R., NRL 8264, Naval research laboratory, April 1979.
10. Mager, T.R., “Feasibility and methodology for thermal annealing an embrittled reactor vessel”, EPRI NP-2712, Electrical Power Research Institute, Vol. 2, November 1982.
11. Hawthorne, J.R., “Exploratory assessment of post-irradiation heat treatment variables in notch ductility recovery of A533-B steels”, NUREG-3229, MEA-2011, NRC, M 1983.
12. A. Kryukov, R.K. Nanstad, M. Brumovsky,,”Common comparison of the irradiation embrittlement of WWER/PWR reactor pressure vessel steels”, Nuclear Engineering and Design, Volume 273, July 2014, 175-180.
13. A. Kryukov, L. Debarberis, P. Haehner, F. Gillemot and F. Oszvald,”Thermal annealing as a method to predict results of high irradiation temperature embrittlement”, Journal of Nuclear Materials, 429 (2012) 190-200.
14. Eason, E.D., Wright, J.E., Nelson E.E., Odette G.R., Mader, E.V., “Models for embrittlement recovery due to annealing of reactor pressure vessel steels”, NUREG/CR-6327, US NRC May, 1995.
15. Miller, M.K., Chernobaeva, A.A., Shtrombakh, Y.I., Russell, K.F., Nanstad, R.K., Erak, D.Y., Zabusov, O.O., “Evolution of the nanostructure of VVER-1000 RPV materials under neutron irradiation and post irradiation annealing”, Journal of Nuclear Materials, 385 (2009), 615-622.
16. P. Pareige, R. Stoller, K. Rassel, M. Miller, “Atom probe characterization of the microstructure of nuclear pressure vessel surveillance material after neutron irradiation and after annealing treatments”, Journal of Nuclear Materials, 249, Issues 2-3 (1997), 165-174.
17. A. Kryukov, L. Debarberis, A. Ballesteros, S. Rogozhkin et al, “Integrated analysis of WWER-440 weld re-embrittlement after annealing”, Journal of Nuclear Materials, 429 (2012), 190-200.

18. M.K. Miller, K.A. Powers, R.K. Nanstad, and P. Efsing, "Atom Probe Tomography Characterizations of High Nickel, Low Copper Surveillance RPV Welds Irradiated to High Fluences," Journal of Nuclear Materials. 437 (2013) 107-115.

19. G. R. Odette, "Microstructural Evolution during Irradiation," p. 137 in MRS Symp. Proc. 373, Materials Research Society, 1995.

20. G.R.Odette, B.D. Wirth, T. Yamamoto, "Late blooming phases and dose rate effects in RPV steels: Integrated experiments and models", Multiscale Materials Modeling (Proc. Second Int. Conf.), Los Angeles, CA(2004) 355.

21. Hawthorne, J. R., "Status of Knowledge of Radiation Embrittlement in USA Reactor Pressure Vessel Steels", NUREG/CR-2511, NRL Memo Rpt.5, 4737, Naval Research Laboratory, Washington, D.C., 1982.

22. Hawthorne, J. R., . "Irradiation-Anneal-Reirradiation (IAR) Studies of Prototypic Reactor Vessel Weldments", NUREG/CR-5469, MEA-2364, Materials Engineering Associates, Inc. Lanham, MD, 1989.

23. Mager, T. R., "Thermal Annealing of an Embrittled Reactor Vessel: Feasibility and Methodology", Nuclear Engineering and Design, Vol. 124, 1990, 43 – 51.

24. Kryukov, A. M. and Sokolov, M. A., "Investigation of Material Behavior under Reirradiation after Annealing Using Subsize Specimens", ASTM STP 1204, Philadelphia, 1993, 417-423.

25. M. Kolluri, , A. Kryukov, , A.J. Magielsen, P. Hahner, V. Petrosyan, G. Sevikyan, Z. Szaraz, Mechanical properties and microstructure of long term thermal aged WWER 440 RPV steel, Journal of Nuclear Materials 486 (2017) 138-147.

26. A.Kryukov, G. Sevikyan, V. Petrosyan, A. Vardanyan "Irradiation embrittlement assessment and prediction of Armenian NPP reactor pressure vessel steels", Nuclear Engineering and Design 272 (2014) 28–35.

RPV integrity assessment – a comparison of regulatory approaches in nine ETSON member countries

Uwe Jendrich / ETSON

Abstract:

In each country operating LWRs stringent regulatory requirements are defined for design, procurement, manufacturing, in-service inspection, surveillance programme, and the structural integrity assessment of the RPV. In the frame of the activities of ETSON, the expert group “Mechanical Systems” decided to compare these regulatory requirements in those ETSON member states represented in the group, i.e. in Belgium, Czech Republic, France, Finland, Germany, Russia, Slovakia, Switzerland and Ukraine. The focus was on the RPV fracture mechanical assessment for the most severe transients, i.e. Pressurized Thermal Shocks. The main objective was to improve the mutual understanding of the different approaches and the identification of differences as well as possible evolutions of the regulations. While most of the regulatory requirements defined in the different countries are based on similar principles, they differ significantly in many details that will be highlighted in this presentation.

1 INTRODUCTION

The integrity of the RPV of each LWR has to be proven with high confidence for the whole lifetime of each NPP. As its failure was not assumed in the design of the plants in operation today, break preclusion is applied to the RPV. This requires ensuring a very low probability (or preclusion) of RPV failure by strengthening the first two levels of the defence-in-depth approach by defining stringent, mostly prescriptive regulatory requirements in the design, procurement, manufacturing, in-service inspection, surveillance programme, and more globally in the structural integrity assessment of the RPV.

The ETSON expert group “Mechanical Systems” chose this key issue as a topic for their first report [1] with a focus on the fracture mechanical analyses. The main objective of the report is to improve the mutual understanding of the different approaches and the identification of differences as well as possible evolutions of the regulations. In the main part, the report describes the general approach and the communalities and differences between the regulations and their application in the participating countries. In the annexes, many details are given that might be most interesting for experts in the field, such as fracture toughness curves, predictive formulas for their changes under irradiation, and a large table comparing the requirements and assumptions made in all nine countries regarding different items such as material properties, prognosis of their irradiation induced changes, scope and technique of non-destructive testing, content and scope of irradiation surveillance programmes, details of the fracture mechanic analyses, selection of transients, postulated crack sizes, and mitigative measures applied.

2 COMMUNALITIES AND DIFFERENCES

2.1 General Approach to RPV integrity analyses

The general approach for the integrity analysis of the RPV is basically the same in all participating countries. At first the RPV design has to take care of all static loadings (internal pressure, dead weight, moments) by strength analyses and of all cyclic loads by fatigue analyses. Both these analyses have to be performed for any pressure vessel and are not addressed in this paper. In addition, for the RPV, fracture mechanical analyses have to be performed, as brittle fracture is a concern due to the embrittlement of the RPV beltline under neutron irradiation.

For this, the most severe loadings of the RPV are analysed for all operating conditions. Thermo-hydraulic analyses of the different transients (including accident scenarios) and the evaluation of the heat transfer to the RPV will result in time dependent temperature distributions within the RPV. The temperature gradients within the RPV create a stress field analysed by structural mechanic codes mostly using finite elements.

As the existence of defects in the RPV cannot be excluded with absolute certainty and to show some defect tolerance, cracks as the most detrimental kind of defects are postulated at the most adverse location and orientation. The loading of the crack during the transient in terms of a stress intensity factor $K_I(t, T)$ is then compared to the fracture toughness of the material $K_{Ic}(T)$ at the end of the lifetime. For some transients and accidents, namely Pressurized Thermal Shocks (PTS), the contribution of the temperature gradients to $K_I(t, T)$ is much larger at some locations than the contribution of the vessel internal pressure. Anyway, both have to be superimposed. If the total loading in terms of K_I is lower than the fracture toughness of the material $K_{Ic}(T)$ at the same location, then no crack initiation will occur.

Showing this is mandatory in most countries. Graded safety factors are applied for the different categories of operating conditions, i.e. larger safety factors are required for more frequent operating conditions. Major differences between the requirements in the participating countries exist in the determination of fracture toughness, the selection of transients and boundary conditions to be considered, the postulated crack size, and applied safety factors.

2.2 Fracture toughness and Ductile-Brittle-Transition

All ferritic steels undergo a transition from brittle behaviour at low temperature to ductile behaviour at higher temperatures, see figure 1 for illustration. The temperature range of the transition between both levels is generally indexed by a ductile-brittle transition temperature (DBTT). In the traditional approach, the DBTT is determined from results of the so-called Charpy test, where a small notched bar is broken by the impact of a hammer. Mainly the Charpy energy, i.e. the energy dissipated to break the notched bar is used as a criterion to define the DBTT. In Western countries the amount of plastic deformation during the Charpy test and the results of a drop weight "Pellini" test in terms of a nil-ductility temperature are also considered to define the DBTT, called here RT_{NDT}.

A generic fracture toughness curve $K_{Ic}(T)$ can be adjusted on the temperature axis by this DBTT of the individual material, i.e. it has the form $K_{Ic}(T - DBTT)$. Close to the upper shelf, where some plastic deformation takes place before fracture, fracture toughness is referred to as K_{Jc}. Next to the curve $K_{Ic}(T)$, that is based on data for crack initiation, the US-American ASME code considers a similar curve based on crack arrest data $K_{Ia}(T)$. As crack arrest takes place at lower K_I-values than initiation, the $K_{Ia}(T)$-curve is below the K_{Ic}-curve. The $K_{Ia}(T)$-curve is also referred to as $K_{IR}(T)$ being a common lower bound to all fracture toughness data.

The degradation of the fracture toughness by neutron irradiation can be represented by a shift of the DBTT to higher temperature, see figure 1. Experimentally, this shift is mostly determined from the shift of the Charpy energy versus temperature curve that also behaves like figure 1 with “energy” on the ordinate. Based on existing data empirical formulas are derived in the form $\Delta DBTT = CF \cdot F^n$ to predict the shift as a function of the fast neutron fluence F and a factor CF that depends on the material. This prediction for design purposes is then validated by test results from surveillance specimens made of materials representative for the beltline materials and subject to accelerated irradiation within the RPV.

Historically, the curve K_{Ic} (T - DBTT) used for the fracture mechanical analyses was created as a “lower bound curve” to a large number of fracture toughness data K_{Ic} (T) by testing rather large, mostly Compact Tension (CT)-type specimens. This type of specimens is considered too big to be integrated into the RPV surveillance program. Therefore, these fracture toughness data were correlated with the DBTT of the same materials determined by testing the much smaller Charpy type specimens that serve as surveillance specimens to be installed in the RPV and that are also used for acceptance tests during manufacturing.

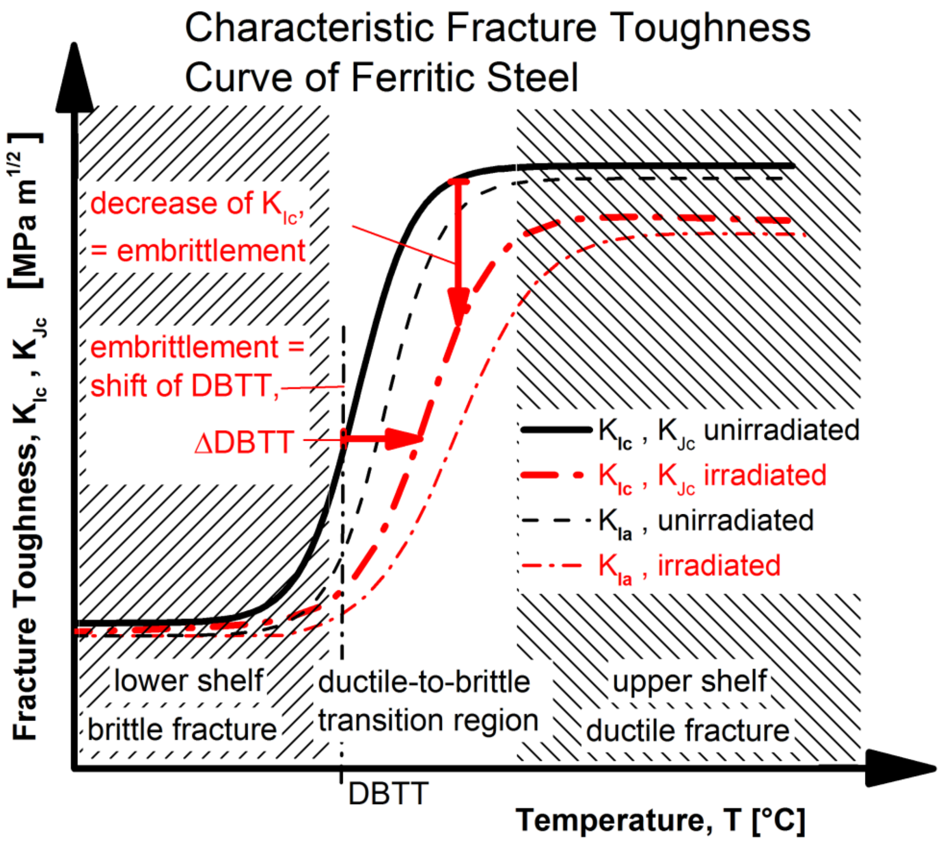

Figure 1: Illustration of the temperature dependence of fracture toughness of ferritic steels: Toughness for crack initiation in the brittle/ductile regime (K_{Ic} /K_{Jc}) and for crack arrest (K_{Ia}). The transition from ductile to brittle is indexed by the Ductile-Brittle Transition Temperature (DBTT). The curves and arrows in red show the changes of these properties due to neutron irradiation (“embrittlement”).

The procedure as described above is common to all countries, while the form of the fracture toughness curves and the way to define the DBTT may differ significantly: Traditionally Western countries basically use the K_{Ic}(T) curve and the “Reference Temperature of Nil-Ductility Transition” RT_{NDT} as DBTT adopted from the US-American ASME code, while countries operating VVER plants used the curves and “Critical Temperature of Brittleness” T_k adopted from the PNAE code of the former Soviet Union. Each of these curves has a fixed shape, regardless of the value of the DBTT, yet PNAE proposes different curves for weld metal, base metal of VVER440, of VVER1000, and a lower bound for all materials. While all the PNAE curves are still in use in Ukraine, Czech and Slovak republic only use the lower bound curve, as proposed by the EU project VERLIFE [2].

In the 21st century new curves and definitions of DBTTs were developed and adopted in some national regulations [1]:

- Some countries allow to or even recommend using the reference temperature T_0 of the “Master Curve”, that is a probabilistic curve with the same shape for all ferritic steels in the transition region. Yet, no lower bound can be defined from the Master Curve but only fractiles, so that for a large number of specimens statistically e.g. 5% of the data fall below these curves. Furthermore, T_0 tends to be lower than RT_{NDT}, especially for base metal, and the irradiation induced shift ΔT_0 tends to be higher than ΔRT_{NDT}. So, if T_0 shall be used as an alternative to RT_{NDT} as an index temperature for the “lower bound” reference curve an additional shift and a margin is used.
- In the new Russian code, the “Unified Curve” was adopted, that becomes flatter with increasing embrittlement by introducing a second parameter Ω. While this curve is considered to be more realistic for highly embrittled RPV steels (i.e. high T_k, low Ω), it is much more complicated to handle and very close to the shape of the Master Curve for steels with low to moderate embrittlement [3].

Conclusion: While all these different fracture toughness curves and definitions of DBTT would give similar values for the same material, the differences between these values are still significant, and a simple comparison of numbers is not always meaningful.

2.3 Prognosis of irradiation induced changes

In the design phase of the plant, a prognosis of irradiation induced changes of the DBTT is needed and a predictive formulae $\Delta DBTT = CF \cdot F^n$ has to be used. The equations in different codes have exponents n between 0.28 and 0.6 and a “chemical factor” CF that depends on the concentration of some of the chemical elements in the individual weld or piece of base metal promoting irradiation embrittlement, e.g. Cu, P, Ni and Mn. For some VVER materials, CF may also be defined as a constant.

For safety assessments of the RPV during operation the predictive formula has to be used in some countries, where the surveillance data only serve to validate the prediction. In other countries, the curve established on the basis of surveillance data can be used for the assessment with a margin added. In Germany a “limit value” RT_{limit} = 40°C that is supposed to be an upper bound for EOL to all surveillance data of German plants in operation is given in the KTA standard. This value or the surveillance data may be used.

As each predictive formula was developed experimentally on the basis of data obtained from vessel materials of a few manufacturers and specifications, it should not simply be transferred to the vessels of other manufacturers or specifications.

2.4 Scope and techniques for non-destructive testing

During manufacturing all the forgings, welded joints and cladding have to be covered to 100% by ultrasonic testing in all countries. Other techniques may apply for surface testing. Pre-service inspections (PSI) mainly serve as a baseline for the in-service inspections (ISI). Their scope covers the whole vessel in some countries while in other countries the inspections are restricted to the welds and surroundings that are also covered by the standard ISI.

The ISI of the RPV in Western countries is restricted to ultrasonic testing of the welds and their surroundings and surface testing of the cladding. In PWRs all inspections are done from the inside of the vessel. In France the area under the cladding in the beltline is checked in addition for underclad cracks. Inspection periods are generally 10 years, 5 years in Germany.

Also, in VVER vessels ISI of the RPV is focussed on welds and their surroundings plus the inner surface of the cladding. In addition, inspections of some part of the base metal in the beltline are performed in some countries. Inspections are performed from the inside and the outside, sometimes in an alternating manner. Inspection periods were initially 4 years, they were extended to 6 or 8 years in some cases.

While inspection strategies in the participating countries are similar in general, differences are apparent with respect to the coverage of base metal during PSI and ISI as well the area under the cladding. In the frame of long-term operation (LTO) a change of inspection scope or intervals may be considered.

2.5 Content and scope of irradiation surveillance programmes

The type of specimens included in the surveillance programmes is almost the same in all countries (tensile, Charpy and small fracture toughness specimens of the base metal(s) and weld in the beltline). There may be some differences in the number of sets, sometimes dependent on the fluence to be covered, and the amount and kind of fracture toughness specimens. In some countries, extra sets were introduced or are foreseen to cover LTO. In addition, the possible embrittlement of RPV support structures close to the core may also be addressed in some VVER1000.

Some VVER 440 units also have some cladding specimens in their programme, as the cladding is particularly thick (9 mm nominal) and RPV fluence very high. So, the embrittlement of the cladding may be significant and have an impact on RPV integrity.

The lead factors, i.e. the ratio of fast neutron flux at the specimen and the maximum at the inner surface of the RPV, differ significantly between the plant types, reflecting different surveillance philosophies or design restrictions: Lead factors are very low (1 to 2) in VVER1000 and French 1300MW plants, about 3 in French a Belgian 900MW units, in the range of 3 to 6 in German plants, and larger than 10 in the original VVER 440 surveillance programs. In most VVER440 "supplementary" surveillance programmes with lead factors in the range of 2 to 6 were introduced later.

While very low lead factors will give results for EOL very late and do not allow for flux reduction as a mitigative action, very high factors may lead to non-conservative results due to a possible flux effect, in case the embrittlement is lower at high flux.

2.6 Postulated crack sizes and locations

In general, generic cracks are postulated separately in the weld and base metal at the most adverse location and orientation assuming material conditions corresponding to the highest fluence at EOL. The form of the cracks is always prescribed as semi-elliptic, mostly with an aspect ratio of 1/3, but sometimes also ratios of ½ or even 2/3 have to be analysed. The postulated size should cover any defect considered possible, i.e. that might have escaped its detection by the non-destructive testing performed. This results in prescribed depths twice the crack size that can safely be detected or in absolute numbers ranging from 5 to 15 mm or in ratios of the wall thickness s for VVERs ranging from 0.07 s to 0.125 s (s = 140 / 190 mm for VVER 440 / 1000).

Nevertheless, even if the ISI can prove the integrity of the cladding surface, cracks penetrating the cladding have to be analysed in some countries, while in other countries only underclad cracks are postulated. Besides, next to brittle fracture of the ferritic base or weld metal, in some countries ductile tearing of the cladding has to be analysed for postulated cracks within the cladding and/or for underclad cracks.

In case larger defects are detected, these have to be justified separately using the local conditions (fluence, temperature, stress). The requirements for the justifications are the same for postulated cracks and detected defects.

2.7 Use of crack arrest and warm pre-stressing (WPS)

In most countries it has to be proven that there is no crack initiation, yet in some countries the integrity might also be proven based on crack arrest after initiation. This opens large margins for fast transients creating a steep temperature gradient in the RPV wall, e.g. large LOCAs. In these cases, the outer parts of the RPV are still in the temperature range of the upper shelf. Yet, the predictability of (multiple) crack jumps are questionable.

Another issue in discussion for a long time is the application of WPS, i.e. the increased K_{Ic} (T) of the material at low temperature after pre-stressing in the temperature range of the upper shelf. While the existence of the WPS effect is generally accepted, it is codified only in the German KTA and also in the current version of VERLIFE /VER 08/. Yet it was also applied in some cases in several countries. The exact boundary conditions to be observed, in particular the question, if WPS can also be applied for non-monotonically decreasing stress during cooling, are still under discussion. The expert group “Mechanical Systems” chose this as one of the next topics for discussion.

2.8 Deterministic versus probabilistic approaches

The general approach described above is a deterministic one in all countries. Probabilistic approaches are applied as supplemental plant specific analyses in many countries. In Switzerland the application of probabilistic fracture mechanics (PFM) is under investigation with the aim to establish PFM for the assessment of RPVs and piping.

Beside these plant specific analyses, a simplified procedure is applied in Belgium following the US-American regulations. Based on generic probabilistic analyses for several representative PWR plants, screening values for the DBTT at EOL (defined as RT_{PTS}) of the different RPV materials (longitudinal / axial welds, base metal (plate or forging)) are defined. As long as these screening values are not exceeded by the materials of the individual RPV, no fracture mechanical analysis is required.

3 CONCLUSIONS

Most of the regulatory requirements related to RPV structural integrity defined in the ETSON countries represented by the participants are based on similar principles, but their approaches differ significantly in many details. Therefore, a direct comparison of results from different analyses should always consider the impact of these details. In the report of the ETSON expert group Mechanical Systems [1] many details regarding the fracture mechanical assessment of RPV integrity are described helping to assess these impacts. This will improve the mutual understanding of the analyses performed in other European countries according to their national regulations and may help their convergence during future evolutions.

4 ACKNOWLEDGEMENT

This report is a result of a network activity based on in-kind contributions and knowledge of the participants. I acknowledge all members of our ETSON expert group for the discussions and contributions to our common report, i.e. F. Balestreri /IRSN, V. Deledicque /Bel V, P. Hermansky /VUJE, A. Kryukov /SEC NRS, M. Niffenegger /PSI, V. Pistora /UJV, Tapio Planman /VTT, O. Shugaylo /SSTC NRS.

5 REFERENCES

1. Comparison of rules-making and practices concerning reactor pressure vessel integrity assessment
   ETSON Technical Report ETSON/2018-001, September 2018

2. Unified Procedure for Lifetime Assessment of Components and Piping in VVER NPPs “VERLIFE”, ver. 2008, 6th Framework Programme of EU, Project COVERS, Contract N° 12727 (FI60), report COVERS-WP4-D4.10

3. B. Z. Margolin, V. N. Fomenko, A. G. Gulenko, V. I. Kostylev, V. A. Shvetsova: On Issue of Comparison of the Unified Curve and Master Curve Methods and Application for RPV Structural Integrity Assessment,
   Strength of Materials (2016) 48: 227. https://doi.org/10.1007/s11223-016-9759-y

Evaluation of computer codes for nuclear safety analyses in the Czech Republic

M. Hrehor, G. Mazzini, A. Flores y Flores, M. Kyncl, A. Musa

Research Centre Řež (CV Řež, s. r. o.) Hlavní 130, Řež, Husinec, 250 68, Czech Republic

Abstract:

The paper informs about the system of evaluation of computational programs for nuclear safety analyses in the Czech Republic as implemented by the State Office for Nuclear Safety (SÚJB) in the Czech Republic. The quality and capability of qualified use of computer programs in nuclear safety assessment processes is as important as the quality and qualification of any nuclear safety-relevant component and is subject to the legislative requirements contained, inter alia, in SÚJB Decree No. 408 on Management System Requirements. The procedure for evaluating computational codes is contained in the SÚJB VDS 030 Internal Guideline for Evaluation of Computer Codes for Nuclear Safety Analyses. A key document of the evaluation process is a test protocol in which the applicant - code user - demonstrates how the code is able to simulate selected test cases (experiments, operational data, simulations with other approved calculation codes), as well as its own ability to apply the code competently without a negative user effect. The test process does not replace validation & verification process done by authors of the code. As examples, results of test cases for the evaluation of TRACE code in high temperature helium application, ATHLET code in supercritical water application, and MELCOR code in the application for selected PHEBUS and THAI experiments are provided.

1 INTRODUCTION

Assessment of nuclear safety using deterministic or probabilistic assessment methods is undoubtedly one of the processes affecting nuclear safety and radiation protection, as it demonstrates the level of compliance with nuclear safety and radiation protection requirements contained in current legislation. The quality and capability of the qualified use of computational codes in nuclear safety assessment processes is therefore as important as the quality and qualification of any component relevant to nuclear safety.

The importance of software products for nuclear safety is covered by the requirements of several separate decrees, which are implementing decrees to Act No. 263/2016 Coll., The Atomic Act of 14 July 2016, in particular

- SÚJB DECREE No. 329 of 26 September 2017 on Requirements for a Nuclear Installation Design, which in § 25 (2) explicitly requires that in the safety assessment verified methods corresponding to the currently achieved level of science and technology should be used

- SÚJB DECREE No. 162 of 25 May 2017 on Safety Assessment Requirements under the Atomic Act, which in § 3 “General Safety Assessment Requirements”, para (1) also requires that safety assessment be performed according to current and practical application proven methodologies in line with current science and technology levels and good practice, and also

- SÚJB DECREE No. 408 of 6 December 2016 on Requirements for a Management System whose general objective is ensuring and improving the level of nuclear safety and radiation protection

The procedure for evaluating computational codes introduced to meet these legislative requirements is contained in the internal SÚJB guideline VDS 030 Evaluation of Computer Codes for Nuclear Safety Analyses. This guideline implements rules for the evaluation of computer programs based on the standards ISO/IEC 9126-1 "Software Engineering - Product Quality" and ISO IEC 14598-1 "Information Technology - Software Product Assessment".

The purpose of this guideline is to ensure an independent evaluation of the quality and suitability of the computer programs used in safety documentation, including those received from other countries, while maintaining the rule that quality of computer programs (their validation and verification) is primarily the responsibility of the origin authoring organization. The SÚJB's independent evaluation of the quality and suitability of the calculation programs does not in any way replace the necessary validation and verification of software products on the part of the author's organization.

2 PROCESS OF EVALUATION OF COMPUTER PROGRAMS

The computer codes used for nuclear safety assessment are divided according to VDS 030 into seven areas:

- Reactor physic calculations
- Thermohydraulic analyses
- Calculations of nuclear fuel behaviour
- Analysis of severe accidents
- Strength calculations of components and piping systems
- Calculations of radioactive products propagation
- Probabilistic safety and reliability analyses.

For each of these areas, an expert evaluation committee has been established, whose members are leading experts of the Czech Republic from the main organizations and research centres in the field of nuclear safety assessment.

The members of the commissions, including their chairmen, are appointed by the SÚJB chairwoman. There is at least one SÚJB representative in all commissions. The members of the committee do not represent their parent organizations in the commission. These members participate in the activities of the Commission as independent experts and their membership is irreplaceable.

The basic purpose of computer codes evaluation is to provide quantitative and qualitative results indicating the quality of the software product and the user's ability to use it in applications to Czech nuclear facilities.

The evaluation of a software product shall commence when an applicant for evaluation asks in a letter addressed to SÚJB to perform the evaluation of the software product. Request for the evaluation of is forwarded to an appropriate Commission. Codes can only be evaluated if the user organizations can prove their legal acquisition.

The request of the submitting organization at SÚJB is documented, inter alia by:

- an evidence that the author’s organization holds a quality assurance document
- an evidence that the authors ' organization agrees to carry out the evaluation, which may be replaced by the submission of a license agreement between the authors' and the user's organizations on use the code.

Other key documents for the evaluation of the code that the submitting organization must provide include:

- Abstract of the code (Code Summary)
- Technical report(s) on code testing
- User Guide - manual instructions for using the program

2.1 Abstract of the Code (Code Summary)

Abstract of the code is elaborated by the user organization using the information of the author's organization. The abstract contains the following information:

a. Description of the problem or function of the code
b. Solution method
   - a brief description of the physical model, listing and discussing all assumptions and limitations used
   - a brief description of the mathematical model used with the analysis of the compatibility of numerical transcription and verification of the convergence and stability of the numerical process
c. Factors, limiting the complexity of the problem (constraints arising from the capacity of memory, maximum number of energy groups, nodes, etc.)
d. Brief characteristics of the code (computer requirements, programming language, structure, memory requirements, calculation speed, etc.)
e. Testing of the code (technical reports references)

2.2 Code testing technical report(s)

Code verification and correct use of the program is usually demonstrated by submitting a range of test cases containing simulations of available experimental, operational or other appropriate reference data, or by a comparison with the results of calculations with other already assessed computer codes. The technical reports shall include a description of the tests used (test characteristics, input data, results) and evaluation of the results. They also include determination of the achieved accuracy of individual computational quantities, specification of the program usability range, etc.

The scope and elaboration of the testing tasks are assessed by 2-3 independent opponents who submit their opinions to the Commission. The Commission has the right to request the processing of additional testing tasks.

If comparative tests do not sufficiently cover the issue (e.g. due to lack of comparative reference data), the scope of the testing is subject to an individual Commission assessment which may result in some restrictions on the application of the code.

2.3 User Guide – instructions for using the program

The User Guide, usually prepared by the authoring organization of the code, contains instructions for the use of the code, (if unreachable, it can be replaced by a description of the quality assurance of input deck, use of the program, etc.). Opponents can get acquainted with the user guide in the user's workplace (or from a publicly available source).

2.4 Evaluation process

Documentation, which is the output of the evaluation process

a) Opponent review - elaborated by 2-3 opponents
b) Minutes of evaluation process - to be provided by the chairperson of the Commission
c) "Position of the Expert Evaluation Commission on the use of the evaluated computer code" signed by the chairperson of the Commission and all opponents. This position becomes valid only after approval by the SÚJB.

The computer codes that have passed the evaluation procedure and for which the “Opinion of the Expert Evaluation Commission” has been approved are recorded and archived at SÚJB.

3 EXAMPLES OF TESTING SELECTED COMPUTER CODES

3.1 Code ATHLET in application for SCW

3.1.1 Code description

ATHLET code (Analysis of THermal-hydraulics of LEaks and Transients) is developed by GRS for the analysis of the whole spectrum of operational conditions, transients, design-basis accidents and beyond design-basis accidents for nuclear energy facilities. [1]

The code was selected for the simulation of the SCWL (Supercritical Water Loop) designed by CVR that is intended to be inserted in the LVR-15 research reactor.

This section will present the simulation of SWAMUP (Supercritical WAter MUltiPurpose loop) facility used in the certification process.

3.1.2 SWAMUP Facility

SWAMUP is a Chinese facility which was built in order to address SCW (Super Critical Water) thermo-hydraulic capabilities, reaching conditions specific to future Super Critical Water Reactors (SCWR). The facility was designed under a Chinese-European nuclear program at Shanghai University. The parameters and operating conditions of the facility were initially proposed by CVŘ based on the SCWR Fuel Qualification Test (FQT) facility. [2], [3]

The aim of the SWAMUP facility, ilustrated in Figure 1 is to provide out-of-pile thermo-fluid-dynamic data for benchmark activities such as code validation and to study the transition phenomena between super critical and sub critical conditions. Such facility is one of the closest research infrastructure to the future Super Critical Water Loop (SCWL) to be inserted in the LVR-15 Research Reactor. [2]

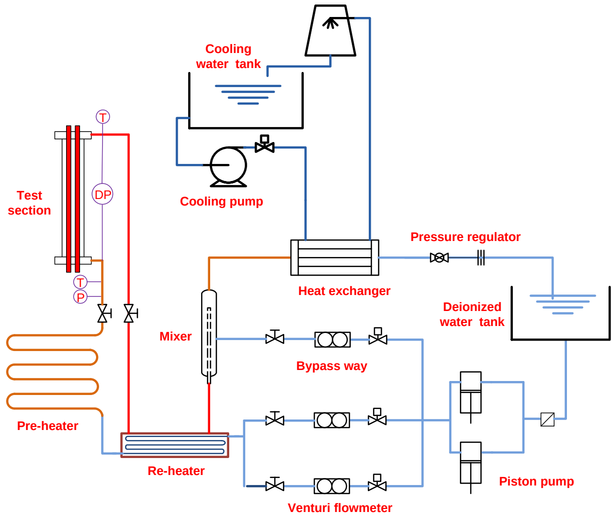

Figure 1: SWAMUP-II facility [2]

Several experiments have been performed and thermal-hydraulic data has been collected for evaluation. Further, the data was used to validate a modified system code ATHLET-SC. The results of the validation concluded that the code can predict SCWR phenomenon.

3.1.3 Test description

The configuration prepared to perform the experiments is illustrated in Figure 2. The loop is designed to a maximum pressure that reaches up to 30 MPa, a maximum outlet temperature of 550 ℃ and a mass flow of 5 t.h^{-1}. The fuel design uses the HPLWR (High Performance Light Water Reactor) fuel assembly as a reference [4]. The active channel nodalization can be seen in Figure 3.

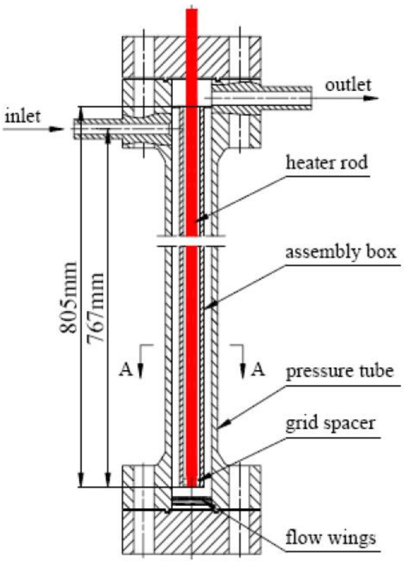

Figure 2 Test Section of SWAMUP Facility [2]

3.1.4 Model description of the active channel using ATHLET 3.1A

Based on the technical specification, geometrical details and thermo-hydraulic parameters from [2], a model was created to simulate the same geometry and SCW conditions using ATHLET 3.1A. The model is simulating steady state conditions and a transient case presented in Table 1. The boundary conditions for the steady state are following: heat flux of 428.5 kW.m^{-2} generated by the electrical coils, water mass flux of 1410 kg.m^{-2} s^{-1}. The maximum gradient is -2 MPa.min^{-1} starting from 25 MPa and arriving to 17 MPa. The whole calculation is performed with a simulation time of 3000 s.

Table 1: Steady state conditions [2]

No.	Initial Pressure [MPa]	Final Pressure [MPa]	Maximal Δ Pressure [MPa.min^{-1}]	Mass flux [kg.m^{-2}s^{-1}]	Heat flux [kW.m^{-2}]	Inlet Temperature [°C]
Case 2-D	25	17	-2	1410	428.5	345

3.1.5 Results and conclusions

The heat transfer correlations for the supercritical water simulation used in these analyses were Gupta, Mokry and Watts-Chou, which according to [5] are capable to predict the steady state conditions, taking into considerations some discrepancies that were detected during the end of the transient.

The results of the test case showed that the CHF (Critical Heat Flux) does not occur during the whole experiment in the transition from super critical to sub critical conditions. The ATHLET 3.1A is able to simulate the steady state conditions before the start of the depressurization at

125 s. The temperatures, measured with the Thermal Couple (TC) number 6 presented in Figure 3, are underestimated by 3-5 °C depending on the correlation and according to the simulation time; the results for TC 6 can be seen in Figure 3.

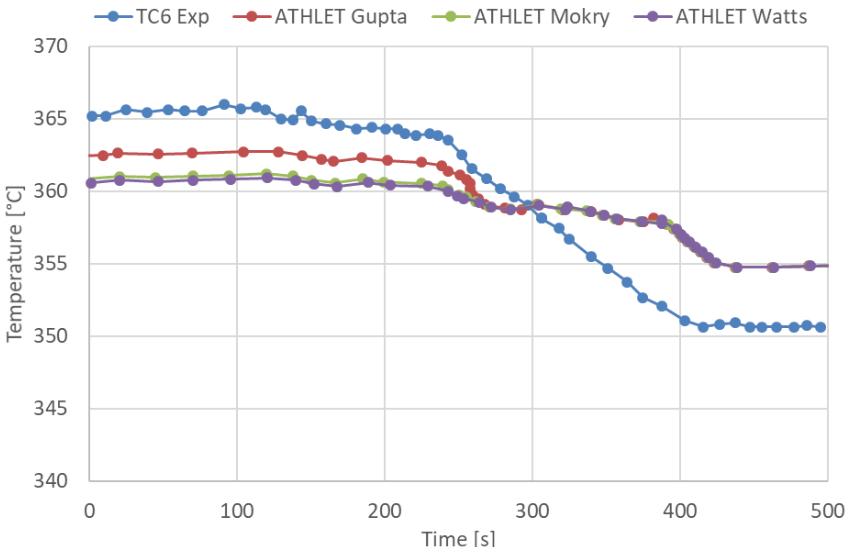

Figure 3: TC6 Rod Temperature

The general results showed that Gupta correlation has a better agreement with the experimental values, while Mokry and Watts-Chou correlations under predict the experimental value up to 5 °C.

The three correlations follow this behaviour until 300 s, as shown in the Figure 3, until they converge in Dittus-Boelter [1]. Also,the code overestimates the experimental temperature at the end of the transient. The reason is due to lack of the dettailed information provided in the deliverables of the project [2] [4].

Generally the DHT(Deteriorated Heat Transfer) phenomenon has still some lack of knowledge that has to be addressed within detailed analyses and new activities such as international projects. Further analyses are required in order to improve the correlations and the capability of the code to predict the heat transfer in supercritical water regime.

3.2 Code TRACE in application for HEFUS3 Facility

3.2.1 Code Description

TRAC/RELAP Advances Computational Engine (TRACE) thermal-hydraulic system code [6] [7] was adopted for simulating the LVR-15 reactor. In particular, it is considered the successor of the Reactor Excursion and Leak Analysis (RELAP) code by the Nuclear Regulatory Commission of United States (US NRC). It is commonly accepted that computational codes can be used properly only within their assessment range. The assessment issue of TRACE system code for thermal-hydraulic analyses of helium cooled systems has been addressed using selected data from the European Helium Cooled Blanket Test Facility (He-FUS3) experiments.

The TRACE has been designed to perform best-estimate analyses of loss-of-coolant accidents (LOCAs), operational transients, and other accident scenarios in pressurized light-water reactors (PWRs) and boiling light-water reactors (BWRs). It can also model phenomena occurring in experimental facilities designed to simulate transients in reactor systems. Models used in the TRACE code include multidimensional two-phase flow, nonequilibrium thermo-dynamics, generalized heat transfer, reflood, level tracking, and reactor kinetics. In addition, TRACE is able to simulate several other coolants such as helium and water in subcooled condition and atmospheric pressure (LVR-15 conditions) [8] [9].

For this reason, TRACE code was selected and used for the simulation of thermohydraulic behavior of Helium at 7 MPa with a temperature rise from 200 °C up to 900 °C (nominal parameters for HTHL). For qualifing the code The correlations adopted in TRACE for simulating the heat transfer from heat structures to the helium coolant and vice versa are Gnielinsky and El Genk [9] [10].

3.2.2 He-FUS3 Experimental facility

Italian National Agency for New Technologies (ENEA) Brasimone Research Center (Italy) was originally created for thermal-mechanical testing of prototypical module assemblies of the DEMO reactor. Within the frame of the Safety Work Package (WP) 1.5 Task 1.5.3 of the GoFastR (Gas Cooled Fast Reactor) European Collaborative Project, ENEA has offered selected experimental data for the organization of a benchmark exercise aimed at the validation of the System Codes and Computational Fluid Dynamics (CFD) codes for the gas reactor transient analyses [11] [12] [13]. During the project, Research Center Řež participated with CFD code application (FLUENT).

The He-FUS3 facility was selected within the frame of the European Fusion Technology Program [14] for the thermal-mechanical and thermal-hydraulic testing of prototypical module assemblies for the European demonstration Helium Cooled Pebble Bed (HCPB) Blanket design reactor [15]. Its eight-shaped loop configuration, described in Table 2 and shown in Figure 4, is trasporting the helium flow to the experimental Test Section (TS). In this section, the International Thermonuclear Experimental Reactor (ITER) module mock-up [16] can be tested. A simplified actively heated test section is available in the facility, which consists of a 7-pin bundle, 3 m high, with a single electrical power of 104 kW. The main performance data of the He-FUS3 facility are reported in Table 2.

Examples of termocouple positions are shown in the Table 3, summerizing the results obtained in [9]. All calculated data was in close agreement with the experimental ones, as shown for the steady state #1 case in Table 4 [9]. The steady state for the case #1 was reached at around 1700 s as shown in Figure 5. The TRACE calculation was run in the null transient mode for 1250 s in order to reach steady state conditions. Measured and calculated helium temperatures along the loop are shown in Table 4. In most cases, the coolant temperatures of interest are within their measurement uncertainty range (estimated at ± 3 °C in [11]) and they present an error <5% with respect to measurements.

Table 2 - He-FUS3 Pipe Lines Main Characteristics [11]

Line	Description	Diameter (m)	Insulation Thickness (m)	Max Temp (°C)
A	From TS to Economizer [orange]	0.130	0.16	520
B	From Economizer to Air-Cooler [yellow]	0.10	0.10	240
C	From Air-Cooler to Compressor [cyan-blue to violet]	0.10	0.06	100
D	From Tank to Cold By-pass T [lime]	0.10	0.06	140
E	From Economizer to Heater 3 [cyan]	0.10	0.16	420
F	From Heater 3 to Heater 1 [blue]	0.130	0.16	530
G	From Heater 1 to TS [orchid]	0.130	0.16	420
	Economizer [purple]			
H	From Cold By-pass T to Economizer and Cold By-pass [sky-blue]	0.10	0.10	240
I	By-pass heater [green]	0.10	0.10	140
L	By-pass Heaters 3-2 [red]	0.10	0.16	420
P	From Compressor to Tank [violet]	0.040	0.06	100
	Tank [olive]	0.81	0.16	140
	Test section [yellow-green]	0.080	0.16	520
	TS inlet [black to red]	0.13 to 0.08	0.16	420
	TS outlet [red to black]	0.08 to 0.13	0.16	520

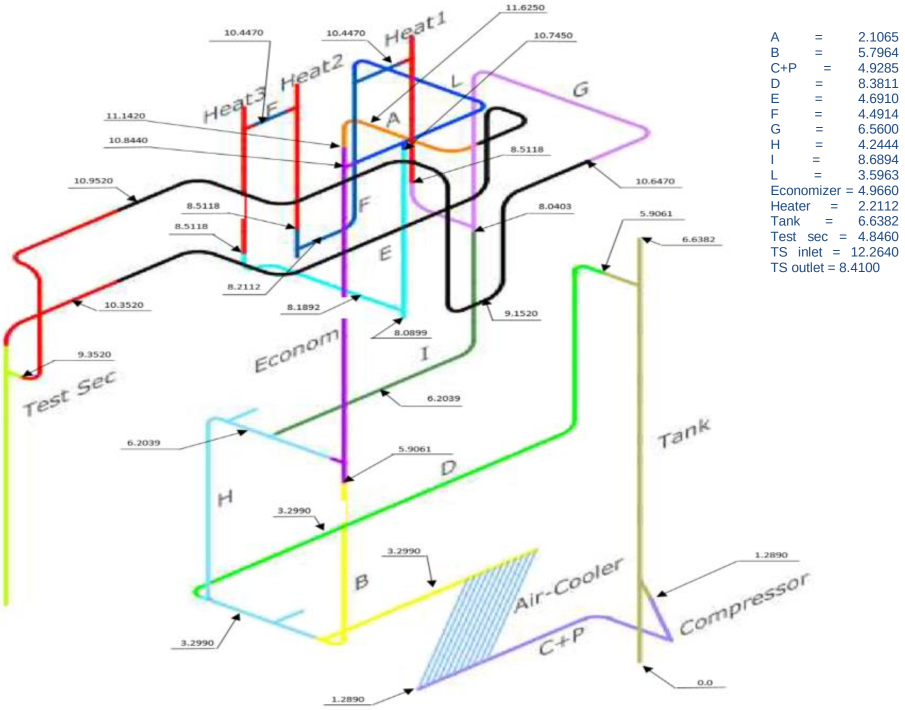

Figure 4 - He-FUS3 Piping Layout 3D Sketch (with height values [m], in black, and length values [m], in blue) [11]

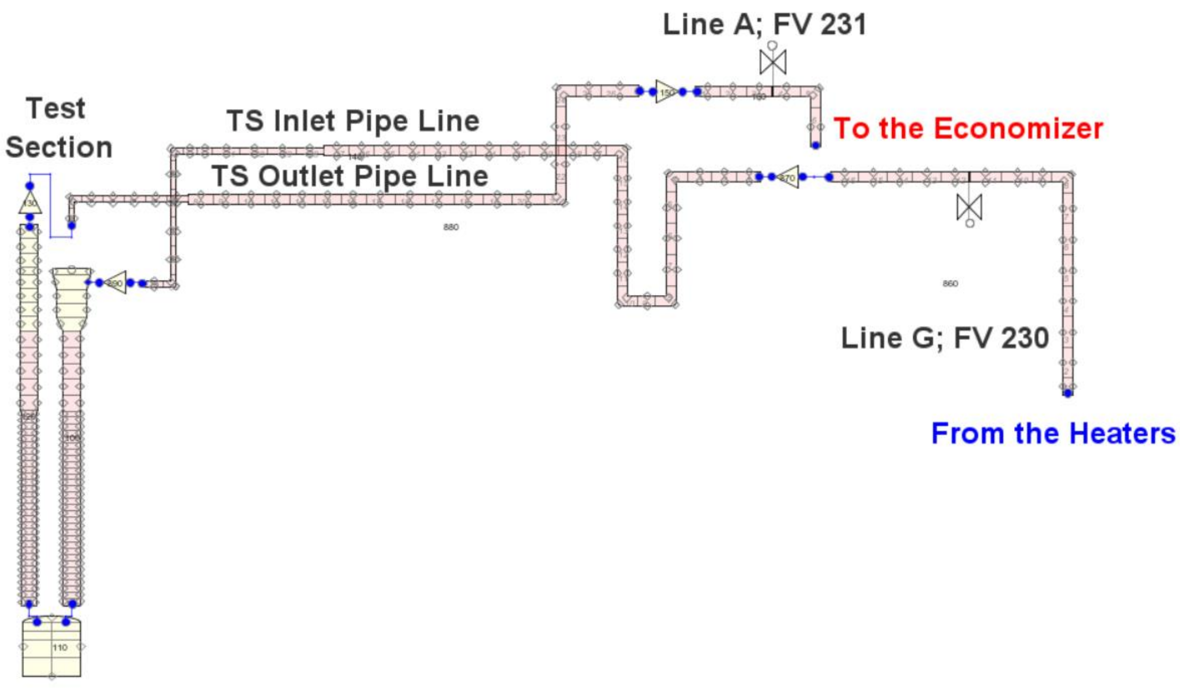

Figure 5 - He-FUS3 nodalization scheme– TS Scheme [9]

Table 3 - Example of He-FUS3 Measured Parameters [9]

He-FUS3 piping layout 3D sketch [9] ***ID***	***Parameter***
TR 218	Economizer Outlet Temperature (Hot Side) [°C]
TR 217	Economizer Inlet Temperature (Hot Side) [°C]
TIC 223X	Heater E219/1 Outlet Temperature for Power Regulation [°C]
TE 101	Test Section Inlet Temperature [°C]
TR 221	Heater E219/3 Outlet Temperature [°C]
TIC 222X	Heater E219/2 Outlet Temperature for Power Regulation [°C]
TIC 232X	Test Section Inlet Temperature for Regulation Valves V234/V213 [°C]
TE 102	Test Section Outlet Temperature [°C]

Table 4 - Example of He-FUS3 Steady State #1 Simulation (a: IDexp-IDcal; b: (IDexp-IDcal)·100/ IDexp) from [9]

He-FUS3 Steady State #1 Selected Parameters					Difference	
Parameter	**ID_{exp}**	**Value [°C]**	**ID_{cal}**	**Value [°C]**	**°C[(a)]**	**%[(b)]**
TS Inlet Helium Temperature	TE 101	230	cb_101	234.1	4.1	1.78
TS Outlet Helium Temperature	TE 102	292	cb_102	294.0	2	0.68
Economizer Inlet Temperature (Hot Side)	TR 217	289	cb_217	291.3	2.3	0.80
Economizer Outlet Temperature (Hot Side)	TR 218	122	cb_218	123.1	1.1	0.90
Heater E219/3 Outlet Temperature	TR 221	237	cb_221	240.0	3	1.27
Heater E219/2 Outlet Temperature	TIC 222X	235	cb_222	239.1	4.1	1.74
Heater E219/1 Outlet Temperature	TIC 223X	235	cb_223	237.5	2.5	1.06
TS Inlet Temperature - Regulation	TIC 232X	233	cb_232	236.7	3.7	1.59

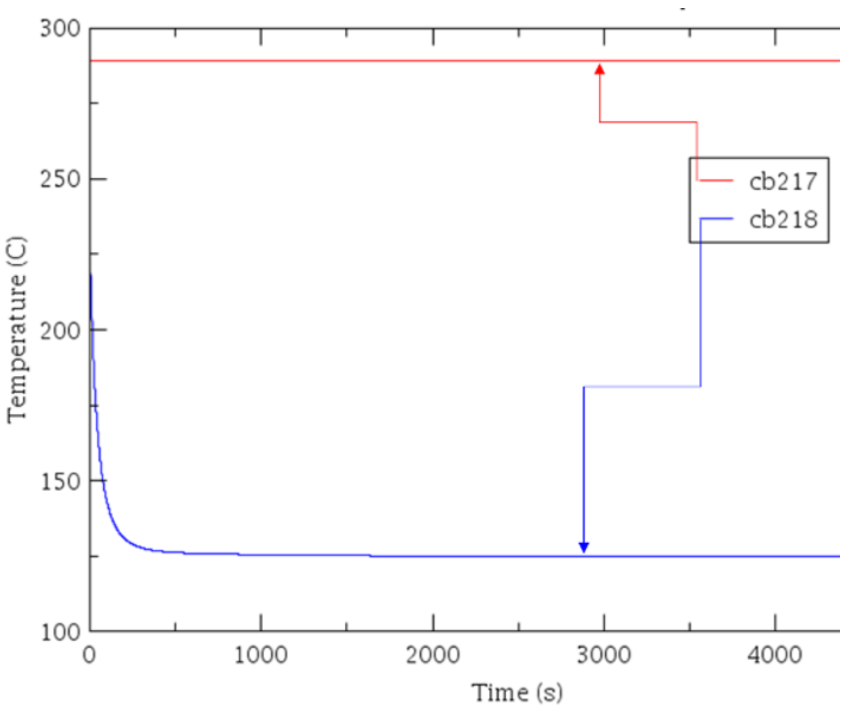

Fig. 6 – Example of TRACE He-FUS3 thermohydraulic model verification – Economizer; Hot Side; Calc #1_2 [9]

3.3 Code MELCOR in application for Phebus-FPT3 and THAI tests

3.3.1 Code description

The MELCOR code is a fully integrated, system computer code which allows to model the progression of severe accidents in light water nuclear power plants. This code is developed by Sandia National Laboratories for the needs of the U.S. (United States) Nuclear Regulatory Commission. MELCOR is also used to perform sensitivity and uncertainty analyses in different applications [17].

The severe accident simulations involve a broad range of phenomena, including thermal-hydraulic response in the reactor coolant system and containment; the core overheating, its degradations and the gradual relocation to the bottom of the vessel; the fission products release, the hydrogen production and deflagration [17].

3.3.2 PHEBUS FPT 3

The PHEBUS FP programme [18] was the core of an international research cooperation by performing several integral in-pile experiments of the relavant key-phenomena, which lead to the progression of postulated severe accidents in LWRs. The FPT-3 experiment was chosen, because in that experiment a B_4C control bar, similar to the VVER models, was used.

In the PHEBUS facility [19] the conditions, similar to those expected in severe accidents of a real power plant, were reproduced, allowing for an in-depth investigation of the basic phenomena that determine the release, transport, deposition and retention of FPs. These phenomena take place in the core region, in the primary circuit and in the containment system and involve a strong coupling between thermal-hydraulics and chemical/physical processes determining nuclear aerosol behaviour.

Figure 7 shows the schematic representation of the PHEBUS facility compared with the nodalization performed with the MELCOR code.

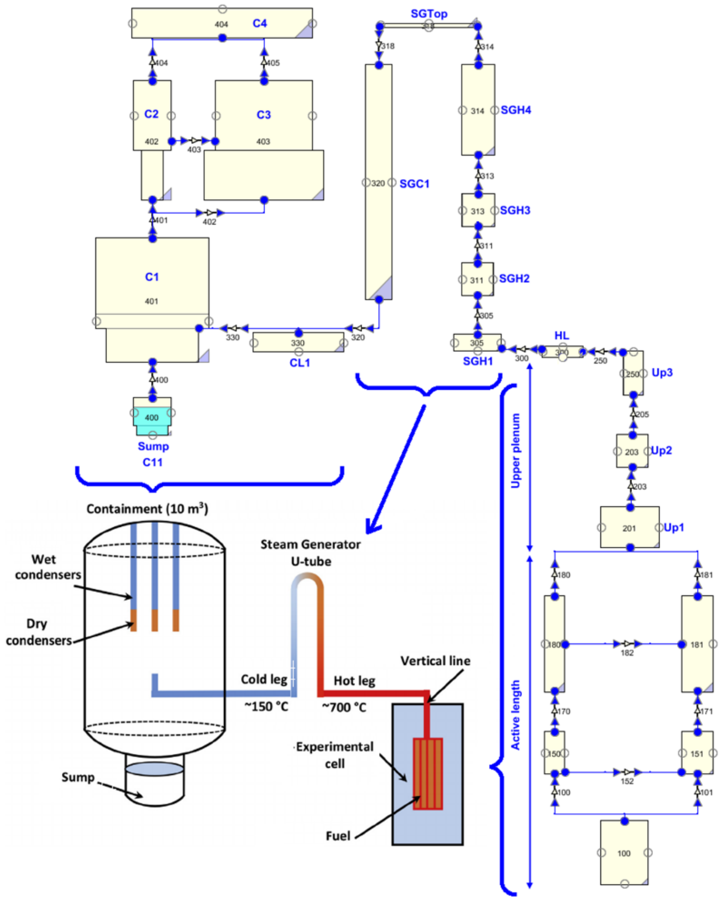

Figure 7. Schematic representation and nodalization of the PHEBUS experimental facility.

The facility provides a reduced-scale representation of the core, the primary circuit (with the steam generator) and the containment system of a nuclear power plant, allowing for a detailed analysis of the prototypical conditions expected during a severe accident sequence. The experimental cell is located in a loop crossing the central part of the PHEBUS driver core which supplies the nuclear power as is shown in the Figure 7.

MELCOR 2.1 code is capable to follow the progression of relocation of bundle materials during the evolution of the degradation phase (up to 18000 s). The bundle profile temperatures, are similar to the reference data, as well as the hydrogen production. MELCOR 2.1 calculation for hydrogen production have a good agreement with the reference value, reaching a total hydrogen production of around 120 g. In addition to the amount of hydrogen production, some other minor differences are due to the the relocation model (such as the secondary candling material) that influenced the B_4C reactions. The MELCOR 2.1 version is using new relocation model in comparison to the previous version (MELCOR 1.8x) corrected by some sensitivity coefficients. However, the simplified model for B_4C oxidation with its sensitivity coefficients leads the MELCOR 2.1 simulation to predict a larger initial reaction for the hydrogen generation.

The simulation shows an early hydrogen release at around 4500 s (see Figure 8-A) this early release in the simulation could be due to the reaction of the control rod (boron carbide) with the steam. A second hydrogen release is detected at around 1000 s (see Figure 8-B) similar to the experiment and finally a third hydrogen release peak is reached at around 12700 s (see Figure 8-C).

Despite to the early hydrogen release and the third hydrogen release, the total amount of hydrogen produced is similar to the experiment.

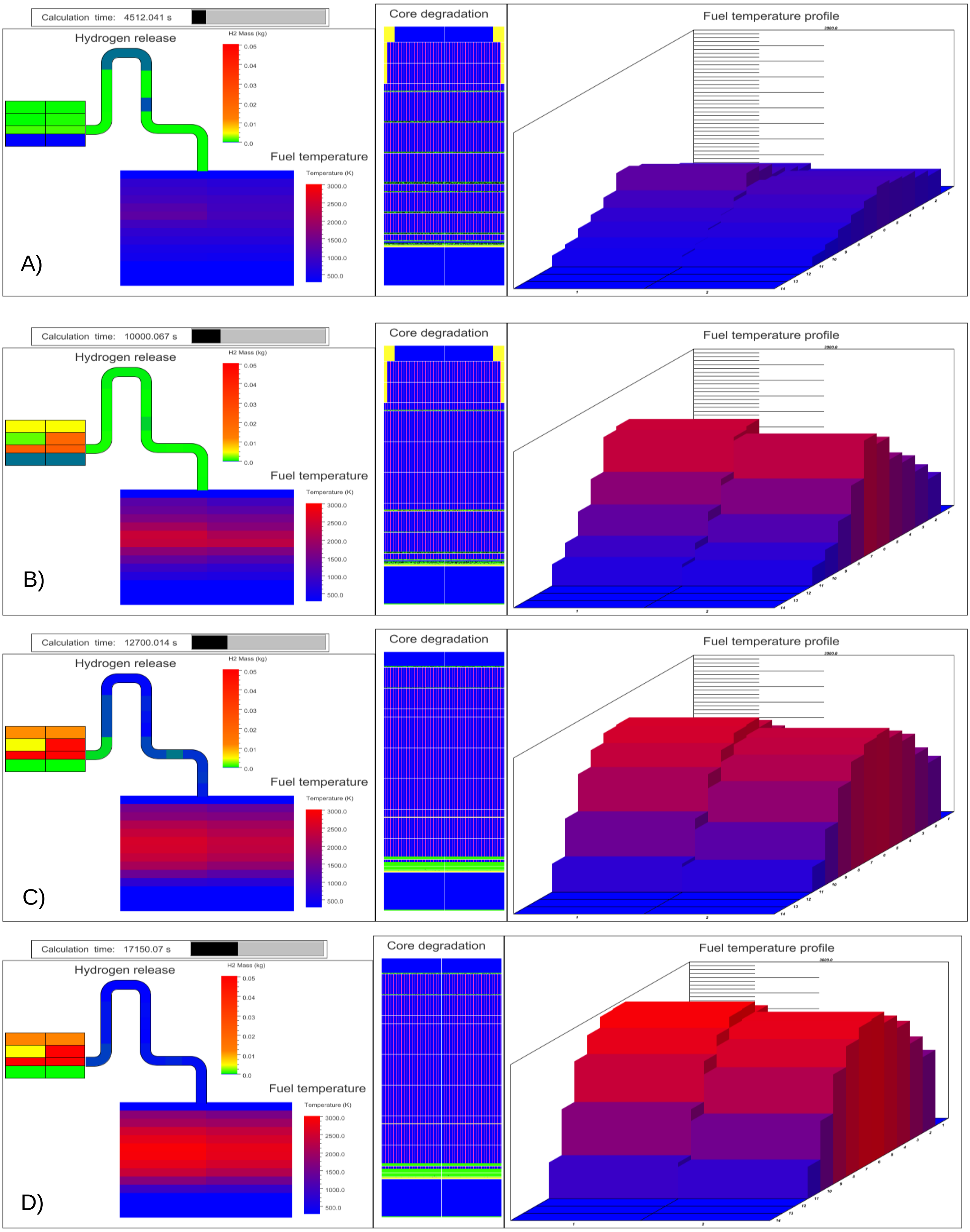

Figure 8. Evolution of the simulation of the FPT3 experiment. A) Early H_2 release, B) 2nd H_2 release, C) 3rd H_2 release, D) Maximum fuel temperature just before SCRAM.

3.3.3 THAI tests

The overall objective of the OECD-THAI project is to address open questions concerning the behaviour of hydrogen, iodine and aerosols in the containment of water reactors during severe accidents. The understanding of the processes taking place during such events is essential for evaluating the challenge posed on containment integrity (hydrogen) and for evaluating the amount of airborne radioactivity (iodine and aerosols) during such severe accidents with core damage [20].

From the set of HD-experiments performed in the THAI campaign, three representative experiments were chosen for the modelling and simulation using the MELCOR code versions 2.1 and 2.2. Hereafter, the simulation with the MELCOR version 2.2 for the HD-24 test is presented.

The THAI HD-24 test consist of experiment involving homogeneous H_2-steam-air mixtures at superheated and saturated conditions.

For the HD-24 test, the THAI facility has been modelled in four different ways in order to point out the influence of nodalization. The models were developed starting from a simple nodalization to a complex one. Two out of four models were discretized by the intersection of several vertical and horizontal planes, while the other two have a toroidal nodalization pattern.

Figure 9 shows the hydrogen burning rate evolution using a specific nodalization, conical in the axial direction and toroidal in the radial direction. Using this conical-toroidal nodalization it was possible to obtain a good agreement between the results and the experiment.

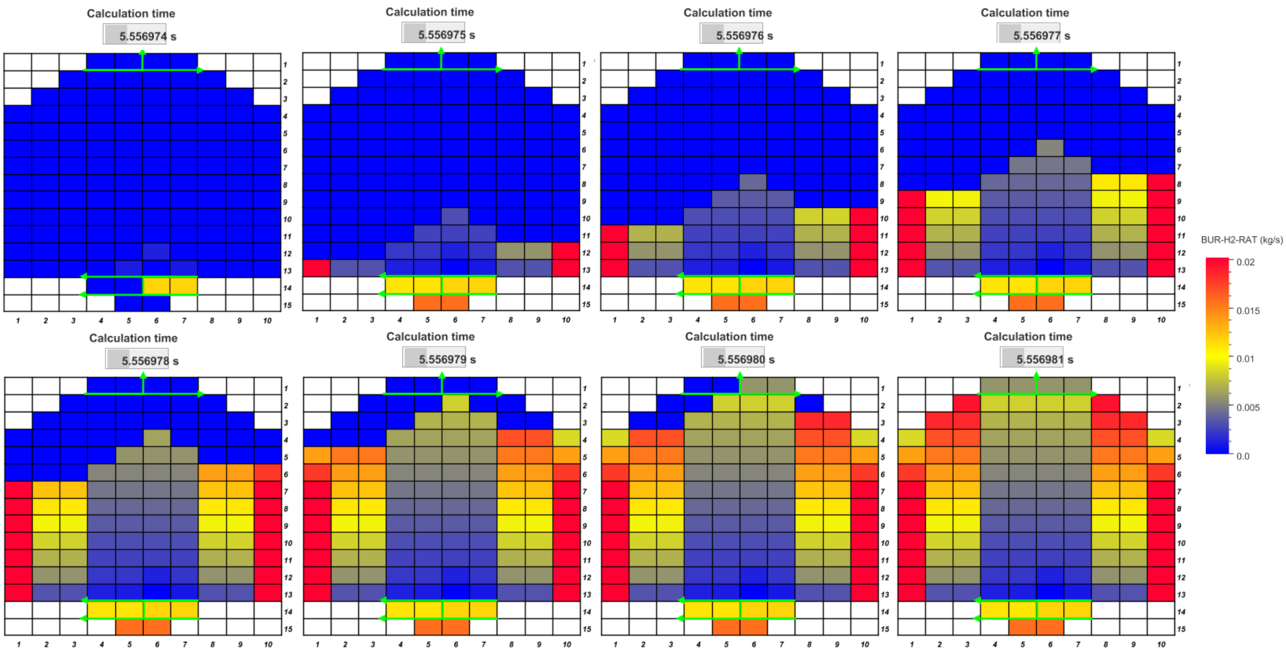

Figure 9. MELCOR 2.2. Model D. H_2 Reaction rate.

4 ACKNOWLEDGMENT

Part of the work was done under the project of Ministry of Interion of the Czech Republic "More accurate prediction of radiological consequences of severe accidents at NPP aimed in identification of their risks" (VI20172020076).

5 REFERENCES

[1] G. Lerchl, H. Austregesilo, P. Schöffel, D. v. d. Cron and F. Weyermann, “ATHLET 3.1A: User Manual,” March, 2016.

[2] China Nuclear Power Technology Research Institute, “SWAMUP, Report on out-of-pile SWAMUP test results and test data base”.

[3] A. Vojáček and G. Mazzini, “Analyses of the start-up and shut-down of SCWR fuel qualification test loop,” in *ICONE 22nd*, Prague, May 2016.

[4] China Nuclear Power Technology Research Institute, “Report on design of the out-of-pile thermal-hydraulic test section for SWAMUP,” 2016.

[5] C. Safety Research Section, “ ATHLET 3.1A Heat Transfer Assessment for Supercritical Water,” Rez,Czech Republic, October, 2016,.

[6] Division of Risk Assessment and Special Projects , TRACE V5.840. Theory Manual. Field Equations, Solution Methods and Physical Model, Washington D.C: U.S. Nuclear Regulatory Commission, 2013.

[7] Division of Risk Assessment and Special Projects, TRACE V5.840 User’s Manual, Volume 1: Input Specification,, Washington D.C.: U.S. Nuclear Regulatory Commission, 2014.

[8] Division of Risk Assessment and Special Projects, TRACE V5.840 User’s Manual, Volume 2: Modeling Guidelines, Washington D.C: U.S. Nuclear Regulatory Commission, 2014.

[9] Guido Mazzini, Miloš Kynčl, Marek Ruščák, Miroslav Hrehor, Alis Musa, Antonio Dambrosio, Vincenzo Romanello, Assessment of the TRACE Code for the He-Cooled Systems Simulation Capability Against Some He-FUS3 Experimental Measurements, ASME. ASME J of Nuclear Rad Sci. July 2019; 5(3): 030914. doi: https://doi.org/10.1115/1.4043377, May 10, 2019.

[10] G. Mazzini, M. Kyncl, M. Ruscak, A. Musa, Experimental and analytical tools for safety research of GEN IV reactors, PAris: EUROSAFE 2017, 2017.

[11] M., Polidori, He-FUS3 Benchmark Specifications, GoFastR-DEL-1.5-01, Rev. 0,, Brasimone: ENEA, 2011.

[12] Meloni P., Polidori M., HE-FUS3 Experimental Campaign for the Assessment of Thermal-Hydraulic Codes : Post-Test Analysis, Brasimone: ENEA, 2009.

[13] M., Polidori, He-FUS3 Benchmark Results, GoFastR-DEL-1.5-6, Brasimone: Enea, 2012.

[14] EUROfusion, European Consortium for the Development of Fusion Energy, vailable: https://www.euro-fusion.org/, Accessed: 20-Aug-2009.

[15] Porfiri M. T., Mazzini G., “DEMO BB Safety Data List (SDL),” SAE 2.22.1-T001-D019-b, EFDA_D_2MF8KU, Frascati, Rome: ENEA, 2018.

[16] ITER, ITER Organization, Available: https://www.iter.org/, 2018.

[17] R. O. Gauntt, "MELCOR Computer Code Manuals - Reference Manual Version 2.0," Sandia National Laboratories, 2008.

[18] P. der Hardt, A. V. Jones, C. Lecomte and A. Tattegrain, "Nuclear safety research: The phebus FP severe accident experimental program," *Nuclear Safety,* vol. 35, pp. 187-205, 1994.

[19] T. Haste, "Specification of International Standard Problem ISP-46 (Phebus FPT1), Revision 0," IRSN, 2011.

[20] OECD/NEA, "Hydrogen and Fission Product Issues Relevant for Containment Safety Assessment under Severe Accident Conditions," 2010.

Improvement on 900 MWe NPPs in the occasion of the 4th 10-year periodic safety review on severe accidents

R. Cozeret, J. Chambarel, S. Phoudiah, D. Corbin, S. Pignet

Institut de Radioprotection et de Sûreté Nucléaire (IRSN), Fontenay-aux-Roses, France

Abstract:

In France, EDF is developing a Plant Lifetime Extension (PLE) program for the Gen. II PWRs, which takes into account the lessons of the Fukushima Dai-ichi accidents and aims at reducing the gaps in terms of safety with the Gen. III PWRs including the EPR™, as requested by the French Safety Authority ASN. This program has been analysed by IRSN in the framework of the 4th 10-years periodic safety review of the 900 MWe series of reactors. The paper presents the main statements of the IRSN review of the upgraded strategies proposed by EDF in order to reduce the consequences of a severe accident on a Gen. II PWR.

1 INTRODUCTION

The French electrical utility EDF is currently operating a fleet of 58 Gen II Pressurized Water Reactors (PWRs) (900, 1300 and 1450 MWe series) built between 1977 and 1999. Periodic Safety Reviews (PSRs) are conducted every 10 years. These reactors were not designed to face a severe accident[1] and several plants reinforcements have been discussed in France and progressively implemented by EDF to improve the management of these accidents.

In 2009, EDF presented to the French Safety Authority (ASN) a Plant Lifetime Extension (PLE) program, in order to extent the Gen II PWRs operation duration beyond 40 years. It included an ageing program but also some reinforcements to reduce the gap with the safety objectives of the new nuclear power plants like the Gen III EPR™. This program has been reviewed by IRSN in addition to the post-Fukushima stress-tests.

In the framework of the operating plant life extension program, the French Nuclear Safety Authority stated to EDF that the safety objectives of the Gen III reactors (for instance the Flamanville 3 EPR) should be used as a reference for safety improvements definition.

Indeed, the EPR™ has been designed notably by including specific devices and accident management procedures to reduce the frequency of occurrence of core melt accidents and to limit their consequences on people and environment in area and time. For this Gen. III reactor, concerning severe accidents, low pressure core melt accident situations have then to be dealt with so that the associated maximum conceivable releases would necessitate only very limited protective measures for the public.

Moreover, in the framework of post-Fukushima stress tests (2014), ASN formulated expectations for Generation II reactors on:

- “improvements allowing residual heat removal from the containment without opening of the containment venting system”;

[1] Accidental situation leading to a significant melt of the reactor nuclear core.

- “a feasibility study of improvements able to prevent melt-through of the basemat in the event of partial or total core melt”.

Today, the PLE and the post-Fukushima programs are combined in a vast industrial project by EDF with also some important efforts from IRSN and ASN to review the project [1] through different prims corresponding to the main safety orientations [2]

Indeed, before the 4th ten-year safety review implementation, a core melt accident leading to a vessel failure without fast safety cooling system recovery would probably cause two main events which would have a strong impact on radiological releases. The first one is the basemat melt-through, strongly polluting ground waters. The second is the opening of the filtered venting of the reactor building to keep containment integrity, resulting in atmospheric releases of non-filtered fission products (FP), especially noble gas and gaseous iodine, leading to emergency evacuations.

In accordance with its initial PLE program, the post-Fukushima lessons and the ASN expectations, EDF has included, in the framework of the 4th 10-years periodic safety review, two important upgrades in its program for severe accident management and mitigation on 900 MWe reactors:

- a strategy to allow corium stabilisation without concrete basemat melt-trough;
- a strategy to remove heat from the containment without venting.

IRSN has assessed these upgrades using a large simulation program based on its Accident Source Term Evaluation Code (ASTEC V2.1) [3]. IRSN has also reviewed the global picture of reactor safety status taking into account these modifications. Conclusions have been presented and discussed with ASN experts standing group on March the 27th and 28th 2019.

The paper summarizes main IRSN statements after the review of the severe accident management and mitigation strategies proposed by EDF for its generation II PWRs (firstly 900 MWe series).

2 STRATEGY TO ALLOW CORIUM STABILIZATION WHITHOUT CONCRETE BASEMAT MELT-THROUGH

2.1 Modifications planned by EDF

To limit the risk of reactor basemat melt-through by the corium after the vessel failure, EDF has retained a strategy based on the following modifications and actions (see Fig. 1 & 2 below):

- The vessel cavity is modified to avoid any water penetration before vessel failure (in the existing design, the spray system activation fills the cavity with water);
- The reactor sumps are filled with water before the vessel failure (taking benefit to the containment spray system if it has worked or preventively by using the new heat removal system);
- In case of vessel failure after core melt, the corium falls and spreads in the dry vessel cavity and in an adjacent area through a dedicated pipe protected by a concrete plug that will be ablated. After complete spreading, some triggers are passively activated, allowing water from the sumps to submerge the spread corium;
- This water contributes to the corium cooling; the corium progression stabilization should be obtained if the sump water is cooled down continuously by a specific ultimate heat exchanger (see section 3).

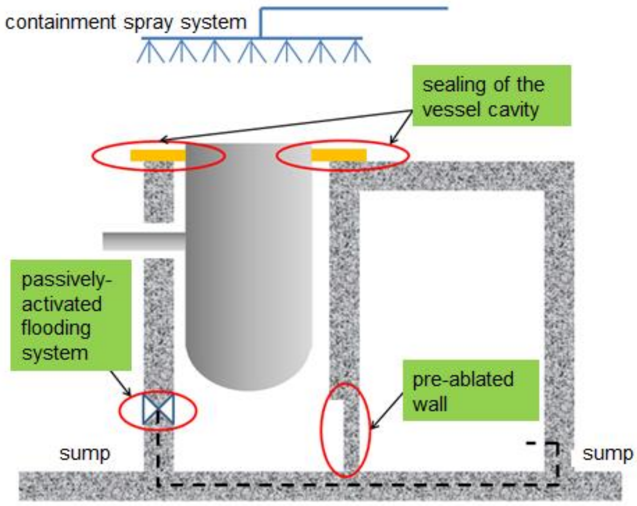

Figure 1: schematic view of modifications to allow dry spreading and passively activated reflooding of the corium

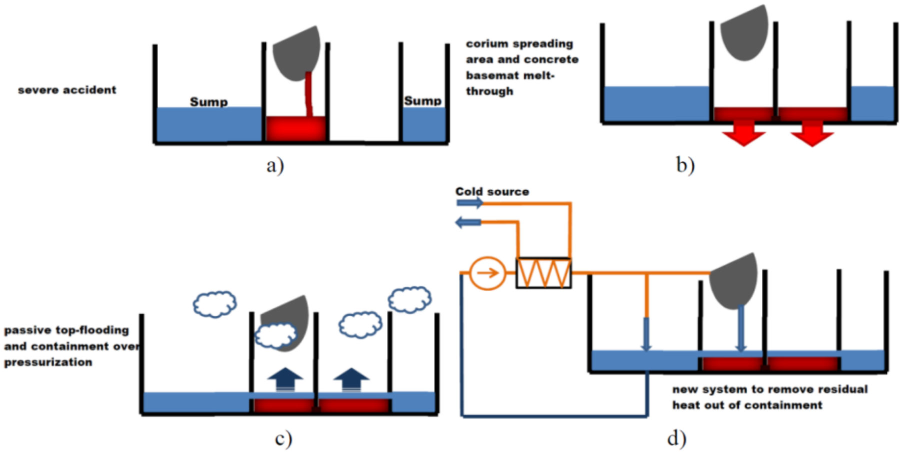

Figure 2: schematic representations of different phases of stabilization of the corium: a) slump from vessel to dry cavitiy, b) spreading in dry cavity and dedicated adjacent room, c) top flooding of corium by water, d) ultimate residual heat removal

2.2 Main issues adressed by IRSN

IRSN has analyzed the different parts of the disposal to ensure that:

- the vessel cavity and the adjacent area remain dry before vessel rupture, in order to avoid fluid-corium interaction (FCI) and to allow a complete spreading of the corium before the passive reflooding;
- the timing of the reflooding is appropriate (too fast limits spreading and increases FCI risk and too slow means a large amount of concrete is ablated);
- the water height in the sump at flooding actuation is sufficient regarding the reflooding flowrate and the height of water flooding the corium;
- the depth of undamaged basemat remains sufficient to prevent a containment failure;
- the top cooling efficiency is sufficient to allow corium stabilization.

This last point is the most complex to evaluate. Water cooling of corium-concrete mix has been characterized thanks to integral corium-concrete interaction (CCI) experiments which have highlighted two different exchange mechanisms **Fehler! Verweisquelle konnte nicht gefunden werden.** between the corium and the water. Their efficiency is strongly dependent on the composition of the basemat concrete progressively incorporated in the corium during the ablation.

These heat exchanges are the exchanges through the corium top crust itself including the water ingression through the cracks and the melt ejection over the crust generating a coolable debris bed. Efficiency of these mechanisms for a reactor configuration is estimated thanks to models included in IRSN tool ASTEC V2.1.

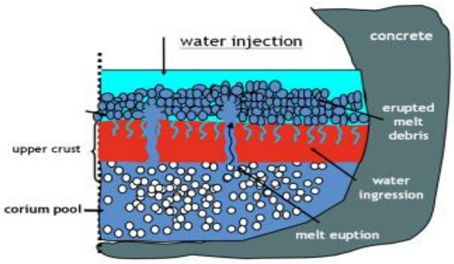

Figure 3: schematic view of MCCI under water mechanisms

For limestone concrete, IRSN and EDF results are consistent and show that the ablated basemat depth is limited (< 1 m). The average basemat thickness being of about 4 meters, the safety margins are sufficiently high to cover remaining uncertainties on the modeling and IRSN so considers that the measures planned by EDF are sufficient to prevent basemat melt-through.

For very siliceous concrete, the amount of gases generated by the concrete ablation is limited and so will be the efficiency of the corium ejection above the corium top crust. Long term stabilization of corium thus relies on the efficiency of water ingression mechanism efficiency that is significantly reduced by the incorporation in the melt of concrete decomposition compounds. IRSN's results show a significant concrete ablation (close to 3 m, as shown in the fig. 4 below), raising doubts on basemat integrity and highlighting again the impact uncertainties on MCCI that are more important for siliceous concrete **Fehler! Verweisquelle konnte nicht gefunden werden.**.

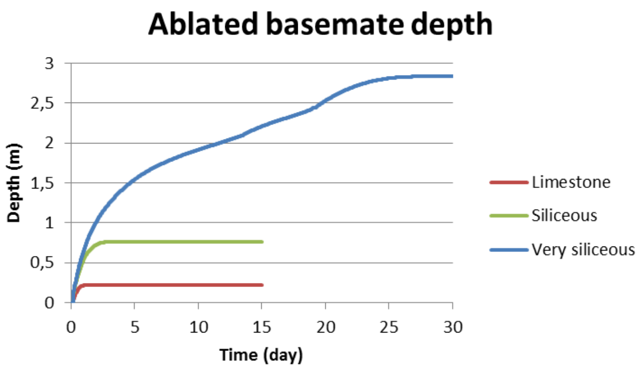

Figure 4: basemat ablation depth vs time for different types of concrete

2.3 Improvement with additional layer

Because of the cooling efficiency uncertainties for very siliceous concrete, IRSN has investigated solutions with addition of a limestone concrete layer on very siliceous concrete basemat in order to limit the ablation in this new layer.

ASTEC simulations performed assuming a 40 cm additional layer of limestone concrete have showed a significant reduction of ablation depth (about 20 cm instead of 3 m).

To conclude, IRSN considers that uncertainties remain for very siliceous concrete ablation and top cooling efficiency. In order to warrant robust mitigation of severe accident, IRSN recommends spreading an additional limestone concrete layer on very siliceous concrete basemat.

Nevertheless, the more efficient is the corium coolability, the faster the energy is transferred to the water and the atmosphere of the reactor building which could lead to an over pressurization of the containment.

3 STRATEGY TO REMOVE HEAT FROM THE CONTAINMENT WHITHOUT VENTING

3.1 Modifications planned by EDF

In order to remove the decay heat from the containment without opening the emergency containment filtered venting system, EDF intends to implement (see Fig. 5 below):

- a fixed circuit (located in the fuel building for the 900 MWe series) including:
  - a pump qualified to extreme external hazards conditions and severe accident situations;
  - an injection line connected to the cold leg of the primary coolant circuit and another feeding the sump of the reactor building;
  - a heat exchanger;
  - actuators enabling the disposal activation from the control room.
- a cooling mobile device (ultimate heat sink) composed of a mobile pump and hoses directly drawing up in the heat sink and lined on the heat exchanger by the EDF rescue team FARN (Nuclear Rapid Response Force).

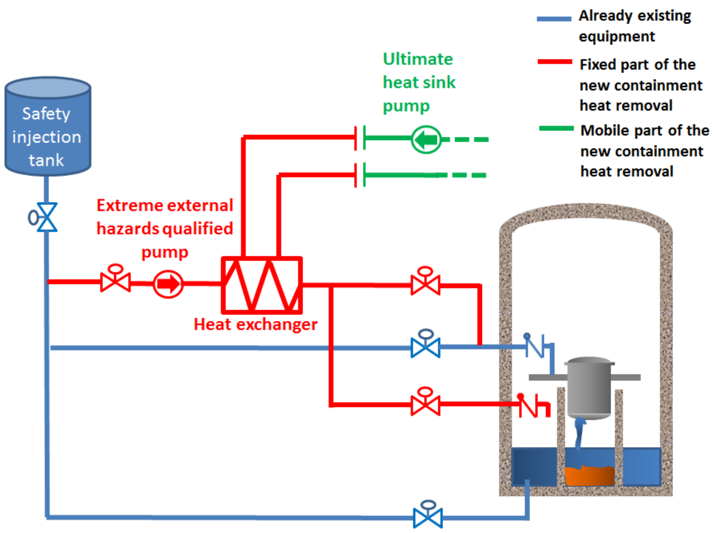

Figure 5: new containment heat removal disposal

3.2 Main issues adressed by IRSN

This new heat removal system operates in two steps:

- direct injection: the pump preventively fills the sump of the reactor building with water coming from the safety injection tank before the vessel failure, allowing to flood the corium when passive flooding system actuates;
- recirculation: once the ultimate heat sink has been lined by the FARN, within 24 hours, the recirculation is activated, allowing to remove decay heat thanks to the heat exchanger.

Two criteria have to be respected to avoid radioactive releases (by containment leakage or filtered venting system opening):

- the containment pressure needs to remain under 5 bar;
- the sump water temperature needs to remain under 140 °C.

IRSN has performed simulations to evaluate the grace period during which the two criteria above are fulfilled, before the ultimate heat sink is settled, thanks to a full coupling modelling (MCCI and containment thermal hydraulics) available in ASTEC V2.1 code. Computations have stressed in some cases a grace period significantly shorter than 24h, highlighting some sensitive parameters.

Firstly, the type of concrete ablated by the corium is an issue. The more the concrete contains limestone, the more efficient the heat transfer from the corium to the water will be, leading to faster containment pressurization.

Then, it appears that the initial mass and temperature of the corium falling down when the vessel failed to be used in the MCCI simulation is an issue. For IRSN, core degradation simulations are uncertain because it is strongly sensitive to very small variation of the accident sequence. This is why, in order to design a new heat removal system, it is necessary to use conservative assumptions for the amount, the temperature and the composition of the corium to be spread.

Finally, the containment wall concrete thermal conductivity, which is difficult to evaluate with accuracy for a reactor building, is a very sensitive parameter in terms of kinetics of pressurization, as shown on the graphic below (Fig. 6). Indeed, during the grace period, heat losses through the reactor building walls is the main phenomena allowing power removal from the containment.

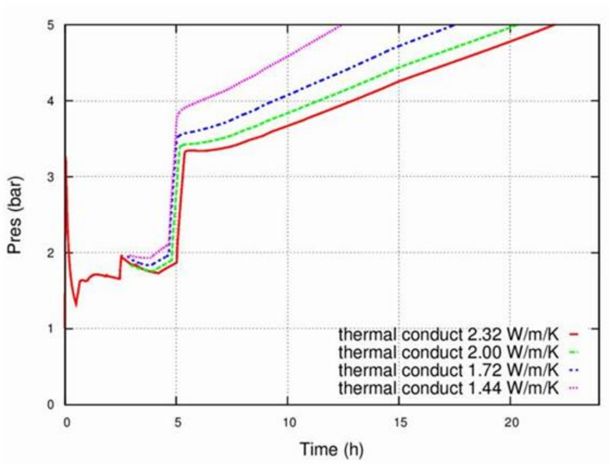

Figure 6: reactor building wall thermal conductivity sensitivity on containment pressurization

3.3 Injection of a second tank of water

Taking into account the various sensitive parameters in the simulations, highlighting uncertainties coming from lack of knowledge on physical phenomenon or difficulty to define one representative case of the worse accident, a pragmatic solution appeared to be an increasing of the quantity of water flooding the corium in order to increase the grace period.

Simulations performed by IRSN show that the injection of a second tank of water in the containment increases significantly the delay before containment over pressurization (see Fig. 7 below). As a consequence, IRSN recommended preventively filling and flowing as soon as possible a second tank of water in the containment.

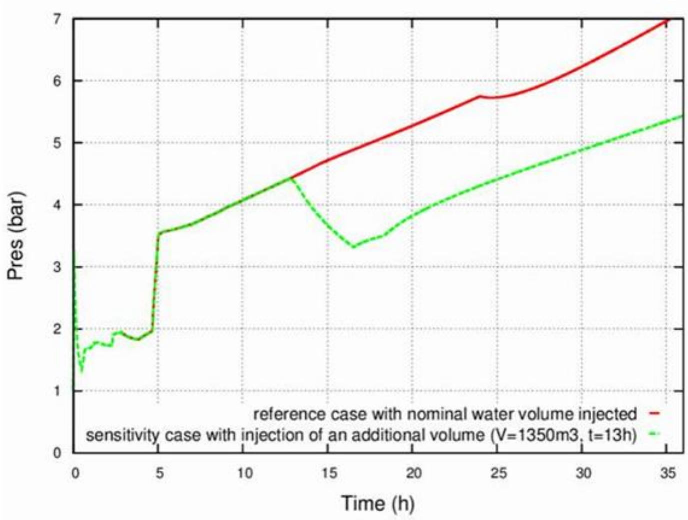

Figure 7: Impact of injection of a second tank of water on the delay before containment over-pressurization

3.4 Sumps clogging issues during recirculation

During a severe accident, various debris are generated and carried towards the sumps by washout. These debris constitute the upstream source term debris (STD). The sumps are equipped with a strainer line, ensuring the filtration of the water circulating in the heat removal system. Debris passing through the strainer line constitute the downstream STD when the heat removal system works in recirculation mode. The water charged with downstream STD will pass through the pump, the heat exchanger and some valves to be reinjected in the primary circuit.

Robustness demonstration of the recirculation function must warrant that:

- upstream STD will not lead to excessive head loss due to the strainer line clogging, resulting in pump cavitation;
- downstream STD does not damage the pump, degrade the heat exchanger performance or clog other equipments of the circuit like valves, diaphragms…

During the review, IRSN analysed the knowledge obtained from experimental programs and recognized a need to characterize the water recirculation system efficiency through experiments performed in more representative conditions and needs of additional analytical activities:

- consolidated upstream STD where the fibers inventory for a primary circuit breach of 12 inches appears to be reasonably conservative;
- representative water chemistry (boric acid or sodium hydroxide) and temperature (> 80°C).

Investigation on chemical effects which could increase the strainer clogging are expected to be specifically targeted. This topic was agreed between EDF and IRSN.

Even if the new heat removal system recirculation dedicated to SA shows more margins for cavitation risk than the recirculation function of the systems dedicated to the design basis accidents, R&D is still on going on the subject of sump clogging issues in case of SA on French Gen. II PWRs.

4 IODINE CHEMISTRY IN THE CONTAINMENT

In order to assess the updated 900 MWe PWR safety demonstration, IRSN has also reviewed EDF evaluation of radioactive releases in the environment in case of a severe accident. This evaluation relies on evaluations of FP releases from the fuel and behaviour during their transport through the primary circuits and the containment up to the environment.

Specific attention is paid to iodine because it is sensitive on doses for people. The review included a focus on iodine chemistry in the sump and in the containment taking into account state of the art knowledges on iodine speciation.

According to previous simplified iodine chemistry models used in ASTEC V2.0, evaluation of iodine species concentrations in the gaseous phase in the containment leads to a fast (~1 day) and complete adsorpsion of molecular iodine (I_2) on painted walls and simultaneously, a fast but partial desorption of organic iodine (ICH_3), resulting in a quite stable gaseous concentration in the containment after about 1 day. Assuming that 5% of iodine core inventory is released at the breach directly in its gaseous form and 95% remains in the liquid phase, a large amount of iodine remains in the water in the sump thanks to interaction with silver coming from the control rods degradation.

Nevertheless, during the last years, knowledge has greatly increased on this topic. Today the vision on iodine speciation is quite different and gives :

- a molecular iodine transfer from liquid phase to gaseous phase, enabled by an acid pH and a partial captation of iodine by silver in the liquid phase;
- an increasing of iodine concentration in gaseous phase involving another iodine specie, iodine oxide (IOx), coming from I2 and ICH3 oxidation by the radiolysis products of air.

Firstly, iodine transfer from the liquid phase to the gaseous is enabled because iodine captation in the liquid phase is not complete, even if the molar ratio seems to be favorable. Two phenomenons explain this result: first, iodine diffuses only in a weak thickness (~400 angströms) of the silver particles, and second, silver particles oxidation is limited. Then, if water pH is acid (typicalement about 5), an important and continuous I_2 release to the gaseous phase would occur.

Secondly, the iodine concentration in the gaseous phase is increased because the main iodine species in the gaseous phase considered with the state of the art model are not the same than those considered with the previous one: iodine oxides IOx are the main specie versus I_2 and ICH_3 in the containment, with a gaseous phase concentration about 10 times the ICH_3 concentration evaluated by the previous model.

These phenomenons, leading to high iodine gazeous species concentration in the containment, do not occur when water pH is basic. Unfortunately, without any specific mitigation system insuring that sump water remains basic, in severe accident conditions, it will be acid.

Iodine concentration in the containment atmosphere evaluated with a state of the art iodine chemistry model is significantly more important in the containment than used to be. This source term is very sensitive on radioactive releases due to contaiment leaks. As a consequence, IRSN recommended measures to significantly reduce iodine releases to the gaseous phase from the liquid phase in the containment. Targetted is a device to alkalinize water sump during the accident until iodine concentration has fully decreased without challenging the water recirculation system efficiency. To that extend the solution that could finally be retained will be constrained by the results of the investigation of the long term efficiency of the sump recirculation system.

5 CONCLUSIONS

Improvements on 900 MWe NPPs in the occasion of the 4th 10-year periodic safety review on severe accidents have been designed in order to tend to safety level of Gen. III reactors. IRSN review has concluded that these improvements enhance significantly safety of 900 MWe NPPs and has stressed some issues that should lead to further updates. Main recommandations of IRSN have dealt with :

- additional limestone concrete layer for very siliceous basemat to prevent melt-though;
- refill of the tank and injection of this additionnal volume of water before rescue team intervention to prevent containment over pressurization;
- modifications to reduce gaseous iodine releases in the containment.

6 REFERENCES

[1] Cozeret, R., et al, “Review of the upgraded severe accident mitigation strategies for the generation II PWRs in France foreseen in the framework of plant life extension”, International Conference on Topical Issues in Nuclear Installation Safety: Safety Demonstration of Advanced Water Cooled Nuclear Power Plants, June 6-9th 2017, IAEA, Vienna, Austria.

[2] ASN, “ASN position statement of 20th April 2016 concerning generic guidelines for the periodic safety review associated with the fourth ten-year inspections for the 900 MWe reactors”, http://www.french-nuclear-safety.fr/Information/News-releases/ASN-position-statement-concerning-generic-guidelines-for-the-periodic-safety-review

[3] Chailan, L., et al, “Overview of ASTEC integral code status and perspectives”, The 9th European Review Meeting on Severe Accident Research (ERMSAR2019), March 18-20th 2019,Clarion Congress Hotel, Prague, Czech Republic.

[4] F. Fichot et al, “Research in support of the 4th 10-year periodic safety review on severe accidents”, EUROSAFE 2019, 4th and 5th November, Cologne, Germany, 2019.

Expert Safety Assessment to Support the Licensing of Accelerator – Driven Nuclear Facility in Ukraine

I.Bilodid, O. Kukhotskyi*, Sv.Nemtsova**, Iu.Ovdiienko*, Iu.Kovbasenko**

*State Scientific and Technical Center for Nuclear and Radiation Safety
35-37 V.Stusa St., 03142 Kyiv, Ukraine

**State Nuclear Regulatory Inspectorate of Ukraine
9/11 Arsenalna St., 01011 Kyiv, Ukraine

Abstract:

The construction and commissioning of a subcritical assembly driven by a linear electron accelerator – a nuclear subcritical facility (NSF) – have been underway in Ukraine for about ten years. This is the first experience in licensing such a facility in Ukraine. Over this time, the relevant regulatory framework was developed and implemented, and documents of the operating organization were developed and agreed by the nuclear regulatory body of Ukraine. In addition, some adjustments were made to the facility design.

Practically from the very beginning (from the feasibility study stage), SSTC NRS successfully works as the Technical Safety Organization (TSO), providing support to the nuclear regulatory body of Ukraine and performing scientific and technical assessments of the documents sent by the operating organization for state review on nuclear and radiation safety. The paper presents the results of calculational studies conducted in the NSF licensing and verifying calculations related to nuclear safety. The calculations are performed for the model of the subcritical assembly core using the up-to-date version of the SCALE code package.

1 FOREWORD

The Neutron Source is an innovative nuclear facility whose main purpose is to conduct scientific and applied research in nuclear physics, radiation materials science, biology and chemistry. In addition, the facility can be used to set up production of medical radioisotopes in Ukraine. The Neutron Source is a pool-type subcritical assembly cooled by light water.

The official start of construction was announced at the Washington Security Summit and set forth in the Joint Statement by the Presidents of Ukraine and the United States of America in April 2010. In May 2013, the facility construction project was approved and later the National Science Center "Kharkov Institute of Physics and Technology" (NSC KIPT) received a construction permit and a license for the construction and commissioning of the Neutron Source.

At the time, the nuclear regulatory body, State Nuclear Regulatory Inspectorate of Ukraine (SNRIU), faced two major challenges. First, there was no experience in assessing the safety of such facilities. Second, there were no legal acts regulating the nuclear and radiation safety of such facilities.

At the beginning of the Neutron Source construction, the Ukrainian regulatory framework included only three valid regulations of the former USSR with regard to NSF:

- Nuclear Safety Rules for Subcritical Stands (PBYa-01-75), which was put into force in 1975;

- Research Reactor Safety Rules (PBYa-03-75), which was put into force in 1975 as well;
- General Safety Provisions for Research Reactors in Design, Construction and Operation (OPB IR), which was put into force in 1988.

However, as seen from the years of their introduction, these regulations did not take into account advances in modern science and technology and latest international experience. Therefore, the priority task for the SNRIU and SSTC NRS experts was to study the international experience in the accelerator – driven systems (ADS). The obtained knowledge was applied to develop a new up-to-date regulation “General Safety Provisions for Nuclear Subcritical Facility” [1], which was put into force in 2012.

Regulatory requirements and approaches to safety assessment were elaborated in parallel with the development of the NSF project. The first steps of interaction between the operator and SSTC NRS under SNRIU supervision began in 2008, when various aspects and potential problems for NSF construction, including regulatory documents, were evaluated.

The actual review activities began in September 2011, when the first state review of the Feasibility Study and the Preliminary Safety Analysis Report (PSAR) was performed. In the light of international experience, it was decided that operation of the facility would be possible only if criterion $k_{eff}^{max} \leq 0.98$ would be met. Besides, the draft regulation “General Safety Provisions for Nuclear Subcritical Facility” was developed and was being prepared for submission for state registration, which the experts relied on.

Upon review of the NSF project, the operational and technical capabilities of the NSC KIPT and potential risks were identified for the NSF construction and operation, in particular:

- involvement of several foreign companies that could complicate interaction and adjustment processes: linear electron accelerator - Institute of High Energy Physics, China; sub-critical assembly - SOSNY R&D Company, Russia; design and manufacture of basic equipment and safety systems - Argonne National Laboratory, USA; the developer of NSF building and services - Kharkiv Design and Development Institute “Teploproekt-Soyuz”, Ukraine; the developer and supplier of I&C systems - Khartron Corporation, Ukraine [2];

- lack of experience at NSC KIPT in the development of licensing, operational, technical and maintenance documentation.

These factors finally led to a delay in project implementation, numerous revisions of documents, project changes and consultations of the operator with the SNRIU and SSTC NRS to make the project safer and more reliable.

For more efficient support to the SNRIU, the SSTC NRS still participates in a number of projects with STUK, BelV and IRSN with support of the European Commission [3], [4] for exchange of experience and training of SSTC NRS experts on aspects of ADS operation and safety assessment. The cooperation covered areas such as gaining a deeper knowledge of the operation principles and physics of processes in ADS, improving the regulatory framework for NSF and improving the computer models of NSF that were developed by SSTC NRS.

2 EXPERT SAFETY ASSESSMENT

The state review on nuclear and radiation safety of nuclear installations is carried out by the SNRIU with support of the TSO represented by the SSTC NRS.

The SNRIU policy of state review of justification materials includes independent verifying calculations that cover as many nuclear and radiation safety aspects as possible. The verifying calculations significantly increase the quality of technical review process as part of the licensing procedure. This provides the regulatory body with reasonable assurance that the justification materials are developed adequately. SSTC NRS intends to confirm its decisions by quantitative assessment of the main neutron kinetic parameters. One of the constituent elements of comparative independent calculations is the use of a computer code that differs from that applied in justification documents and a computer model developed at SSTC NRS.

The VVR-M2 fuel assemblies (FAs) are planned to be used in the subcritical assembly. In the early stages of project development, the maximum loading of NSF was planned to be 43 FAs with a tungsten target or 38 FAs with a uranium target.

VVR-M2 assemblies have been used in nuclear research facilities since 1963. However, there are no open sources with validation material such as benchmarks or comparative calculations for test installations or stands. Nevertheless, SSTC NRS and ANL experts gained good knowledge of the VVR-M2 assemblies in the transfer to low-enriched fuel of the VVR-M research reactor of the Nuclear Research Institute in Kyiv (2005-2012) within the Russian Research Reactor Fuel Return (RRRFR) Program.

An example is the calculation for the most critical situation in terms of criticality safety assuming the removal of a tungsten target. The SSTC NRS calculations were performed using the KENO-VI code from the SCALE 6 software package [5], which implements the Monte Carlo method. The calculations were performed for the NSF core with 38 FAs for the 238-group cross-section library based on ENDF/B-VI for NSF with design parameters and taking into account tolerances in the fuel manufacture according to technical specifications.

Table. Results of Verifying Calculations

	$k_{eff}\pm\sigma$
PSAR (MCNPX [6])	0.97739 ± 0.00012
SSTC NRS calculation (SCALE), average design parameters	0.97533 ± 0.00016
SSTC NRS calculation (SCALE), consideration of fuel enrichment and density tolerances	0.98477 ± 0.00020

The above table demonstrates a good match between the results of the verifying calculations and the results reported in the PSAR.

However, since Ukrainian regulatory documents require that accident analysis calculations be performed taking into account the conservative side (e.g., worst case) of all technological tolerances and considering only manufacture tolerances for fuel mass and enrichment, the result of calculating such an accident exceeds 0.98.

To prevent the exceedance of the established criticality criteria, two absorbing rods were introduced into the NSF project. Their location and absorbing features allow $k_{eff}\leq0.95$.

The NSF criticality safety was discussed many times at meetings with representatives of the NSC KIPT and Argonne National Laboratory. In the framework of close cooperation between the SSTC NRS, NSC KIPT and ANL, approaches to NSF neutronic calculations were developed and agreed with the SNRIU.

Moreover, the verifying calculations were and are performed currently not only for the neutronic analysis but also for the evaluation of thermal hydraulic characteristics (see the Figure below), radiation exposure and strength analysis of structures.

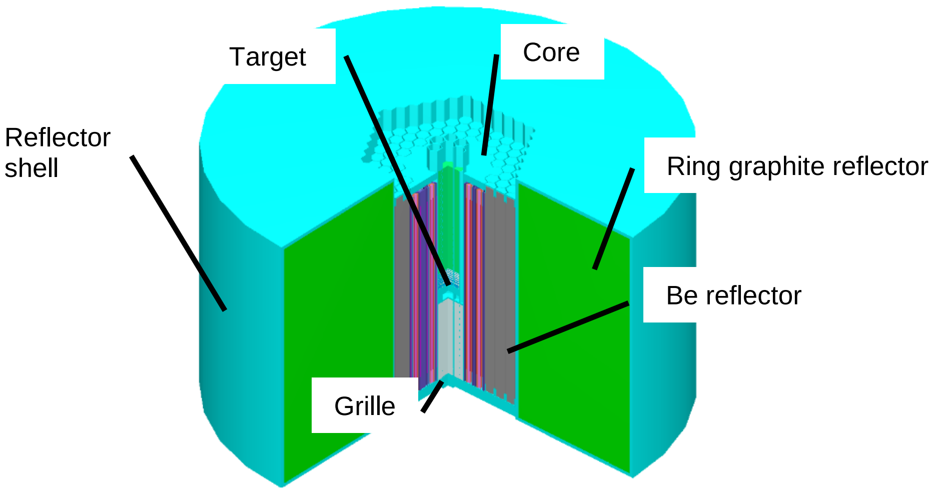

Figure – SSTC NRS model for criticality analysis

3 RECENT ACTIVITIES

All construction activities, installation and functional tests of equipment and systems important to safety have been completed at the NSC KIPT site. The comprehensive tests (with dummy fuel assemblies) were conducted successfully at the end of November 2018. The operator developed necessary technical and operational documentation, such as specifications, instructions, programs, etc., passed their state review and agreed them with the SNRIU. Along with the development of documents and construction activities, changes were made to the design.

In particular, the following significant design changes were made to the NSF project:

- the number of FAs to be loaded into the core with a tungsten target was reduced (38 FAs versus 43/42 FAs prior to modification);
- the internal reflector material was changed to two-component beryllium–graphite material instead of single graphite;
- the biological shielding design was modified;
- the number of hinged racks in the NSF tank was reduced from five to three.

Finally, as a result of the above activities, an individual permit for the first nuclear fuel delivery to the NSC KIPT industrial site was issued by the SNRIU on 12 April 2019, fuel was delivered to the NSC KIPT site in May 2019 and the NSC KIPT placed the fuel for storage. The next step now is to obtain an individual permit for the initial startup. In this regard, the NSC KIPT and the regulatory body with TSO are dealing with new tasks and challenges. One of them is to update the PSAR based on the construction activities and tests. The implementation of this task primarily depends on the NSC KIPT's hard and careful efforts to account for all project changes, latest operating documents and state review comments. The second task is to perform subcriticality calculations to justify the safety of the first core loading. The second task involved both the NSC KIPT and the SSTC NRS. The SSTC NRS proposed approaches to subcriticality calculations for the first Neutron Source core loading, performed state review of nuclear and radiation safety of the Technical Decision on the composition of the first loading (35 FAs) and performed relevant verifying calculations. In 2012-2019, structural elements and actual FA data were obtained from the NSC KIPT, resulting in the improvement of the NSF model and more accurate simulation of the system. The results of the SSTC NRS verifying calculations and NSC KIPT calculations comply with the regulatory requirements and show good correlation, but slight differences were found for 35 FAs. Based on the review findings, the SNRIU agreed the Technical Decision on the composition of the first loading (35 FAs) of the NSF core.

This allows the NSC KIPT to load the first 35 FAs to the core according to the agreed procedure set forth in the Initial Startup Program, with all necessary measurements and comparisons of the experimental results and calculations performed with the MCNPX code. After completion of the first stage, the NSC KIPT will prepare a report on the results of initial startup with 35 FAs and send it for agreement. Upon analysis, the computer models will be refined and forecast calculations for the loading of the next three FAs with realistic approach will be performed. After agreement with the SNRIU, the final stage of loading 36-38 FAs will be completed in accordance with the procedure set forth in the Initial Startup Program.

The NSC KIPT is currently preparing to obtain individual permits for the initial startup and trial operation of NSF. The tentative date for commissioning of the Neutron Source is the end of 2020.

4 SUMMARY

As a technical safety organization of the regulatory body, the SSTC NRS participates in the state review of the NSF Neutron Source upon request of the regulatory body throughout the facility life cycle.

The construction of the NSF Neutron Source has become a challenge not only for the operator and regulatory body but also for the SSTC NRS. On the one hand, over the years of construction and commissioning, the SSTC NRS experts gained extensive new knowledge and became acquainted with the latest international experience in safety justifications of ADS, which was immediately applied in the review and regulatory activities. This experience continues to ensure an appropriate level of technical support to the regulatory body. On the other hand, expert safety assessment significantly increased the quality of the licensing procedure for the accelerator – driven nuclear facility.

5 REFERENCES

[1] General Safety Provisions for Nuclear Subcritical Facility: NP 306.2.183-2012, SNRIU (2012).

[2] Y. Gohar et al. Safety Justification of KIPT Neutron Source Facility Based on Electron Accelerator Driven Subcritical Assembly. Proc. of the 6th Regional Lessons Learned Workshop on Russian Research Reactor Fuel Return Program, Tihany, Hungary, 12-15 June, 2012.

[3] INSC U3.01/12 “Support to the Ukrainian Regulatory Authorities”, Component UK/TS/49 "Licensing of new nuclear subcritical facility - neutron source based on an electron accelerator-driven subcritical assembly".

[4] INSC U3.01/14 & U3.01/15 “Strengthening of State Nuclear Regulatory Inspectorate of Ukraine (SNRIU) capabilities relevant for the regulation of nuclear activities and in licensing and severe accident management of Nuclear Installations”, Component UK/TS/51 “Strengthening of SNRIU Capabilities in Licensing of New Nuclear Installations (Except NPPs)”.

[5] B. T. Rearden and M. A. Jessee, Eds., SCALE Code System, ORNL/TM-2005/39, Version 6.2.3, Oak Ridge National Laboratory, Oak Ridge, Tennessee (2018).

[6] L. WATERS, ed., “MCNPX User's Manual Version 2.4.0,” Los Alamos National Laboratory document LACP-02-408 (2002).

Safety research at GRS to enhance nuclear safety in Europe

Andreas Schaffrath, Jérémy Bousquet, Klaus Heckmann, Joachim Herb, Robert Kilger, Berthold Schramm, Armin Seubert, Jürgen Sievers, Andreas Wielenberg

Gesellschaft für Anlagen- und Reaktorsicherheit (GRS) gGmbH, Forschungszentrum, Boltzmannstrasse 14, 85748 Garching near Munich, andreas.schaffrath@grs.de

Abstract

The Safety Research Division of the Gesellschaft für Anlagen- und Reaktorsicherheit (GRS) gGmbH develops, validates and applies computer codes as well as coupling interfaces between individual codes or codes modules, which can be used for the safety assessment of nuclear power plants and other nuclear installations. Due to the German phase out of nuclear energy for electricity generation by the end of 2022, the research priorities shift from issues mainly relevant for German reactors to issues relevant for existing or planned reactors in the vicinity of Germany. At a national level, open questions relevant for the decommissioning phase and selected issues on radioactive waste, particularly in connection with (prolonged) interim storage, are increasingly gaining importance. With view to international developments, GRS will retain and increase its expertise related to safety analyses of evolutionary reactor designs with advanced safety features (Gen III/III+ reactors) including passive safety systems, innovative (Gen IV) reactor concepts as well as small modular reactors (SMRs) that are being developed internationally and have different safety concepts than the plants currently operated in Germany. Other important, internationally relevant research topics are related to long-term operation, ageing of components and structures, alternative nuclear fuel and cladding concepts as well as new core loading patterns. This article presents selected research results from the above-mentioned topics.

1 INTRODUCTION

After the Fukushima nuclear disaster the German Federal government decided to terminate the use of nuclear energy for electricity production at the latest in 2022 (13th amendment of the atomic energy law in March 2011, [BMU11]). The government decided to immediately shut down permanently eight Nuclear Power Plants (Biblis A/B (KWB-A/B), Brunsbüttel (KKB), Isar 1 (KKI-1), Krümmel (KKK), Neckarwestheim 1 (GKN-1), Philippsburg 1 (KKP-1), Unterweser (KKU)). Nine Nuclear Power Plants (NPP) continued operation, but the points in time when the operation permission of the respective NPP expires has been fixed (2015: Grafenrheinfeld (KKG), 2017: Gundremmingen B (KGG-B), 2019: Philippsburg 2 (KKP-2), 2021: Brokdorf (KBR), Grohnde (KWG) and Gundremmingen C (KGG-C), 2022: Emsland (KKE), Isar 2 (KKI-2), Neckarwestheim 2 (GKN-2)). Under these special political conditions it is important to illustrate to our numerous national and international partners how the Gesellschaft für Anlagen- und Reaktor-sicherheit (GRS) gGmbH continues its safety research [SCH17].

One of the main tasks of the approximately 70 technical experts at GRS's Safety Research Division is developing and validating the codes that form GRS's nuclear simulation chain [SCH18], which allows the simulation and assessment of all relevant phenomena for the analysis of operational states, anticipated operational transients, accidents and severe accidents in NPP and in other nuclear facilities. The scientific basis for the code development and validation activities is built on reliable plant and experimental data, as well as information gained from operational occurrences or accidents and considers new insights on physical phenomena. Because GRS operates no test rigs, monitoring and evaluating the results of national and international reactor safety research network projects, and particularly the participation in experimental programs, are essential parts of the work. Through its national and international research and expert activities, GRS is able to consider, in this context, the current state of science and technology.

In the following contribution selected activities and results in the working fields of neutron kinetics, thermal hydraulics and structural mechanics are presented.

2 NEUTRON KINETICS

The neutron kinetic activities of GRS are currently pursuing several different lines of research. Current national and international developments are the planned transition to cores with longer fuel cycle length, higher burn-up and/or higher fuel enrichment, advanced loading pattern, and the increasing use of burnable absorbers. Furthermore, new fuels, claddings, and fuel assemblies are developed or already used, which requires further development and validation of the GRS evidence tools. This is not just a matter of providing new models and procedures that work on same scale previously considered in simulations. Often the spatial resolution used in the analyses so far are no longer sufficient for an in-depth analysis of the advanced fuel elements and core loading patterns. Therefore, GRS develops high-fidelity multi-physics pin-by-pin models for the simulation of the aforementioned applications. In the first section of this chapter an example of such a development will be presented with the simulation of a SVEA-96 Optima2 fuel assembly.

Fast reactors are experiencing a renaissance today. In the past, many of the fast reactor developments have been terminated due to lack of economic efficiency in countries like United States of America, United Kingdom, Germany and Italy. Only the Russian Federation, Japan and France are still actively pursuing the development of fast reactor technology. Currently a set of 6 nuclear reactor designs is being researched for commercial applications by the Generation IV International Forum motivated by a variety of goals including improved safety, sustainability, efficiency, and cost competetiveness. Four out of six concepts proposed by the Generation IV International Forum (GIF) are fast reactors. These are the:

- sodium cooled fast reactor (SFR),
- lead cooled fast (LFR),
- gas cooled fast reactor (GFR) and
- molten salt fast reactor (MSFR).

The technology readiness level vary extremely. GRS’s motivation for the development of safety assessment tools is to continuously follow these developments, to review these designs, and to develop, validate and apply computational tools for (preliminary) safety assessments for performing preliminary safety assessments at an early stage. The development of safety assessment tools for fast reactors is therefore the topic of the second section of this chaper.

2.1 High-fidelity Multi-physics Pin-by-pin Modeling of a SVEA-96 Optima2 Fuel Assembly with TORT-TD/CTF

Simulating the physics of BWRs has become more complicated in recent years because modern fuel assemblies exhibit new sophisticated design features, given by, e.g., part length fuel rods, strongly varying radial fuel enrichment, and Gadolinium-bearing burnable absorber pins. The SVEA-96 Optima2 fuel assembly is an example of a complex BWR assembly design which consists of four sub-bundles separated by a cruciform internal structure (water cross) in the channel including a central canal. It features fuel rods with 1/3 and 2/3 active length, a not strictly regular pin lattice and four Gd_2O_3-bearing fuel rods in each sub-bundle with different Gd contents (see Figure 2.1). This quarter-channel design may have consequences on the void fraction distribution across the assembly, e.g., if it is subject to the influence of absorber blades or if there are different flow conditions between the four sub-bundles. The study of such local phenomena requires the application of high-fidelity coupled multi-physics simulations at pin and subchannel scale for accurate and realistic predictions of local safety parameters.

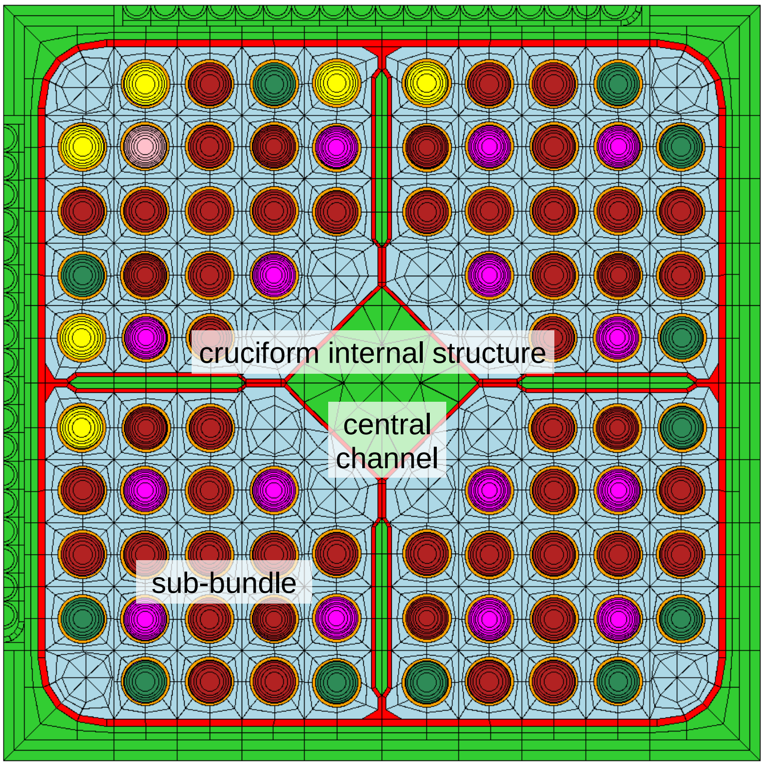

Figure 2.1 HELIOS model of the upper axial section of SVEA-96 Optima2. Varying enrichment and Gadolinium contents are characterized by different colors.

For the coupled code system TORT-TD/CTF [CRI10], a 3D pin-by-pin neutronic and subchannel thermal hydraulic model of a SVEA-96 Optima2 fuel assembly has been developed. The thermal hydraulics is simulated by the subchannel code CTF which uses a two-fluid and three-field representation of the two-phase flow. Originating from COBRA-TF [AVR06], CTF is jointly developed by North Carolina State University (NCSU) and Oak Ridge National Laboratory (ORNL) and provides the best available sub-channel methods. The neutron kinetics is treated at pin-by-pin level by the transient 3D few-group transport code TORT-TD developed at GRS [SEU08]. TORT-TD solves the time-dependent 3D few-group transport equation in discrete ordinates representation with arbitrary number of energy groups, arbitrary Legendre scattering expansion order and arbitrary number of delayed neutron precursor groups. In addition, it also contains a fine-mesh diffusion solver which operates on the same arbitrary space-time-energy discretization of the diffusion equation. Both codes are coupled using an explicit coupling scheme [CRI10] wherein both codes are compiled to a single executable with a newly developed coupling supervisor. The lattice and depletion code HELIOS-1.12 [CAS91] is used for the generation of pin cell-homogenized macroscopic cross section libraries. HELIOS is a 2D general geometry lattice and depletion code which solves the multi-group transport equation using the current coupling colission probability (CCCP) method. The cross sections have been generated in eight energy groups, which are parameterized with respect to fuel temperature, channel water density and bypass water density. For the validation of the neutronics model, multiplication factors and pin power distributions obtained with TORT-TD using the HELIOS-generated cross section libraries have been compared to those calculated by an equivalent Monte Carlo Serpent model using continuous energy nuclear data. It is found that the multiplication factor obtained by HELIOS differs from the Serpent reference result by 278 pcm, 275 pcm and 226 pcm for the lower, middle and upper axial zone of the fuel assembly. Regarding the pin-wise power distribution, the deviation of the HELIOS solution from the Serpent reference result about 1.1% (RMS) with a maximum of 2.7%. Using the pin cell-wise homogenized macroscopic cross sections in TORT-TD, the deviation of the TORT-TD pin power distribution from the Serpent solution is of similar order as shown in Table 2.1 for the controlled state and in Table 2.2 for the uncontrolled state. It is emphasized that TORT-TD implements a direct pin-by-pin solution method, i.e. no pin power reconstruction is applied.

Table 2.1 Deviation of TORT-TD pin power distribution from the HELIOS result (lower axial section, uncontrolled).

	1	2	3	4	5	6	7	8	9	10
A	1.6%	-0.4%	-1.4%	-1.3%	-1.0%	-1.0%	-1.5%	-1.3%	-0.5%	1.9%
B	-0.4%	1.3%	1.0%	1.4%	-0.4%	-0.3%	0.2%	0.6%	1.1%	-0.6%
C	-1.5%	1.0%	1.4%	1.3%	0.6%	1.1%	0.2%	1.6%	1.1%	-1.7%
D	-1.3%	1.3%	1.3%	0.7%	0.3%	0.5%	0.5%	1.2%	1.5%	-1.6%
E	-1.0%	-0.4%	0.6%	0.2%			0.2%	0.6%	-0.3%	-1.4%
F	-1.0%	-0.3%	1.1%	0.5%			0.4%	1.0%	-0.2%	-1.2%
G	-1.6%	0.2%	0.3%	0.5%	0.1%	0.4%	0.3%	0.1%	0.3%	-1.7%
H	-1.5%	0.5%	1.7%	1.2%	0.6%	1.0%	0.2%	1.7%	0.5%	-1.5%
I	-0.4%	1.1%	1.1%	1.5%	-0.2%	-0.3%	0.3%	0.5%	1.0%	-0.4%
J	2.0%	-0.6%	-1.7%	-1.6%	-1.4%	-1.2%	-1.7%	-1.5%	-0.4%	2.2%

Table 2.2 Deviation of TORT-TD pin power distribution from the HELIOS result (lower axial section, controlled).

	1	2	3	4	5	6	7	8	9	10
A	0.6%	0.7%	2.1%	2.5%	2.0%	2.3%	2.0%	2.3%	-2.6%	2.5%
B	0.8%	-1.6%	-1.1%	0.1%	-0.3%	-0.5%	-0.5%	-1.8%	-0.9%	0.9%
C	2.1%	-1.1%	-0.1%	-0.1%	0.1%	0.5%	-0.7%	0.3%	0.4%	-0.7%
D	2.5%	0.1%	-0.2%	0.0%	-0.3%	-0.3%	-0.1%	0.7%	1.2%	-1.1%
E	2.0%	-0.3%	0.1%	-0.4%			-0.2%	0.2%	-0.4%	-1.0%
F	2.2%	-0.6%	0.5%	-0.2%			0.0%	0.8%	-0.4%	-1.0%
G	1.7%	-0.6%	-0.6%	0.0%	-0.2%	0.1%	-0.2%	-0.3%	-0.1%	-1.7%
H	1.6%	-1.8%	0.4%	0.6%	0.2%	0.8%	-0.2%	1.3%	0.2%	-1.7%
I	-2.7%	-0.7%	0.5%	1.2%	-0.4%	-0.3%	-0.1%	0.2%	0.7%	-0.6%
J	3.3%	1.2%	-0.6%	-0.9%	-1.0%	-1.0%	-1.7%	-1.7%	-0.5%	2.2%

Initial coupled steady state TORT-TD/CTF simulations of the SVEA-96 Optima2 fuel assembly in infinite lattice arrangement converge after 5 iterations between TORT-TD and CTF. Axial and radial distributions of pin power and moderator density have been investigated and appear physically plausible. It is found that the pin power distribution is highly peaked (see Figure 2.2 left side). In the middle and upper axial sections, the latter without the 1/3 length rods at the corners, the pin power is maximum at the next-to-corner rods. The relative differences between the power of the next-to-corner rods and its neighbors exceeds 20%. It is shown that the presence of absorber blades leads to a strong radial tilt of the pin power distribution (see Figure 2.2, right side), which results in different conditions between the sub-bundles of the same fuel assembly. First test calculations of a transient of partially rodded assembly initiated by a small control blades movement show physically plausible power excursions as shown in Figure 2.3 for a 4-by-4 mini core configuration, for which the converged coupled steady state pin power distribution in the lower axial section is depicted in Figure 2.4.

With the improved 3D coupled neutron kinetics and subchannel thermal hydraulics code system TORT-TD/CTF, GRS has developed an advanced tool for high-fidelity multi-physics simulation of local neutron physical and thermal hydraulic phenomena in complex modern BWR assemblies and so provides a contribution to improved assessment of local safety parameters in LWR. It is envisaged to transfer the respective know-how and experience to future applications for the high-fidelity safety assessment of local phenomena in innovative designs, e.g., liquid metal-cooled reactor systems including SMR.

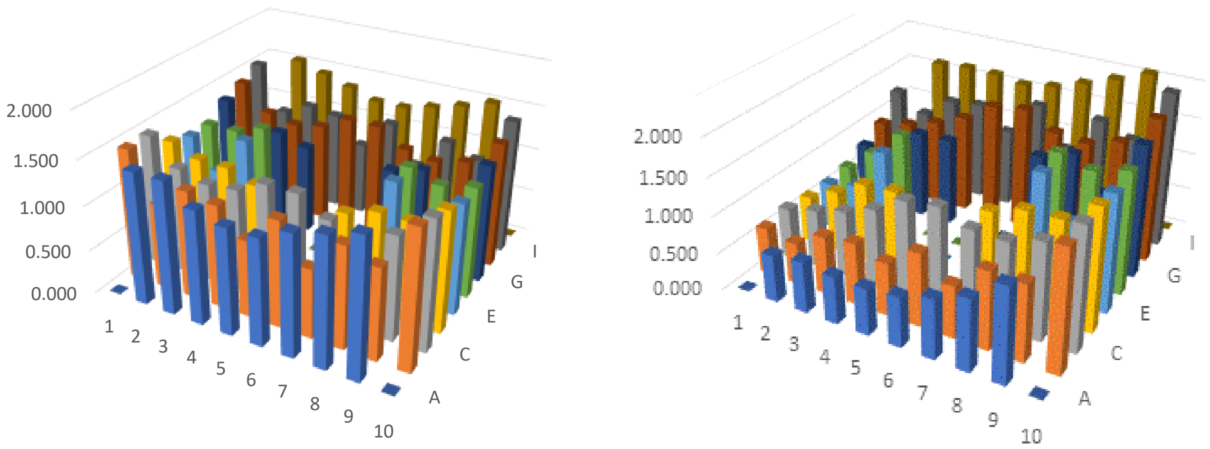

Figure 2.2 Normalized pin power distribution in the middle axial section of SVEA-96 Optima2 (left side: unrodded, right side: rodded).

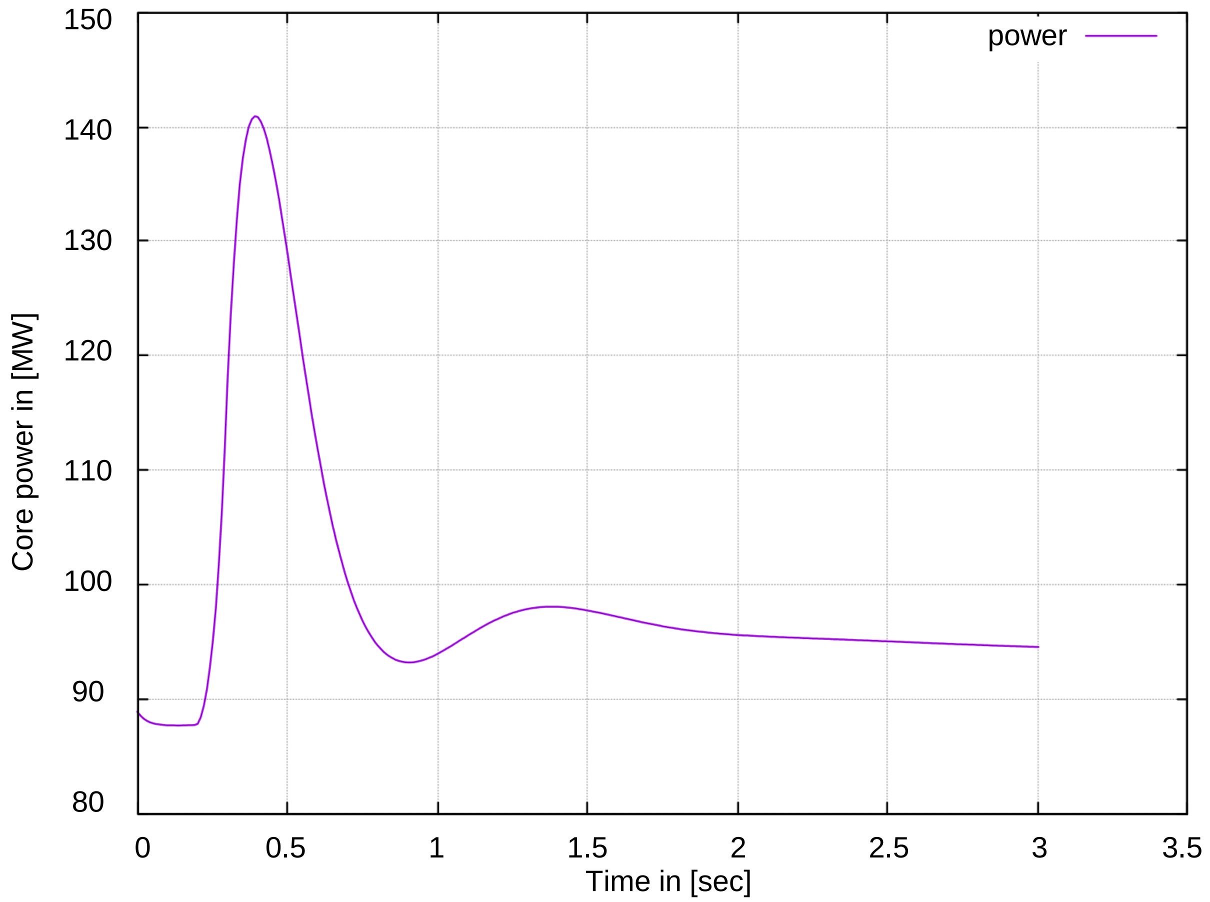

Figure 2.3 Transient response by TORT-TD/CTF of a 12,5 cm withdrawal of a partially inserted control blade (start at 0.2 sec. and end at 0.3 sec.) in the lower axial section of one assembly in a 4-by-4 mini core configuration.

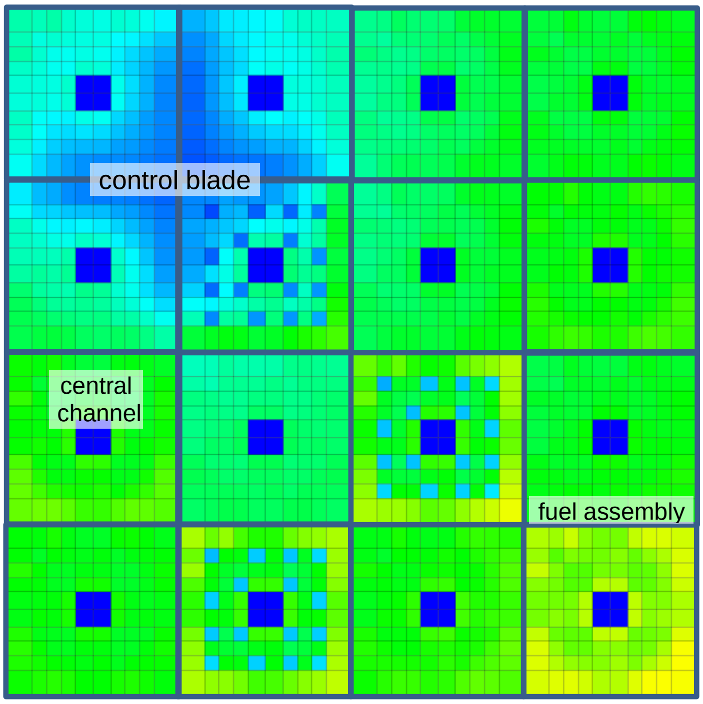

Figure 2.4 Converged TORT-TD/CTF steady state pin power distribution in the lower axial section of a 4-by-4 arrangement of Svea-96 Optima2 fuel assemblies with different burnups and one control blade inserted (blue/yellow: low/high power).

2.2 Development of Safety Assessment Tools for Fast reactorS

In fast reactors, the fission chain is sustained by fast neutrons. For this reason they do not use a moderator (e.g. water, graphite) to slow down neutrons. Fast reactors require fuel with higher enrichment than thermal reactors and different coolants other than water such as liquid metal.

At GRS, methods and tools for safety assessment for fast reactors were developed in the last few years. They are based on further developments and improvements of the thermal hydraulic system code ATHLET [LER19] developed at GRS within the AC^2 code package [SCH18] and on developments and improvements of 3D neutron kinetics codes like PARCS [DOW12] or DYN3D-MG [ROH16].

Since version Mod 3.1A, ATHLET contains coolant properties for sodium, lead and lead-bismuth-eutectic (LBE), helium and different molten salts, accounting also for sodium boiling and sodium two-phase flow simulation. However, further validation of the closure equations of ATHLET is required.

Furthermore, the working temperature range for SFR is higher than PWR. While the typical inlet/outlet temperatures are 290°C/320°C for PWR, they are 400°C/550°C for SFR. Elevated fuel temperatures cause the axial expansion of the fuel and cladding and their density decreasing. This leads to more parasitic absorptions by the cladding and a slight insertion of the control rods. The typical observed values for this effect are around -0.6 pcm/°C. A rise in the core coolant inlet temperature causes thermal expansion of the diagrid plate (which is the core support structure) thus increasing the fuel assembly pitch. This results in more sodium between fuel assemblies which leads to higher axial leakage and more scattering and parasitic absorptions by the coolant. The typical observed values for this effect are around -1 pcm/°C. Material thermal expansion thus plays an important role in reactivity feedback effect in SFR and has to be taken into account in safety assessment. GRS has extended the PARCS code to simulate thermal expansion in the 3D neutron kinetics, e.g. radial (diagrid) and axial (fuel, cladding) expansion, which plays an important role in fast reactors [BOU19]. For the safety assessment of external source driven subcritical fast reactors, PARCS was also extended by GRS to simulate time-dependent external neutron sources. More recently, a new diffusion code, based on few-group 3D finite element solver [SEU16], is under development at GRS for future safety assessment of small modular (SMR) with their irregular geometries. Moreover, the core simulator KMACS [ZIL18], developed by GRS, was also updated for the generation of few-group macroscopic cross section using the Monte-Carlo Code Serpent [LEP15].

GRS was involved over the past years in several activities regarding SFR and LFR. As participant of the EU project MAXSIMA, GRS has performed analyses [BOU16] of the reactor MYRRHA. MYRRHA is the *Multi-purpose hYbrid Research Reactor for High-tech Applications* planned to be built at the SCK-CEN research center in Mol (Belgium) around 2026 and is cooled by Lead-Bismuth Eutectic (LBE).

Currently, Russia has two out of three SFR in operation in the worldwide. In the framework of the scientific collaboration between the Russian technical safety organization SEC-NRS and GRS, several safety analy-ses and simulations were performed using the coupling system code ATHLET/DYN-3D-MG on those two SFR, the BN-600 [IVA16] and the BN-800 [IVA18].

GRS is participating in the currently ongoing EU project ESFR-SMART, in particular safety and performance parameters assessments including quantification of nuclear data uncertainties, assessment of transition from forced to natural circulation using ATHLET/OpenFOAM (system thermal hydraulic and CFD) coupled simulations and also contri-butes to 3D neutronic codes calibration and validation by participating in the neutronics and thermal hydraulics benchmark exercise for the large-power Superphénix core, which was a 1,242 MW_{el} fast breeder reactor in France, using PARCS and ATHLET [HEN19]. Further ongoing activities are the participation in the

- IAEA CRP on neutronics benchmark on start-up tests of the CEFR, which is the China Experimental Fast Reactor (65 MWth).
- OECD/NEA Sodium Fast Reactor Uncertainty Analysis in Modelling for the Qualifica-tion of best-estimate codes and data with uncertainty evaluation for Generation-IV so-dium fast reactors in a series of static and transient benchmarks,
- IAEA Fast Reactor Knowledge Preservation (FRKP) initiative that aims at preventing the ongoing loss of information related to fast reactors and to collect, retrieve, preserve and make accessible already existing data and information on fast reactors.

3 THERMAL HYDRAULICS

Different approaches are used at GRS for thermal hydraulic simulations in the reactor coolant system (RCS) and the containment. These are the application of

1. the system code suite AC^2 with its thermal hydraulics codes ATHLET, ATHLET-CD and COCOSYS stand alone,
2. the computational fluid dynamic (CFD) codes ANSYS-CFX or OpenFOAM stand alone,
3. a coupled system and CFD code approach (AC^2 codes and ANSYS/CFX or AC^2 codes and OpenFOAM).

The selection of the appropriate approach and code for the investigation of a specific issue is based on the necessary spatial resolution and current code capabilities.

The AC^2 code suite integrates the thermal hydraulics codes ATHLET [LER19], ATHLET-CD [AUS19] and COCOSYS [ARN19] at the centre of GRS's simulation chain [GRS19] for the analysis of nuclear reactors at normal operation, anticipated operational occurrences and design basis accidents up to severe accident conditions with radionuclide releases from the containment. Its current version AC^2 2019 was released this year in June [WIB19]. The objec-tive for this suite is to provide a state-of-the-art tool for the integral simulation of plant behavior that can explicitly consider the interactions between reactor core, cooling circuit and contain-ment. AC^2 is distributed with further programs, tools and libraries, e.g.

- NuT library (Numerical Toolkit) [STE19], which provides an easy access to dedicated numerical libraries to speed up the internal computations of ATHLET and ATHLET-CD,

- ATLAS version 5.1 [CES15], which provides a GUI for both interactive control and post-processing of AC2 code simulations,
- OpenFOAM interface [LER19], a hydrodynamic interface for single phase flow between ATHLET 3.2 and OpenFOAM simulation domains allowing multiple coupling locations between ATHLET and OpenFOAM calculation domains.

The GRS system codes ATHLET, ATHLET-CD and COCOSYS have been developed for four decades. For validation, GRS uses well-balanced validation matrices with separate effect tests and integral tests that are derived from OECD/CNSI test matrices for thermal hydraulic codes [NEA87], [NEA96] and for containment codes [NEA14] and considers relevant state-of-the-art reports. The validation is complemented by selected plant transient as well as postulated fault condition simulations, which are checked against available data or for plausibility.

ATHLET and ATHLET-CD simulate the coolant flows of reactors with a one-dimensional approach very efficiently. ATHLET's newly developed 3D model allows the simulation of selected phenomena (coolant mixing) in selected components (e.g. the downcomer and the lower plenum) of a PWR. Using a parallel channel nodalisation the 1D flow model, explicit momentum terms for the two additional directions (x- and y) are added to the conservation equations, thus allowing the simulation of complex flow patterns. Relying on the system code models, 1- and 2-phase flow can be handled. Furthermore, the ATHLET 3D model has been successfully validated for application to large water pools with free water surface [BUS19]. Although these result are very promising, the space resolution of these models is limited so that local phenomena that need high resolutions to investigate in detail such as turbulence or stratification of flows are not accessible for these system codes. Similarly, COCOSYS also employs a lumped parameter approach and is not able to resolve local phenomena or simulate complex three-dimensional flow problems in the gas phase and also for water pools.

To overcome these limitations, computational fluid dynamic codes (CFD) can be used. These allow the in-depth investigation of local and highly complex flow phenomena, particularly for single-phase flows and with specific capabilities for 2-phase flow conditions. However, these codes are often several orders of magnitude more expensive in terms of CPU time than system codes. Therefore, it is usually necessary to limit CFD models to parts of a plant or facility, thus neglecting the feedback of the overall system. For some issues, this is sufficient in which case the CFD tool needs to be properly validated.

Using a coupled code approach, it is possible to determine the overall reactor coolant system behaviour by a system code while those parts of a facility being of special interest can be calculated in a detailed 3D solution. This combines the advantages of system code and CFD tools, but also requires to split calculational domains and develop an interface between the two codes that is numerically stable and efficient. In general, the same considerations can be applied also for the containment [SCH17].

Numerous publications on the development strategy of the GRS Code AC² [WEY19] and the simulation of advanced reactor designs of Gen III/III+ and light water cooled SMRs [SCH18], as well as conventional and renewable applications [WIB18] e.g. heat pipes [KRA18] have been recently published. Therefore, the focus in the following sections is on ongoing and planned OpenFOAM activities on containment-specific issues (section 3.1) and on the coupling of the AC² code ATHLET with computational fluid dynamic codes ANSYS CFX and OpenFOAM (section 3.2).

3.1 Ongoing and Planned OpenFOAM Activities on Containment-Specific Issues

The German nuclear research community considers the increased use of the open-source CFD code OpenFOAM (Open Source Field Operation and Manipulation) for research purposes as an important strategic objective for the future. This decision was ultimately driven by freely accessible source code, which is not the case for commercial CFD codes.

The major advantage of the open source solution is that the source code is available and new models can be integrated. Since the implementation and validation of all models required for containment issues are very extensive in terms of time, man-power and costs, this work shall be carried out within a framework of a national initiative together with partners of the German CFD network (especially universities and other research institutes).

With regard to the model development and validation of OpenFOAM, GRS is currently working on the

- simulation of the flow and the composition of gases (in particular H2 concentration),
- simulation of wall and volume condensation,
- thermal radiation modelling and
- simulation of passive catalytic hydrogen recombiners.

In the following results of the first two items are presented.

3.1.1 Simulation of the flow and the composition of gases

An important safety-related issue in severe accidents with H_2 release is the investigation if the gas mixture exceeds the flammability or detonation limits both overall as well as for specific (containment) compartments. For this it is necessary to be able to correctly simulate the gas flow with all relevant phenomena. Especially the turbulent flow and mixing must be calculated with a sufficient accuracy. In particular, GRS dealt with model extension and validation of the following phenomena:

- influence of walls and other structures (validation of wall functions and heat transfer wall / gas),
- diffusion modeling (extension and modification of the transport equations for energy and species mass fractions),
- validation of turbulence modeling.

In addition to the verification of individual phenomena using simple test examples, a series of large-scale THAI and Panda experiments (e.g. Panda ST1-4 [MIG10], OECD / NEA-Panda Benchmark [ADR13]) were carried out, focusing on the dissolution of a stable light gas stratification. In the OECD / NEA-Panda Benchmark a stable helium-layer in the upper part of the vessel (see Figure 3.1, left side) is slowly eroded by a vertical steam jet (see Figure 3.1, right side). The gas volume (~90 m^3) is discretized using a structured mesh with 1.2 million cells. The size of the cells differs significant due to local grid refinement in the jet region and in the region of the Helium cloud. OpenFOAM calculates the erosion time of the helium cloud in good agreement with experimental data.

3.1.2 Simulation of wall and bulk condensation

In a severe accident with hydrogen release, a large amount of steam is usually released into the containment. This steam can condense on cold walls or bulk condensation occurs due to mixing processes. Although a two-phase modeling of these processes within a CFD model would be possible, the computational effort required for this is not practical, in particular because of the very fine grid that is required for this approach. To overcome this problem simplified models can be used. In the basic version of OpenFOAM, there are currently no models for the simulation of wall and volume condensation suitable for containment questions. Based on the models developed in past BMWi funded projects and already implemented in ANSYS CFX, corresponding models have also been implemented in OpenFOAM. Previous results - with condensation models that may still have to be improved - of recalculations of small-scale CONAN wall condensation experiments [AMB09] and large-scale THAI experiments (TH-2 [KAN03], TH-24 [FIS11]) are promising, but further work is needed.

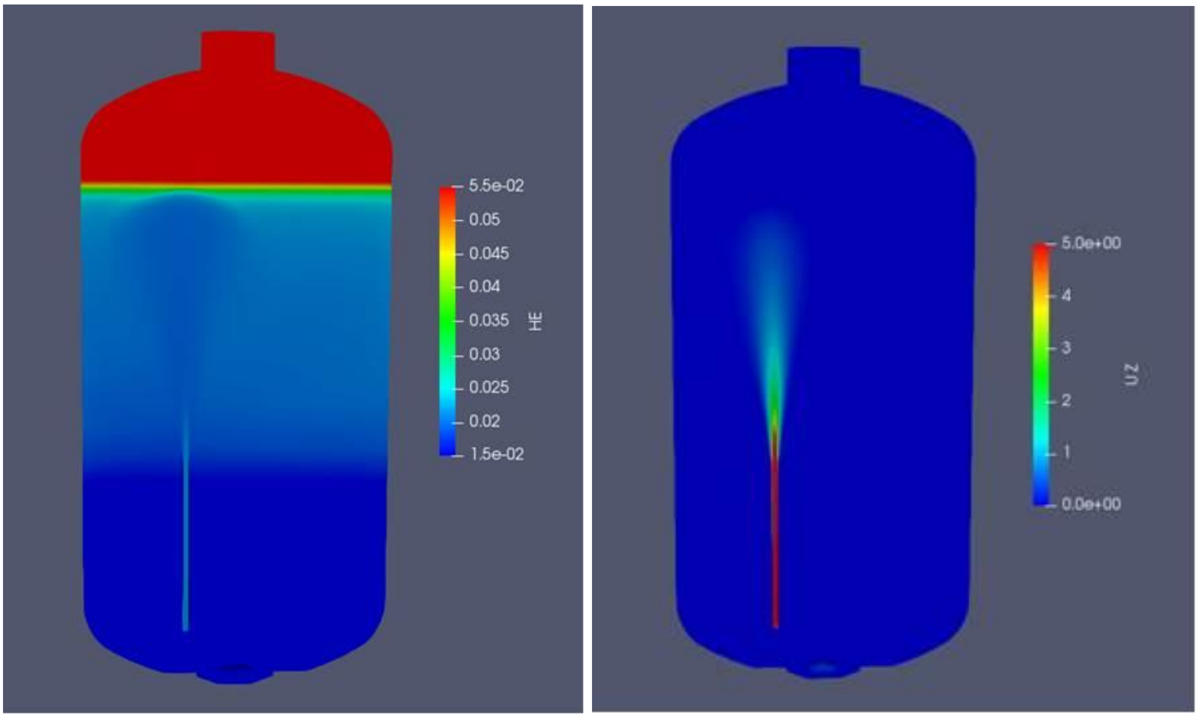

Figure 3.1 Helium concentration (left) and velocity (right) in an OpenFOAM simulation of the OECD/NEA-Panda benchmark at t = 1000 s.

3.2 Coupling of AC² system codes with Computational Fluid Dynamic Codes

In the last ten years, GRS has developed methods to couple its system codes ATHLET and ATHLET-CD with both the commercial CFD code ANSYS CFX [PAP10] and the open source CFD code OpenFOAM [HER16]. The coupling facilitates the exchange of fluid thermal hydraulic data at the coupling interfaces and the control of the coupled calculation. Special care has been taken to ensure a stable common solution of the coupled solvers. The numerical methods implemented in the coupling schemes include under-relaxation and quasi-Newton methods approaches. Two types of coupling interfaces are needed to achieve stable calculation models. In the first type the CFD-code provides scalar variables (like pressure, fluid temperature, quality, etc.) and ATHLET responds with vector variables (mass flow or velocity and related temperature, etc.) whereas in the second interface type the roles are reversed.

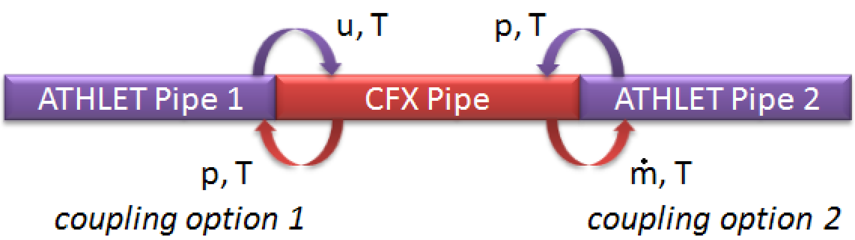

Figure 3.2 Multiscale single-phase coupling: fluid dynamic exchange parameters [PAP14]

The developed coupling methods have been applied by GRS and external organizations to different reactor relevant geometries. The ATHLET-ANSYS CFX coupling was validated on the geometry of the TALL-3D experiment [PAP15] within the EU THINS and SESAME projects [PAP16]. This experiment used lead-bismuth-eutectic as fluid and had a well-instrumented test section, which was a source of complex 3D flow phenomena, affecting the thermal hydraulics behavior of the whole primary loop. It was simulated with ANSYS CFX, while the rest of the loop was calculated with ATHLET. In the coupled simulation in the CFD flow domain not only the fluid flow was simulated but also the heat transfer with the walls.

The ATHLET-ANSYS CFX coupling was also applied for the calculation of the Double T-Junction experiment [PAP14] of the Paul Scherrer Institut (PSI). The computational results show a good agreement with measured data. Furthermore, this coupled system was applied for the investigation of experiments with density variations of the fluid in the ROCOM facility.The ROCOM test facility is a 1:5 scaled model of a German pressurized water reactor (PWR). The ROCOM experiments were also simulated with ATHLET-OpenFOAM with good accuracy. Additionally ATHLET-Open-FOAM was also sucessfully applied for the flow simulation of the cooling circuit of the fast sodium cooled Phénix reactor [HER19].

All simulations described in this section were numerically extremely challenging. They included one or more closed circuits, decomposed in 1D and 3D calculation domains, which were split up between the different solvers. Physical oscillations can be avoided only with suitable numerical methods. The simulations also differ in the number of coupling interfaces. While for the simulation of the ROCOM test facility six coupling interfaces were sufficient, the simulation of the Phénix reactor required seventeen interfaces (for an illustration see Figure 3.3).

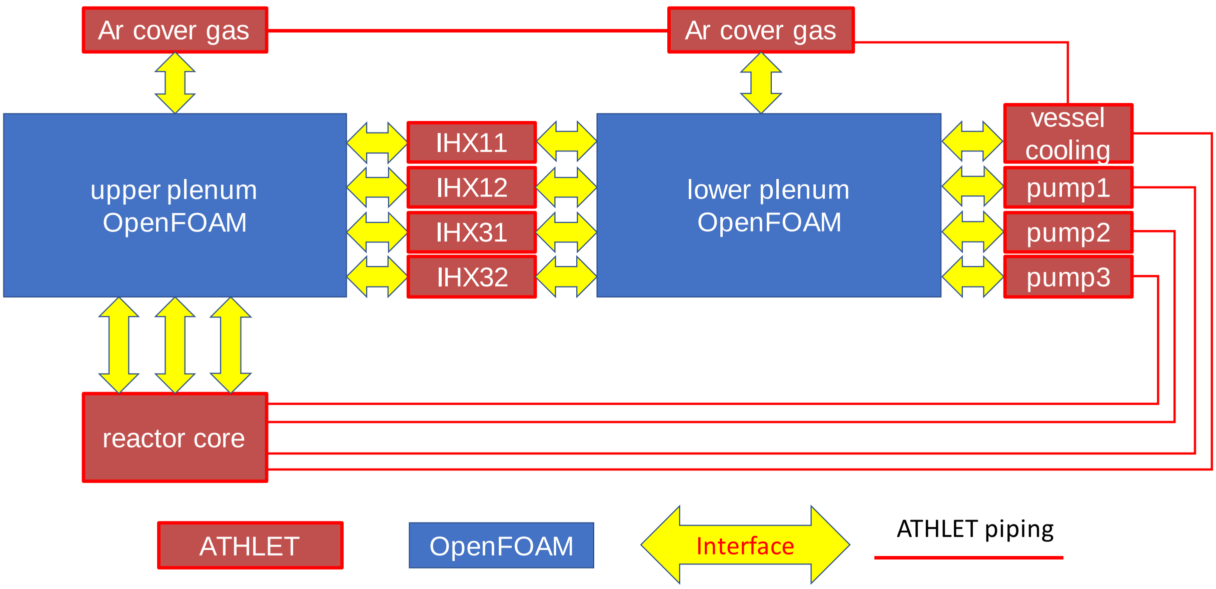

Figure 3.3 Scheme of calculational domains and interfaces for the Phénix reactor simulation [HER19]

GRS continues with the further development and validation of the coupling methods for system and CFD codes. Important improvements will focus on a more systematic approach to the numerical approaches at the coupling interfaces and the extension of the coupling capabilities schemes for multi-components and multi-phase flows in future. Particularly two-phase flows pose significant challenges for the thermal hydraulic coupling of system codes and CFD-codes and there are still a lot of open questions regarding physical models within the coupling interface and suitable numerical methods for an effective and stable simulation. In this regard, GRS is also pursuing a collaboration with TU München that explores the use of the generic preCICE [BUN16] coupling interface between ATHLET and OpenFOAM.

4 STRUCTURAL MECHANICS

In the framework of research on structural mechanics issues GRS develops, validates and applies analysis methods to investigate the behaviour of metallic components (vessels, piping, fuel assemblies) and building structures (containment, interim waste storage) under operational, accidental and severe accident loads. This includes safety relevant issues like the integrity assessment of reactor pressure vessels (RPV) in case of emergency core cooling events, leak before break assessment of piping, and investigations on vibrations of fuel assemblies coupled with RPV internals. The structural mechanics codes used are included in the simulation chain of GRS [GRS19] and are based on analytical methods or the finite element method. In the following sections, two codes developed by GRS are described and an application example is given.

4.1 Integrity Assessment of Piping and Vessels with consideration of Ageing Mechanisms

For the assessment of integrity and ageing of pipework, vessels and components in NPPs, GRS develops the fast running computer codes PROST (PRObabilistic STructure Analysis) and WinLeck based on analytical approaches as an alternative to the finite element and the CFD analysis techniques, which need much more effort.

PROST is a fracture mechanics computer code for the evaluation of crack formation, crack growth, leak and break probabilities of pipe components. These approaches allow the consideration of ageing phenomena, such as corrosion, fatigue, and ductile crack growth as well as the combination of ageing mechanisms under operational or (severe) accident loads. The code's fields of application are deterministic and probabilistic fracture mechanical analysis, assessment of ageing and degradation, as well as analysis of sensitivities and uncertainties with consideration of technical standards such as the nuclear safety standard (KTA-rule) 3206 [KTA16]. The failure assessment diagrams (FAD) according to the structural integrity assessment procedures for European industry (SINTAP) are applied to evaluate the transition from a crack to a leak. The growth of wall-penetrating cracks, i.e. leaks, can be treated in PROST, too. Leak rates can be calculated with consideration of leak detection systems. Deterministic applications are useful for a fracture mechanical assessment of a safety-relevant finding in the form of a crack at a facility with prognosis on possible crack growth, leak formation, leak growth, leak detection and quantification of margins against a break (see Figure 4.1).

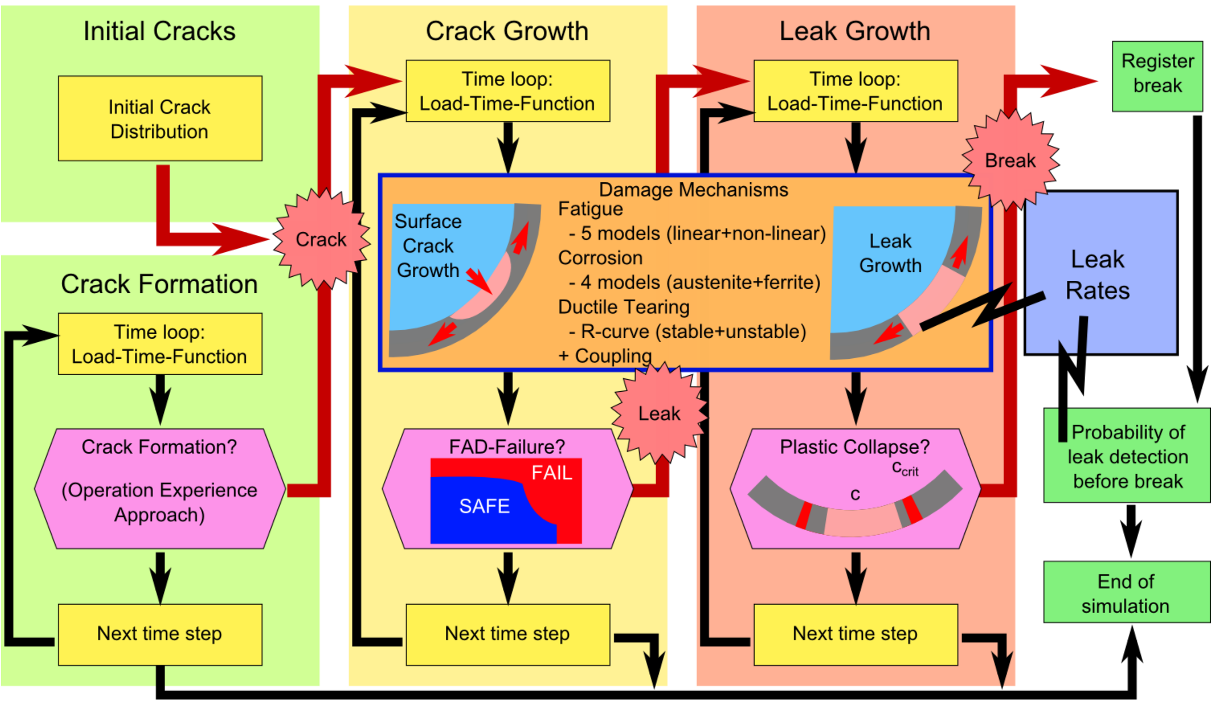

Figure 4.1 Schematic illustration of the work flow in PROST with the steps of crack formation and growth of cracks / leaks due to ageing mechanisms [HEC19]

Probabilistic applications on the other hand allow the consideration of statistical distributions of relevant parameters like geometry, material properties and loadings. In this case the code calculates leak and break probabilities as function of the operation time. The deterministic models of PROST have been validated by calculations on experiments, on tasks within international benchmark activities, and by comparison with results of finite element calculations. The probabilistic capabilities were compared successfully in international round robins with comparable codes. The PROST documentation includes a user and a theory manual and a validation report. A more technical overview of the individual models, corresponding references and generic applications are given in [HEC15].

4.2 Assessment of Leakage in Piping

Pressurized components and building structures may lose their tightness, for example due to manufacturing defects, ageing effects or overloads. Prominent leakage cases are loss-of-coolant accident scenarios due to postulated crack-like leaks in a main coolant line and loss of contaminated gas mixtures from the containment building during severe accident scenarios. Two quantities are essential for the leak rate calculation: the size of the leak area, and the fluid flow through the leak. Leakages can be found during on-site-inspections and with the help of leakage monitoring systems in power plants. Thus, a small but detectable leakage could warn the operators of the plant, allowing shut-down and repair actions to be taken. In this context the verification of leak-before-break (LBB) behavior is an additional safety attribute. LBB means the property of a pressure-retaining system area, which ensures that a leakage arising from a wall-penetrating crack is detected in time and under the operational loadings of steady-state normal operation, and that such a leak is sub-critical regarding instability under all operational and postulated design basis accident loadings so that safe shut-down of the plant is ensured before global component failure occurs [KTA16]. In different country-specific regulations, the LBB demonstration is a supplementary safety assessment step, following the defense-in-depth strategy. In addition to design and manufacturing quality standards, with operational surveillance and regular maintenance it is prevented that any safety-relevant component may catastrophically fail during the specified operational and exceptional load conditions (e.g. safe-shutdown-earthquakes, SSE). The leak-before-break assessment com-pares the (circumferential) length of postulated leaks, considering the installed leak monitoring systems, and the stability of the leak (crack) against catastrophic component failure (break). Any leak should be detected before it can reach a critical size. Figure 4.2 shows a typical scenario for leakage rate calculation.

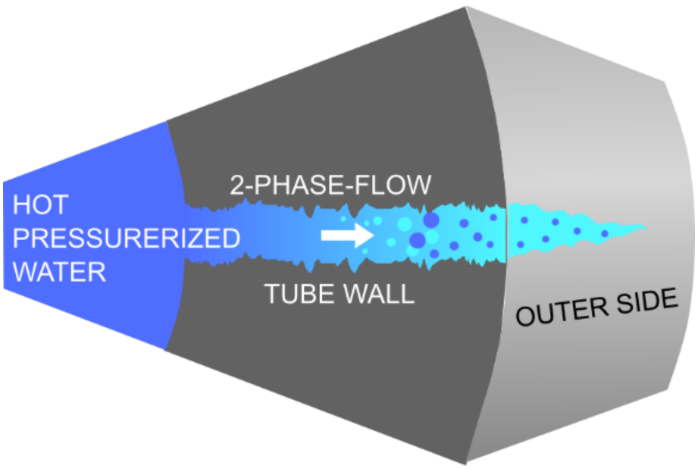

Figure 4.2 **Schematic illustration of two-phase discharge flow of subcooled water through a crack-like leakage in a pressurized tube**

The GRS code WinLeck includes several simplified models for the computation of the leak areas and leak rates, based on geometry, material properties, and medium. The optional coupling to the GRS code ATHLET [LER19] provides additional analysis procedures for the assessment of accidental and severe accident scenarios. The options to compare different models and their predictions are powerful features of WinLeck, which help to identify sources of deviations and systematic trends, independent of the shortcomings of single models. The code includes different country-specific assessment strategies for an appropriate computation of a postulated leakage, especially the procedure in KTA 3206 [KTA16]. The code is a model collection for the calculations of leak sizes and leak rates in piping components as well as gas leak rates through reinforced concrete structures with different analytical approaches. For the validation of the leak rate models within WinLeck, comparisons with numerous experimental tests have been performed, showing a good agreement between the measured data and the models predictions. A more technical overview of the individual models, corresponding references and generic applications are given in [HEC16] and [HEC18]. The WinLeck documentation includes a user manual and a validation report.

4.3 Example of LBB analysis

For a parametric investigation of influences to the LBB behaviour of nuclear piping, generic components with different pipe diameter were analyzed. For the investigated cases the critical length of a leak (usually: circumferential length) under accident conditions as well as the length of the smallest detectable leak under operating conditions have been computed. If the smallest detectable leak is sufficiently smaller than the critical leak, leak-before-break behavior is confirmed, i.e. the leak can be detected by the monitoring installations before a catastrophic failure. If the detectable leak is larger than the critical leak, unnoticed leaks may exist, which may fail by rupture under sudden exceptional design basis loads.

Circumferential leaks in straight pipes, covering inner diameters from 12.5 to 800 mm have been analyzed. The material is characterized by a yield stress of 150 MPa and a Young's modulus of 180 GPa. An operating pressure of 15.6 MPa at a temperature of 320 °C was assumed. The wall thickness is designed such that the nominal membrane stress due to operational loads corresponds to half the level of the yield stress. No additional loads (like bending) are assumed for the computation of the detectable leak length, i.e. pipe deadweight and thermal extension during normal operation are neglected. Dependent on the position of the leak, this may be conservative since the leak opening (and hence the flow rate) is smaller without additional tensile stresses, which implies that the leak detection is more challenging. It is assumed that a leak rate of 1 gal/min (63 g/s) can be detected by the monitoring system. The Henry model implemented in WinLeck was used for the flow computations and for the critical length, a flow stress concept also included in WinLeck was applied, taking the yield stress as input. Based on the assumed design criteria the procedure results in a constant critical angle of 45° independent from the pipe diameter. Figure 4.3 shows that for the detection threshold 63 (g/s) the pipes of 200 mm inner diameter or larger turn out to show leak-before-break behavior, while for the pipes of 100 mm inner diameter or less, leak-before-break behavior cannot be verified. Notably, the assumed detection threshold of the installed monitoring system plays a significant role in the LBB analysis. Beside the generic value of 63 g/s, the values of 200 g/s and 20 g/s are taken in the parametric study (see Figure 4.3). More details are given in [HEC16].

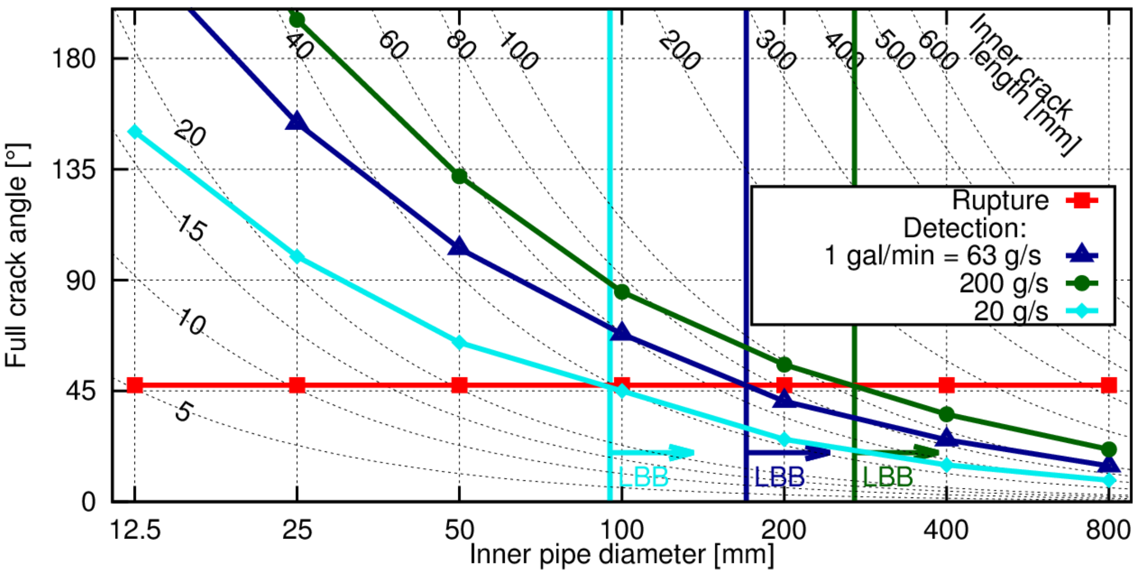

Figure 4.3 LBB Analysis of piping with variation of the detection threshold for the mass flow rate

5 SUMMARY

Despite the decided termination of the use of nuclear energy for electricity production in Germany, the German Federal government will support further nuclear safety research at GRS. Through this GRS remains a stable partner in this area, especially for all topics of code development, validation and application. But the research priorities will shift at a national level towards open questions relevant for the decommissioning phase and selected issues on radioactive waste, particularly in connection with (prolonged) interim storage. With view to international developments, GRS will retain and increase its expertise related to safety analyses for currently operated reactors abroad and their long-term operation. Furthermore GRS will further build up competence related to evolutionary reactor designs with advanced safety features (Gen III/III+ reactors) including passive safety systems, innovative (Gen IV) reactor concepts as well as small modular reactors (SMRs) currently in the commissioniong phase, under construction or in the planning stage. The codes of the GRS nuclear simulation chain, are being further developed and validated in this respect. Thus, GRS will continue to substantially contribute to enhancing the worldwide nuclear safety standards.

6 ACKNOWLEGDEMENTS

The presented study was sponsored by the German Federal Ministry of Economic Affairs and Energy (BMWi) within the projects RS1540, RS1547, RS1551 and RS1562.

7 REFERENCES

[AMB 09] Ambrosini, W., et al.,
SARNET-2 condensation benchmark No. 2, Data for a Numerical Benchmark on Condensation Modelling proposed in the frame of the SARNET-2, Universität di Pisa, 2009.

[ADR13] Adreani, M.,
OECD/NEA – PSI CFD Benchmark Specifications,
Paul-Scherrer-Institut, 2013.

[ARN19] Arndt, S., et al.
COCOSYS 3.0 – User’s Manual, March 2019.

[AUS19] Austregesilo, H., et al.
ATHLET-CD 3.2 – User’s Manual, March 2019.

[AVR06] M. Avramova, D. Cuervo, K. Ivanov, Improvements and Applications of COBRA-TF for Stand-Alone and Coupled LWR Safety Analyses,
International Conference on the Physics of Reactors (PHYSOR) - Advances in Nuclear Analysis and Simulation
September 10 – 14, 2006, Vancouver, (Canada).

[BOU16] Bousquet, J., Seubert, et al.,
Neutronic modeling of the MYRRHA minimum critical core with PARCS and Serpent.
International Conference on the Physics of Reactors (PHYSOR) - Unifying Theory and Experiments in the 21st Century,
May 1 – 5, 2016, Sun Valley, Idaho (USA).

[BOU19] Bousquet, J., Seubert, A., Henry, R.,
3-D Coupled PARCS/ATHLET Transient Simulation of SFR using Detailed Expansion Modeling.
International Conference on Mathematics & Computational (M&C) - Methods Applied Bridging Theory and Applications,
August 25 – 29, 2019, Portland, Oregon (USA).

[BMU11] Bundesministerium für Umwelt, Naturschutz, Bau und Reaktorsicherheit (BMUB),
Dreizehntes Gesetz zur Änderung des Atomgesetzes, BGBL. I, p. 1704 - 1705, August 2011.

[BUN16] H.-J. Bungartz, F. Lindner, B. Gatzhammer, M. Mehl, K. Scheufele, A. Shukaev, B. Uekermann,
preCICE – A Fully Parallel Library for Multi-Physics Surface Coupling,
Computers and Fluids, Vol. 141 (2016), pp. 250 - 258.

[BUS19] Buchholz, S., Schöffel, P., Schaffrath, A.,
Exemplification of AC²'s Multidimensional Capabilities to the Application of Large Pools within the Frame of the German EASY – Project
Nuclear Engineering and Design, Vol. 346 (2019), pp. 46 - 53.

[CAS-91] Casal, J.J., Stamm'ler, R.J., Villarino, E.A., Ferri A.A.,
HELIOS: Geometric Capabilities of a New Fuel Assembly Program,
International Topical Meeting on Advances in Mathematics and Computation, Pittsburgh (USA), 1991.

[CES15] Cester, F., et al.,
Entwicklung neuer Methoden zur Modellierung technischer Systeme und zur Ergebnisauswertung für Simulationsprogramme der Reaktorsicherheit,
GRS-368, GRS, April 2015.

[CRI10] Christienne, M., Avramova, M., Perin, Y., Seubert, A.,
Coupled TORT-TD/CTF Capability for High-Fidelity LWR Core Calculations,
International Conference on the Physics of Reactors (PHYSOR) – Advances in Reactor Physics to Power the Nuclear Renaissance,
May 9 – 14, 2010, Pittsburgh, Pennsylvania (USA).

[DOW02] Downar, T. J., Barber, et al.,
PARCS: Purdue Advanced Reactor Core Simulator,
International Conference on the Physics of Reactors (PHYSOR) - New Frontiers of Nuclear Technology: Reactor Physics, Safety and High-Performance Computing
October 7-10, 2002, Seoul (Korea).

[FIS11] Freitag, M., Gupta, S.,
Specification Report for Blind Simulations of THAI Test TH-24 (CFD V5) – Dissolution of a Steam Stratification by Natural Convection,
Becker Technologies GmbH, Eschborn, October 2011.

[GRS19] Gesellschaft für Anlagen und Reaktorsicherheit (GRS) gGmbH
Development and Validation of Simulation Codes,
https://www.grs.de/en/content/development-and-validation-simulation-codes,
last accessed 7 June 2019.

[HEC15] Heckmann, K., Sievers, J.,
Code development for piping integrity assessment with respect to new German safety standard,
Transactions of 23rd Conference on Structural Mechanics in Reactor Technology (SMiRT-23), Division II
August 10-14, 2015.

[HEC16] Heckmann, K., Sievers, J.,
Analysis methods for leakage rates in pressurized components,
42nd MPA-Seminar, p. 283 - 301,
October 4-5, 2016, Stuttgart (Germany).

[HEC18] Heckmann, K., Sievers, J.,
Leak-Before-Break Analyses of PWR and BWR Piping Concerning Size Effects.
Nuclear Engineering and Design 326 (2018), p. 383 - 391.

[HEC19] Heckmann, K., Bläsius, C., Arndt, J., Sievers, J.,
PROST 4.7 documentation: User's Manual, Theory Manual, Validation Report, and Programmer's Manual.
GRS-P-7 Vol. 1-4, 2019.

[HEN19] Henry, R., Seubert, A.,
3-D Modelling of a Superphénix with Serpent and PARCS for Coupled simulation with PARCS/ATHLET
International Conference on Mathematics & Computational (M&C) - Methods Applied Bridging Theory and Applications,
August 25 – 29, 2019, Portland, Oregon (USA).

[HER16] Herb, J., Chiriac, F.,
One- and Two-Phase Coupling of OpenFOAM with the Thermal Hydraulic Code ATHLET for Nuclear Safety Analyses,
11th OpenFOAM® Workshop,
June 26-30, 2016, Guimarães (Portugal).

[HER19] Herb, J.,
Coupled OpenFOAM-ATHLET simulatios of the primary circuit of a liquid sodium cooled reactor,
14th OpenFOAM Workshop 2019,
July 23 – 26, 2019, Duisburg (Germany),

[IVA16] Ivanov, V., Bousquet, J.,
Assessing reactor physics codes capabilities to simulate fast reactors on the example of the BN-600 Benchmark.
Kerntechnik, Bd. 81, Vol. 5, p. 512 - 519, 2016.

[IVA18] Ivanov, V., Khrennikov, et al.,
SFR transient calculations with ATHLET-DYN3D on the example of BN-type reactor,
International Conference on the Physics of Reactors (PHYSOR) - Reactor Physics paving the way towards more efficient systems,
April 22 – 26, 2018, Cancun (Mexico).

[KAN03] Kanzleiter, T. et al.,
Abschlussbericht – Versuchsanlage und Programm zur Untersuchung offener Fragen zum Spaltproduktverhalten im Sicherheitsbehälter,
Teil 1: Versuchsanlage und Thermohydraulik-Versuche,
Becker Technologies GmbH,
Oktober 2003, Eschborn (Germany).

[KRA18] Krüssenberg, A.-K., et al.,
Validation of AC² for Calculation of Passive Heat Removal with Heat Pipes
Joint 19th IHPC und 13th IHPS,
June 10-14, 2018, Pisa (Italy).

[KTA16] Nuclear Safety Standards Commission (KTA): Break Preclusion Verifications for Pressure-Retaining Components in Nuclear Power Plants. Technical Report KTA 3206, Safety Standards of the Nuclear Safety Standards Commission (KTA), Salzgitter, Germany, November 2016

[LEP15] Leppänen, J., Pusa, M., Viitanen, T., Valtavirta, V., Kaltiaisenaho, T.,
The Serpent Monte Carlo code, Status, development and applications in 2013.
Annals of Nuclear Energy, Bd. 82, p. 142 - 150, 2015.

[LER19] Lerchl, G., et al.,
ATHLET 3.2 – User's Manual,
Gesellschaft fuer Anlagen- und Reaktorsicherheit (GRS) gGmbH, March 2019.

[MIG10] Mignot, G., et al.,
OECD/SETH-2 Vertical Fluid Release Test, Test Series Report,
Paul Scherrer Institut, 2010.

[NEA87] OECD/NEA, CSNI,
Code Validation Matrix of Thermal Hydraulic Codes for LWR LOCA and Transients,
OECD-NEA-CSNI Report 132, March 1987.

[NEA96] OECD/NEA, CSNI,
Integral Test Facility Validation Matrix for the Assessment of Thermal Hydraulic Codes for LWR LOCA and Transients,
Report NEA/CSNI/R(96)17, July 1996.

[NEA14] OECD/NEA, CSNI,
Containment Code Validation Matrix,
Report NEA/CSNI/R(2014)3, May 2014.

[PAP10] Papukchiev, A., et al.,
Development and Implementation of Different Schemes for the Coupling of the System Code ATHLET with the 3D CFD Program ANSYS CFX
8th International Topical Meeting on Nuclear Thermal Hydraulics, Operation and Safety (NUTHOS-8)
October 10 – 14, 2010, Shanghai (China).

[PAP14] Papukchiev, A., et al.,
Assessment of Coupled Multiscale and Stand Alone System Code Simulations Based on a Double T-Junction Mixing Experiment
45th Annual Meeting on Nuclear Technology
May 6 – 8, 2014, Frankfurt am Main (Germany).

[PAP15] Papukchiev, A., et al.,
Comparison of different coupling CFD–STH approaches for pre-test analysis of a TALL-3D experiment
Nuclear Engineering and Design 290 (2015), p. 135 - 143.

[PAP16] Papukchiev, A.,
Application and Validation of the Multiscale Code ATHLET-ANSYS CFX for Transient Flows in Next Generation Reactors
CFD4NRS-6 Workshop,
September 13-15, 2016, Cambridge, MA (USA).

[ROH16] Rohde, U., Kliem, S., et al.,
The reactor dynamics code DYN3D – models, validation and applications.
Progress in Nuclear Energy, Vol. 89, p. 170 - 90, 2016.

[SCH17] Schaffrath, A., et al.,
The Nuclear Simulation Chain of GRS
IAEA International Conference on Topical Issues in Nuclear Installation Safety: Safety Demonstration of Advanced Water Cooled Nuclear Power Plants,
June 6 – 9, 2017, Vienna (Austria).

[SCH18] Schaffrath, A., Wielenberg, A., Sonnenkalb, M., Kilger, R.,
The Nuclear Simulation Chain of GRS and its Improvements for New ALWR and SMR Typical Phenomena,
12th International Topical Meeting on Nuclear Reactor Thermal Hydraulics, Operation and Safety (NUTHOS-12),
October 14 – 18, 2018, Qingdao (China).

[SEU08] A. Seubert, K. Velkov, S. Langenbuch,
The time-dependent 3D discrete ordinates code TORT-TD with thermal-hydraulic feedback by ATHLET models,
International Conference on the Physics of Reactors (PHYSOR) – Nuclear

Power: A Sustainable Resource,
April 22 – 26, 2008, Interlaken (Switzerland).

[SEU16] Seubert, A., Velkov, K.,
Fast Reactor Diagrid and Axial Expansion Models for the Diffusion Equation,
International Conference on the Physics of Reactors (PHYSOR) – Unifying Theory and Experiments in the 21st Century,
May 1 – 5, 2016, Sun Valley, Idaho (USA).

[STE19] Steinhoff, T., Jacht, V.,
NuT 1.0 Numerical Toolkit User's Manual,
GRS-P-10, Rev. 1,
February 2019.

[WEY19] Weyermann, F., Schaffrath, A.
Development Strategy of the GRS Code AC²,
Technical Session Development, Validation and Application of the GRS Code System AC² for Currently Operated and Future NPP,
50th Annual Meeting on Nuclear Technology,
May 7 – 8, 2019, Berlin (Germany).

[WIB18] Wielenberg, A., Schaffrath, A.,
Adaption of the GRS Simulation Chain for Conventional and Renewable Applications,
8th International Energy Conference & Workshop REMOO,
May 29 – 31, 2018,
Venice (Italy).

[WIB19] A. Wielenberg, L. Lovasz, et al.,
Recent Improvements in the System Code Package AC² 2019 for the Safety Analysis of Nuclear Reactors,
Nuclear Engineering and Design, Vol. 354 (2019). available online.

[ZIL18] Zilly, M., Perin, Y.,
KMACS Validation Report,
Gesellschaft fuer Anlagen- und Reaktorsicherheit (GRS) gGmbH,
GRS-P-8/Vol. 2, Rev. 0, 2018.

Research in support of the 4th 10-year periodic safety review on severe accidents

F. Fichot, P. Chatelard, L. Bosland, S. Pignet

IRSN, Institute of Radioprotection and Nuclear Safety (France)

Abstract:

In France, the utility EDF is developing a Plant Lifetime Extension (PLE) program for the operating Gen. II PWRs, which takes into account the lessons from the Fukushima Dai-ichi accidents and aims at reducing the gaps in terms of safety with the Gen. III PWRs including the EPR™, as requested by the French Safety Authority ASN. To review this program in the framework of the 4th 10-years periodic safety review of the 900 MWe series of reactors, the IRSN collected important R&D data through international collaborative programs. The interpretation of those data has led to the development of new models that are implemented in a new version of the ASTEC evaluation code. Moreover new experiments are planned to fill the gap of knowledge in certain area which will led to additional validation work and increase the code capability to predict the evolution of a reactor severe accident.

1 INTRODUCTION

The French electrical utility EDF is currently operating a fleet of 58 Gen. II Pressurized Water Reactors (PWRs) (900, 1300 and 1450 MWe series) built between 1977 and 1999. Periodic Safety Reviews (PSRs) are conducted every 10 years.

These reactors were not designed to face a core melt accident and several reinforcements have been discussed in France and progressively implemented by EDF to allow for the management of severe accidents. Now, in the framework of the 4th 10-years periodic safety review of the 900 MWe series of reactors, EDF performs an ambitious modifications program to reduce off-site consequences in case of a severe accident. These reinforcements target the protection of the containment notably by an ex-vessel stabilization of the corium before an excessive basemate ablation is reached. Another concern was the evaluation and mitigation of fission products releases where the EPR has been designed to limit in space and time the population protection measures. This article presents the R&D activities conducted by IRSN to support its safety evaluation and can be considered as a mirroring article of [10]. Evaluation of bounding scenarios using the ASTEC code is an essential ingredient of IRSN severe accident evaluation.

Section 2 highlights how the ASTEC code was developped to take into account all the latest knowledge. Then sections 3 and 4 give an overview of the main R&D results obtained on corium ex-vessel stabilization mechanisms and fission products (FP) releases evaluation and mitigation respectively and show how those results are used to estimate EDF strategies efficiency. Some points where uncertainties remain that deserve additional R&D activities are mentionned in conclusions.

2 ASTEC CODE

The ASTEC code (Accident Source Term Evaluation Code), developed by IRSN, aims at simulating an entire severe accident sequence in a nuclear water-cooled reactor from the initiating event up to the release of radioactive elements out of the containment [6,7]. The ASTEC code structure is modular, each of its modules simulating a reactor zone or a set of physical phenomena. Two different running modes are possible: stand-alone mode for running each ASTEC module independently (particularly useful for module validation) and coupled mode where all (or a subset) of the ASTEC modules are run sequentially within a macro-time step. The current version on production is the V2.1.1 .

Focusing on the three main issues that are discussed in this paper, the ASTEC main modules of concern are those relating to the containment behaviour, i.e. CPA for the thermalhydraulics in the containment, MEDICIS for molten core concrete interaction (MCCI) and SOPHAEROS for iodine chemistry and aerosol transport.

Furthermore, one may notice that the MDB (material data bank) library, shared by all ASTEC modules, groups together all material properties under a unique simple readable format. This includes: all simple materials of a water-cooled reactor (solid, liquid and gas) and associated usual properties (enthalpy, conductivity, density…); ideal chemistry (equilibrium reactions); iodine chemistry (kinetics); FP isotopes (decay heat, transmutation rates…); complex materials such as molten corium. The MDB library includes all the recent research on the nuclear material properties done in international projects: for FP, CIT and ENTHALPY FP4 projects, and for corium OECD RASPLAV and MASCA projects. The evaluation of corium properties is based on the NUCLEA database [3] for corium thermo-chemistry. It also benefits from a continuous validation at IRSN of the database contents.

The ASTEC V2.1 CPA module simulates thermal-hydraulics behaviour in containment including hydrogen and carbon oxide combustion [7]. The discretization through a "lumped-parameter" approach (0D zones connected by junctions and surrounded by walls) simulates simple or multi-compartment containments (tunnels, pit, and dome) with possible leakages to the environment or to normal buildings, with specified openings to the environment. Several real compartments can either be combined to become one CPA zone or large compartments can be divided into several zones to cover flow peculiarities more realistically, e.g. steam or hydrogen plumes. CPA thermal-hydraulics models describe phenomena such as pressure and temperature build-up, local temperature and pressure distributions, local gas distributions (steam and different non-condensable gases), local heat transfer to walls (free and forced convection, radiation, condensation), 1D heat conduction in structures (plate or cylinders, consisting of several material layers), as well as gas (hydrogen and carbon monoxide) combustion. The thermal-hydraulic state of a node is described according to the non-equilibrium model where deposited and airborne water are separately balanced. Mass transfer between zones is described separately for gas and liquid flows by momentum equations (unsteady, incompressible or steady compressible) accounting for the height differences between zone centres.

The ASTEC V2.1 MEDICIS module simulates MCCI phenomena using a lumped-parameter 0-D approach with averaged melt/crust layers [8]. This module assumes either a well-mixed oxide/metal pool configuration or possible pool stratification into separate oxide and metal layers. It describes concrete ablation, corium oxidation, release of incondensable gases (H_2, CO, CO_2) and steam into the containment. Most convective heat transfer correlations available in literature for the corium/concrete interface and the interface between corium layers are implemented. A robust algorithm for cavity erosion was developed, including the possibility to represent a multi-layered concrete basemat. In particular, the MEDICIS module includes the following key-models: 1) a model for the structure of the corium/concrete interface taking into account, from the pool bulk to the concrete interface, a convective zone, a possible conductive zone described as a crust and a slag layer; 2) models of evolution of corium pool configurations, depending on criteria using the superficial gas velocity and on differences between oxide and metal densities determining the switch between homogeneous and stratified pools; 3) models of corium coolability in case of water injection upon the corium pool surface, that notably consider the modelling of a dedicated debris bed layer above and apart from the upper crust, the modelling of water ingression through the upper crust and the modelling of corium eruption through the upper crust towards the overlying water pool.

Moreover, one may underline that MEDICIS uses the MDB package to evaluate the corium layers thermo-physical properties and to treat the corium oxidation: in that respect, metals are oxidized instantaneously in proportion to the mass of available gases with a priority rank (Al_2O_3, CaO, MgO, UO_2, ZrO_2, SiO_2, Cr_2O_3, NiO, FeO).

Besides, in order to adequately take into account the feed-back from MCCI on the containment thermalhydraulics, a specific prediction-correction coupling approach was developed in ASTEC V2 between MEDICIS and CPA when representing the cavity as a CPA volume. First, in the prediction step, MEDICIS calculates the whole behaviour of the cavity and notably evaluates the gas temperature in the cavity. Besides, the gas flow rates coming from the MCCI are also taken into account as well as heat exchanges between the upper crust layer and covering water in case of top flooding. All these heat fluxes are then transferred to CPA which, in the correction step, calculates again the cavity thermal-hydraulics in the same time as the other containment zones, taking into account the gas mass flow rates entering into this zone (in particular the gaseous sources issued from the MCCI process) or going out of this zone.

The ASTEC V2.1 SOPHAEROS module [9] simulates the fission products evolution in the reactror coolant system (RCS) and the iodine chemistry in the containment (Figure 2 and Figure 3). The thermal hydraulics conditions are given by CPA whereas the dose rate in each containment zone is calculated by ISODOP and DOSE modules. In the RCS, except for the I-O-H system for which kinetics are considered, the other species formation (CsI, AgI, Cs2I2…) are considered based on their equilibrium thermodynamics properties (Figure 2). In the containment, kinetics are considered for each reactions on Figure 3. It includes the iodine chemistry in the sump, in the gaseous phase and on the surfaces (Epoxy paint, steel and concrete).

As to the validation of the containment thermalhydraulics models, the matrix that has been retained for the ASTEC V2.1 CPA module has been specified to follow a progressive approach in terms of physical phenomena, from separate effect tests to coupled effect tests, and to cover the following aspects: gas distribution inside the containment; mitigation systems (spray and passive autocatalytic recombiner); hydrogen combustion [4]. In particular, the tests TOSQAN ISP-47, TOSQAN T115, THAI HM-2, PANDA T9, T9bis and PE1 have been simulated with the ASTEC V2.1.1 version to assess the physical relevance of the CPA models on gas distribution (gas mixing and stratification) and mass transfers (condensation and evaporation) [4].

As to the ASTEC V2.1 models dealing with MCCI top quenching, they have been mostly assessed vs. CCI-7, CCI-8 and CCI-9 experiments [12,21]. FP models chemical and physical models are strongly coupled. They have been the subject of intense development validation efforts that have been supported by a large set of experimental programs including large scale to separate effect tests. Main programs are the PHEBUS-FP program and the subsequent R&D programs devoted to source term EC/ISTP, OECD/STEM, OECD/BIP and OECD/THAI programs and follow-up.

3 CORIUM COOLABILITY AND INTERACTION WITH CONCRETE

This section describes the main issues associated with the spreading and cooling of corium in the reactor pit and in an adjacent room, in order to have a larger exchange surface area. The type of reactor considered in this paper is the French PWR-900.

3.1 Modelling of corium coolability under water

The total area S of corium spreading (reactor pit and neighbouring room) is about 80 m^2 for an initial corium height of 30 cm (assuming an initial corium mass of 200 tons). The stabilization of corium is therefore essentially a 1D problem, which amounts to estimating three main quantities: the fraction of residual power transmitted downwards leading to the ablation of concrete $P_{abl} = S.\varphi_{abl}$, the fraction of power transmitted to the water $P_{wat} = S.\varphi_{wi}$. and the thickness of the solidified corium layer (crust) δ. Depending on the accident scenario, the residual power of corium P_{res} is estimated at the time of complete spreading of corium. It varies in the range between 20MW if spreading occurs 1h after scram (LBLOCA) and 15MW if spreading occurs 5h after scram (SBO). After 3 days, the residual power is reduced by a little more than half, at approximately 7-8 MW. Before spreading, there is a phase of corium-concrete interaction in the reactor pit that leads to add about 10 wt.% of concrete in the corium when it fully spreads.

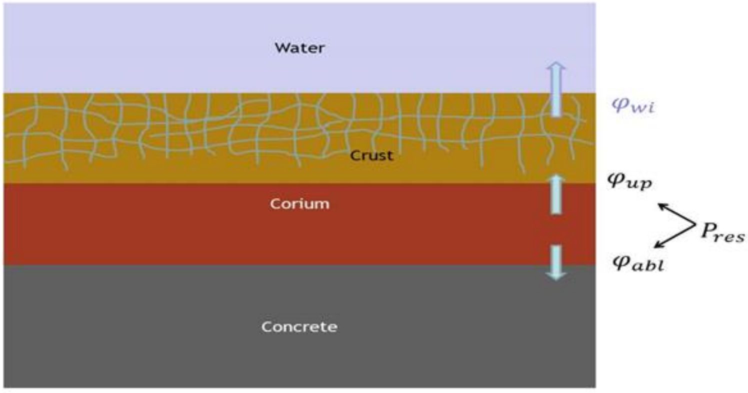

Figure 1: Schematic view of corium and porous crust under water

3.2 Top/bottom partition of power

One of the main uncertainties of the problem is the distribution of corium power in the liquid pool between the top (upper crust) and the bottom (concrete). In previous CCI tests, this partition ranged from 90% -10% (CCI-6) to 70% -30% (CCI-3, CCI-8), depending on the type of concrete and the experimental conditions [12]. For an order of magnitude calculation, in this paper, we assume a residual power P_{res} =16 MW, distributed in 75% ($P_{up=}$ 12 MW) upwards and 25% (4 MW) downwards. This gives a heat flux to the top $\varphi_{up} = P_{up}/S$ =150 kW/m^2, and a heat flux of ablation $\varphi_{abl} = 50$ kW/m^2. After 3 days, all those values are reduced by half.

3.3 Early phase of quenching and limitations of conduction through the crust

Shortly after contact with water, some of the corium solidifies rapidly: it is the phenomenon of corium quenching (or "bulk cooling") that is very poorly known because it is a fast process which is difficult to identify in the experimental measures (since experimental images show only the final state and on-line measurements of steam production cumulate all the processes). In order to be conservative in the evaluation of corium stabilization, we maximize the energy of the corium interacting with concrete by neglecting this initial and fast "bulk cooling". With this assumption, during the first 2-3 hours, the main cooling phenomenon is the conductive transfer through the corium crust which grows until it stabilizes around 4-5 cm, when the conductive flux through the crust becomes equal to the heat flux from the corium. If no additional phenomenon is considered, crust growth remains limited by φ_{up} and the crust progresses only slowly because of the decrease of residual power, which is quite slow. As a consequence, there remains an unextracted power P_{abl} which would lead to an ablation of the basemat at a velocity $v_{abl} = \varphi_{abl}/\rho\Delta h_{abl} =$ 4 cm/h (or 0.8 m/day). After 3 days, it would still be 0.4 m/day and this would lead to an inevitable failure of the containment basemat. With the value of 4 cm/h, it takes only 2 hours to reach the mass fraction of 15 % of concrete (ablation of about 6-8 cm, in addition to concrete already ablated in the reactor pit), which appears to be an important threshold for water ingression (discussed below).

Therefore, the strategy of stabilizing the corium by flooding it under water can be considered as reliable only if phenomena such as water ingression or melt ejection are able to continuously solidify (and maintain solid) a portion of the corium which therefore no longer participates in the ablation of the concrete. Part of the residual power is then transmitted directly to the water, which gradually reduces the power transmitted downwards, until the cessation of ablation if all the corium is made "permeable" by one of those phenomena (or both).

Water ingression

Water ingression is a phenomenon highlighted in the SSWICS (ANL,[20]) and CCI (ANL,[11]) tests. SSWICS results indicate that water ingression is not much dependent on the type of concrete and leads to the formation of a permeable crust into which the water flows. To evaluate this rate of solidification, it is necessary to know the "critical heat flux" φ_{wi} that can be extracted by the water entering this permeable crust. This velocity is proportional to $(\varphi_{wi} - \dot{Q}\delta - \varphi_{up})$ according to the theoretical models [11,13] which means that this phenomenon cannot occur as long as the power transmitted by the corium is too high: the condition for crust growth is $\varphi_{wi} > \dot{Q}\delta + \varphi_{up}$.

For a value of $\varphi_{wi} = 200$ kW/m^2, the velocity of crust progression is about 7 mm/h, which would lead to stabilization in about 6 to 8 hours. But for $\varphi_{wi} = 100$ kW/m^2, water ingression would not occur until the residual power is lower than 10 MW, i.e. after about one day. Therefore, complete stabilization would not be possible before 2 to 3 days.

3.4 Melt ejection

Corium ejection is a phenomenon also highlighted in some CCI tests (ANL, [12]), when the concrete contains a large fraction of CO2 (limestone or siliceous-limestone concrete). This phenomenon results in violent but intermittent eruptions, leading to the cooling of a portion of the corium in the form of debris ejected above the crust. For concrete containing a lot of CO2, this can lead to a debris bed formation rate of about 5 mm/h (with the Ricou-Spalding model [23]), which is slower than the crust growth by water ingression. For very siliceous concrete (absence of CO2), this phenomenon contributes little to cooling (approximately 1 to 2 mm/h). Moreover, this phenomenon decreases with time (in proportion to the velocity of ablation which also decreases).

3.5 Maximum heat flux to water

The maximum heat flux that can be extracted through the porous crust is the second main uncertainty of the problem. For water ingression, the extrapolation of SSWICS data indicate that the critical heat flux could reach values higher than 400 kW/m^2 in the absence of concrete in the corium but it goes down to 100 kW/m^2 for a concrete mass fraction of 15%. If we consider that the mass fraction of concrete is at least 10% after complete spreading, φ_{wi} is in the narrow range 100-150 kW/m^2. Experimental uncertainties may be estimated as +/- 50 kW/m^2. In principle, this uncertainty is of the same order at the reactor scale since it is a 1D problem and the experimental corium thickness is approximately equal to the thickness at the reactor scale. For concrete containing CO_2, the extracted fluxes are always higher (because of contribution of the corium ejection in particular). So very siliceous concretes constitute the case for which the stabilization of the corium is the most difficult.

3.6 Conclusions and limitations of extrapolation to the reactor case

Available experimental data show that both water ingression and corium ejection phenomena may contribute to stop the ablation of the basemat by solidifying an increasing amount of corium and thus reducing the fraction of power ablating the concrete.

But, in case of very siliceous concrete, it should be noted that corium ejection does not make a significant contribution. Moreover, for water ingression, there is no obvious margin between the residual power to be evacuated and that which can be dissipated by the quenched crust and/or debris: a threshold value of 100 kW/m2 is insufficient to demonstrate a stabilization for sure (for a highly siliceous concrete).

Below are listed the points which raise uncertainties about the water ingression efficiency for the reactor cases:

- In CCI test, to simulate the decay power $\dot{Q}$, sustained heating is provided by DEH. Such method only heat the liquid phase and there is no heating in the solid crust. The crust thickness evolution $\frac{d\delta}{dt}$ modeling is then only validated on cases for which $\dot{Q}\delta$ is null, which is more favorable for water ingression than in the reactor case; CCI-9 test does not last long enough to validate the potential growth of the crust up to a few tens of centimeters which would correspond to the complete stabilization. More generally, there are no data in the literature about long term (more than 12h) stabilization of corium;

- During the test, the mean concrete mass fraction does not exceed 25% whereas reactor calculations lead to larger amount, after only a few hours. This can affect the mechanical behavior of the crust and so the water ingression efficiency. Moreover, there are no data available to distinguish between the amount of concrete in the crust and in the melt;
- Some reactor accident scenarios can lead to important amount of metal in corium. This is not included in the CCI tests. The effect of such metal in the crust is still undetermined: thermal conductivity of the crust would be larger but the less brittle mechanical behavior and molten metal in cracks could lead to significantly decrease the water progression in the fractured crust.

4 EVALUATION AND MITIGATION OF FISSION PRODUCTS RELEASES

R&D about the FP behaviour has led to better understand and model the phenomenology of the fission products in the reactor coolant system (RCS) and of Iodine chemistry in the containment. The phenomenology of the FP behaviour in the RCS is shown on **Figure 2**. It highlights the main physical and chemical phenomena modeled in ASTEC [9] in order to consider the behaviour of the FP from the hot leg (left part) to the cold leg of the RCS (right part).

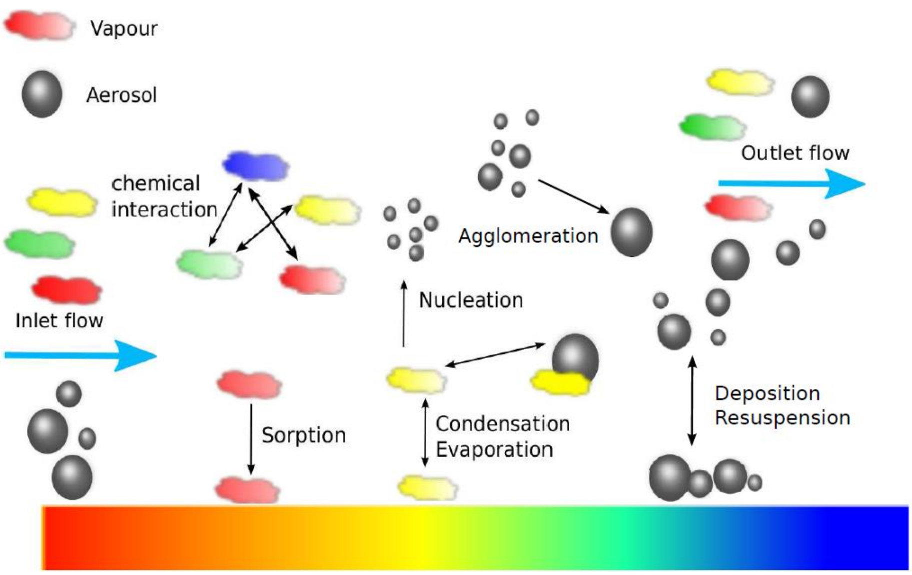

Figure 2: phenomenology of the fission products behaviour in the reactor coolant system (RCS) in ASTEC V2.1 code

The state of the art of the iodine chemistry modeling in ASTEC [9] for the containment is shown on **Figure 3**. It highlights the thermal and radiolytic chemical reactions for the sump and the gaseous phase (including the effect of surfaces) and is the result of more than 30 years of R&D that is capitalized in ASTEC/SOPHAEROS.

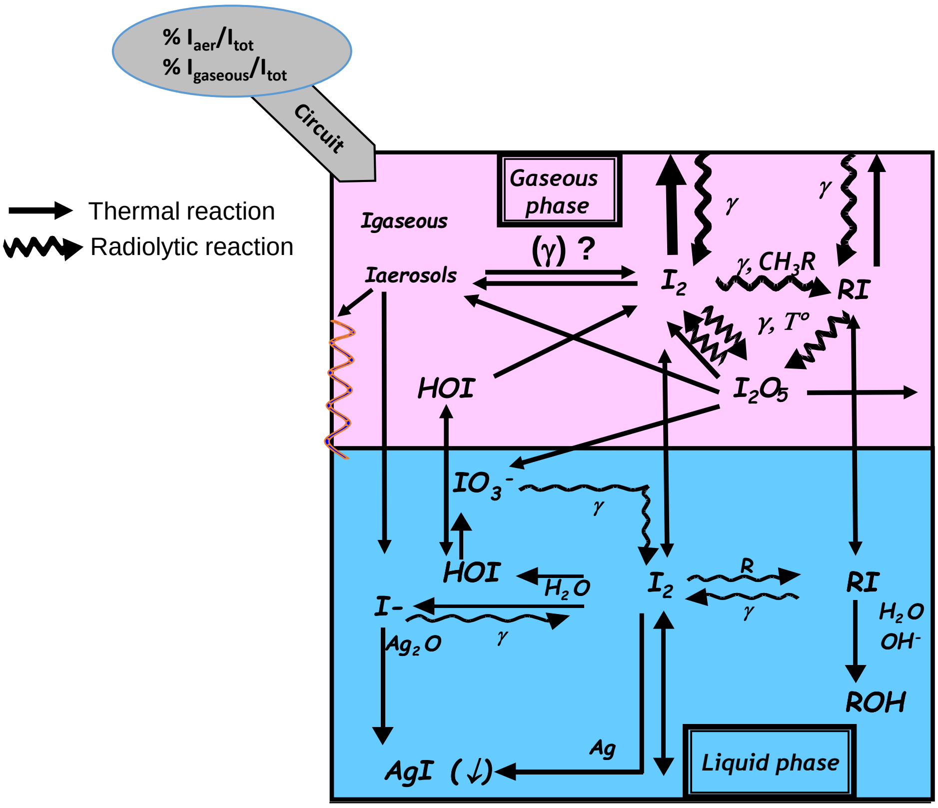

Figure 3: phenomenology of Iodine behaviour in the containment in ASTEC V2.1 code

Silver used to be considered as an efficient iodine trap in the sump. Nevertheless, this has been recently questioned and it is discussed below as it could lead to more gaseous releases than expected.

The filtration efficiency of the containment venting procedure on French reactors is also presented for gaseous iodine (organic iodides and I_2) and iodine oxides aerosols. In order to envisage a better mitigation of these gaseous releases, the filtration efficiency of new devices is presented.

4.1 Influence of the non-complete capture of iodine by silver particle in the sump

For 900 MWe reactors, the degradation of the control rods (made with Silver, Indium and Cadmium) is expected to bring significant enough amount of Silver into the containment sump so that dissolved iodine would be efficiently trapped even for an acidic sump. Nevertheless, PHEBUS FPT-1 test [14] has shown that containment aerosols (coming from the reactor coolant system and that settle down into the sump) are mostly made with the control rods degradation material: Silver, Indium and Cadmium and by other fission products (Iodine, Cesium…). Based on the PHEBUS FPT1 aerosols analysis, it has been shown that silver oxide (Ag_2O) was mostly found in the outer shell of the aerosols whereas silver (Ag) was mostly found in the inner part of the aerosols. Silver oxide is a soluble compound that can be dissolved in the sump and react with iodides ions (I^-) whereas silver reacts with molecular iodine (I_2). Both reactions lead to the formation of non-soluble silver iodide (AgI) that is an efficient way to capture iodine, as long as silver is in excess towards iodine. However, some silver-iodine experiments have shown that, despite an excess of silver, all the dissolved iodine does not react with silver. It can be explained by the particulate form of silver aerosols coming from the containment into the sump: the diffusion of iodine into the silver particles is assumed to be limited by an outer shell and thus limits the availability of the total silver mass for reaction with dissolved iodine. The outer shell thickness was estimated to be ≈ 400 Å and implemented in ASTEC code [9] as shown on **Figure 4**.

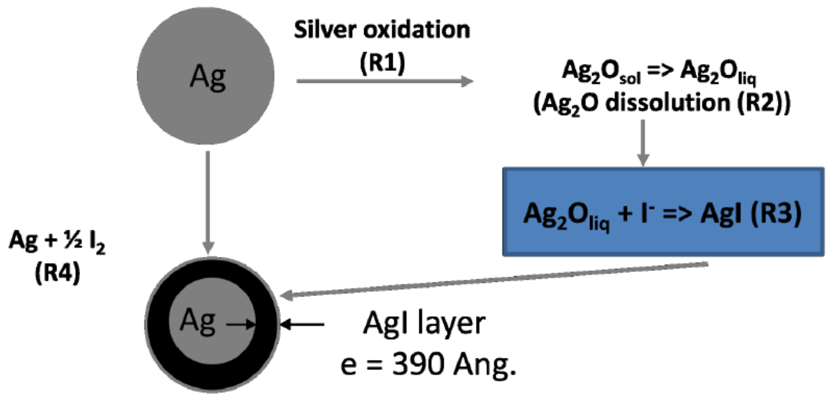

Figure 4: model of Ag2O reaction with I- and of Ag reaction with I2, leading to the formation of AgI

As a consequence, the total silver mass available for reaction with iodine is limited. Even if the silver amount is in large excess towards iodine, the complete iodine sump inventory might not react totally with silver/oxidized silver, especially in an acidic sump, leaving iodides ions (I^-) available for oxidation into I_2 and its transfer to the gaseous phase [15,5]. Under irradiation, gaseous molecular iodine is then converted into iodine oxide aerosols compounds (IOx, known as small aerosols particles) whose formation is continuous, as long as there is a source of I_2 from the sump. Recent IRSN evaluations with ASTEC code have shown that the suspended IOx mass in the gaseous phase could reach a steady-state (up 250 g in the containment atmosphere after 7 days) as there is a balance between their formation and decomposition reactions. In case the containment depressurization needs to be used, IOx aerosols would be transferred to the sand filter and decompose into gaseous iodine under the effect of the temperature and irradiation. It is thus necessary to address IOx aerosols amount in the Source Term evaluation of 900 MW reactors.

On the opposite, in case of an alkaline sump, the faster I_2 hydrolysis in the sump [5,1] would strongly reduce I_2 volatility which would limit IOx formation in the gaseous phase which lead to a specific recommandation of IRSN in his review [10].

4.2 Improvement of the efficiency of the filtered containment venting system (FCVS)

The filtered containment venting system installed on French PWRs (metallic pre-filter followed by a sand filter) was designed to keep the containment integrity and trap aerosols for which the decontamination factor (DF, defined as the ratio between the concentration in the upstream gas and the concentration in the downstream gas) is high. Nevertheless, it is rather low for gaseous organic iodides [16]. For the specific case of molecular iodine (I_2) capture by the sand filter, the FUCHIA tests have indicated a value of DF ≈ 10 but it was found that iodine is mostly retained in the steel surfaces of the pipes rather by the sand itself. Recent experiments highlighted that I_2 is not well captured by the pre-filter (DF < 10) and not retained by the sand [16] (as DF ≈ 1). The filtration efficiency of the gaseous species by the sand filter installed on French reactors is thus low. For iodine oxides aerosols capture by the sand filter, values of DF ≈ 500 were estimated using a simulant having the same granulometry [18]. However, as trapped IOx aerosols are not stable (thermal and radiolytical decompositions) on the sand and decompose into inorganic iodine by the temperature and irradiation effect [17], delayed gaseous iodine release into the environment are expected.

In order to limit the need to use this containment venting procedure, some post-Fukushima modifications on the reactors are being discussed (like the ultimate containment heat removal system [10]). Despite the possible implementation of this complementary safety device, IRSN still estimates the probability (coming from IRSN PSA2 outcomes) to use the containment venting procedure in case of severe accident at (at least) 18% (at least) in order to preserve the containment integrity. The improvement of the filtration efficiency of the venting procedure remains thus an important issue that has to be addressed. To fix ideas a reduction by one order of magnitude of the iodine release amount to the environment would reduce by a factor of three the distance from the reactor within which the distribution of iodine tablets would be needed.

Some new insights coming from recent R&D programs focused on filtration efficiency of aerosols and gaseous iodine species are now available [2,16,19,22]. For organic iodides capture, a commercial silver containing zeolite (with a 35% silver content) has been added to a sand matrix whose total height is lower than 4 cm. A representative gaseous flow containing methyl iodide has been passed through at temperature ranging from 80°C to 140°C and representative expected humidities, varying the zeolite mass content in the sand from 9 to 100%. It was found that DF(CH_3I) > 10 for all the configurations tested [22]. As the sand height in the sand filter installed on PWRs is 80 cm, we might even expect higher DF(CH_3I) values for a representative sand height. These tests demonstrate the ability of silver containing zeolite to effectively trap methyl iodide. For molecular iodine capture, even though no specific tests have been performed with zeolite, I_2 is well captured by deposited silver on sand [16], so that we expect DF(I_2) > DF(CH_3I) for I_2 capture by silver containing zeolite.

The reversibility of molecular iodine capture by a MOF was also studied under irradiation [19,2] and has shown a very good retention at 120°C and 20% relative humidity as no iodine was released despite the carrier gas flow.

Whatever the gaseous iodine species considered (methyl organic iodides or molecular iodine), the PWRs containment depressurization (through the existing sand filter) would lead to potential significant gaseous iodine releases into the environment. Nevertheless, the irreversible capture of gaseous I_2 and CH_3I has been demonstrated in the lab-scale but with representative conditions with efficient filtration systems like zeolites. IRSN has thus recommended to implement complementary filters on the existing sand filters on French PWRs , in order to limit the iodine releases into the environment.

5 CONCLUSIONS

IRSN supports its SA risk assessment by participating and developing R&D programs (analytical, separate effects and integral experiments) covering the main issues on accident progression and consequences including their mitigation. Most of the results are then valorized in the in-house evaluation code ASTEC.

The safety evaluation process led by the ASN is continuous, an important step has been passed for this 4th PSR of the 900Mwe conducted in the plant life extension and post-Fukushima Daiichi context.

In particular, the modelling developed on the ex-vessel corium stabilization by top flooding has been used to review the strategy proposed by the French utility, EDF. This review led to identify important uncertainties on the efficiency of the thermal exchanges through the corium top crust in case of siliceous concrete MCCI. The impact of large fraction of metal in the corium also deserve additional R&D. These topics will be covered by the starting OECD ROSAU program conducted by ANL. This program will also investigate the corium spreading underwater.

Also the evaluation of the FP releases in the large range of potential SA accidents scenarios (identified through deterministic analyses completed by probabilistic evaluation) confirmed the complexity of the associated modelling as well as the potentiality to mitigate the consequences of an accident. Proposing new mitigation devices and procedures impose to develop predictive evaluations. That’s the reason why the IRSN decide to propose the OECD ESTER program tackling still open issues such as mid to long term releases.

6 REFERENCES

1 C. B. Ashmore, D. J. Brown et al., "Measurements of the radiolytic oxidation of aqueous CsI using a sparging apparatus." Nucl. Tech. 129(3): 387-397, 2000.

2 B. Azambre, M. Chebbi, et al., "Effects of Zeolitic Parameters and Irradiation on the Retention Properties of Silver Zeolites Exposed to Molecular Iodine" Ind. Eng. Chem. Res. 57, 1468-1479, 2018

3 S. Bakardjieva, M. Barrachin, S. Bechta, P. Bezdicka, D. Bottomley, L. Brissonneau, B. Cheynet, O. Dugne, E. Fischer, M. Fischer, V. Gusarov, C. Journeau, V. Khabensky, M. Kiselova, D. Manara, P. Piluso, M. Sheindlin, V. Tyrpekl, T. Wiss, Quality improvements of thermodynamic data applied to corium interactions for severe accident modelling in SARNET2, Annals of Nuclear Energy, 74, pp. 110-124, 2014.

4 A. Bleyer, L. Maas, ASTEC V2.1 – CPA Module: Validation Report, IRSN/PSN-RES/SAG/2018-00080, 2018

5 L. Cantrel, "Radiochemistry of iodine : outcomes of the CAIMAN program." Nucl. Tech. 156: 11-28, 2006

6 P. Chatelard, S. Belon, L. Bosland, L. Carénini, O. Coindreau, F. Cousin, C. Marchetto, H. Nowack, L. Piar, L. Chailan, Main modelling features of the ASTEC V2.1 major version, Annals of Nuclear Energy, Volume 93, pp. 83-93, 2016

7 L. Chailan, A. Bentaïb, P. Chatelard, Overview of ASTEC code and models for Evaluation of Severe Accidents in Water Cooled Reactors, IAEA Technical Meeting on the Status and Evaluation of Severe Accident Simulation Codes for Water Cooled Reactors, Vienna (Austria), October, 9-12, 2017

8 C. Marchetto, ASTEC V2.1 MEDICIS MCCI module : Theoretical manual, Technical report IRSN/PSN-RES/SAG/2015-00333

9 F. Cousin, L. Bosland, ASTEC V2.1.1 SOPHAEROS module, Theoretical manual, Rapport IRSN/PSN-RES/SAG/2017-00215

10 R. Cozeret, J. Chambarel et al., “Improvement on 900 MWe NPPs in the occasion of the 4th 10-year periodic safety review on severe accidents”, EUROSAFE 2019, 04th and 05th November, Cologne, Germany, 2019

11 M. Epstein, Review of Water Ingression Models, EPRI Report ACEX-TR-C31, 1999

12 M. Farmer, C. Gerardi, N. Bremer, S. Basu, Key Findings and Remaining Questions in the Areas of Core-Concrete Interaction and Debris Coolability, Nuclear Technology, Vol. 196, 2016

13 H. Hardee, Solidification in Kilauea Iki Lava Lake, Journal of Volcanology and Geothermal Research, 7, 1980

14 D. Jacquemain, S. Bourdon et al., ”FPT-1 final report”, CEA/IPSN/DRS/SEA/PEPF - rapport SEA 1/100 - Report PHEBUS FP IP/00/479, 2000

15 C.C. Lin, "Chemical effects of gamma radiation on iodine in aqueous solutions." J. Inorg. Nucl. Chem 42: 1101-1107, 1980

16 O. Leroy and C. Monsanglant-Louvet, Trapping measurements of volatile iodine by sand be and metallic filters, J. Radioanalytical and Nuclear Chemistry, accepted, 2019

17 O. Leroy, Experimental investigations on sand bed (SF3, SF4) – Release under irradiation of volatile iodine species from IOx aerosols trapped in a sand filter, IRSN/PSN-RES/SEREX/2017-00742, MIRE 85-2017, 2017

18 O. Leroy, C. Monsanglant-Louvet, "Synthesis of the tests, at the laboratory scale, of molecular iodine, organic iodide and fine aerosols retention by existing filtering media representative of the French venting line", IRSN/PSN-RES/SEREX/2018-00522 - MIRE 112-2018, 2018

19 O. Leroy, "Investigations expérimentales sur les Metal-Organic Frameworks (MOFs)", IRSN/PSN-RES/SEREX-2019-00247 - MIRE 123-2019 ind. 2, 2019

20 S. Lomperski, M. Farmer, Experimental evaluation of the water ingression mechanism for corium cooling , Nuclear Engineering and Design, Vol. 237, 2007

21 R. Meignen, S. Garrier, Résultats et interprétation de l'essai d 'ICB sous eau CCI-8, Rapport IRSN PSN-RES/SAG/2015-00412, 2015

22 C. Monsanglant-Louvet, A. L. Teppe et al., "Etude du coefficient d'épuration de matériaux de type sable et zéolite dans des conditions ambiantes proches de l'accident grave ; cas de la filtration de CH3I et de nanoparticules", IRSN/PSN-RES/SCA/2018-00009

23 F. B. Ricou and D. B. Spalding, Measurements of Entrainment of Axisymmetrical Turbulent Jets, J. Fluid Mechanics, 11, 21, 1961

RELAP5-3D Code Simulation of the Effect from Complex In-Vessel Flow Patterns on the Performance of Reactor Coolant Temperature Sensors Located at the Core Outlet and Different In-Core Elevations

Alex Matev

Bel V, Walcourtstraat 148, Brussels, Belgium

Abstract:

Results from experimental programs [2, 3] have revealed limitations in the use of core exit thermocouples' (CETC) measurements to diagnose core cooling degradation. These tests indicated that significant delays might appear in the CETC response to changes in the temperature of the coolant exiting the core. This might hinder the use of CETC readings to both diagnose the onset of an inadequate core cooling (ICC) condition and to track the evolution of accident scenarios with breaks in the RPV upper or lower head [3]. One should thus try to examine by using computer codes with state-of-the-art modeling capabilities how the evolution of such transients affects the sensors' readings, especially in conditions with tripped reactor coolant pumps, when multi-dimensional fluid flow patterns could be established, both in the core and in the upper plenum of the reactor vessel.

Nuclear instrumentation vendors [5, 7] have recently proposed alternatives to CETC, such as thermocouples inserted in the fuel assemblies' instrumentation thimbles. Such in-core coolant temperature sensors may provide the NPP operators with an early indication of the appearance of an ICC condition and may serve as a means to assess how effective are the operators' actions to manage the accident. There has been considerable interest lately in using both system-analysis and CFD computer codes for the assessment of the expected benefits from the use of such in-core thermocouples for accident management [8, 9, 13, 14].

The objectives of this analysis are:

- To test the RELAP5-3D code's ability [10] to simulate successfully free convection of multi-dimensional coolant flows in both of the core and the reactor vessel upper plenum;
- To simulate the performance of coolant temperature sensors placed either above the core outlet (CETC), or at in-core elevations, inserted into the instrumentation thimbles (IITA)
- Compare different Accident Management (AM) strategies and grade them by using as a criterion the degree of core damage, defined by parameters as Peak Cladding Temperature (PCT), thickness of the maximum Local clad Metal Oxidation layer (LMO), mass of hydrogen produced in a Core Wide Oxidation (CWO), and blockage of flow through the bundles of fuel pins in the core

This study presents the results from the simulation of Small-Break LOCA scenarios in a generic 3-loop PWR power plant with an assumed failure of the high-head safety injection capability. The operators need to depressurize the primary system in response to the onset of an ICC condition, so that the hydro-accumulators and the low-head safety injection systems can provide for sufficient coolant makeup to recover the core.

KEYWORDS

CETC, COT, in-core instrumentation, RELAP5-3D, MULTID, SBLOCA

1 INTRODUCTION

1.1 Accident management in NPP

The NPP accident management (AM) concept uses both “preventive” and “mitigation” measures to implement pre-defined accident management strategies [11]. These measures may include both manual operator actions and automated sequences of equipment operation, e.g. primary and secondary systems‘ depressurization, control of the hydrogen concentration inside containment, containment venting, flooding the reactor cavity to cool and retain in-vessel the molten corium and thus prevent MCCI, etc.

The guidance, given to the operators in the AM “preventive” domain, is in the form of prescriptive procedures, often referred to as Emergency Operating Procedures, (EOPs). The EOPs include descriptions of specfic actions, the timing, and the methods for their implementation by the operators *before* significant fuel rods’ damage occurs. The EOPs can be either *“event-based“*, i.e. they include sets of instructions how to respond to certain events, e.g. reactor scram or actuation of safety injection, or are *“symptom-oriented“*, i.e. they aim to prevent the loss, or restore critical safety functions, such as core subcriticality, core cooling, secondary heat sink, etc.

Many PWR plants use the emergence of an ICC condition as a suitable symptom to enter specific “symptom-oriented“ EOPs and carry out actions to restore core cooling and prevent fuel damage. If these actions fail to arrest the accident progression, so that extensive core damage occurs or is imminent, the operators then promptly transit from the EOPs to severe accident management guidelines (SAMGs) that should prescribe adequate measures how to mitigate the consequences from extensive core damage. Since the presence of an ICC condition indicates the imminent onset of fuel clad runaway overheating, the EOPs actions should be able to terminate it while the core geometry is still amenable to cooling, i.e. before the cladding of a large fraction of all pins in the core becomes so brittle as to fail during, or after core quenching.

If the fuel clad overheats, it may balloon and rupture, and thus cause significant blockage of some coolant flow in-core channels. The clad in the blocked channels may consequently overheat and may eventually start to oxidize. In its output, RELAP5-3D provides information where in the core the ballooned clad has blocked the flow and indicates the relative contraction of that channel’s flow area. The successful implementation of a given AM strategy should result in placing the reactor in a safe end state, i.e. one for which the calculated by RELAP5-3D code fuel temperatures remain at an acceptably low value and the core decay heat can be safely removed for the extended period of time.[4]

One may use RELAP5-3D calculated parameters to characterize the margins to core safety limits [4]:

1) Peak Cladding Temperature (PCT) – the safety limit is 1477 K
2) Local Maximum Oxidation (LMO) – the maximum local relative thickness of the cladding oxide layer; the respective safety limit is 17% of the initial clad thickness
3) Core Wide Oxidation (CWO) – characterized by the mass of hydrogen, produced by the vapor-Zirconium oxidation reaction; the limit is 1% of the mass produced if all fuel clad oxidizes.
4) Blocked flow channels in the core as a fraction of the total in-core flow channels – there is no quantitative limit on the core blockage, but the changes, calculated by the RELAP5-3D code, in the core geometry shall be such that the core remains amenable to cooling. [4]

1.2 Limitations in the use for accident management of in-vessel coolant temperature measurements

The fuel pins' cladding heats up as a result of an ICC and the saturated steam, surrounding the fuel rods, superheats and may rise out of the core into the upper plenum and reach the CETC. These temperature sensors indicate to the operators the onsert of rapid fuel cladding overheating by detecting the superheated vapor when it flows past them. The timing of the ICC indication by the CETCs is adequate if it occurs early enough, so that the operators have sufficient time to recognize the overheated condition of the core, initiate, and complete successfully all AM actions, needed to restore core cooling core and *prevent* fuel damage *in excess of* the licensing safety limits, i.e. PCT, LMO, and CWO.

The assessment of the CETCs performance, in conditions with deep core uncovery and significantly overheated fuel, has involved the use of data from a number of experiments in integral test facilities [3]. Two general CETC limitations appeared during experiments at the LOFT facility [2] regarding the ability of CETCs to monitor the core uncovery and to indicate the ICC appearance:

- Large time delay from the moment of core uncovery until the time when CETC respond to it.

The LOFT data analysis led to the conclusion that the CETC's delay came from the formation of a film of liquid water that coats the CETCs hot junctions. Consequently, the sensors can respond to the presence of superheated vapor only after this liquid film gets either evaporated or stripped away from the hot junction by steam flowing past it.

When an ICC condition arises in commercial PWR systems, such large time delay in the CETC performance may impede the implementation of AM procedures that use CETC readings to indicate the appearance of ICC and monitor its evolution. Therefore, one may need to use a system code as RELAP5-3D to simulate in detail the core and the reactor vessel internals and assess the effect of multi-dimensional fluid flows on the performance of the temperature sensors used for accident management.

- CETC readings are much lower than the maximum fuel clad temperature.

The CETC indication in one of the LOFT tests was about 450 K lower than the maximum cladding temperature, measured during the transient. A possible explanation [2] is that the maximum COT reading is rather close to the temperature of the cladding at the top of the core, while the maximum fuel cladding temperature may be at, or below, the elevation of the core belt line. Moreover, the "hot spot", i.e. the location of the maximum PCT, may change in the course of the transient – it may move away from the core high-power region to a region where the clad may have ballooned and blocked significantly the coolant flow, [3]. In addition to the reduced heat removal in the in-core region with blocked coolant flow and ballooned fuel pins, fragments of fuel pellets may relocate inside the fuel pin to its region with ballooned cladding and increase the heat flux from the fuel to the cladding.

The LOFT tests led to the conclusion that AM procedures that rely on the response of the CETCs to monitor the core cooling degradation and fuel overheating, should take into account the above two limitations. Moreover, the LOFT tests [2] indicated that there might be accident scenarios in which the CETCs would eather not detect at all the appearance of an ICC, or reveal it too late to the operators, when the transient would be rapidly escalating towards a stage with a large-scale fuel damage.

The assessment of other sets of test results [3] led to conclusions similar to those derived from the LOFT experiments:

- When CETC readings indicate the presence of superheated vapor, it happens in nearly all cases with a certain time delay - it may range from twenty to several hundred seconds - and these readings are always significantly lower (up to several hundred degrees Kelvin) than the maximum cladding temperature at that very same moment.

- The CETC performance is strongly affected by the accident scenario that has led to ICC and the flow conditions established in the core and in that part of the upper plenum, where the CETC are.
- Both delays in the CETC readings and large differences between the sensor measurement and the maximum fuel clad temperature in the core have appeared in tests on all experimental facilities and in nearly all studied transient scenarios.

The main causes for these delays are the following [3]:

(i) Fluid temperatures along the core radius differ significantly during the approach to ICC, both at elevations below and above the upper core plate, where the CETC are located.
(ii) Cooling effect on the vapor from the unheated metal structures in the RPV upper internals: The massive metal structures in the RPV upper plenum may cause some of the saturated steam in the upper plenum to condense into liquid and then flow downwards along the CETC thimbles. The liquid can envelop the CETC hot junction and block the contact between the CETC and the superheated vapor rising from the core top.
(iii) The low rate of convection heat transfer from the clad surface to the low-velocity steam that flows past the fuel pins results in having a large temperature difference between the cladding and the fluid. Low steam velocity inside the fuel pins bundle and in the location of the CETC increase the significance of 3D flow patterns, e.g. superheated vapor may flow sideways and thus miss the hot junction of the CETC located above the core upper support plate.
(iv) Reflux cooling in the SG produces some liquid that flows in reverse direction, (i.e. from SG towards RPV), along the bottom of the hot legs into the RPV upper plenum. This liquid may provide some cooling effect that brings down the CETC measurements. This cooling effect on the CETC is stronger for PWR plants with injection into the hot leg of cold ECCS water.

The CETC indications can be strongly dependent on the actual accident scenario that has resulted in an ICC. For example, for SBLOCA scenarios with a break located in the top RPV head, the control rods guide tubes (CRGT) serve as conduit that may direct hot superheated vapor towards the break, thus allowing it to bypass the CETC located nearby. This “chimney” effect may lead to having an advanced ICC condition, while at the same time the CETC readings remain low and may even not indicate the presence of superheated vapor in the upper plenum. Another example of the significant effect of the accident scenario on the CETCs readings is the downward fluid flow, away from the CETC, in case of SBLOCA with break location in the lower RPV head, [3].

2 PWR SYSTEM MODEL DESCRIPTION

2.1 Multi-Dimensional Model of the Reactor Core and Upper Internals Plenum

2.1.1 RELAP5-3D Multi-Dimensional Fluid Flow Modeling Capability

The multi-dimensional component “MULTID” in RELAP5-3D allows the user to model the reactor vessel (i.e. the core, the downcomer) and the steam generator. These components have solid structures in the fluid path (i.e., core, steam generator), or have a short length in the radial direction (i.e., downcomer) that cause the coolant flow form loss, coolant-to-wall friction, and the interphase friction to be the primary source terms in the momentum equations that define the coolant fluid flow. For these code applications, the viscous stress and turbulence terms in the fluid flow equations are not as important and they have not been not included in the RELAP5-3D multi-dimensional flow model.

The functionality of the RELAP5-3D multi-dimensional MULTID component has been under testing and refinement since it was first applied [16] to study the K reactor at Savannah River in the early 1990s. A set of approximately twenty verification test problems was devised to demonstrate the correctness of the numerical conservation equation formulation. All of these problems have closed form solutions. Until recently, application of the model to experiments was limited to tests carried out in the L reactor at Savannah River. A program is currently underway to expand the validation base to include a wide variety of experiments that exhibit multi-dimensional flow behavior. One example is a series of experiments conducted at the Rensselaer Polytechnic Institute [17] to examine the flow patterns in a two-dimensional test section connected to an air-water loop.

The capability of the RELAP5-3D computer code to perform multi-dimensional analysis of a pressurized water reactor was assessed [15] by using data from the Loss-of-Fluid Test (LOFT) L2-5 experiment. The LOFT facility was a 50 MW PWR that served to simulate the response of a commercial PWR during a loss-of-coolant accident (LOCA). Test L2-5 simulated a 200% double-ended cold leg break with an immediate primary coolant pump trip. A three-dimensional model of the LOFT reactor vessel was developed. Calculations of the LOFT L21-5 experiment were performed using the RELAP5-3D computer code. The calculations simulated the blowdown, refill, and reflood portions of the transient. The calculated thermal-hydraulic response of the primary coolant system was generally in reasonable agreement with the test. The results, calculated by using the RELAP5-3D three-dimensional model of the LOFT reactor vessel, were generally as good as, or better than those obtained previously with the one-dimensional RELAP5/MOD3 model.

2.1.2 RELAP5-3D Core and Upper Internals Model

Figures 1 and 2 represent an arbitrary in-core relative power distribution of a three-loop generic PWR with 157 fuel assemblies in the core, where each fuel assembly has a 17x17 lattice of 264 fuel pins and 25 hollow thimbles. The nominal core thermal power is set at 2775 MW.

	R	P	N	M	L	K	J	H	G	F	E	D	C	B	A
01							0,377	0,546	0,377						
02					0,373	0,708	1,156	1,242	1,154	0,704	0,372				
03				0,438	1,08	1,304	1,128	1,153	1,127	1,303	1,078	0,436			
04			0,436	1,057	1,039	1,099	1,432	1,122	1,434	1,093	1,039	1,057	0,438		
05		0,372	1,078	1,039	1,119	1,396	1,012	1,4	1,015	1,399	1,119	1,039	1,08	0,373	
06		0,704	1,303	1,093	1,399	1,055	1,08	1,088	1,083	1,055	1,396	1,093	1,304	0,708	
07	0,377	1,154	1,127	1,434	1,015	1,083	1,026	1	1,026	1,08	1,012	1,432	1,128	1,156	0,377
08	0,546	1,242	1,153	1,122	1,4	1,088	1	0,842	1	1,088	1,4	1,122	1,153	1,242	0,546
09	0,377	1,156	1,128	1,432	1,012	1,08	1,026	1	1,026	1,083	1,015	1,434	1,127	1,154	0,377
10		0,708	1,304	1,093	1,396	1,055	1,083	1,088	1,08	1,055	1,399	1,093	1,303	0,704	
11		0,373	1,08	1,039	1,119	1,399	1,015	1,4	1,012	1,396	1,119	1,039	1,078	0,372	
12			0,438	1,057	1,039	1,093	1,434	1,122	1,432	1,093	1,039	1,057	0,436		
13				0,436	1,078	1,303	1,127	1,153	1,128	1,304	1,08	0,438			
14					0,372	0,704	1,154	1,242	1,156	0,708	0,373				
15							0,377	0,546	0,377						

Figure 1. Relative Fuel Assemblies Powers in Core

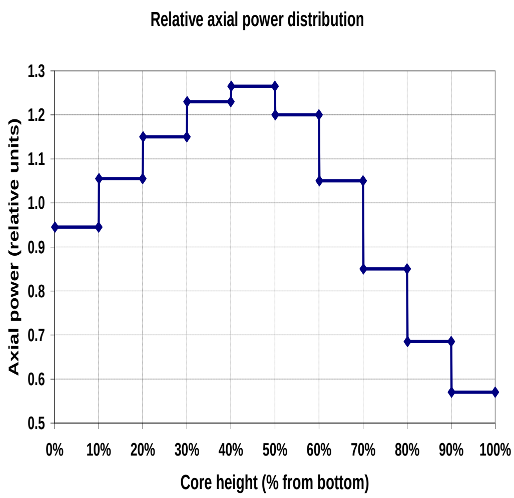

Figure 2 Relative Axial Power Distribution in Core

There are twelve fuel assemblies (Fig.1) with relative powers in the range of 1.40 to 1.434, or 140% to 143.4% of the average power assembly in the core. Each of these twelve assemblies has eight fuel pins with an assumed relative power of 120% of the average pin power in the respective fuel assembly. Therefore, the highest assumed relative power, (ie 1.434*1.2=1.7208) of these fuel pins is nearly equal to the limiting value of the maximum allowed fuel rod power, as given by the limiting “enthalpy rise peaking factor” ($F_{\Delta H}$=1.732) in the operating technical specifications of many currently operating PWR. The relative power axial distribution is given on Fig.2 and the axial power maximum peaking factor is F_Z=1.265. Therefore, the highest assumed relative power of the core‘s ‘hot spot‘ is: $F_Q=F_{\Delta H}*F_Z$=1.7208*1.265=2.177, which is close to the limiting value of the volumetric power peaking factor, maxF_Q= 2.3

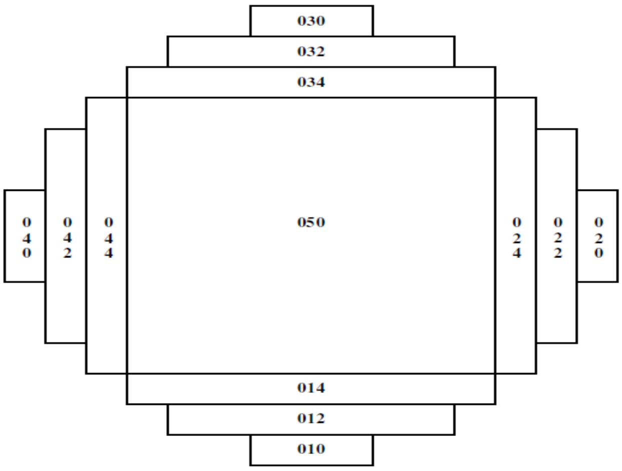

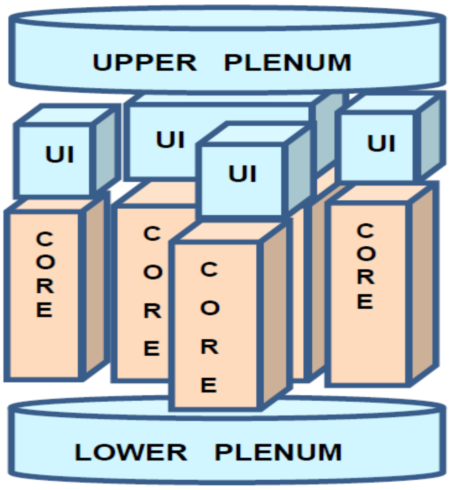

Figure 3. Core Model with RELAP5-3D MULTID components

Figure 4. RPV nodalization with cylindrical and orthogonal MULTID components

The RELAP5-3D multidimensional "MULTID" component [10] defines a three-dimensional array of nodes, i.e. volumes, and the internal junctions connecting these volumes. This RELAP5-3D model uses cartesian "MULTID" components, Fig.3 and Fig.4, to nodalize the core, so that each fuel assembly, i.e. a bundle of 264 fuel pins, sits in a separate coolant flow channel. Cylindrical "MULTID" components (Fig.4) represent the lower plenum, ie the volume below the core, and the volume below the reactor vessel upper head and above the plenum with the upper internals – these are modeled by using cartesian MULTID components that have the same x-y nodalization meshes as the cartesian MULTID components used to model the core.

A cylindrical MULTID component with two radial and six azimuthal meshes represents the annulus between the reactor vessel inner wall and the core barrel. Such nodalization allows simulating the circulation of coolant rising along the hot core barrel wall and descending along the colder reactor vessel wall. Such coolant's circulation facilitates the movement downwards of cold water, injected by ECCS, in the downcomer, when a mixture of saturated liquid and steam fills it up.

For example, the RELAP5-3D component MULTID-010 (and Fig.3) represents three fuel assemblies: J15, G15, and H15 (Fig.1); hence, its orthogonal nodalization parameters are MULTID-010: x=1 to 3, y=1, z=1 to 13. MULTID-020 represents also three fuel assemblies: A07, A08, and A09 (Fig.1) and has nodalization parameters: MULTID-020: x=1, y=1 to 3, z= 1 to 13. Component MULTID-050 represents 81 fuel assemblies and, consequently, its nodalization parameters are MULTID-050: x=1 to 9, y=1 to 9, z = 1 to 13.

The cartesian MULTID components, used to simulate the upper internals plenum, comprise, or are "perforated" by forty-eight RELAP5-3D "PIPE" components that represent the volumes enclosed by the Control Rods Guide Tubes, (CRGT). These "PIPE" components play an important role in simulating the coolant flows circulation inside the upper plenum and the important effect this coolant circulation may have on the performance of the CETC sensors, especially in the course of a SBLOCA transient with a break location in the top of the RPV.

2.2 Coolant Temperature Sensors Modeling

Modeling the coolant flow past each CETC, or in-core temperature sensor IITA, allows to compare their performance and to evaluate the effect from a failure of a number of sensors in the course of the analyzed transient on the timing and efficiency of operators' AM actions.

Instead of using COT, i.e. the calculated by RELAP5-3D liquid or vapor temperature at the core outlet, the CETC sensor model uses the RELAP-3D component *"heat structure"* that serves to simulate the transfer of heat to the CETC sensor from fluid inside a mixing device, a "bowl", Fig.5A, mounted on top of the Upper Core Plate, (UCP), [12].

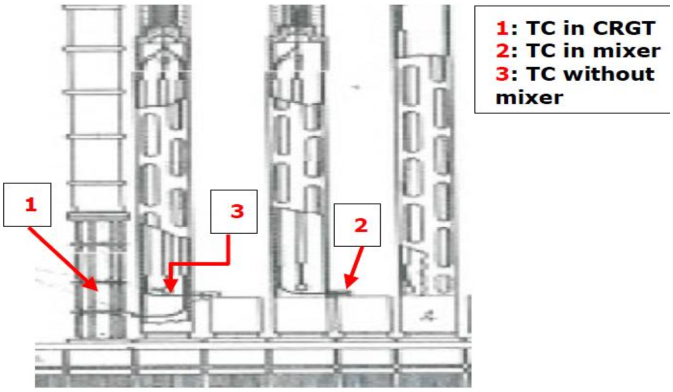

Figure 5A. CETC are mounted on top of Mixing Devices, sitting on UCP (Upper Core Plate) [12]

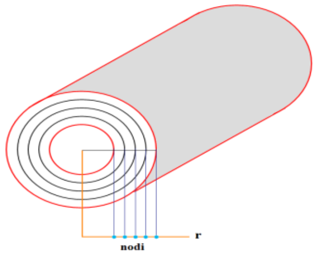

Node	Outer Radius	Materials along CETC radius	
1	0.5 mm	34	Chromel
2	1.5 mm	34	Chromel
3	2.0 mm	37	Arbitrary material, used to set TC thermal constant to τ=2 sec
4	3.0 mm	38	Gap, filled either with stagnant liquid or water vapor
5	3.5 mm	36	Inconel-690

Figure 5B. Radial nodalization of heat structure model of CETC and IITA sensors [12]

The model of the CETC "hot junction" heat structure, Fig.5B, is a solid cylinder of "chromel" alloy (RELAP5-3D material ***'34'***) with radius of 0.0015 m, surrounded by a layer of artificial substance (material ***'37'***) that serves to adjust the thermo-couple time constant to t= 2 sec. Material ***'38'*** represents the actual gap between the thermocouple and the inner wall of the instrumentation thimble in the fuel assembly, or the thermo-well in the CETC sensor. Material ***'38'*** has the thermal properties either of stagnant saturated liquid, if the adjacent fluid is at temperature less than 623 K, or the properties of superheated vapor at pressure 2 Mpa, if the adjacent fluid is at temperatures higher than 623 K. The so-defined thermocouple "heat structure" has an outside radius of 0.0035 (m) and its outer mesh represents a cylindrical wall of 0.0005 (m) made of inconel-690 (RELAP5-3D material ***'36'***).

In many operating PWR plants the instrumentation thimbles, inside the array of fuel pins of the fuel assemblies, currently house only movable neutron flux sensors. Some NPP vendors have considered the possibility to use the instrumentation thimbles for placing there a set of sensors [5], hereafter referred as IITA, Fig. 5C, to measure both the in-core neutron flux and the coolant temperature - these IITA sensors are located in core cells given on Fig. 6B.

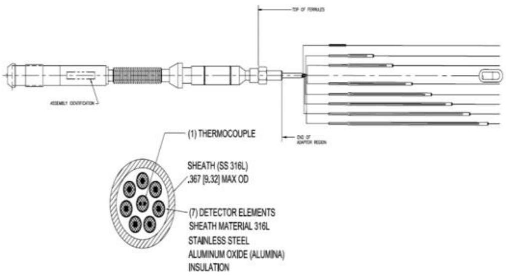

Figure 5C. In-core neutron flux and coolant temperature sensor (IITA) [5]

The RELAP5-3D model of the IITA sensors' design uses the following assumptions:

- The "hot junction" of in-core thermocouple ***IITA-W*** is placed at the elevation of the topmost node of the fueled part of the pins in the respective assembly, Fig. 6B
- The "hot junction" of in-core thermocouple ***IITA-K*** is placed at the elevation of the fuel-free part of the fuel pins in the respective assembly, Fig. 6B

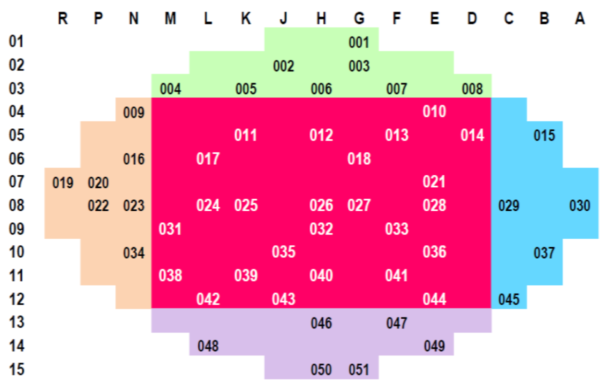

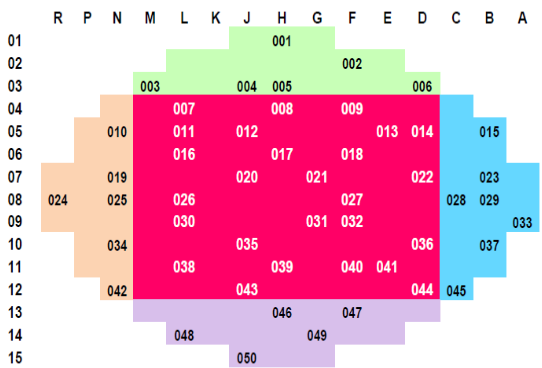

Figure 6A. Core Exit Thermo-Couples (CETC) Distribution

Figure 6B. Core locations of in-core neutron flux and coolant temperature IITA sensors

Figure 6A shows the assumed CETCs locations at the core outlet. Although the IITA thermocouple model is a RELAP5-3D *'heat structure'*, identical to the CETC one, there is important difference between IITA-W and IITA-K sensors - since IITA-W is at the elevation of the *fuel top node* in the core, (Fig. 7C), its heat structure exchanges heat not only with the adjacent reactor coolant via convection, but with the nearest fuel pins via thermal radiation. To model the radiation heat transfer, each IITA is included in a RELAP5-3D “radiation enclosure” [10] - a schematic is shown on Fig. 7A, where (1) is the IITA sensor, and (2), (3), (4), …(10) are fuel pins. For the derivation of the view factors between the radiation enclosure elements, one can use data from [6].

The schematic on Fig.7C shows the arrangement in the RELAP5-3D model to represent the CETC and the IITA sensors.

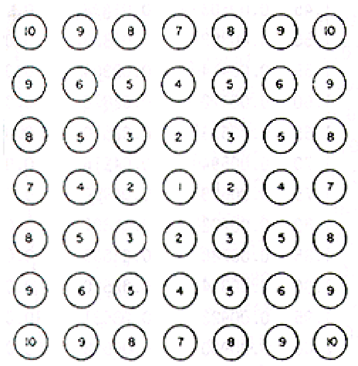

Figure 7A. Actual arrangement of IITA (1) and fuel pins (2), (3), (4), …, (10) [6]

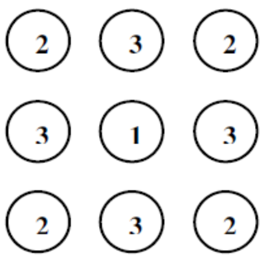

Figure 7B. Simplified RELAP-3D “radiation enclosure” model: IITA (1) and fuel pins (2), (3)

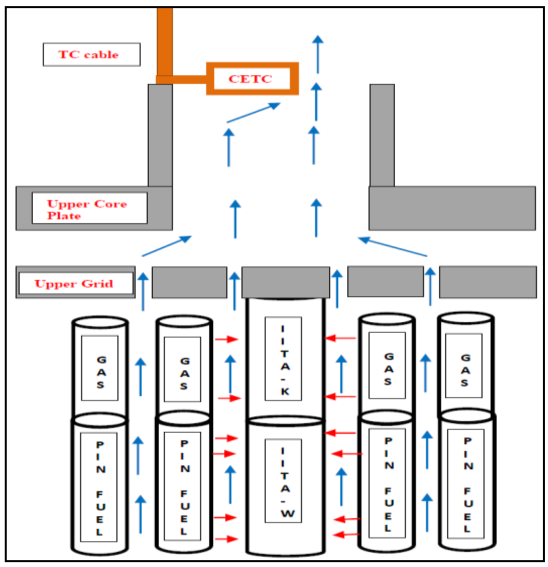

Figure 7C. CETC in Upper Internals plenum

2.3 RELAP5-3D Fuel Performance Model

One can use the data, given on Fig. 8A and 8B, to define the axial nodalization of the core region.

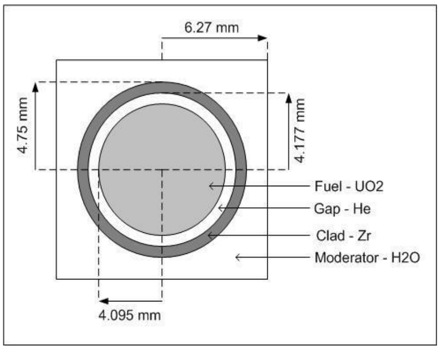

Figure 8A. Fuel pin dimensions [18]

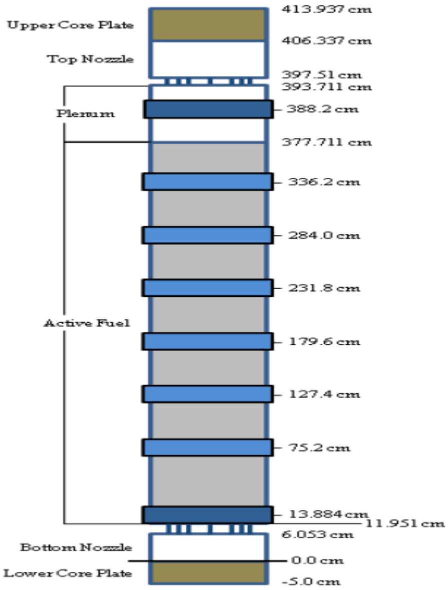

Figure 8B. Fuel assembly dimensions

The RELAP5-3D model for the simulation of the fuel behavior in the course of overheating accidents, takes into account fuel clad ballooning and clad burst, the blockage of coolant flow that clad rupture may cause, clad oxidation, and hydrogen generation. The RELAP-3D fuel model [10] can indeed simulate the reduction in flow area due to blockage caused by fuel cladding's rupture, but it cannot represent the deformation, i.e. the change in geometry of the RELAP5-3D "heat structure" components that represent the fuel pins. Therefore, RELAP5-3D cannot simulate the appearance of contacts between the heat structures representing ballooned adjacent fuel pins. Neither can the code represent how loose fuel pellets' crumbs may relocate into pockets, formed by ballooned fuel cladding that has detached from the fuel pellets. Ignoring these phenomena leads to some underestimation of the peak cladding temperature that RELAP5-3D cannot quantify.

2.4 Reactor Coolant System Modeling

The RELAP5-3D model represents the SG secondary side depressurization by simulating the operation of the SG relief valves for steam dump to atmosphere. The RELAP5-3D model uses for these valves the component *"srvvlv"*, or servo-valve. Another RELAP5-3D *"srvvlv"*, servo-valve component, represents the operation of the three pressurizer PORV valves. A separate RELAP5-3D component *"accum"* represents each of the three ECCS hydro-accumulators that discharges into a RCS cold leg via a RELAP5-3D component "ECCMIX".

The reflux flow of condensate, from the SG hot side channel head, along the bottom of the pretty wide hot leg pipes, Fig.9 [13], can contribute to the removal of heat from the core. When the low-velocity reflux stream enters the RPV, it slides down the inner wall of the core barrel and eventually reaches the peripheral rows of fuel assemblies in the core. This inflow of liquid into the core serves to drive in-core natural circulation loops where high-quality mixture of saturated liquid and steam rises in the core hottest regions. A stream with lower steam quality moves then downwards in fuel assemblies in the cooler peripheral regions towards the bottom of the core hot regions. This circulation serves to distribute heat from the core hot regions to the adjacent cooler ones. The nodalization of all hot legs and SG primary side, i.e. its hot channel head and tubes' bundles facilitates the simulation of the reflux flow from the SGs back to the reactor vessel by using two parallel *"pipe"* RELAP5-3D components on top of each other to represent the separate coolant streams to and from the SG.

The RELAP5-3D model represents all main heat structures inside the reactor vessel in order to describe correctly the thermal inertia and the exchange of heat between fluids and structures, especially near the in-vessel coolant‘s temperature sensors.

3 TRANSIENT DESCRIPTION AND SIMULATION RESULTS

3.1 Operators accident management actions in response to ICC condition

The presence of superheated steam inside the reactor vessel indicates the existence of either a *degraded*, i.e. a prolonged loss of subcooling, or *inadequate* core cooling condition, when the fluid in the core is superheated by several hundred degrees Kelvin. Since the temperature of saturated steam in the RCS of a PWR plant can never exceed 643 K, one should interpret a CETCs reading of a COT equal or greater than 643 K as an indication that a certain part of the core is uncovered, i.e. the heat transfer there is from fuel clad to superheated vapor. When the CETCs readings reach a COT = 923 K, this indicates that the core cooling condition has worsened from “*degraded*” to “*inadequate*”, i.e. the fuel uncovery is deeper and runaway core overheating is either imminent or has already begun.

The operator shall then execute sequentially the following AM actions:

a) Re-initiation of the HHSI
b) Rapid SG secondary side depressurization
c) RCPs restart and/or opening of all available pressurizer PORV to depressurize the RCS

“Re-initiation of HHSI“ is the most effective EOP action to recover the core and restore core cooling. If HHSI flow to RCS cannot resume, or is ineffective in restoring adequate core cooling, then the operators should reduce the RCS pressure in order to let the ECCS accumulators and the LHSI pumps deliver sufficient amount of coolant to quench and recover the core. One of the means to depressurize the RCS is to carry out a *rapid SG secondary side depressurization* by opening all available SG atmospheric relief, or condenser dump valves. The decrease in the SG secondary coolant pressure and temperature will increase primary-to-secondary heat transfer and will cause steam inside the SG tubes to condense. When the steam condensation rate exceeds the rate of coolant evaporation in the core, the RCS will begin to depressurize. The liquid in the RPV lower plenum and downcomer will begin to evaporate and a mixture of liquid steam and liquid will rise into the core, displace the superheated vapor enveloping the fuel pins, and will thus improve the heat removal from the fuel.

The continued RCS depressurization will eventually let the ECCS accumulators inject and temporarily recover the core. To prevent nitrogen ingress into RCS from the ECCS accumulators, the operators isolate them when the RCS pressure becomes sufficiently low. After the ECCS accumulators have been isolated, the operators depressurize the SG secondary side to atmospheric pressure. The RCS pressure will follow the decreasing SG secondary side pressure and eventually will descend below the LHSI pumps shut-off pressure, so that make-up coolant can finally begin to enter the RPV and recover the core.

If SG secondary depressurization is not possible, or primary-to-secondary heat transfer degrades significantly due to a loss of SG secondary heat sink, then the operators may attempt to start the RCPs. As long as these pumps can run, they will provide a two-phase coolant flow through the core and temporarily improve the core cooling until the operators restore some form of make-up flow to the RCS. It is unlikely that the RCPs can run for very long time under highly voided RCS conditions. Even if the pumps run, one still needs a coolant makeup source to replenish the lost coolant and recover the core. Such source can be the ECCS accumulators and the LHSI pumps, provided they are available, and the RCS is depressurized.

If the COT readings still indicate the presence of an ICC condition, i.e. COT= 643 K (for plants equipped with RVLIS), or COT=923 K (for plants without RVLIS), the operators should *accelerate the RCS depressurization by opening all available pressurizer relief valves* (PORVs), RPV head vents, and any other vent paths that can help to reduce the RCS pressure. One of the safety concerns related to the presence of an ICC condition is the generation of hydrogen that can escape into the containment through the pressurizer relief valves when the operators begin to vent the RCS. High hydrogen concentrations in the containment can lead to hydrogen deflagration, or even detonation that can produce a large pressure spike and thus cause loss of containment integrity, and/or damage to vital structures, e.g. essential pipework, PAR for hydrogen control, safety-related sensors, etc. If the operators do not succeed to restore core cooling after depressurizing RCS and initiating some makeup flow to the core, i.e. the ICC condition is still present, then the AM control over the accident moves from the "preventive" domain to the "mitigation" one. When selecting the optimum sets of operator response actions to a transient leading to an ICC, one can evaluate the adequacy and efficiency of proposed alternatives by comparing the margin to safety limits, once a safe plant end-state has been achieved after implementing of a given sequence of AM actions. One can optimize a given EOP by comparing how alternative AM strategies affect RELAP5-3D calculated parameters such as:

- **PCT**: the peak cladding temperature reached until the reactor has been brought to a safe end-state
- **LMO**: the maximum thickness of the oxide layer on the clad wall
- **CWO**: the amount of hydrogen produced by clad oxidation until the accident ends.
- **Core Blockage**: Fraction of the core that has been blocked by ruptured fuel tods' cladding

Since the operators will need some time to implement the entire AM strategy, i.e. identify the onset of ICC, depressurize both the primary and secondary sides, line up and start the LHSI system, and place the hydrogen PARs into service, one may also have to compare the time required to complete the implementation of alternative AM strategies, or single actions.

3.2 Transient description

The transient is initiated by the opening of a break with a throat area of $81*10^{-4}$ (m^2) in RPV lower head. All "High-Head Safety Injection" (HHSI) pumps and the SG auxiliary feedwater pumps fail to start up. Two "Low-Head Safety Injection" (LHSI) pumps are assumed available and each pump is modeled to have a shut-off head of 1.17 (MPa) and is being able to deliver a flow rate of 360 (kg/s) at a backpressure of 0.38 MPa. The accident scenario includes the assumption that the reactor coolant pumps (RCPs) are tripped when voiding appears in the node representing the pump's volute and after completing their coastdown, remain idle for the entire duration of the transient. Assuming the SG auxiliary feedwater pumps have failed, results in a loss of the secondary heat sink and, bars the operators to initiate controled SG depressurization at the rate of 55 K/hour.

Since HHSI remains unavailable, and controled SG depressurization is not allowed due to lack of feedwater flow to the SGs, the operators can respond to the appearance of an ICC only by depressurizing simultaneously both the primary and secondary sides at the maximum possible rate.

3.3 Transient study objective

The study objectives are:

- to evaluate the performance of CETC and IITA coolant temperature sensors in the course of a SBLOCA
- to compare two alternative AM strategies by using as a criterian the degree of core damage

Consider the following definition of "core damage":

- Peak cladding temperature becomes greater than 1475 (K);
- The thickness of the oxide layer on the fuel cladding wall exceeds 17% of the cladding thickness
- The amount of hydrogen produced in the course of the accident exceeds 10 (kg)

This study presents the plant responses to an ICC condition when the operators restore core cooling by using two different entry symptoms to initiate the same EOP:

a) Case-1: Core Outlet Temperature indications, produced by the CETC sensors are becoming greater than 923 (K)

b) Core Outlet Temperature indications, measured by the CETC sensors, are becoming greater than 643 (K), while the level of the saturated liquid-steam mixture in the core is less than 30%

One can use the respective values of the maximum clad temperature, the thickness of oxidation layer, and the mass of generated hydrogen as parameters to decide which entry symptom to the emergency procedure is better suited to take the plant to a safe end-state for a given accident scenario at the cost of a minimum, or no core damage.

3.4 Transient simulation results

The transient begins at time T_O=0 sec with the opening of the break at the RPV bottom. The coolant mass in the core begins to decrease and by time T_O+8 (min) the core is nearly fully voided - one may refer for details to Figures 10-1 and 11-1. If the operators begin to depressurize RCS at COT=923 K (Case 1), the primary pressure begins to decrease quickly when the break at the RPV bottom clears of liquid and starts to discharge mainly steam at time T_O+11 (min), Fig.10-2. The RCS pressure becomes lower than the pressure in the ECCS hydro-accumulators at time T_O+27 (min); Fig.10-2.

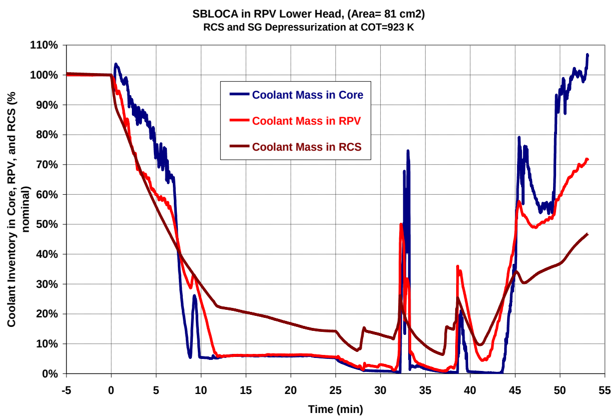

Figure 10-1. Case 1: Coolant mass in Core, RV, RCS, and ECCS delivery

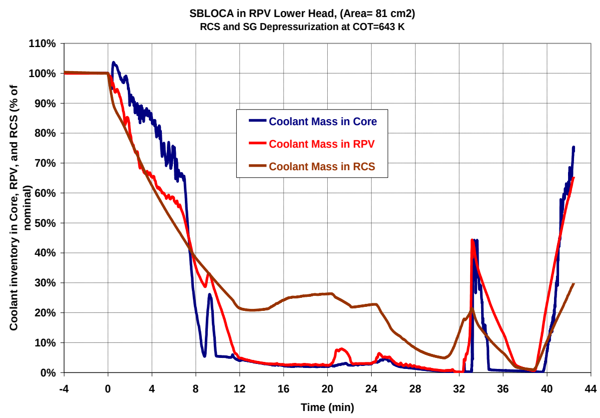

Figure 11-1. Case-2: Coolant mass in Core, RPV, RCS, and ECCS delivery

The coolant, delivered by ECCS hydro-accumulators, does not, however, reach the core (Fig 10-1) until time T_O+33(min) – it flows mainly into the lowest section of the RCS cold legs, i.e. the U-bent pipe between the RCPs inlet and the SGs outlet. Opening the pressurizer relief valves at time T_O+33 (min), together with the SG secondary side depressurization, accelerate the decrease of the primary pressure.

The discharge from the ECCS hydro-accumulators at time T_O+33 (min) fills up the core to level 70%, Fig. 10-1. Eventually, the primary pressure becomes lower than the LHSI pumps shut-off head at time T_O+33 (min), Fig.10-2, so that the core can be then re-flooded.

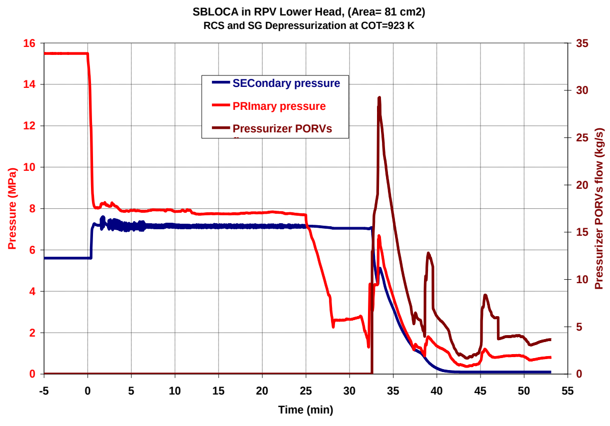

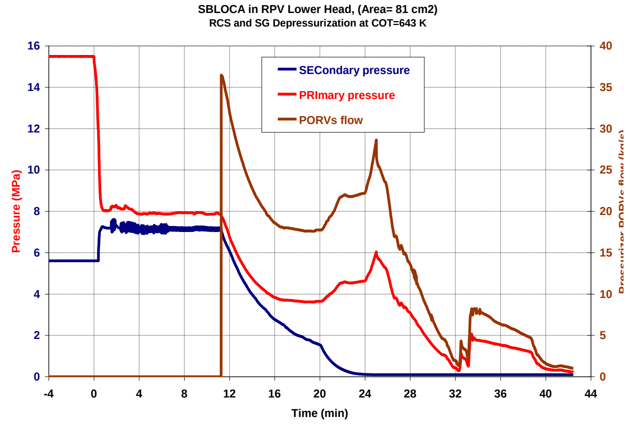

Figure 10-2 Case 1: RCS and SG pressure and pressurizer PORVs discharge

Figure 11-2 Case 2: RCS and SG pressure and pressurizer PORVs discharge

When the RCS depressurization is started at COT=643 K (Case 2), all SG and pressurizer PORVs are opened at time T_O+11(min), Fig.11-2, and the core is re-flooded by time T_O+42.5 (min) when the core level reaches 75%, Fig. 11-1. When the RCS pressure decreases below the LHSI shut-off head at time T_O+32 (min), Fig.11-2, the incoming coolant quenches the core. When the RCS depressurization is started at COT=923 K, the peak cladding temperature (PCT) exceeds the first of the acceptance criteria, i.e. PCT=1477 (K), at time T_O+27.5 (min), Fig.10-3.

The remaining two acceptance criteria exceed their respective assumed limits, Fig. 10-4:

- at time TO+27 (min): the relative thickness of the oxide layer on the cladding becomes > 17%;
- at time TO+30 (min): the mass of hydrogen, generated by clad oxidation, exceeds 10 (kg), which has been assumed to be equal to 1% of the total amount of hydrogen that can be produced in the reactor by zirconium oxidation

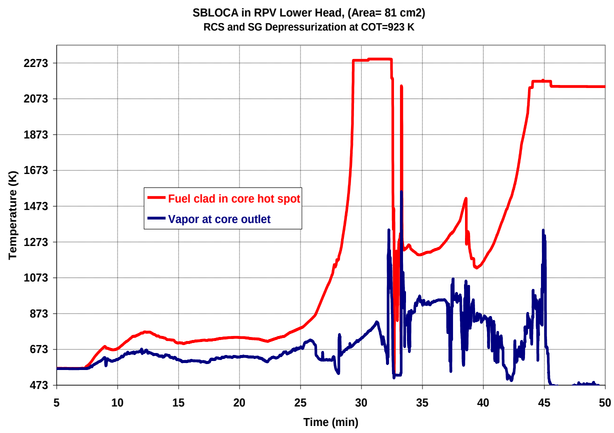

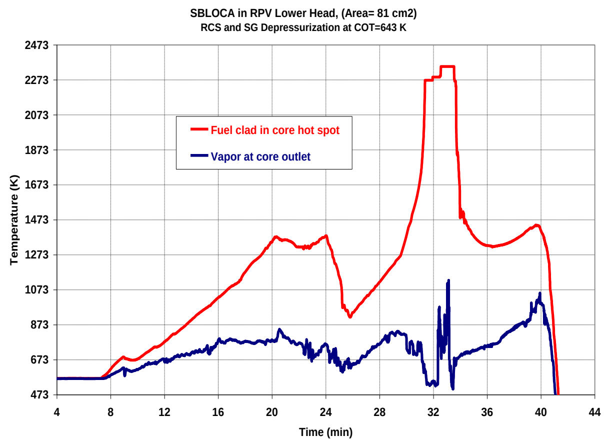

Figure 10-3 Case 1: Peak temperatures: fuel cladding and vapor at core outlet

Figure 11-3 Case 2: Peak temperatures: fuel cladding and vapor at core outlet

The onset of an ICC condition in the time interval between T_O+33 and T_O+37 (min) is signaled to the operators when the CETC reading exceeds at time T_O+33 (min), Fig. 10-5, the setpoint of 923(K), so that the operators may enter then the repective emergency procedure.

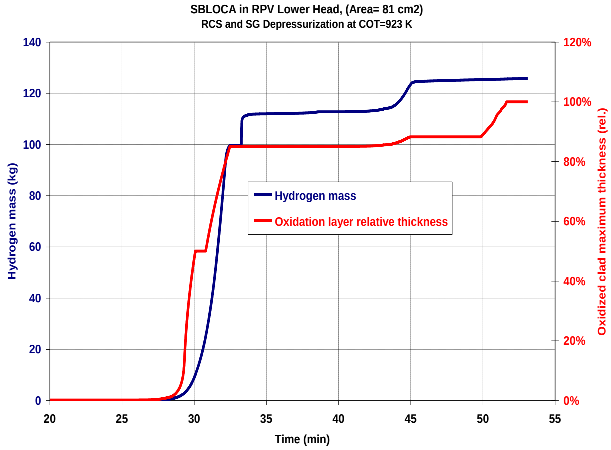

Figure 10-4 Case 1: Hydrogen mass and clad oxide layer relative thickness

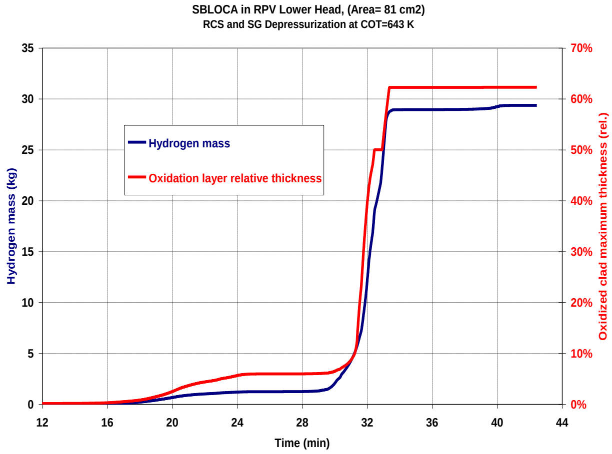

Figure 11-4 Case 2: Hydrogen mass and clad oxide layer relative thickness

Note that if the criterion COT=923 K were provided not by CETC, but by the IITA-W sensor, the operators would enter the procedure at time T_O+27 (min); refer to Fig.10-5. When the RCS depressurization is started at COT=643 K, the peak cladding temperature (PCT) does not exceed the first of ECCS Acceptance Criteria, i.e. PCT=1475 (K), until time T_O+30 (min); Fig.11-6. The thickness of the oxidized cladding layer is 62.5%, Fig.11-4, i.e. well over the limit of 17%, and the amount of hydrogen from clad oxidation is 29 (kg) - that is also above the respective limit of 10 (kg).

For the case when operators commence RCS depressurization at COT=643 K, all COT sensors have similar trends, Fig.11-5, while in Case-1 the CETC and the IITA-K sensors are unable to track the rise in the peak cladding temperature.

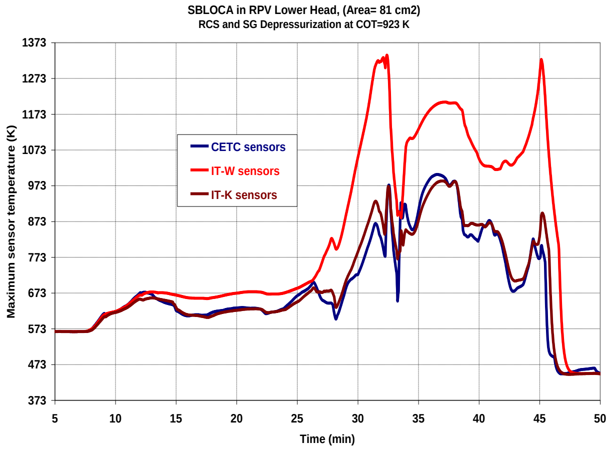

Figure 10-5. Case 1: Comparison of COT sensors performance: CETC, IITA-W, and IITA-K

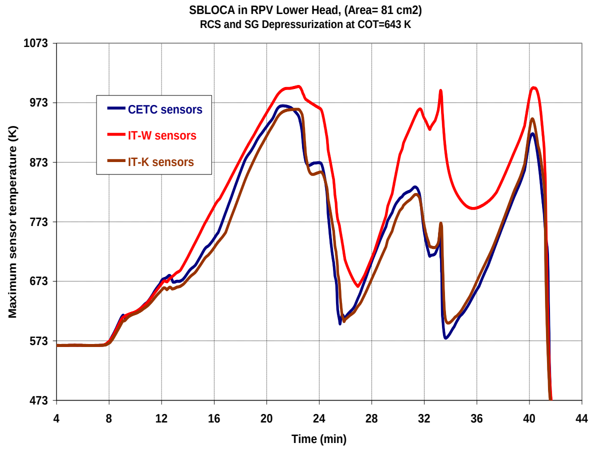

Figure 11-5. Case 2: Comparison of COT sensors performance: CETC, IITA-W, and IITA-K

Since both IITA-K and CETC sensors rely only on convective heat exchange with the adjacent fluid, their readings lag considerably behind the IITA-W indications that are influenced not only by convection, but also by heat exchange via thermal radiation with the neighboring fuel pins. The readings of IITA-W sensor show greater stability than these of the other two sensors Fig.10-5, once the ECCS hydro-accumulators start discharging into the RCS after time T_O+27 (min). The inflow of cold coolant into the RCS produces, apparently, large changes in the temperature of steam that is near the CETC and IITA-K sensors. If the rate of zirconium clad oxidation reaction intensifies substantially – as it is the case when operators commence RCS depressurization at COT=923 K – the readings from all COT sensors follow a trend that does *not* track any longer the trend of how the peak clad temperature changes - refer to Fig.10-6 and 10-7.

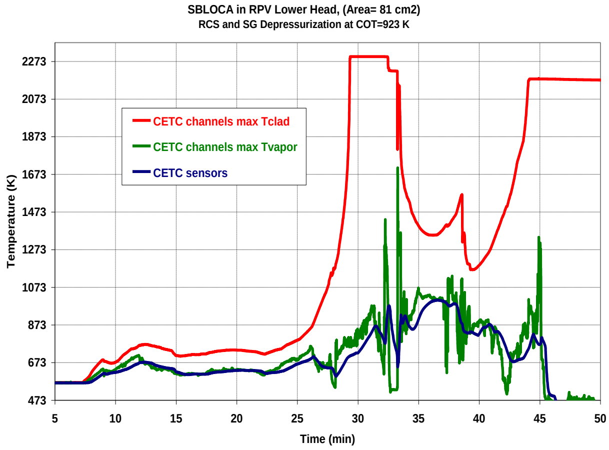

Figure 10-6. Case 1: Temperatures of cladding, vapor, and sensors in flow channels with CETC

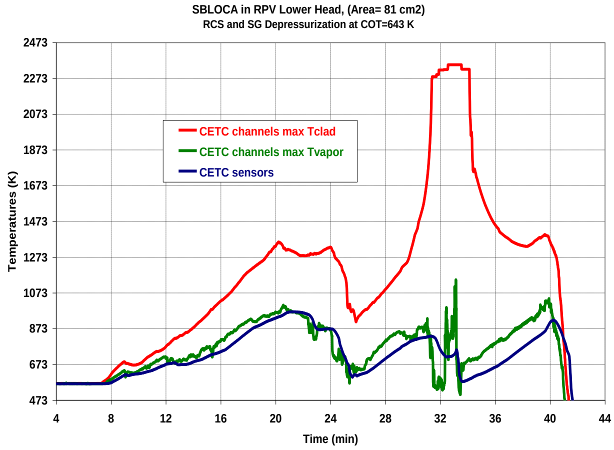

Figure 11-6. Case 2: Temperatures of cladding, vapor, and sensors in flow channels with CETC

When the RCS depressurization is started at COT=643, the rate of clad oxidation reaction is much smaller than in other case, so the COT sensors indications have the same trends as the peak cladding temperature until the time when the discharge from the ECCS accumulators begins to affect the temperature of the steam next to CETC and IITA-K sensors.

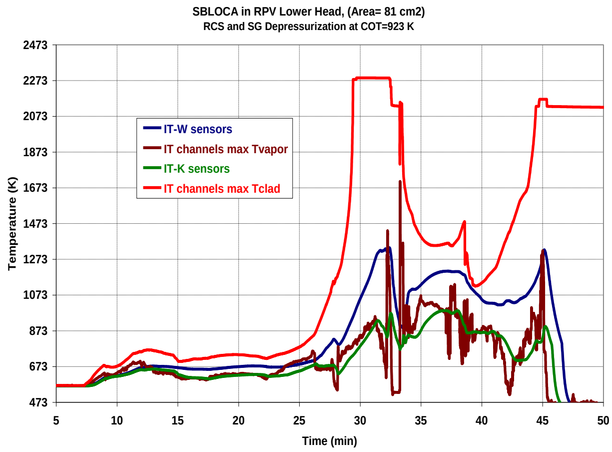

Figure 10-7. Case 1: Temperatures of cladding, vapor, and sensors in flow channels with IITA

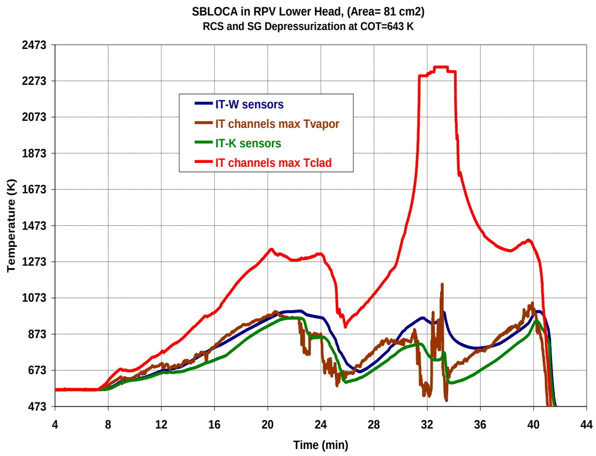

Figure 11-7. Case 2: Temperatures of cladding, vapor, and sensors in flow channels with IITA

The IITA-W sensor continues to track the rise in the peak fuel cladding temperature even after the ECCS discharge has started – refer to Fig.10-7 and Fig.11-7. Figures 10-8 and 11-8 present how the rupture of cladding affects the relative flow area in each fuel assembly in the core.

In Case 1 (Fig.10-8) the fuel pins cladding rupture begins at T_O+34.2 (min) and ends at T_O+45.1 (min) when the average flow area per fuel assembly in the core has reduced to 83.2% of the niminal, i.e. unblocked, area.

In Case 2 (Fig.11-8) the fuel pins cladding rupture begins at T_O+21.4 (min) and ends at T_O+41.1 (min) when the average flow area per fuel assembly in the core has reduced to 84.8% of the niminal, i.e. unblocked, area.

						100	81.3	81.3						
				100	100	100	29.3	100	36.6	100				
			100	100	28.9	100	29.4	100	100	100	100			
		100	100	100	100	100	28.9	28.8	100	100	100	100		
	100	100	100	28.9	28.7	100	100	100	100	100	100	100	100	
	100	100	28.7	28.7	100	100	100	100	100	100	100	100	100	
40.5	100	100	28.9	100	100	100	100	100	100	100	28.8	100	100	100
41	29	28.9	28.8	28.8	100	100	100	100	100	100	100	100	100	32.6
100	28.5	100	29.5	28.7	100	100	100	100	100	100	100	100	28.9	80.5
	100	28.9	28.9	28.5	100	29.2	100	100	100	100	100	28.9	100	
	100	100	100	28.8	28.8	100	100	100	100	100	100	100	100	
		100	100	100	28.7	28.8	100	100	100	100	100	100		
			29	100	28.7	100	100	100	100	100	100			
				100	100	100	30.4	28.9	100	100				
						82.1	60	100						

Figure 10-8. Case 1: Relative Fuel Assembly Coolant Flow Area at time To+45.1 (min)

						100	38.6	65.1						
				100	100	100	100	100	54.9	100				
			100	100	100	100	62	100	53.8	100	100			
		100	100	100	100	45.6	47.4	43.3	100	100	100	100		
	100	100	100	31.4	34	100	100	100	100	100	100	100	100	
	100	100	100	28.8	100	100	100	100	100	100	100	29.1	100	
100	100	100	29	100	100	100	100	100	100	100	31.1	100	100	100
69.8	38.6	33.6	32.1	30	100	100	100	100	100	100	100	32.1	33.9	78
74.9	39.5	38.7	33.2	29.1	100	100	100	100	100	100	100	100	32.1	100
	100	100	100	29	100	30.6	100	100	100	100	100	100	100	
	100	100	100	100	28.9	100	30.2	100	100	100	100	100	100	
		100	100	100	100	28.6	100	29.9	31.3	100	100	100		
			100	100	28.8	100	100	100	30.6	100	100			
				100	100	100	31.9	29.8	100	100				
						100	100	100						

Figure 11-8. Case 2: Relative Fuel Assembly Coolant Flow Area at time To+41 (min)

4 CONCLUSIONS

- The RELAP5-3D code is capable of implementing a multi-dimensional approach to modeling complex flow patterns inside the core and in the upper internals plenum. This allows to simulate individual CETC and IITA sensors and to evaluate the impact on operator actions from the postulated failure of a number of sensors;
- The proposed modeling approach allows to track for the entire duration of the accident how phenomena such as: in-core power radial and axial distribution, appearance of coolant circulation loops inside the core and the upper internals, and inflows of ECCS coolant into the RCS, influence the readings of individual CETC and IITA sensors.
- In addition to the fuel's peak cladding temperature, (PCT), one may the use of other RELAP5-3D calculated parameters, e.g. LMO, CWO, and the fraction of blocked in-core flow channels to compare the effectiveness of alternative AM strategies and to optimize the selection of certain setpoints in the AM procedures.
- RELAP5-3D code is able to simulate the performance of in-core coolant temperature sensors of type IITA-W, i.e. those having heat exchange with neighboring fuel pins via thermal radiation in addition to convection with adjacent fluid. The comprehensive comparison of the performance of the IITA-W and CETC sensors requires a detailed description of the sensors design and characteristics and a consideration of a wider set of accident scenarios.
- Future activities, related to the topics investigated in this study, may include the validation of the developed modeling multi-dimensional approach by using experimental data obtained in the framework of international research projects in which Bel V participates.

5 NOMENCLATURE

AM	Accident Management	**LHSI**	Low-Head Safety Injection
CETC	Core Exit Thermo-Couple	**MCCI**	Molten Corium Concrete Interaction
CFD	Computational Fluid Dynamics	**PAR**	Passive Autocatalytic Re-combiner
COT	Core Outlet Temperature	**PCT**	Peak Cladding Temperature
CWO	Core Wide Oxidation	**PORV**	Pilot Operated Relief Valve
ECCS	Emergency Core Cooling System	**PWR**	Pressurized Water Reactor
EOPs	Emergency Operating Procedures	**RCP**	Reactor Coolant Pump
HHSI	High-Head Safety Injection	**RCS**	Reactor Coolant System
ICC	Inadequate Core Cooling	**RVLIS**	Reactor Vessel Level Indication System
IITA	In-core Instrumentation Thimble Assembly	**SG**	Steam Generator
LMO	Local Maximum Oxidation	**SAMG**	Severe Accident Management Guidelines

6 ACKNOWLEDGMENTS

The author wishes to express his gratitude to his colleagues at Bel V for their help and valuable advice throughout his work on completing this study.

7 REFERENCES

1. US NRC Generic letter “Inadequate Core Cooling Instrumentation System,” https://www.nrc.gov/reading-rm/doc-collections/gen-letters/1982/gl82028.html
2. NUREG/CR-3386, “Detection of Inadequate Core Cooling With Core Exit Thermocouples: LOFT PWR Experience”, https://www.nrc.gov/docs/ML1303/ML13032A566.pdf
3. NEA/CSNI/R(2010)9, “Core Exit Temperature Effectiveness in Accident Management of Nuclear Power Reactor”, October 2010; https://www.oecd-nea.org/nsd/docs/2010/csni-r2010-9.pdf
4. 10CFR50.46 “Acceptance criteria for emergency core cooling systems for light-water nuclear power reactors”, August 29, 2017; https://www.nrc.gov/reading-rm/doc-collections/cfr/part050-0046.pdf
5. WINCISE (Westinghouse In-Core Information Surveillance & Engineering); https://patentimages.storage.googleapis.com/c3/d8/fa/51cafcc5a71648/WO2013103405A1.pdf
6. http://www.thermalradiation.net/sectionc/C-72.html
7. http://us.areva.com/home/liblocal/docs/Catalog/PWR/ANP_U_250_V4_14_ENG_FixedIncoreMonitoring.pdf
8. Song Hae Ye, et al., “Three-Dimensional Temperature Indication for the Reactor Core by Using Multiple Thermocouples,” *Proceedings of 8-th International Conference on Sensing Technology,* Liverpool, UK, Sep 2–4, 2014.
9. Liping Cao, et al. “Core Exit Thermocouple Response to Inadequate Core Cooling Using CFD Dynamic Mesh,” NURETH-16, Chicago, IL, Aug. 30-Sep. 4, 2015
10. RELAP5-3D Home, https://relap53d.inl.gov/SitePages/Home.aspx
11. IAEA SSG-54 “ACCIDENT MANAGEMENT PROGRAMMES FOR NUCLEAR POWER PLANTS”, https://www-pub.iaea.org/MTCD/Publications/PDF/P1834_web.pdf
12. W. L. SERVER, “Reactor Vessel Internals Embrittlement”, Joint ICTP/IAEA Workshop on *Irradiation-induced Embrittlement of Pressure Vessel Steels,* 23-27 Nov. 2009, http://indico.ictp.it/event/a08189/session/27/contribution/18/material/0/0.pdf
13. M. SUZUKI and H. NAKAMURA, “Reliability of Core Exit Thermocouple for Accident Management Action during SBLOCA and Abnormal Transient Tests at ROSA/LSTF,” *Journal of Nuc. Sci. and Techn.*, Vol. **47**, No. 12, p. 1193–1205 (2010)
14. J. FREIXA, et al. “Core Exit Temperature Response During an SBLOCA Event in the ASCÓ NPP,” NURETH-16, Chicago, IL, Aug. 30-Sep. 4, 2015
15. C. B. DAVIS, “Assessment of the RELAP5-3D Multi-Dimensional Component Model Using Data From LOFT Test L2-5,” INEEL/CON-98-00400, July 09, 1998
16. K.E. CARLSON et al., Theory and Input Requirements for the multidimensional Component in RELAP5 for Savannah River Site Thermal Hydraulic Analysis, EGG-EAST-9803, Rev. 0, July 1992
17. K. M. BUKHARI and R. T. LAHEY, "The Measurement of Countercurrent Phase Separation and Distribution in a Two-Dimensional Test Section," Rensselaer Polytechnic Institute, Department of Nuclear Engineering, NUREG/CR-3577, Jan. 1984.
18. https://syeilendrapramuditya.wordpress.com/2009/04/14/standard-pwr-nuclear-fuel-assembly-17x17-technical-specification/

Digital I&C – the Analysis and Test System (AnTeS) of GRS

Christian Müller, Ewgenij Piljugin, Hervé Mbonjo, Felix Gärner, Jaroslaw Shvab, Dagmar Sommer

Gesellschaft für Anlagen- und Reaktorsicherheit (GRS) gGmbH, Boltzmannstraße 14, 85748 Garching bei München, Germany

Abstract:

This paper introduces the Analysis and Test System (AnTeS) of GRS. AnTeS can be used for investigations, research and method developments in the field of digital I&C of nuclear power plants. It consists of a real digital I&C (DI&C) system (based on Teleperm XS from Framatome, formerly Areva), a simulated DI&C system and an additional module for generating and monitoring input and output signals, including simulated and real front-line systems. AnTeS is used in several research projects for the development and validation of model-based analysis methods.

1 INTRODUCTION

Instrumentation and control (I&C) systems are applied to monitor, control and protect nuclear power plants and research reactors. The ongoing shift from analogue hardwired I&C systems to digital I&C (DI&C) systems is increasing as they allow an easy access to process optimization, self-monitoring, fault tolerant features, very compact designs and very high performance /NRC04/, /BFE18/. On the other hand, the reliability of DI&C systems represents a challenge with respect to test and assessment. These challenges are characterized by, for example, unrecognized software errors, faulty updates, cyber security gaps and limited available operating experience /RSK11/. In particular, the lack of operating experience necessitates a model-based approach to assessing the reliability of DI&C systems.

2 SYSTEM DESCRIPTION

Figure 1 shows a schematic overview of the functional structure of the instrumentation and control of a nuclear power plant. The conditioned signals (e.g. pressures, temperatures) from the field are used by the I&C system to drive the actuators (e.g. valves, pumps), either automatically or as specified by the shift personnel. For this purpose, the corresponding commands from the I&C system are first prepared (within the drive controls), then optionally prioritized and then routed via the switchgear to the appropriate actuators.

AnTeS allows the investigation of the overall structure in Figure 1 and consists of three modules:

- **Module 1**: Real I&C system
- **Module 2**: Simulated I&C system
- **Module 3**: Generation and monitoring of input and output signals

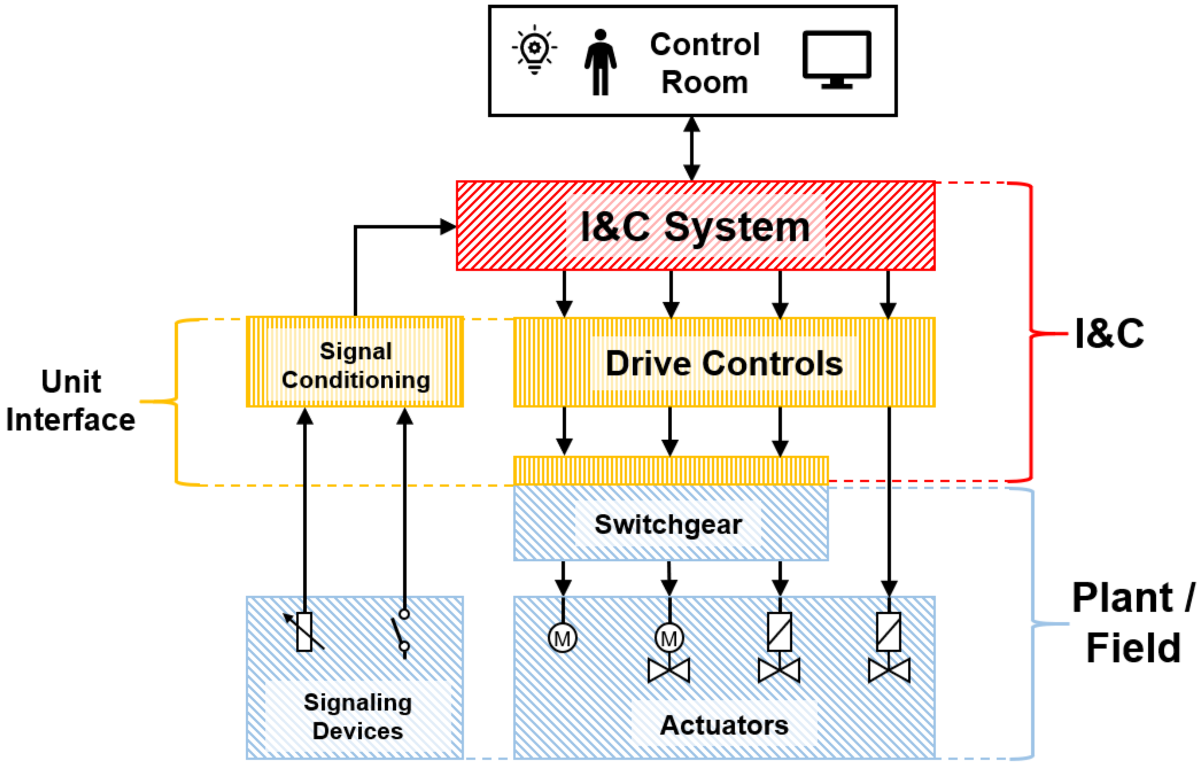

Figure 1: Functional structure of the instrumentation and control of a nuclear power plant

Both module 1 (real I&C system) and module 2 (simulated I&C system) cover the area marked "I&C" (including "Unit Interface") in Figure 1. The lower area in Figure 1 ("Plant / Field") is covered by module 3 of AnTeS. The following sections describe these three modules in more details. An application example of AnTeS is given in chapter 3.

2.1 Module 1: Real I&C System

The hardware and engineering software of the real I&C system of AnTeS (module 1) is based on components of the Teleperm XS system (TXS) from Framatome (formerly Areva) /TXS19/. It allows to flexibly realize different I&C architectures and network topologies to implement typical I&C functions (for the process automation or safety tasks). There are three cabinets available at GRS (Figure 2 a), b)), thus it is possible to operate a couple of redundant or (functional) diverse divisions at the same time.

The programming (engineering) of I&C functions takes place via SPACE (SPecification and Coding Environment of TXS) and can be adapted easily to any requirements. In addition, all signals within the system can be monitored online (Figure 2 c)). Module 1 can be used to examine and verify I&C functions in a real environment. For this purpose, among other things, it is possible to inject faults (for fault injection methods see for example /KIM06/) together with module 3 and, for example, carry out automatic failure modes and effects analyzes (FMEA – see for example /LEE17/, / NEA15/).

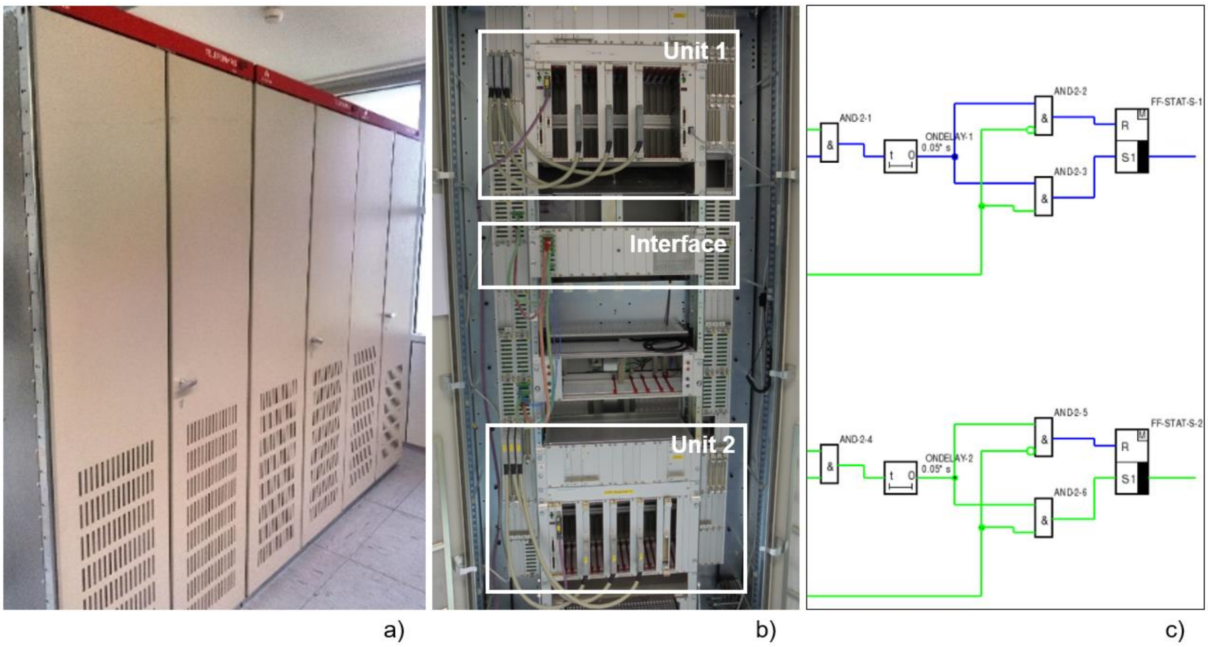

Figure 2: a) TXS cabinets at GRS in Garching, Germany b) Interior view of one of the cabinets; c) Detail of a dynamic function diagram (signal status indicated by different colors)

2.2 Module 2: Simulated I&C System

The simulated I&C system of AnTeS (module 2) is based on Matlab / Simulink /MAT19/. This module allows to replicate 1:1 all functions of module 1 or to build up simulated stand-alone I&C systems. For this purpose, the functionalities of the function blocks of the TXS system and some basic hardware features have been reproduced using Simulink (Figure 3).

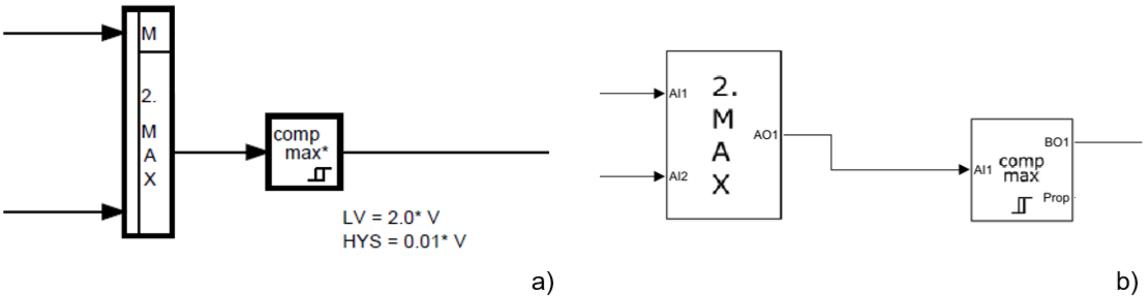

Figure 3: The same detail of an I&C function in module 1 (real I&C system, a)) and module 2 (simulated I&C system, b))

There is no necessary restriction to the functionality of the TXS system when using the module 2 of AnTeS. If desired, the behavior of alternative or generic I&C systems can also be simulated here. Simulated I&C systems can be used in Simulink directly, distributed on dedicated hardware (e.g., microcomputers, microcontrollers) or compiled as Windows libraries (dll – dynamic link library), depending on the current research task and desired combination with other systems. The same types of examinations as with module 1 can also be carried out with the module 2 of AnTeS (e.g., fault injection, automated failure modes and effects analyzes).

Due to the possible very fast execution velocity compared to module 1, module 2 also allows, among other things, Monte Carlo simulations over relatively long simulated time periods (e.g. simulated 1 million years of operation in about 1 hour of computing time).

2.3 Module 3: Generation and monitoring of input and output signals

Module 3 of AnTeS consists of additional hardware (e.g. “interface” in Figure 2b)), self-developed software for the generation of input and monitoring of output signals and real and simulated front-line systems. It is the basis for controlling all analyzes using modules 1 and 2 (e.g., automated failure effects analyzes, Monte Carlo simulations) und comprises the following components:

- Interface between the front-line systems and modules 1 and 2
    - Connection of simulated front-line systems
    - Connection of real front-line systems
- Simulation of a generic fuel pool (Figure 4 b))
- Simulation of a generic pool reactor (under development)
- Real valve drives (4 pieces available for AnTeS, Figure 4 a))
- Real signaling devices (e.g. feedback signals from real valve drives)
- Self-developed software (in Python, fexibly changeable)
    - Manual or automatic presetting of input signals and recording of the output signals generated by modules 1 and 2
    - Manual or automatic fault injection into modules 1 and 2
    - Automated failure modes and effects analysis for all input signal combinations and predefined failure modes within modules 1 and 2
    - Monte Carlo simulations within module 2 of AnTeS
- SIVAT (SImulation-based Validation Tool)
    - Software from Framatome (formerly Areva) which allows to dynamically test functions before implementing in TXS hardware

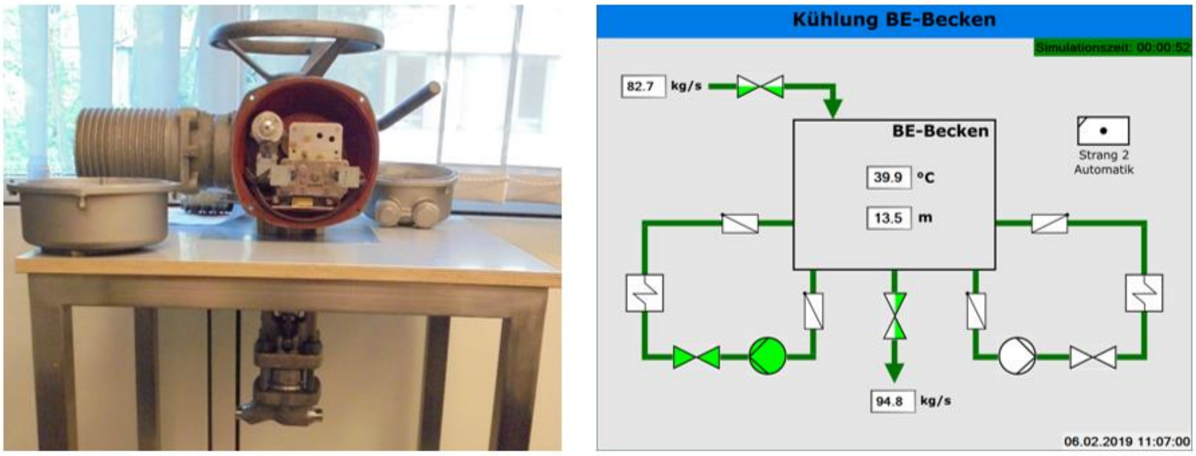

a) b)

Figure 4: Examples for real (a) and simulated (b) front-line systems of module 3 of AnTeS

3 EXAMPLE APPLICATION

AnTeS is a versatile research environment that can be flexibly adapted to a wide variety of requirements and is currently being used by GRS in a number of different projects /GRS17/, /GRS18b/, /GRS18c/, /GRS19/. This chapter exemplifies the application of AnTeS to a simple case.

In a previous project /GRS18a/, a number of different I&C architectures have been examined for their sensitivity to different paramters using fault tree analyzes. For demonstration purposes, one of the model systems of this project has been recreated using AnTeS modules 1 and 2. The selected model system is a dual-redundant I&C system for monitoring a pressure value exceeding a limit value (with appropriate triggering of an actuator). Both modules (1 and 2) allow an automated analysis of the effects of predefined failure modes.

A comparison of the results obtained with AnTeS with results from the previous project shows a perfect match concerning the so-called minimal cuts. In Figure 5 a) the minimal cut sets (Event 1 and Event 2) obtained with module 2 from AnTeS are listed in tabular form, Figure 5 b) shows the same cut sets obtained with a fault tree analysis using RiskSpectrum /RIS19/ in the previous project (see columns Event 1 and Event 2). AnTeS module 1 gives identical results, but due to the limitation to real time in module 1 and the very large number of failure modes to be investigated (131071 combinations of single faults) in a much longer time (computation time module 2: approx. 1 s, recording and analysis with module 1: approx. 6 days 10 hours 22 minutes). The specified events in Figure 5 represent predefined failure modes of the two redundancies of the model system. The abbreviations SF and NSF stand for self-signaling failures and non-self-signaling failures of specific components (AU – acuisition unit, PU – processing unit, VU – voting unit) of the model system. For more details see /GRS18a/.

Event 1	Event 2
AU1.A NSF	
AU2.A NSF	
CCF VU	
CCF ALL	
CCF PU	
CCF AU	
AL NSF	
AU1.A SF	AU2.A SF
PU1.A SF	PU2.A SF
PU1.A NSF	PU2.A SF
PU1.A SF	PU2.A NSF
PU1.A NSF	PU2.A NSF
VU1.A NSF	VU2.A NSF
VU1.A NSF	VU2.A SF
VU1.A SF	VU2.A NSF
VU1.A SF	VU2.A SF

a)

Top Event probability Q = 1,151E-04

No	Probability	%	Event 1	Event 2
1	5,60E-05	48,66	AU1.A NSF	
2	5,60E-05	48,66	AU2.A NSF	
3	7,46E-07	00,65	CCF VU	
4	7,46E-07	00,65	CCF ALL	
5	7,46E-07	00,65	CCF PU	
6	7,46E-07	00,65	CCF AU	
7	3,44E-08	00,03	AL NSF	
8	2,82E-08	00,02	AU1.A SF	AU2.A SF
9	1,58E-08	00,01	PU1.A SF	PU2.A SF
10	7,03E-09	00,01	PU1.A NSF	PU2.A SF
11	7,03E-09	00,01	PU1.A SF	PU2.A NSF
12	3,14E-09	00,00	PU1.A NSF	PU2.A NSF
13	3,14E-09	00,00	VU1.A NSF	VU2.A NSF
14	3,12E-09	00,00	VU1.A NSF	VU2.A SF
15	3,12E-09	00,00	VU1.A SF	VU2.A NSF
16	3,11E-09	00,00	VU1.A SF	VU2.A SF

b)

Figure 5: Minimal Cut Sets (MCS) of failures leading to a failure on demand of the model system obtained with AnTeS (a) and fault tree analysis with RiskSpectrum (b)

One parameter that has been varied in terms of a sensitivity analysis in the previous project is the time interval between periodic tests of the different redundancies of the model system. Figure 6 compares the results of Monte Carlo simulations using AnTeS modules 2 and 3 with those of the previous project (using fault trees). Also this comparison shows a nearly perfect match.

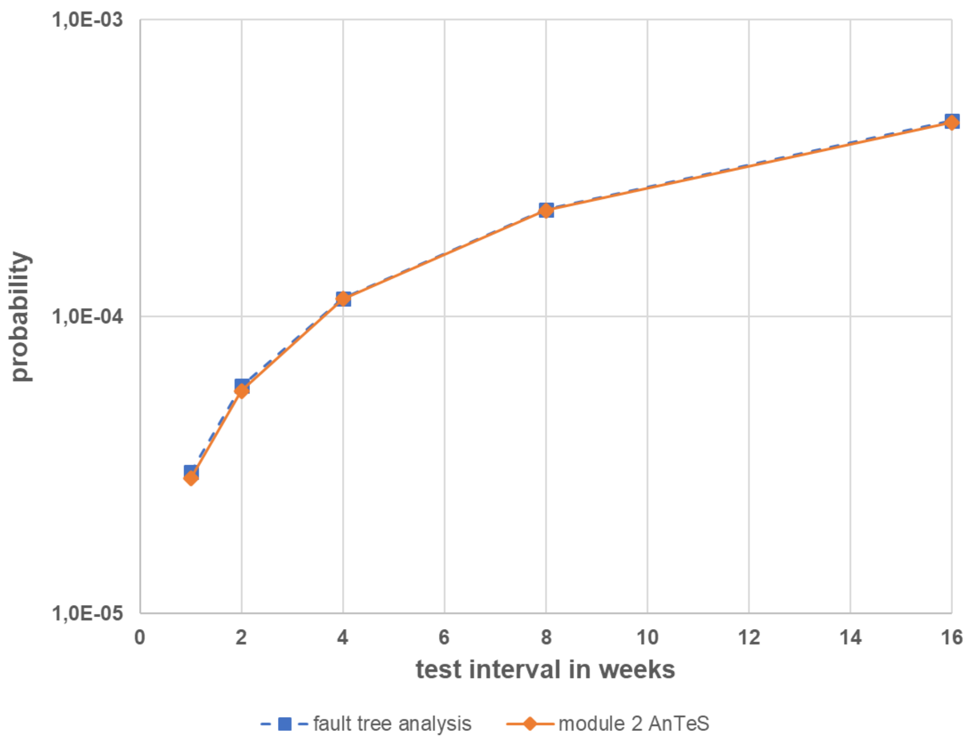

Figure 6: Sensitivity analysis of the effects of different test intervals on the probability of failure on demands of a dual redundant model system using fault tree analysis and module 2 of AnTeS

4 CONCLUSION

With the Analysis and Test System (AnTeS) presented here, a flexible and powerful tool for research and method development in the field of digital I&C is available at GRS. Depending on the analysis requirements, the modules of AnTeS can be variably combined and adjusted to the required extent for a wide variety of projects considering different I&C architectures and components. Conceivable automatic and manual analyzes with AnTeS include, for example, failure modes and effects analyzes and Monte Carlo simulations. As demonstrated by an example, these analysis methods are an objective complement to existing external and GRS developed methods.

5 REFERENCES

/BFE18/ Bundesamt für kerntechnische Entsorgungssicherheit (BfE): „*Licensing of safety critical software for nuclear reactors. Common position of international nuclear regulators and authorized technical support organizations*”
© 2018 Bel V, BfE, CNSC, CSN, ISTec, KAERI, KINS, ONR, SSM, STUK, NSC

/GRS17/ „*Erforschung von Ausbreitungswegen von Softwarefehlern in softwarebasierter Leittechnik in Kernkraftwerken*“, BMU 3617R01331

/GRS18a/ C. Müller, J. Peschke, E. Piljugin: „*Entwicklung und Erprobung eines Werkzeugs zur Sensitivitätsanalyse der Fehlerauswirkungen in der sicherheitsrelevanten digitalen Leittechnik*“, GRS report, GRS – 494, March 2018

/GRS18b/ „*Forschungsarbeiten zur Weiterentwicklung der Methode der Sensitivitätsanalyse zur Bewertung von Fehlerauswirkungen auf ein Leittechnik-Testsystem*“, BMU 4718R01314

/GRS18c/ „*Entwicklung einer Bewertungsgrundlage für rechnerbasierte und programmierbare Leittechniksysteme in kerntechnischen Anlagen und Erforschung des Weiterentwicklungsbedarfs der dazugehörigen Anforderungen in der Leittechnik*“, BMU 4718R01530

/GRS19/ Entwicklung einer Methode zur Bewertung von Vorkehrungen gegen potentielle Fehler bei Softwareänderungen sicherheitsrelevanter Leittechnik, BMU 4719R01374

/KIM06/ Kim, Suk Joon: “*A method for evaluating fault coverage using simulated fault injection for digitalized systems in nuclear power plants”*, Reliability Engineering & System Safety, Volume 91, Issue 5, S. 614-623, May 2006

/LEE17/ Lee, S. J.: “*Fault-weighted quantification method of fault detection coverage through fault mode and effect analysis in digital I&C systems*”, Nuclear Engineering and Design, Volume 316, S. 198-208, May 2017

/MAT19/ https://de.mathworks.com/products/simulink.html

/NEA15/ OECD/NEA: “*Failure Modes Taxonomy for Reliability Assessment of Digital Instrumentation and Control Systems for Probabilistic Risk Analysis”*, NEA/CSNI/R(2014)16, February 2015

/NRC04/ US NRC: “*Advanced Reactor Licensing: Experience with Digital I&C Technology in Evolutionary Plants*”, NUREG/CR-6842, April 2004

/RIS19/ http://www.riskspectrum.com/, Lloyd’s Register Consulting – Energy AB, Sweden, August 2019

/RSK11/ RSK/ESK-Geschäftsstelle: „*Rechnerbasierte Sicherheitsleittechnik für den Einsatz in der höchsten Sicherheitskategorie in deutschen Kernkraftwerken, Darstellung der Beratungsergebnisse der RSK-Arbeitsgruppe (ERL)*“

http://www.rskonline.de, 2011

/TXS19/ https://www.framatome.com/EN/customer-1324/teleperm-xsbased-modular-safety-ic.html, August 2019

2 WASTE MANAGEMENT, DECOMMISSIONING & DISPOSAL

Methodology of an explosion safety assessment of sorption processes for SNF and waste treatment

Alexey Rodin

Scientific and Engineering Centre for Nuclear and Radiation Safety / Russia, Moscow, 107140, Malaya Krasnoselskaya st. 2/8, bld. 5, E-mail: rodin@secnrs.ru

Abstract:

Sorption processes are widely used for spent nuclear fuel and waste treatment to separate radionuclides and reduce the activity of aqueous solutions. Organic resins may interact with a nitric acid and nitrates and generate gases and heat that could lead to an explosion and release of radioactive material. The presence of heat generating radionuclides in a media increases the potential hazards of sorption systems. The approach for safety assessment of sorption processes is developed and described in detail. It includes several steps which assist to assess safety with different levels of conservatism. The developed approach allows analysing failures such as lack of heat removal or operator errors as well as setting safety limits at an acceptable level. Examples for the main assessment steps and their implementation are given.

1 INTRODUCTION

Nowadays the problems of spent nuclear fuel (SNF) and radioactive waste (RW) are limiting the development of nuclear energy. SNF reprocessing and RW volume reduction are the options to solve these problems by implementations of efficient methods such as an extraction and re-use of the major part of the radionuclides and subsequent sorption processes used for a sophisticated cleaning of water solutions. The most developed technology for the partitioning of radioactive elements and reduction of RW activity are still based on hydrometallurgical processes with nitric acid solutions [1, 2]. However, these processes have some disadvantages such as the possibility of interactions of organic components with nitric acid and nitrate ions. These interactions could lead to the release of significant amounts of gaseous products and heat and should be limited by using safety measures as for example, the setting of safety limits, the design of emergency heat removal systems, properly designed valves etc. Examples for consequences of such interactions in sorption systems were reasons of incidents mentioned in [3 - 7]:

- 26/06/1962 Fontenay-Aux-Roses Dowex 1-X4 resin with Pu in nitric acid
- 14/07/1963 Rocky flats. Dowex 1-X4 resin with Pu in nitric acid
- 6/11/1963 Plutonium processing facility, Hanford, USA – Exothermic reactions in a plutonium-loaded anion exchange resin;
- 23/07/1964 Brookhaven National Laboratory
- 30/08/1976 Hanford, USA - Chemical reactions of nitric acid with cation ion-exchange resin;
- 17/07/1993 Mayak, Russia - Thermal-chemical explosion at an ion-exchange column.

Assessment of such hazards is complicated due to the technical impossibility of investigation of these interaction reactions in full-scale experiments and with radioactive elements because of extremely high costs and due to the need to ensure the safety of the experimentalists. For this reason, only a few options are available. One of them is thermodynamic modelling, but with its own limitations. Another one is the investigation of small real samples with subsequent simulation of the chemical interactions at full-scale. The combination of these methods is recommended for the safety assessment of sorption systems for SNF reprocessing processes by the developed guide RB-125-17 «Fire- and explosion safety assessment of sorption systems for reprocessing SNF» [8]. The scheme of safety assessment is shown in Fig. 1.

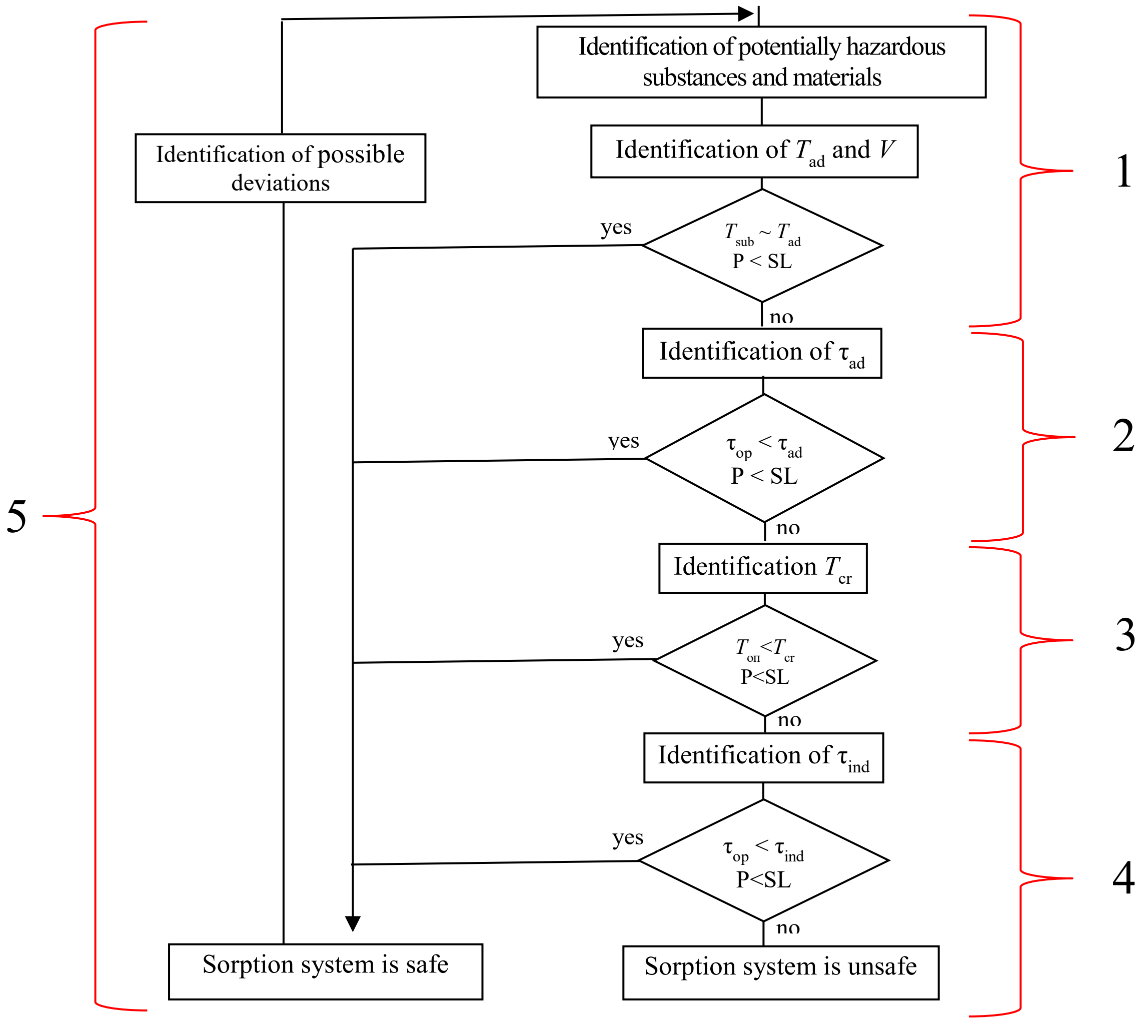

Fig. 1 The safety assessment scheme for sorption systems is implemented in the safety guide

2 SAFETY ASSESMENT STEPS

The approach implemented in the document is based on gradually decreasing conservatism in the assessment. On one hand it assists to save resources when parameter values for processes are far away from the critical points, but on the other hand it allows the safety specialist to set operational limits on acceptable parameter value levels and justify them. The scheme could be divided in five general parts shown in Fig. 1 (1-5), and each of them may be executed using different methods.

2.1 Identification of potentially hazardous materials and maximum parameter values

The first part (1) is executing the analysis of the processes such as sorption, desorption, flushing to determine potential hazardous chemicals. Firstly, it is recommended to find the most dangerous substance. It might be mixtures with highest concentration of reductants and oxidants, or heat generating radioactive elements, or the most degraded one, or with lowest heat transfer coefficient or other with critical properties. Afterwards, parameters such as the adiabatic temperature (T_{ad}) and the volume of the gaseous products (V) should be calculated using a conservative approach. Here, it is necessary to make a decision about the acceptance of the decomposition this substance by comparison of these parameters (P) with safety limits (SL) such as the pressure value for the damage of the sorption column or others.

For example, for the sorption processes including sulfonic acid ion-exchange resin (KU-2*8, scheme of chain is shown in Fig. 2) one of the potential hazardous combinations could be the mixtures of resin and nitric acid solution.

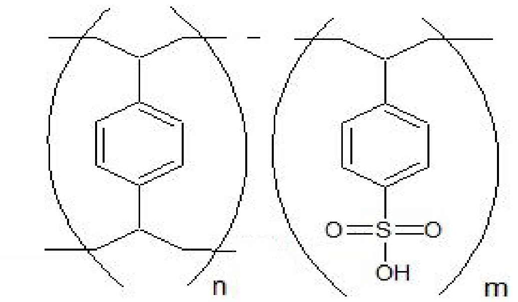

Fig. 2 The sulfonic acid ion-exchange resin KU-2*8

If data about the products of initial components interaction are absent, energy of decomposition of resin mixtures and nitric acid solution could be estimated by a conservative calculation methods of heat release maximization, as used in software [9], or other ones, primarily supposing H_2O, CO_2, N_2 formation. The problem of the estimation of heat of resin formation may be solved by using Benson group methods [10] or similar. The conservatively calculated heat of decomposition diagram for the mixture of KU-2*8 with nitric acid for isochoric conditions is shown in Fig. 3. The following combination of reactions are considered:

$$C_{18}H_{16}SO_3H_s + nHNO_{3_l} \xrightarrow{n=1.5} 16.875C_s + 0.75N_{2_g} + S_s + 4.5H_2O_l + 1.125CH_{4_g}$$

$$C_{18}H_{16}SO_3H_s + nHNO_{3_l} \xrightarrow{n=7} 12.25C_s + 3.5N_{2_g} + S_s + 12.5H_2O_l + 5.75CO_{2_g}$$

$$C_{18}H_{16}SO_3H_s + nHNO_{3_l} \xrightarrow{n=20} 9N_{2_g} + 17H_2O_l + 18CO_{2_g} + 2HNO_{3_l} + H_2SO_{4_l}$$

It was suggested that the higher the ratio of resin and nitric acid, the higher the formation of more oxidized components; lower ratios lead primarily to the formation of water, and the remaining oxygen forms carbon dioxide.

A conservative calculation shows that for mixtures of KU-2*8 with 4 and 12 mol/l nitric acid the heat of decomposition is between 1000 and 2000, and 2000 and 4000 kJ/kg, respectively.

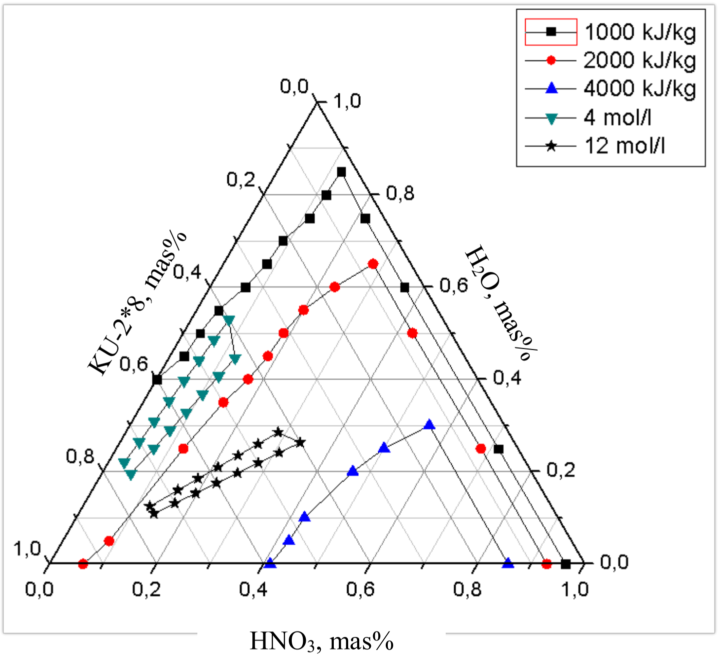

Fig. 3 The composition diagram of the mixture KU-2 * 8 and nitric acid with isolines of the heat of decomposition

These calculations show that with rapid energy release, the temperature can increase by hundreds of degrees Celsius (heat capacity less than 4 kJ/kg*°C, which can be dangerous for the equipment. This means that the kinetics of heat release should be investigated to show that the reactions do not become a runaway. For this, the following part of the assessment is provided.

2.2 Assumption of adiabatic conditions

The second part (Fig. 1 (2)) focuses on the determination of the time to reach the maximum rate of chemical decomposition under adiabatic conditions (τ_{ad}). In this part information about the kinetics of the chemical reactions occurring in technical media is needed. There is essential step of assessment necessary to provide the mathematical kinetic model for the chemical reactions, which is also most complicated one. In [11] an approach to develop kinetic model is described.

A formal kinetic description of the thermal analysis data has been used to develop a kinetic model. Using the data of differential scanning calorimetry (DSC), a mathematical reaction model for decomposition of pyridine resin (VP-1AP) in the nitrate form has been developed, which produced results that are in good agreement with the experimental data. DSC data and the model prediction are shown in Fig. 4.

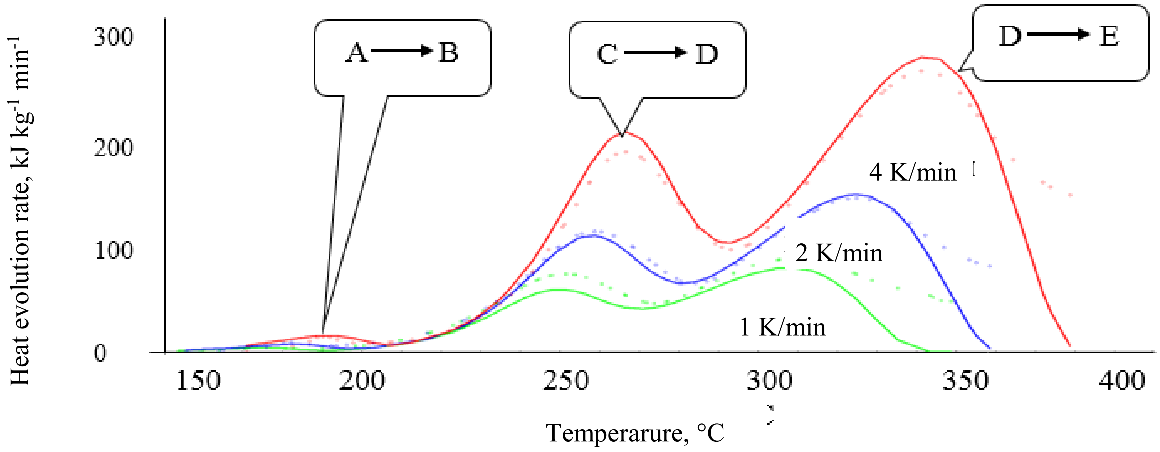

Fig. 4 Temperature dependence of the specific heat evolution rate at different heating rates (points: experimental data; lines: calculation)

The parameters of decomposition reactions are shown in Tab. 1 [11].

Tab. 1 The parameters of decomposition reactions

Parametr	(A → B) $w_1 = k_{01} * \exp\left(-\frac{Ea_1}{RT}\right) * (1-\alpha)^{n_1}$	(C → D) $w_2 = k_{02} * \exp\left(-\frac{Ea_2}{RT}\right) * (1-\alpha)^{n_2}$	(D → E) $w_3 = k_{03} * \exp\left(-\frac{Ea_3}{RT}\right) * (1-\alpha)^{n_3} * (z_0 + \alpha^m)$
$\ln(k_{0i})$, ln(1/s)	31,1±1,1	33,2±1,2	24,6±0,9
Ea_i, kJ/mol	140,0±4,2	172,1±4,4	151,2±3,9
n_i	0,80±0,06	1,35±0,12	3,05±0,35
m	-	-	1,8±0,35
$\ln(z_0)$	-	-	0,55±0,021
Q_i, kJ/kg	130±18	2090±120	6450±270

where w_i is heat evolution rate (s^{-1}) for i step of decomposition reaction

The predictions of runaway reactions in grams scale tests using the kinetic model based on differential scanning calorimetry data are shown in Fig. 5 [11].

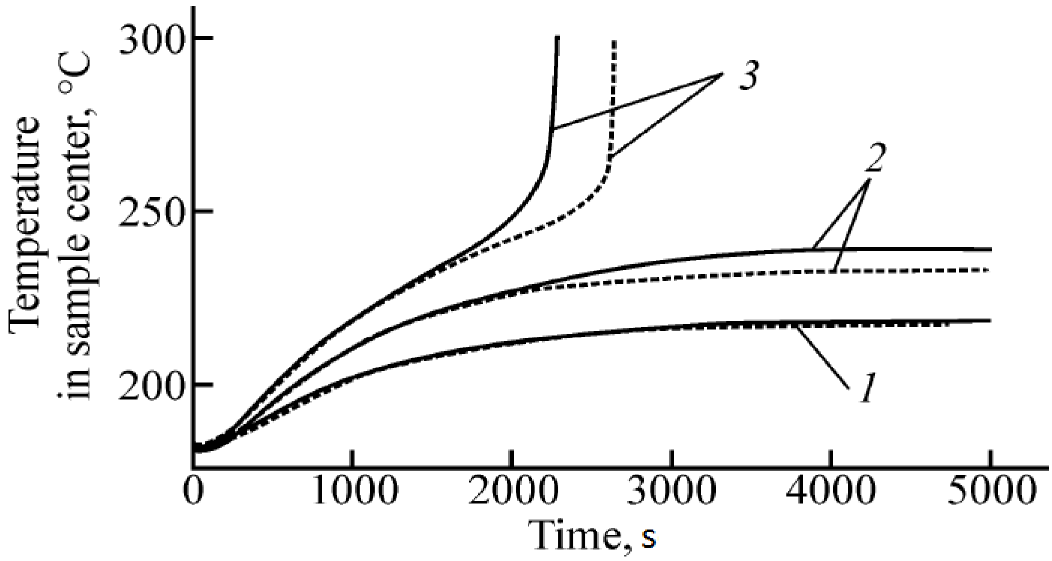

Fig. 5 Experimental and calculated variation of temperature in the center of a sample of VP-1AP resin in the nitrate form at different thermostat temperatures. Thermostat temperatures in °C: (1) 220, (2) 230, and (3) 243. Solid lines: model calculations; dashed lines: experimental data

This example also shows that critical conditions can be found with accuracy acceptable for technical purposes. It was demonstrated by mathematical modeling the critical temperature is about 240 °C, and experiments confirmed that at 230 °C there is no explosion, but at 243 °C explosion has been observed. This shows the possibility of developing kinetic models that could be used for safety assessment.

Using finite element methods or similar for the development of decomposition models for mixtures, it is possible to calculate the temperature dependence of mixtures as a function of time for adiabatic conditions. A general view of such a dependence is shown in Fig. 6.

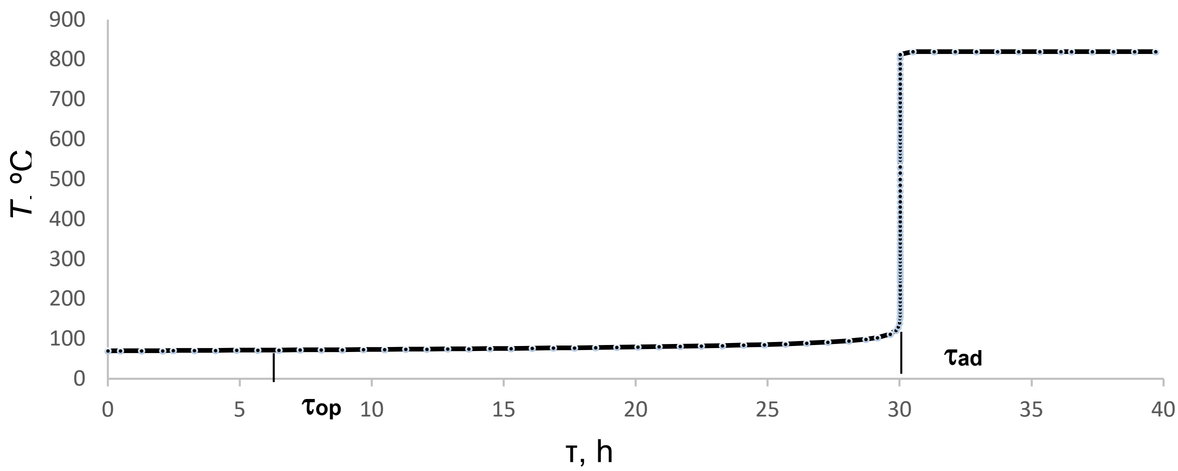

Fig. 5 The temperature of the mixture as a function of time

By comparing the estimated τ_{ad} with the time for normal operation (τ_{op}), a decision can be made whether safety ($\tau_{ad} >> \tau_{op}$) is ensured or not. If there is a high risk for runaway reactions (τ_{op} > or $\simeq \tau_{ad}$) the next stage of assessment may be carried out.

2.3 Evaluation of critical temperature and time to maximum rate

The third and the fourth part (Fig. 1 (3,4) are related to each other and for both of them it is necessary to create a full model of the processes. This model should include all of the heat sources and losses. In some cases, when the kinetic model of decomposition is simple, simplified analytical solutions and criteria can be used to evaluate safety as described in Semenov [12], Frank-Kamenetsky [13] or Todes [14]. In other case, when the kinetic model of decomposition is complex, numerical simulations are necessary.
The criteria are similar to the previous part, but in the third part, it should be additionally estimated if there is a general possibility for an explosion under initial conditions. That means the critical temperature (T_{cr}) has to be found and compared with operational one (T_{op}).
An example for temperature curves for super- and sub- critical conditions are shown in Fig. 6.

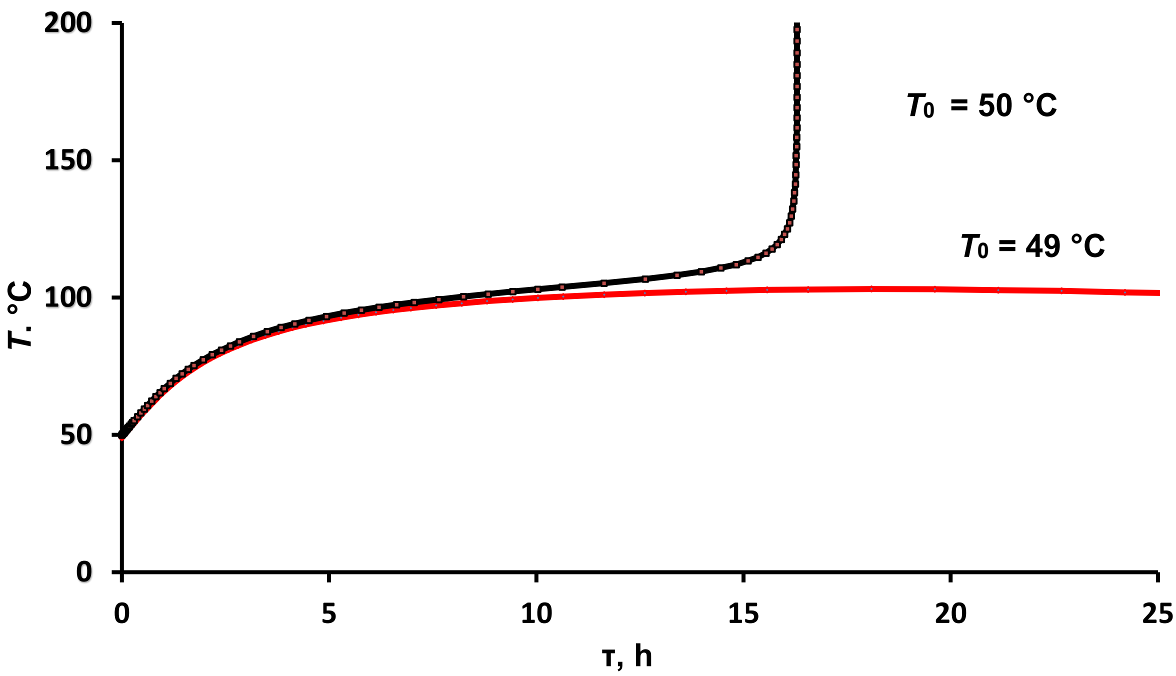

Fig. 6 The evolutions of temperature for super- and sub- critical conditions

For supercritical conditions, the temperature increases exponentially while for subcritical conditions, the reactions slow down without an explosion. If the safety limits are violated after the fourth part, the initial conditions are recommended to be considered as dangerous.

2.4 Analysis of deviations

An essential part of each safety assessment is the analysis of possible process parameter deviation or uncertainties. It is rare under “normal” parameters and without any failures, the reactions can become the runaway. More often only the combination of equipment failures or operator errors lead to an accident. For this reason, the analysis should aim to identify such events or their combinations in order to develop safety measures.

Following major events are recommended to be considered:

- errors or failures that lead to the loading of additional heat sources (increased concentration of radionuclides);
- process shutdown for a long period;

- contact of the resin with high concentration nitric acid;
- errors in reagent dosing sequence.

Other events should be considered, if there is a risk that they can lead to the formation of unexplored mixtures or affect critical conditions. The safety assessment scheme under additional conditions (failures) is the same as at the beginning.

3 CONCLUSIONS

For the nuclear industry, the problem of assessing the safety of reactive hazards, as it is called in [15], is an important part of radiation safety, since such to runaway related reaction events can have radiological consequences. Evaluation methods should be developed taking into account the latest achievements of science and technology. The developed approach can be used to assess safety, since it is based on a scheme of gradual decreasing of conservatism and implements both time-tested approaches and methods of mathematical simulation. For a technical support organization, the approach allows to have a choice whether to save resource when process parameters are far away from critical points, or to carry out detailed safety evaluation with taking into account many aspects. For sorption systems, the developed approach allows the operator to determine the critical conditions and enhance safety by designing additional safety systems.

Developing reactive hazard identification approaches can be associated with improvement of calculations methods that could solve the problems of the initial separation of a potentially hazardous substance from a safe one. The improvement of the approach is also associated with the introduction of methods for determining the consequences, such as the calculation of shock waves and the prediction of the release of radioactive elements beyond the barriers. The implementation of probabilistic analysis methods in the safety assessment scheme is necessary to determine the priorities of the facility modernization from the safety point of view.

4 REFERENCES

[1] Advanced Nuclear Fuel Cycles and Radioactive Waste Management, OECD NEA No. 5990 (2006).

[2] State-of-the-Art Report on the Progress of Nuclear Fuel Cycle Chemistry, OECD NEA No. 7267 (2018)

[3] Nuclear Safety 1968, Vol.9 №5 p.395

[4] Significant incidents in nuclear fuel cycle facilities, IAEA-TECDOC-867, IAEA, Vienna (1996).

[5] Calmon C. «Explosion hazards of using nitric acid in ion-exchange equipment», Chemical engineering, 1980, №23, 271 p.

[6] Milest F.W. «Lon-Exchange-Resin System Failures in Processing Actinides», Isotopes and Radiation Technology, 1969, Vol.6, N 4., p. 428-440

[7] Glagolenko Yu.V. «Analysis the causes of depressurization of the sorption column, dedicated to obtain Pu238 on radioisotope plant» MS «MAYAK», Radium institute named after V.G.Khlopina, ATOMINFORM, 1996

[8] Safety guide «Fire- and explosion safety assessment of sorption systems for reprocessing SNF» RB-125-17, Rostechnadzor (2017).

[9] The ASTM Computer Program for Chemical Thermodynamic and Energy Release Evaluation CHETAH

[10] Benson S. W., Cruickshank F. R., Golden D. M., Haugen G. R., O'Neal H. E, Rodgers A. S., Shaw R., Walsh R. «Additivity rules for the estimation of thermochemical properties» Department of Thermochemistry and Chemical Kinetiks, Stanford research institute. Menlo park, California. April 24, 1968. p .279-324

[11] V. V. Kalistratova, A. V. Rodin at al / Kinetics of Thermal Degradation of VP-1AP Anion-Exchange Resin in the Nitrate Form // Radiochemistry, Vol. 60, No. 3, pp. 287–293 (2018).

[12] Semenov N.N. Thermal theory of combustion and explosion. Usp Fiz Nauk 23:25–292 (1940).

[13] Frank-Kamenetskii, D.A. Diffusion and heat transfer in chemical kinetics, in The Theory of Thermal Explosion (ed.J.P.Appleton), Plenum Press, New York (1969).

[14] Todes OM, Melentev PV Theory of thermal explosions III. Thermal explosion for autocatalytic reactions. Zh Fz Khim 14:1026–1042 (1940).

[15] U.S. Chemical Safety and Hazard Investigation Board. Hazard Investigation. Improving Reactive Hazard Management. Report No 2001-01-H (2002).

Long-term chemical evolution of wasteforms predicted by geochemical modelling

E. Wieland

Paul Scherrer Institut, Laboratory for Waste Management, 5232 Villigen PSI, Switzerland

Abstract:

In Switzerland, the currently favoured concept for disposing of low- and intermediate-level radioactive waste (L/ILW) envisages storage of waste packages in a deep geological repository. The near field of the L/ILW repository will consist of very different waste materials with very different reactivity, such as metallic and organic wastes, which are encapsulated in cementitious matrices. The barrier function of the cementitious near field is expected to change with time due to degradation of the waste materials with time and the interaction of the degradation products with cement paste. This study aims to present an approach based on geochemical modelling that allows the degradation processes and, related to that, alteration of the solidifying cementitious matrix in a cement-stabilised model wasteform to be predicted over the entire period of concern for the L/ILW repository. For the geochemical modelling it was assumed that the cementitious matrix used to condition the wasteform is fabricated either with siliceous or calcareous aggregates.

1 INTRODUCTION

The Swiss disposal concept for low- and intermediate-level waste (L/ILW) envisages that waste packages will be placed in the vaults of a deep geological repository and then surrounded by cementitious backfill, thus allowing waste isolation by a multi-barrier system in a stable geologic formation [1]. Cementitious materials will be used as encapsulants and backfill as well as for construction. The variety of waste materials to be disposed of in the L/ILW repository and their degradation with time may be of importance in conjunction with long-term performance of the repository system. Waste degradation and the interaction of the degradation products with cementitious materials could alter performance of the multi-barrier system with time while it is acknowledged that the impact on radionuclide release may be limited as the inventory of radionuclides in the L/ILW repository and the radiotoxicity associated with L/ILW are much less than those in the planned repository for spent fuel and high-level waste.

To the best of our knowledge the effect of degradation processes of waste on the evolution of the chemical conditions in waste packages has not yet been explored in detail while it was suggested that state-of-the-art modelling of the performance of waste containers and waste packages may support safety assessment (SA) [e.g. 2]. Recently, an approach has been proposed which allows the long-term evolution of the chemical conditions of cemented wasteforms to be assessed by geochemical modelling [3]. The approach is based on the use of the Gibbs energy minimisation selektor (GEMS) software package for thermodynamic modelling and the development of appropriate models for the degradation of waste materials and the interaction of the degradation products with the cementitious matrix used as encapsulate. The degradation processes include i) (bio)chemical degradation of organic waste and the interaction of CO_2 (and it bases) with hydrated cement, ii) corrosion of the metallic waste materials, and iii) internal degradation of hydrated cement due to interaction of alkaline cement pore water with reactive siliceous aggregate in concrete and backfill [4].

In this study, the effect of different types of aggregates used to fabricate the solidifying cementitious matrix on the chemical evolution was explored with the aim of assessing design options for a model wasteform. Geochemical modelling was performed on the assumption that either siliceous or calcareous aggregates are employed. The modelling provides geochemical information (volume and chemical composition of solid, liquid and gaseous phases) over the period of concern for the L/ILW repository, which is assumed to be 10^5 years. Note, however, that the modelling approach is based on the conceptual assumption of a "mixing tank", i.e. all materials are evenly distributed in the waste package and further, that transport processes are not rate-limiting. Hence, the approach does not provide information on the spatially resolved evolution of the chemical conditions in a waste package and, in particular, it does not account for the effect of gas production on transport processes in the waste package.

2 WASTEFORM

A potential wasteform produced during decommissioning of nuclear power plants was considered for this study. Its inventory has been selected from the database for a model wasteform (Table 1) [5]. The waste will be placed in concrete containers and stabilised by a solidifying cementitious material. The wasteform mainly contains metals while the inventory of low molecular weight (LMW) organics and polymeric polyvinylchloride (PVC) is small.

Table 1: Alphabetic order of the materials present in the model wasteform.

Material	Mass (kg)	Material	Mass (kg)
Aluminium	3.17	PVC	0.752
Brass	124	Quartz sand	1950
Cement (unhydrated)	1250	Silica fume ("Micropoz")	375
Clinoptilolite	187	Steel	5930
Copper	139	Urea	4.49
Iron (cast)	210	Water	757
LMW organics	12.92	Zinc	0.557

The solidifying cementitious matrix is made by adding water to a mixture consisting of sulphate-resisting ordinary Portland cement (OPC), clinoptilolite, silica fume and aggregate (water-to-cement (w/c) ratio of ~ 0.5). It should be noted that only the solidifying cementitious matrix was taken into account for the modelling while other concrete structures were not considered, in particular concrete of the emplacement container.

3 DEGRADATION PROCESSES

The relevant degradation processes are schematically summarised in Figure 1. Internal degradation of the solidifying cementitious matrix is one of the deterioration processes considered in this study. Silica release from siliceous aggregates is a commonly observed process in ageing concrete structures. Presence of significant amounts of alkalis in OPC gives rise to high pH of the pore solution, which promotes the dissolution of the siliceous aggregates. The modelling scenario implies that the solidifying cementitious matrix will be fabricated either by using siliceous aggregate (e.g. quartz sand) or calcareous aggregate (e.g. limestone), respectively. In contrast to quartz and silicates, calcite is stable in cementitious environments and therefore, the use of calcareous aggregate does not promote internal degradation of concrete.

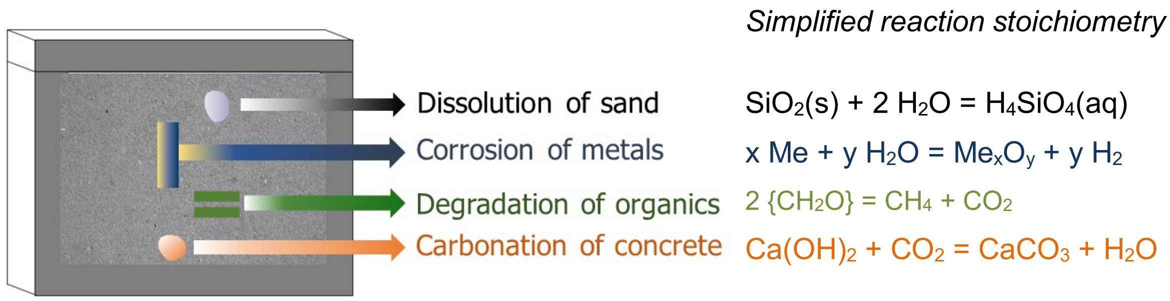

Figure 1: Schematic presentation of degradation processes in the waste package.

The dissolution of quartz, used as surrogate for siliceous aggregate (e.g. sand), was modelled in terms of a (simplified) pH-dependent rate for neutral and alkaline conditions by considering grain size and inventory of the aggregate used to fabricate the solidifying cementitious matrix.

The cement-stabilised wasteform contains metals (aluminium, brass, iron/steel, zinc) and likely air due to voids present in the waste package while no information on the exact volume of air is available. Oxic corrosion of the metals is likely to occur in the early stage of the evolution of the wasteform while this stage is expected to be short as the inventory of oxygen is limited and residual oxygen will be consumed shortly after sealing the waste package. Therefore, oxic corrosion of metals is considered to be negligible and the corrosion of metals will be anoxic in humid/wet conditions in the long term, which produces hydrogen gas ($H_2(g)$) (Figure 1). The corrosion rates correspond to reference values used in connection with SA. They were estimated by considering the surface areas of the various metallic wastes [5]. In particular, the rates account for faster iron/steel corrosion in weakly alkaline conditions compared to strongly alkaline conditions while no pH dependence of corrosion was considered in the case of aluminium, brass and zinc. The behaviour of copper was considered in terms of thermodynamic equilibrium as no corrosion rates have been reported for the given conditions.

Decomposition of organic matter is one of the most important deterioration process in wasteforms [3]. Organic wastes have been classified as either readily degradable, such as cellulose and LMW organics or slowly degradable, such as acrylic glass, bitumen, plastics, polystyrene, PVC, resins and rubber which may be resistant to complete degradation. Decomposition of organic waste, presumably catalysed by microbes, will produce methane (CH_4) and carbon dioxide (CO_2) according to the specific reaction stoichiometry of the individual organics [3]. To this end, organic matter was characterised in terms of the mean oxidation state of carbon and the carbon content, which were determined from appropriate monomeric components. The degradation rates of the organics were estimated on the basis of reference gas generation rates currently used in conjunction with SA. The rates were converted into degradation rates of organic matter in accordance with first-order kinetics [3]. Carbon dioxide produced in the course of the decomposition of organics dissolves in the alkaline porewater, deprotonates to form its bases (HCO_3^{2-}, CO_3^{2-}) and, upon supersaturation, precipitates as calcium carbonate. Reaction with CO_2 (and its bases) gives rise to the conversion of Ca-bearing cement phases, in particular portlandite and calcium silicate hydrates, into calcium carbonate (Figure 1).

4 GEOCHEMICAL MODELLING

The modelling approach corresponds to that reported in detail elsewhere [6] and it is based on the following step-by-step procedure: i) The inventory of waste materials was selected from the database and arranged for modelling, e.g. by merging the inventories of urea and LMW organics for the current wasteform (Table 1), ii) the initial composition of the solidifying cementitious matrix used to condition the waste was modelled (Figure 2), and eventually iii) the effect of the degradation of organic waste, metal corrosion and internal degradation of the cementitious matrix in the presence of siliceous aggregate on the temporal evolution of the chemical condition in the waste package was modelled (Figure 3). It is to be noted that the latter process is not relevant in the case of calcareous aggregate.

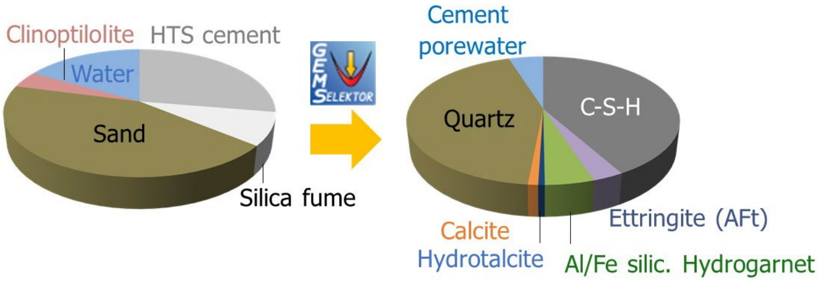

Figure 2: Initial composition of the mix (left) and modelled composition of the solidifying cementitious matrix after hydration (right).

The phase assemblage and solution composition of the cementitious matrix correspond to a “low pH” cement as portlandite was completely converted into C-S-H phases by the reaction with silica fume and clinoptilolite (Figure 2). The initial pH was 12.68 while the initial Ca/Si ratio of the C-S-H phases was low (Ca/Si ratio = 1.01). Ettringite (AFt), Al/Fe siliceous hydrogarnet (Fe(III)-bearing phase), hydrotalcite (Mg-bearing phase) and calcite were the main constituents of the cement paste in addition to C-S-H phases. A positive E_h indicated initially oxidising conditions. Replacing siliceous by calcareous aggregate had, besides differences in the quartz and calcite contents, no significant effect on the mineral composition of the paste as well as the composition of the pore solution at equilibrium. Modelling the composition of the solidifying cementitious material implicitly assumes that the time required to reach the equilibrium state of the cement paste is much shorter than the period of concern for the L/ILW repository.

Geochemical modelling of the wasteform was performed by assuming the following scenarios: 1) Use of either siliceous or calcareous aggregate, 2) formation or absence, respectively, of zeolites, 3) limited or unlimited water availability. Limited water availability implies that only free water entrapped in the pore space of the solidifying cementitious matrix is available for reaction while in the case of unlimited water availability, the containment of the wasteform does not remain “intact” and gas (or water) can exchange through one or more small openings or by vents, such as small holes drilled in the walls of the drums (mm diameter or smaller). In this case, availability of water is not limited by free water in the waste package but by the humidity outside the containment as vapour (or liquid) transport from the surrounding backfill into the waste package occurs.

Selected results from the modelling scenario with unlimited water availability and the use of calcareous aggregate are exemplarily displayed in Figure 3.

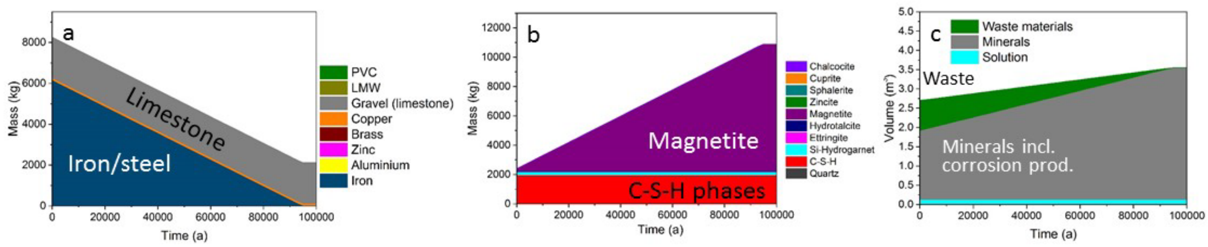

Figure 3: Time-dependent evolution of the wasteform at unlimited water content, calcareous aggregate, and possible formation of zeolites, a) waste materials and gravel, b) cement phases and minerals, c) volume of waste, cement phases and minerals, and porewater.

At unlimited water availability the wasteform was found to react over the entire period of concern for the L/ILW repository while reactivity of the wasteform already stopped after a few thousand years if the availability of water was limited [3, 6]. The results further showed that the use of calcareous aggegate instead of siliceous aggregate prevents formation of zeolites as conditions in the wasteform remain hyperalkaline (pH ~ 12.7). By contrast, zeolite formation was observed if siliceous aggregate was used. In addition, a decrease of the Ca/Si ratio of the C-S-H phases was observed due to the reaction of silica released during the dissolution of siliceous aggregate with C-S-H phases. Zeolite formation and alteration of C-S-H phases further alkali binding by solids which lowers the pH (OH^- activity) as the alkalis are the main charge-compensating cations in solution. In the resulting weakly alkaline conditions, iron/steel corrosion was accelerated and consequently H_2 production. Using calcareous aggregate, however, iron/steel corrosion occurred at the very low rate relevant to strongly alkaline conditions (Figure 3a). As a consequence of this, magnetite (Figure 3b) and H_2 were steadily produced with time. Furthermore, production of magnetite with time resulted in a continuous increase in the volume of the wasteform (Figure 3c).

5 CONCLUSION

The geochemical modelling approach reported in this study allows for an assessment of the effect of degradation processes of waste materials on the long-term performance of waste-forms. The approach is well suited for “screening” applications as it allows relevance and consequences of individual chemical processes on the chemical evolution of a wasteform to be assessed at various initial conditions, such as varying waste inventories and varying compositions of the solidifying cementitious matrix. However, the approach is of limited use if exact predictions of the long-term evolution of wasteforms in time and space are required as the model has been conceptualized on the basis of a “mixing tank”. In particular, the approach does not account for spatially resolved evolution of the chemical conditions in a waste package and the effect of gas production on transport processes in the waste package, which requires new developments in the framework of coupled two-phase reactive transport modelling [7].

6 REFERENCES

[1] Nagra, 2016. Waste management programme 2016 of the waste producers. Nagra Technical Report NTB 16-01E, Nagra, Wettingen, Switzerland.

[2] T. Sullivan, 2004. Waste container and waste package performance: Modeling to support safety assessment of low- and intermediate-level radioactive waste disposal. Report BNL-74700-2005-IR, Brookhaven National Laboratory, Upton, New York, USA.

[3] E. Wieland, G. Kosakowski, B. Lothenbach, D.A. Kulik, V. Cloet, 2018. Preliminary assessment of the temporal evolution of waste packages in the near field of the L/ILW repository. Nagra Work Report NAB 18-05, Nagra, Wettingen, Switzerland.

[4] G. Kosakowski, U. Berner, E. Wieland, M.A. Glaus, C. Degueldre, 2014. Geochemical evolution of the L/ILW near field. Nagra Technical Report NTB 14-11, Nagra, Wettingen, Switzerland.

[5] Nagra, 2014. Modellhaftes Inventar für radioaktive Materialien MIRAM 14. Nagra Technical Report NTB 14-04, Nagra, Wettingen, Switzerland.

[6] E. Wieland, G. Kosakowski, B. Lothenbach, D.A. Kulik, 2019. Geochemical modelling of the effect of waste degradation processes on the long-term performance of wasteforms. Appl. Geochem. (in prep.).

[7] Y. Huang, H. Shao, E. Wieland, O. Kolditz, G. Kosakowski, 2018. A new approach to coupled two-phase reactive transport simulation for long-term degradation of concrete. Constr. Build. Mater. 190, 805-829.

7 ACKNOWLEDGEMENT

Partial funding for this project was provided by the National Cooperative for the Disposal of Radioactive Waste (Nagra), Switzerland. The author wishes to thank G. Kosakowksi, D.A. Kulik and B. Lothenbach for their helpful contribution to this project.

8 DISCLAIMER

The findings and conclusions in this paper are those of the author and do not necessarily represent the official position of Nagra. The kinetic parameters, materials and inventories used in this study are not necessarily those of future license applications.

Assessing the performances of engineered barrier systems and rock masses from large scale in situ tests at the Tournemire underground research laboratory

DICK P, MATRAY J.M*, DYMITROWSKA M*, MOKNI N*, CABRERA J*, DELERUYELLE F*, DAUZERES A**

IRSN, 31, avenue de la Division Leclerc, 92260 Fontenay-aux-Roses-France

Abstract:

The institute for Radiological Protection and Nuclear Safety (IRSN) develops a wide range of scientific research programmes related to deep geological disposal safety issues in order to support their technical assessment for the French Nuclear Safety Authority (ASN). The research programmes are organised along key safety questions, drawn from the regulatory review on the “feasibility of reversible geological disposal in clay”. They deal with various scientific disciplines such as geology, hydrogeology, geomechanics, geochemistry or physics and are implemented in national and international partnerships. In this framework and during the last decade, IRSN has carried out several large scale in situ experiments in its underground research laboratory (URL) located at Tournemire (South France), to develop and assess new repository monitoring technologies, to quantify the performance assessment of different engineered barrier systems as well as the confinement capabilities of sound and fractured shale host rocks. The experimental results gained from these tests have provided IRSN with valuable independent knowledge and scientific skills in order to assess whether the scientific results, gained by the waste management organisation and their integration for demonstrating the safety of the geological disposal, are acceptable with regard to the safety issues to be dealt within the Safety Case.

1 INTRODUCTION

In-situ investigations within the field of deep geological repositories play a fundemental role in understanding geological, hydrogeological, geochemical, structural and mechanical processes that occur in or around a potential host rock. The data gained from these experiments allow to test various parameters in several situations (nominal or altered) to verify the efficiency and subsequently the safety of specific designs or concepts.

Contrary to laboratory tests, that have well-defined and well-regulated boundary conditions, and thus, a more theoretical explanation of the processes, in-situ experiments are commonly constructed in a more pragmatic and simple manner. Nevertheless, in-situ experiments test a much larger volume of material and are consequently more realistic in terms of representativeness for evaluating the processes that could occur in a real underground repository. Though different, the data obtained from these two methods must not be opposed but combined if one aspires to characterise the long-term properties governing a repository’s evolution.

In this framework and in order to maintain and develop its expertise function in the field of radioactive waste management, IRSN has carried out, for more than 30 years, studies and experiments in its own facilities using a multiscale approach from laboratory, in-situ to modelling investigations. This approach guarantees IRSN an independent and global understanding of a wide range of technical skills and complete datasets necessary to ensure a consistent and high quality technical assessment. The works performed by IRSN with regards to large-scale field tests are located in the Underground Research Laboratory (URL) at Tournemire (South France). The URL is located in a former railway tunnel built over 130 years ago and provides access to a shale formation that has similar geological characteristics to the site chosen by Andra at the Meuse/Haute Marne URL (France).

The objective of this paper is to provide an overview of several large scale in-situ experiments carried out at the Tournemire URL during the last 5 years and to show how they have assisted IRSN in their assessment of the Cigeo project, from a safety point of view. The different projects presented hereafter deal with the confinement properties of a fractured shale rock (Fluids and Faults project), the effeciency of shaft sealing systems (VSEAL) and the near field monitoring of an engineered barrier system (Modern2020 project). The objectives, layouts and main outcomes of each project will be presented as well as their implication to long-term safety.

2 FAULT SEAL INTEGRITY TEST: "FLUIDS AND FAULTS" PROJECT

The objectives of the "Fluids and Faults" project was to constrain a relationship linking permeability, pressure, stress and strain in fault zones in order to assess the long-term performance of fractured shale formations within the context of deep geological disposal of radioactive waste as well as reservoir and basin modelling for CO_2 sequestration. The project comprised (i) In-situ injection tests performed in the Tournemire URL (ii) Laboratory experiments on core samples from the Tournemire URL at the ENS Paris, Université Cergy-Pontoise and CEREGE (iii) Numerical modeling of hydromechanical coupling at the University of Grenoble and CEREGE (iv) Seismic monitoring of the injection tests lead by the université of Nice (Geoazur).

The Tournemire site was selected for this project as it enables an easy access to a strike-slip fault zone that cross-cuts the entire Jurassic sedimentry cover and extends lateraly across the URL for more than 100 m.

2.1 Experimenatal layout

The experiments were carried out in 2014 and consisted of a series of water injections tests in different intervals of the fault zone, from a central injection borehole surrounded by a network of sensors installed in observation boreholes (Figure 1). This network included a fluid pressure measuring chamber, a deformation probe, an electrical resistivity streamer and an array of seismic sensors (accelerometers and 3-component geophones). The injection borehole was equipped with a step-rate injection method for fracture in-situ properties (SIMFIP) probe [1]. The SIMFIP probe was designed to isolate an interval of 2.5 m and included an anchoring system and measurement of optical fiber deformation allowing to measure, with a resolution of a few microns, the relative movements through the injected fracture zone.

The stress field in the vicinity of the test was defined with a series of leak off tests performed in a vertical borehole [2] at 50m from the current experiment. The stress regime is characterized with a σ_1=4 ±2 MPa, horizontal and oriented N162° ±15°, σ_2=3.8 ±0.4 MPa 7-8° inclined from the vertical in the N72° direction and σ_3=2.1 ±1 MPa 7-8° inclined from the horizontal in the N72° direction.

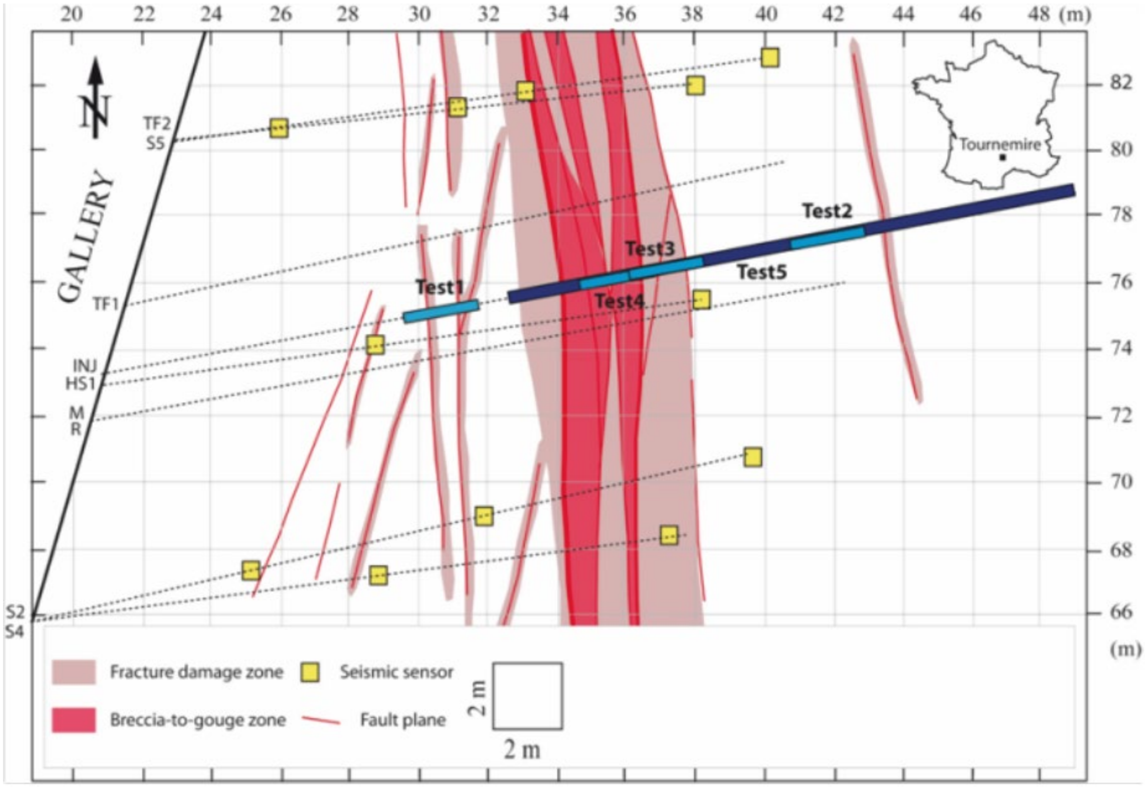

Figure 1: Fault zone architecture and distribution tested intervals along the injection well (de Barros et al. 2016).

2.2 Main results

Two series of tests were performed on the pre-existing fractures within the fault zone. The first series used the SIMFIP probe (Test 1 to 4), while then second series (Test 5) was performed with a single packer system after the partial collapse of the injection borehole.

Two main hydromechanical thresholds were identified from the hydromechanical tests, the first one FPmin (minimum Fracture Pressure) estimated at 2 MPa corresponds to the state of stress along the borehole walls and the second one FOP (Formation Opening Pressure), varying from 1.5 MPa to 4.4 MPa, corresponds to the hydraulic opening of the formation beyond, which fluid injection can be sustained with a steady flow rate. The wide range of FOP in response to the hydraulic pressurisation of the fault zone appears to reflect the different lithologies on either side of the fault and the nature of different cements within fractures (calcite, clay smear). Indeed, the higher FOP pressure measured in Tests 3, 4, and 5 (values of 3.1 to 3.6 MPa) could be related to the higher strength of the calcite sealed fractures, compared to the highly polished and striated surfaces enhanced by pressure solution stimulated in Test 1.

This interpretation is also supported by the Tournemire focal mechanisms assymetric distribution [3] which is seemingly controlled by the structural hetrogeneity within the fault zone. The focal mechanisms are generally located in the eastern damage zone of the fault where the lithology is slightly more carbonate rich and the presence of a high density network of calcite sealed fractures [3]. The aseismic behaviour of the western and damage zone and fault core is probably the consequence of clay fractions exceeding 50 % and the presence of a few calcified structures.

The flow channels induced by the pressurisation of the fault never allowed fluid to cross the entire fault zone, as the flow channels in the western damage zone were never connected with flow channels in the eastern damage zone and core [4]. However, fluid exchanges were noticed within the fault damage zones between natural and induced fractures (excavation damage zone) appear to have taken place and this in spite of the complex architecture of the fault zone and large lateral variations of the fault core thickness [4]. Furthermore, the boundary between the two flow systems (western and eastern zone) doesn't coincide with the whole core but rather the western core/damage zone interface.

The results obtained from this in-situ test indicate that the Tournemire fault zone acts as a fluid barrier and shows heterogeneous hydromechanical properties. This induces modifications on how stress is transferred from the pressure build up. Furthermore, heterogeneity seems to be the main controlling factor for the seismic, mechanical and flow distribution. The experiment suggests that the permeability across such a fault still corresponds to the diffusive regime and thus remains several orders of magnitude below the permeability of channelised flow system over a certain time and/or length scale [4].

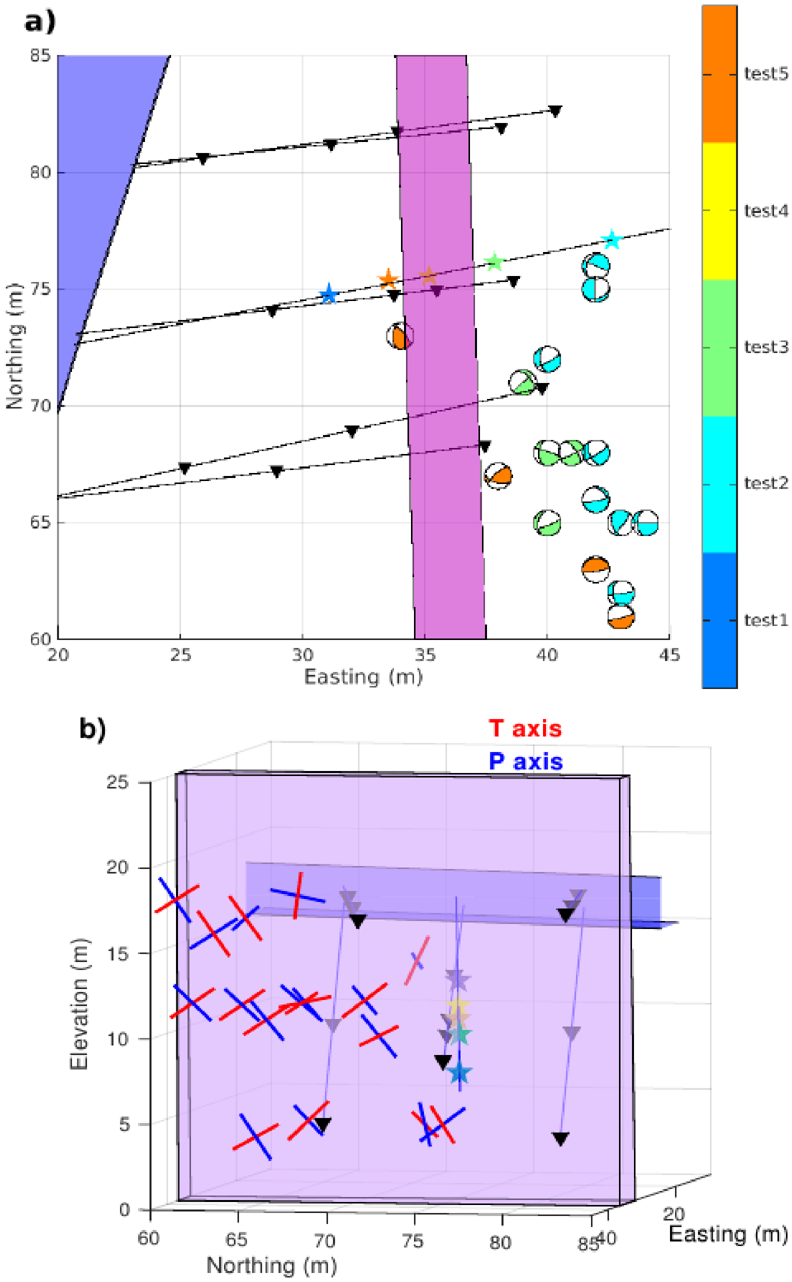

Figure 2: (Top) Focal mechanisms determined from 16 events (see DeBarros et al., 2016 and seismic monitoring report). A majority of events have a nodal plane coinciding with the most frequent orientation of calcite veins and small faults (N-S steeply dipping W). Map view from the east of the location of the microseismic events (P and T axises). Triangles show the sensor positions, purple area is a schematic representation of the fault core and the injection zone for test 5 as stars.The slip direction does not correspond to a coherent stress field, indicating that the stress perturbation caused by the injection of the fluid is sufficiently large to influence induced seismicity [4].

3 PERFORMANCE ASSESSMENTS OF SEALS

Vertical sealing systems of a deep geological disposal are one of the key elements in the containment of this facility, since they constitute the main potential pathway between the nuclear wastes and the biosphere. Understanding migration processes of gas is of great importance for performance assessment and long-term evolution of such facilities. If the gas production rate exceeds the dissolved gas diffusion rate in the pore water of the host rock and the engineered barriers, a gas phase will form and accumulate until the associated pressure buildup becomes sufficiently large to migrate through the surrounding material. The transport of gases in clay-based sealing systems has been the subject of different international research programs during the last two decades (FP7 FORGE Project). Evidence from laboratory experiments suggests that transport in bentonite is controlled by the saturation history of the material, which strongly affects its microstructural features. These changes in the pore network play an important role on the two-phase flow properties and on the initiation of localized pathways during the gas phase invasion. Thus it is important to explore these gas migration properties under different saturation states that can be reached under varying water pressurisation rates. In this context, IRSN has launched the VSEAL project to investigate the impact of gas migration on the long term performance of bentonite based vertical sealing systems, which play a major role. This project relies on two in-situ experiments that will be emplaced in the Tournemire URL and small-scale tests conducted in laboratory.

3.1 VSEAL layout

The generic layout of VSEAL in-situ experiments is based on a bentonite based swelling core confined between two lids. The clay core is composed of a mixture of MX 80 bentonite high density pellets and powder (Figure 3) which are being evaluated as possible sealing materials in deep geological repositories. All these elements will be inserted in a vertical large diameter borehole (1 m diameter, 10 m depth), excavated in Tournemire shale. Water will be injected from the top surface through injection lines connected to the top lid which will slowly saturate the bentonite core. The upper face of the core will undergo a very rapid hydraulic loading while the lower part will remain strongly initially desaturated and will gradually saturate itself in a few years. Under these conditions gas will be injected from the bottom surface to observe the induced perturbations.

Two VSEAL in situ tests are foreseen. The first in situ test VSEAL_1 will be a reference tests, used to observe bentonite re-saturation without gas injection to be able to estimate gas effects. For the second in situ test VSEAL_2 gas will be injected from the bottom surface during the re-saturation phase at time $t0+\Delta t$ to observe the perturbation induced by gas. In each borehole multiple pore pressure, total pressure, and RH sensors will be installed to follow, as best as, possible swelling pressure evolution and water saturation. Various injection gas phases could be performed once the bentonite reaches full saturation.

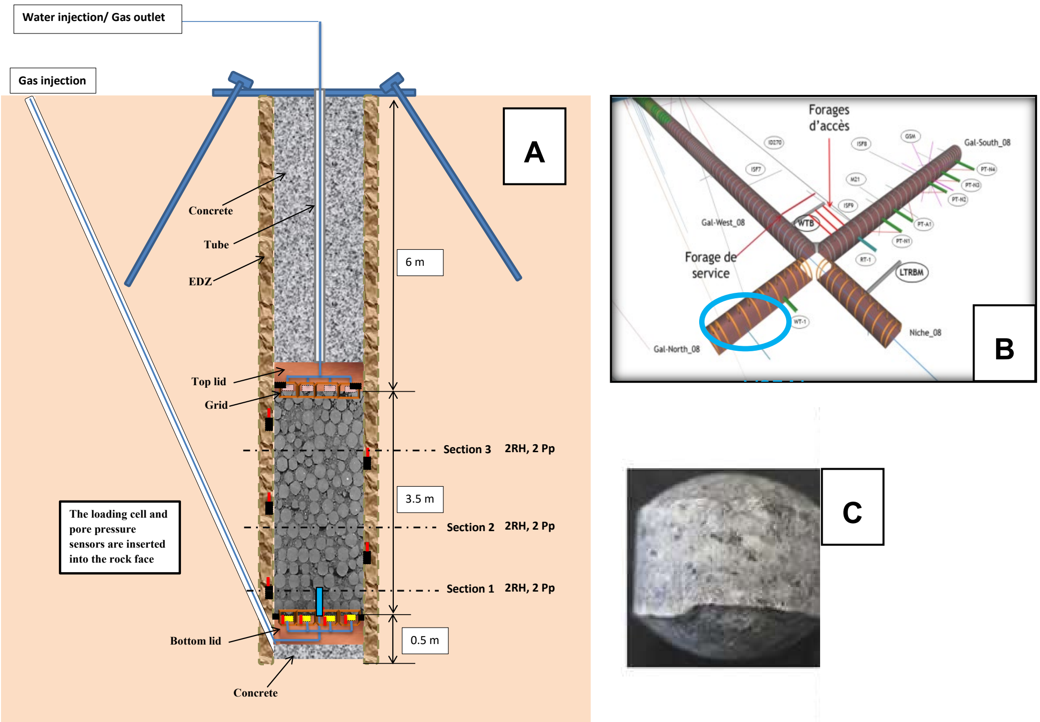

Figure. 3: A- Schematic diagram of the main components of VSEAL in situ tests. B- Location of the VSEAL tests in the Tournemire URL. C- View of 32 mm pellet used in the test.

Prior to the in-situ tests a series of laboratory mock up tests have already been undertaken. Two types of tests have been carried out: (i) mock-up tests focussing on the global behaviour of the bentonite (fast hydration and gas migration) and (ii) interface tests focussing on the hydromechanical behaviour of the bentonite/argillite interface. The results gained from these experiments have enabled to build a quantitative model to gain insight into the coupled hydro-mechanical response of the mixtures.

The aim of these experimental programs is to provide quantitative data to improve process understanding and validate / test modelling approaches used in repository performance assessment. The installation of the in situ test is planned for the end of 2019 and first results should be available by 2022.

4 MODERN2020 IN SITU EXPERIMENTS

The Modern2020 project (funded by the EU's Horizon 2020 research and innovation programme (2014–2020), co-ordinated by Andra) focuses on providing the means in developing and implementing an effective and efficient repository operational monitoring programme for specific national programmes. The work carried out has enabled to define which parameters could be monitored within an underground repository and to provide a methodology on how data can be used to support decision making and to plan the response. In this framework, several full-scale in situ demonstrations of innovative monitoring techniques have been implemented in 4 different URLs across Europe (France, Switzerland and Finland) to enhance the knowledge on disposal monitoring techniques and to demonstrate the performance of new innovative sensors.

The demonstration of technologies in the Modern2020 project is considered as an essential step to validate the work performed to implement a monitoring strategy into a practical plan and the development and field assessment of innovative sensing systems, as well as to establish confidence amongst both technical and nontechnical stakeholders. This need has led the different partners of the Modern2020 project to build in the Tournemire URL joint generic in situ tests that aim to assess the performance of new monitoring devices developed in the project (mainly wireless devices and new sensors) for conditions as close as possible to those expected in a real repository as well as refining and developing non-invasive monitoring techniques. The tested prototypes were placed in or around a multi-barrier system (shale, bentonite buffer and cement plug) to monitor key safety and performance assessment parameters (saturation, humidity, temperature, pore and total pressures, deformation and chemical composition).

4.1 General layout of the tests

The experiment tests (Figure 4) were all based on a series of performance assessment sealing experiments called SEALEX [5], implemented in IRSN'S Tournemire URL. The general setup of each in situ test consists in a main horizontal borehole (MB) measuring 60 cm in diameter and ≈10 m in length backfilled with a 4 m long bentonite buffer and confined by means of a 2 m long bentonite-cement plug. The buffers are composed of bentonite-sand (highly compacted bentonite-sand blocks and a granular bentonite-sand mixture) or pure bentonite. The buffers were equipped with several independent artificial saturation mats to accelerate the buffers saturation.

In addition, auxiliary boreholes were drilled perpendicularly and parallel to each MB:

- Boreholes drilled perpendicularly to the MB were used to pass the hydration lines and wired cables from the buffer to the data acquisition system, thus avoiding cables to run through the buffer and create preferential pathways. These boreholes were PVC cased and cemented with a high performance resin to avoid any water flow inside the boreholes;
- Boreholes drilled around the MB, and were used to house geophysical streamers for electrical resistivity tomography (ERT).

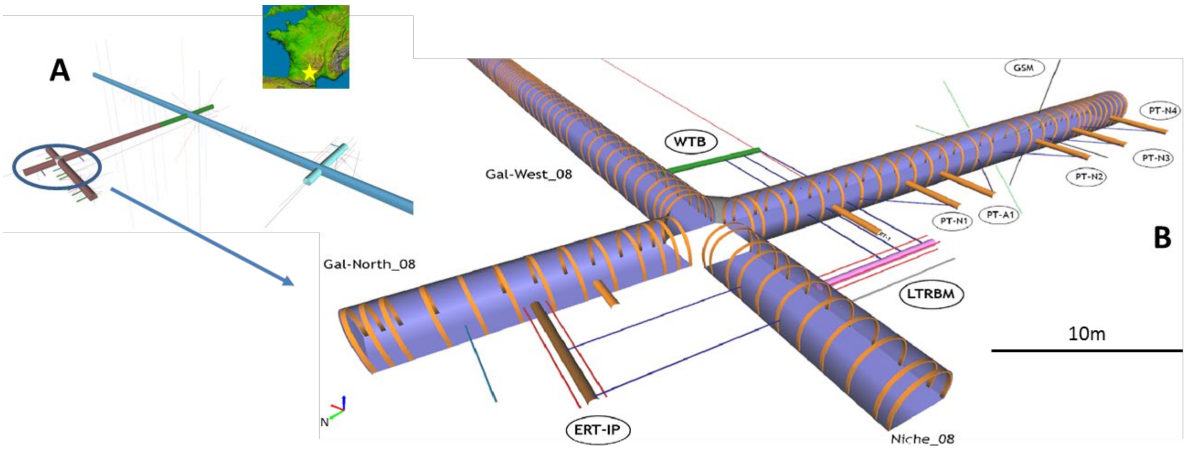

Figure 4: Location of the Modern2020 experiments in the Tournemire URL. A- General view of the Tournemire URL and B- borehole layout of the 3 in situ tests (ERT, LTRBM and WTB)

4.2 The Long Term Rock Buffer Monitoring (LTRBM) experiment

The LTRBM experiment (Figure 5) aims to assess the performance of new wireless devices and new sensors developed in Modern2020 that have never been tested before in a bentonite buffer under realistic in situ conditions. When possible, the new sensors were installed next to standard commercial ones to validate their performance.

4.2.1 Data transmission

In addition to the wired sensors that were directly cabled to a single data acquisition unit, three wireless data acquisition systems were used to transfer data measured inside LTRBM to receivers placed outside the buffer. Two different types of wireless units were installed inside the bentonite buffer and were designed to extract data recorded from within the buffer to wireless receivers located in the adjacent gallery. One (provided by ARQUIMEA) was based on a high frequency transmission (2.2 MHz), while the other (provided by Andra/ Sakata Denki) used a low frequency transmission (below 10 kHz). A third wireless transmission system, developed by NRG, was installed (temporarily) in the main Tunnel (transmitter) of the Tournemire URL and on top of the plateau (receiver). The objective of this third wireless transmission device was to demonstrate in a combined effort a full data transmission solution that allows transmitting wirelessly sensor readings out of the LTRBM borehole to the earth's surface (e.g. across 275 m of clay and limestone rock).

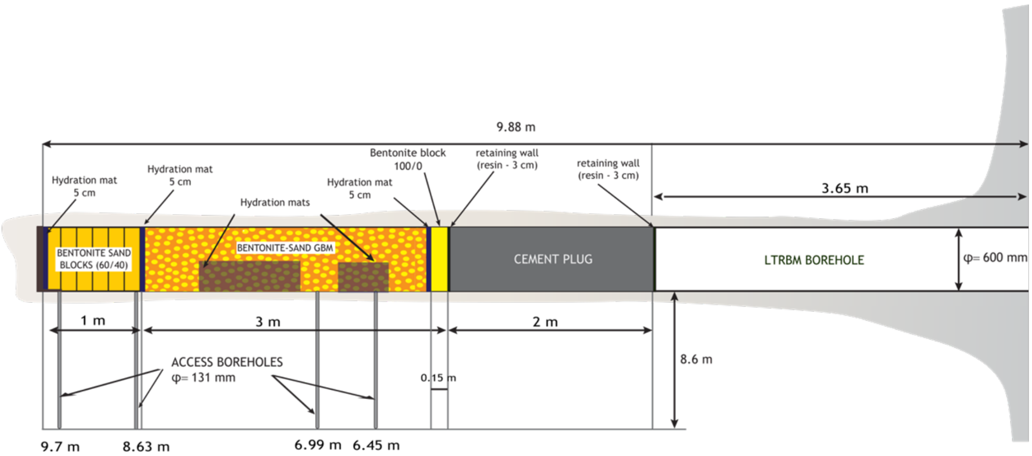

Granular Based Bentonite-Sand Material (GBM)

- Length 3 m, composition: 75% bentonite (MX 80-Expangel SP7) pellets and 25% sand. Target dry density pellets + sand:1.4 g/cm^3

Cement plug

- 55% cement (Portland type IV) + 40% water + 5% bentonite (sodic)

Bentonite-Sand compacted blocks (moulds from SEALEX PT-N2)

- Diameter φ=560 mm, divided in 4 sections, length 1 meter
- Composition: 60% bentonite (MX 80) and 40% sand. Dry density 1.88
- 1 block 100% bentonite with a dry density of 1.5 g/cm3

Figure 5: Conceptual view of the engineered barrier layout distribution inside LTRBM main borehole (sensors are not shown).

4.3 The Electrical Resistivity Tomography (ERT) experiment

The ERT experiment was designed to assess the capabilities of Electrical Resistivity Tomography (ERT) as a non-intrusive technique to monitor the resaturation of a bentonite buffer. The bentonite buffer composed of bentonite pellets and powder was provided by NAGRA. The buffer has been artificially saturated and is equipped with a heater to mimic heat transfer from waste packages. Local sensors were installed into the bentonite buffer to measure water content and temperature and are used as a way to perform cross-checking with geophysical measurements. Two boreholes were drilled on either side of the MB, each borehole was equipped with an electric probe containing 32 electrodes (0.29 m spacing). For research purposes, 2 parallel lines of electrodes were also buried inside the main shaft within the buffer, each line contains 16 electrodes (0.24 m spacing).

4.3.1 Preliminary ERT results

Blank test surveys carried out before the drilling of the main ERT borehole show that the resistivity of the host rock is homogeneous and less than 100 Ωm. ERT inversions performed after the installation of the engineered barrier system and after the first phase of hydration, enables to distinguish clearly the bentonite buffer and cement plug. Additionally, it seems to be able to detect the narrow rock section between the shaft and electrodes boreholes around the cement plug section, but not around the bentonite section. This is a consequence of the high resistivity of the dry bentonite material [6].

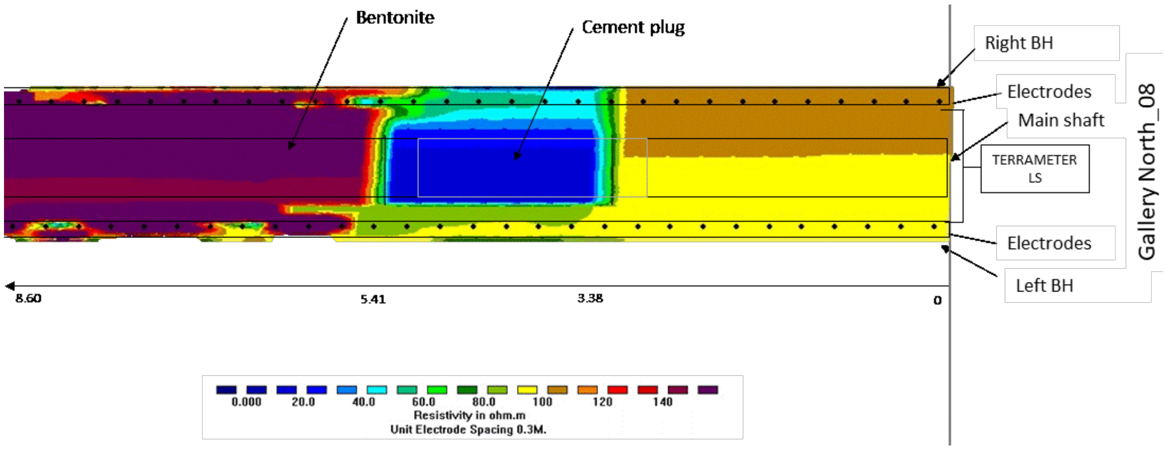

Figure 6: ERT cross borehole survey [3]. The resistivity shown in this survey, from depths 0 to 3.4m are not real, corresponds to the empty borehole. The high resistivity located above the cement plug towards the borehole mouth corresponds to a highly fractured zone.

4.4 The Wireless testing bench (WTB)

The Wireless Testing Bench (WTB) provides the possibility to evaluate signal transmission parameters of different wireless technologies for data transmission (short- and long-range radio waves) under representative in situ conditions. The experimental design enables wireless units to be introduced and removed within the bentonite buffer. A watertight access to the bentonite cores (transparent to radio waves), allows testing and continuous improvement of the wireless units under different saturation conditions. The radio transmission units to test do not require incorporating sensors, given that the sensors signal is converted to digital data before being transmitted, but to send equivalent data that will be received at different locations around the emission point to determine the transmission parameters of interest (length, quality, strength of signal, etc.).

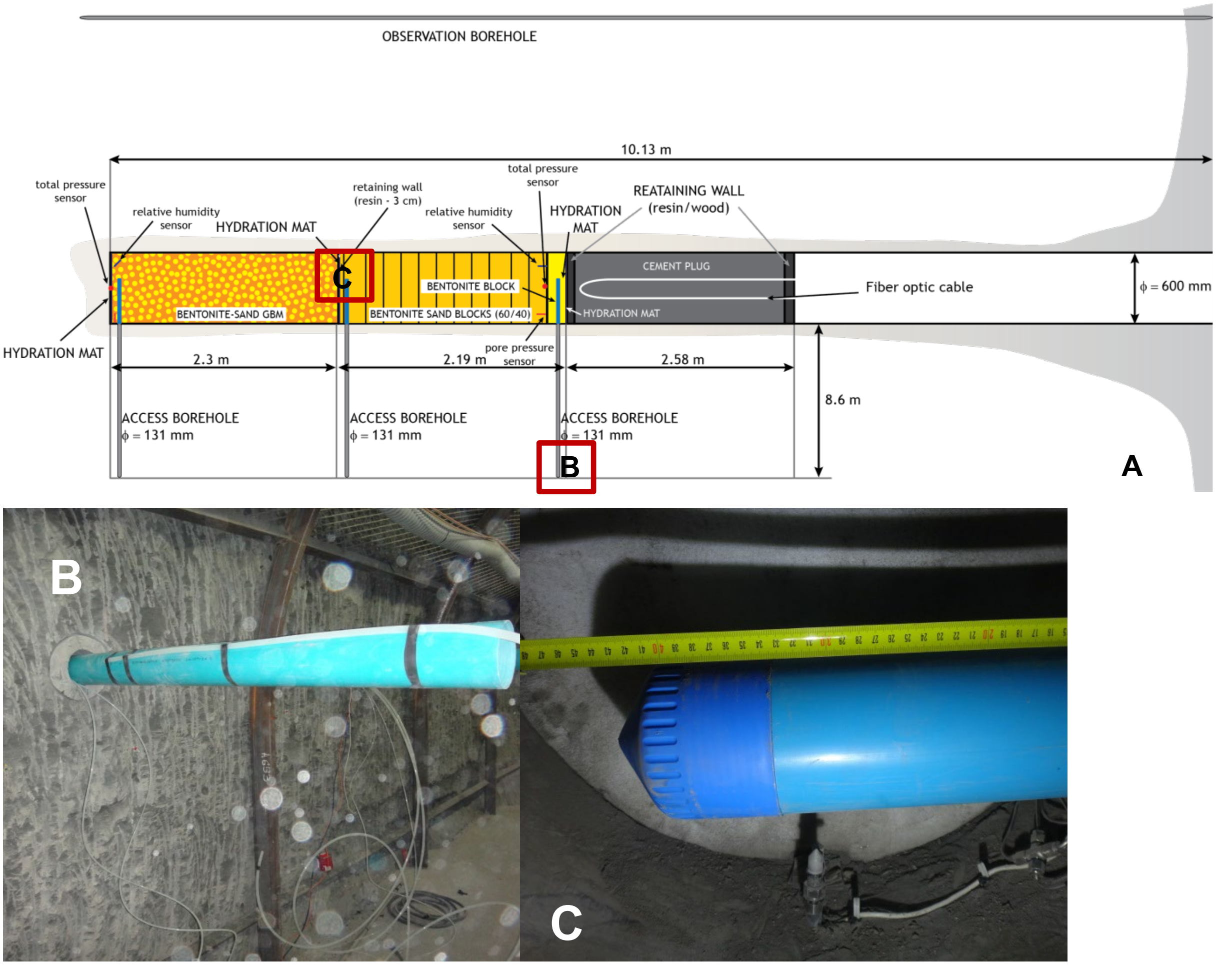

Figure 7: PVC casing inside WTB access boreholes. A- Conceptual view of the engineered barrier layout distribution inside WTB main borehole. B- Access borehole from the Gal_South_08. C- access borehole end inside the MB before insertion of bentonite buffer.

4.5 Lessons learned for Modern2020 in situ tests

The preliminary performance assessment of the new sensors and wireless transfer units implemented in LTRBM shows encouraging results. The data recorded from the new sensors are in general close to the ones measured from the standard commercial ones. Though some results differ from the general predicted trend, their validity is not questioned as it could be the consequence of heterogeneous swelling in the bentonite buffer and short monitoring time. Two out of four wireless transmitters placed in the bentonite buffer worked continuously during the monitoring period. The lack of received signal from the two nonworking units could be related to damaging caused by the buffer installation. These results highlight that the performance assessment of the sensors should be carried out during each step of the installation in order to prevent possible dysfunctions due to improper handling. LTRBM illustrates the difficulties in testing new sensors under realistic conditions (embedded in the rock or buffer) as if they fail no solution is currently available to remove them and repair the defect. A newly proposed qualification methodology developed in Modern2020 should improve greatly and speed up the required development process.

The preliminary ERT results during the water injection period are promising, different materials within the installation are identifiable and changes in resistivity due to saturation and temperature increase are also visible. Interpretation of resistivity results could benefit from time-lapse inversions, which are not currently possible [6].

The WTB has offered the possibility of several companies and research institutes to improve wireless transmission systems. The WTB design not only enables the development of wireless devices but also allows a better understanding of the transmission attenuation physics under different hydromechanical conditions.

5 CONCLUDING REMARKS

Certain types of information and experience that play an important role in ensuring the long-term safety of a deep geological repository can only be obtained through access to the underground environment. The technical feasibility of such a facilitiy, including it's design, material construction, geological environment can only be assessed through carefull verification and demonstration in an underground facility. The use of such tools are generally managed by waste management organisations due to their relatively expensive costs of running. However, generic URLs such as the Tournemire URL, provide an economically affordable possibility for TSOs to carry out an independent assessment of their national projects and also preserve and increase their knowledge with their own challenging and thoughtful in-situ experiments.

The development of large-scale in-situ experiments at the Tournemire URL has provided IRSN with important technical knowledge in determining the confinement properties of sound and fractured clay-based rocks as well as the performance of various engineered barriers. The research carried out has enabled IRSN to understand fundamental mechanisms in representative conditions which are used to consolidate scientific and technical foundations for a better safety evaluation.

6 REFERENCES

[1] Guglielmi, Y., Cappa, F., Lanc¸on, H., Janowczyk, J.B., Rutqvist, J., Tsang, C.F., Wang, J.S.Y., 2013. ISRM suggested method for step-rate injection method for fracture in-situ properties (SIMFIP): Using a 3-components borehole deformation sensor. In: The ISRM Suggested Methods for Rock Characterization, Testing and Monitoring: 2007–2014. 179–186.

[2] Cornet, F. H. (2000), Détermination du champ de contrainte qu voisinage du laboratoire souterrain de Tournemire. Contrat GEOSTRESS_IPSN, n°: 4060 9B038960/SH, ECODEV-CNRS n°:98N33/0073.

[3] De Barros, L., Daniel, G., Guglielmi, Y., Rivet, D., Caron, H., Payre, X., Barbieri, E., 2016. Fault structure, stress, or pressure control of the seismicity in shale? Insights from a controlled experiment of fluidinduced fault reactivation. J. Geophys. Res.: Solid Earth 121 (6), 4506–4522.

[4] P. Henry, Y. Guglielmi, C. Gout, R. Castilla, P. Dick, F. Donzé, A. Tsopela, D. Neyens, L. De Barros and J. Durand., 2019. Strain and Flow Pathways in a Shale Fault Zone: An In-Situ Test of Fault Seal Integrity. Fifth International Conference on Fault and Top Seals., 8-9 September 2019. DOI: 10.3997/2214-4609.201902318.

[5] Barnichon J.D, Dick P., Bauer C., 2012. The SEALEX in situ experiments: Performance tests of repository se. In: Harmonising Rock Engineering and the Environment – Qian & Zhou (eds), © 2012 Taylor & Francis Group, London, ISBN 978-0-415-80444-8, pages 1391-1394.

[6] Lopes, B., Dick P., Bertrand, J., García-Siñeriz, J-L., Tarantino, A., 2019. Modern2020 Final Conference, 9-11 April 2019, Paris.

International overview of investigated alternatives to deep geological disposal of high-level waste and long-lived intermediate-level waste

Muriel Rocher, François Marsal*, Didier Gay*, Marc Philippe*, Delphine Pellegrini**

*Institute for Radiological Protection and Nuclear Safety (IRSN, France), 31, avenue de la Division Leclerc, 92260 Fontenay-aux-Roses – France

Abstract:

In the frame of the public debate on the national plan for the management of radioactive materials and waste, IRSN carried out a literature review of the main alternatives to deep geological disposal that have been investigated around the world, up to now, for the long-term management of high-level waste and long-lived intermediate-level waste. This overview, based on public documents from international or national organisations and on scientific literature, gives historical and scientific keys to understand in which context the different options have been examined.

Six main options were identified: storage for centuries, partitioning-transmutation, borehole disposal, seabed disposal, launching into outer space and disposal in polar ice sheets. The extent of the international work on each of these is highly variable. All of these have, however, been the subject of investigations carried out by official bodies, often involving several countries, as well as involving experimental devices and tests. The present review summarizes the main principles and objectives, the historical studies performed in the world, as well as the issues encountered for each alternative, leading to the abandonment of the option or to perspectives and current research programs.

1 INTRODUCTION

Within the framework of the preparation for the public debate on the national plan for radioactive materials and waste (PNGMDR, 2019-2021), the President of the National Commission for Public Debate asked the French Institute for Radiological Protection and Nuclear Safety (IRSN) to provide an international panorama of the research conducted on alternatives to the geological disposal of high-level (HLW) and intermediate-level long-lived radioactive waste (ILW-LL).

In line with this request, the literature review conducted by IRSN, based on the use of freely available information published by international agencies (IAEA, OECD/NEA in particular) or national organizations, as well as in scientific journals, is not intended to provide IRSN's point of view (available through IRSN review reports on irsn.fr) on the relevance or feasibility of the technical options identified. The resulting panorama identifies the main alternatives to geological disposal explored around the world, historically or currently, to ensure the long-term management of HLW and ILW-LL (including spent fuel (SF) for countries that consider it as waste). It provides historical and scientific evidence to appreciate the context within which the various options emerged and were explored. It also identifies the concerns of technical and societal natures associated with these options.

The panorama highlights the diversity of alternatives to geological disposal explored since the 1950s. These can be grouped into six major families: storage for centuries, partitioning-transmutation, borehole disposal, seabed disposal, launching into outer space and disposal in polar ice sheets. The extent of the international work on each family is highly variable. All of these have, however, been the subject of investigations carried out by official bodies, often involving several countries, as well as involving experimental devices and tests.

The use of desert areas or volcanoes has also been suggested by scientists but without substantial documentation to support them, thus considered herein to be too anecdotal to merit specific development. Ceasing to produce radioactive waste, sometimes cited as an alternative, is also not covered by the panorama proposed since it does not, strictly speaking, constitute an alternative to geological disposal for waste that has already been produced.

For each of the six families aforementioned, the main principles are successively presented, together with the history of the research carried out worldwide and the current state of the art, including, where applicable, current research underway and, finally, the work and discussions more specifically conducted in France in connection with each of the options considered.

2 THE INVESTIGATED ALTERNATIVES TO DEEP GEOLOGICAL DISPOSAL

2.1 Storage

In nuclear terminology, the storage of radioactive waste constitutes a temporary management solution (as opposed to disposal, considered as a definitive solution) and falls under a so-called "active safety" principle, that is to say, requiring human intervention (maintenance, monitoring) to ensure its proper operation, while disposal is based on “passive safety” after its closure. Many conventional storage facilities for radioactive waste of all categories, located on the surface or underground, are aleady in operation in the world; they are authorised to operate for periods on the order of a few decades. For example, the figure below is an illustration of the Oskarshamm underground underwater storage facility in Sweden (CLAB). Thus, storage is not, strictly speaking, an alternative to geological disposal as a definitive waste management solution, since it implies an intent to remove waste again.

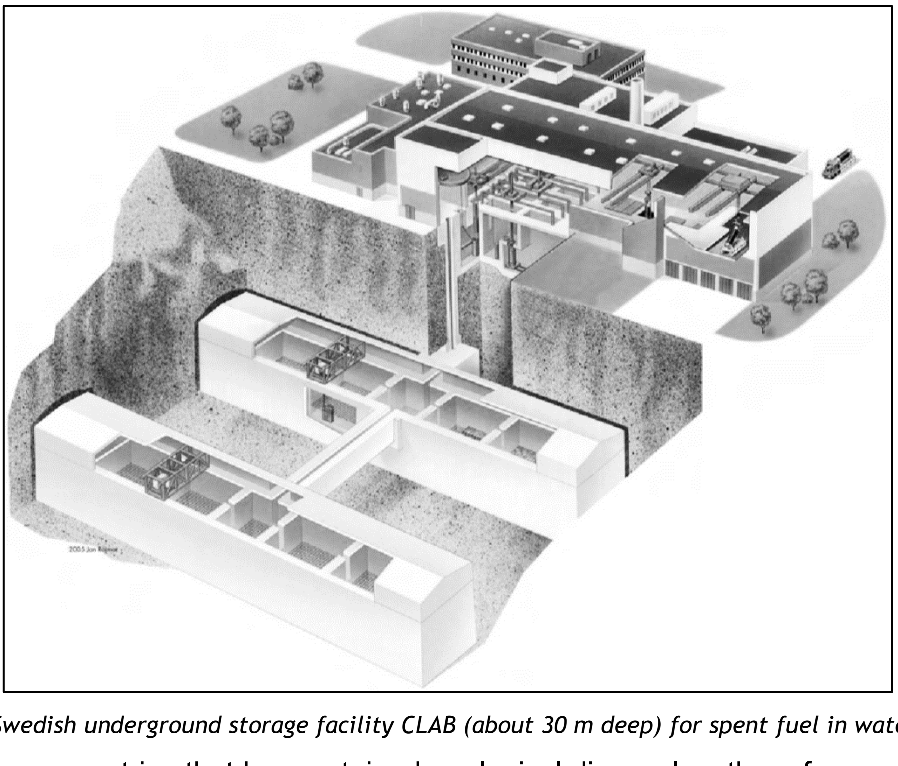

The Swedish underground storage facility CLAB (about 30 m deep) for spent fuel in water [1]

However, many countries that have retained geological disposal as the reference solution for the management of their HLW/ILW-LL, have opted for "long-term storage" (LTS) for the duration needed to develop their disposal project. In other countries, opting for "permanent storage" can be a deliberate alternative to respond to the desire to give future generations the time and opportunity to opt for solutions other than those currently available. Both cases may require to extend the duration of the storage period beyond a century. A LTS can last up to a few hundred years and may correspond to one maintained facility or to successive use of conventional storage facilities. A permanent storage, sometimes called a "monolith" or "mausoleum", is likely to remain intact over up to tens of thousands of years.

Unlike the permanent storage [2] which has not really been subject to technical studies, researches on LTS were notably carried out until the mid-2000s in the United Kingdom [3], Switzerland [4] and Canada [5]. Finland and Sweden have also examined situations called "zero-option" that could lead to a lack of decision with regard to the creation of a geological repository [6]. In France, it has been studied by the CEA [7] as required by the Act of 30th December 1991, until 2005, but the assessment of these studies pointed out a number of long term issues, such as the natural ventilation, the durability of concrete, and the long-term monitoring of the facilities, which cannot be guaranteed for periods longer than a few hundred years and which postpone the burden of waste management onto future generations. It has also been suggested by an independant expert in 2006 to build an underground LTS facility that could be transformed into a repository, after a secular period of observation of the waste and the environment [8].

Nowadays, LTS is considered as a part of the management of HLW in some countries like Netherlands [9] and Italy [10] and is examined in the United States [11].

2.2 Partitioning-transmutation

The goal of transmutation is to transform the very long radioactive half-life radionuclides contained in the spent fuel of nuclear reactors, notably minor actinides (like neptunium, americium and curium), some fission products (mainly iodine, cesium and technetium) and activation products, into stable or shorter-lived atoms. It first requires their partitioning from the other elements in the SF, then their conversion to an oxide or metal element and incorporation into fuels or "transmutation targets" for irradiation. Transmutation generally consists in causing neutron absorption by the nucleus of a radionuclide ("neutron capture"), as shown of the figure below. Such reactions can be induced in thermal or fast neutron power reactors or in dedicated systems.

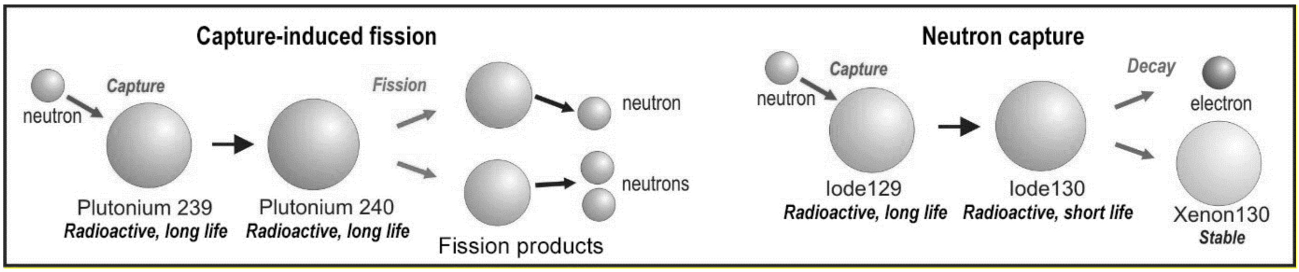

Transmutation of an actinide by fission (left) or of a fission product by simple capture of a neutron (right) (according to [12], modified)

Regarding partitioning, the hydrometallurgical processes benefit from important industrial experience in Japan and Europe, notably by the CEA in France [6], in continuity of the PUREX process developed since 1947 in the United States. They have been tested at laboratory scale for minor actinides and for some fission products, even if new techniques are still investigated nowadays for improving the performances. Pyrochemical techniques, of potential interest for the treatment of the strongly irradiating spent fuels of fast type reactors, were developed in Russia, the United States and France.

The manufacture of targets or fuels for transmutation are nowadays the subject of numerous studies aimed, in particular, at adapting the processes to the particular constraints of thermal powers and the high neutron emissions attributable to actinides (in particular americium and curium), inducing stringent requirements in terms of radiation protection.

Transmutation of activation products is of little interest, because of their presence in limited quantities in the waste.

Fission products could be transmuted through neutron capture (see figure above) in thermal neutron power reactors, which constitute most of the reactors installed worldwide. However, according to experience feedback [13], the transmutation yields of technetium 99 are low, the transmutation of iodine 129 raise safety concerns for reactors (unstable under irradiation, fuel corrosion) [14] and transmutation of caesium 135 would require complex isotopic partitioning with its stable isotope [15].

The transmutation of minor actinides requires fast neutrons, favouring capture-induced fission: (see figure above) to obtain sufficient yields. Fast neutrons can be produced inside a fast neutron reactor (FNR), in which the transmutation targets can be inserted, as studied in the frame of the “Generation IV International Forum” [16]. Only 4 FNR are currently in operation in Russia, China and India but nearly 15 have been operated in the past (as Phénix and SuperPhénix in France), and several are in project in the world. Therefore, a potential industrial deployment of this option would probably require the development of a new fleet of reactors. In France, the study of a potential industrial development of a FNR technology is assigned to the CEA through the project Astrid.

Fast neutrons can also be generated by a linear particle accelerator technology such as the LINAC (ionized particles accelerated by an electric field), then injected in a reactor dedicated to transmutation of minor actinides: these dedicated systems are called Accelerator Driven Systems (ADS). Such concept is the result of researches carried our by the teams of K. Furukawa, C.D. Bowman and C. Rubbia in the 1980s and the CERN in the 1990s. Several projects are currently developed in China [17], South Korea, India and Europe, as the MYRRHA project developed in Belgium.

Finally, an alternative technology to the LINAC for generating fast neutrons would rely on a laser-generated-plasma-based particle accelerator concept, called Laser Wakefield Acceleration (LWFA [18]), extremely powerful with reduced dimensions, based on the technique Chirped Pulse Amplification (CPA) which won the 2018 Nobel Prize in Physics for G. Mourou and D. Strickland [19]. Recently, the use of this laser technology has been proposed to accelerate deuterium ions intended to cause a fusion reaction. The neutrons produced would then feed a molten salt reactor for transmutation [20].

2.3 Borehole disposal

Various disposal concepts involving rock melting have been explored in the United States in the 1970s for exothermic waste placed in boreholes drilled into magmatic rocks (e.g., [21]). The heat that waste generates leads to the melting of the surrounding rock, the objective being that, during cooling, the mixing of waste and rock forms a vitreous mass that traps the radionuclides. As an example, the Deep Self Burial concept, where the waste sinks deep into the liquefied rock, is given below.

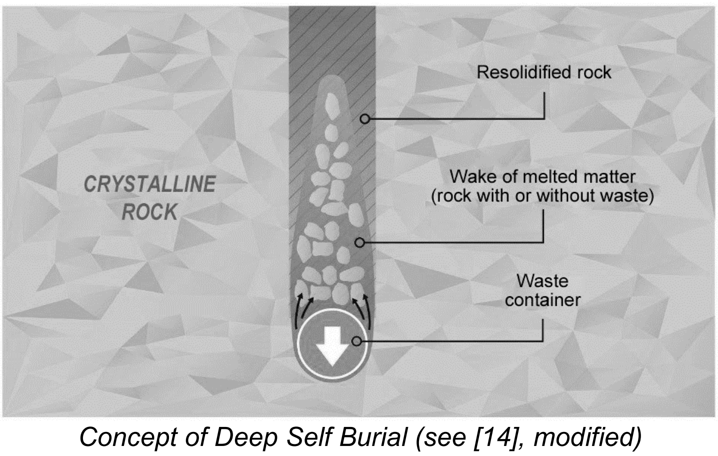

Concept of Deep Self Burial (see [14], modified)

These concepts are currently no longer the subject of official studies and have not been the subject of significant work in France. However, a derived option is still under study in the United States for Hanford caesium and strontium sources, based on the partial melting of a granite-based material ("rock welding”, see e.g. [22]) placed around the waste packages so as to seal the boreholes.

It should be recalled that direct injection of waste in liquid form by borehole in porous and permeable rocks at several 100s metres depth has been operated in the United States between 1959 and 1979 [23] and is still operated in Russia since 1962 [24]. In France, various investigations with non-radioactive effluents or of hydraulic fracturing were gradually abandoned at the end of the 1980s. To our knowledge, rock injection is now not being considered by any country as a definitive management option for HLW/ILW-LL.

Finally, a first concept of disposal of solid and packaged waste in boreholes of several 1000s metres depth was developed by the National Academy of Sciences of the United States in 1957 [25]. Following the significant technological advances of the past thirty years, this option, even if not the reference solution for the management of HLW or SF, is still the subject of R&D in the United States [26], closely followed in several countries such as Germany, Denmark, Switzerland, Sweden [27], Finland and the United Kingdom [28].

None of these options of borehole disposal have been the subject of particular work in France.

2.4 Sub-seabed disposal

The present paper will not further deal with the disposal operations at sea, carried out by most nuclearised countries in the 1950s-1970s: such operations did not involve ILW-LL/HLW and it is now prohibited by a moratorium on dumping adopted in 1983. The option of burying waste in the marine sediments was considered more acceptable, in that it consists in confining the waste in a thick layer of sediments on the seabed with the capacity to absorb the radioactive substances.

Several options of disposal of radioactive waste in the seabed have been considered, mainly by depositing the waste in the abyssal plains of the oceans, placed on the seabed in anticipation of being covered by sedimentation, or sunk in the unconsolidated sediments that cover the bedrock (generally basalts) by means of boreholes or "penetrators" (heavy containers falling in free-fall: see figure below), or buried in the bedrock.

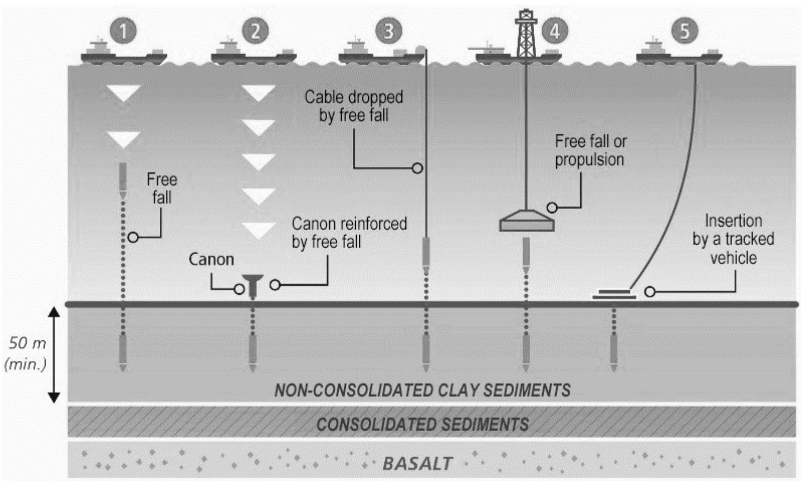

Various concepts for placing the waste in seabed sediments using a penetrator (according to Sandia under the Sub-seabed Disposal Program, modified)

Sediment burial studies began in 1973 in the United States, then at international level in 1976 with the NEA "Sub-seabed Disposal Programme", which notably involved the United States, France, the United Kingdom, Japan and several other countries [29]. The international initiatives undertaken to protect the oceans have progressively led to a slowdown in research on the disposal of waste under the seabed from a boat or an offshore structure and then to their ceasing [30] following the moratorium on the disposal of waste at sea in 1983 [3, 5, 31] and the end of the Sub-seabed Disposal Programme in 1986 subsequent to United States' withdrawal.

Another examined option was to place the waste in of the so-called "subduction" trenches, where an oceanic plate sinks into the Earth's mantle. It was initially proposed in the 1970s in the United States [32] and also considered in Canada and in the United Kingdom in the 1980s

[3, 5]. However, the geologists brought to light the slowness of the subduction phenomenon [33] as well as signs of strong seismic activity and observed that in some cases, the sediments on the subducted plate might not penetrate the mantle, but might rather be levelled off during the sinking of the plate and accumulated on the surface. The subduction zone disposal option is, to our knowledge, currently not being studied by any of the agencies in charge of radioactive waste management.

2.5 Launching into outer space

The shipment of HLW resulting from reprocessing of SF into outer space was mainly studied in the United States notably by NASA [34] in the 1970s and early 1980s for the US authorities [35], and secondarily by the USSR [36] and Kazakhstan [37]. NASA examined the launching of packaged waste into a low Earth orbit (150-500 km) on board a space shuttle, and then its transport to its final destination using a space tug. Several destinations were examined, like the surface of the moon and an orbit around the sun.

These projects have been progressively abandoned, given the difficulty of reliable space technology [5], the heavy weight of the waste as well as the requirements for robust packaging in which it would be necessary to place them, and therefore the energy and financial cost [3, 35] of sending such cargoes into space.

This option has not been specifically developed in France.

2.6 Disposal in polar ice sheets

The disposal of exothermic radioactive waste in the thick ice sheets of Antarctica or Greenland consists in placing the containers either on the ice or at shallow depths, so as to cause them to sink gradually by the melting of the ice around them. Several options were investigated by the United States until the 1980s [35, 38]: disposal in the ice, allowing the waste packages to gradually descend in the ice or restraining them with cables in order to allow their retrievability, or at the surface, allowing the heat to dissipate and the waste packages to be retrievable until the snow finally buries the facility, as illustrated below.

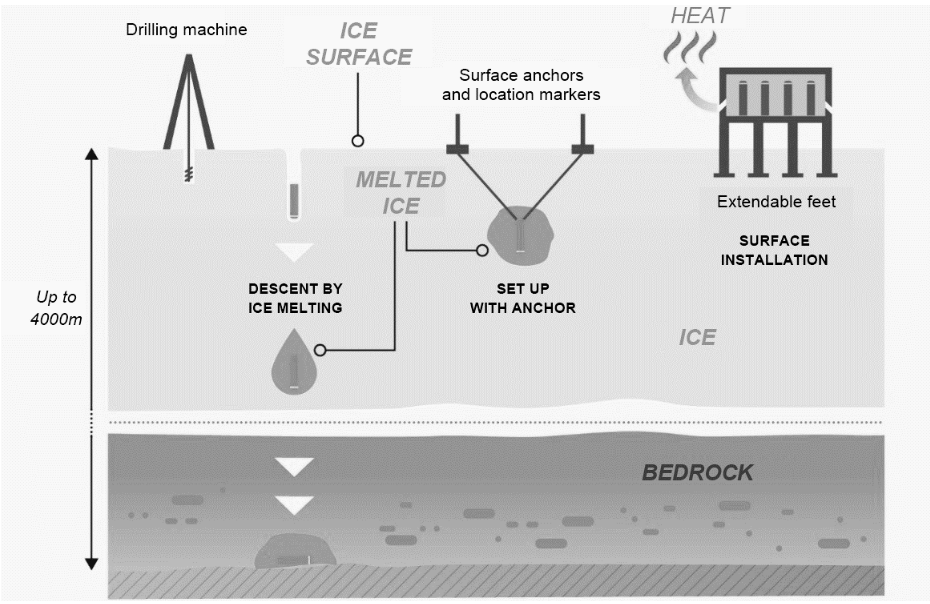

Various concepts of exothermic waste disposal in ice sheets envisaged in the United States in 1974 ([1], modified)

After the first investigations, the glaciologists revealed the presence of salted pockets trapped in the ice that could cause an extremely rapid corrosion of steels, stability problems associated with the movement of ice as well as the impossibility to rest assured that the ice caps will remain for the hundreds of thousands of years necessary for the decay of the waste (e.g., [5, 39]). Finally, the possibility of disposal of radioactive waste in the South Pole ice sheets is formally excluded by the 1959 Antarctic Treaty and is unworkable for countries committed to managing their radioactive waste within their national borders [3, 5].

This option has not been contemplated in France.

3 CONCLUSION

The technical difficulties of implementation, as well as the changing ethical considerations and their legal extrapolation led to the abandonment of several of the options considered historically. This is the case of seabed disposal, launching into outer space, and disposal in polar ice sheets, which are no longer the subject of studies and research.

Discussions continue, however, on storage, partitioning-transmutation and borehole disposal. Regarding storage, which is generally perceived as a standby solution, the work is aimed at evaluating the possibilities of extending the lifetimes of the facilities and at reinforcing their robustness. For partitioning-transmutation, the work covers a very broad field of scientific knowledge and combines developments in fundamental research and studies to establish the feasibility of deploying the technologies envisaged on an industrial scale. Studies on borehole disposal deal with the handling and transfer of waste from the surface to the containment area and with the sealing of boreholes after the waste has been placed inside them.

4 REFERENCES

[1] Sweden, 2008. Sweden's third national report under the Joint Convention on the Safety of Spent Fuel Management and on the Safety of Radioactive Waste Management. Ds 2008:73, Ministry of Environment.

[2] Greenpeace, Friends of the Earth, Cumbrians Opposed to a Radioactive Environment, 1987. Radioactive Waste Management: The Environmental Approach. Briefing paper. Nov. 1987.

[3] CoRWM, 2006. Managing our radioactive waste safely – CoRWM's recommendations to Government. CoRWM Doc 700, 195 p.

[4] EKRA, 2000. Disposal Concepts for Radioactive Waste, Final Report. Swiss Federal Department of Environment, Transport, Energy and Communication, Federal Office of Energy, Bern.

[5] NWMO, 2005. Chosing a way forward – The Future Management of Canada's Used Nuclear Fuel. Draft study report, 304 p.

[6] Topical Session on Overall Waste Management Approaches. NEA/RWMC (2002)6, Paris, France, 14th March 2002, p. 13-14.

[7] CEA, 2005. Les déchets radioactifs à haute activité et à vie longue – Recherches et résultats. Axe 1– Séparation-transmutation des éléments radioactifs à vie longue, Axe 3– Conditionnement et entreposage de longue durée. Enjeux, questions et réponses. Débat public, juin 2005, 20 p.

[8] CNE, 2006. Rapport global d'évaluation de recherches conduites dans le cadre de la loi du 30 décembre 1991. Janvier 2006, 38 p.

[9] Netherlands, 2010. Net-Enabled Radioactive Waste Management Database (NEWMDB), Country Waste Profile Report for Netherland for IAEA. July 8. 2011, 29 p.

[10] Italy, 2017. Joint Convention on the Safety of Spent Fuel Management and on the Safety of Radioactive Waste Management - Fifth Italian National Report. ISPRA, Oct. 2017, 193 p.

[11] NRC, 2014. Generic Environmental Impact Statement for Continued Storage of Spent Nuclear Fuel - Final Report- Public Comments. NUREG-2157 Vol. 2, Published September 2014, 717 p.

[12] DOE, 1999. A Report to Congress: A Roadmap for Developing Accelerator Transmutation of Waste. (ATW) Technology, DOE/RW-0519. Washington, D.C., U.S. Department of Energy, Office of Civilian Radioactive Waste Management, October 1999, p. 1–4.

[13] OCDE, 2012. Vers un cycle du combustible nucléaire durable. AEN n°6981, 203 p.

[14] Ichimura E. et al. , 2004. Iodine transmutation studies using metal iodide targets. *Journal of Nuclear Materials*, 334, p. 149–158.

[15] Nash, K.L, Lumetta, G.J., 2011. Advanced separation techniques for nuclear fuel reprocessing and radioactive waste treatment. Woodhead Publishing Limited, 15th March 2011, 512 p.

[16] GIF, 2014. Technology roadmap update for Generation IV Nuclear energy systems - GIF, jan. 2014.

[17] CIAE, 2017. The Progress of the Gen-IV Reactor in China. Fast Reactor Development Council Strategy Working Group (4). Sept. 14, 2017, Ministry of Economy, Heisei, Japan.

[18] Tajima T., Dawson J.M., 1979. Laser electron accelerator. *Physical Review Letters*, 43, p. 267.

[19] Strickland D., Mourou G., 1985. *Optics Communications*. Vol. 56 (3), p. 219-221.

[20] Necas A. et al., 2018. A Beam-Fusion-Triggered Transmutator; Transparent, Monitored and Controlled Realtime. *Bulletin of the American Physical Society*, 2018/11/7.

[21] Heuze, F.E., 1981. On the Geotechnical Modelling of High-Level Nuclear Waste Disposal by Rock Melting. Lawrence Livermore Laboratory, Livermore, CA, USA. UCRL-53183, 54 p.

[22] Gibb F.G.F., 2003. Granite recrystallization: the key to the nuclear waste problem? *Geology*, 31, p. 657–660.

[23] Weeren H.O., Coobs J.H., Haase S.C., Sun RJ. Tamura I., 1982. Disposal of Radioactive Wastes by Hydraulic Fracturing Rep. ORNL/CF-81/245, Oak Ridge, Tennessee, May 1982.

[24] Compton K. L. et al., 2000. Deep Well Injection of Liquid Radioactive Waste at Krasnoyarsk-26: Vol. I. Int. Institute for Applied Systems Analysis, Laxenburg, Austria, RR-00-1, Feb. 2000, 113 p.

[25] National Academy of Sciences, 1957. The Disposal of Radioactive Waste on Land. Report of the Committee on waste disposal of the division of earth science. NAS, NRC, Publ. 519, Sept. 1957.

[26] Arnold B.W. et al., 2011. Reference Design and Operations for Deep Borehole Disposal of High-Level Radioactive Waste. SAND2011-6749. Albuquerque, NM: Sandia National Laboratories.

[27] Juhlin C. et al., 1998. The Very Deep Hole Concept – Geoscientific Appraisal of Conditions at Great Depth. SKB Technical Report 98-05, Stockholm, Sweden.

[28] Chapman N., Gibb F., 2003. A truly final waste management solution – is very deep borehole disposal a realistic option for HLW or fissile material? *Radwaste Solutions*, 10 (4), p. 26–35.

[29] Talbert D.M., 1980. Subseabed Radioactive Waste Disposal Feasibility Program: Ocean Engineering Challenges for the 80's. Conference OCEANS '80, Oct. 1980.

[30] Nadis, 1996. The Sub-Seabed Solution. *The Atlantic Monthly*, Oct.1996; Vol. 278, 4, p. 28–39.

[31] Miles E.L., 2014. Sub-seabed disposal of high level radioactive waste: The policy context then and now. The Oceans in the Nuclear Age: Legacies and Risks, p. 125–143.

[32] Bostrom R. C., Sheriff M. A., 1970. Disposal of Waste Material in Tectonic Sinks. *Nature*, vol. 228, p. 154–156.

[33] Silver E.A. 1972. Subduction Zones: Not Relevant to Present-day Problems of Waste Disposal. *Nature*, Vol. 239, p. 330-331.

[34] NASA, 1978. Nuclear Waste Disposal in Space. NASA technical paper 1225, 178 p.

[35] Battelle, 1974. High-level radioactive waste management alternatives. *Ed*. K. J. Schneider & A. M. Platt, BNWL-1900. 4 volumes.

[36] Egorov N. N. et al., 1991. Fuel Management in the USSR and New Way to Solve the Problem. Moscow Radio-Technical Institute of the USSR Academy of Sciences, ISBN 5-201-09424 4.

[37] Pshenin, E., Suimenbaev, B., 1996. Selection of the trajectory for radioactive wastes disposal in the outer space. International Science and Technology Center, Kazakhstan, 22-26 Oct 1996; *Ed.* Akhmetov *T.* et al., p. 110–111.

[38] Bentley C. et al., 1975. The disposal of radioactive wastes in the Antarctic ice sheet. *Polar Record*, Vol. 17, 110, May 1975, p. 578–579.

[39] Zeller E.J. et al.,·1973. Putting Radioactive Wastes on Ice- A Proposal for an International Radionuclide Depository in Antarctica. *Bulletin of the Atomic Scientists*, Vol. 29, 1.

Update on the Status of Deep Borehole Disposal of High-Level Radioactive Waste in Germany

Guido Bracke, Wolfram Kudla**, Tino Rosenzweig***

*GRS gGmbH; Schwertnergasse 1, 50968 Cologne; guido.bracke@grs.de

**Technische Universität Bergakademie Freiberg, Institut für Bergbau und Spezialtiefbau; Wolfram.Kudla@mabb.tu-freiberg.de, Tino.Rosenzweig@mabb.tu-freiberg.de

Abstract:

The phase-out of nuclear energy in Germany will take place in 2022. A site for final disposal of high-level radioactive waste (HLRW) has not yet been provided, but a site selection process was restarted by Act on the Search for and Selection of a Site for a Disposal Facility for High-Level Radioactive Waste (Site Selection Act - StandAG 2017). This act was based on a recommendation by a commission which also advised to follow up the development of deep borehole disposal (DBD) as a possible option for final disposal of HLRW. This paper describes briefly the status of DBD in Germany and if this option should be pursued in Germany. Although there are some merits of DBD, it can only be a real option if research and development is supported. The technical equipment for larger boreholes of the required size will only be developed if there is funding and a feasibility test. Furthermore, any concept of DBD must be detailed further, and some requirements of the act must be reconsidered. The paper concludes that despite the possible merits of DBD, that political and financial support through R&D will only be provided for the time being if it is pushed by interested parties. Alternatively, if the site selection procedure is not progressing well, than the alternative option of DBD may find greater interest in the future.

1 INTRODUCTION

The geological disposal of radioactive waste is well set at an international level with the deep borehole disposal DBD being one of the long known options /CHA 03/, /OJO 14/, /APT 17/. It is referred by the IAEA as well /INT 03/, /IAEA 17/. DBD for larger volumes of high-level radioactive waste (HLRW) has not yet been applied and is a controversial topic. Some authors are supportive /BES 17/, /GIB 14/, /ARN 14/, /DEE / to this technology whereas others are reluctant to accept this idea for Germany /BOL 18/. It is obvious that the idea of disposal of HLRW in deep boreholes has some merits in geological disposal, but it also has disadvantages which need to be discussed and weighted. After a thorough look at it, one can form an opinion of whether or not there is a possible use of a concept and technology for DBD for the specific type and amount of waste to be disposed of. The radioactive waste inventory, technology and a concept, which may be applicable to Germany, have been presented already in /BRA 16a/, /BRA 17a/ and /BRA 17b/. This paper wants to give a minor update of /BRA 19/ and overview of the status of DBD for HLRW, discussions and recent developments in Germany as DBD could be part of the concept of geological disposal of HLRW within the site selection process. The disposal of LLW and ILW is not considered here.

2 REGULATORY FRAMEWORK IN GERMANY AS OF 2019

2.1 General

Nuclear Power has a long history in Germany. The first nuclear power plant was put into operation in 1962. The Atomic Act has been updated several times since then. In the year 2000 an update included the phase-out from nuclear energy /ATG 18/. The last reactor will cease operation in 2022. Therefore, the question of disposal of high-level radioactive waste has been becoming more and more urgent. In 2002 a commission was set up to make a proposal for a site selection process /AKE 02/. Their proposal was not implemented for political reasons. After a long political debate, an act on site selection was issued in 2013 /STA 13/, foreseeing a commission to define a detailed site selection process. Subsequently, a new commission was set up in 2015 to develop a site selection process. The proposed process is laid down in/KOM 16/ and was issued as a revised site selection act in 2017 /STA 17/. As the regulatory framework and funding /ENT 17/ was revised in parallel, the institutions (implementer and regulator) were founded and could commence their activities in 2017. The site selections process and the actors are described briefly in the following.

2.2 Site Selection Act

The Site Selection Act /STA 17/ aims to find the best possible site for final disposal high-radioactive waste in the geological formation of rock salt, clay or crystalline rock in Germany. It foresees actors, phases for the site selection process and several criteria for the site selection. A short description of the process is given below. This is needed for understanding the status and possibility of DBD in Germany.

2.2.1 Actors in the site selection

The main actors of the site selection procedure include

- German Parliament
- Federal Ministry for the Environment, Nature Conservation and Nuclear Safety (BMU)
- Federal Office for the Safety of Nuclear Waste Management (BfE)
- Federal Company for Radioactive Waste Disposal (BGE)
- National Accompanying Body (NBG)

These actors have different roles (Figure 1). The BGE being implementer performs the site selection and hands over the results of each phase (see below) with proposals to the BfE. The BfE as regulatory authority ensures participation of the public and approves a final proposal for each phase. The BMU submits this proposal to the German Parliament for a final decision and issuance of an act. Currently the BMU is preparing the ordinances on safety requirements and safety analyses /BMU 19/. During the site selection process, the NBG has the right to insight and to act as mediator. The NBG is composed of members of the public selected by the German parliament.

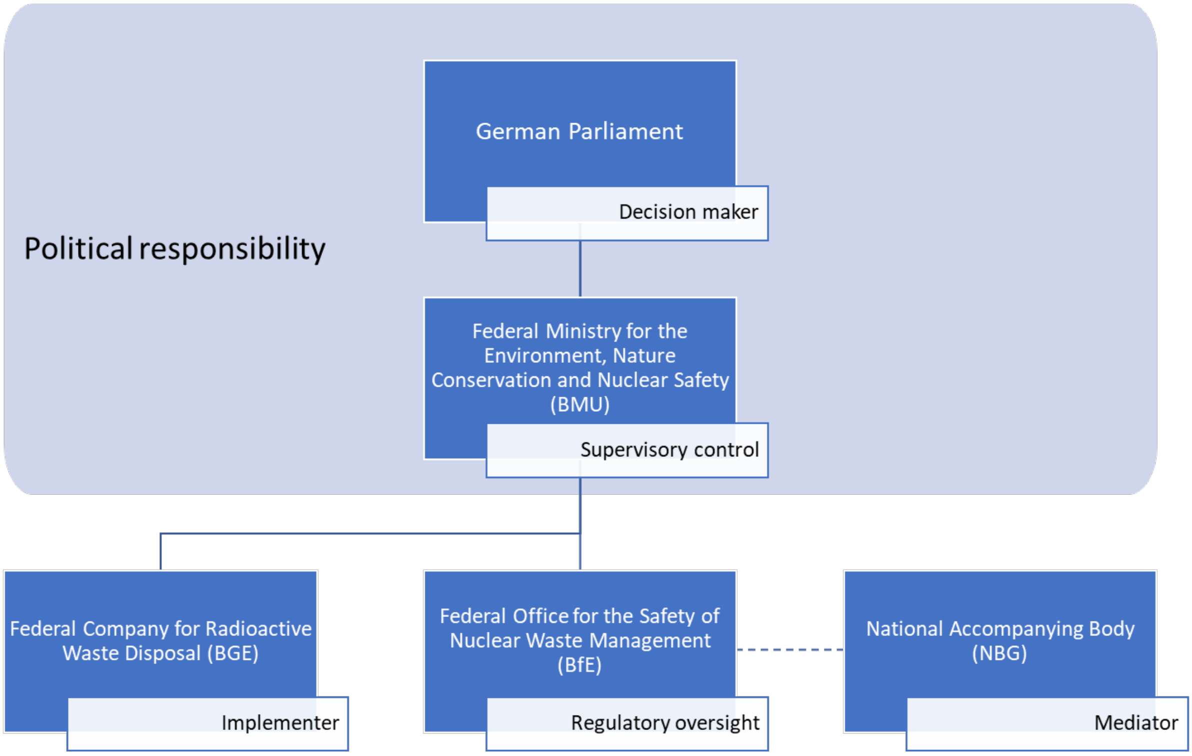

Figure 1. Roles of main actors in the site selection procedure.

2.2.2 Phases of the site selection process

The site selection process was divided into three main phases as shown in the Figure 2:

Phase 1: Identification of possible regions

Phase 2: Exploration from the surface

Phase 3: Underground explorations and decision for a site

The site selection process started in 2017 with phase 1 and shall be finalized in 2031 with phase 3 according to /STA 17/. As the "Decide/Declare/Defend" approach failed for the former intended repository in Gorleben in Germany, a public participation and debates are foreseen for all phases. This is to be organized by the BfE according to the site selection act. Phase 1 shall find regions for exploration from the surface applying exclusion and weighing criteria set in the act. After performing preliminary safety analyses on concepts to be developed, planning criteria may be assessed. Once the regions have been decided by the German parliament, phase 2 will start with an exploration from the surface to find sites for underground exploration. After application of geo-scientific criteria, advanced preliminary safety analyses, consideration of secondary planning criteria, socio-economics and an environmental assessment, the sites for underground exploration can be decided by the German parliament. Phase 3 shall be finished with a proposal of sites based on the results of underground exploration, application of criteria and detailed preliminary safety analyses and again considering in second order planning criteria, socio-economics and an environmental assessment. The German parliament will decide on the site based on the proposal of two sites, which are the result of phase 3.

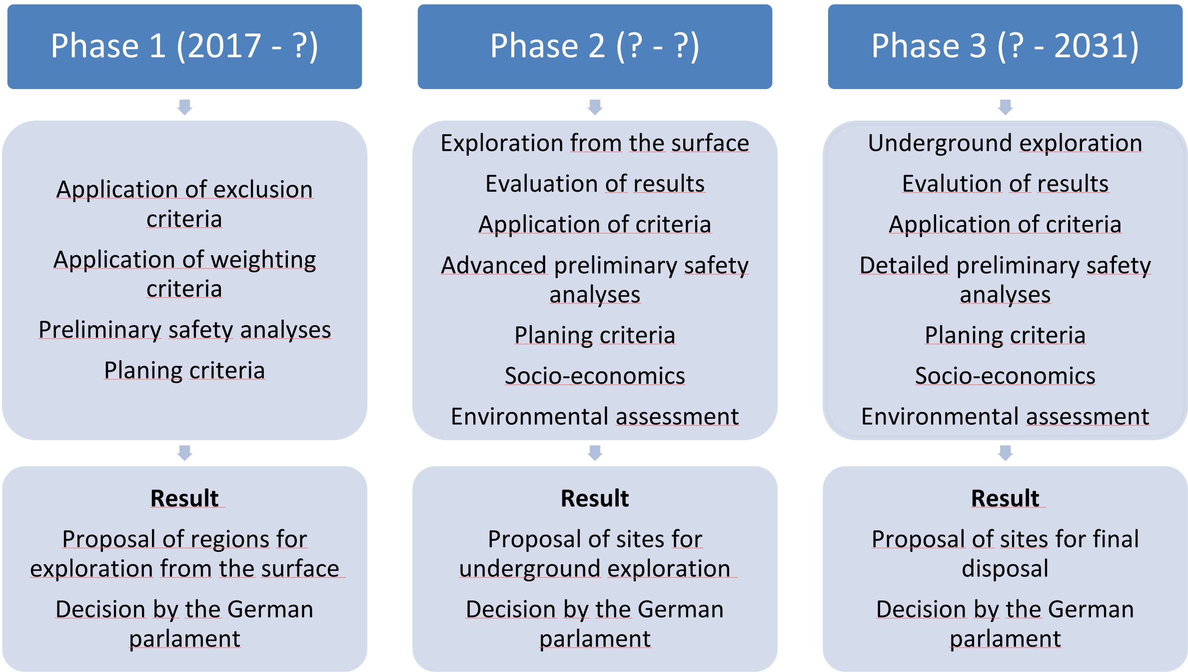

Figure 2. Phases within the site selection process.

2.2.3 Containment providing rock zone and deep borehole disposal

The containment providing rock zone (CPRZ) is an important term by the German site selection act /STA 17/ describing the part of a rock formation in which disposal systems, which are mainly based on geological barriers, ensure the safe containment of radioactive waste in a disposal facility in coaction with the technical and geotechnical seals. Minimum and weighing requirements and criteria have been set for the CPRZ in /STA 17/. Some possible configurations of a CPRZ are shown in Figure 3.

A containment providing technical barrier is permissible for crystalline rock as given in §23 (1) of /STA 17/.

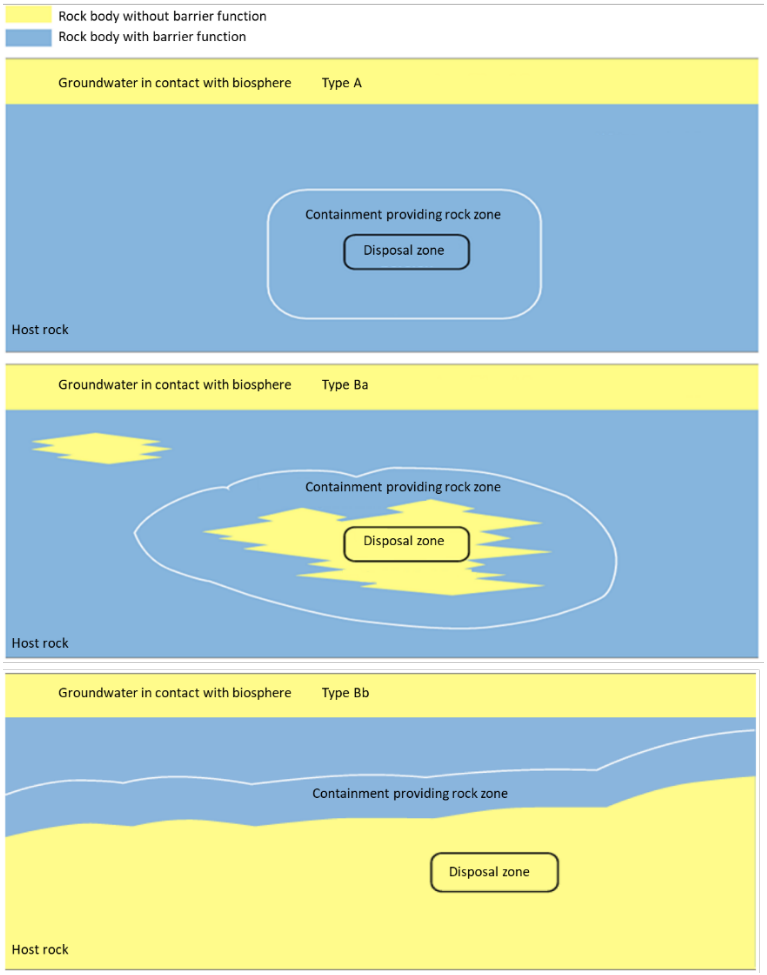

Figure 3. Types of containment providing rock zones (not to scale).

2.2.4 Requirements, Criteria, Indicators

The site selection must consider clay rock, crystalline rock and rock salt as possible host rocks in all phases. Exclusion criteria are applied in the first step. To further narrow down regions (phase 1) to subareas or specific sites, a preliminary safety and disposal concept is obviously needed. These concepts will consider either a containment providing rock zone and / or technical barriers for containment. If these concepts are not available, suitable subareas may not be assessed. The discussion on safety concepts or disposal concepts has not currently been started in detail.

The site selection act foresees geo-scientific criteria for exclusion (large scale vertical movements, active faults, impact from mining, seismic and volcanic activity, age of groundwater), which can be applied directly to any site in a geological formation even without a disposal concept.

The minimum geo-scientific criteria provided (permeability of formation, thickness of the possible containment providing rock zone (CPRZ), depth of possible CPRZ) are to be applied to rock salt and clay rock in order to narrow down regions with suitable geological formations. Since a CPRZ is not required for crystalline rock and technical barriers are favored in the site selection act, not all minimum geo-scientific criteria apply to crystalline rock. This leads to an inequality for the different host rocks concerning the criteria and complicates the development and comparison of concepts.

The site selection act lists eleven weighting geo-scientific requirements in three groups based on /KOM 16/: quality of containment and reliability of its evidence; validation of containment, and; additional safety-relevant features (see Table 1–3).

These criteria may be used the compare the different sites and their quality but might not be decisive in detail as the overall safety is assessed in preliminary safety analyses.

Table 1. Requirements of the weighting group 1: Quality of containment and reliability of its evidence.

	Requirement	Comment by the author regarding DBD
1.	No or slow transport with groundwater in the CPRZ	achievable
2.	Favorable configuration of rock body, host rock and CPRZ	achievable
3.	Good spatial characterization	Tools to characterize host rock properties are available for greater depths but may pose a larger effort compared to lower depth. The volume of rock to be characterized for a CPRZ for DBD may be lower than for a repository depending on the concept.
4.	Good predictability of the long-term stability of favorable conditions	achievable

Table 2. Requirements of weighting group 2: Validation of containment.

	Requirement	Comment by the author regarding DBD
1.	Favorable rock mechanics	achievable
2.	Low tendency to generation of groundwater flows in host rock and CPRZ	achievable

Table 3. Weighting group 3: Further safety relevant features.

	Requirement	Comment regarding DBD
1.	Protective composition of overlying rocks	achievable
2.	Good conditions to avoid or minimize gas generation	The draft concept for container and casing is using steel, which will inevitably lead to gas generation. Gas generation may be minimized or slowed down by choice of suitable borehole fluid or cementation of containers. A future concept may also minimize the use of steel or may provide physical gas traps. Gas generation cannot be completely avoided.
3.	Good temperature compatibility	The temperature in the disposal zone will be higher than 100 °C due to the depth. Any safety analyses must consider the temperatures and its compatibility for DBD.
4.	High radionuclide retention capability of CPRZ	achievable
5.	Favorable hydrochemistry	achievable

The requirement “Good temperature compatibility” has been discussed intensely. Since there is a dedicated § 26 in /STA 17/, a maximum temperature of 100 °C at the outer surface of the containers must be considered in preliminary safety analyses. A strict application of 100 °C as a requirement would render many safety and disposal concepts as obsolete. However, there is the clause, that further research may yield other results. A recent study concluded that setting a regulatory temperature limit prior to the assessment of safety and disposal concepts would hamper optimization of safety and disposal concepts /BRA 18/.

2.3 Safety requirements and safety analyses

Furthermore, any disposal site must comply with the upcoming ordinance for safety requirements on final disposal /BMU 10/, which is under revision and has published as a draft in 2019 for public discussion /BMU 19/. The ordinance outlines how to consider the requirements and criteria within a site selection for geological disposal. Clearly this ordinance is drawn up against the background, even mind-set, of a mined repository and is nearly inapplicable in some respects to other forms of geological disposal (like DBD). An additional ordinance will outline requirements on preliminary safety analyses.

The author thinks that most requirements of these ordinances can be met by a concept for DBD if confinement of radionuclides, integrity and criticality are concerned. The requirement to provide retrievability of the waste container may also be complied with. Only the requirement for a possible recovery of the disposed waste for 500 years after closure may not be reasonably achievable in larger depths even with corrosion resistant containers. This permanence can be seen as one of the advantages of DBD for safeguards etc. but is a contradiction to this requirement.

If there were a requirement for a maximum temperature of 100 °C or for a preset assumption in safety analyses to be applied, this would be nonsense for DBD since the ambient temperatures at the depths involved can be much higher than this. The capacity to cope with elevated temperatures, including waste-generated, is one of the advantages of the DBD concept.

3 GEOLOGY IN GERMANY

Several studies /BRÄ 94/, /JOB 16/, /REI 14/, /HOT 07/, /SCH 15/ have been done to find geological formations in Germany which could be considered suitable for the final disposal of HLRW.

The study on crystalline rocks for final disposal showed only the outcrops of crystalline rocks on the surface /BRÄ 94/. Recently an update for concepts in crystalline rocks was created referring to the crystalline basement in Germany /JOB 16/. A disposal concept for crystalline rock could be based on the containment by technical and geotechnical barriers like the KBS-3 concept /SKB 15/.

Previous concepts considered mainly domal rock salt for final disposal in Germany /BRA 15/. Recently a study was done which considered layered rock salt /REI 14/.

Also, concepts for clay rock have been developed in the past /HOT 07/.

Only one study considered layered rock salt as a confining rock zone above a mine /SCH 15/. One study considered alternative concepts below rock salt formations /SCH 15/.

Although different requirements have been set, all studies have one thing in common - that a disposal mine is foreseen for disposal. None of the studies considered disposal deeper than 1 500 m depth due to the technological challenges of mining.

4 INVENTORY OF HIGH LEVEL RADIOACTIVE WASTE (HLRW) IN GERMANY

The HLRW consists mainly of spent fuel elements, currently stored in CASTOR containers, canisters with vitrified waste and spent fuel pebbles. These waste types are shown in Figure 4. These waste types must fit into a container for deep borehole disposal as they cannot be handled or disposed of as they are.

The volume of HLRW is limited in Germany due to the phase-out of nuclear energy in 2022 /KOM 16/, /PEI 11/, /BMUB 18a/, /BMUB 18b/. The waste forms are mainly spent fuel elements from power reactors (approximately 35 000 pieces with about 10 500 Mg spent fuel or approximately 7 600 m^3 if considered as fuel rods only), canisters with vitrified waste from reprocessing (approximately 8 000 pieces, approximately 2 000 m^3) and some spent fuel elements from research reactors (approximately 2000 m^3).

The total volume of high-level radioactive waste in POLLUX containers and canisters is projected to be around 27 000 m^3 in 2080 /BMUB 18a/.

The vitrified waste canisters are unlikely to be changed or reconditioned. This means that a disposal container must have a minimum diameter to accommodate vitrified waste canisters or another disposal option must be found for the vitrified waste canisters.

The reconditioning and repackaging of the spent fuel elements are necessary as the direct disposal of CASTOR container in boreholes is considered practically impossible and would require shaft sinking. To minimize the effort for reconditioning and repackaging the spent fuel rods should remain intact. This is considered possible. Therefore, the container to accommodate the intact spent fuel rods must have minimum length of about 5 m.

The spent fuel pebbles can be repacked easily because of their size in any container type.

For all containers subcriticality must be ensured.

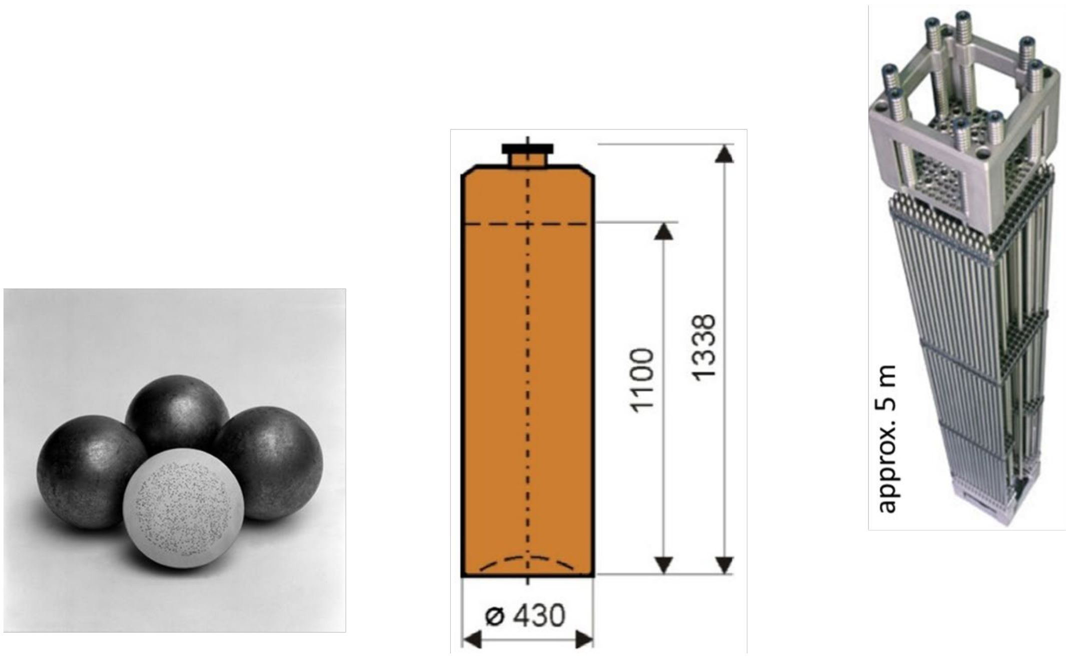

Figure 4. Types of high-level radioactive waste in Germany.

5 DRILLING TECHNOLOGY AND ITS CONSEQUENCES ON THE DISPOSAL CONCEPTS

The drilling technology in the field of conventional deep drilling in the oil and gas industry is well advanced. This led to several proposals to use deep boreholes for disposal for radioactive waste (see e.g. /BES 17/, /GIB 14/, /NWT 16/, /HAR 15/) and even large diameters were considered /RIG 17/. These tests were aborted for political reasons /HEI 17/.

The actual maximum borehole diameter that can be drilled depends on the rock type. The state-of-the-art deep drilling technology allows for the drilling of depths of 5 000 m in crystalline rock with diameters of up to 17.5'' (44.5 cm). This can be ordered off-the-shelf. For larger boreholes, larger roller bits must be developed. Alternatively, drilling techniques in hard rock (e.g. the electric impulse method) would have to be developed or further developed. However, larger borehole diameters cannot currently be drilled using state-of-the-art deep drilling technology at 5 000 m. Adapting deep drilling equipment for drilling into hard rock and for diameters considerably larger than 17.5'' (44.5 cm) would require considerable developmental and testing work. The particular challenges are; to provide the large-sized part with the necessary contact pressure (drill rod design); to continuously clean the cuttings from the borehole (capacity of the pumps); to manage the heavy drill string (development and engineering of a special deep drilling rig); and to develop a well design that can cope with a minimal drilling diameter in the first drilling section (lean casing or mono bore method). Drilling and disposal technologies are presented and discussed in detail in /BOL 18/ and /BRA 16b/.

Some concepts have been considered for DBD in Germany in these studies. They vary in the size of the container and the depth of disposal /BOL 18/, /BRA 16b/ and /BRA 17c/. Three concepts with the approximate technical data are summarized below which differ mainly in borehole diameter and depth of the borehole (Table 4).

The first concept is limited by the biggest possible borehole diameter at 5 000 m according to the state-of-the-art deep drilling technology. The second and third concept for 5 000 m and 3 500 m depth is based on the minimum diameter needed to be able to dispose of the vitrified waste canisters, which are unlikely to be changed or reconditioned as stated before. All three concepts consider a container length of 5.6 m so that the length of the spent fuel rods of approx. 5 m fits into the container.

The pressure on the container results from the load of the stacked containers and the hydrostatic pressure of the liquid column (during operation, the borehole must be filled with fluid for stability reasons). The rock pressure is not considered, as it is assumed that the borehole casing, together with the fluid-filled borehole, will withstand the rock pressure until the borehole seal is fully functional. To withstand the loads at a maximum burial depth taking into consideration the fluid and the casing in the borehole but not the bridge plugs, the steel containers would need a wall thickness of about 4.5 cm to 10 cm depending on the concept.

The advantage of the first concept of smaller borehole diameter of 44.5 cm is that a further development of the drilling technology is not necessary and that the state-of-the-art deep drilling technology can be used. However, the first concept has the disadvantage that a relatively large number of boreholes is required. Furthermore, this concept cannot accommodate the radioactive waste, which is already vitrified, from reprocessing as this would require the containers to have an inner diameter of at least 43 cm. Thus, only the fuel rods of spent fuel elements from power reactors could be emplaced. If one borehole is filled with 180 containers, approx. 150 boreholes would be required for about 27 000 containers. There is still potential for optimization.

The advantage of the second and third concept is that with 31 boreholes (11 000 containers), the number of boreholes is considerably lower than in the first concept. The disadvantage is that without considerable further developments in the deep drilling equipment, these concepts cannot be implemented.

Furthermore, the additional advantage of third concept is that if a lower depth for disposal is selected, the necessary diameter of the borehole can be reduced significantly. This is due to the lower hydrostatic pressure of the liquid column on the container. Therefore, a lower wall thickness of container is needed.

This draft concepts could be used within the site selection process to find suitable regions and sites.

Table 4. Technical data for different concepts in Germany (/BOL 18/, /BRA 16b/, /BRA 17c/).

Concept #	1*	2	3
Reference	/BOL 18/	/BOL 18/	/BRA 16b/, /BRA 17c/
Diameter of borehole	17.5“ / 44,5 cm	35.4“ / 90 cm	29.5“ / 75 cm
Maximum depth of borehole	5 000 m	5 000 m	3 500 m
Disposal zone	3 000 – 5 000 m	3 000 – 5 000 m	1 500 – 3 500 m
Space for cementation	44.5 mm	44 mm	25 mm
Outer diameter of casing	14“ / 356 mm	32“ / 812 mm	27.6“ / 700 mm
Wall thickness of casing	21.6 mm	63.5 mm	62.5 mm
Space between casing and container	24 mm	25 mm	25 mm
Outer diameter of container	265 mm	635 mm	525 mm
Inner diameter of container	175 mm	435 mm	435 mm
Wall thickness of container	45 mm	100 mm	45 mm
Length of container	5.6 m	5.6 m	5.6 m
Number of containers	27 000	11 000	11 000
Number of containers per borehole	180	356	356
Minimum number of boreholes	150	31	31

* Spent fuel rods and pebbles only

A proposed container for the second and third concept is shown in Figure 5. This container would fit the pebbles, the vitrified waste canisters and the spent fuel rods from the disassembled fuel bundles.

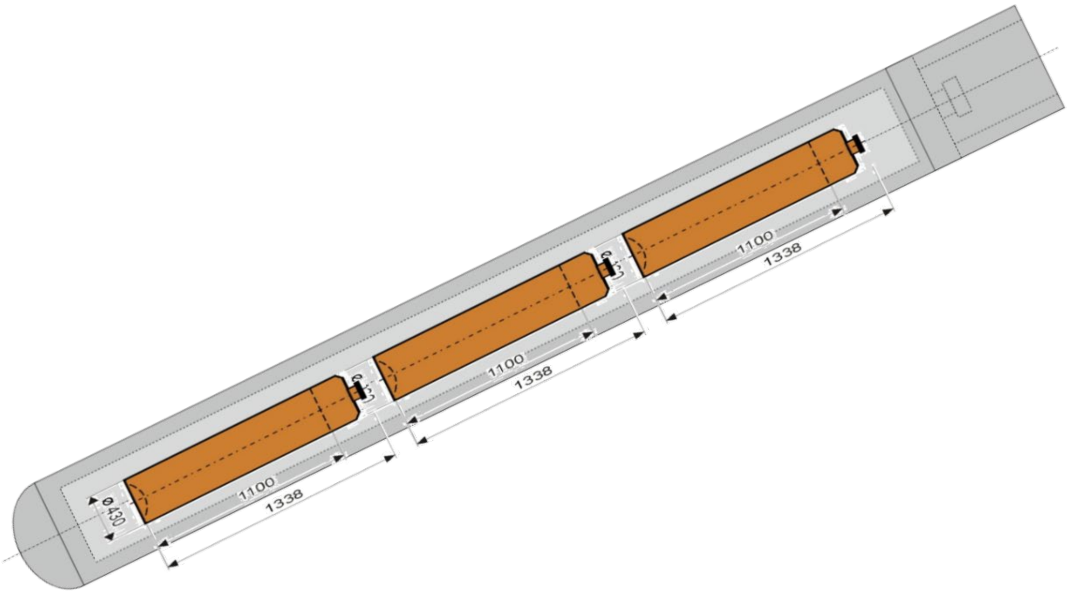

Figure 5. Sketch of the proposed container for deep borehole disposal.

Drilling technology using fluids and a casing for stability for boreholes going down to 5 000 m with a diameter of 37.5 cm can be ordered off-the-shelf. This would cost about 30 million Euro /BRA 17b/. A diameter of 70 cm to 3 500 m depth or even 90 cm to 5 000 m depth would require special equipment which is not currently available off-the-shelf but can be developed, according to drilling engineers. The price has not yet been calculated but will be less than a dry borehole with a diameter of 111 cm down to 5 000 m. A dry borehole of that size would be considered shaft sinking instead of drilling a borehole. A cost estimate yielded more than 500 million Euro /BRA 17b/. It seems to be out of the question because costs alone are too high, without even considering its feasibility.

The Table 5 shows a cost estimate, if the HLRW of Germany were to be disposed in 35 boreholes for about 11 000 containers based on the concept outlined in chapter 6. Clearly, such cost estimates have a high level of uncertainty and are hypothetical, but it would be less than the 24,1 billion € which has been paid by the utilities to a fund for disposal of HLRW /FON 19/.

Initially, a feasibility demonstration is considered mandatory. The effort for site selection and explorations could be limited if several boreholes were installed at one site. Not every borehole will be successfully installed, therefore 35 boreholes are assumed. The steel containers are relatively simple in their design and should not be as costly as CASTOR or POLLUX containers (each approx. up to 1 million €). This figure may change, if the concept is modified.

Reconditioning of the HLRW is necessary, but similar costs would also apply for any other disposal concept. Since the disposal must be performed complying with operational safety requirements and radiological protection, installation and operational costs are relatively high, but the operating time is only 2 years per borehole.

The total costs could be less than 10 billion €.

Table 5. Cost estimate.

Task	Number	Costs	Sum
Feasibility Demonstration	1	500 Mio €/each	0,50 billion €
Site Selection and Exploration	5	200 Mio €/each	1,00 billion €
Borehole	35	50 Mio €/each	1,75 billion €
Containers	11 000	0,1 Mio €/each	1,10 billion €
Reconditioning	1	1 Billion €	1,00 billion €
Installation and Operating Costs	35 / 2 years	50 Mio €/each	3,50 billion €
Licensing / safety analyses	35	5 Mio € /each	0,175 billion €
Total	**-**	**-**	**9,025 billion €**

6 OUTLINE OF A CONCEPT FOR DEEP BOREHOLE DISPOSAL IN GERMANY

6.1 Safety concept

A proposed concept for DBD should comply with the site selection act, which foresees a CPRZ. Disposal using boreholes in rock salt or clay rock could be type A. Whereas, disposal using boreholes in crystalline rock would be at least type Bb if overlaying rock salt or clay rock formations are considered as CPRZ. If exploration can characterize crystalline rock well enough the assignment of type A could be possible. The disposal technology, whether using mines or deep boreholes should not be relevant for the assignment of these types. overlaying of rock salt and clay rock formations are available in Germany /SCH 15/, it seems possible to have a redundant and diverse multiple barriers system of type Bb when using DBD.

Therefore, the use of multiple, independent geological barriers formed by e.g. clay and salt layers together with seals, should provide the main safety functions of a generic concept for DBD. This means that boreholes must be sealed effectively to restore the functionality of the geological barriers.

The study /BOL 18/ outlined that it may be possible to install a borehole seal into a dry borehole. The borehole will be stable while lowering the liquid column in a way that the sealed area is dry. This allows the use of different materials to create redundant and diverse borehole seals. Some materials were considered as possible backfilling or sealing materials like bentonite, bitumen / asphalt, and cement as well as salt suspensions and eutectic molten salt and barite /BOL 18/. First considerations about how to feed the material into the boreholes or voids have also been presented /BOL 18/. However, all these technologies still need to be developed and tested with regard to the special conditions of DBD.

Furthermore, only very slow groundwater movement should be probable at great depths which ideally restricts radionuclide migration to diffusion alone. The generalized concept foresees disposal in the geological bed-rock (which is most likely a crystalline rock) which should be overlain by at least two redundant or diverse geological barriers acting as CPRZ. Ideally, an additional geological feature could act as gas trap below these barriers.

The minimum depth for DBD is selected at 1 500 m to allow a suitable geological setting with barriers /BRA 17c/ to be found. Furthermore, at lesser depths technical features of a mine could outweigh DBD features. The greater depth of DBD compared to disposal in a mine will facilitate the finding of sites with several independent geological barriers and exclude glacial impacts on barriers and waste with greater certainty. The maximum depth for DBD is set at 3 500 m. This is due to the large diameter of the borehole. The technical challenge and costs increase greatly with depth. A disposal length of 2 000 m seems to be sufficient for an outline of a concept. Inclined, deviated or horizontal boreholes are not considered at that stage.

The minimum and maximum depth should be optimized by considering geological setting, state-of-the art drilling, disposal technology and the outcome of safety analyses. A vertical borehole is preferred over inclined boreholes but multiple and deviating boreholes are possible.

Possible geological barriers overlying the disposal zone (designated zone) are:

- Clay rock: bedded clay which can ensure retardation and containment.
- Salt rock: bedded salt with high sealing capacity and self-sealing ability based on its visco-plastic characteristics.

These barriers should be combined ideally. At least two independent barriers should be available. A further possible feature would be porous rock (e.g. sandstone) acting as a trap for gases which could be released from the disposal zone. Such settings occur naturally in Germany and can be found undisturbed. A schematic figure is shown in /BRA 17c/.

An alternative concept of DBD was proposed in /BOL 18/ considering a disposal in boreholes in salt rock (domal salt) at depths of 2 500 to 4 000 m. This would take advantage of some features of rock salt. For example, the self-sealing features of rock salt are useful as it creeps under stress. This process becomes even faster with increasing temperatures. Therefore, it is possible to seal the boreholes very quickly by using the creeping feature of the salt rock. This is not possible in any other host rock.

6.2 Other aspects for concepts in Germany

Besides challenges such as drilling large boreholes in great depth, borehole stability, operational safety on disposal and retrieval technology are important when disposing high-level radioactive waste. Incidents such as the sticking of containers and leakage of radionuclides from containers must be discussed and managed.

Considering the concept for containment, three rock zones can be defined:

- Disposal zone where containers are supposed to be disposed of
- Retention zone, which is the containment providing rock zone (CPRZ)
- Transfer zone to which the container must pass.

If a container becomes stuck in the designated disposal zone and cannot be recovered, the container may stay in place and the borehole is abandoned and sealed.

If a container becomes stuck in the transfer zone, a removable liner should have been foreseen. The liner including the container is recovered.

If a container leaks, the contaminated fluid must be dealt with. Contamination in the designated or retention zone alone would imply abandonment and sealing of the borehole without handling of the fluid.

If a container leaks within the transfer zone, the liner with container and the fluid can be recovered and treated. A gate / valve using a hydraulic control pipe to separate the fluid in the liner from the remaining borehole fluid must be foreseen.

This implies monitoring of fluids for radioactivity at any time to detect leakage and to provide enough storage and treatment facilities.

This concept is supposed to show that technical solutions are available to handle such incidents. A schematic figure is shown in /BRA 17c/.

7 DISCUSSION

A detailed safety analysis and assessment of a general concept for DBD in Germany has not been performed. A study on borehole disposal in the U.S. considered a radionuclide transport around the borehole /ARN 11/. The radionuclide transport from that depth would exhibit an extremely low release of radionuclides to the biosphere. Still, it must be shown for a generic concept or site with CPRZ in Germany.

The commission handed over their report /KOM 16/ to the German government recommending preferably a geological disposal with a mined repository. They also recommend following up on developments in DBD as the only alternative option as other options (e.g. partitioning and transmutation) were excluded. Based on this report, the German Parliament updated the site selection act in 2017 and restructured the duties of the different actors. The act provided many requirements which must be fulfilled in each phase prior to the selection of regions, areas or sites.

There are exclusion and minimum criteria which must be fulfilled by any region, area or site. These criteria can also be met by a site using DBD. Furthermore, the site selection act does not limit the depth.

Weighting criteria are applied if there are several possible sites. Only three aspects of about 12 criteria must be considered more specifically in detail for DBD.

The first one is the gas compatibility. There is a lot of steel put underground using containers and casings which may generate gas. This can be addressed in a concept.

The second one concerns the temperature. The site selection act requires that a safety analysis should be done for temperatures of 100°C on the outside of the container. If the temperature is higher, further research must show that it is also safe and feasible. At depths of more than 1 500 m, the temperature underground is already high and will raise in most cases beyond 100°C when disposing HLRW. Therefore, detailed safety analyses on this are needed for DBD compared to disposal in a mine.

The third aspect refers to the requirement of geochemistry of the disposal zone and CPRZ. These zones do not coincide in the configuration of type Bb. Therefore, an interpretation is needed, and how it can apply to DBD must be discussed in detail.

Apart from these weighting requirements, recovery of radioactive waste for up to 500 years after sealing of the boreholes is required in the site selection act. This will remain a challenge once the waste is disposed of in deep boreholes and the boreholes are sealed. This requirement could be changed as it can been seen to be in contradiction to safeguards and possible proliferation.

The requirements stipulated by the relevant legal regulations in Germany are listed and analyzed also in /BOL 18/. It was concluded that applying current legal provisions and requirements to DBD would cause an impediment as these provisions refer to disposal in mines. Thus, some legal requirements can and should be revised or redrafted in such a way that they also apply to DBD. This is political and not a technical issue.

The site selection process is performed in several steps to find the best suitable site. In later steps draft concepts are needed to select regions, sites for underground exploration and to perform the required (provisional) safety analyses. If a draft concept for DBD is not included, this may exclude favourable regions and sites.

Research and development is needed for DBD if it should ever become a feasible option for Germany. This concerns the conceptual design and safety concept as the former studies were general. Moreover, a technical feasibility study with practical demonstration is required. The container design can be further improved and optimized. It is still necessary to discuss the requirement of recovery.

Further open issues are: Is long-term monitoring needed and how can it be done? Also, there is a need for an operational safety analysis.

Some advantages of DBD are; a multiple barrier system due to its great depth; the fact that no man must go underground as it is man-less disposal technology; several sites being possible provided that the geology is suitable; proliferation not being likely once the waste is disposed of; the cost possibly being less, and the implementation possibly being quicker.

However, the biggest issue for DBD in Germany is that no major actor (which are BGE and BfE) is currently interested in following up developments in DBD nor in supporting further research on it. All actors intend to stick to the exact wording of the site selection act. Although it is not foreseen in the site selection act to follow or support developments of DBD, it is also not forbidden to do so. Any work on DBD could rely only on the recommendation of the commission /KOM 16/. Therefore, it will be difficult for any organization to get enough funds for further research, development or feasibility studies on DBD in Germany.

Disposal of high-level radioactive waste remains a very political topic. The political agreement, which has been made when issuing the site selection act, seems to be stable. If the site selection procedure performs successfully in the next few years, no one will seek an alternative option. Therefore, it is not expected by the authors that politics will change details (e.g. requirement on recovery, temperature issue) to facilitate pursuing DBD.

8 SUMMARY AND CONCLUSIONS

The present article summarizes the background and status of DBD in Germany as it can be concluded from two studies /BOL 18/, /BRA 16b/, final report of the commission /KOM 16/ and the site selection act /STA 17/. Supporting ordinances to site selection act are to be issued soon in 2019. These regulations will not likely prescribe the follow-up of other options such as DBD, which has been mentioned in /KOM 16/.

As no major actor (BGE, BfE) in Germany is currently interested in following up developments in DBD or in supporting further research on it, DBD is likely to only be followed up at a very low-level in Germany. That is, if there are significant developments or progress in other countries. Even then, active support in DBD by research, development or feasibility studies is not expected in Germany as skepticism is high, especially when considering the requirement of recovery and the discussion of maximum container temperatures. Nevertheless, the German oil and gas industry has a lot of know-how and the appropriate specialists to carry out developments of DBD if asked.

Only if the site selection procedure is going to fail for whatever reason by 2031, may DBD become an interesting option. Results of the site selection procedure from later phases will hardly apply fully to this option, as the geological settings have not been considered in the concepts which are needed to perform a site selection for DBD.

9 OUTLOOK

There is still a chance that DBD to be followed up on at a very low level in Germany. If the site selection procedure is not progressing well, than the alternative option of DBD may find greater interest in the future.

10 REFERENCES

/AKE 02/ Bundesamt für Strahlenschutz (BfS) (Hrsg.): Auswahlverfahren für Endlagerstandorte, Empfehlungen des AkEnd, Abschlussbericht. Arbeitskreis Auswahlverfahren Endlagerstandorte (AkEnd), 260 S.: Köln, Dezember 2002.

/APT 17/ Apted, M. J., Ahn, J. (Hrsg.): Geological repository systems for safe disposal of spent nuclear fuels and radioactive waste. Woodhead Publishing Series in Energy, 778 S., ISBN 9780081006528, Woodhead Publishing: Cambridge, UK, 2017.

/ARN 11/ Arnold, B. W., Brady, P. V., Bauer, S. J., Herrick, C., Pye, S., Finger, J.: Reference Design and Operations for Deep Borehole Disposal of High-Level Radioactive Waste. SANDIA National Laboratories (SNL), SAND2011-6749, 67 S.: Albuquerque, New Mexico, 2011.

/ARN 14/ Arnold, B. W., Brady, P. V., Sutton, M., Travis, K. P., MacKinnon, R., Gibb, F. G. F., Greenberg, H.: Deep Borehole Disposal Research: Geological Evaluation, Alternative Wasteforms, and Borehole Seals. Hrsg.: Sandia National Laboratories, SAND2014-17430R, 99 S.: Alburquerque, NM, USA, 5. September 2014.

/ATG 18/ Gesetz über die friedliche Verwendung der Kernenergie und den Schutz gegen ihre Gefahren (Atomgesetz - AtG) in der Fassung vom 15. Juli 1985 (BGBl. I 1985, Nr. 41, S. 1565-1583), zuletzt geändert durch Artikel 1 des Gesetzes vom 10. Juli 2018 (BGBl. I 2018, S. 1122–1124).

/BES 17/ Beswick, A. J.: Borehole Construction and Operation for Disposal in Crystalline Rocks. Radwaste Solution, Bd. 24, Nr. 1, S. 28–32, 2017.

/BMU 10/ Federal Ministry for the Environment, Nature Conversation and Nuclear Safety (BMU): Safety Requirements Governing the Final Disposal of Heat-Generating Radioactive Waste. 21 S.: Bonn, Germany, 30. September 2010.

/BMU 19/ Bundesministerium für Umwelt, Naturschutz und nukleare Sicherheit (BMU): Referentenentwurf, Verordnungen über die sicherheitstechnischen Anforderungen an die Entsorgung hochradioaktiver Abfälle. 49 S.: Berlin, 11. Juli 2019.

/BMUB 18a/ Federal Ministry for the Environment, Nature Conversation, Building and Nuclear Safety (BMUB): Joint Convention on the Safety of Spent Fuel Management and on the Safety of Radioactive Waste Management. Report of the Federal Republic of Germany for the Sixth Review Meeting in May 2018, 340 S., Mai 2018.

/BMUB 18b/ Bundesministerium für Umwelt, Naturschutz, Bau und Reaktorsicherheit (BMUB): Verzeichnis radioaktiver Abfälle, Bestand zum 31. Dezember 2017 und Prognose. 84 S.: Bonn, August 2018.

/BOL 18/ Bollingerfehr, W., Dieterichs, C., Herold, M., Kudla, W., Reich, M., Rosenzweig, T.: Untersuchungen zu Chancen und Risiken der Endlagerung wärmeentwickelnder radioaktiver Abfälle und ausgedienter Brennelemente in Tiefen Bohrlöchern (CREATIEF), Abschlussbericht. Technische Universität Bergakademie Freiberg (TUBAF), BGE TECHNOLOGY GmbH (BGE TEC), 182 S.: Freiberg / Peine, 31. Juli 2018.

/BRA 15/ Bracke, G., Fischer-Appelt, K.: Methodological approach to a safety analysis of radioactive waste disposal in rock salt, An example. Progress in Nuclear Energy, Bd. 84, S. 79–88, DOI 10.1016/j.pnucene.2015.01.012, 2015.

/BRA 16a/ Bracke, G., Hurst, S., Merkel, B., Müller, B., Schilling, F. (Hrsg.): Proceedings of the Workshop “Final Disposal in Deep Boreholes Using Multiple Geological Barriers: Digging Deeper for safety”, 5-6 June 2015, Berlin. Gesellschaft für Anlagen- und Reaktorsicherheit (GRS) gGmbH, GRS-405, 278 S., ISBN 978-3-944161-87-7: Köln, 2016.

/BRA 16b/ Bracke, G., Charlier, F., Geckeis, H., Harms, U., Heidbach, O., Kienzler, B., Liebscher, A., Müller, B., Prevedel, B., Röckel, T., Schilling, F., Sperber, A.: Tiefe Bohrlöcher. GRS-423, 316 S., ISBN 9783946607052, Gesellschaft für Anlagen- und Reaktorsicherheit (GRS) gGmbH: Köln, Garching b. München, Berlin, Braunschweig, Februar 2016.

/BRA 17a/ Bracke, G.: Endlagerkonzept einer tiefen Bohrlochlagerung (Deutschland), Anforderungen an aktuelle Endlagerkonzepte für unterschiedliche Wirtsgesteinsformationen, Bericht zum Arbeitspaket 1. Gesellschaft für Anlagen- und Reaktorsicherheit (GRS) gGmbH, GRS-471 Anhang 7, 61 S.: Köln, August 2017.

/BRA 17b/ Bracke, G., Charlier, F., Liebscher, A., Schilling, F., Röckel, T.: Does Deep Borehole Disposal of HLRW has a Chance in Germany? atw - Internationale Zeitschrift für Kernenergie, Bd. 62, Nr. 1, S. 46–53, 2017.

/BRA 17c/ Bracke, G., Charlier, F., Liebscher, A., Schilling, F., Röckel, T.: About the Possibility of Disposal of HLRW in Deep Boreholes in Germany. Geosciences, Bd. 7, Nr. 3, S. 58, DOI 10.3390/geosciences7030058, 2017.

/BRA 18/ Bracke, G., Weyand, T., Hartwig-Thurat, E., Meleshyn, A., Larue, J., Fischer-Appelt, K.: Untersuchungen zu den “maximalen physikalisch möglichen Temperaturen” gemäß § 27 StandAG im Hinblick auf die Grenztemperatur an der Außenfläche von Abfallbehältern. Gesellschaft für Anlagen- und Reaktorsicherheit (GRS) gGmbH, 1. Statuskonferenz Endlagerung von hochradioaktiven Abfällen, DOI 10.13140/RG.2.2.23328.: Berlin, 8. November 2018.

/BRA 19/ Bracke, G., Kudla, W., Rosenzweig, T.: Status of Deep Borehole Disposal of High-Level Radioactive Waste in Germany. Energies, Bd. 12, Nr. 13, S. 2580, DOI 10.3390/en12132580, 4. Juli 2019.

/BRÄ 94/ Bräuer, V., Reh, M., Schulz, P., Schuster, P., Sprado, K.-H.: Endlagerung stark wärmeentwickelnder radioaktiver Abfälle in tiefen geologischen Formationen Deutschlands, Untersuchung und Bewertung von Regionen in nichtsalinaren Formationen. Bundesanstalt für Geowissenschaften und Rohstoffe (BGR), Archiv-Nr.: 112642 Hannover; 2025039 Berlin; Tgb.-Nr.: 12437/91, 147 S.: Hannover, November 1994.

/CHA 03/ Chapman, N., McCombie, C.: Principles and Standards for the Disposal of Long-lived Radioactive Wastes. Waste Managment Series, Bd. 3, 277 S., ISBN 0080441920, Elsevier Science Limited: Oxford, 2003.

/DEE / Deep Isolation Technical Team: Technology - Deep Isolation. http://www.deepisolation.com/about/, erreichbar unter https://www.deepisolation.com/ technology/, abgerufen am 22. März 2019.

/ENT 17/ Gesetz zur Errichtung eines Fonds zur Finanzierung der kerntechnischen Entsorgung (Entsorgungsfondsgesetz - EntsorgFondsG) (EntsorgFondsG), zuletzt geändert 2017 (BGBl. I 2017, 114, 1672).

/FON 19/ Fonds zur Finanzierung der kerntechnischen Entsorgung: erreichbar unter http:// www.entsorgungsfonds.de/, abgerufen am 23. Juni 2019.

/GIB 14/ Gibb, F. G. F., Beswick, A. J., Travis, K. P.: Deep borehole disposal of nuclear waste, Engineering challenges. Proc. Inst. Civ. Eng.-Energy, Bd. 167, Nr. 2, S. 47–66, DOI 10.1680/ener.13.00016, 2014.

/HAR 15/ Hardin, E. L.: Deep Borehole Field Test Requirements and Controlled Assumptions. SANDIA National Laboratories (SNL), SANDIA Report, SAND2015-6009, 31 S.: Albuquerque / New Mexico / USA, 2015.

/HEI 17/ Heidelberger, C. A.: Energy Dept. Cancels Deep Borehole Field Test. erreichbar unter https://dakotafreepress.com/2017/05/23/energy-dept-cancels-deep-borehole-field-test/, abgerufen am 24. Juni 2019.

/HOT 07/ Hoth, P., Wirth, H., Reinhold, K., Bräuer, V., Krull, P., Feldrappe, H.: Endlagerung radioaktiver Abfälle in tiefen geologischen Formationen Deutschlands, Untersuchung und Bewertung von Tongesteinsformationen. Hrsg.: Bundesanstalt für Geowissenschaften und Rohstoffe (BGR), 118 S.: Berlin / Hannover, 1. April 2007.

/IAEA 17/ International Atomic Energy Agency (IAEA): Selection of Technical Solutions for the Management of Radioactive Waste. IAEA TECDOC Series No. 1817, v.1817, 1114 S., ISBN 9789201047175, IAEA: Vienna, 2017.

/INT 03/ International Atomic Energy Agency (IAEA): Scientific and technical basis for the geological disposal of radioactive waste. Technical Report Series, Bd. 413, STI/DOC/010/413, 80 S., ISBN 9201001037, International Atomic Energy Agency: Vienna, 2003.

/JOB 16/ Jobmann, M., Becker, D.-A., Hammer, J., Jahn, S., Lommerzheim, A., Müller-Hoeppe, N., Noseck, U., Krone, J., Weber, J. R., Weitkamp, A., Wolf, J.: Projekt CHRISTA: Machbarkeitsuntersuchung zur Entwicklung einer Sicherheits- und Nachweismethodik für ein Endlager für Wärme entwickelnde radioaktive Abfälle im Kristallingestein in

Deutschland. Gesellschaft für Anlagen- und Reaktorsicherheit (GRS) gGmbH, Bundesanstalt für Geowissenschaften und Rohstoffe (BGR), DBE TECHNOLOGY GmbH (DBETEC), TEC-20-2016-AB: Peine, 20. Oktober 2016.

/KOM 16/ Kommission Lagerung hoch radioaktiver Abfallstoffe: Abschlussbericht, Verantwortung für die Zukunft - Ein faires und transparentes Verfahren für die Auswahl eines nationalen Endlagerstandortes. Drucksache der Kommission Lagerung hoch radioaktiver Abfallstoffe, K-Drs. 268, 683 S.: Berlin, 30. August 2016.

/NWT 16/ Ewing, R. C., Bahr, J. M., Becker, S. M., Brantley, S. L., Croff, A. G., Foufoula-Georgiou, E., Frankel, G. S., Nozick, L. K., Peddicord, K. L., Turinsky, P. J., Zoback, M. L.: Technical Evaluation of the U.S. Department of Energy Deep Borehole Disposal Research and Development Program, A Report to the U.S. Congress and the Secretary of Energy. Hrsg.: U.S. Nuclear Waste Technical Review Board (NWTRB), 32 S.: Arlington, VA, USA, 27. Januar 2016.

/OJO 14/ Ojovan, M. I., Lee, W. E.: An introduction to nuclear waste immobilisation. 2. Aufl., 512 S., ISBN 9780080993928, Elsevier: Kidlington UK, Oxford, UK, Waltham, MA, USA, 2014.

/PEI 11/ Peiffer, F., McStocker, B., Gründler, D., Ewig, F., Thomauske, B., Havenith, A., Kettler, J.: Abfallspezifikation und Mengengerüst. Basis Ausstieg aus der Kernenergienutzung (Juli 2011), Bericht zum Arbeitspaket 3, Vorläufige Sicherheitsanalyse für den Standort Gorleben. GRS-278, 89 S., ISBN 978-3-939355-54-0, Gesellschaft für Anlagen- und Reaktorsicherheit (GRS) mbH: Köln, 2011.

/REI 14/ Reinhold, K., Hammer, J., Pusch, M.: Verbreitung und Eigenschaften flach lagernder Salzschichten in Deutschland (BASAL), Verbreitung, Zusammensetzung und geologische Lagerungsverhältnisse flach lagernder Steinsalzfolgen in Deutschland - Zwischenbericht. Bundesanstalt für Geowissenschaften und Rohstoffe (BGR), 9Y2013030000, 111 S.: Hannover, 2014.

/RIG 17/ Rigali, M. J., Hardin, E. L., Stein, E. R., Su, J.-C.: Large Diameter Deep Borehole Disposal Concept for HLW Glass. In: American Nuclear Society (ANS) (Hrsg.): Proceedings. International High-Level Radioactive Waste Management Conference, Charlotte, NC, 9. - 13. April 2017, S. 536, 2017.

/SCH 15/ Schreiber, U., Jentzsch, G., Ewert, T.: Geologische Potentiale zur Einlagerung von radioaktiven Abfallstoffen unterhalb von stratiformen Salzformationen, Konzeptstudie für ein alternatives Endlagermodell. Kommission Lagerung hoch radioaktiver Abfallstoffe, Material für die Kommission Lagerung hoch radioaktiver Abfallstoffe, K-MAT 42, 28 S., 22. April 2015.

/SKB 15/ Birgersson, L.: The barriers in the KBS-3 repository in Forsmark. Svensk Kärnbränslehantering AB (SKB), SKB Public Report, Nr. 1520261, 18 S., 10. Dezember 2015.

/STA 13/ Gesetz zur Suche und Auswahl eines Standortes für ein Endlager für Wärme entwickelnde radioaktive Abfälle (Standortauswahlgesetz – StandAG) in der Fassung vom 23. Juli 2013 (BGBl. I 2013, Nr. 41, S. 2553-2561).

/STA 17/ Gesetz zur Suche und Auswahl eines Standortes für ein Endlager für hochradioaktive Abfälle (Standortauswahlgesetz – StandAG) in der Fassung vom 5. Mai 2017 (BGBl. I 2017, Nr. 26, S. 1074-1100), zuletzt geändert 20. Juli 2017 (BGBl. I 2017, Nr. 52, S. 2808–2838).

Lessons learned during planning and first phases of decommissioning of the Finnish TRIGA FiR 1[1]

M.I. Airila, I. Auterinen, P. Kotiluoto, A. Räty

VTT Technical Research Centre of Finland Ltd, PO Box 1000, 02044 VTT, Finland

Abstract:

The operation of the FiR 1 reactor ended in 2015, after which the reactor has been in permanent shutdown, used fuel still at the facility and partly in the core. VTT as the operator applied for a license for decommissioning in June 2017. FiR 1 is the first nuclear facility to be decommissioned in Finland. Going from operation to decommissioning requires organizational changes and improvements in the quality management system of the reactor. New procedures for free or controlled release of materials and equipment from the reactor are being developed and implemented. We review the evolution of FiR 1 decommissioning plan, waste management plans and project duration and cost estimates over years 1988-2018. The estimates for manpower, duration and costs have increased significantly along with more detailed planning and identification of additional needs. Lack of operational services for the nuclear waste from FiR 1 has caused project delays after 2014, implying additional cost increases, e.g. in planning and in maintaining the reactor facility.

1 INTRODUCTION

The State of Finland procured the 250 kW TRIGA Mk II reactor FiR 1 from the United States in 1960 for educational and research purposes at the Helsinki University of Technology. VTT Technical Research Centre of Finland has administered the reactor since 1971. The reactor has been operated in the Otaniemi campus area located in Espoo, Finland, about 10 km from the Helsinki city centre, since 1962. In the early days, the reactor was mainly used for neutron and reactor physics research and national education. At a later stage, intensive use was made of its radiation for chemical element analyses, including soil and lunar soil samples. In the 1990's, the reactor was complemented with a boron neutron capture therapy (BNCT) facility using moderator material technology developed by VTT, and utilised for patient care. Radiotherapy ended in January 2012, when the company organising it went bankrupt. We describe the history in more detail in [2].

2 LICENSING FIR 1 FOR DECOMMISSIONING

VTT shut down the reactor permanently on 30 June 2015, and two years later, in June 2017, submitted to the Finnish Government an application according to Section 20 of the Nuclear Energy Act [3,4] to decommission the FiR 1 research reactor[2] and to possess, use, handle and store nuclear waste and existing nuclear materials as is necessary for decommissioning [5].

[1] Published previously in the RRFM2019 Conference [1]. Minor updates have been made to this version.

[2] In the 2018 amendment of the Nuclear Energy Act, an additional Section 20a *Licensing - Decommissioning of a nuclear facility* was introduced. However, as VTT submitted the application prior to the amendment, the applied license is formally an *operating license* (for decommissioning) as defined in Section 20.

The contents of the application follow the requirements of the Nuclear Energy Decree [6,7] as described in Fig. 1. Already prior to the shutdown, VTT carried out an environmental impact assessment (EIA) for decommissioning in 2013–15. As the competent authority, the Ministry of Economic Affairs and Employment of Finland (MEAE) gave its final statement on the EIA report in February 2015. A few stakeholders provided MEAE with their remarks on the report, which VTT has accounted for in the detailed decommissioning planning and replied to in the license application.

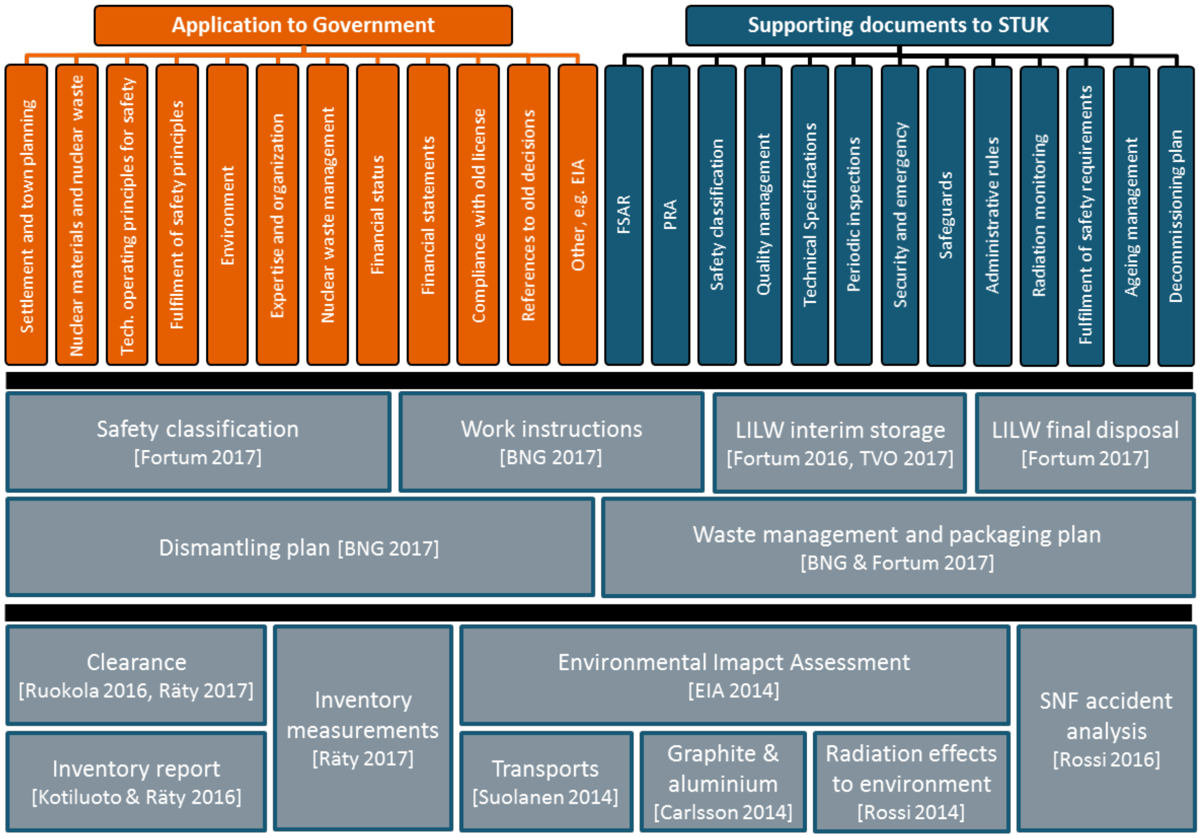

Fig 1. Structure of the licensing documentation for FiR 1, following the Finnish Nuclear Energy Decree. Orange: application and appendices according to Section 34 of the Decree. Blue: Technical documentation according to Section 36 of the Decree. Grey (bottom layer): Fundamental topical reports prepared mostly by VTT for the EIA and license application. Grey (middle layer): Detailed technical plans contracted by VTT, forming the basis for the decommissioning plan.

3 ITERATIVE REFINEMENT OF DECOMMISSIONING PLANS

3.1 Finnish requirements for waste management and decommissioning planning of nuclear facilities

The Finnish Nuclear Energy Act regulates decommissioning and nuclear waste management planning during the operation of a nuclear facility.

The purpose of the *decommissioning plan* is to assess the sufficiency and appropriateness of the technical solutions for dismantling and waste management. Unless otherwise provided in the licence conditions, a plan for the decommissioning of the nuclear facility shall be presented every six years. Therefore, all operators, including VTT, have prepared several editions of preliminary decommissioning plans for their facilities. As an exception from these rules, during the last years of operation and during preparation for decommissioning of FiR 1, the authority has required VTT to update the plans annually.

The *waste management plan* includes basic (final) solutions for SNF and decommissioning waste, and the authority uses it also to quantify the financial provision obligation (amount of deposit in the national nuclear waste management fund VYR) of the licensee. The plan for carrying out nuclear waste management shall be presented to the authority (MEAE) every three years, unless otherwise provided in the licence conditions. The plan shall also include a general plan for the following six years.

3.2 Evolution of VTT's technical decommissioning plans

During operations, VTT maintained a generic decommissioning plan, which discusses possible dismantling methods and available waste management options as well as gives rough estimates for the cost and duration of decommissioning and for doses to the workers. As an example of that plan, we show a planned dismantling sequence and schedule in Fig. 2. The plan relies on inventories and other data that have been obtained from other reactors and scaled to the dimensions, thermal output etc. of FiR 1. In waste management planning, the underlying assumption has been that VTT (being a state research centre at that time) would have access to the waste management facilities of Finnish NPP's in a relatively straightforward and inexpensive manner.

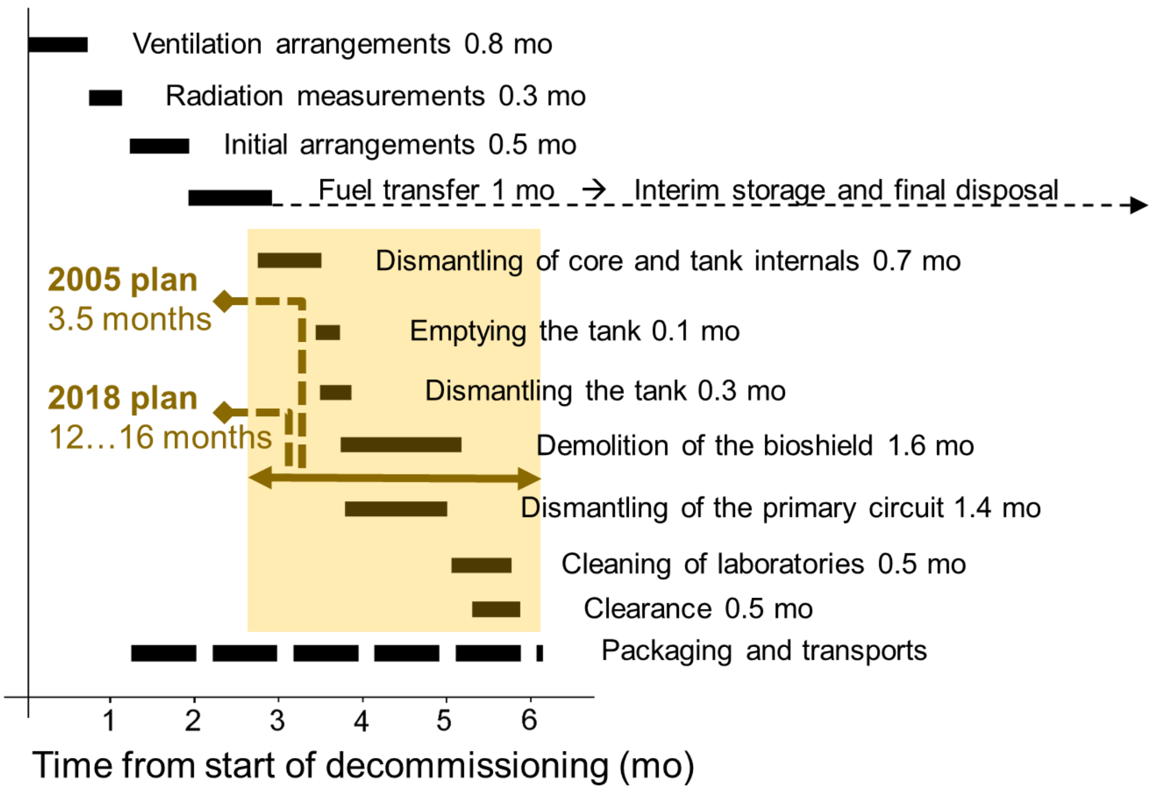

Fig 2. An example of an estimated project schedule from 2005 (originally from 1988). In the 2018 plan, the duration of the highlighted phase (reactor dismantling) has expanded about 4-fold due to more detailed consideration of all sub-tasks.

In 2007, VTT contracted from the Finnish company Platom a consultation on potential decommissioning strategies, including various options to execute the project, and a review of VTT's decommissioning plan for FiR 1. This work yielded suggestions for developing the plan, in particular by using experiences from Frankfurt TRIGA decommissioning in Germany.

In 2013, VTT contracted Platom a preliminary dismantling plan, which reviews available dismantling and demolition techniques and gathers systematically experiences and data from several decommissioned foreign research reactors (German HD-2, Danish DR-2 and Korean KRR-1). This work constituted one of the background reports for the EIA.

In 2016, VTT contracted the German company Babcock Noell GmbH to carry out detailed dismantling planning, using all specific background information from FiR 1, in order to obtain a documentation suitable for the procurement of the dismantling works. The work was completed early 2017, and the resulting technical reports and work instructions (about 540 pages) constitute a significant part of the topical reports submitted to the Finnish Radiation and Nuclear Safety Authority (STUK) as part of the decommissioning licensing process. On a more general level, VTT prepared the first version of the decommissioning plan to be approved by STUK and a draft safety assessment report (SAR) for decommissioning. These documents were largely based on the dismantling plan but included additional information on waste management.

There are further needs to refine the detailed dismantling plan in order to include all practical considerations related to site logistics, taking waste acceptance criteria fully into account, and integrating the dismantling, waste management, radiation protection and security operations at the site. The remaining planning work belongs to the scope of decommissioning and nuclear waste management services that VTT is currently contracting. As a prerequisite for starting the dismantling, STUK requires that the final planning documentation has been delivered for review 6 months earlier and approved by STUK. VTT estimates that this allows starting the dismantling in mid-2021, provided that the SNF has been repatriated to US by that time.

3.3 Evolution of VTT's cost estimates for decommissioning

The financial provisions for decommissioning and nuclear waste management are based on plans presented by the licensees and approved by MEAE. VTT's approved estimates between 1988–2018 are presented in Fig. 3.

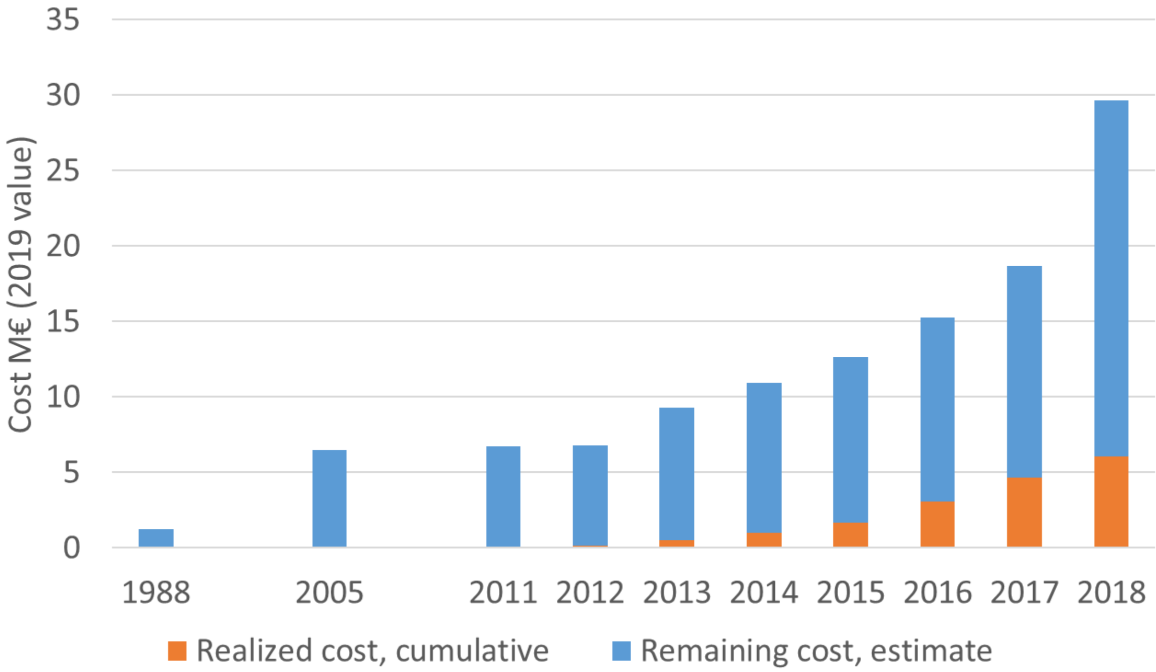

Fig. 3. Evolution of decommissioning cost estimate 1988–2018. In 2018, VTT revised the cost estimate radically by including SNF interim storage with necessary licensing, investments and related further time delay at a Finnish NPP site.

The cost estimate of the spent nuclear fuel (SNF) management has been based on the other hand on published US DOE SNF return fee for TRIGA fuel [8,9] and on references of shipping costs in similar cases in Europe; on the other hand on an estimation of FiR 1 share in the Posiva SNF final repository in Finland. In the past, cost estimates on the domestic option have been lower than the US option, so in the waste management plan the costs of the US option have been used for conservatism.

The cost estimates for decommissioning waste have evolved from 0.758 M€ (2005) to 3.413 M€ (2018). Main cost drivers are: (i) inclusion explicit costs of a separately licenced intermediate storage phase before final disposal; (ii) explicit inclusion of the licensing and construction costs; (iii) recognizing that NPP operators are presently indicating pricing on a commercial basis (while early estimates assumed that they would service VTT essentially on a cost price basis); and (iv) adding an uncertainty of 30 % on top of the base estimate.

The amount of realized planning and paperwork exceeds significantly the original estimates. In the original plans, the need for a full re-license for nuclear facility was not foreseen, but VTT assumed that an amendment of the conditions of the existing license would be sufficient. In 2016, MEAE required that VTT must apply for a new license, which triggered the preparation of all documentation described in Fig. 1.

From 2014, the project has suffered from prolonged schedule due to uncertainties in waste management solutions (both SNF return to US and decommissioning waste in Finland). Maintaining the project and the fully licenced nuclear facility requires several hundred thousand euros annually. Analogously, the cost of decommissioning work increased mainly due to the longer execution time.

4 BEST PRACTICES AND ACHIEVEMENTS DURING PLANNING AND LICENSING PHASE

4.1 Impact on national regulation and practices

As FiR 1 is the first nuclear facility to be decommissioned in Finland under contemporary legislation[3], also many parts of the legislation and regulation are now entering practical testing for the first time. To facilitate efficient preparation and review of the licensing documentation, VTT carries out regular information exchange with authorities (MEAE and STUK). In addition to the official correspondence between licensee and authority, VTT and authorities arrange technical expert-level meetings to discuss the licensing process and regulatory details, which need interpretation. In many cases, VTT's hands-on experience has yielded interpretations on how to apply specific requirements to achieve the safety goals while maintaining reasonable means to implement the requirements in practice. MEAE and STUK have also already used experiences from VTT's project in the development of legislation (the 2018 amendment of the Nuclear Energy Act put significant focus on decommissioning). In addition, MEAE recently reported on the results of a national working group aiming at enhancing the practices for nuclear and radioactive waste management in Finland [12]. As one outcome of the work, MEAE added a license condition to Olkiluoto NPP's operating license for years 2019–38, which allows the licensee to store on the site nuclear and radioactive low- and intermediate level waste originating also from other sources than NPP itself. The operating and decommissioning waste from FiR 1 and VTT's radioactive structural materials' research laboratory are the largest such waste streams in Finland.

4.2 Experience gained in the project organization

Already VTT's early decommissioning plans include benchmarking to foreign research reactor decommissioning projects (inventories and doses). Much of the existing decommissioning experience has been imported from Germany, a significant step in the project being the detailed decommissioning planning by a contractor with experience on the decommissioning planning and execution for a similar reactor. During this planning project, VTT took a role of an active owner, investing significant effort of own employees, which created a fruitful interaction with the contractor and facilitated efficient transfer of knowledge to VTT's project organization.

VTT simulated radionuclide inventories in an early phase [13], which has proven to be an invaluable basis for several planning tasks related to dismantling methods, packaging, waste management (space requirements), radiation protection, measurements for waste classification and clearance as well as long-term safety analyses. However, the modelling

[3] The predecessor of FiR 1, a subcritical pile YXP (Ydin Exponential Pile), operated next to the FiR 1 site between 1958–1974 and was dismantled in a quick and practical manner before present legislation [10,11]. Decommissioning of YXP was completed in 2018 by delivering the fuel (natural and enriched uranium) for further use in the Czech Republic.

suffered from insufficient information on materials compositions. Some minor impurities like chlorine and europium are often neglected in in materials specifications, but their activation products may have a significant contribution to the total activation or long-term safety in disposal.

Based on the simulated inventories and improved measurement capabilities, new procedures for free or controlled release of materials and equipment from the reactor are being developed and implemented. A more thorough approach is required during decommissioning than during operation when the yearly waste production has been minimal.

4.3 Adapting the organization to decommissioning

While VTT has retained all personnel of the operating organization, a few key recruitments have been important in strengthening the competences in waste management planning, licensing framework knowledge and radionuclide measurements. The project organization is relatively small and involves all staff of the previous, still maintained part-time operating organization. In 2017–18, VTT carried out a safety culture assessment [14] by VTT's own independent experts. The assessment confirms that the organization is competent and committed, but that the systemic uncertainties described in this paper (time and cost) can also jeopardize the safety culture by creating tension between economic and safety aspects. In addition, the assessment recommends VTT's organization to put additional attention on competence and information management to ensure that no critical knowledge is lost during the long decommissioning project.

5 MAIN CHALLENGES AND LESSONS LEARNED DURING PLANNING AND LICENSING PHASE

VTT's main challenge in FiR 1 decommissioning has turned out to be the uncertainty over waste management solutions (both SNF and dismantling waste) at the time of final shutdown. This reflects to licensing as long preparation and review times and to planning as slow convergence of the plans due to the lack of fixed boundary conditions for waste management and project timeline.

The earlier plans for the waste management of FiR 1 decommissioning were based on rational engineering solutions and plans made in the 1980's. An example is storing all the decommissioning waste in containers in an appendix of the Loviisa NPP underground storage facility until moving them to the large final disposal space of the NPP itself. None of these solutions was licensed. Now all relevant plans have changed and require extensive licensing work.

Current radioactive waste management regulation and practices at the waste receiving sites require a good knowledge on the waste constituents and all the included radionuclides. To produce all this data on a nearly 60 years old facility is a cumbersome task. Especially the requirement for the data in the planning phase are tedious to meet.

The Finnish radioactive waste management system does not yet have any operational or ready solutions for the dismantling waste. The above-mentioned change in the licensing policy to open the radwaste facilities of the NPP´s also for other than their own waste – including the FiR 1 decommissioning waste – is a first step, but the technical solutions and their licensing still lie ahead.

6 SUMMARY

We have reviewed the experiences gathered up to now in the FiR 1 TRIGA research reactor decommissioning project, still in the licensing phase. The reactor in Otaniemi university campus, Espoo, Finland, has been a key nuclear energy training and research facility for almost two generations. The first decommissioning of a nuclear reactor in Finland will be implemented safely, and the waste management will be performed in collaboration with NPP operators. The lessons learned during the decommissioning of the research reactor can be applied to the preparations for the decommissioning of nuclear power reactors.

7 REFERENCES

[1] M.I. Airila, I. Auterinen, P. Kotiluoto, A. Räty, *Lessons learned during planning and first phases of decommissioning of the Finnish TRIGA FiR 1,* Proceedings of RRFM 2019 (https://www.euronuclear.org/newsletter/RRFM2019/Proceedings/RRFMIGORR2019-A0182-fullpaper.pdf)

[2] M.I. Airila, I. Auterinen, P. Kotiluoto, T. Vanttola and O. Vilkamo, *The glow of Finland's first reactor fades*, Nuclear Engineering International, December 2015 (https://www.neimagazine.com/features/featurethe-glow-of-finlands-first-reactor-fades-4760842/).

[3] Nuclear Energy Act with all amendments implemented, in Finnish (https://www.finlex.fi/fi/laki/ajantasa/1987/19870990)

[4] Nuclear Energy Act, unofficial English translation dated 28 April 2009 (https://www.finlex.fi/fi/laki/kaannokset/1987/en19870990_20080342.pdf)

[5] Ministry of Economic Affairs and Employment of Finland, *VTT Technical Research Centre of Finland Ltd's licence application for decommissioning* (https://tem.fi/en/vtt-technical-research-centre-of-finland-ltd-s-licence-application-for-decommissioning, accessed 14 February 2019).

[6] Nuclear Energy Decree with all amendments implemented, in Finnish https://www.finlex.fi/fi/laki/ajantasa/1988/19880161

[7] Nuclear Energy Decree, unofficial English translation dated 2009 (https://www.finlex.fi/fi/laki/kaannokset/1988/en19880161_20090732.pdf).

[8] US Department of Energy, *61 FR 26507 - Establishment of the Fee Policy for Acceptance of Foreign Research Reactor Spent Nuclear Fuel*, Federal Register Volume 61, Issue 103 (May 28, 1996).

[9] US Department of Energy, *77 FR 4807 - Revised Fee Policy for Acceptance of Foreign Research Reactor Spent Nuclear Fuel From High-Income Economy Countries*, Federal Register Volume 77, Issue 20 (January 31, 2012).

[10] D. Jåfs, *Introduktionen av kärnkraften i Finland – En undersökning med fokus speciellt på vår verkstadsindustris roll*, Doctoral dissertation, Åbo Akademi University, 2009, in Swedish (http://urn.fi/URN:ISBN:978-951-765-474-6).

[11] B. Bärs, *Drag ur FiR 1 reaktorns historia – del 2/2*, ATS Ydintekniikka **37**(4), 2008, in Swedish (https://ats-fns.fi/images/files/ydintekniikka/atsyt_2008_4.pdf).

[12] L. Kumpula and O. Slant, *Kansallisen ydinjätehuollon yhteistyöryhmän loppuraportti*, Ministry of Economic Affairs and Employment, 2019, in Finnish (http://urn.fi/URN:ISBN:978-952-327-435-8).

[13] P. Kotiluoto and A. Räty, *FiR 1 activity inventories for decommissioning planning*, report VTT-R-03599-16 (2016).

[14] M. Ylönen and M. Airola, *FiR 1 -tutkimusreaktorin käytöstäpoiston turvallisuuskulttuuriarviointi*, report VTT-R-0216-18 (2018), in Finnish.

On Temperature Limits in a Disposal Facility for High-Level Radioactive Waste

G. BRACKE, E. HARTWIG-THURAT, J. LARUE, A. MELESHYN, T. WEYAND*

GRS gGmbH; Schwertnergasse 1, 50968 Cologne; guido.bracke@grs.de

Abstract

Section 27(4) of the Act on the Search for and Selection of a Site for a disposal facility for high-level radioactive waste (Site Selection Act - StandAG 2017) sets a **draft** temperature limit of 100 °C on the outer surface of the containers with high-level radioactive waste in the disposal facility. This **draft** temperature limit shall be applied in the preliminary safety analyses provided that the "*maximum physically possible temperatures*" in the respective host rocks have not yet been determined due to pending research.

This paper discusses the temperature dependence of thermohydraulical, mechanical, chemical and biological processes as well as on issues related to retrievability and recovery.

Based on databases for features, events and processes (FEP-databases), several temperature-dependent processes have been identified and assessed for possible impacts of temperature on the processes. Based on these impacts, temperature limits for different components (e. g. the outer surface of the containers) can be derived. However, the interactions of safety relevant processes must be considered in a disposal concept in order to determine a temperature limit on the outer surface of the containers.

The temperature limits may vary for disposal facilities in the following host rocks: rock salt, claystone and crystalline rock.

Technical solutions for retrieval and design options for recovery seem to be viable up to 200 °C with different downsides. Therefore, no temperature limits could be deduced from issues of retrieval and recovery.

However, technical solutions and design options for containers must still be developed and checked for their practicability and feasibility.

The conclusion is that temperature limits on the outer surface of the containers should be derived specifically for each safety concept, design of the disposal facility and the respective host rock. General temperature limits without reference to specific safety concepts or the disposal facility design may narrow down the possibilities for optimisation of the disposal facility and could adversely affect the site selection process in finding the best site.

1 INTRODUCTION

1.1 Motivation

The current **draft** limit on the temperature at the outside of containers for highly radioactive waste in a disposal facility is stipulated by the site selection act § 27 (4) /STA 17/. This value must be used for drafting disposal concepts and performing safety analyses until further research shows that higher temperatures are feasible. This requirement is based on a recommendation made by the commission on storage of high level radioactive waste /KOM 16/, which has been a political comprise. This compromise has been heavily disputed and criticized /FIS 16/, /KUD 16/, /REI 17/. The main statements were:

- Temperatures below 100 °C are not necessarily advantageous for safety /RÖH 17/.
- Advantages and disadvantages of disposal concepts with different design or **draft** temperatures shall be shown in order not to exclude potential sites /WAT 17/.
- Research and development concerning this issue was recommended, since the requirement of a temperature limit has a large impact on the development of concepts (e. g. size of the facility, dimension of the barriers) for the site selection process /RÖH 17/.

The following paper presents and exemplifies some of the temperature depending themohydraulic-chemical-mechanical-biological processes (THCMB-processes), which could be considered for the development of concepts and for assignment of temperature limits in different components.

1.2 High-level radioactive waste (HLRW) in Germany

The volume of HLRW is limited in Germany due nuclear energy being phased-out in 2022 /KOM 16/, /BMUB 18a/, /BMUB 18b/. The waste forms are mainly: spent fuel elements from power reactors (approximately 35 000 pieces with about 10 500 Mg spent fuel or approximately 7 600 m^3, if considered as fuel rods only); canisters with vitrified waste from reprocessing (approximately 8 000 pieces, approximately 2 000 m^3) and spent fuel elements from research reactors (approximately 2000 m^3). The HLRW generates heat and will raise the temperature in a disposal facility after closure.

The total volume of HLRW, if conditioned in POLLUX containers and canisters, is projected to be around 27 000 m^3 in 2080 /BMUB 18/.

If these containers are disposed, the heat generation will lead to an increase of the temperature in the disposal facility (Fig. 1). As a temperature increase may lead to failure of the barrier systems, a maximum design temperature at a specific point (e. g. container surface) must be set.

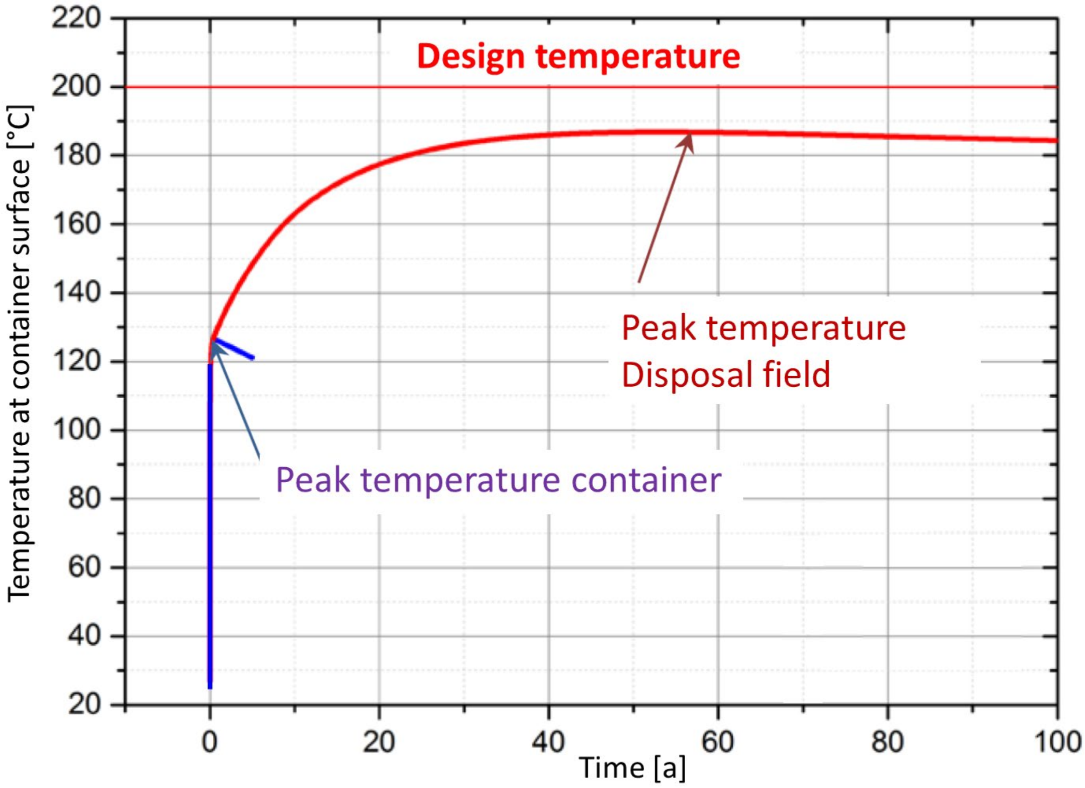

Fig. 1 Temperature on the outer surface of a single container and in a disposal field in a generic HLRW-concept for rock salt (modified after /DBE 16/)

1.3 Background

Temperature limit

The term "*temperature limit*" is provided by the § 27 (4) of the Site Selection Act /STA 17/. This section specifies that "*for precautionary reasons a temperature limit of 100 °C at the outer surface of containers shall be assumed as long as the temperatures, which are maximal physically possible in the host rocks, have not been determined by pending research work*". As there is literally no "*maximal physically possible*" temperature available in physics, the understanding of this paragraph must relate to safety analyses based on safety concepts, to which a specific temperature limit must be applied, designed or developed for. Therefore, the "*maximum physically possible*" temperature must be related to a maximum temperature, which must not be exceeded in a safety concept by considering safety requirements and technical measures in its design.

On the one hand, the precautionary reasons have not been outlined in the act or in its explanatory statement /BT 17/. However, it can be assumed that for higher temperatures unfavourable outcomes in safety investigations may be expected. This could affect long-term safety, operational safety, retrieval or recovery.

On the other hand, based on results from research, it can be concluded that it is possible to apply temperature limits higher than 100 °C.

Design temperature

Apart from the "*temperature limit*" at the outer surface of containers, "*design temperatures*" for components are needed for the planing and optimisation of the design of a disposal facility. These temperatures shall ensure a safe operation and long-term safety. The latter must neither be exceeded nor fall below the designated temperature (ranges) at certain areas and/or components of the facility or at certain times. The design temperatures at reference points may differ from the temperature limit at the outer surface of containers.

Weighting criteria

The site selection act § 24 (5) refers to safety relevant features, which are assessed by weighting criteria. One of the weighting criteria is dedicated to temperature compatibility:

> *The rock formations affected by temperature changes due to the emplacement of radioactive waste should be such that the resulting changes in rock properties and thermomechanical rock stresses do not lead to a loss of integrity and the formation of secondary permeabilities in the repository area.*
>
> *Indicators for this are the tendency to form heat-induced secondary permeabilities and their expansion as well as the temperature stability of the host rock with regard to mineral transformations.*

Apart form the indicators, /BT 17/ also explains the following criteria:

> *Since temperature changes in geotechnical barriers and surrounding rock can trigger, accelerate or intensify processes with different positive or negative consequences for repository safety, the determination of host rock-specific or even generally valid temperature limits and their application are only conditionally suitable for the reliable avoidance of adverse consequences for repository safety.*

Therefore, the requirement of a "*temperature limit*" by § 27 (4) of the Site Selection Act is somewhat in contradiction to this statement for § 24 (5), which restricts the applicability of a "*temperature limit*". It is outlined further in /BT 17/, that safety requirements will be issued for the application of temperature limits for the design of the disposal facility. Furthermore the current draft of the safety requirements /BMU 19/ is in accordance with /BT 17/ regarding the requirement on "*temperature limits*" for safety analyses, without specifying a value for the temperature limit on the outer surface of containers.

Retrievability/Recovery

§ 2 StandAG /STA 17/ requires that the disposed waste containers with radioactive waste must be retrievable during the operating phase. The retrievability must be planned (§ 13 /BMU 19/) and refers to the active process of removing waste containers from the repository during the operating period (Fig. 2).

According to § 2 StandAG /STA 17/, recovery is defined as the unplanned retrieval of radioactive waste from a repository after closure of the disposal facility. This must be possible for 500 years /BMU 19/. It is considered as an emergency measure. Furthermore, the discoverability, identificability, the manageability of the waste containers (tightness for aerosols) is required.

This distinction between retrievability and recovery on the basis of the period under consideration exists in this form exclusively in Germany.

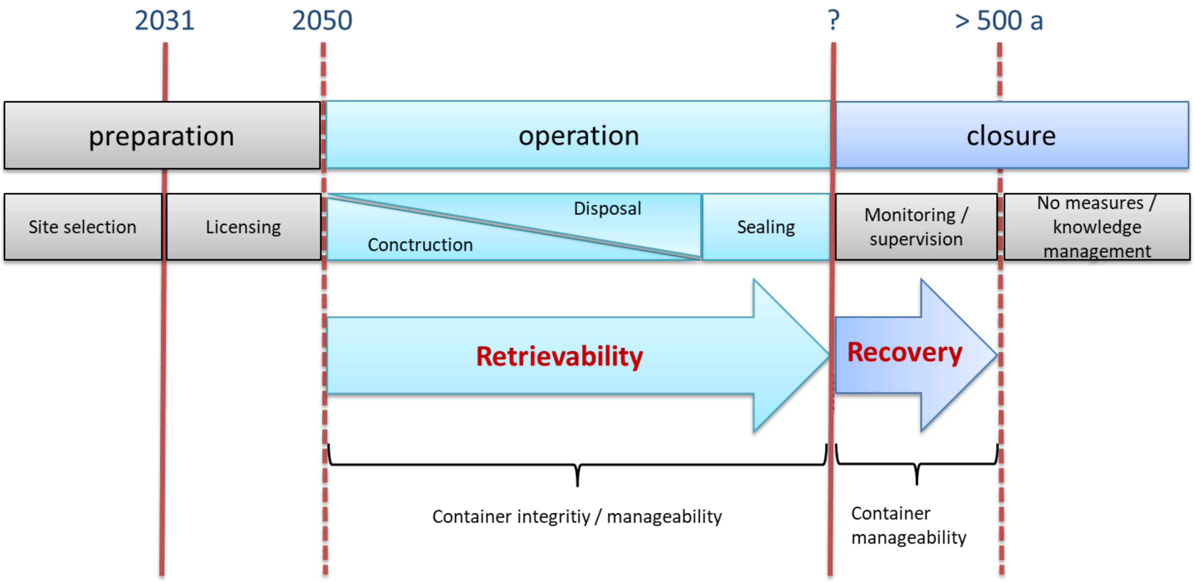

Fig. 2 Time frame for retrievability and recovery (modified after /ESK 11/)

Components

Repository components are: waste, canister, container, geotechnical barriers (backfill, buffer, drift and shaft seals), geological barriers (host rock) and geological environment. Repository components (e.g. the outer surface of a container, buffer, host rock, etc.) serve frequently as reference points as the repository components are subject to a temperature influence due to the heat input of the high-level radioactive waste. The Site Selection Act refers in § 27 (4) to a temperature limit with the reference point at the outer surface of a container. From a safety point of view, however, temperature limits may also be based on other reference points.

Temperature field

The storage of containers with HLRW leads to a heat input within the repository due to radioactive decay and thus to an increase in temperature of the host rock and its geological environment compared to the original rock temperature. The specific temperature at the outer surface of the container depends mainly on: the loading of the containers; the thermal capacity of the waste (after burn-up and interim storage); the storage design and the thermal material properties of the geotechnical barriers as well as of the host rock and the heat flux in the geological environment. The temperature field calculations (numerical model calculations) determine the (peak) temperatures in time and space, e.g. on repository components. Temperature field calculations are a necessary part of the technical design of a disposal concept and are used for its optimisation regarding e.g. size, spacing, etc.

2 NATIONAL REGULATIONS REGARDING TEMPERATURE IN A DISPOSAL FACILITY

Some site selection procedures (as in Switzerland) consider the thermal compatibility of host rocks as a criterion to be considered in the selection of a site. This is similar to Annex 8 § 24 (59) StandAG /STA 17/. Other countries (Belgium, the Netherlands, Finland, Sweden) consider the safety-related effects of an increase in temperature or the heat effect of the heat-generating waste on the repository components. However, this is done within the scope of the design and optimisation of a disposal facility. The regulations of these countries do not provide concrete temperatures in the sense of a " temperature limit " prior the determination of a concept, site or a host rock.

Only in France a temperature of 100 °C at the boundary of the container and its surroundings is recommended in a guideline by the Autorité de Sûreté Nucléaire (ASN), due to it being considered as favourable for safety /BOD 08/. However, this temperature limit does not represent a regulatory requirement. It is seen as an orientation value for further optimisation of disposal concepts and this temperature is related only to the host rock-specific disposal concepts in clay rock.

Germany has set a unique requirement by § 27 (4) /STA 17/ that a temperature limit on the outer surface of the containers has to be applied for preliminary safety analyses without specifiying the host rock, disposal concept or site. In all other evaluated regulations such a temperature pre-determination is missing.

3 DISPOSAL CONCEPTS REGARDING TEMPERATURE

In the following, the statements on the design temperatures, which have been determined by the disposal concepts of various countries, are summarised with regard to the resulting temperature on the outer surfaces of the waste containers.

The disposal concepts in Belgium, Switzerland and France for clay rock and in Spain for crystalline rock were initially based on the temperature limit of max. 100 °C for the backfill material bentonite. The reason was that the buffer material loses sealing properties at higher temperatures. In the Swiss concept, the design temperature for the outer half of the buffer was increased from 100 °C to 125 °C /JOH 02/. The peak temperatures for the outer surface of the containers could therefore reach 140 - 160 °C according to /JOH 02/. In France, it was stipulated that for the specific disposal design that a maximum temperature of 90 °C is permissible at the buffer/claystone contact in order to fall below a temperature of 100 °C in the buffer /WEI 08/.

Most concepts which use clay-containing materials as barrier material are designed for a temperature of up to 100 °C in the clay-containing material (design temperature). In Switzerland, higher temperatures in the clay-containing buffer are also regarded as conceptually feasible. Accordingly, peak temperatures in the range of 80 - 150 °C are permissible on the outer surfaces of the containers in disposal concepts with mainly clay-based barrier systems.

The literature survey revealed some significant differences for the peak temperatures on the outer surface of the containers related to the disposal concepts. The highest peak temperature in a disposal concept is up to 230 °C, which was derived from an inner temperature of 350 °C in a waste container. This peak temperature was applied for the design of the disposal concept in tuff (Yucca Mountain), which does not consider backfill in its disposal design /PAP 99/, /REC 14/. For Great Britain, Japan, Russia, Spain and South Korea, no statements on temperatures on the outer surface of the containers were found which were related to a disposal design.

No indications were found in the evaluated literature which would require a maximum temperature to be specified on the outer surface of the containers based on the features of containers or processes which lead to the failure of the container as barrier (e.g. corrosion). Furthermore, the melting of barriers, for example, would need much higher temperatures than those discussed and considered reasonable in the disposal concepts.

Tab. 1 lists the area required for generic disposal facilities in different host rocks for the inventory of HLW in Germany according to /DBE 16/. It shows an increase of the disposal area when the temperature in rock salt is lowered from 200 °C to 100 °C. The area is increased further when clay or crystalline rock is considered for this temperature.

Tab. 1 Size of disposal facilities depending on temperature and host rock /DBE 16/

	Unit	Rock salt	Rock salt	Clay rock	Crystalline rock
Temperature	**°C**	**200**	**100**	**100**	**100**
Minimum disposal area for containers	km²	0.80	1.63	4.87	2.21
Minimum disposal area applying safety distance	km²	0.23	0.40	1.08	1.03
Minimum area for infrastructure facility	km²	0.25	0.25	0.63	0.32
Total area for disposal	**km²**	**1.28**	**2.28**	**6.58**	**3.56**

4 TEMPERATURE AND THCMB PROCESSES

A change in temperature (or heat flux) does not only affect the specific thermal properties (heat conductivity, specific heat capacity), but can simultaneously have effects on:

- Mineralogy (e.g. structural changes due to illitization, mineral composition, sorption capacity),
- Hydraulics (e.g. viscosity, density and surface tension; relative permeability of the water phase),
- Mechanics (e.g. strength properties; cracking due to drying out; swelling capability),
- Chemistry (e.g. diffusive transport; cation exchange; pH value, reactions)

Since the temperature impacts all processes, the entire system behaviour can only be studied by considering thermo-hydromechanical-chemical-biological coupled processes.

With regard to different host rocks, FEP-catalogues (features, events and processes) have been compiled for disposal concepts. These FEP-catalogues are supposed to cover all relevant processes for systems analyses, including those features and processes which have a temperature dependence. Geological or climatic events are not considered here as temperature dependent, as those are not triggered by the heat flux of the disposed radioactive waste. The available FEP-catalogue for crystalline rock was generated differently compared to rock salt and clay rock.

As the relevance of specific temperature dependent processes for long-term safety depends on the host rock and the disposal concept, some examples are given and discussed for their relevance for different host rocks.

4.1 Salt rock

Crushed salt is used for backfill of drifts in disposal concepts in rock salt /BOL 11/. The process of compaction of the backfill restores the sealing capacity of rock salt to confine the containers.

Immediately after being placed in the repository, crushed salt has a porosity of approx. 35 % /ROT 99/. The porosity (or pore volume) decreases as a result of the compaction due to the convergence. The compaction rate depends on the specific conditions at the site (e.g. stress conditions, humidity, fluid pressure, offset resistance and temperature). High temperatures increase the convergence and thus accelerate the process of compaction. With increasing compaction (i.e. decreasing porosity), the thermal properties of crushed salt approach those of undisturbed rock salt. This increases the thermal conductivity of the backfill of crushed salt with progressing compaction.

The relationship between the imposed pressure (stress) and the porosity (void ratio, the quotient of pore volume to solid volume) describes the compaction behaviour of crushed salt down to small void ratios of 0.1 (Fig. 3). This relationship also depends on the temperature. Higher temperatures have a favourable effect, i.e. small porosities (void ratios) can be achieved with a lower stress (pressure) at a constant compaction rate. Nevertheless, as the porosity decreases, the stress must increase to achieve compaction.

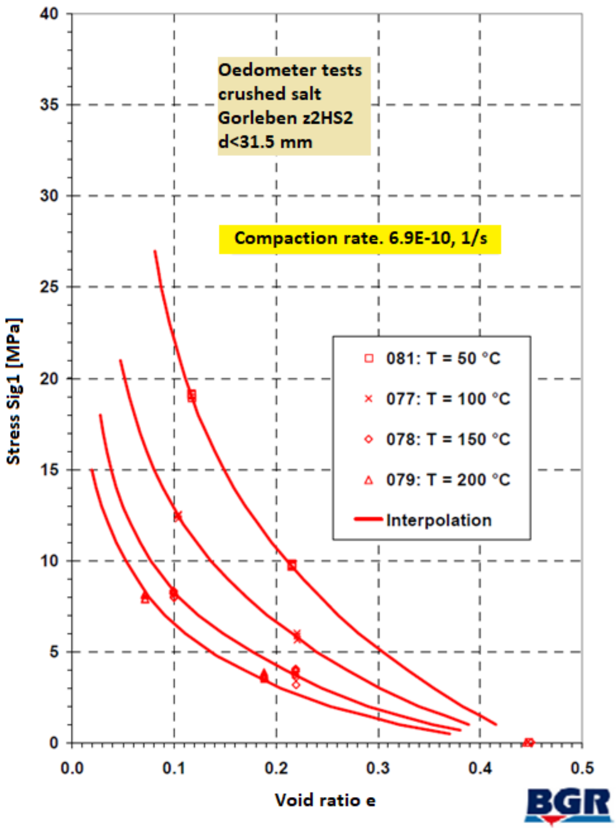

Fig. 3 Stress versus void ratio of crushed salt for different temperatures in compaction tests with constant compaction rate /STÜ 04/.

Since the input of heat has a positive effect on lowering the void ratio of crushed salt (which is desirable from safety considerations for the enclosure of the containers) this process does not require an explicit maximum temperature limit to be set. However, a minimum temperature could be desirable for this process to achieve the containment in a specified time period. This may be demanded by a safety concept. The detailed determination of parameters is only possible with knowledge of the site specific conditions and the disposal concept.

4.2 Clay rock

Bentonite is commonly used in disposal concepts in clay rocks as buffer for geotechnical barriers and backfill. Smectites and Illites are two clay mineral groups which compose bentonite. The cation exchange capacity of smectites is much higher than that of illites and more favourable for the sorption of radionuclides. In addition, smectites have a high swelling capacity, which also give bentonite a high plasticity and sealing capacity, while illites are less swellable. The conversion of smectite into illite in a so-called smectite-illite reaction in a geotechnical barrier (bentonite) or in the host rock (clay rock) can, therefore, have a negative effect on the favourable properties of bentonite or clay rock.

The smectite-illite reaction is clearly detectable under geological conditions at temperatures above approx. 60 °C /THY 11/, /GOU 16/. When a clay rock has reached a temperature of approx. 100 – 120 °C during its diagenetic immersion history, its pure smectite-containing mineral phase is lost and the proportion of smectite-layers in the illite-smectite intercalation is reduced to approx. 35 - 50 % /POL 93/, /ŠUC 93/, /SCH 96/, /COL 11/, /VÁZ 14/ (Fig. 4).

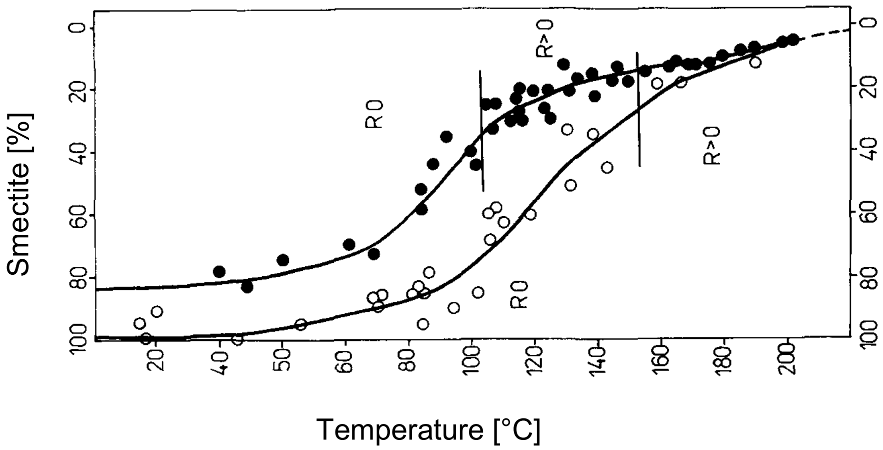

Fig. 4 Smectite fraction of the illite-smectite intercalation (I/S) of a bentonite rich clay rock (○) and other clay rock / shale (•) as a function of the in-situ temperature (depth) /ŠUC 93/.

The smectite-illite reaction in bentonite-rich clay rock progresses much more slowly than in other clay rock /ŠUC 93/, /MAS 01/. Therefore, the transition of bentonite-rich clay rock to low proportion of smectite (35 %) shifts to a temperature of approx. 150 °C. Then, the difference of the swelling capacity between bentonites and clay rocks becomes negligible /ŠUC 93/. According to the literature on diagenesis, the next transition takes place at a smectite content of less than 15 % at 150 - 190 ºC /POL 93/, /VÁZ 14/. If the potassium supply is insufficient, this transition temperature shifts to 240 °C /ARO 06/. Furthermore, a complete transformation of the smectite layers into illite layers was only detected at approx. 270 °C /ARO 06/.

In addition, a high salinity in interaction with a temperature above 80 °C was recognized as an accelerating factor influencing the smectite-illite reaction /HON 04/. At high pH values, (e.g. 13.4) and a potassium concentration of 1 M, the smectite-illite reaction is observed in the laboratory at 50 °C over 30 days /DRI 02/. These site-specific effects must be assessed when a disposal concept is developed.

4.3 Crystalline rock

During its genesis, crystalline rock was exposed to very high temperatures over very long periods of time. For example, the rock units in the area of continental deep drilling are characterized by a medium pressure metamorphosis at approx. 600 - 800 MPa and 650 - 700 °C /ROH 11/. Therefore, no significant safety-relevant THMCB processes are expected for the crystalline rock in the range of the design temperatures discussed in disposal concepts. The properties *thermal conductivity* and *thermal capacity* (as e.g. described in /KNU 83/, /SKB 10/) are to be considered for the repository design. Possible implications from other temperature-dependent processes would result rather from the materials used in the repository and the (geotechnical) barriers (e.g. bentonite, containers), fluids (geochemical environment) and fissure fillings, if the latter were assigned a safety-relevant barrier function in the disposal concept.

Corrosion refers mainly to the chemical or electrochemical reaction of a metal with substances from its environment. In the case of steel corrosion of container, corrosion reactions are controlled by the pH and the availability of oxygen. Anaerobic corrosion of steel generates mainly hydrogen gas. The aerobic corrosion rate is much faster than the anaerobic corrosion rate. However, the corrosion rate and corrosion products depend not only on the composition of the metal, the prevailing geochemical environment but also – since it is a chemical reaction – on the temperature.

Therefore, the impact of metal corrosion depends on the disposal concept (in particular the container materials and design) and the geochemical conditions in the host rock. However, corrosion processes have never been used to justify a temperature limit according to our knowledge.

In disposal concepts for crystalline rock, bentonite is used as a buffer and assigned as a barrier function. In principle, the temperature dependencies and limitations mentioned for clay rock or bentonite also apply for disposal concepts in crystalline rock if they consider clay-containing buffers as barriers. Temperature-dependent processes of clay-containing barriers are already known (microbial activity, saturation and swelling behaviour, flow processes, diffusion) and are therefore not covered here. Since disposal concepts in crystalline rock (Sweden, Finland) consider the clay-containing buffers and containers as essential geotechnical barriers for long-term safety, the temperatures for the design of a repository is reviewed more restrictively than in other disposal concepts (Switzerland).

The hydrothermal alteration processes may have an impact on fissure fillings. If the features of the fissure fillings have been assigned a safety relevant barrier function (e.g. sorption) in a disposal concept, the design of a repository has to consider these processes by means of THMC calculations, e.g. in order to avoid undesired mineral transformations.

5 DISCUSSION AND SUMMARY

For most disposal concepts using clay-based materials as barriers, a maximum design temperature of up to 100 °C was set for the clay-based material (buffer). Only in Switzerland higher temperatures in the clay-based buffer are considered in the disposal concept. The maximum temperatures on the outer surface of the containers in different disposal concepts using clay-based materials range between 80 - 150 °C. This shows that there is some flexibility.

Apart from the positive impact of higher temperatures on the compaction process, the temperatures for a disposal concept in rock salt were justified by the mineral properties of the minerals containing water (so-called hydrate salts) to exclude the release of water from the hydrate salts. These salts may occur in the surroundings of the disposal area. The minimum distance of disposed containers to the hydrate salt formations was determined for the disposal concept by means of a temperature field calculation. This took into account the temperature limit on the outer surface of the containers (e.g. 200 °C). This example shows that the applicable temperature limit depends on safety and disposal concepts, which may include a minimum distance to hydrate salt formations.

In addition, the literature review revealed some significant differences with regard to the maximum temperatures on the outer surface of the containers in various disposal concepts.

No indications were found in the literature to justify a disposal concept exclusively on the basis of a given temperature limit at the outer surface of the containers or the properties of the containers.

There are many other THMCB processes for the host rocks; rock salt, clay rock and crystalline rock which can be used to derive temperature limits for disposal concepts /MEL 16/. Almost all relevant processes are listed in FEP catalogues (e.g. /NEA 19/).

With the exception of the temperature behaviour of gap fillings in crystalline rock, the temperature-dependent processes for crystalline rock are identical to those for clay rock. If gap fillings are considered as a barrier in safety concepts for repository systems in crystalline rock, a more detailed evaluation is needed.

6 CONCLUSIONS

On the basis of the temperature-dependent properties and individual processes considered for known disposal concepts in different host rocks /MEL 16/, a general temperature limit can not be justified. Any temperature limit will depend on specific safety and disposal concepts considering advantages and disadvantages of barriers /BRA 18/.

The temperatures discussed so far - related to the outer surface of the containers and used for design of a disposal facility - are in the range of approx. 80 to 230 °C. Overall, this temperature range appears to be plausible from a safety point of view according to the current state of knowledge.

Temperature limits on the outer surface of the containers which can be justified as being safe can only be derived on the basis of a (possibly provisional) safety and disposal concept. This can take into account the various temperature-dependent properties and processes of barriers as well as impacts on retrievability/recovery.

For this reason, any general "temperature limit" for the host rocks; rock salt, clay rock and crystalline rock would hamper the development of safety and disposal concepts and their optimisation in the course of a site selection (see also /ALT 16/).

7 OUTLOOK

Using a safety concept and a preliminary disposal concept, "design temperatures" can be derived using comprehensible assumptions based on the state of the art in science and technology for host rocks, barriers and other components. These design temperatures can be justified in terms of safety and can be used to set a specific temperature limit by the regulatory authority.

It became obvious that temperatures and effects **within** the containers after disposal have not been investigated or extrapolated. However, knowledge is required in order to be able to ensure container manageability for recovery. Evidence for sufficient manageability of containers, which have experienced high(er) temperatures externally and internally in the long term, has not been found in a literature review. Corresponding conceptual work and material research appear necessary.

8 REFERENCES

/ALT 16/ Alt, S., Kallenbach-Herbert, B., Ustohalova, V.: Bewertung der Einführung einer wirtsgesteinsunabhängigen Grenztemperatur unter Vorsorgeaspekten, Rev. 02, BMUB-Vorhaben UM16E03210. Öko-Institut e.V., 69 S.: Darmstadt, 31. Oktober 2016.

/ARO 06/ Arostegui, J., SanGüesa, F. J., Nieto, F., Uriarte, J. A.: Thermal models and clay diagenesis in the Tertiary-Cretaceous sediments of the Alava block (Basque-Cantabrian basin, Spain). Clay Minerals, Bd. 41, Nr. 4, S. 791–809, DOI 10.1180/0009855064140219, 2006.

/BMU 19/ Verordnung über die sicherheitstechnischen Anforderungen an die Entsorgung hochradioaktiver Abfälle - Artikel 1 Verordnung über Sicherheitsanforderungen an die Endlagerung hochradioaktiver Abfälle (Endlagersicherheitsanforderungsverordnung – EndlSiAnfV) - Referentenentwurf (EndlSiAnfV) in der Fassung von Referentenentwurf, zuletzt geändert 4. Juli 2019.

/BMUB 18/ Bundesministerium für Umwelt, Naturschutz, Bau und Reaktorsicherheit (BMUB): Verzeichnis radioaktiver Abfälle, Bestand zum 31. Dezember 2017 und Prognose. 84 S.: Bonn, August 2018.

/BOD 08/ Bodenez, P., Rieu, J., Niel, J. C.: Guide de sûreté relatif au stockage définitif des déchets radioactifs en formation géologique profonde. Autorité de Sûreté Nucléaire (ASN), 32 S., 12. Februar 2008.

/BOL 11/ Bollingerfehr, W., Filbert, W., Lerch, C., Tholen, M.: Endlagerkonzepte, Bericht zum Arbeitspaket 5, Vorläufige Sicherheitsanalyse für den Standort Gorleben. DBE TECHNOLOGY GmbH (DBETEC), GRS-272, 187 S., ISBN 978-3-939355-48-9, Gesellschaft für Anlagen- und Reaktorsicherheit (GRS) mbH: Köln, 2011.

/BRA 18/ Bracke, G., Weyand, T., Hartwig-Thurat, E., Meleshyn, A., Larue, J., Fischer-Appelt, K.: Untersuchungen zu den “maximalen physikalisch möglichen Temperaturen” gemäß § 27 StandAG im Hinblick auf die Grenztemperatur an der Außenfläche von Abfallbehältern. Gesellschaft für Anlagen- und Reaktorsicherheit (GRS) gGmbH, 1. Statuskonferenz Endlagerung von hochradioaktiven Abfällen, DOI 10.13140/RG.2.2.23328.: Berlin, 8. November 2018.

/BT 17/ Deutscher Bundestag (BT): Gesetzentwurf der Fraktionen CDU/CSU, SPD und BÜNDNIS 90/DIE GRÜNEN, Beschlussvorlage, Entwurf eines Gesetzes zur Fortentwicklung des Gesetzes zur Suche und Auswahl eines Standortes für ein Endlager für Wärme entwickelnde radioaktive Abfälle und anderer Gesetze. Drucksache des deutschen Bundestages, 18/11398, 77 S.: Berlin, 7. März 2017.

/COL 11/ Collo, G., Dávila, F. M., Nóbile, J., Astini, R. A., Gehrels, G.: Clay mineralogy and thermal history of the Neogene Vinchina Basin, central Andes of Argentina, Analysis of factors controlling the heating conditions. Tectonics, Bd. 30, Nr. 4, S. n/a-n/a, DOI 10.1029/2010TC002841, 2011.

/DBE 16/ DBE TECHNOLOGY GmbH (DBETEC): Gutachten Flächenbedarf für ein Endlager für wärmeentwickelnde, hoch radioaktive Abfälle. Material für die Kommission Lagerung hoch radioaktiver Abfallstoffe, K-MAT 58, 92 S., 2016.

/DRI 02/ Drief, A., Martinez-Ruiz, F., Nieto, F., Sanchez, N. V.: Transmission Electron Microscopy evidence for experimental Illitization of Smectite in K-enriched seawater solution at 50°C and basic pH. Clays and Clay Minerals, Bd. 50, Nr. 6, S. 746–756, DOI 10.1346/000986002762090146, 2002.

/ESK 11/ Entsorgungskommission (ESK) - Ausschuss Endlagerung radioaktiver Abfälle (EL): Rückholung/Rückholbarkeit hochradioaktiver Abfälle aus einem Endlager - ein Diskussionspapier. 45 S., 2. September 2011.

/FIS 16/ Fischer, B., Jäger, G.: Sondervotum zu dem Abwägungskriterium "Gute Temperaturverträglichkeit". In: Kommission Lagerung hoch radioaktiver Abfallstoffe: Abschlussbericht, Verantwortung für die Zukunft - Ein faires und transparentes Verfahren für die Auswahl eines nationalen Endlagerstandortes. Drucksache der Kommission Lagerung hoch radioaktiver Abfallstoffe, K-Drs. 268, S. 506: Berlin, August 2016.

/GOU 16/ Goulty, N. R., Sargent, C., Andras, P., Aplin, A. C.: Compaction of diagenetically altered mudstones – Part 1, Mechanical and chemical contributions. Marine and Petroleum Geology, Bd. 77, S. 703–713, DOI 10.1016/j.marpetgeo.2016.07.015, 2016.

/HON 04/ Honty, M., Uhlík, P., Sucha, V., Caplovicova, M., Francå, J., Biron, A.: Smectite-to-illite alteration in salt-bearing bentonites (the East Slovak Basin). Clays and Clay Minerals, Bd. 52, Nr. 5, S. 533–551, DOI 10.1346/CCMN.2004.0520502, 2004.

/JOH 02/ Johnson, L., Schneider, J., Zuidema, P., Gribi, P., Mayer, G., Smith, P.: Project Opalinus Clay - Safety Report, Demonstration of disposal feasibility for spent fuel, vitrified high-level waste and longlived intermediate-level waste (Entsorgungsnachweis). Nationale Genossenschaft für die Lagerung radioaktiver Abfälle (NAGRA), Nagra Technischer Bericht, NTB 02-05, 360 S.: Wettingen, 1. Dezember 2002.

/KNU 83/ Knutsson, S.: On the thermal conductivity and thermal diffusivity of highly compacted bentonite. Svensk Kärnbränslehantering AB (SKB), SKBF/KBS Technical Report, TR 83-72, 55 S., 1983.

/KOM 16/ Kommission Lagerung hoch radioaktiver Abfallstoffe: Abschlussbericht, Verantwortung für die Zukunft - Ein faires und transparentes Verfahren für die Auswahl eines nationalen Endlagerstandortes. Drucksache der Kommission Lagerung hoch radioaktiver Abfallstoffe, K-Drs. 268, 683 S.: Berlin, 30. August 2016.

/KUD 16/ Kudla, W.: Sondervotum zum "Temperaturkriterium". In: Kommission Lagerung hoch radioaktiver Abfallstoffe: Abschlussbericht, Verantwortung für die Zukunft - Ein faires und transparentes Verfahren für die Auswahl eines nationalen Endlagerstandortes. Drucksache der Kommission Lagerung hoch radioaktiver Abfallstoffe, K-Drs. 268, S. 506–508: Berlin, August 2016.

/MAS 01/ Masuda, H., Peacor, D. R., Dong, H.: Transmission electron microscopy study of conversion of smectite to illite in mudstones of the Nankai Trough: contrast with coeval bentonites. Clays and Clay Minerals, Bd. 49, S. 109–118, 2001.

/MEL 16/ Meleshyn, A., Weyand, T., Bracke, G., Kull, H., Wieczorek, K.: Wärmeentwicklung / Gesteinsverträglichkeit. Hrsg.: Kommission Lagerung hoch radioaktiver Abfallstoffe, Gesellschaft für Anlagen- und Reaktorsicherheit (GRS) gGmbH, K-MAT 64, 172 S., DOI 10.13140/RG.2.1.1882.8406, Mai 2016.

/NEA 19/ Nuclear Energy Agency Radioactive Waste Management Committee: International Features, Events and Processes (IFEP) List for the Deep Geological Disposal of Radioactive Waste, Version 3.0. NEA Radioactive Waste Management and Decommissioning, 166 S.: Paris, France, 2019.

/PAP 99/ Papp, R.: GEISHA, Gegenüberstellung von Endlagerkonzepten in Salz und Hartgestein. Hrsg.: Projektträgerschaft des BMBF für Entsorgung (PTE), Forschungszentrum Karlsruhe GmbH (FZK), Wissenschaftliche Berichte, FZKA-PTE Nr. 3, 200 S.: Karlsruhe, Mai 1999.

/POL 93/ Pollastro, R. M.: Considerations and Applications of the Illite/Smectite Geothermometer in Hydrocarbon-Bearing Rocks of Miocene to Mississippian Age. Clays and Clay Minerals, Bd. 41, Nr. 2, S. 119–133, DOI 10.1346/CCMN.1993.0410202, 1993.

/REC 14/ Rechard, R. P., Voegele, M. D.: Evolution of repository and waste package designs for Yucca Mountain disposal system for spent nuclear fuel and high-level radioactive waste. Reliability Engineering & System Safety, Bd. 122, S. 53–73, DOI 10.1016/j.ress.2013.06.018, 2014.

/REI 17/ Reichert, B.: Stellungnahme aus Sicht des ESK-Ausschusses "Endlagerung radioaktiver Abfälle" zur öffentlichen Anhörung des Umweltausschusses am 08.03.2017 zur Fortentwicklung des StandAG. Rheinische Friedrich-Wilhelms-Universität Bonn, Entsorgungskommission (ESK) - Ausschuss Endlagerung radioaktiver Abfälle (EL), Ausschussdrucksache, 18(16)526-L, 3 S.: Berlin, 6. März 2017.

/ROH 11/ Rohrmüller, J., Mielke, H.-G., Gebauer, D.: Tektonik. Bayrisches Geologisches Landesamt, Kapitel 7, 8 S., 2011.

/RÖH 17/ Röhlig, K.-J.: Stellungnahme anlässlich der öffentlichen Anhörung zu dem Entwurf eines Gesetzes zur Fortentwicklung des Gesetzes zur Suche und Auswahl eines Standortes für ein Endlager für Wärme entwickelnde radioaktive Abfälle und anderer Gesetze. Hrsg.: Deutscher Bundestag (BT), Technische Universität Clausthal-Zellerfeld, Ausschussdrucksache, 18(16)526-H, 8 S.: Berlin, 1. März 2017.

/ROT 99/ Rothfuchs, T., Feddersen, H.-K., Kröhn, K.-P., Miehe, R., Wieczorek, K.: The DEBORA-Project: Development of Borehole Seals for High-Level Radioactive Waste, Final Report, BMWi-Vorhaben, FKZ 02E8715. 124 S.: Braunschweig, Dezember 1999.

/SCH 96/ Schegg, R.: Clay Mineral Diagenesis and Thermal History of the Thonex Well, Western Swiss Molasse Basin. Clays and Clay Minerals, Bd. 44, Nr. 5, S. 693–705, DOI 10.1346/CCMN.1996.0440513, 1996.

/SKB 10/ Svensk Kärnbränslehantering AB (SKB): Buffer, backfill and closure process report for the safety assessment SR-Site. SKB Technical Report, TR-10-47, 361 S., 2010.

/STA 17/ Gesetz zur Suche und Auswahl eines Standortes für ein Endlager für hochradioaktive Abfälle (Standortauswahlgesetz – StandAG) in der Fassung vom 5. Mai 2017 (BGBl. I 2017, Nr. 26, S. 1074-1100), zuletzt geändert 20. Juli 2017 (BGBl. I 2017, Nr. 52, S. 2808–2838).

/STÜ 04/ Stührenberg, D.: Compaction and Permeability Behaviour of Crushed Salt and Mixtures of Crushed Salt and Bentonite. In: Brazier, D. (Hrsg.): DisTec 2004. DisTec2004, International Conference on Radioactive Waste Disposal, Berlin, 26. - 28. April 2004, Nr. 24, S. 511–515, 2004.

/ŠUC 93/ Šucha, V.: Smectite to Illite Conversion in Bentonites and Shales of the East Slovak Basin. Clay Minerals, Bd. 28, Nr. 2, S. 243–253, DOI 10.1180/claymin.1993.028.2.06, 1993.

/THY 11/ Thyberg, B., Jahren, J.: Quartz cementation in mudstones, Sheet-like quartz cement from clay mineral reactions during burial. Petroleum Geoscience, Bd. 17, Nr. 1, S. 53–63, DOI 10.1144/1354-079310-028, 2011.

/VÁZ 14/ Vázquez, M., Nieto, F., Morata, D., Droguett, B., Carrillo-Rosua, F. J., Morales, S.: Evolution of clay mineral assemblages in the Tinguiririca geothermal field, Andean Cordillera of central Chile, An XRD and HRTEM-AEM study. Journal of Volcanology and Geothermal Research, Bd. 282, S. 43–59, DOI 10.1016/j.jvolgeores.2014.05.022, 2014.

/WAT 17/ Watzel, R.: Stellungnahme zur öffentlichen Anhörung des Umweltausschusses am 08.03.2017 zur Fortentwicklung des StandAG. Hrsg.: Deutscher Bundestag (BT), Bundesanstalt für Geowissenschaften und Rohstoffe (BGR), Ausschussdrucksache, 18(16)526-G, 2 S.: Berlin, 1. März 2017.

/WEI 08/ Weiß, E., Lommerzheim, A.: Entwicklung und Umsetzung von technischen Konzepten für geologische Endlager in allen Wirtsgesteinen - EUGENIA, AP 6 – Bau und Betrieb von Endlagerbergwerken. Hrsg.: DBE TECHNOLOGY GmbH (DBETEC), TEC-26-2008-AP, 186 S.: Peine, September 2008.

Combining geostatistics and physically-based flow-and-transport simulations to characterize contaminated soils

Mathieu Le Coz, Léa Pannecoucke**, Xavier Freulon**, Charlotte Cazala*, Chantal de Fouquet***

*Institute for Radiological protection and Nuclear Safety (IRSN), PSE-ENV/SEDRE, 31 avenue de la Division Leclerc, 92260 Fontenay-aux-Roses, France

**MINES ParisTech, PSL University, Centre de Géosciences, 35 rue Saint-Honoré, 77300 Fontainebleau, France

Abstract:

Characterization of contamination in soils resulting from nuclear activities is a crucial issue for site remediation. A classical approach consists in delineating the contaminated zones based on a geostatistical estimation calibrated from measured activities, but it results in high uncertainties when the number of measurements is low and/or the spatial variability of the studied variable is governed by complex processes. In order to reduce these uncertainties, a novel approach, called Kriging with Numerical Variogram (KNV), is developed: the variogram is computed from a set of physically-based flow-and-transport simulations rather than from the measurements.

The KNV approach is assessed on a two-dimensional synthetic reference test case reproducing the migration of a tritium plume within an unsaturated soil with hydraulic properties highly variable in space. In this case, the KNV method reduces the mean absolute error by 50% to 75% compared to classical geostatistical approaches, depending on the sampling scenario. The performance of KNV regarding the classification into contaminated or not-contaminated zones is yet sensitive to the contamination threshold.

The KNV approach could thus help to better estimate volumes of soils to be decontaminated in the context of remediation of nuclear sites. This approach can be transposed to other scales of heterogeneities, such as systems with several geological units, or other pollutants with a more complex chemical behaviour, as soon as a numerical code that simulates the phenomenon under study is available.

1 INTRODUCTION

Kriging is used to map contamination in soils and groundwater by providing estimates of pollutant concentration at unsampled locations (e.g., [1] and [2]). However, the quality of the kriging estimator strongly depends on the ability to model the spatial structure of the studied variable through the variogram or the covariance function. In particular, the kriging estimator is often poorly accurate if the number of sampled values is low or if the spatial variability of the studied variable is governed by complex processes ([3] and [4]).

Physically-based numerical simulations of flow and solute transport are another widely used approach to assess contaminated soils and groundwater (e.g., [5] and [6]). Such simulations take into account complex processes governing contamination spread but they require a relevant definition of initial and boundary conditions, as well as internal hydraulic properties. Within the unsaturated zone, the inference of these hydraulic properties is difficult, time-consuming and the induced uncertainties result in a lack of accuracy in the characterization of the contaminated areas ([7]).

The present study aims at combining kriging and flow-and-transport simulations, by computing the mean of experimental variograms from outputs of numerical simulation (hence they are called numerical variograms), in order to improve the characterization of a contaminant plume under a complex configuration, i.e., by considering transient unsaturated flow and highly variable hydraulic properties.

2 KRIGING WITH NUMERICAL VARIOGRAM (KNV)

Ordinary kriging is widely used to map pollutant concentrations in soil and groundwater. The estimate of the variable of interest Z at a target point x_0, $Z^*(x_0)$, is a linear combination of the observations:

$$Z^*(x_0) = \sum_{a=1}^{N} \lambda_a Z(x_a)$$

where λ_a are the kriging weights to be determined and x_a are the locations of the N observations. Ordinary kriging assumes that (i) the mean of the regionalized variable (Z) under study is constant but unknown; and (ii) the variance of any increments, i.e. the variogram function is known for any pairs of points in the studied domain ([8]).

Instead of computing the variogram from observations, numerical variograms are computed from several realizations of Z. These realizations result from a physically-based model, e.g., flow and transport simulations of a contaminant plume for the application presented in this study. The numerical variogram γ between two points x and x' is the average of the increments computed on the P realizations:

$$\gamma(x, x') = \frac{1}{P} \sum_{p=1}^{P} \frac{1}{2} \left[Z_p(x) - Z_p(x') \right]^2$$

where $Z_p(x)$ (resp. $Z_p(x')$) is the value of Z at location x (resp. x') for the p-th simulation.

3 METHOD

In order to assess the KNV approach, a synthetic reference test case is considered. This reference case consists in a two-dimensional vertical domain of 100 m large by 15 m deep in an unsaturated zone contaminated with a point source of tritiated water, and it is built as follows:

- A triplet of random fields describing the proportions of sand, silt and clay (i.e., soil textural properties) are generated by considering (i) a normal distribution of these proportions; and (ii) a spatial variability implemented through an exponential variogram with anisotropy between the horizontal and vertical directions.
- The textural properties are converted into Mualem-van Genuchten hydraulic parameters, governing unsaturated flow ([9] and [10]), by means of the rosetta3 pedo-transfer function ([11]).
- The hydraulic parameter fields are used as inputs to MELODIE flow-and-transport numerical code ([12]) for simulating the evolution of the tritium plume during five years.

Both the soil texture and the tritium activity are sampled in seven boreholes crossing the reference case (Fig. 1). The KNV approach is then carried out to estimate the tritium activity within the whole domain from these punctual sampling:

- The sampled soil textures are used to compute experimental variograms, which allow the generation of 2,000 triplets of conditional fields of sand, silt and clay contents.
- The textural property fields are converted into hydraulic parameter fields by means of rosetta3 pedo-transfer function.

- The hydraulic parameter fields are used as inputs to the flow-and-transport code to simulate 2,000 tritium plumes (all the other model parameters are kept constant compared to the reference test case).
- The set of 2,000 simulated plumes is used to compute the numerical variograms between each couple of points needed to build the kriging system.

The KNV estimates are compared to the activities of the reference test case and two other kriging methods are used as benchmarks, ordinary kriging (OK, [8]) and kriging with an external drift (KED, [13]).

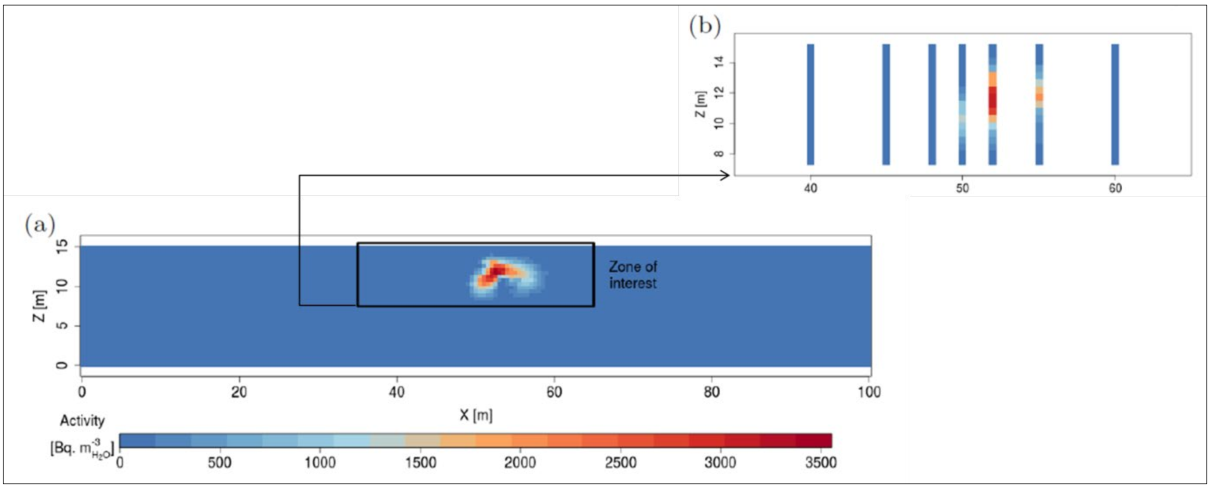

Fig. 1. Reference test case: simulated tritium plume (a); and activities sampled for assessing the KNV approach (b).

4 RESULTS

The maps of estimation are almost similar for the three methods (Fig. 2). Yet, the errors are higher for OK (Root Mean Square Error, RMSE = 161 Bq.m^{-3}H$_2$0) and KED (RMSE = 138 Bq.m^{-3}H$_2$0) than for KNV (RMSE = 89 Bq.m^{-3}H$_2$0).

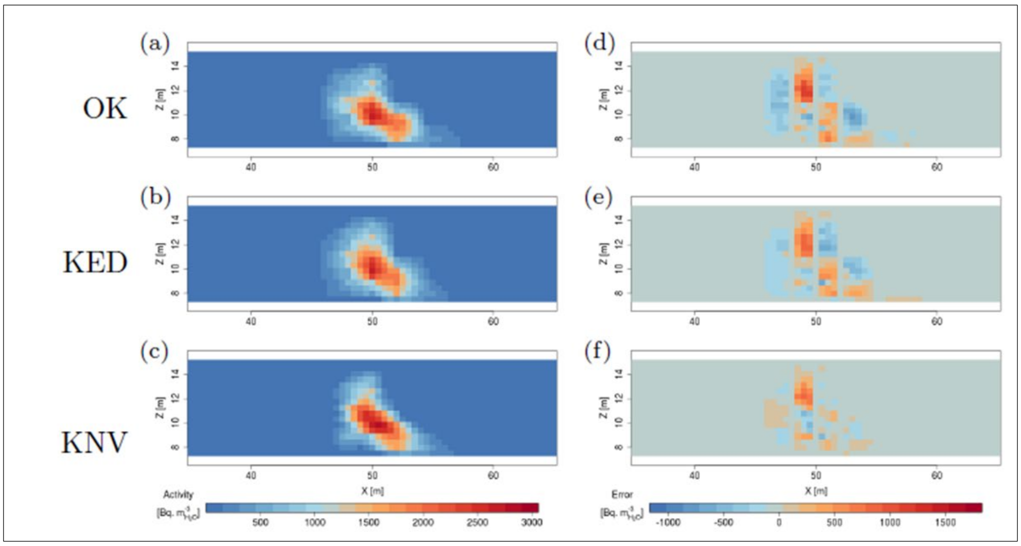

Fig. 2. Map of estimation obtained with the OK (a), KED (b) and KNV (c) approaches; and maps of corresponding estimation errors (d, e and f).

The proportion of false-positive (i.e., contaminated on the estimation, not contaminated on the reference) surface is smaller for KNV that for OK, whatever the contamination threshold (Fig. 3a). This proportion is reduced of 10%, except for contamination thresholds above 1,000 Bq.m^{-3}H$_2$0. The proportion of false-positive surface is smaller for KED than for KNV for very low contamination thresholds (below 20 Bq.m$^{-3}H_2$0); for higher contamination thresholds, KNV leads to smaller proportion of false-positive surfaces than KED.

The proportion of false-negative (i.e., contaminated on the reference, not contaminated on the estimation) surface is slightly higher for KNV than for OK and KED for contamination thresholds below 500 Bq.m$^{-3}H_2$0 (Fig. 3b). For higher contamination thresholds, KNV performs better than OK and KED.

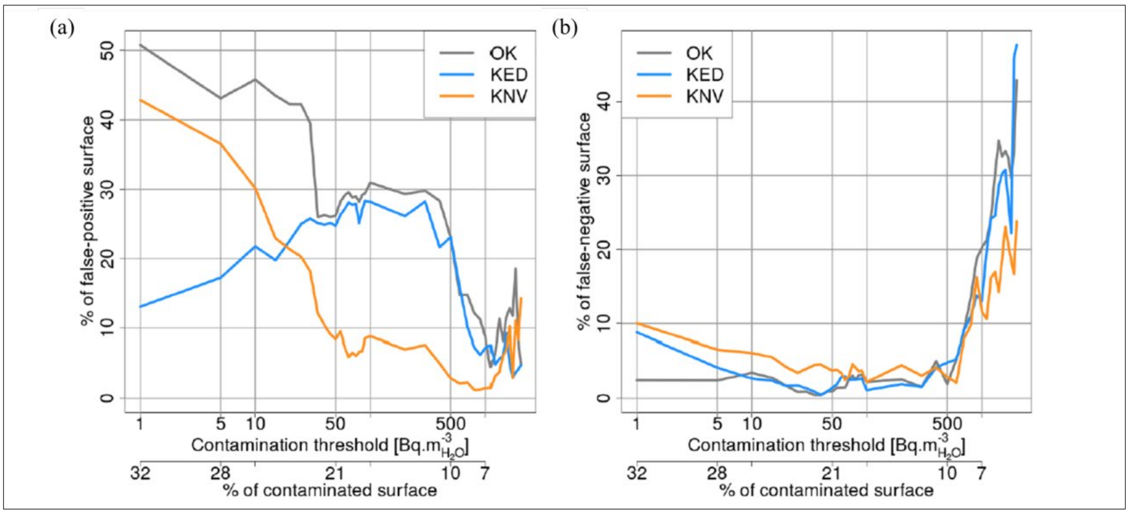

Fig. 3. Proportion of false-positive (a) and false-negative (b) surfaces in function of the contaminated threshold.

5 CONCLUSION

The KNV approach, consisting in using flow-and-transport simulation outputs to compute numerical variograms, appears to perform better than standard geostatistical tools to improve plume characterization. Additional tests show that KNV appears to be particularly interesting when the available observations are scarce (when reference test case activity is sampled in four boreholes, OK RMSE is 348 Bq.m$^{-3}H_2$0; KED RMSE is 174 Bq.m$^{-3}H_2$0; and KNV RMSE is 147 Bq.m$^{-3}H_2$0).

The assessment procedure detailed in this study is based on a synthetic case study with boundary conditions supposed to be exactly known. The next step will be to carry out the method on an actual contaminated site.

This work is part of the Kri-Terres project, supported by the French National Radioactive Waste Management Agency (Andra) under the "Investments for the Future" Program.

More details about this work are given in a research article submitted for publication in a scientific peer-review journal ([14]).

6 REFERENCES

[1] Pelillo, V., Piper, L., Lay-Ekuakille, A., Lanzolla, A., Andria, G., Morello, R., 2014. Geostatistical approach for validating contaminated soil measurements. Measurement 47, 1016-1023.

[2] Liang, C.-P., Chen, J.-S., Chien, Y.-C., Chen, C.-F., 2018. Spatial analysis of the risk to human health from exposure to arsenic contaminated groundwater: A kriging approach. Science of The Total Environment 627, 1048-1057.

[3] Webster, R., Oliver, M. A. Geostatistics for Environmental Scientists, 2nd Edition. Statistics in Practice. Wiley edition, 2007.

[4] Wang, Y., Akeju, O. V., Zhao, T., 2017. Interpolation of spatially varying but sparsely measured geo-data: A comparative study. Engineering Geology 231, 200-217.

[5] Bugai, D., Skalskyy, A., Dzhepo, S., Kubko, Y., Kashparov, V., Van Meir, N., Stammose, D., Simonucci, C., Martin-Garin, A., 2012. Radionuclide migration at experimental polygon at Red Forest waste site in Chernobyl zone. Part 2: Hydrogeological characterization and groundwater transport modeling. Applied Geochemistry 27 (7), 1359-1374.

[6] Testoni, R., Levizzari, R., De Salve, M., 2017. Coupling of unsaturated zone and saturated zone in radionuclide transport simulations. Progress in Nuclear Energy 95, 84-95.

[7] Pannecoucke, L., Le Coz, M., Houze, C. Saintenoy, A., Cazala, C., de Fouquet, C., 2019. Impact of spatial variability in hydraulic parameters on plume migration within unsaturated surficial formations. Journal of Hydrology 574, 160-168.

[8] Chiles, J.-P., Delfiner, P. Geostatistics: Modeling Spatial Uncertainty, 2nd Edition. Wiley series in probability and statistics. Wiley edition, 2012.

[9] Mualem, Y., 1976. A new model for predicting the hydraulic conductivity of unsaturated porous media. Water Resources Research 12 (3), 513-522.

[10] van Genuchten, M. T., 1980. A closed-form equation for predicting the hydraulic conductivity of unsaturated soils. Soil Science Society of America Journal 44 (5), 892-898.

[11] Zhang, Y., Schaap, M. G., 2017. Weighted recalibration of the Rosetta pedotransfer model with improved estimates of hydraulic parameter distributions and summary statistics (Rosetta3). Journal of Hydrology 547, 39-53.

[12] IRSN, 2009. MELODIE Modèle d’Evaluation à LOng terme des Déchets Irradiants Enterrés. Notice théorique du code de calcul MELO version 5.0. (in french).

[13] Rivest, M., Marcotte, D., Pasquier, P., 2008. Hydraulic head field estimation using kriging with an external drift: A way to consider conceptual model information Journal of Hydrology 361 (3), 349-361.

[14] Pannecoucke, L., Le Coz, M., Freulon, X., de Fouquet, C., 2019. Combining geostatistics and simulations of flow and transport to characterize contamination within the unsaturated zone. Science. of the Total Environment, under review.

STATE-OF-THE-ART MICROSPECTROSCOPIC CHARACTERISATION OF CEMENTITIOUS MATERIALS USED FOR THE ENGINEERED BARRIER OF A DEEP GEOLOGICAL REPOSITORY

Dähn R., Vespa M.**and Wieland E.**

* Paul Scherrer Institut, Laboratory for Waste Management, 5232 Villigen PSI, Switzerland
** Brenk Systemplanung, 52080 Aachen, Germany

Abstract:

Synergetic use of state-of-the-art synchrotron-based measurement techniques from the macro- down to the nano-scale together with standard laboratory analytical methods are a unique approach to determine uptake processes of radionuclides onto cementitious materials and to explore micro-scale processes supporting predictions on the long-term performance of cement-based structures. Cement is foreseen in many countries as an engineered barrier within the concept of geological disposal of radioactive waste and it is also used for the solidification of low- and intermediate-level waste.

1 INTRODUCTION

Synchrotron radiation-based analytical techniques embrace a high number of powerful methods capable of providing molecular-level information of chemical speciation, mineralogical composition and mechanical properties of cementitious materials. Among these techniques, X-ray absorption spectroscopy (XAS) probes the local environment of an X-ray absorber atom, while X-ray diffraction (XRD) experiments probe the long-range order of crystalline samples.

The strength of the XAS technique lies in the wide application possibilities: it is non-destructive and it can provide in-situ measurements in different sample environments, such as solid, liquid, suspension and gaseous as well as crystalline and amorphous materials. The information gained from XAS concerns the type of neighbouring atoms, bond length and coordination numbers from the absorbing atom. Furthermore, the method is capable of distinguishing different oxidation states of the X-ray absorber by the X-ray absorption near-edge spectra (XANES). The latter enables also the identification of the coordination environment by using the fingerprinting method. During the past years, with the further development of powerful codes, the synergetic use of XANES and ab initio calculations enables to get detailed molecular-level information comparable to extended X-ray absorption data (EXAFS). The approach is very useful in those cases where EXAFS data are not collectable. This is, for example, the case when chemical elements contained in the system are energetically to near to each other or the absorber concentration is very low (as low as a few tens of ppm). The approach is applicable from the macro-, to the nano-scale. On the micro- and nano-scale the synergy with synchrotron-based micro-XRF (microXRF) is desired in order to determine spatially resolved elemental distributions and elemental correlations, which then can be complemented with the simultaneous registration of micro X-ray diffraction (microXRD) patterns. The latter are complex images in which many crystal grains from different structures can contribute. The quality of the diffraction data ranges from almost perfect individual single crystals to microfine powders or even non-crystalline materials. This study presents several applications of synchrotron radiation-based techniques to answer pertinent questions related to the safe disposal of radioactive waste.

2 IDENTIFICATION OF THE CONTAMINANT SPECIATION WITHIN CEMENT-BASED WASTE MATERIAL

The use of synchrotron-based techniques on the macro-scale and, in particular, of XAS enables to detect the major speciation of an absorbing atom. Vespa et al. [1] have shown, that in the case of Ni within hardened cement pastes (HCP) a Ni-layered double hydroxide was the major component formed within the highly heterogeneous system and was the solubility limiting phase for thermodynamic processes. These results obtained from the macro-scale rely on the assumption that immobilisation processes and the fate of contaminants are primarily determined by sorption reactions on the most predominant mineral phase in the investigated system. However, this assumption breaks down when highly reactive mineral phases are present as minor components. Neglecting the major role of such minor minerals would result in significant errors in calculations of the retardation of contaminants in the environment. The work on Co uptake by HCP by Vespa et al. [2] and Dähn et al. [3] indeed showed that different processes are responsible at the macro- and nano-scale. At the macro-scale the major detected speciation were $Co(OH)_2$ and CoOOH with oxidation state 2+ and 3+, respectively. On the micro-scale (5x5 μm^2) elemental distribution maps performed by synchrotron micro-XRF combined with micro-XAS investigations revealed that the two oxidation states were spatially resolved. The Co^{3+} phases were always present in form of a ring, whereas the Co^{2+} as highly enriched Co spots. The originally Co^{2+} added to the cementitious system had partly oxidized due to oxygen entering the system during the cement production processes, in particular the mixing of clinker phases with water [2]. Nevertheless, due to the heterogeneity of the cement system and its particle size, which can reach the nanometer range, not all Co-containing regions observed by micro-XRF could be identified as $Co(OH)_2$ and CoOOH. The breakthrough was achieved by using highly spatially resolved absorption techniques, i.e. scanning transmission X-ray microscopy (STXM). The technique enables to radiograph the material at the nano-scale (20x20 nm^2) along the absorption edge range of the element of interest creating absorption distribution maps of the region of interest. From every single pixel of such a map, a XANES can be extracted. By using the finger-printing method, i.e. comparison of experimental and reference spectra, the speciation can be pinned down. These studies have shown that at the nano-scale a further Co^{2+} speciation was present, i.e. Co-pyllosilicate [3]. Therefore, three different speciation have to be considered for Co immobilisation processes in cementitious system and for thermodynamic calculations.

3 CHARACTERISATION OF CEMENTITIOUS PHASES

Cementitious materials are very heterogeneous with discrete particles, typically in the size range of about a few hundred nanometers up to a few hundred micrometers, which may vary in crystallinity from crystalline to amourphous state. In many cases, well-established laboratory techniques, such as XRD, thermogravimetric analysis/differential thermogravimetry, solid-state nuclear magnetic resonance or scanning electron microscopy [e.g., 4] are suitable to pin down the physical and chemical properties of the cement structure. These techniques allow gaining information on the elemental distribution, but are limited towards speciation. For the latter, XAS is the tool of choice. EXAFS is possible when the absorber atoms, such as transition metals, are energetically far from the major elements present in cement, such as Al, Ca, Si. The latter are energetically so near that only XANES can be collected. Wieland and co-workers [5] have employed this technique combined with micro-XRF in order to investigate the spatial resolution of ettringite and monosulfate on the macro-scale. They have used the fingerprinting method combined with different specific XAS analytical tools, such as principle component analysis, target transformation in order to identify the Al and S-bearing phases. The study revealed that on the micro-scale the monosulfate was hardly co-existing with ettringite, and that the latter was a minor component. Additionally the hydrotalcite was identified in few reactions zones of the cement.

XANES data are very complex and contain a large number of information. Over the past years, the amelioration of computational codes and increase in computer power allowed to developed advanced computational codes specifically to pin down the information included in XANES data. Recent studies have shown that by combining XANES with ab initio calculations using the FDMNES code new possibilities open up for the identification and characterization of the local chemical arrangement of the elements that dominate the cement matrix [6]. The identified semi-amorphous Mg-bearing phases (M-S-H) formed at the reactive interface between cement and clay material. Due to the great similarity between natural Mg-silicate bearing phase and the M-S-H phases the use of the fingerprinting method is limited. The latter allows identifying the oxidation state of the investigated phase, but it cannot pin down the molecular structure. The use of the FDMNES code enables to calculated XANES spectra from a well-defined starting model, which is subsequently redefined during several steps, until the model reflects the experiment. Vespa and co-workers [7] have shown that in the case of the M-S-H phases Mg is present in at least two geometrically distinct octahedral sites arranged in a structured layer. This layering is composed of a tetrahedral-octahedral-tetrahedral and a Mg-hydroxide layer, organized similarly to the structure of talc and brucite, respectively. Furthermore, they have proofed that Ca may be enclosed in the structure. A question, which has been strongly debated in the literature [8-15]. This technical and methodological approach opens up new possibilities for the identification and characterisation of the local chemical arrangement of the light elements that dominate the cement matrix.

4 IDENTIFICATION OF ALKALI-SILICA REACTION PRODUCTS

The complexity of cementitious materials is related to its highly heterogeneous physical and chemcial system and its extreme variation in particles sizes. Many chemical reactions within the cementitious system are related to processes at the micrometre scale. The alkali-silica-reaction (ASR) is a deterioration of concrete in outdoor structures exposed to water or moisture, e.g. dam walls or bridges. ASR takes place over decades and damages are initially only visible on the micro-meter scale. The understanding of the processes leading to the ASR products and the expansion mechanisms within the concrete have been very challenging, especially due to the small sizes in the micrometre range of these products.

Recent technical developments performed by Dähn and co-workers [16] in the setup of synchrotron micro-XRD measurements for spatially resolved samples open up a large number of possibilities. Dähn et al. have applied a particular experimental set up for the synergetic use of synchrotron-based micro-XRF with micro-XRD techniques on thin sections. The micro-XRF was employed in order to identify the regions of the reaction products mainly present in veins, whereas by micro-XRD the crystalline phase was identified. The particularity of the technique is that the thin section was rotated during the collection of several micro-XRD frames in order to gain the maximum of characteristic reflections from the investigated phase. The challenge, which has to be overwhelmed, is to keep a steady X-ray beam position on the spot of interest while rotating the sample and collecting micro-XRD frames at each point of rotation. All these frames are than convoluted into a composite patter and transformed to a conventional one-dimensional XRD pattern to be used for Rietveld analysis.

This methodological approach was applied to investigate a Swiss infrastructure built in 1969. The results show that the ASR products form a new layered-framed phase with the chemical composition $\{Ca_{5.34}\ K_{4.6}Na_{0.74}\cdot Fe_{0.22}\cdot 7.66H_2O\}[Si_{19.34}Al_{0.66}O_{48}]$ similar to minerals of the mountainite family. The identification and understanding of the crystalline structure of phases formed by ASR will unequivocally contribute to the development of new technical treatments inhibiting the formation of these products.

5 REFERENCES

1. Vespa, M., R. Dähn, D. Grolimund, E. Wieland, and A.M. Scheidegger, *Spectroscopic investigation of Ni speciation in hardened cement paste.* Environmental Science and Technology, 2006. **40**: p. 2275-2282.

2. Vespa, M., R. Dähn, D. Grolimund, E. Wieland, and A.M. Scheidegger, *Co speciation in hardened cement paste: A macro- and micro-spectroscopic investigation.* Environmental Science and Technology, 2007. **41**: p. 1902-1908.
3. Dähn, R., M. Vespa, T. Tyliszczak, E. Wieland, and D.K. Shuh, *Soft X-ray spectromicroscopy of cobalt uptake by cement.* Environmental Science and Technology, 2011. **45**(5): p. 2021-2027.
4. Skibsted, J. and C. Hall, *Characterization of cement minerals, cements and their reaction products at the atomic and nano scale.* Cement and Concrete Research, 2008. **38**(2): p. 205-225.
5. Wieland, E., R. Dähn, M. Vespa, and B. Lothenbach, *Micro-spectroscopic investigation of Al and S speciation in hardened cement paste.* Cement and Concrete Research, 2010. **40**(6): p. 885-891.
6. Vespa, M., R. Dähn, T. Huthwelker, and E. Wieland, *Soft X-ray absorption near-edge investigations of Mg-containing mineral phases relevant for cementitious materials.* Physics and Chemistry of the Earth, Parts A/B/C, 2017. **99**: p. 168-174.
7. Vespa, M., B. Lothenbach, R. Dähn, and E. Wieland, *Characterisation of magnesium silicate hydrate phases (MSH): A combined approach using synchrotron-based absorption-spectroscopy and ab initio calculations.* Cement and Concrete Research, 2018. **109**: p. 175-183.
8. Fernandez, L., C. Alonso, C. Andrade, and A. Hidalgo, *The interaction of magnesium in hydration of C_3S and CSH formation using ^{29}Si MAS-NMR.* Journal of Materials Science, 2008. **43**(17): p. 5772-5783.
9. Shrivastava, O.P., S. Komarneni, and E. Breval, *Mg^{2+} uptake by synthetic tobermorite and xonotlite.* Cement and Concrete Research, 1991. **21**(1): p. 83-90.
10. Pytel, Z. and J. Malolepszy, *DTA studies of phases synthesized in the system CaO–MgO–SiO_2–H_2O.* Silicate Industrials, 2000. **65**: p. 81-85.
11. Bernard, E., B. Lothenbach, F. Le Goff, I. Pochard, and A. Dauzères, *Effect of magnesium on calcium silicate hydrates (C-S-H).* Cement and Concrete Research, 2017. **97**: p. 61-72.
12. Lothenbach, B., D. Nied, E. L'Hôpital, G. Achiedo, and A. Dauzères, *Magnesium and calcium silicate hydrates.* Cement and Concrete Research, 2015. **77**: p. 60-68.
13. Chiang, W.S., G. Ferraro, E. Fratini, F. Ridi, Y.Q. Yeh, U.S. Jeng, S.H. Chen, and P. Baglioni, *Multiscale structure of calcium- and magnesium-silicate-hydrate gels.* Journal of Materials Chemistry A, 2014. **2**(32): p. 12991-12998.
14. Bernard, E., B. Lothenbach, C. Cau-Dit-Coumes, C. Chlique, A. Dauzères, and I. Pochard, *Magnesium and calcium silicate hydrates, Part I: Investigation of the possible magnesium incorporation in calcium silicate hydrate (C-S-H) and of the calcium in magnesium silicate hydrate (M-S-H).* Applied Geochemistry, 2018. **89**: p. 229-242.
15. Bernard, E., A. Dauzères, and B. Lothenbach, *Magnesium and calcium silicate hydrates, Part II: Mg-exchange at the interface "low-pH" cement and magnesium environment studied in a C-S-H and M-S-H model system.* Applied Geochemistry, 2018. **89**: p. 210-218.
16. Dähn, R., A. Arakcheeva, P. Schaub, P. Pattison, G. Chapuis, D. Grolimund, E. Wieland, and A. Leemann, *Application of micro X-ray diffraction to investigate the reaction products formed by the alkali–silica reaction in concrete structures.* Cement and Concrete Research, 2016. **79**: p. 49-56.

3 RADIATION PROTECTION, ENVIRONMENT & EPR

Emergency preparedness and response: a review of EURATOM actions

Roberto Passalacqua

European Commission, DG RTD D4, EURATOM Research
21 rue du Champ de Mars, 1050 Brussels, Belgium

Abstract:

Since its signature in 1957, EURATOM has promoted improvement and harmonization of emergency preparedness and response to potential radiological accidents. The FP7 EURATOM NERIS-TP project, through a collaboration of industry, research and governmental organisations, has further consolidated a self-sustaining “European Technology Platform” to improve EU response by coupling the decision support systems with the early notification system ECURIE (the JRC’s highly reliable web-application for the creation of notifications under the 87/600/EURATOM Council Decision).

EURATOM has also liaised with IAEA for the implementation of the FASTNET (FAST Nuclear Emergency Tools) project: knowledge management, dissemination and education & training through the set-up of a database of all potential severe accident scenarios.

FASTNET is improving the methodology and the tools required for rapid response to emergencies at nuclear power plants. These tools will enable emergency centres to provide a quicker and more appropriate response to radiological risks. In particular, the capabilities of tools and methods have been extended to cover a complete set of “reference accident scenarios” for the main types of operating water-cooled nuclear power plants in Europe (including a generic concept for spent-fuel pools). By the end of this H2020 project, the database of potential nuclear accident scenarios will be transferred to the IAEA where it will be maintained and extended to non-European nuclear technologies, and finally made available to emergency centres in all IAEA’s member countries.

The current EURATOM Work Programme 2019-2020 is further focussing on the need to minimize radiological risks by improving plants’ operational safety by use of Emergency Mobile Equipment (EME) and adapting emergency preparedness and response to these challenging scenarios (topics NFRP-02, NFRP-03 and NFRP-12: http://ec.europa.eu/research/participants/data/ref/h2020/wp/2018-2020/euratom/h2020-wp1920-euratom_en.pdf). This area will be also tackled by the MUSA project, started last July, by investigating the practical elimination of risks, with related uncertainties, of operational EU nuclear plants.

Furthermore, the regulatory guidelines of several EU countries call for a continuous development of safety in plants under operation, as well as in construction and in design such to guarantee that “any event that may result in a release requiring measures to protect the population in the early stages of the accident shall be practically eliminated”. In other words, current legislation and regulatory guidelines require the elimination of evacuation plans around the plant. EURATOM has tackled this issue for Gen II&III operational plants (for example with the sCO2-4-NPP and the R2CA projects) as well as for Gen III+ as the European Pressurised Reactors (EPRs) under construction (e.g. with the “Network of Excellence” SARNET). Currently EURATOM is also focussing on safety assessments for Gen IV new designs of Small Modular Reactors (the SAMOSAFER project).

Future EURATOM work programs might need to further focus on social science and humanities (SS&H): the very recent HoNESt project has concluded that nuclear energy could become accepted as a viable low-carbon source of power, and therefore remain an important contributor to the energy mix, only if safety assessments and EU emergency procedures would be able to demonstrate the elimination of any potential power plant impact on surrounding population.

1 EURATOM RESEARCH

Since the signature of the EURATOM treaty in 1957, the European Commission has focussed on the improvement of the safety of nuclear installations by promoting integration and harmonization of research at EU level.

As from the same year, EURATOM has been the legal basis for:

1) the establishment of the first EU joint research organization, the Joint Research Centre, JRC where EU scientists have been directly working together to provide independent scientific advice and support to EU policy, and

2) the work of the Directorate-General for Research & Innovation (RTD) which focusses on the definition of the European Union's research and innovation policy and the coordination of research activities (with a view to achieving the goals of the Europe 2020 strategy and its key flagship initiative, the Innovation Union (Ref.1).

Under the current EURATOM programme, research and training in nuclear safety and security, radiation protection, radioactive waste management and fusion energy is implemented through (Ref.2):

– direct actions in fission — i.e. research performed by the Commission's Joint Research Centre (JRC), and

– indirect actions in fission and fusion — i.e. via competitive calls for proposals (fission safety, waste management and radiation protection), and a comprehensive named-beneficiary co-fund action (fusion energy) managed by the Commission's Directorate-General for Research & Innovation (RTD).

EURATOM fission research falls under both direct and indirect actions, while all Euratom fusion research falls under indirect actions managed by the RTD.

The 2014-2018 Council Regulation provides a budget of EUR 1 603 329 000 for the implementation of the Euratom programme. This amount is distributed as follows:

- indirect actions for fusion research: EUR 728 232 000;
- indirect actions for fission, safety and radiation protection: EUR 315 535 000;
- direct actions: EUR 559 562 000.

The adoption of the EURATOM work programme for 2019-2020 (Ref.2) foresees the financing of DG RTD indirect actions with a maximum Union contribution set at EUR 477 167 500.

For the next long-term EU budget 2021-2027, the Commission is proposing EUR 100 billion for research and innovation. The indicative budget distribution for Euratom (2021-2025) shall be (EUR 1 675 million):

- for fusion research and development (indirect actions): EUR 724 563 000
- for nuclear fission, safety and radiation protection (indirect actions): EUR 330 930 000
- for direct actions undertaken by JRC: EUR 619 507 000

The new programme – Horizon Europe – will build on the achievements and success of the previous research and innovation programme (Horizon 2020) and keep the EU at the forefront of global research and innovation. Horizon Europe is the most ambitious research and innovation programme ever.

Carlos Moedas, Commissioner for Research, Science and Innovation, has recently stated: "Horizon 2020 is one of Europe's biggest success stories. And the new "Horizon Europe" programme aims even higher. As part of this, we want to strengthen the EU's global scientific leadership and reengage citizens by setting ambitious new missions for EU research as well as modernise funding for ground-breaking innovation in Europe".

2 THE CURRENT BASELINE FOR EMERGENCY AND PREPAREDNESS RESPONSE: THE FP7 EURATOM NERIS-TP PROJECT

The NERIS-TP project (Towards a self-sustaining European Technology Platform on Preparedness for Nuclear and Radiological Emergency Response and Recovery) has, since February 2011, combined eleven leading research organisations in the nuclear emergency management area with four SMEs and four governmental organisations from 13 countries. Within the three years of operation, the project has achieved results in the following areas:

- Operation of a European platform on emergency and post-accident preparedness and management (The NERIS Platform) to further improve emergency response and recovery preparedness in Europe;
- Development of a screening model to test the new International Commission Radiological Protection (ICRP-103) recommendations in respect to national implementation plans;
- Improvement of the two late phase modes ERMIN (inhabited areas) and AgriCP (agricultural production) to better deal with the request from the end users;
- Coupling of the emergency information system of the IAEA with the existing European Decision Support Systems (RODOS/ARGOS) by developing an interface and a meteorological model chain that provides meteorological data from freely available world-wide data;
- Strengthening of the preparedness at the local/national level by setting up dedicated fora for the improvement/adaptation of the tools developed within the EURANOS projects.

Besides, several dissemination workshops and exercises have been conducted to distribute the information on the new tools to all interested parties. This resulted in national exercises testing the new tools and providing feedback to the developers. A dissemination workshop with 82 participants was conducted at the end of the project bringing together national and international experts as well as local stakeholders from 20 countries.

A good sustainability was achieved as 49 members joined the NERIS platform (and so far 20 of them are "supporting members" providing fees for the operation of the secretariat). The platform will also play an important role in identifying future research needs at European level. In this way, the NERIS-TP projects helped to achieve a greater harmonisation in Europe by improving European decision support systems and establishing a sustainable platform that combines all important players in emergency and post-accident preparedness and management in one single organisation.

2.1 Early warning information systems

The European Community Urgent Radiological Information Exchange (ECURIE), and internationally, the Unified System for Information Exchange in Incidents and Emergencies (USIE) of the IAEA are the two most used early warning information systems. The country where an incident/accident happens, issues an early warning message that is immediately further distributed by one or both of these systems. Information includes its location and potential releases of radioactive materials.

ECURIE is the interface to the EU early notification and information exchange system for radiological emergencies. It is the technical implementation of Council Decision 87/600/EURATOM, which obliges EU Member States to urgently inform the European Commission of any radiological emergency for which they intend to take countermeasures. In addition ECURIE may be used to disseminate information regarding other events with radiological consequences on an urgent basis.

The system is operated by the Directorate-General Energy (DG ENER) of the European Commission in Luxembourg. Access is restricted to nominated national Competent Authorities (CAs) and Contact Points (CPs) as well as to international organisations with responsibilities regarding the response to radiological emergencies.

3 THE H2020 EURATOM FASTNET PROJECT

FASTNET is improving the methodology and the tools required for rapid response to emergencies at nuclear power plants. These tools will enable emergency centres to provide a quicker and more appropriate response to radiological risks. In particular, the capabilities of tools and methods have been extended to cover a complete set of “reference accident scenarios” for the main types of operating water-cooled nuclear power plants in Europe (including a generic concept for spent-fuel pools). By the end of this H2020 project (end of 2019), the database of potential nuclear accident scenarios will be transferred to the IAEA where it will be maintained and extended to non-European nuclear technologies, and finally made available to emergency centres in all IAEA’s member countries (http://ec.europa.eu/research/infocentre/article_en.cfm?artid=50311).

When dealing with emergency, two issues with fully different time requirements and operational objectives, and thus different methods and tools, have to be considered: emergency preparedness and emergency response. The FASTNET project has addressed both issues by combining the efforts of organizations active in these two areas to improve the capabilities of identified deterministic reference tools and methods to categorize accident scenarios in main types of operating water-cooled NPPs in Europe.

After the identification of several main categories of scenarios and the formulation of a methodology for the description and the development of a database (of scenarios), the diagnosis of accidental situations has been also performed with probabilistic approaches based on Bayesian Belief Networks (BBN) in order to complement operational deterministic methodologies and tools.

By the end of the project, both approaches should be assessed against the above mentioned database of scenarios. Finally a comprehensive set of emergency exercises has been developed and proposed to be run by a large set of partners.

4 RELEVANT PROJECTS UNDER THE EURATOM WORK PROGRAMME 2019-2020

The lesson learnt from the Fukushima accident has further pushed towards emergency responses relying on the use of mobile equipment. Consequently, the current EURATOM Work Programme 2019-2020 is explicitely focussing on the need to minimize radiological risks by improving plants’ operational safety thanks to the use of Emergency Mobile Equipment (EME) and adapting emergency preparedness and response to these challenging scenarios. Topics NFRP-02, NFRP-03 and NFRP-12 of the last EURATOM work programme are tackling these issues: http://ec.europa.eu/research/participants/data/ref/h2020/wp/2018-2020/euratom/h2020-wp1920-euratom_en.pdf.

However, it is clear that EME should be available from the very onset of the accident and, above all, plant personnel must be well trained to its use.

4.1 The Fukushima lesson

Following the tsunami (Ref.7) and the total station black-out (SBO), there were multiple equipment failures on-site, and a range of portable equipment and heavy machinery was provided to cope with the situation. Some of this equipment was supplied by TEPCO and some other heavy equipment was provided by local and prefectural organizations (e.g. firefighting brigades).

Many types of portable equipment were delivered, such as: mobile AC power generators; equipment for power restoration (mainly cables and transformers); mobile pumps (engine driven), such as fire engines with all of the associated fittings and equipment; mobile air compressors; radiation monitoring vehicles; batteries of different types, voltages and sizes; and portable lighting equipment. In some cases (especially for batteries and equipment to restore electric power supply), a logistical procurement team was established near the Fukushima Daiichi site to manage the request and/or procurement of the equipment needed.

However, the delivery of equipment was hampered by multiple problems. Fear of contamination from radioactive material deposited on vehicles impeded the transport of supplies necessary for the response. On-site emergency workers encountered difficulties in obtaining authorization from the police to travel on roads leading to and from the site. Truck drivers abandoned deliveries or retreated, requiring on-site emergency workers with driving licences to replace them. Receiving, managing and organizing the arrival of deliveries was logistically very challenging.

In conclusion, the emergency response at the Fukushima Daiichi plant has been ineffective with the inability to inject water into the reactor from ECC systems.

A different result was obtained at the Fukushima Daiini plant, only 10 km far away, also thanks to the partial availability of electric supply (Ref.8). There, the plant staff was able to cope with the situation and updated strategies for emergency preparadness and response have indeed benefitted of this lesson.

4.2 Elimination of events leading to an impact on population

As stated above, the Fukushima lessons are at the basis of important improvements in the field of emergency preparedness and response.

Furthermore, the regulatory guidelines of several EU countries call for a continuous development of safety in plants under operation, as well as in construction and in design such to guarantee that “any event that may result in a release requiring measures to protect the population in the early stages of the accident shall be practically eliminated”. In other words, current legislation and regulatory guidelines require the elimination of evacuation plans around the plant also for Gen II & III plants under operation.

As an example, efficient provisions have been implemented at Finnish operating NPP units, constructed a long time ago, in order to significantly decrease the frequencies of early releases and large releases (Ref.9): “*It is a significant achievement of Finnish licensees that the core damage frequencies of older NPP units approach and even reach the quantitative criteria set for new NPP units. The definitions and interpretations related to “practical elimination” may sometimes be vague, but it can be demonstrated that the results and practical applications can be robust and not sensitive to the definitions*”.

To be noted that the Finnish nuclear research organization VTT, as well as the FORTUM operator have contributed to the demonstration and dissemination of the “practical elimination of risks” in the framework of the EURATOM “In-Vessel Melt Retention”, IVMR project (the IVMR strategy was already adopted for the VVER 440 type 213 based on thorough research work for the Finnish Loviisa NPP: https://cordis.europa.eu/project/rcn/196923/factsheet/en).

The in-vessel melt retention and coolability is based on the idea of flooding the PWR vessel cavity or the BWR drywell with water to either submerge the vessel completely or at least submerge the lower head. The PWR or BWR lower head containing the melt pool is cooled from outside, which keeps the outer surface of the vessel wall cool enough to prevent vessel failure. As said, this concept is employed in the Loviisa VVER-440 in Finland, where it has been approved by the regulatory authority STUK. More recently the IVMR concept was adopted at all VVER-440 units operated in Central Europe.

The concept is also employed in the Gen-III PWR designs: AP-600, AP-1000, Korea's Advanced PWR-1400, Mitsubishi's 1700 MW APWR, in the 1000 MWe BWR design of AREVA, and Hitachi's ABWR which was already approved by the US-NRC.

The state-of-the-art of the demonstration of the IVMR concept for these reactors of higher power (>600MWe) is well summarised in one of the deliverables of the IVMR project: "In-Vessel Melt Retention Analysis of a VVER-1000 NPP, JRC technical report" (file:///C:/Users/passart/AppData/Local/Packages/Microsoft.MicrosoftEdge_8wekyb3d8bbwe/TempState/Downloads/ivr-jrc_tech_report_final_online.pdf).

4.3 Current EURATOM projects (WP 2019-2020)

EURATOM has always promoted safety improvements i.e. a constant reduction/elimination of risks, through for example, two "networks of excellence", the SARNET and SARNET2 projects.

SARNET2 (Severe Accident Research NETwork of Excellence - Phase 2) has involved most of the "severe accident" expertise in Europe, plus Canada, Korea and the United States (41 partners). In particular, the project has optimised the use of the available means, e.g. the European ASTEC computer code able to predict NPP behaviour during a postulated severe accident (to be noted that the above-mentioned FASTNET project has largely benefitted of the results of the SARNET network of excellence and in particular of the development of the ASTEC code).

A further "practical elimination of risks" is currently tackled in a number of new EURATOM projects:

- MUSA, sCO2-4-NPP and R2CA projects for Gen II&III operational plants, and
- SAMOSAFER and ELMSOR projects for Gen IV new designs of Small Modular Reactors.

4.3.1 The MUSA (Management and Uncertainties of Severe Accident) project

CIEMAT is coordinating an innovative approach for accident mitigation means in operating plants (including storage pools) by fostering and coupling BEPU (Best Estimate Plus Uncertainties) assessments in the severe accident (SA) domain with accident management (AM).

The MUSA project proposes an innovative research agenda in order to move forward the predictive capability of SA analysis codes by combining them with the best available/improved UQ (Uncertainty Quantification) tools and embedding accident management as an intrinsic aspect of SA analyses.

The target is to avoid adopting conservative assumptions and allow identifying safety margins, quantify likelihood of reaching specific acceptable values and, through the distribution variance, provide insights into dominating uncertain parameters.

To do so UQ methods are to be used, with emphasis on the effect of already-set and innovative accident management measures on accident unfolding, particularly those related to ST (Source Term) mitigation. Therefore, ST related Figures Of Merit (FOM) are to be used in the UQ application.

Given the focus of FOM on source term, the project will identify variables governing ST uncertainties that would be worth investigating further. All the ingredients necessary to conduct the project are already available: analytical tools, experimental data, postulated reactor accidental scenarios and, technical and scientific competences.

4.3.2 The R2CA (Reduction of Radiological Consequence in design-based Assessments) project

The R2CA, led by IRSN, is focussing on the radiological consequences of design accidents and their management strategy.

The project targets the development of harmonized methodologies and innovative management approaches, as well as safety devices able to support evaluation and reduction of consequences of Design-Based Accidents (DBA) and DEC-A accidents in operating and foreseen nuclear power plants in Europe. DEC accidents are Design Extension Conditions which fall into two different subdomains: the DEC-A for which the prevention of significant core degradation can be achieved and DEC-B (significant core melting) which has a much lower probability of occurrence.

The R2CA project will reassess the safety margins of DBA and DEC-A using less conservative approaches and considering for relevant accident scenarios the gap, and associated risks, between the original design and the design extension phases (beyond design accidents). This will reinforce the confidence on these safety margins for conditions up to the extended design domain, will allow the identification of new accident management measures, new potential devices/barriers and new insights for the optimization of the potential emergency response to reduce the burden of population protection measures.

The project will include also innovative actions to estimate the pros and cons of potential new accident management measures and devices, to explore the potential switch of prognosis evaluation tools to the diagnosis of on-going fuel cladding failure and to explore the potentiality for these accidental situations for advanced fuels.

4.3.3 The sCO2-4-NPP (Innovative SCO2-based Heat Removal Technology for an Increased Level of Safety of Nuclear Power Plants) project

The main aim of the EDF-led sCO2-4-NPP is to bring an innovative technology based on supercritical CO2 (sCO2) for heat removal in nuclear power plants (NPPs) closer to the market. sCO2-4-NPP builds on results of the previous H2020 sCO2-HeRo project, where the technology was first developed and brought to TRL3.

The sCO2-4-NPP technology will be a backup cooling system, attached to the principal steam-based cooling system, which will considerably delay or eliminate the need for human intervention (>72 hours) in case of accidents such as Station Black-Out, thus replying to the need for increased safety in NPPs.

Thanks to the compact size and modularity of the system, it can be retrofitted into existing NPPs but also included in future NPPs under development. Through a close collaboration between major industrial actors and highly-skilled academic institutions, the sCO2-4-NPP partners will bring the full system to a TRL5 (while parts of the system will reach a TRL7) by carrying out experiments, simulations, design, upscaling and validation of the technology in a real NPP PWR simulator.

Regulatory requirements will be considered in the conceptual design of components and the system architecture to increase the chances of acceptance by European nuclear safety authorities and speed up the road to the market. Detailed technical, regulatory, financial and marketing roadmaps will be developed for bringing the technology to industrial uses after the project. The sCO2-4-NPP technology will increase NPP safety, decrease the plant overall environmental footprint, thus increasing the competitiveness of European NPP operators.

4.3.4 The SAMOSAFER (Severe Accident Modelling and Safety Assessment for Fluid-fuel Energy Reactors) project

The Molten Salt Reactor (MSR) is considered a game-changer in the field of nuclear energy and a strong asset in the combat against climate change. The expanding R&D programmes in China, EU, Russia, and the USA, lead to a vibrant atmosphere with many bright students entering the scene and new start-up companies eager to commercialize this technology.

The MSR typically consists of a reactor core with a liquid fuel salt, and an integrated treatment unit to clean and control the fuel salt composition. Due to the liquid fuel, the MSR excels on safety and can operate as a breeder with thorium or uranium, or as a burner of spent fuel actinides.

The SAMOSAFER projects targets the demonstration of the inherent safety of the reactor, the feasibility of the fuel cycle facilities, and the path towards licensing and deployment. In particular, safety assessments will be performed to determine if new safety barriers are required as well as to verify the reactor behaviour during severe accident contitions. New simulation models and assessment tools will be developed and validated with experiments.

The project will cover the modelling, analysis and design improvements for:

- Prevention and control of reactivity induced accidents;
- Redistribution of the fuel salt via natural circulation and draining by gravity;
- Freezing and re-melting of the fuel salt during draining;
- Temperature control of the salt via decay heat transfer to the environment;
- Thermo-chemical control of the salt to enhance the radionuclide retention;
- Nuclide extraction processes, such as helium bubbling, fluorination, and others;
- Redistribution of the source term in the fuel treatment unit;
- Assessment and reduction of radionuclide mobility;
- Barriers against severe accidents, such as fail-safe freeze plugs, emergency drain tanks, and gas hold-up tanks.

The main objective is to ensure that the MSR can comply with all expected safety requirements in a few decades from now.

4.3.5 The ELSMOR (Towards European Licencing of Small Modular Reactors) project

The VTT-led ELSMOR project aims to create methods and tools for the assessment and verification of the safety of light-water small modular reactors (LW-SMR).

ELSMOR advances the understanding and technological solutions pertaining to light-water SMRs on several fronts:

• Collection, analysis, and dissemination of the information on the potential and challenges of Small Modular Reactors to various stakeholders, including the public, decision makers and regulators;

• Development of the high level methods to assess the safety of LW-SMRs;

• Improvement of the European experimental research infrastructure to assist in the evaluation of the novel safety features of the future LW-SMRs;

• Improvement of the European nuclear safety analysis codes to demonstrate the capability to assess the safety of the future LW-SMRs.

Establishing education and training in the field of innovative nuclear reactors for young professionals is also emphasized.

The ELSMOR industrial partners include utilities, small medium sized enterprises as well as the consortium in charge of the development of the French LW-SMR (F-SMR design). The licencing approaches and methods used by the partners of the ELSMOR project are expected to be directly utilized by SMR designers like the French consortium. The outcomes should make the licensing process more fluid and comprehensive; this should also be true from the regulator point of view.

5 NUCLEAR ENERGY, SOCIAL SCIENCE AND PUBLIC ACCEPTANCE: THE HONEST PROJECT

HoNESt (History of Nuclear Energy and Society) was a three-year interdisciplinary research endeavour funded by EURATOM (the project ended in March 2019).

HoNESt's central objective was to understand how societies have engaged with nuclear energy, and how the nuclear energy sector has engaged with societies, and how this has changed over the course of the past 60 years.

Based on a critical examination of past experiences, HoNESt has underlined the need of "*a transition to a sustainable, secure, and clean energy provision in the future*"… including safe innovative nuclear energy systems as stated in several HoNESt deliverables (http://www.honest2020.eu/).

HoNESt has also confirmed that nuclear acceptance is possible only in countries where there is a good public participation to the decision process AND a good level of trust towards decision-makers.

Therefore, the results of the HoNESt project should be used by the nuclear community in order to correct the public-perceived «psychological irrationality» of the nuclear sector (i.e. the image of a dangerous and unsustainable energy source) and tackle the main, simple, incorrect question of the large public: if risks are unavoidable, why to use nuclear energy?

The nuclear community should take into account the two main reactions of the large public:

- the loss aversion, in other words the negative psychological impact we feel from a specific issue if interpreted as a danger/ loss rather than interpreted as a gain (this is a cognitive bias that arises from heuristics which makes the negative impact estimated at least twice as strong as the positive impact);
- the challenge of knowledge, i.e. the polarized attitude of people who believe that they are knowledgeable on a specific issue. Thus, in a context of a general opposition/ negative opinion towards nuclear energy, telling people about the benefits of nuclear energy is more likely to generate protest rather than support.

For the above reasons, the nuclear community should put in place a bottom-up public engagement by supporting the so-called « Citizen Science » (the quest for truth by the large public) with « Scientist Science » and, above all, by adopting a common, coherent communication providing quality over quantity (HoNesT: "*only increasing the amount of engagement, if the methods employed are ineffective or unjust in the experiences of the large public, is unlikely to build knowledge, trust or support*").

Future EURATOM work programs might need to further focus on social science and humanities (a potential follow-up of the HoNESt project?) by suggesting to assess whether nuclear energy could become accepted as a viable, clean source of power and therefore remain an important contributor of the clean energy revolution (Ref.12). According to this target, safety assessments and harmonization of EU emergency procedures must demonstrate the "practical elimination of risks" associated to the use of the nuclear technology.

EU citizens have the right to access the results, for example, of half a century of studies in the field of radioprotection which have underlined that cellular adaptive responses are conveying beneficial effects to the organism exposed to low doses (million of years of adaptation to natural doses). This view is reflected in a statement by the US Health Physics

Society: “*for doses below 100 mSv (10 rem) risks of health effects are either too small to be observed or are non-existent*“ (Ref.10).

Besides, the fear of (low) radiation doses could even impair the use and development of medical nuclear applications, therefore there is a need for correct information: “*there is no evidence of [medical applications] low-dose carcinogenicity. These claims themselves have adverse public health impacts by frightening the public away from medically justified exams. It is time for the medical and scientific communities to be more assertive in responding to sensational claims of health risks*” (Ref.11).

6 CONCLUSIONS

EURATOM has the mission to guarantee and improve the safety of nuclear installations which are part of the energy mix of sovrain EU member countries. In particular, the EC has “shared competences” inferred by the EURATOM treaty and, under this principle, may only act to attain shared objectives.

Therefore, within this framework, EURATOM, through the Work Programs implemented by DG RTD, has put in place a “shared” strategy aiming at a viable and safe use of nuclear energy in those EU countries which intend to use this energy source.

In the last 30 years EURATOM has funded world-leading research and scientific cooperation (e.g. the PHEBUS FP programme which has been the largest severe accident research programme carried out in the world). During this period of time, the total EC financial contribution in the area of severe accidents and emergency preparedness has been more than EUR 200 million (without including funding of research in radioprotection).

EURATOM research is currently demonstrating the further reduction of radiological risks thanks to the use of Emergency Mobile Equipment (EME) for example during Fukushima-like Station BlackOut scenarios and promoting specific emergency preparedness and response to these challenging scenarios: it is clear that “standardized“ EME should be available from the very onset of the accident and, above all, plant personnel must be well trained to its use.

Last but not least, in today’s battle for reduction of CO2 emissions, climate policy experts believe that it's time to overcome longstanding fears of the nuclear technology: the nuclear community could indeed contribute by providing “Scientist Science” against “Citizen Science” (a justified quest for truth).

In conclusions, nuclear stakeholders must guarantee high level of plant operational safety but also pay attention to a coherent, “psycologically rational” communication aiming at an improvement of public acceptance, by underlining for example, that:

- the use of nuclear power rather than fossil fuels has saved some 1.84 million air pollution-related premature deaths, while saving the emission of 64 billion tonnes of carbon dioxide (with up to a further 7 million lives to be potentially saved over the following four decades should a "reasonable" new nuclear programme be initiated globally, Ref.13),
- future nuclear builds (as the Gen III+ European Pressurised Reactor, EPR and Gen IV innovative designs), as well as plants in operation (Gen II & III for which measures of “practical elimination of risks” have been implemented) will not impact on surrounding population since all potential accidents will not allow releases requiring evacuation plans, and
- the consequences of any potential accident at EU plants (i.e. low doses to the population) are comparable to the effects of natural doses (and often much lower than the effects implied by linearity from high doses).

7 REFERENCES

1. Innovation Union: Aims of the Innovation Union, state of progress and related policy, January 2016 -https://ec.europa.eu/info/research-and-innovation/strategy/goals-research-and-innovation-policy/innovation-union_en
2. Report from the Commission to the European Parliament, the Council and the European Economic and Social Committee: Interim evaluation of the Euratom Research and Training Programme 2014-2018, Brussels, 1.12.2017 COM(2017) 697 final.
3. Commission Implementing Decision of 14.12.2018 on the financing of indirect actions within the framework of Council Regulation (Euratom) No 2018/1563 and on the adoption of the work programme for 2019-2020, Brussels, 14.12.2018 C(2018) 8412 final.
4. Final Report Summary - NERIS-TP (Towards a self sustaining European Technology Platform (NERIS-TP) on Preparedness for Nuclear and Radiological Emergency Response and Recovery), 31 Januar 2014 (https://cordis.europa.eu/project/rcn/97429/reporting/de).
5. The European Community Urgent Radiological Information Exchange ECURIE: https://ecurie.jrc.ec.europa.eu/
6. FAST Nuclear Emergency Tools (FASTNET), CORDIS, 1 October 2015 https://cordis.europa.eu/project/rcn/198668/factsheet/en
7. The Fukushima Daiichi Accident, IAEA Technical Volume 3/5: Emergency Preparedness and Response (https://www-pub.iaea.org/MTCD/Publications/PDF/AdditionalVolumes/P1710/Pub1710-TV3-Web.pdf).
8. Harvard Business Review: How the other Fukushima plant survived, August 2014 (https://hbr.org/2014/07/how-the-other-fukushima-plant-survived)
9. I. Niemelä et alii: Practical Elimination - Experiences for Units in Use, in Construction and in Design, STUK, Helsinki, Finland, Probabilistic Safety Assessment and Management PSAM 14, September 2018, Los Angeles, CA (file://net1.cec.eu.int/HOMES/106/passart/Desktop/VTT_practical_elimination.pdf)
10. Nuclear science: a guide to the nuclear science wall chart, Appendix F, 1918 (https://www2.lbl.gov/abc/wallchart/teachersguide/pdf/~AppF.pdf)
11. Are risks from medical imaging still too small to be observed or nonexistent? (https://www.ncbi.nlm.nih.gov/pmc/articles/PMC4674180/)
12. Michael Shellenberger : How fear of nuclear is hurting the environment, TED Summit, June 2016 (https://www.ted.com/talks/michael_shellenberger_how_fear_of_nuclear_power_is_hurting_the_environment?language=zh).
13. Kharecha P. and Hansen J.: Prevented mortality and greenhouse gas emissions from historical and projected nuclear power. Environmental Science and Technology, 2013 (https://pubs.giss.nasa.gov/abs/kh05000e.html)

EU SUPPORT TO ESTABLISH AN EARLY WARNING RADIATION MONITORING NETWORK AND TO ENHANCE NUCLEAR AND RADIATION EMERGENCY RESPONSE CAPABILITIES OF THE REPUBLIC OF ARMENIA

G. Lizin[1], N. Kelly[2], J. Végh[3], R. Dielmann[4], M. Helmecke[4], W. Raskob[5], V. Grigoryan[6], A. Amirjanyan[7], M. Simonyan[7], K. Haroyan[7]

[1]EC DEVCO, Rue de la Loi 41, B-1049 Brussels, Belgium
[2]Lattanzio Advisory SPA, KIBS, Via Cimarosa 4, 20144 Milano, Italy
[3]EC JRC, P.O.Box 2, 1755 ZG Petten, The Netherlands (janos.vegh@ec.europa.eu)
[4]Bertin GmbH, Heerstrasse 149, D-60488 Frankfurt am Main, Germany
[5]KIT, Hermann-von-Helmholtz Platz 1, D-76344 Eggenstein-Leopoldshafen, Germany
[6]ANRA, Tigran Mets 4, 0010 Yerevan, Armenia
[7]NRSC, Tigran Mets 4, 0010 Yerevan, Armenia

Abstract:

The European Commission recently launched a cooperation project in the frame of the Instrument for Nuclear Safety Cooperation (INSC) to support the ANRA, the nuclear regulator of Armenia, to establish a state-of-the art automatic on-line Early Warning Radiation Monitoring Network (EWRMN) around the Armenian nuclear power plant (NPP) and to install and customize the JRODOS decision support system at the Emergency Response Centre (ERC) of the regulator. The monitoring stations of the ERWMN will be located around the Metsamor NPP (mostly at distances between 2 km and 5 km with others at more distant strategic locations or centres of population) and will provide gamma dose rate and gamma spectrometric data, as well as meteorological data through a GSM (3G) network. Measured data will be transferred to the Monitoring and Management Centre (MMC), located at the ERC of the ANRA) and will be further processed and displayed. The ERC will also include a JRODOS installation for supporting the experts of the ANRA and its technical support organisation (TSO) in their accident prediction and decision making activities during nuclear and radiation emergencies. The internationally acknowledged and widely used JRODOS tool will be customized to the specific conditions in Armenia, e.g. hydrological, meteorological, map (geographical), population and radio-ecological data, and JRODOS will be updated according to the local conditions. The new network will be able to exchange monitoring data with the European Radiological Data Exchange Platform (EURDEP). The ERWMN is designed, equipped and integrated by the Bertin Technologies Gmbh (Germany) as winner of the EU tender for the supply of equipment and provision of services. The Karlsruhe Institute of Technology (KIT) – as the official JRODOS developer and supplier – was contracted to install and customize JRODOS at the ERC of the ANRA. The Nuclear and Radiation Safety Center (NRSC, the TSO of ANRA) participates in both projects as a local subcontractor.

The paper first provides a brief overview of INSC activities, focusing on cooperation projects implemented in Armenia during the last 5 years in the areas of nuclear and radiation safety and radioactive waste management. Then the current state of environmental radiation monitoring and the present Armenian nuclear emergency preparedness and response (EP&R) provisions are outlined. Details of the ERWMN are then discussed, focusing on network architecture and functions, the state-of-the-art measuring equipment, as well as data communication and processing methods. JRODOS implementation details are also outlined, together with some details of its customization and the intended future use of the system during nuclear or radiation emergencies in Armenia. The paper concludes with a brief evaluation of the expected benefits of the EWRMN and JRODOS on the EP&R capabilities of Armenia.

1 INSTRUMENT FOR NUCLEAR SAFETY COOPERATION AND RECENT INSC PROJECTS IN ARMENIA

1.1 Instrument for Nuclear Safety Cooperation

The Instrument for Nuclear Safety Cooperation (INSC) is a funding instrument established [1] and operated by the European Union (EU). The INSC supports the promotion of a high level of nuclear safety, radiation protection, and the application of efficient and effective safeguards of nuclear material in eligible third countries. The geographical scope of the INSC covers all third countries, but priority is given to accession and neighbouring countries. The INSC finances projects supporting

- the promotion of an effective nuclear safety culture and implementation of the highest nuclear safety and radiation protection standards, and continuous improvement of nuclear safety;
- responsible and safe management of radioactive waste and spent nuclear fuel and remediation of former nuclear sites and installations;
- the establishment of frameworks and methodologies for the application of efficient and effective safeguards for nuclear material.

In the current implementation period (i.e. between 2014 and 2020) the instrument provides support to enhancing regulatory frameworks in African countries, as well. The basic aim in Africa is to ensure that ongoing and future uranium mining activities respect high safety and environmental standards. Initiatives to improve the situation of the population around Chernobyl (Ukraine) continue. A special programme for dealing with the uranium mining legacy in the most affected parts of Central Asia shall be implemented together with the European Bank for Reconstruction and Development (EBRD). The instrument disposes a financial budget amounting to €225 million in the current 7 year period.

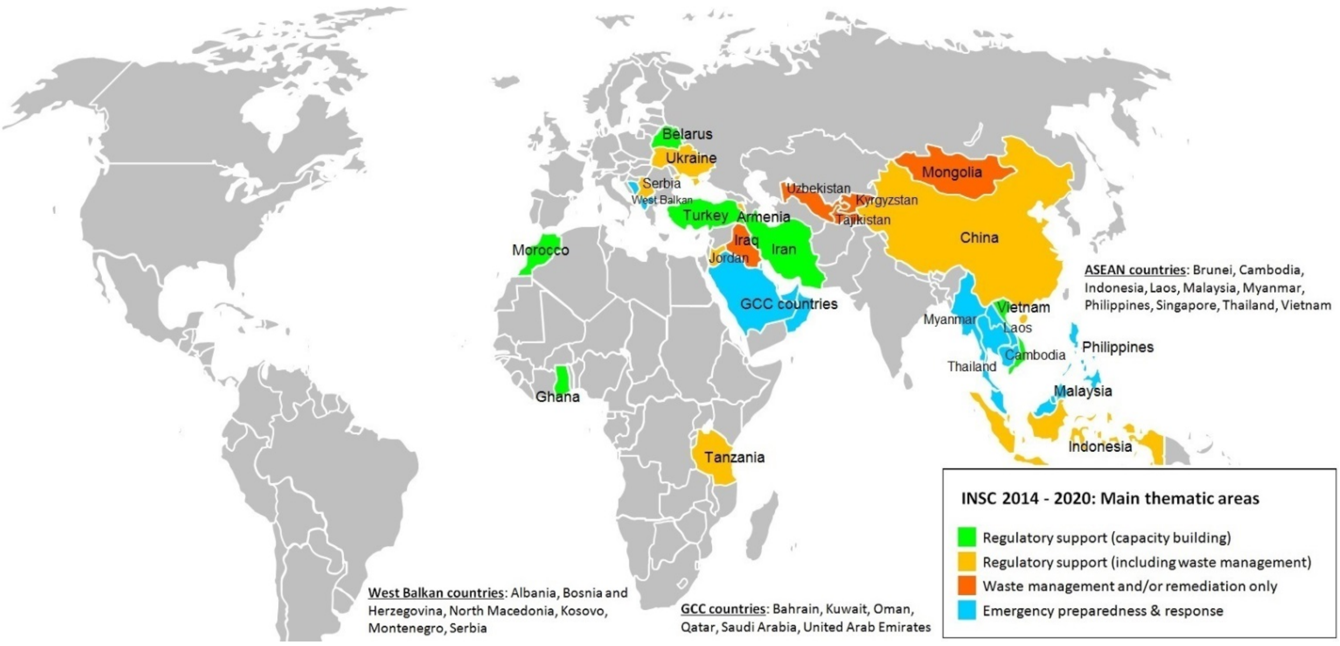

Figure 1-1. Main thematic areas of the current INSC projects around the world

1.2 Recent INSC projects supporting Armenia

One of the INSC focal areas is the cooperation with national nuclear regulatory authorities and their technical support organisations (TSOs) to enhance their regulatory skills by improving licensing and safety assessment capabilities, to reinforce the national nuclear safety infrastructure and to transfer of best EU practice and international experience. Starting from 1991 Armenia continuously received EU nuclear safety assistance in the frame of the TACIS project. In addition to the cooperation with the Armenian Nuclear Regulatory Authority (ANRA) and its TSO, the Nuclear and Radiation Safety Centre (NRSC), considerable efforts were targeted to improve the safety of the Armenian nuclear power plant (ANPP) by providing support to the Armenian nuclear operator.

The ANPP is located at the Metsamor site, 30 km west from Yerevan, the capital of Armenia (see Fig. 1-2). The plant has two power generating units, but only Unit 2 is in operation, while Unit 1 is kept in long-term shutdown condition since 1989. Although the ANPP did not suffer damages, both units were shut down in early 1989, as a precaution after the Spitak earthquake occurring in December 1988.

Figure 1-2. View of the Armenian NPP with the cooling towers in the background

In the early 1990s Armenia suffered an extreme shortage of energy and the Government of Armenia decided the restart Unit 2 in order to tackle the energy crisis by using a domestic option. Unit 2 was restarted in November 1995, following a preparatory period when a large number of safety upgrade measures had been implemented.

Both ANPP units are VVER-440/V-270 type reactors; their design is based on the first generation of Soviet VVER-440/V-230 reactors. Due to the seismic features of the Metsamor site, the original V-230 design was seismically reinforced and this resulted in the V-270 variant. Note that Unit 2 started its commercial operation in 1980. On the average the operating Unit 2 accounts for about 40% of the domestic electricity production in Armenia.

According to the decision of the Government of Armenia, activities aimed to extend the ANPP Unit 2 design service time have been started. No INSC support is provided to the ANPP in connection with the planned long-term operation (LTO), but the Armenian nuclear regulator is assisted in performing its tasks arising from reviewing and assessing the large number of licensing documentation submitted during the preparation and implementation of the LTO.

As mentioned above, Armenia received substantial INSC support in the past and the nuclear safety cooperation is being continued today with concrete and ambitious plans for the future.

Table 1-1 summarizes the Armenian INSC projects in the last 5 years, indicating projects supporting the ANRA and the nuclear operator, as well.

Table 1-1. Overview of recent INSC projects supporting Armenia (2014 – 2019)

Beneficiary	Project ID	Project title / description	Contractor	Status
ANRA	A3.01/16A	Enhancing the capabilities of the Armenian NRA and its TSO in reviewing	RISKAUDIT + SÚJB, IRSN,	On-going

		documents demonstrating the long-term safety of Unit 2 of the Metsamor NPP	GRS, SSTC, TECNATOM	
ANRA	A3.01/15A	Supply of an Early Warning Radiation Monitoring System (EWRMS) and computer hardware equipment for the implementation of JRODOS in Armenia	Bertin GmbH	On-going
ANRA	A3.01/15B	Enhancing the capabilities of the Armenian NRA in preparedness for and response to a nuclear or radiological emergency	Karlsruhe Institute of Technology (KIT)	On-going
ANRA	A3.01/13	Enhancement of ANRA and NRSC capabilities for safety review and assessment of radioactive waste management facilities and activities	ITER Consult + ISPRA, VTT, SOGIN	Finished
Ministry of Energy and Natural Resources	A4.01/09	Development of radioactive waste and spent fuel management strategy for Armenia	ITER Consult + SOGIN, STUK, ARAO	Finished
ANPP	A1.01/16B	Support to the Nuclear Operator of Armenia – Provision of on-site assistance to the ANPP	ENCO	On-going
ANPP	A1.01/11	On-Site Assistance to Armenian NPP – Contributions to the ANPP operator for the implementation of the Stress Tests for Armenian NPP, Unit 2	ENCO	Finished
ANPP	A1.01/09 (components C&D)	Decommissioning planning and licensing development at ANPP and pilot decommissioning project at ANPP	NUKEM + EWN, Worley Parsons	Finished

2 CURRENT STATUS OF NUCLEAR AND RADIATION EMERGENCY PREPAREDNESS AND RESPONSE IN ARMENIA

2.1 Current status of radiation monitoring around the ANPP

The environmental radiation monitoring aspects are addressed in and regulated by laws and governmental decrees [2-7]. The “Radiation safety norms” stipulates the dose limits for the public and the risk for workers and public from radiological point of view [5]. The issues related to radiation safety at ANPP, including release criteria, monitoring requirements, measures to complete the radiation safety requirements and dose constraints for the relevant critical group, the optimized levels of airborne releases for noble gases, iodine and long-lived radionuclides, as well as the optimized level of liquid effluences are established in and are regulated by [7].

The initial assessment of environmental radiation situation ("zero background measurements") at the ANPP site was performed before the construction of power plant in middle of 1970s.

The radiation monitoring at ANPP site is implemented in accordance with the “Technical specification on radiation monitoring of Armenian NPP” which specifies the conditions and limits of radioactive releases and effluents (source term). Currently, the environmental radiation monitoring implemented at ANPP for the supervised area within 10 km is performed according to a program approved by the ANRA. The monitoring incudes periodic (the periodicity depends on the subject: weekly, monthly, quarterly and yearly basis) measurements of atmospheric air, fallouts, water and the sediments from open pools, soil, grasses and the vegetation, dose rate at the sampling points, total beta and total alpha, gamma spectrometry and concentration of ^{90}Sr in the environmental samples. The monitoring results in monthly, quarterly and yearly bases are submitted to ANRA for review and assessment. The stationary gamma dose rate monitoring stations (BABUKA system) were installed around ANPP in the end of 1990s. Currently, the BABUKA system is out of operation because of technical reasons, and it is impossible to restore/re-operate it.

The environmental radiation monitoring of facilities in the Armenian NPP supervised area and the methodology to distribute the areas for taking samples are determined taking into account the climatic, geographic, economic, demographic and other factors of the area where the Armenian NPP is located.

The external exposure control of the population in the Armenian NPP supervised area is performed by regular dosimetric measurements. According to the results of the periodical measurements the gamma dose rate in the supervised area (external exposure) varied within 0.097 μSv/h - 0.13 μSv/h (open areas), which is almost the same as mentioned in the report on radiation situation surveillance dated 1976, i.e. before the Armenian NPP commissioning (0.10 - 0.12 μSv/h).

The airborne releases from the Armenian NPP are controlled by the measurement devices located on the ventilation stack (150m height), and the liquid effluents are controlled by taking samples from the bore-holes located outside the boundary of the Armenian NPP rainwater and sewerage systems. The measurement frequency is described in the technical specification for radiation monitoring. The airborne releases volumetric beta activity trends are 100 times lower than the authorized levels of releases from the Armenian NPP.

The main contribution to the releases comes from the following radionuclides: ^{60}Co (25.2%), ^{137}Cs (8.2%), ^{90}Sr (0.5%), ^{131}I (20.0%), ^{58}Co (1.9%), ^{110m}Ag (41.0%), ^{54}Mn (0.21%) and ^{103}Ru (2.1%). The ^{60}Co, ^{58}Co, ^{110m}Ag and ^{54}Mn isotopes are corrosion products, while the ^{137}Cs, ^{131}I and ^{90}Sr isotopes are produced in the fission process.

There are no laboratory capabilities available to ANRA for independent monitoring of atmospheric and liquid releases of radiation pollutants (ANPP, RWM facility and others), as well as to monitor the environmental radiation situation in Armenia, including ANPP supervised area. There are a few hand-held radiation measuring equipment at the NRSC (technical support organization of ANRA), that are also available to ANRA for environmental radiation monitoring. These are mainly used to monitor the radiation protection conditions of facilities using ionizing radiation sources (for instance medical facilities). A mobile gamma dose rate monitoring system SPARCS (Spectral Advanced Radiological Computer System) is also available to monitor the in-situ gamma dose rates (see Fig. 2-1). Actually, the current monitoring program is only a small part of the national environmental radiation monitoring program and doesn't cover overall objectives of the environmental radiation monitoring activities. Currently ANRA is verifying the ANPPs environmental radiation monitoring results only by means of regulatory inspections without independent monitoring capacities.

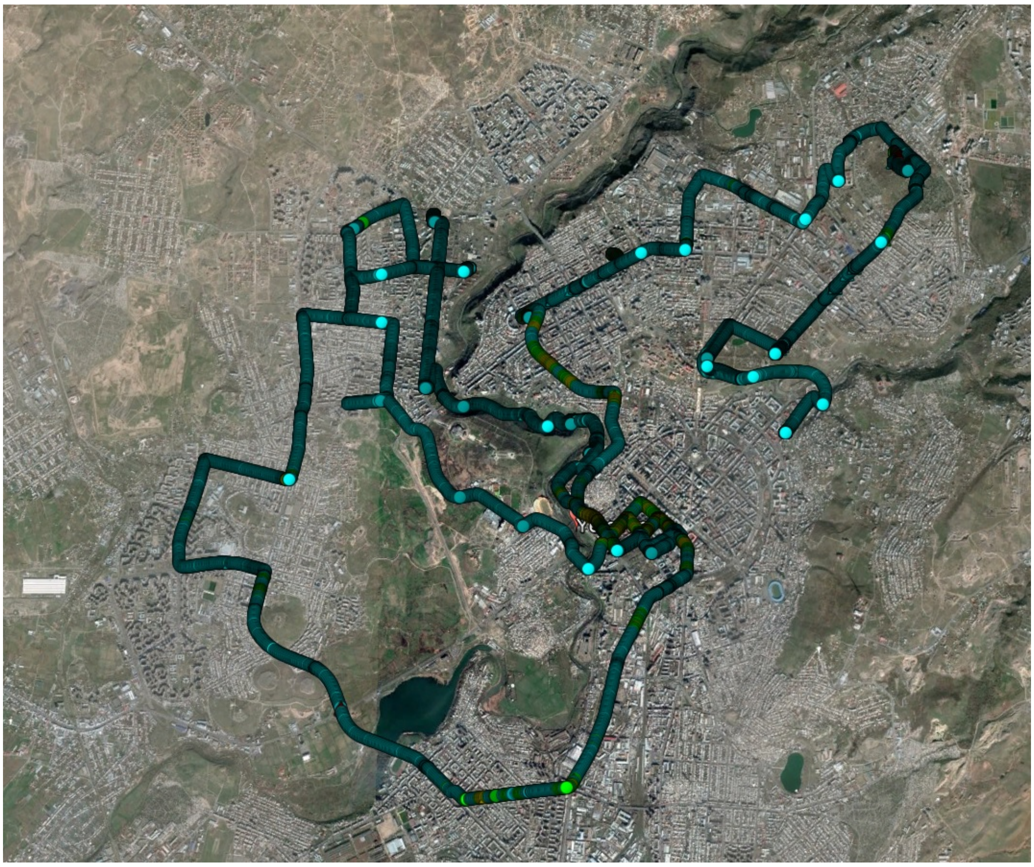

Figure 2-1. Gamma dose rate scanning implemented by NRSC in Yerevan using SPARCS

2.2 Current organisation and functions of the emergency preparedness and response in Armenia

The basic framework for preparedness and response to nuclear and radiation emergencies in Armenia is established in a number of legal acts dealing with separate issues concerned with the emergency preparedness (notification, organization and implementation of evacuation, transportation, emergency radiation monitoring, medical response, possible agricultural countermeasures and so on) [2-3, 5-11]. According to the existing framework the emergency preparedness and response plans are divided into on-site and off-site parts. The National Plan on Population Protection in case of nuclear and radiological emergencies at Armenian NPP (off-site plan) provides with the detailed assessment of organizational measures and allocation of the functions and responsibilities of the operator and the national and local authorities implementing response measures in case emergencies at the ANPP [8].

For the effective implementation of emergency planning and response actions, currently, according to existing regulations, the area around nuclear installations is divided into emergency planning zones as follows:

- Precautionary action zone (PAZ). This is a predesignated area around a facility in threat category I where urgent protective action has been preplanned and will be implemented immediately upon declaration of a general emergency.
- Urgent protective action planning zone (UPZ). This is a predesignated area around a facility in threat category I or II where preparations are made to promptly implement urgent protective actions based on environmental monitoring data and assessment of facility conditions, the goal being to avert doses specified in international standards.
- Long-term protective action planning zone (LPZ). A zone around a facility in which plans and procedures are in place for taking effective protective actions to reduce the long-term exposure due to deposited radionuclides in the event of an accident.

The main actors and corresponding functions based on National Plan on Population

Protection (the off-site plan) are listed below:

- The Armenian NPP is responsible for classification of emergency situation at NPP, prompt notification on the occurrence of emergency situation, bringing the reactor into a safe condition and NPP personnel protection.
- The Ministry of Emergency Situations of the Republic of Armenia (MES) is responsible for warning the national response organizations and the population, coordination of population protection measures, organization of emergency radiological monitoring and performing rescue actions in emergency situations.
- The ANRA is the national advisor in the organization of response and also the National Warning Point under the Convention on Early Notification of a Nuclear Accident. The actions to be carried out by ANRA in case of a nuclear and (or) radiological accident at the ANPP are as follows:
    - Assessment of the situation at the ANPP and its adjacent territories based on the data received from the ANPP and emergency radiological monitoring results.
    - Prediction of the possible change of the situation based on situation assessment.
    - Submission of recommendations on implementation of necessary protective measures to the Ministry of Emergency Situations of the Republic of Armenia.
    - International operative warning on the nuclear accident in accordance with the convention on operative informing on a nuclear accident.
- The Ministry of Foreign Affairs of the RA is responsible for providing information received from the ANRA Emergency Response Centre (ERC) on the emergency to the embassies, foreign representative offices and the embassies of the RA in other countries.
- The Ministry of Defense of the RA is responsible for conducting emergency radiological monitoring, deployment of forces and resources necessary for rescue operations and deployment of decontamination and special treatment units.
- The Police of the RA are participating in the warning and notification of the population, responsible for protection of property and assets of the settlements in the contaminated area and maintaining public order in the settlements, organizations, evacuation points, and transportation routes.

To cope with its task the ANRA operates an appropriately equipped Emergency Response Center and has appropriately trained emergency personnel. The functions of the ANRA ERC groups are:

- The Emergency Commission – management of the ERC operations;
- The NPP technological assessment group – assessment of nuclear reactor condition, prognosis on possible changes of the reactor condition, estimation of radioactive releases and discharges and conditions based on on-line access to the NPP control parameters;
- The Radiation Situation Assessment and Prognoses Group – assessment of situation at the facility or place where the accident took place, prognosis on possible changes of situation, development of recommendations on protective measures based on a simplified assessment tool (PUMA).
- The Information and Public Relations Group – receiving from and sending to information of the emergency commission, providing information to the IAEA, communication with public and mass media.

There are relevant emergency procedures established to ensure functioning of the ANRA ERC groups. Among others there are procedures specifying the sequence of implementation of reactor condition and source term assessment, assessment of radiological situation of the Armenian NPP and adjacent territories, prognosis on situation change, development recommendations on radiation protection of the Armenian NPP personnel, emergency personnel, population and other.

These procedures are periodically revised during/after the regular table-top exercises within the ANRA. The Emergency Response Structure of the ANRA is provided in the Figure 2-2.

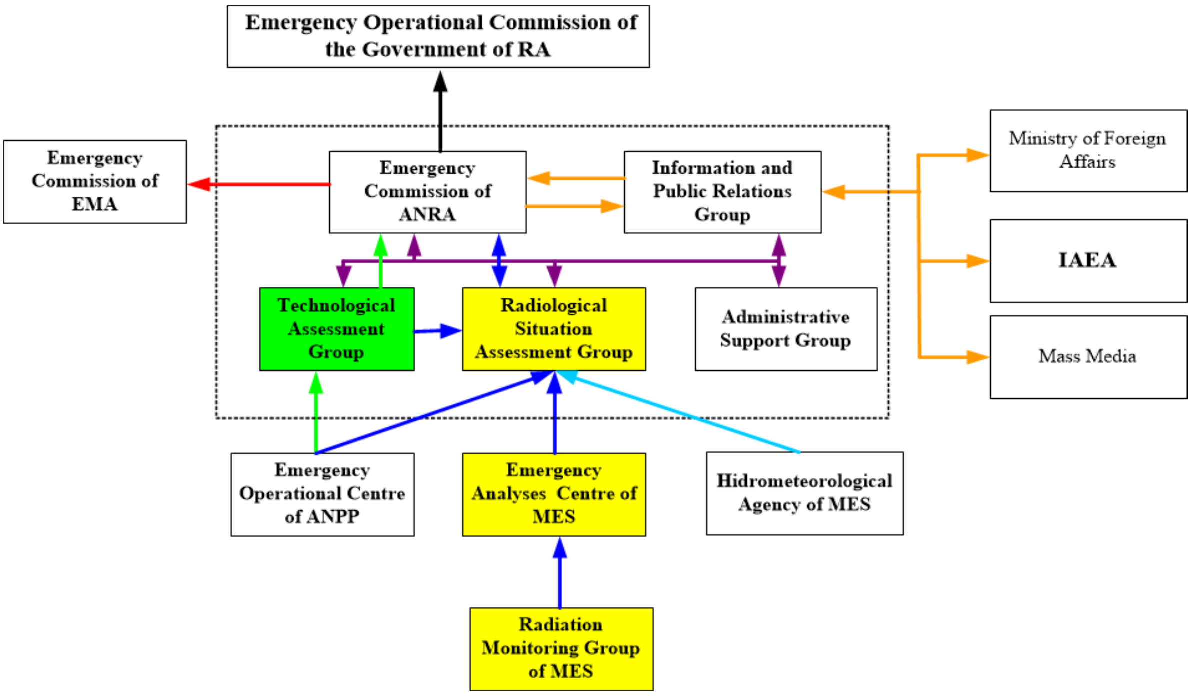

Figure 2-2. Scheme of ANRA's emergency response and interaction with external organizations

3 DESIGN AND IMPLEMENTATION OF THE EARLY WARNING RADIATION MEASUREMENT SYSTEM

3.1 Design architecture, configuration and functions of the EWRMS

The objective of Bertin is the design and installation of a complete EWRMS, which will be established around Metsamor NPP (in two circles at distances of about 2 and 5 km) in order to obtain the necessary data to be used by national and international experts for an effective response to any future nuclear or radiological emergency. In addition computer hardware and related equipment will be delivered by Bertin. On this real-time decision support system the JRODOS will be installed (see chapter 4 for details).

In general the radiation monitoring systems of Bertin are developed for continous monitoring in routine conditions and for the case of emergency. Especially in cases of emergency it is very important that the system continues to operate in order be able to inform the population and to support decision makers.

The system around Metsamor NPP will consist of 32 gamma dose rate measurement probes (GammaTRACER XL2-2) and two mobile devices for radionuclide identification (SpectroTRACER Air/Soil). All probes can be connected to external power and in addition they are equipped with an autonomous power supply via batteries and solar panels. The data transmission of the probes is performed via 3G and radio transmission. All probes are equipped with internal sensors (for temperature, humidity, movement, etc.) and an external rain sensor.

The stations will be installed inside and outside of the secured area of the NPP and for each site local demands are considered: in some cases (for 14 stations at least) concrete sockets and fences have to be installed for theft protection. 17 probes will be fixed at walls and one probe installation is on the top of a roof. External public displays can be used, so the ambient dose rate is also directly readable at a distance of about 5 meters.

The on-site installations have to be in accordance to local regulations and will be performed by NRSC (ANRA's TSO and subcontractor of Bertin). Also a study about the radio transmission signal quality of each site had been carried out by Bertin together with NRSC in order to ensure best signal availability. Beforehand a simulation of the radio signal propagation was performed, taking into account the topography of Armenia and the surroundings of the Metsamor NPP. Concerning the mobile network availability each site was visited and the signal quality was tested. It turned out that different cellular providers have to be used at different stations and that only 3G is available, which is sufficient for a reliable data transmission of the Bertin stations.

3.1.1 The GammaTRACER XL2-2

The GammaTRACER XL2-2 is equipped with two Geiger-Mueller-tubes – a low dose tube and a high dose tube – to measure the ambient equivalent dose H*(10) covering a range from 10 nSv/h to 10 Sv/h. It has got a hermetically sealed housing (IP68), which is covered by nano paint. This paint contains nano particles in order to reduce the adhesion of radioactive particles. The dimensions are: Ø 98 mm, Ø of flange 130 mm, length depends on interface configuration (minimum 580 mm). The parts of the GammaTRACER XL2 are shown in Fig. 3-1.

The probe is designed for operation under harsh environmental conditions: the operating temperature range is from -40°C to +60°C. It is seismic tested according to IEEE Std. 344:2013, par. 8, IEC 980: 1993, par. 6 and IEC 17025:2005. It is fully galvanic isolated at 3000V for RS232/485 and power supply, to assure a very high level of safety against EMC influences, according to IEC61000. Thanks to the ultra low power consumption, very small solar panels can be used. Even without solar panel the station can be operated for several months. To ensure availability of data specially in emergencies, a redundant data transmission using radio modem and 3G cellular modem is implemented.

Table 3-1. Radiological data of the GammaTRACER XL2-2 device

Measurement range	10 nSv/h to 10 Sv/h
Energy- and angular response	45 to 2000 keV (±40%)
Calibration accuracy	0 to 0.1 mSv/h < 6% > 0.1 mSv/h < 15 %

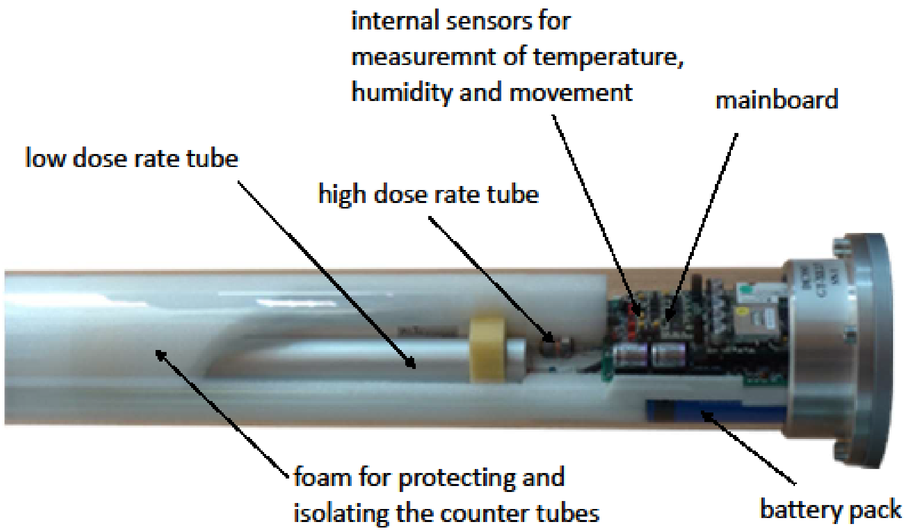

Figure 3-1. All electronic and sensitive parts of the GammaTRACER station are inside the hermetically sealed enclosure, including rechargeable battery

3.1.2 The SpectroTRACER Air/Soil

The properties of the two SpectroTRACERs, which will be delivered, are given in Table 3-2. Similar to the GammaTRACER it has got a hermetically sealed enclosure. The housing has got a length of 540 mm and a diameter of 120 mm and 160 mm at the flange. Two independent measurement cycles (free adjustable) are available. The transmission cycle is also free adjustable. The SpectroTRACER operates fully automatic and autonomous. The station calculates the dose rate from the gamma spectrum, performs nuclide identification and calculates the soil activity (Bq/m^2), as well as air activity (Bq/m^3). All measurement data and spectra are transmitted to the central system using a 3G cellular modem.

Table 3-2. Radiological data of SpectroTRACER Air/Soil

Crystal type	NaI(Tl) 2'' x 2'' inches
Measurement range of ambient dose rate	1 nSv/h to 200 µSv/h
Energy range	30 keV to 3 MeV
Resolution	< 7% for ^{137}Cs

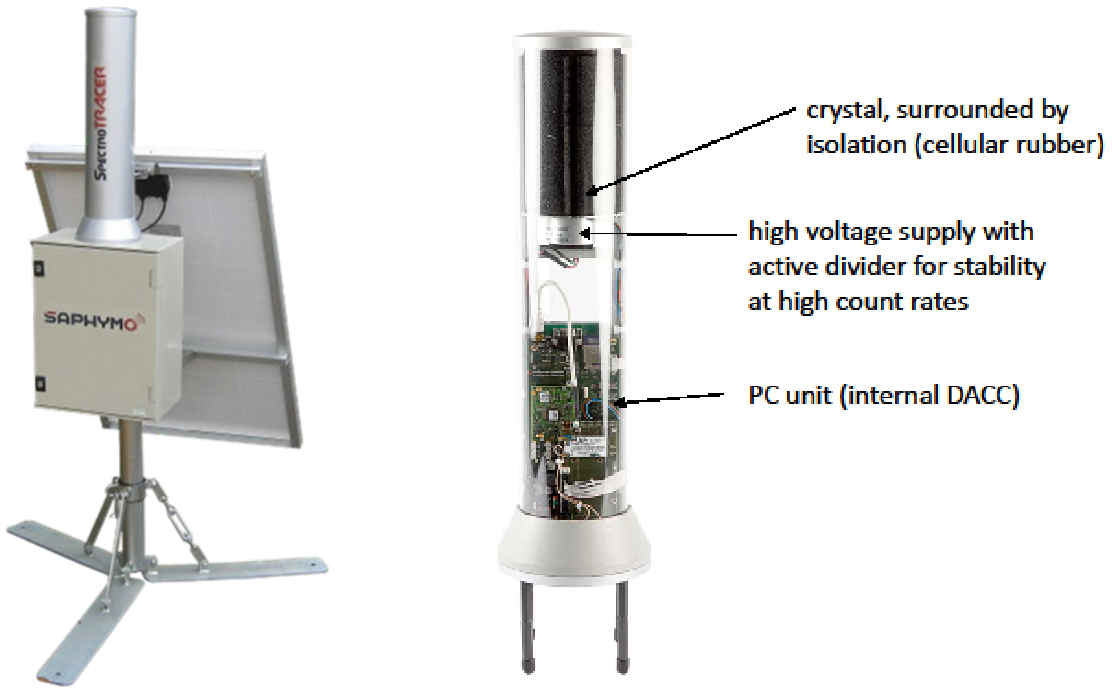

Figure 3-2. Left: SpectroTRACER Air/Soil with connection box (with solar charger and battery, solar panel and heavy tripod stand); Right: Inner parts of the device

3.1.3 Data transmission

Past experience showed that large area powerdown and outage of the public cellular network are the most critical topics for availability of data during emergencies. To ensure high reliability and availability a redundant transmission using radio modem and 3G cellular transmission will be implemented.

A mast for the radio data transmission will be installed on top of the roof of the ANRA building at the NPP as it is shown in Fig. 3-3. The received measurement data is then forwarded to the ANRA control center using a fixed line. The transmission cycle is adjustable for specific needs and the GammaTRACER can automatically switch from standard to alarm mode. The data transmission via radio is secured by using a proprietary protocol encrypted by AES128. Each transmitted protocol contains a history of past dose rate values to be able to observe any inconsistency.

The data transmission by 3G cellular modem is secured by using a standardized secure ftp/s protocol (for Gamma- and SpectroTRACER). Bidirectional communication allows simple remote setup by the central software DATAEXPERT 10.

Table 3-3. Data storage and transmission

Storage capacity	Up to 10.000 values (GammaTRACER XL2), ≥ 2 GB (SpectroTRACER)
Interfaces for data transmission	Infrared, RS 232, radio, 3G/4G/GSM
Radio transmission power (GammaTRACER)	100 mW
Radio frequency used in Armenia	157,025 MHz

Figure 3-3. Left: Antenna with mast, receiver and weather station, Right: One station with GammaTRACER XL2-2, external display with small solar panel, rain sensor and antenna

3.2 System implementation and the use of the measured information in the EP&R activities

The main architecture of the system is shown in Fig. 3-4.

The measurements at the NPP are collected at ANRA's office on the NPP site. The data measured at public sites and the data of the SpectroTRACER Air/Soil are sent to ANRA Emergency Response Center (ERC) in Yerevan. The central supervision software DataEXPERT 10 performs automatic collection, storage and analysis of data. All data is checked for technical or radiation treshold violations, alarms are automatically generated and can be forwarded to the responsible team members. The completely web-based design of the user interface allows data analysis from different workplaces, even from internet and by tablet or mobile phone. Visualization of data in tables, charts and on maps allow comfortable analysis and report generation. All measurement data are exported using IRIX 1.0 format to the JRODOS decision support system and EURDEP platform.

The installation and operation of a comprehensive and integrated state-of-the-art system within ANRA will allow Armenia in general and ANRA in particular providing a timely and effective response to nuclear and/or radiation incidents/accidents at ANPP site. The final locations of monitoring stations provide the possibility of 7/24 technical decision support and control of a radiation emergency situation in PAZ, in the nearest populated sites from ANPP and in the biggest city of Armenia, Yerevan (see Fig. 3-5). EWRMS provides a valuable tool for ANRA emergency response center personnel and decision makers, in particular in displaying informatively the forecast or actual extent and levels of radiation and radioactive material in the environment and how these may vary with time, and for evaluating how remedial measures (e.g., sheltering, evacuation, iodine prophylaxis, food restrictions, decontamination, etc.), in both the short and longer terms, can mitigate the radiological impact.

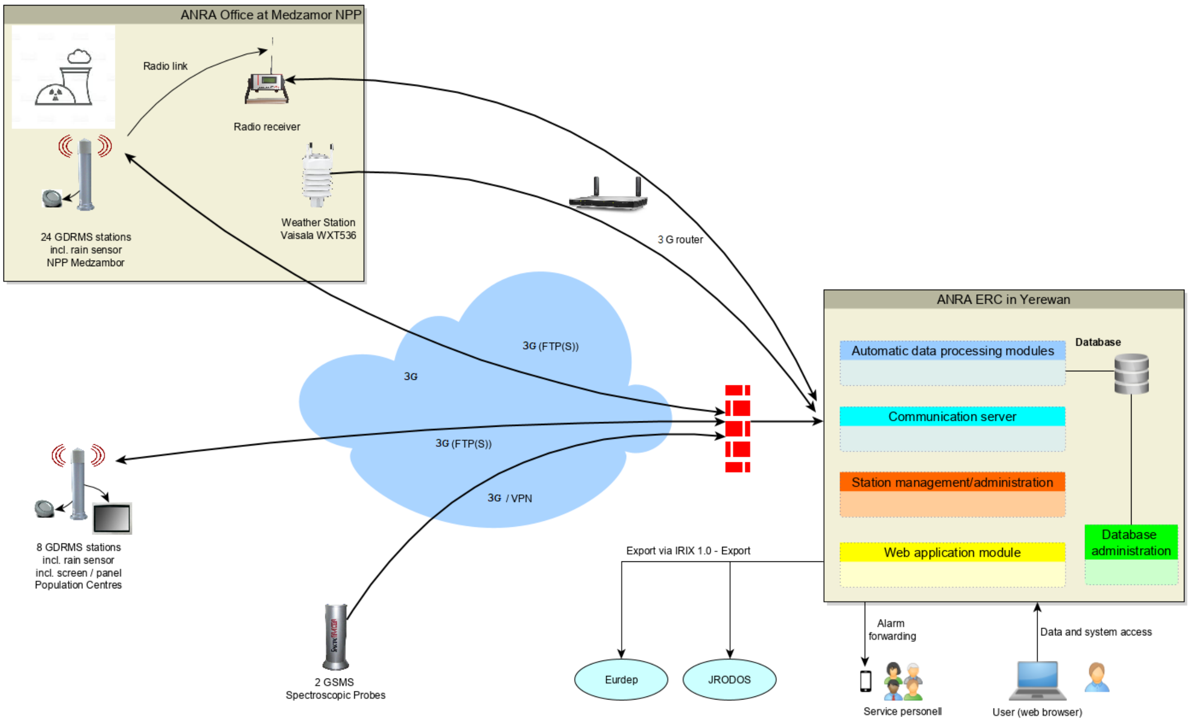

Figure 3-4. Overview of system and data transfer

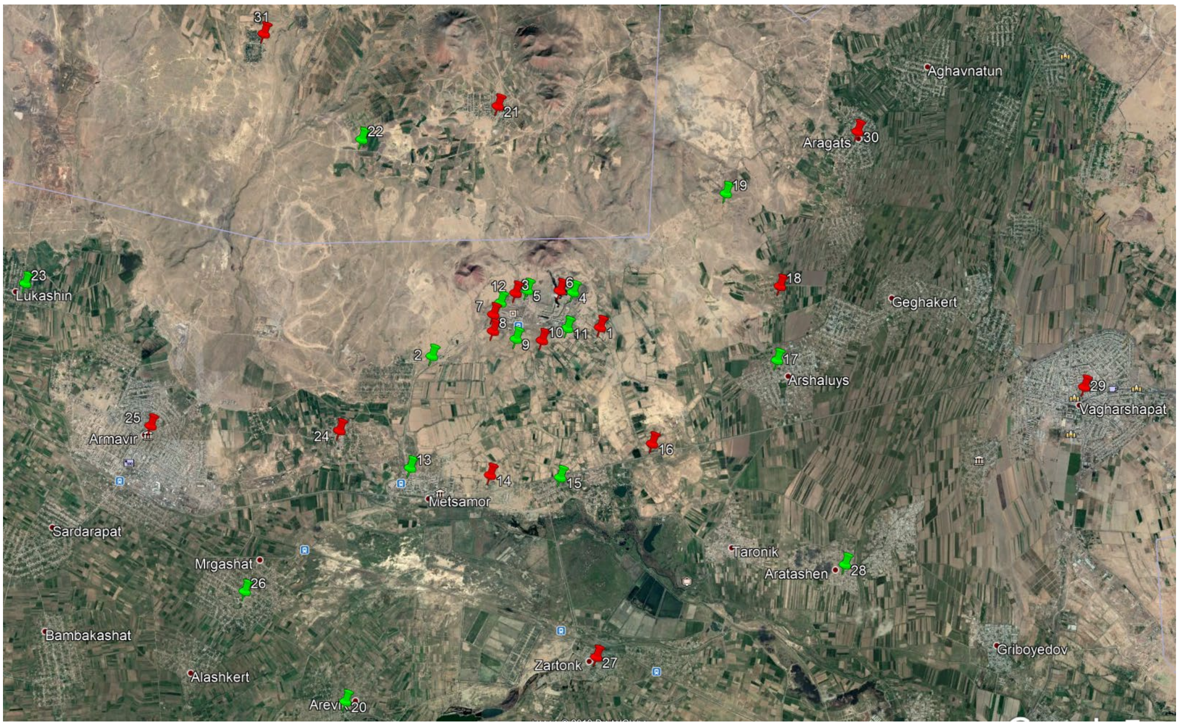

Figure 3-5. Final locations of the monitoring stations (the red and green signs indicate the two different cell providers that will be involved in the data transmission)

The configuration and the design of EWRMS will allow providing information from the monitoring stations at two different sites (ANRA emergency center and ANRA's backup emergency center) which will allow making a data backup and performing an independent assessment of the radiation situation.

The system allows the provision of restricted information from the monitoring stations to other involved parties of the emergency response off-site plan through separate data channels, and to public throw ANRA's web site.

3.3 Outlook

The final installation, commissioning and the Site Aceptance Test (SAT) of the complete system is planned for March 2020. In parallel a training program of local staff is carried out in order to optimise the maintenance of the system.

4 INSTALLATION AND CUSTOMIZATION OF THE JRODOS DECISION SUPPORT SYSTEM IN ARMENIA

4.1 JRODOS decision support functions and the configuration installed in Armenia

During the Chernobyl accident in April 1986, many deficits in emergency management and response were revealed in how to deal with an event of such magnitude. As a consequence, actions were initiated within the European Union's research and development programmes. One of these programmes has led to the development of the non-commercial real-time on-line decision support system RODOS (Real-time On-line DecisiOn Support, [12]). At present, its successor, the JAVA based RODOS system named JRODOS is the operational version to be installed in emergency centres [13]. At present JRODOS is operated by about 30 organisations in more than 20 countries in Europe and elsewhere [14]. Installations in China and Ukraine were completed recently, installations in 8 ASEAN countries and Armenia, supported by the European Commission, are ongoing. INSC support to enhance EP&R capabilities is also provided to the six Gulf countries (members of the GCC), as well as to six West Balkan countries (see Fig. 1-1).

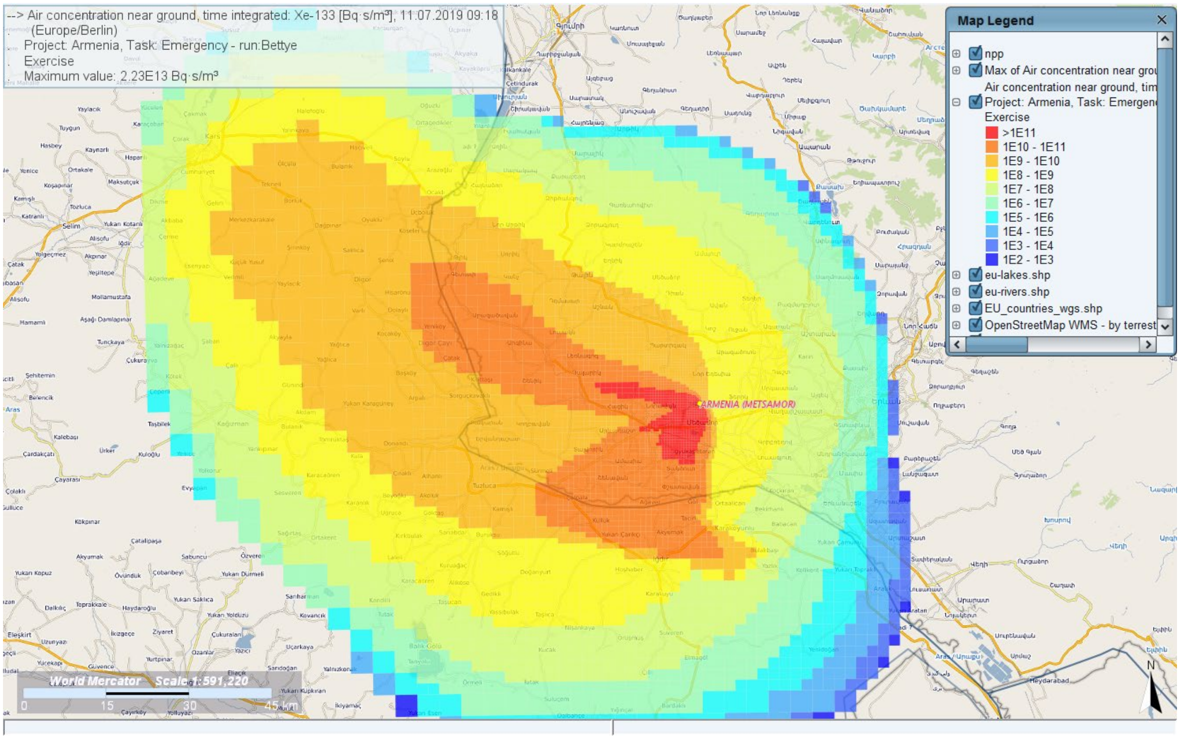

Figure 4-1. Time integrated air concentration of Xe-133, following a hypothetical release from the Metsamor NPP

The JRODOS system contains a suite of simulation models for the terrestrial and aquatic environment. Forecasting modules predict how radioactive contamination would spread following atmospheric and aquatic releases of radiation. A set of models calculate the best estimate of the current and evolving radiological situation in contaminated inhabited and agricultural areas. Dose models predict the dose to individuals and communities for all exposure pathways not related to ingestion, both with and without the application of countermeasures. Special food chain models predict the contamination of terrestrial and aquatic food stuffs and the resulting dose to people. Additional decision aiding components can facilitate the ranking and selection of alternative options using decision analysis procedures.

To respond quickly to an emergency, the Emergency Model Chain (EMC) was created as the main module of JRODOS to be operated in the early phase of an event. This EMC facilitates the operation of an atmospheric dispersion model, a dose model, the early countermeasure model and the food-chain model in one instance with a user interface that guides to operator from input to input. Fig. 4-1 shows a characteristic result of the dispersion model of the EMC. In the later phases, countermeasure models for food production systems and inhabited areas allow developing countermeasure strategies for long-term post accidental remediation of the affected areas.

One important aspect of the operability of the system is the set of features and tools that allow adapting models and data bases, as well as the user interface to national conditions and user preferences.

4.2 Customization of JRODOS to the Armenian conditions and the related data needs

The adaptation of JRODOS to national conditions is the key task when installing the system in a country. By default, JRODOS contains databases allowing operation all over the world. However, these databases were developed using openly available data. National data typically have a higher quality and are most up-to-date. Customisation is performed for the following categories:

- **Nuclear power plant and site data**: This comprises typically the location of the NPP, building geometries, installed capacity, radioactive inventory, default source terms and further characteristics of the site.
- **Prognostic meteorological data**: JRODOS supports several common formats (e.g. GRIB1 and GRIB2, netCDF) for numerical weather forecast data. The system foresees coupling to data from national weather services and supports the use of globally applicable weather data that are publicly available from the American NOMADS server[1].
- **On-site meteorological data**: Meteorological real-time data from the site (tower of SODAR) are typically provided in an arbitrary format. JRODOS uses internally a specific format, thus a conversion routine has to be developed for integration of these data into JRODOS.
- **Measurements (source term monitor data, radiological data)**: JRODOS supports the EURDEP format[2] as well as the IRIX format[3]. In Armenia, the IRIX format will be used.
- **Map data**: Map data with information on political boundaries, streets, important buildings etc. can be integrated in geo-referenced TIFF format. Thus national data will be collected in the “shape” GIS exchange format that can be converted in any GIS system to the geo-referenced TIFF format.
- **Statistical data (e.g. population, food production)**: Statistical data, in particular population distribution should be collected at least around the NPP. Format of the data is also geo-referenced TIFF.
- **Parameters for food-chain models and radio-ecological regions**: The foodchain and dose model terrestrial (FDMT) has the ability to be operated under different conditions. To facilitate this, so called radioecological regions can be defined. They are characterized by similar vegetation and dietary conditions assuming that the model parameters are constant. For each region the full set of parameters has to be defined for all food- and feedstuffs; the parameters are then applied for all locations within the region. The parameters encompass foodstuff related data like consumption rates or food processing factors, vegetation related data such as growing times of crops or the transfer factor soil-to-plant, and animal related data, for example typical feeding diets for domestic animals producing milk and meat. JRODOS currently models 34 types of terrestrial foodstuff and 21 types of terrestrial feedstuff. Data collection will concentrate on main feed- and foodstuffs. For the remaining ones, default data from the database will be used.
- **Hydrological data**: JRODOS contains a suite of hydrological models ranging from a compartment model describing the contamination in a lake up to a three-dimensional model for complex flows and the marine environment. Unlike the foodchain models, no baseline customization is available here. Therefore, any river, catchment or lake system has to be defined from scratch. Customisation strongly depends on the link with the national hydrological service and data availability. To demonstrate the functionality of the hydrological model chain, customization is envisaged for a river close to the Metsamor NPP. This will also include the catchment that is linked to that river.
- **National criteria for intervention or protective actions following a nuclear or radiological emergency**: These data will become part of the countermeasure simulation model.

[1] data from the Global Forecast Systems (GFS), cf. http://www.emc.ncep.noaa.gov/index.php?branch=GFS

[2] https://eurdep.jrc.ec.europa.eu

[3] wwwns.iaea.org/downloads/iec/info-brochures/13-27431-irix.pdf

- **User Interface**: JRODOS provides the means to customise the user interface to the national language. This includes any character type including Armenian.

To support the customisation, the Contractor provides all the necessary documentation and performs workshop to discuss the data to be selected as well as workshops demonstrating the integration into the JRODOS database.

The customisation process starts with the first installation of the system in the premises of ANRA. Fig. 4-2 provides an overview of the hardware used and the links to external data such as the monitoring system and the weather data.

The first installation with the default database on the hardware indicated in Fig. 4-2 is accompanied by the basic training of the system and the first customisation workshop that highlights the most important parameters to be collected and how the data collection should be performed. In the frame of the project, further workshops are envisaged to discuss the progress in the data collection and focus the support of the Contractor to topics needed.

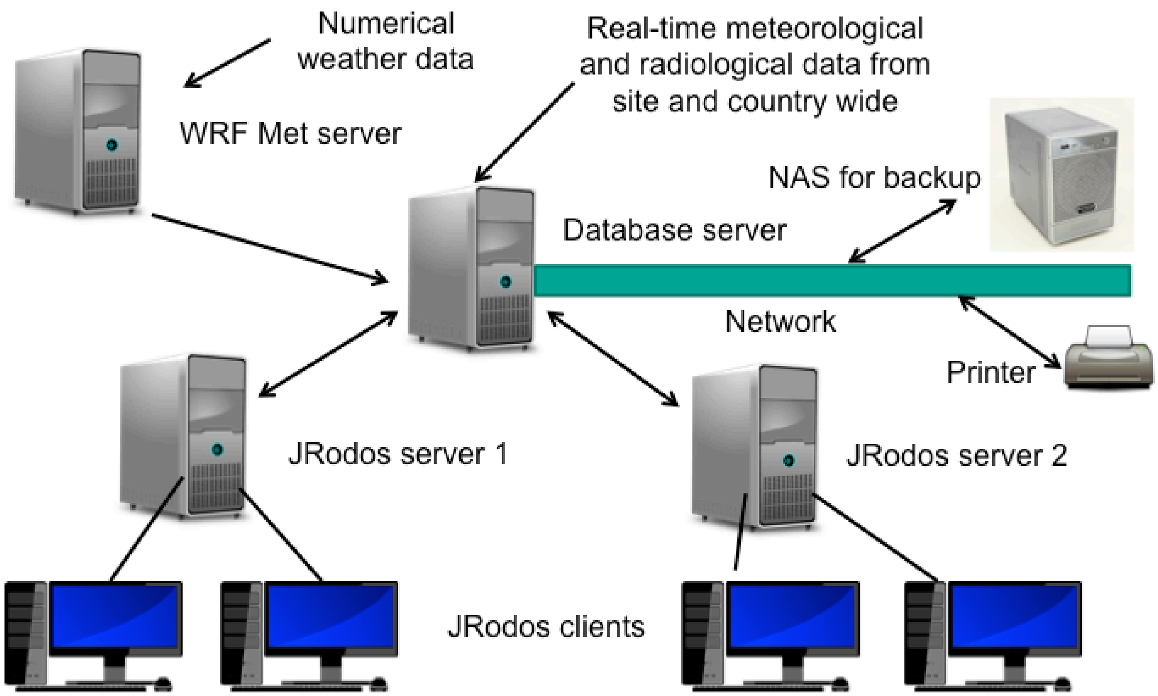

Figure 4-2. Indicative configuration of the JRODOS hardware (without showing UPS and with arrows indicating network connections)

Further work activities comprise methodological support in applying JRODOS to nuclear and radiological emergencies, training for operators and system administrators, demonstration to end users, testing of the customised system and final verification at the end of the project. In this respect, the operational and customised JRODOS system, connected to monitoring and weather data, should become available to ANRA 24 months after the start of the project.

5 SUMMARY AND CONCLUSIONS

The technical desing and implementation details of a new environmental radiation monitoring system were summarised in our paper, including the expected effect of this state-of-the-art monitoring tool on the Armenian nuclear emergency preparedness and response capabilities. It is believed that the advanced radiation monitoring network, as well as the installation and customisation of the JRODOS decision support system will enhance EP&R capabilities in Armenia to a great extent and it will be raised to a level comparable to other European countries utilising nuclear energy. The local experts of the Beneficiary and its TSO participate in the project with great enhusiasm and provide valuable input to the design, installation, customisation and utilisation activities. According to the – rather tight – project schedule, the site acceptance test will be in March 2020 and the complete system should be operational before the end of 2020. Selected experts of the Beneficiary and its TSO will receive a comprehensive training on the use, maintenance, configuration and further customisation of the monitoring network and the associated JRODOS configuration, thus ensuring the long-term sustainability of the new system.

6 REFERENCES

[1] Council regulation (EURATOM) No 237/2014 of 13 December 2013 establishing an Instrument for Nuclear Safety Cooperation

[2] Law on safe utilization of atomic energy for peaceful purposes (Republic of Armenia, RA)

[3] Law on population protection in case of emergency situation (RA)

[4] Law on licensing (RA)

[5] Government Decree 1219-N on approval of “Radiation safety norms” (RA)

[6] Government Decree 1489-N on approval of “Radiation safety rules” (RA)

[7] Sanitary rules for NPPs design and operation, SPAES-2013, Russian Federation

[8] Government Decree 2328-N on approval of “The population protection plan in case of nuclear and radiation emergencies at Armenian NPP (off-site emergency plan of the Armenian NPP)” (RA)

[9] Government Decree 943-N on approval of “Establishing of regime of implementing rescue works in the areas of radioactive contamination” (RA)

[10] Government Protocol 8 on approval of “National plan of civil protection in case of radiological and nuclear accidents in the territory of Republic of Armenia” (RA)

[11] The Armenian NPP emergency response plan to nuclear and/or radiation emergencies (on-site emergency plan of the Armenian NPP), RA

[12] Ehrhardt J, Weis A (editors) (2000) RODOS: Decision Support System for Off-site Nuclear Emergency Management in Europe, European Commission, Brussels, Report EUR 19144

[13] Ievdin I, Trybushnyi D, Zheleznyak M, Raskob W (2010) RODOS re-engineering: aims and implementation details, Radioprotection, Volume 45, No. 5, Supplement 2010, S181-S189

[14] Landman C, Päsler-Sauer J, Raskob W (2014) The RODOS System as an Instance of a European Computer-Based Decision Support System for Emergency Management after Nuclear Accidents, in: G. Kessler et al., The Risks of Nuclear Energy Technology, pp 337-348, Science Policy Reports, DOI 10.1007/978-3-642-55116-1_19, © Springer-Verlag Berlin Heidelberg.

7 LIST OF ABBREVIATIONS

AES – Advanced Encryption Standard

ANPP – Armenian Nuclear Power Plant

ANRA – Armenian Nuclear Regulatory Authority

ASEAN - Association of Southeast Asian Nations

DG DEVCO - Directorate-General for International Cooperation and Development (EC)

EC - European Commission

ENCO - Austrian expert company providing consultancy services in areas related to nuclear safety

EMC – Emergency Model Chain (in the context of RODOS only)

EMC – Electromagnetic Compatibility

EP&R - Emergency Preparedness and Response

ERC – Emergency Response Centre

EU - European Union

EURDEP – European Radiological Data Exchange Platform

EWRMN - Early Warning Radiation Monitoring Network

EWRMS - Early Warning Radiation Measurement System

FDMT – Foodchain and Dose Model Terrestrial

FTP – File Transfer Protocol

GCC – Gulf Cooperation Council

GDRMS – Gamma Dose Rate Measuring System

GIS – Geographic Information Systems

GFS – Global Forecast Systems

GRS - Gesellschaft für Anlagen- und Reaktorsicherheit, the German TSO

GSM – Global System for Mobile Communications

IAEA – International Atomic Energy Agency

INSC - Instrument for Nuclear Safety Cooperation

IP68 – Ingress Protection housing (6 = protected against solids; 8 = protected against liquids)

IRIX - International Radiological Information eXchange data standard (IAEA)

IRSN - Institut de Radioprotection et de Sûreté Nucléaire, the French TSO (established in 2002)

ISPRA - Istituto Superiore per la Protezione e la Ricerca Ambientale (Italian NRA)

ITER Consult - Independent Technical Evaluation and Review (Italian expert company)

JRC- Joint Research Centre (EC)

JRODOS – Java version of RODOS

KIT – Karlsruhe Institute of Technology

LPZ – Long-term Protective Action Planning Zone

NOAA - National Oceanic and Atmospheric Administration (USA)

NOMADS - NOAA Operational Model Archive and Distribution System

NPP - Nuclear Power Plant

NRSC - Nuclear and Radiation Safety Center (Armenian TSO)

MES – Ministry of Emergency Situations of RA

MMC – Monitoring and Management Centre

PAZ – Precautionary Action Zone

RA – Republic of Armenia

RODOS - Real-time On-line DecisiOn Support

RWM – Radioactive Waste Management

SAT – Site Acceptance Test

SODAR – SOnic Detection And Ranging

SOGIN - State owned company responsible for the decommissioning of nuclear facilities (Italy)

SPARCS – Spectral Advanced Radiological Computer System

STUK- Säteilyturvakeskus (Radiation and Nuclear Safety Authority, Finland)

SSTC NRS - State Scientific and Technical Center for Nuclear and Radiation Safety (Ukraine)

SÚJB - Státní Úřad pro Jadernou Bezpečnost (State Office for Nuclear Safety, Czech Republic)

TACIS - Technical Assistance to the Commonwealth of Independent States

TIFF – Tagged Image File Format

ToR - Terms of Reference

TSO - Technical Support Organisation (in this article used in its broadest sense)

UPZ – Urgent Protective Action Planning Zone

VPN – Virtual Private Network

VTT - Teknologian Tutkimuskeskus (Technical Research Centre), Espoo, Finland

VVER - Pressurized water reactor of Russian (Soviet) design

The FASTNET project for structured and faster responses to nuclear emergencies

I. Devol-Brown (*), O. Isnard (*), E. Urbonavičius (**), E. Tengborn (***), M. Dowdall (****), F. Rocchi (*****)

* Institut de Radioprotection et de Sûreté Nucléaire, IRSN, France
** Lithuanian Energy Institute, LEI, Lithuania
*** Swedish Radiation Safety Authority, SSM, Sweden
**** Norwegian Radiation and Nuclear Safety Authority, DSA, Norway
***** Agenzia nazionale per le nuove tecnologie, l'energia e lo sviluppo economico sostenibile, ENEA, Italy

Abstract:

The H2020 FASTNET (FAST Nuclear Emergency Tools) project, coordinated by IRSN (France), started in October 2015 for a period of four years. The project involves a Consortium of 20 partners from 18 countries (including Unites States of America, Canada and the Russian Federation) as well as the IAEA as a third party. When dealing with nuclear emergency, two issues of very different timeframes and operational objectives, thus including the use of different methods and tools, have to be considered: the emergency preparedness and the emergency response. The FASTNET project addresses both of these issues by combining the efforts of several organizations to make substantial progress on already identified reference tools and method. In particular, the capabilities of these method and tools will be extended to tackle the main categories of accident scenarios in the main types of operating or foreseen NPPs in Europe (PWR, EPR, BWR, VVER and CANDU), including a generic concept of Spent Fuel Pools (SFP). Current expertise methodology (3D/3P method) as well as tools to assess source terms used in France (PERSAN) and in Sweden (RASTEP) were extended to these 5 NPPs' designs operated in Europe. The project partners also worked on the inclusion of functionalities to produce or integrate atmospheric releases data in a standard format (IRIX) in order to link them with other initiatives focused on atmospheric transport, radiological consequence assessments and data assimilation. In addition, an accident scenarios database was developed and contains more than one hundred description of scenarios including assessment of atmospheric releases performed by partners using best-estimate computer codes like ASTEC, MELCOR and MAAP for the 5 NPPs' designs operated in Europe and a generic concept of SFP. At the end of the project, a comprehensive set of emergency exercises was developed and proposed to a large set of partners in order to demonstrate the operational capabilities of the FASTNET method and tools for emergency response. This demonstration was achieved through two distinct exercise activities: (i) A first exercise addressed source term evaluations, to be compared to the reference source terms from the scenario database; (ii) A second exercise focused on the main emergency objective of protecting the population. These FASTNET method and tools will enable Emergency Centers to provide a fast, organized and reliable prediction of accident development and the anticipation of the atmospheric releases in order to protect better the population around most of European NPPs.

1 INTRODUCTION

The H2020 FASTNET (FAST Nuclear Emergency Tools) project, coordinated by IRSN (France), involves a Consortium of 20 partners from 18 countries (including USA, Canada and the Russian Federation) as well as the IAEA as a third party. The project implementation is over four years (October 2015 to September 2019) [1]. It is one of the two EURATOM-funded projects on Emergency Preparedness and Response in the last 6 years [2].

When dealing with nuclear emergency, two issues of very different timeframes and operational objectives, thus including the use of different methods and tools, have to be considered: the emergency preparedness and the emergency response. The FASTNET project addresses both of these issues by combining the efforts of several organizations to make substantial progress on already identified reference tools and methodologies. In particular, the capabilities of the current expertise methodology (3D/3P method) as well as tools to assess source terms used in France (PERSAN) and in Sweden (RASTEP) were extended to tackle the main categories of accident scenarios for the main types of operating or foreseen NPPs in Europe (PWR, EPR, BWR, VVER and CANDU), including a generic concept of Spent Fuel Pools (SFP). The project partners also worked on the inclusion of functionalities to produce or integrate atmospheric release data in a standard format (the IAEA IRIX format [3]) in order to link them with other initiatives focused on atmospheric transport, radiological consequence assessments and data assimilation.

A database was developed to contain the detailed descriptions of accident scenarios including assessment of atmospheric releases. The results to the database were provided by project partners who performed accident analyses using computer codes (ASTEC, MELCOR and MAAP) for the main types of NPP in operation in Europe and a generic concept of SFP.

At the end of the project, a set of emergency exercises was developed and proposed to a large set of partners in order to demonstrate the operational capabilities of the FASTNET method and tools for emergency response. Two distinct exercises were implemented: (i) a first exercise addressed at source term evaluations, to be compared to the reference source terms from the scenario database; (ii) a second exercise focused on the main safety objective of population protection.

This paper provides qualitative information on the key outputs of the project.

2 SEVERE ACCIDENT SCENARIO DATABASE

In the severe accident scenario database [4], more than one hundred scenarios are stored covering 4 types of NPPs (PWR, VVER, CANDU and BWR). The pre-calculated data for the database were provided by 10 project partners, who agreed to share their results. The main advantage of this database is that it includes much more information than a source term of radionuclides to the environment. The database includes all the supporting information produced by the accident analysis performed with best-estimate SA computer codes. It includes all information on the response of the reactor core, the reactor coolant system (primary and secondary circuits), and the containment as well as the status of the safety systems. It also includes the timing of the key events during accident progressions, e.g. core uncovery, rupture of reactor pressure vessel, etc.

All the above mentioned behavior data can be viewed in graphs or downloaded as xml file and opened in tabulated format with MS Excel for further analysis. All the information stored in the database provides many opportunities for the development of the training programs of the emergency response teams in all countries around the world. As well, such detailed information may enable further validation of the predicted accident progression and the efficiency of the accident management actions assumed to be taken during the accident scenario.

The isotopic composition of the source term is based on the recommendations of IAEA, which includes a list of 55 isotopes in total to be used for the assessment of the radiation doses to the population [4].

Access to the database was provided for all project partners who were able to test it and provided comments for improvements. The partners’ comments helped in developing the final version of the database.

3 3D/3P METHODOLOGY

3.1 Overview of the French methodology

More than 12 years ago IRSN, together with the main French NPP operator, developed a methodology with the objective of:

- giving structure to the evaluation process of the Emergency Technical Teams,
- allowing focusing on key parameters for a pertinent and global assessment,
- facilitating dialogue and information sharing with other Emergency Teams,
- allowing anticipating the potential evolutions of the situation
- answering the main question: “What about releases”?

The IRSN approach 3D/3P (triple diagnosis/triple prognosis) is based on the design of the French nuclear reactors (PWRs), where there are three physical barriers set up between the radioactive products and the environment.

From the analysis of the three barriers it is possible to define the actions on the plant to mitigate the accident and to calculate the consequences in the environment in order to decide the most effective actions to protect the population. The aim of this methodology is to detect, as soon as possible, any different event likely to lead to a future release of radioactivity into the environment. The ease to extend this methodology to other reactors or nuclear facilities is its strength. The first and most important step to extend the methodology is to know how to identify the different barriers set up between the fission products and the environment and the safety functions associated with them.

3.2 3D/3P methodology

The 3D/3P methodology consists of periodically assessing the status of the three barriers (triple diagnosis) and forecasting their developments (triple prognosis) to characterize the present and/or possible future release of activity into the environment. For each barrier, a diagnosis phase followed by a prognosis phase can be distinguished:

- diagnosis phase:
  - ✓ the condition of the barrier is assessed,
  - ✓ the barrier’s protecting functions are characterized in terms of margins and,
  - ✓ the systems fulfilling the barrier’s protecting functions are identified;
- prognosis phase:
  - ✓ the future availability of the systems supporting the barrier’s protecting functions is examined (without taking into account additional failures whose cause might be independent of the accident),
  - ✓ the future development of the protecting functions is then deduced from the future availability of the systems and,
  - ✓ the future condition of the barrier is deduced from the future condition of the associated protecting functions.

In addition, it is necessary to quantify the available time delay prior to the beginning of the possible radioactive releases and to assess the quantity of nuclear activity released into the environment.

For a PWR reactor, the traditional three barriers are shown in Figure 1.

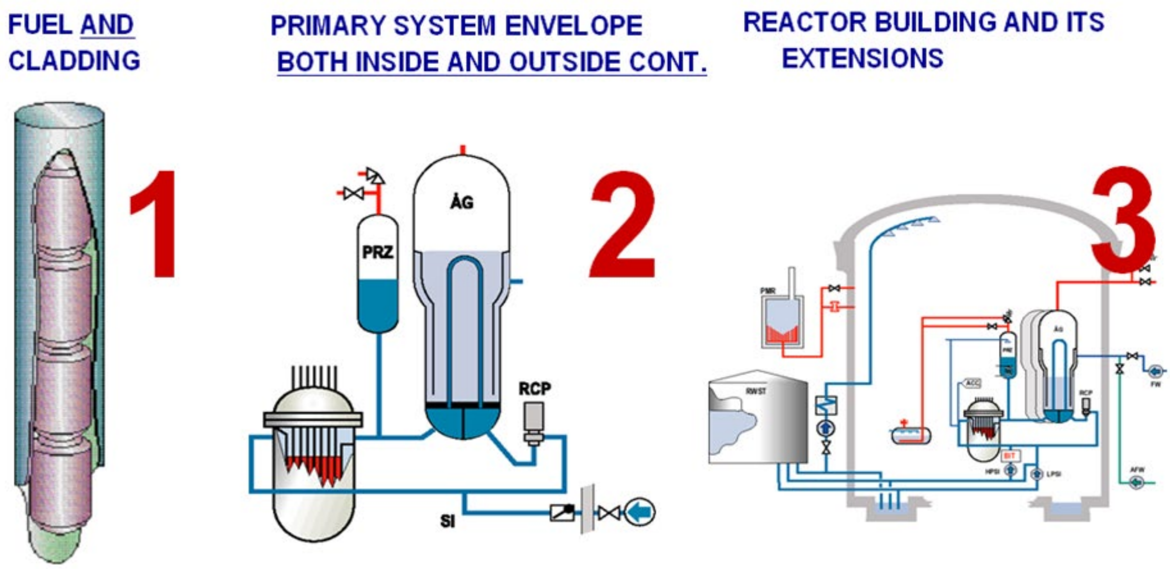

Figure 1 – The three barriers of a PWR

The first barrier consists of the cladding of the fuel rods and the fuel matrix itself. The second barrier is comprised of the reactor coolant system (RCS) envelope (waste tank and connected circuits included). Lastly, the third barrier is made up of the containment and its extensions that isolate the nuclear steam supply system from the environment. The containment is constituted by the building itself, the penetrations of this building (equipment hatch, lock chamber, penetrations, transfer tube), their isolation organs and its extensions.

A nuclear reactor accident is characterized by the failure or risk of failure of one or several of these three barriers. It can thus be noted that there can be a significant release of radioactive particles into the environment only if the integrity of at least two barriers is compromised.

Once the barriers for a given reactor type have been identified, the associated "safety functions" need to be recognized. Several safety functions are associated with each barrier. When these safety functions are assured, the integrity of the barrier is assured. In other terms, the safety function(s) associated with each barrier relate to one or more conditions that must be checked so as to maintain the integrity of the barrier itself (see Table 1).

Table 1. Safety barriers and associated safety functions

3 barriers	#1 Fuel and cladding	#2 Primary system envelope	#3 Reactor building and its extensions
Associated safety functions	Subcriticality Primary liquid inventory	Removing heat from the primary system Removing heat from primary pump seals	Containment Removing heat from the reactor building

The diagnosis and prognosis are then collected into appropriate tables, or "grids", for ease of use. Within FASTNET, the 3D/3P methodology has been extended to the following reactor types or facilities:

- VVER (three barriers are defined),
- BWR (three barriers are defined),
- CANDU (four barriers are defined),

- Spent fuel pool (three barriers are defined) and,
- EPR (same three barriers as for the PWR).

In Appendix 1 the grids for these reactor types are reported.

4 DETERMINISTIC APPROACH USING PERSAN

4.1 Overview of the PERSAN software

PERSAN (Program for Evaluation of Radiological Source term in case of Accident on a Nuclear power plant) is part of the SESAME software system developed by IRSN. This system of emergency evaluation tools is used at the Technical Crisis Centre (TCC) of IRSN to produce in real-time an assessment of any accidental situation on a nuclear power plant, based on a diagnosis of the situation and a prognosis of its evolution through the application of the 3D/3P method, previously described.

Within the SESAME system, PERSAN is the “final” module, dedicated to performing a fast (few minutes) deterministic evaluation of the real or potential atmospheric radiological release, taking into account the real-time data from the installation, and/or their predicted values provided by other SESAME modules.

The PERSAN source term is computed for a set of more than 1800 isotopes and is given in terms of release kinetics and chemical speciation, namely for halogen elements, with consideration of ingrowth/decay on the overall set of isotopes, during their migration from damaged fuel of the core or spent fuel to the atmosphere.

Once the source term is computed, it can then be forwarded to the Radiological Consequences Unit of IRSN TCC, as an input to dispersion models to produce consequence mapping, then iterated with on-site dose measurements, etc. This mapping underpins recommendations of the French regulatory body (ASN) to local authorities in charge of population protection countermeasures.

The underlying physics and chemistry of PERSAN are based on state-of-the-art knowledge of severe accident phenomena. Namely, PERSAN includes:

- a predictor of core, or spent fuel, degradation and melting kinetics,
- a physical model of fission product release from damaged fuel to primary circuit,
- a chemical model of halogen (iodine and bromine) speciation in the reactor building (homogeneous chemistry in the liquid and gas phases, heterogeneous chemistry of chemisorption on organic compounds),
- a physical model of aerosols deposition and re-emission from corium during molten core concrete interaction, coupled with containment spray system operation,
- a leak distribution model from reactor building to auxiliaries buildings,
- a general mass balance equation that takes into account the above computed phenomena coupled with ventilation/filtration systems operation,
- a generalized ingrowth/decay model that operates on this general equation at each time step and in each building.

Each model has been treated to give a conservative response towards residual uncertainty of the evaluation of each phenomenon with a best-estimate approach. The global validation of PERSAN has been achieved by benchmarking results with integral codes, namely the ASTEC code, which is developed by the Severe Accident Department of IRSN. A comparison of results between PERSAN and the US-NRC fast-running code RASCAL is given in [5].

4.2 Input and output interfaces of PERSAN

Figure 2 shows the main input interface of PERSAN, where the fuel degradation events, containment pressure and containment spray system flow are set (by the user, or automatically from the real-data stream, when available).

Ventilation/filtration parameters of auxiliary buildings are also set in this interface and other assumptions, such as molten core concrete interaction, ultimate containment venting systems or user-defined leaks, in case, for instance, of failure in containment isolation.

Figure 2 – Main assumption interface of PERSAN

Figure 3 and 4 exhibit the main output interface of PERSAN, where results are compiled at a given time (Fig. 3) or from the beginning of the accident (Fig. 4). Beside these visualization interfaces, some .txt and .csv files are also created, containing the overall source term.

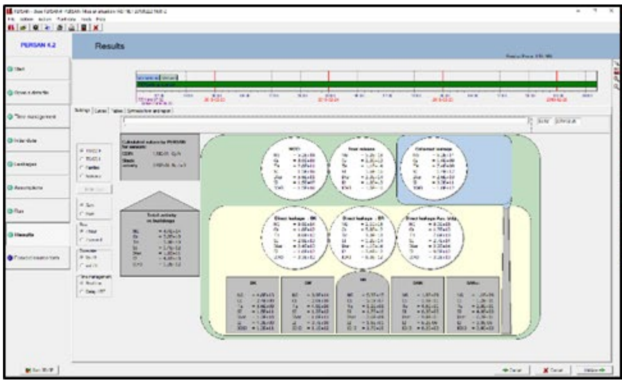

Figure 3 - Results interface of PERSAN (at required time)

Figure 4 - Results interface of PERSAN (from beginning)

4.3 Development of PERSAN within the FASTNET project

4.3.1 New plant models

PERSAN includes a powerful nuclear power plan editor, which was used to develop new power plant models within the FASTNET project, using data and parameters provided by various partners. Seven new plant models have been created, with their containment systems specificities, and their typical radiological inventories (core and spent fuel pool):

- BWR ABB-II
- BWR ABB-III
- BWR Mark-1
- CANDU-6
- VVER V213 440
- VVER V320 1000
- EPR

These new models are illustrated in Figure 5.

4.3.2 Response analysis of the new models

Several accidental sequences were provided within the FASTNET project. They were used by IRSN to perform a response analysis of the newly implemented models and check whether they give satisfactory results with respect to those from integral computer codes (e.g. MELCOR, ASTEC and MAAP). This analysis is summed up here after.

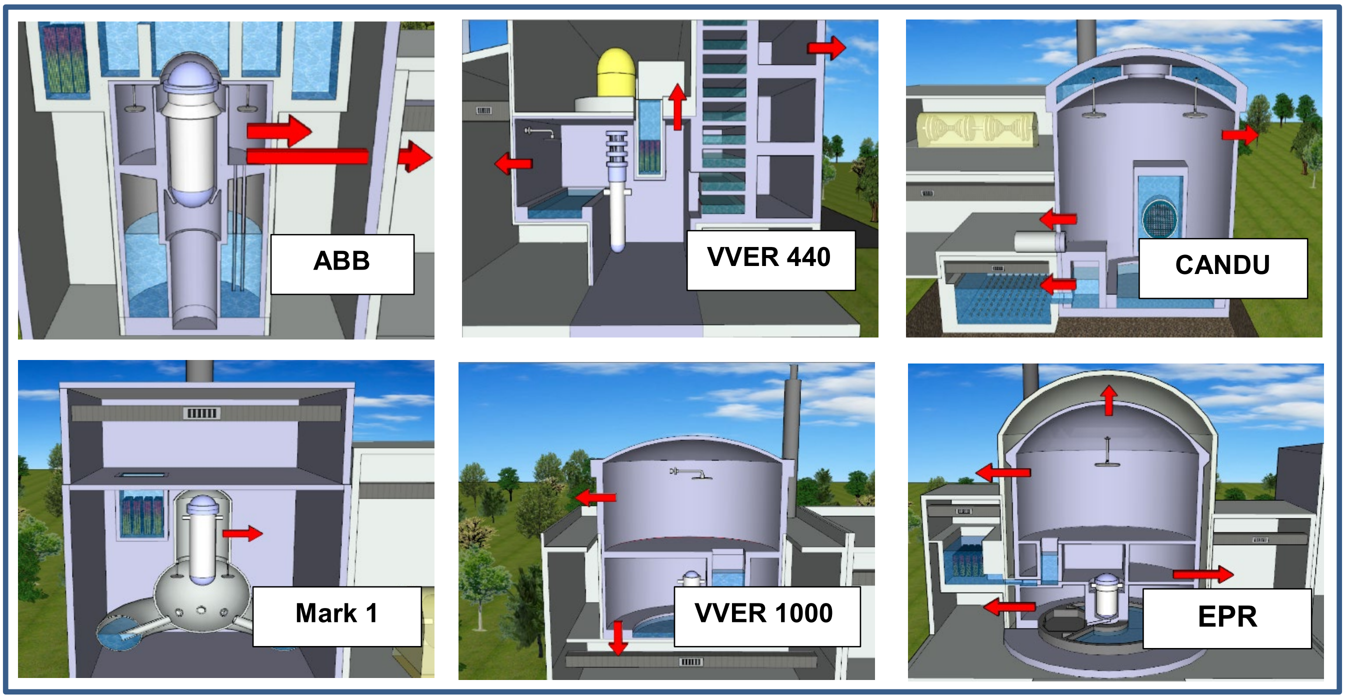

Figure 5: New power plant models developed in PERSAN within the FASTNET project

The new models implemented in PERSAN were found to match the results given by integral codes with a very good agreement (see Figure 6). Therefore, IRSN has concluded that no further developments are presently required to consider the direct operability of these new models in emergency situations.

Figure 6: Comparison of PERSAN results with integral code results for different reactor types

4.3.3 New output results export (IRIX file)

As part of the FASTNET project, the PERSAN computed source terms can now be exported in the international IRIX format, which can be used by many atmospheric dispersion codes. The functionality has been added directly to the output interface (Figure 7).

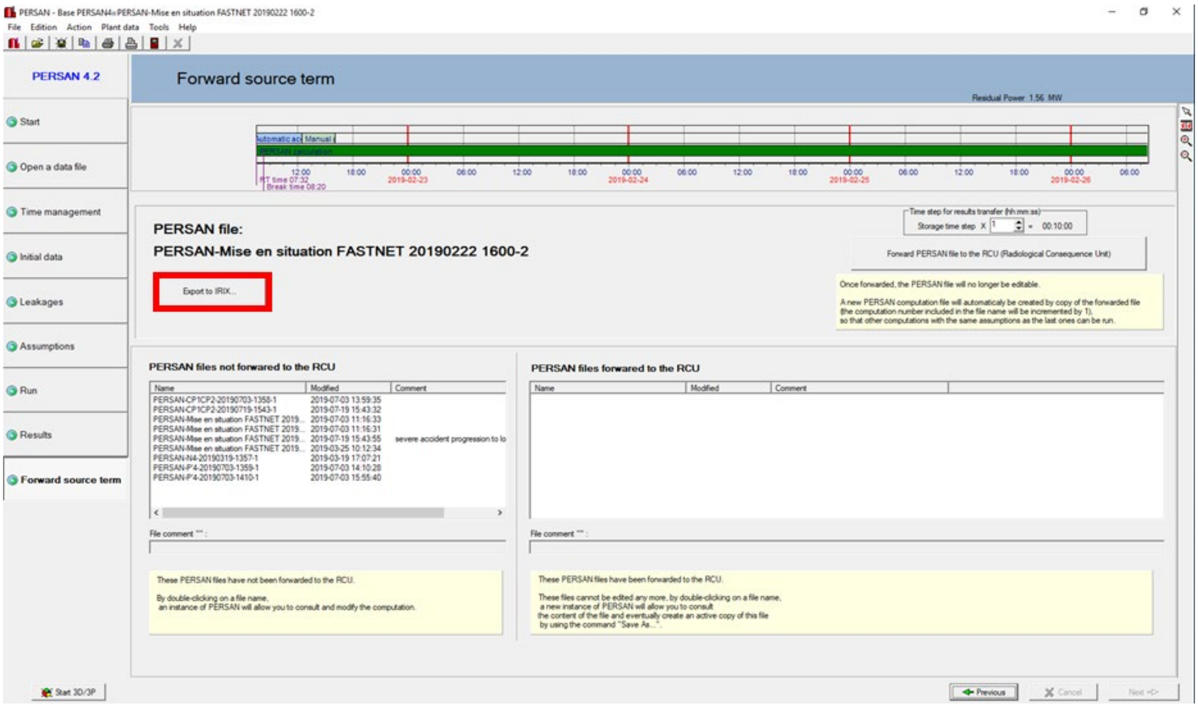

Figure 7: New IRIX source term export interface

5 PROBABILISTIC APPROACH USING RASTEP

5.1 The RASTEP tool

RASTEP (RApid Source TErm Prediction) is a software tool, developed by Lloyd's Register in cooperation with the Swedish Radiation Safety Authority (SSM), with the aim of providing state-of-the-art decision support in nuclear emergency situations [6]. RASTEP is a dynamic tool capable of modelling causes and effects in complex cases with lots of free variables, missing or incomplete information and where the level of uncertainty is high. The tool combines a Bayesian Belief Network (BBN), representing uncertainty as probabilistic relations among observations, events and variables, with deterministically pre-calculated source term data. BBNs represent an established method of modelling uncertain relations among random variables and capturing the relationships between these variables using Bayes' theorem. The BBN approach is to take prior beliefs at the outset and when information on the progression of an event becomes available, modify and update those beliefs. In the nuclear power plant accident application, BBNs can collect a multitude of probabilistic relations between an observation and different events and can become a "filter" that is fed with observations and creates a likelihood-ordered ranking of a list of pre-calculated accident scenarios – and of the source term connected to these scenarios. The tool thereby provides a best estimate of the atmospheric release for the situation at hand even though data may be sparse and the level of uncertainty high. The RASTEP user answers a series of questions regarding the status of the affected nuclear power plant. The questions can be answered without highly specialized severe accident and plant knowledge. The answers are fed into the BBN, mapping the interconnections between significant systems. As circumstances develop, new or updated information on specific system parameters are entered by the user, creating a continuously updated diagnosis, including the atmospheric releases. Today, RASTEP is in use at the emergency response center of SSM together with plant specific models for the nuclear power plants currently in operation in Sweden.

The graphical user interface is shown in Figure 8. Different panels provide real-time information on system status, predictions of source terms and visualization of radiological releases over time, with one section set aside for dialogue with the user. Data for off-site radiation dose assessment and atmospheric dispersion calculations can be easily exported e.g. using the internationally used IRIX format.

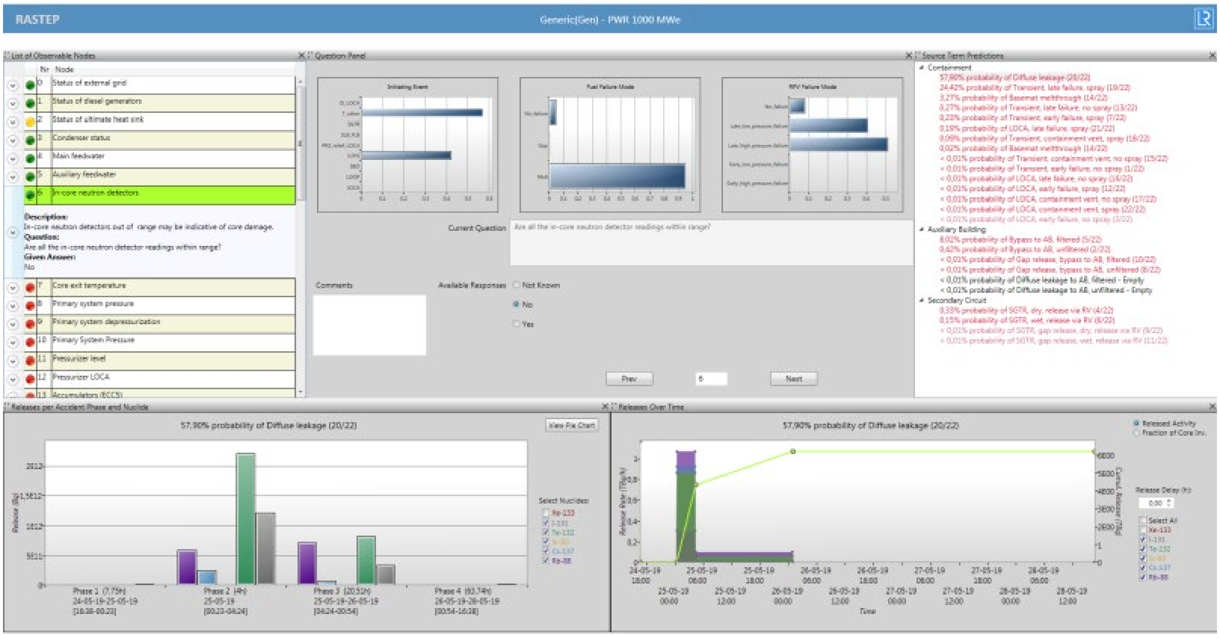

Figure 8: RASTEP graphical user interface

5.2 Method

A RASTEP plant model is built around a selection of key plant features:

- Source term volumes and release routes, as shown in Figure 9. Here, the volumes can represent features related to the release and transport (including trapping, re-suspension etc.) of fission products. Connections between the volumes represent the failure of fission product barriers or, in case of venting, deliberate mitigation actions; they define the release path created during a severe accident.
- Key safety functions are defined to build information on mitigation options into the model. Plant safety systems related to the specified safety functions are defined, along with the parameters used to monitor the system. In addition, probabilities for operability or availability of these systems are defined to fit them into a BBN model.
- Observable parameters that are monitored during an accident are identified. This type of information is relevant to the BBN in order to determine the plant status and corresponds to the questions asked by the RASTEP user interface. In order to correctly determine the state of the plant, it is essential to know which information is reliable during accident conditions as well as which information is possible to obtain.

RASTEP models include two main components:

- A BBN including initiating events, barriers, safety functions and a number of predefined release categories.
- Customized, pre-calculated source terms based on deterministic simulations of pre-defined plant-representative release categories.

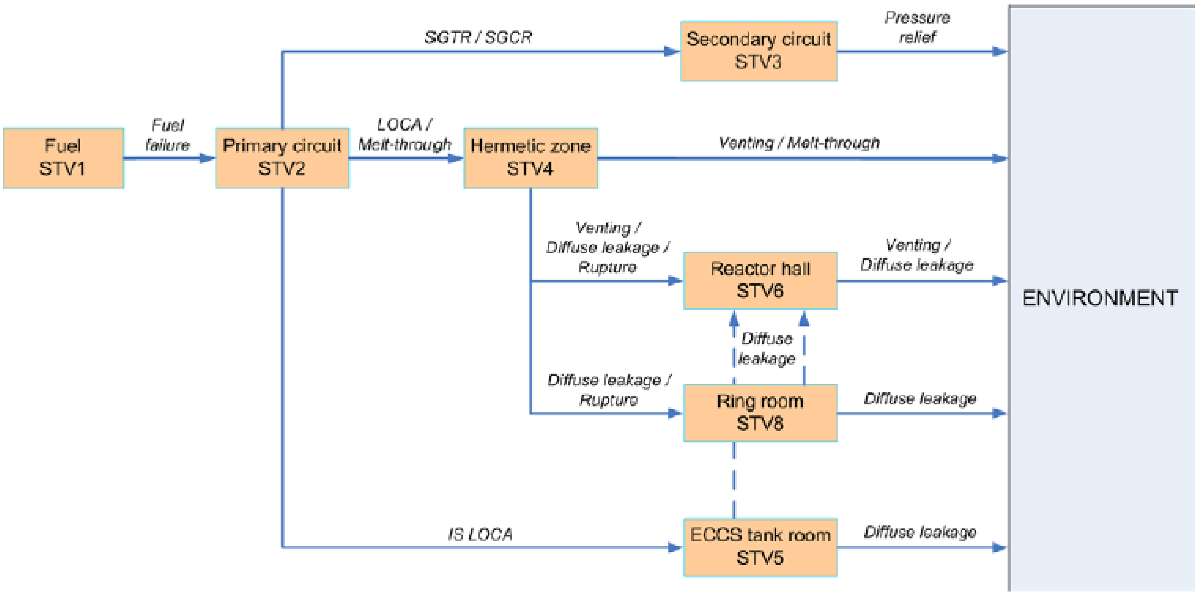

Figure 9: Example of a release path diagram (VVER440-213)

5.3 Development of RASTEP within the FASTNET project

Within the FASTNET project, existing models for Swedish BWR and PWR plants have been modified to create generic reactor models for BWR, PWR, VVER-440, CANDU and for an SFP. For these reactor types, FASTNET project partners have provided detailed information on (i) source term volumes and release routes; (ii) key safety functions and plant systems; (iii) observable parameters; and, (iv) initiating events. Based on the information gathered from the partners and from publicly available information sources, Lloyd's Register has created specific BBNs for each generic plant type.

The material generated in FASTNET comprises, for the different reactor types,

- release path diagrams;
- BBN models, with explanatory tables of nodes in the model, see Figure 10 left. These nodes have a conditional probability that can
  - ✓ be based on generic PSA data ("PSA")
  - ✓ be based on expert judgment ("BELIEF")
  - ✓ contain only zeros and ones ("DETERMINISTIC")
- a list of questions for providing observations and measurements from the affected plant (see Figure 10 right).

The input used for the calculation of source terms for the models within the FASTNET project is collected from the database created in WP1. This database contains calculations performed by severe accident codes such as MAAP, MELCOR or ASTEC.

As part of the FASTNET project, the RASTEP software can now export the result into the international IRIX format which can be used by most atmospheric dispersion codes available.

TITLE	TYPE
AB exhaust system filtration	BELIEF
Auxiliary building mode	BELIEF
Auxiliary building (Source term 2)	**DETERMINISTIC**
Auxiliary building extract	DETERMINISTIC
Auxiliary building leakage indication	BELIEF
Auxiliary building pressure	BELIEF
Auxiliary building temperature	BELIEF
Auxiliary feedwater	BELIEF
Boron solution from accumulators	DETERMINISTIC
Condenser status	BELIEF
Containment long-term pressure trend	DETERMINISTIC
Containment bypass	DETERMINISTIC
Containment cavity waterlevel	DETERMINISTIC
Containment gamma activity	BELIEF
Containment hydrogen combustion	BELIEF
Containment hydrogen concentration	BELIEF
Containment hydrogen level	BELIEF
Containment isolation	BELIEF
Containment mode	DETERMINISTIC
Containment pressure	BELIEF
Containment rupture due to phenomena	DETERMINISTIC
Containment source term (Source term 1)	**DETERMINISTIC**
Containment spray	BELIEF
Containment steam concentration	BELIEF
Containment sump state	BELIEF
Containment temperature	BELIEF
Containment threat	DETERMINISTIC
Containment vent / overpressure protection	BELIEF
Core cooling sufficiency	DETERMINISTIC
[illegible]	[illegible]

#	Question
0	Is offsite power available?
1	What is the core exit temperature?
2	Are all the in-core neutron detector readings within range?
3	Has the hydrogen concentration in the containment exceeded 8 %?
4	Is the auxiliary feedwater system available?
5	Is the ECCS high pressure injection available?
6	What is the current pressure trend in the primary system?
7	What is the current trend in steam generator water level?
8	What is the long-term pressure trend in the containment?
9	Are the emergency diesel generators available?
10	What is the status of the containment spray system?
11	What is the containment cavity water level?
12	Is the main feedwater system available?
13	What is the status of the containment sumps?
14	Has a high containment dose rate reading occurred?
15	Has a high containment pressure reading occurred?
16	What was the early trend in secondary circuit pressure?
17	Is the ECCS low pressure injection available?
18	Has a high containment temperature reading occurred?
19	What is the containment hydrogen concentration?
20	Are the ECCS accumulators available?
21	What was the early trend in pressurizer water level?
22	What is the containment humidity?
23	Has primary system depressurization been initiated?
24	What was the early trend in primary system pressure?
25	What is the status of the hydrogen recombiners?
26	Is the main heat sink available?
27	What was the early trend in steam generator water level?

Figure 10: PWR BBN model. Extract from the list of network nodes (left), and extract from the list of questions posed to the user (right).

6 EMERGENCY PREPAREDNESS EXERCISES

6.1 The FASTNET Exercises

Another objective of the FASTNET project was the demonstration of the operational capabilities of the proposed methodology for emergency preparedness and response. In addition, an important step in the dissemination of the approach was through the two exercise activities focused on, in the first instance, generation and evaluation of best source term estimates and the evolution of the scenarios and, in the second instance, the protection of populations.

The first exercises was based on scenarios derived from the database developed during the FASTNET project. It consisted in the digital distribution of technical data to participants who were then required to respond with a series of estimates of the released activity at various times after the initiating event. Participants were also required to provide information as to the nature of the accident and the progression of the situation. The second exercise was a table top activity where participants were asked to progress from developing an understanding of the accident sequence, through an estimation of the released activity and ultimately providing descriptions of the preventative measures required to protect the population and an estimate of the extent, spatial and temporal, over which these measures would be necessary. Prior to these exercises, a 3-day training was organized at the IRSN in Paris in May 2018 to introduce participants to the FASTNET method and the tools developed within the project for evaluation of source terms, namely, the BBN-based tool RASTEP and the deterministic tool PERSAN and its associated 3D/3P method.

6.2 Exercise 1 – Estimation of source terms

The first exercise was held during December 2018 with the specific objective of comparing the FASTNET tools (RASTEP & PERSAN) with respect to the generation of source term estimates for a series of accident scenarios and collation of feedback from users as to their experience with the tools in this context. Four accident sequences were selected from FASTNET database for use in the exercise:

- Case 1: PWR 1300 MW: 6 inches LOCA

- Case 2: ABB BWR: Steam line break
- Case 3: CANDU: single unit SBO
- Case 4: VVER 440: SBO

All necessary information to characterize the scenarios were provided to participants (safety system availability, chronological sequence, core temperatures, water levels, etc.). Participants were required to report on template forms the following: estimates of the releases of 52 different isotopes at three different times after the accident (PERSAN) and estimates of a shorter list of isotopes over four phases after the accident (RASTEP). Participant results were compared with those generated by a reference user (primarily the developers of the tools) and those contained in the FASTNET database. Participants were also asked to complete a questionnaire as to their experiences with the tools and methodology. In total, 23 organizations participated. The exercise commenced on the 1st of December 2018 with a reporting deadline on the 31st of the same month. An overview of participant responses as compared to those of the PERSAN reference user are displayed in Figure 11. A majority of participants were able to generate results from PERSAN and/or RASTEP indicating the benefit of the 3-day training period before the exercise which facilitated the participants being in a position to use the tools unaided during the exercise itself. Analysis of reported source term estimates indicated some gaps linked to the misinterpretation of sequence data provided during the exercise, user inexperience, or in relation to specific technology types, which was highlighted as a source of deviation in the source term predictions. Targeted training would be required to improve the use of the tools and consequently the confidence in their output. The extension of PERSAN and RASTEP, from PWR and BWR respectively, to other reactor types was demonstrated satisfactorily. Results obtained by both tools were coherent with estimates yielded by integral codes (MAAP, MELCOR, ASTEC), extant differences being not significant regarding the application of the FASTNET tools in emergency situations. Participant feedback suggested specific improvements that could be made to the tools and formed an important basis for the developers in further enhancement of the tools.

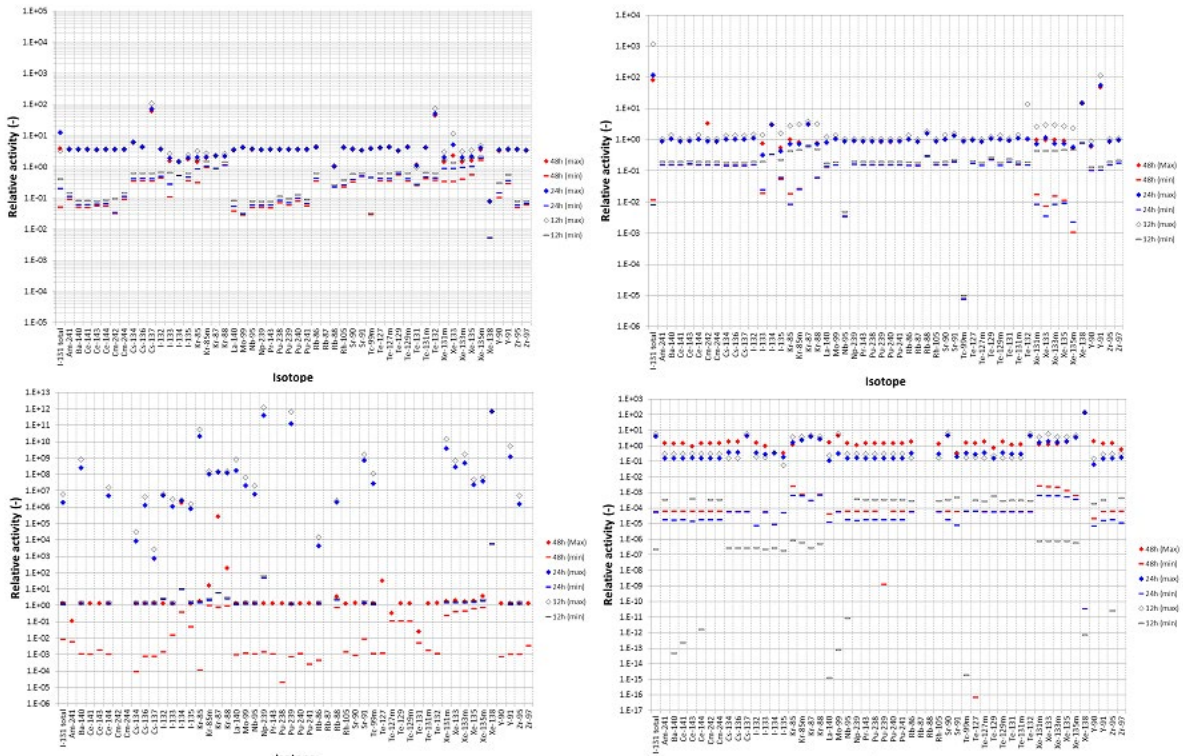

Figure 11: Dispersion range for participant responses relative to those for the reference user for PERSAN. Clockwise from top left: Case 1, Case 2, Case 3, Case 4.

6.3 Exercise 2 – emergency preparedness

The second FASTNET exercise, held on the 22nd of February 2019 at the University of Natural Resources and Life Sciences (BOKU) in Vienna, was a 1-day table top activity focused on implementation of the tools within response to an emergency situation. In all, 18 different organizations participated in the exercise, being divided into a series of discrete groups for the actual exercise. Preparation of Exercise 2 was conducted at four separate meetings between September 2018 and February 2019. Exercise 2 differed from Exercise 1 in contextualizing the use of the FASTNET tools and methodology within emergency response oriented towards protecting populations and the processes and procedures in fulfilment of that objective. For Exercise 2, the predefined exercise scenario, based on PWR technology but not drawn from the FASTNET database, was happening in "real time". The scenario was focused on the Gravelines facility in France and the meteorological data to be used was that from the week starting on the 7th of February (participants having stored the relevant data in advance). Participants played the role of the French authorities in responding to the accident and French regulatory limits were employed throughout. Prior to the exercise, a briefing was held to establish the rules of the exercise.

Each participating group was required to analyze the data delivered regularly during the exercise and then apply the FASTNET methodology based on the appropriate use of the 3D/3P method, if needed, and one of the FASTNET tools. The participants then had to provide one or several estimations of a source term suitable for consequence evaluations for the given scenario. The source terms were to be provided in IRIX format to allow for interfacing the FASTNET tools with relevant dispersion models. In addition, participants were required to provide estimations of consequences with the different decision support systems and dispersion models usually employed by participants and to report regularly throughout the day to hypothetical decision makers and suggest protective actions based on their deliberations.

The scenario that formed the basis for Exercise 2 was a fire in an electrical building of the facility at 07:00 on the exercise day, which progressed through a series of developments, resulting in core melt at 13:20 and failure of the vessel at 16:30. Technical information typical of that which would be available was provided periodically throughout the day and participants were required to report on the results of their assessments and discussions at various times. In addition to reporting on the day of the exercise, participants were required to provide comprehensive analyses of the situation and its likely consequences within 1 week of the exercise and complete a detailed questionnaire as to their experiences with the FASTNET tools and methodology. These data could then be compared with equivalent information generated by the developers of the exercise material. Examples of the results generated by different groups are displayed in Figure 12.

Most participants successfully estimated source terms with the FASTNET tools while there was some evidence of a lack of experience with the 3D/3P method. The tools outputs were successfully incorporated with the decision support and dispersion systems used by the participants. Regardless of the decision support system used, there was a general agreement among groups as to the affected geographical area of the scenario and the suggested protective measures. The exercise indicated that with well-established and mature tools such as those of the FASTNET project, all groups were in a position to generate consistent and fit-for-purpose results. Both PERSAN and RASTEP were deemed by the participants as useful components in an emergency preparedness system and could be used as a support tool directly during crisis situations. The advantages and disadvantages of both tools were highlighted during the exercise and this information was fed forward to the developers for incorporation in future versions.

The exercise indicated the utility of the IRIX format in exporting and importing data from the PERSAN and RASTEP tools to decision support systems such as ARGOS and JRODOS. Specific problems in using the IRIX format with certain dispersion modelling systems were identified and could be addressed satisfactorily by the groups.

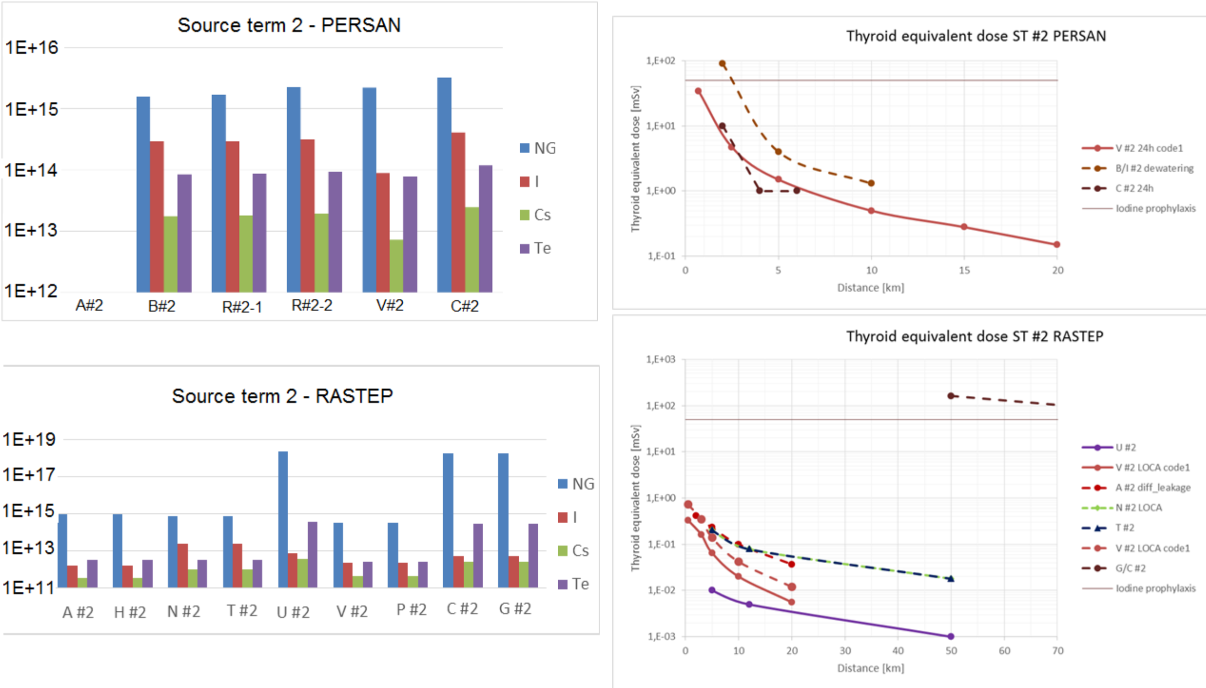

Figure 12: Comparison of group responses for estimation of the second source term of Exercise 2 (left) and estimation of consequences as a function of distance from the facility based on those estimates as inputs to the dispersion tools employed (right).

The exercise functioned to highlight the importance of experience and practice in effectively using the FASTNET tools and while both tools were capable of providing fast and reliable estimates of source terms, further training would be advantageous in establishing confidence amongst the user base. The usefulness of the 3D/3P method in examination of accident data and in the early stages of diagnosing what is happening was adequately demonstrated by the exercise and the necessity to iterate the method application with the on-site evolution of the accident and off-site environmental and radiological data was viewed as an important aspect to be addressed.

7 CONCLUSIONS

An accident scenarios database was developed, containing more than one hundred descriptions of scenarios, including assessment of atmospheric releases performed by partners using reference computer codes (ASTEC, MELCOR and MAAP) for four designs of NPPs operated in Europe (PWR, BWR, VVER and CANDU) and a generic concept of SFP. At the end of the FASTNET project, the database will be hosted by IAEA and extended to other NPP designs.

Current expertise methodology (3D/3P method) as well as tools to assess source terms used in France (PERSAN) and in Sweden (RASTEP) were extended to five (PERSAN) or four (RASTEP) designs of NPPs operated in Europe. The project partners also developed the functionality to produce or integrate atmospheric releases data in a standard format (IRIX) in order to link them with other initiatives focused on atmospheric transport, radiological consequence assessments and data assimilation.

The extension of these method and tools was improved and validated through:

- a training session which was organized in May 2018 in Paris, gathering 38 participants from 22 European or non-Europeans countries;
- the realization of two exercises:
  - ✓ the first dedicated to the best calculation of atmospheric releases and held in December 2018. 23 participating organizations registered; 18 using PERSAN, 19 using RASTEP and 13 using both;

- ✓ the second including more widely the management of the protection of the population and organized on February 22, 2019 in Vienna. 17 participating organizations; 5 using PERSAN, 9 using RASTEP and 3 using both.

The extended version of the rapid source term tool PERSAN is now implemented in the Technical Crisis Centre of IRSN (France). SSM uses plant specific RASTEP models for the NPPs in operation in Sweden.

The social and economic benefits arising from the project are, on the one hand, the capitalization and the dissemination of an accident scenarios database including a uniform description of all scenarios. On the second hand, these FASTNET method and tools will enable Emergency Centres to provide a fast, organized and reliable prediction of accident development and the anticipation of the atmospheric releases in order to better protect the population around most of European NPPs.

The high ambition of this large project was met through the organization of numerous meetings, workshops, trainings and exercises, to enhance the interaction between experts from the areas of severe accident management and of emergency management. All these occasions gave them the opportunity to develop a common language and facilitate their appropriation of the FASTNET tools and method. The implementation of the two exercises added an enormous value of the project.

In order to strengthen the developed links between these two communities, it would be interesting to organize in the future:

- further operational trainings based on every technologies and the feedback of these exercises;
- a new series of exercises targeting the protection of population and having a higher level of reality (table-top or full-scale formats, scenarios based on every technologies and provided by different partners …).

The scenarios database could be further extended by including more CANDU and VVER scenarios.

8 REFERENCES

[1] D. Vola, I. Devol-Brown, F. Di Dedda, J.E. Dyve, O. Isnard, F. Rocchi, E. Urbonavicius, FASTNET H2020 project: qualification of a harmonized response methodology for diagnosis and prognosis of severe accident situations, 8th ERMSAR Conference, Warsaw, Poland, May 2017.

[2] F. Rocchi, I. Devol-Brown, W. Raskob, Nuclear and radiological emergency management and preparedness, Proceedings of the FISA 2019 Conference, 4-7 June 2019, Pitesti, Romania, accepted for publication in EPJ-N.

[3] International Radiological Information Exchange (IRIX) Format, Version 1.0, Reference Description, IAEA Incident and Emergency Centre, 2013-03-31.

[4] F. Mascari et al., Fastnet Scenarios Database Development and Status, 9th ERMSAR Conference, Prague, Czech Republic, March 18-20, 2019.

[5] A. Guglielmelli, A. Cervone, F. Rocchi, V. Creach, G. Ortega Nicaise, Intercomparison of PERSAN 4 and RASCAL 4.3 Source Term evaluations for a PWR LOCA Scenario, Proceedings of EUROSAFE 2019, Köln, 3-4 November 2019.

[6] M. Knochenhauer, V. Hedtjärn Swaling, F. Di Dedda, F. Hansson, S. Sjökvist, K. Sunnegård, Using Bayesian Belief Network (BBN) Modelling for Rapid Source Term Prediction – Final Report, Report NKS-293, October 2013.

APPENDIX 1

In this Appendix the 3D/3P grids developed within the project for PWR, VVER, BWR, CANDU and SFP are reported. It should be noted that for CANDU reactors the method and grid have been renamed to 4D/4P, given the four barriers present in this reactor design.

Site:	Unit:	Date: 2015-01-09	Time: 08:20	Visa:	Sender:	Receiver:

FORM "DIAGNOSIS-PROGNOSIS" — INSTALLATION OPERATION — #

3D / 3P

STATUS AT __:__	DIAGNOSIS		PROGNOSIS		
Barriers status	Safety functions status	Safety functions control systems	Forecast of systems availability	Forecast of safety functions status	Forecast of the barriers status
CLAD - FUEL **No clad failure** ☐ **Clads failures** ☐ **Core melt** ☐	Reactivity control Comfortable Low Insufficient Doubtful	• Control rods • Boration : ECCS, CVCS, RBWMS,	• Control rods • Boration : ECCS, CVCS, RBWMS,	Reactivity control Comfortable Low Insufficient Doubtful	**CLAD - FUEL** **No clad failure** ☐ **Clads failures at __:__** ☐ **Core melt at __:__** ☐
	RCS water inventory Satisfactory Degraded Dewatering Doubtful	• SI (HPSI/MPSI, LPSI pumps), CVCS, … • Water reserves (IRWST, BRS, …)	• SI (HPSI/MPSI, LPSI pumps), CVCS, … • Water reserves (IRWST, BRS, …)	RCS water inventory Satisfactory Degraded Dewatering Doubtful	
PRIMARY SYSTEM **Intact** ☐ **Doubtful** ☐ **Primary break** ☐ ☐inside containment ☐PZR relief lines ☐outside containment ☐SGTR ☐MCCP seals	RCS heat removal Sufficient/Not sufficient Doubtful Controlled/Not controlled RCS Heat removal through MCCP seals Sufficient/Not sufficient Doubtful	• Steam generators • Break • ECCS • Feed and Bleed • RHRS • CCWS/ESWS	• Steam generators • Break • ECCS • Feed and Bleed • RHRS • CCWS/ESWS	RCS heat removal Sufficient/Not sufficient Doubtful Controlled/Not controlled RCS Heat removal through MCCP seals Sufficient/Not sufficient Doubtful	**PRIMARY SYSTEM** **Intact** ☐ **Doubtful** ☐ **Primary break** ☐ ☐inside containment ☐PZR relief lines op. at __:__ ☐outside containment ☐SGTR isolated at __:__ ☐MCCP seals
CONTAINMENT **Normal leak** ☐ **Doubtful** ☐ **Direct leak** ☐ ☐penetration ☐PTR tank ☐secondary systeme **Leak to aux. buildings** ☐ ☐penetration ☐connected system **U5 system On** ☐	Containment (isolation systems efficiency, atmosphere composition control) Safe Not assured Doubtful	• Containment isolation • H2	• Containment isolation • H2	Containment (isolation systems efficiency, atmosphere composition control) Safe Not assured Doubtful	**CONTAINMENT** **Normal leak** ☐ **Doubtful** ☐ **Direct leak** ☐ ☐penetration ☐PTR tank ☐sec. system isolated at __:__ **Leak to aux. buildings** ☐ ☐penetration ☐conn. sys. isolated at __:__ **U5 the ____-__-__at__:__** ☐
	RB heat removal Sufficient Not sufficient Doubtful	• CSS • CCWS/ESWS • Steam generators • U5	• CSS • CCWS/ESWS • Steam generators • U5	RB heat removal Sufficient Not sufficient Doubtful	

Figure 13: 3D/3P grid for PWR.

Site :	Unit :	Date :	Time :	Visa :	Sender :	Receiver :

FORM "DIAGNOSIS – PROGNOSIS" : **INSTALLATION OPERATION** N° ....

STATUS AT __:__	DIAGNOSIS		PROGNOSIS		
Barriers status	**Safety functions status**	**Safety functions control system**	**Forecast of system avaibality**	**Forecast of safety function**	**Forecast of the barrier status**
Fuel matrix - Clad No clad failure ☐ Clads failures ☐ Core melt ☐	Reactivity control Comfortable Endangerd Insufficient Doubtfull	•Control rods •Boron injection	•Control rods, •Boron injection	Reactivity control Comfortable Endangered Insufficient Doubtfull	**CLAD - FUEL** No clad failure ☐ Clads failures at __:__ ☐ ☐ Fuel handling accident Core melt at __:__ ☐
	Core cooling&water inv. Satisfactory Degraded Dewatering Doubtfull	•CVCS •ECCS •Water reserves IRWST+ BRS	•CVCS •ECCS •Water reserves IRWST+ BRS	Core cooling&water inv. Satisfactory Degraded Dewatering Doubtfull	
Primary system Intact ☐ Doubtfull ☐ Primary break ☐ ☐ Inside the containment ☐ Inadvertent opening of one or several safety relief valves ☐ Outside the containment ☐ SGTR ☐ MCCP seals	RCS Heat removal Satisfactory degraded Doubtful	•Steam Generators •Feedwater system •ECCS •Feed & Bleed •RHR •CCWS	•Steam Generators •Feedwater system •ECCS •Feed & Bleed •RHR •CCWS	RCS Heat removal Satisfactory degraded Doubtful	**Primary system** Intact ☐ Doubtfull ☐ Primary break ☐ ☐ Inside the containment ☐ Inadvertent opening of one or several safety relief valves ☐ Outside the containment ☐ SGTR ☐ MCCP seals
	Pressure relief Satisfactory Not satisfactory Doubtful	•Safety relief valves •Suppression pool	•Safety relief valves •Suppression pool	Pressure relief Satisfactory Not satisfactory Doubtful	
	MCCP sealing Satisfactory Not satisfactory Doubtful	•CVCS •CCWS	•CVCS •CCWS	MCCP sealing Satisfactory Not satisfactory Doubtful	
Containment Intact ☐ Leak to reactor building ☐ ☐ Due to damage to containment ☐ Steamline or feedwater line breaks outside containment ☐ IS LOCA outside containment Filtered containment venting at _ _:_ _ ☐ Unfiltered containment venting at _ _:_ _ ☐	Containment Isolation efficiency Atmosphere control Safe Not assured Doubtful	• Containment isolation • CSS •H2 recombiners •Venting system	• Containment isolation • CSS •H2 recombiners •Venting system	Containment Isolation efficiency Atmosphere control Safe Not assured Doubtful	**Containment** Intact ☐ Leak to reactor building ☐ ☐ Due to damage to containment ☐ Steamline or feedwater line breaks outside containment ☐ IS LOCA outside containment
	Containment Heat Removal Satisfactory Not satisfactory Doubtful	•Containment spray system •CSS Cooler •CCWS/ESWS •Venting system	•Containment spray system •CSS cooler •CCWS/ESWS •Venting system	Containment Heat Removal Satisfactory Not satisfactory Doubtful	

Figure 14: 3D/3P grid for VVER.

Site :	Unit :	Date :	Time :	Visa :	Sender :	Receiver :

FORM"DIAGNOSIS – PROGNOSIS" : **INSTALLATION OPERATION** N° ....

STATUS AT __:__	DIAGNOSIS		PROGNOSIS		
Barriers status	**Safety functions status**	**Safety functions control system**	**Forecast of system availability**	**Forecast of safety function**	**Forecast of the barrier status**
Fuel matrix - Clad No clad failure ☐ Clads failures ☐ Core melt ☐	Reactivity control • Comfortable • Endangered • Insufficient • Doubtful	Control rods, recirculation pumps, boron injection	Control rods, recirculation pumps, boron injection	Reactivity control • Comfortable • Endangered • Insufficient • Doubtful	**CLAD - FUEL** No clad failure ☐ Clads failures at __:__ ☐ ☐ Fuel handling accident Core melt at __:__ ☐
	Water inventory • Satisfactory • Degraded • Dewatering • Doubtful	Safety injection, External SI water tank, Other injection/pump	Safety injection, External SI water tank, Other injection/pump	Water inventory • Satisfactory • Degraded • Dewatering • Doubtful	
Primary system Intact ☐ Doubtful ☐ Primary break ☐ ☐ Inside the containment ☐ Inadvertent opening of one or several safety relief valves ☐ Outside the containment	Heat removal Satisfactory Degraded Doubtful	Safety injection Safety relief valves	Safety injection Safety relief valves	Heat removal Satisfactory Degraded Doubtful	**Primary system** Intact ☐ Doubtful ☐ Primary break ☐ ☐ Inside the containment ☐ Inadvertent opening of one or several safety relief valves ☐ Outside the containment
	Pressure relief Satisfactory Not satisfactory Doubtful	Suppression pool Safety relief valves	Suppression pool Safety relief valves	Pressure relief Satisfactory Not satisfactory Doubtful	
	Containment isolation Satisfactory Not satisfactory Doubtful	Containment isolation valves	Containment isolation valves	Containment isolation Satisfactory Not satisfactory Doubtful	
Containment Intact ☐ Leak to reactor building ☐ ☐ Due to damage to the containment ☐ Steamline or feedwater line breaks outside containment ☐ IS LOCA outside containment Filtered containment venting ☐ Unfiltered containment venting ☐	Pressure suppression Satisfactory Not satisfactory	Blow-down lines Suppression pool level and temperature	Blow-down lines Suppression pool level and temperature	Pressure suppression Satisfactory Not satisfactory	**Containment** Intact ☐ Leak to reactor building ☐ ☐ Due to damage to the containment ☐ Steamline or feedwater line breaks outside containment ☐ IS LOCA outside containment Filtered containment venting at __:__ ☐ Unfiltered containment venting at __:__ ☐
	Suppression pool heat removal Satisfactory Not satisfactory	Suppression pool heat removal system	Suppression pool heat removal system	Suppression pool heat removal Satisfactory Not satisfactory	
	Containment pressure relief Satisfactory Not satisfactory Doubtful	Containment spray system Containment venting systems	Containment spray system Containment venting systems	Containment pressure relief Satisfactory Not satisfactory Doubtful	
	Drywell flooding Satisfactory Not satisfactory Doubtful	Water level	Water level	Drywell flooding Satisfactory Not satisfactory Doubtful	
	Nitrogen atmosphere Satisfactory Doubtful	Nitrogen gas system	Nitrogen gas system	Nitrogen atmosphere Satisfactory Doubtful	

Figure 15: 3D/3P grid for BWR.

Status at XX :XX Status of barriers	Diagnosis (Assessment) Safety function status	Systems used for function control	Prognosis Forecast of function control systems availability	Forecast of safety function status	Forecast of the barriers status
FUEL-SHEATH: ☐ **No systematic failure** ☐ **Systematic sheath failure** ☐ **Fuel melt** ☐ **Fueling machine accident**	☐ **Reactivity** ☐ Shutdown ☐ Reactivity control	☐ *Active:* ☐ Shutdown System 1 ☐ Shutdown System 2 ☐ Reactivity control devices		☐ **Reactivity Control** ☐ Shutdown Status	**FUEL-SHEATH:** ☐ **No systematic failure** ☐ **Systematic sheath failure** **at __:__** ☐ **Fuel melt** **at __:__**
	☐ **Water Coverage** ☐ Fuel sheath water coverage	☐ *Active:* ☐ Shutdown cooling ☐ ECC/ECI high pressure injection ☐ ECC/ECI medium pressure injection ☐ ECC/ECI low pressure injection ☐ Emergency Mitigating Equipment* ☐ *Passive:* ☐ HTS header level (measure)		☐ **Water Coverage** ☐ Fuel sheath water coverage	
		*Refer to technical basis document			
HEAT TRANSPORT SYSTEM: ☐ **Intact** ☐ **Doubtful** ☐ **Leakage** ☐ **HTS break** *Where:* ☐ *In-core* ☐ *Out-core* ☐ *Out-core (End fitting failure)* ☐ *Containment bypass* **SAMG Entry** ☐ **Loss of subcooling margin**	☐ **Energy Removal** ☐ Capability ☐ Control of heat removal ☐ Overpressure protection	☐ *Active:* ☐ ECC/ECI System ☐ Shutdown cooling ☐ Emergency Mitigating Equipment* ☐ *Passive:* ☐ Thermosyphoning (Steam Generator level) ☐ Emergency Water Supply (refill HTS) ☐ Moderator inventory (level) ☐ *Uncontrolled:* ☐ HTS barrier status (break status, size, location) ☐ Liquid relief valve		☐ **Energy Removal** ☐ Capability ☐ Control of heat removal ☐ Overpressure protection	**HEAT TRANSPORT SYSTEM:** ☐ **Intact** ☐ **Doubtful** ☐ **Leakage** ☐ **HTS break** *Where:* ☐ *In-core* ☐ *Out-core* ☐ *Out-core (End fitting failure)* ☐ *Containment bypass* **SAMG Entry** ☐ **Loss of subcooling margin** **at __:__**
		*Refer to technical basis document			
CALANDRIA VESSEL: ☐ **Intact** ☐ **Doubtful** ☐ **Calandria Break** *Where:* ☐ *Calandria failure* ☐ *Rupture disk burst* **SAMG Entry*** ☐ **Low moderator level**	☐ **Heat Removal** ☐ Capability ☐ Control of heat removal	☐ *Active:* ☐ Shield cooling system (shield tank and end shields) ☐ Moderator cooling ☐ *Passive:* ☐ Calandria vault (water level) ☐ *Uncontrolled:* ☐ Calandria Vessel Rupture disks		☐ **Heat Removal** ☐ Capability ☐ Control of heat removal	**CALANDRIA VESSEL:** ☐ **Intact** ☐ **Doubtful** ☐ **Calandria Break** *Where:* ☐ *Calandria failure* ☐ *Rupture disk burst* **SAMG Entry*** ☐ **Low moderator level** **at __:__**
	☐ **Water Coverage** ☐ Moderator Level	☐ *Active:* ☐ ECC/ECI Recirculation ☐ Emergency Mitigating Equipment* ☐ Emergency Water Supply (refill calandria vessel)		☐ **Water Coverage** ☐ Moderator Level	
		*Refer to technical basis document			
CONTAINMENT: ☐ **Normal Leak** ☐ **Doubtful** ☐ *High hydrogen concentration* ☐ **Direct Leak/failure** ☐ *Enhanced Leak* ☐ *Direct penetration* ☐ *Secondary side* ☐ *Leak to other buildings* ☐ *IFB penetration* ☐ *Airlock* **SAMG Entry*** ☐ **High containment radiation**	☐ **Containment Fission Product Control** ☐ Isolation ☐ Fission production retention	☐ *Passive:* ☐ Vacuum Building (capacty)* ☐ Isolation ☐ Dousing Tank Inventory* ☐ *Uncontrolled:* ☐ Core Coverage (pool scrubbing)		☐ **Containment Fission Product Retention** ☐ Isolation ☐ Fission production retention	**CONTAINMENT:** ☐ **Normal Leak** ☐ **Doubtful** ☐ *High hydrogen concentration* ☐ **Direct Leak/failure** ☐ *Enhanced Leak* ☐ *Direct penetration* ☐ *Secondary side* ☐ *Leak to other buildings* ☐ *IFB penetration* ☐ *Airlock* ☐ **Leakage - Vacuum building capacity depleted at __:__** **SAMG Entry*** ☐ **High containment radiation** **at __:__**
	☐ **Containment Energy Removal** ☐ Capability ☐ Control of containment cooling ☐ Control of containment pressure	☐ *Active:* ☐ Air Cooling Units ☐ Containment Filtered Venting ☐ Emergency Filtered Air Discharge ☐ *Passive:* ☐ Vacuum Building (capacty)* ☐ *Uncontrolled:* ☐ Containment barrier status		☐ **Containment Energy Removal** ☐ Capability ☐ Control of containment cooling ☐ Control of containment pressure	
	☐ **Containment Flammability** ☐ Hydrogen gas control ☐ Control containment condtions	☐ *Active:* ☐ Containment Filtered Venting ☐ Emergency Filtered Air Discharge ☐ Inert gas injection ☐ Air Cooling Units (turn off to steam containment ☐ *Passive:* ☐ Hydrogen Igniters ☐ Passive Autocatalytic Recombiners ☐ *Uncontrolled:* ☐ Combustible gas burn		☐ **Containment Flammability** ☐ Hydrogen gas control ☐ Control containment condtions	

Figure 16: 4D/4P grid for CANDU.

Site :	Unit :	Date :	Time :	Visa :	Sender :	Receiver :

FORM"DIAGNOSIS – PROGNOSIS" : **INSTALLATION OPERATION (Pool Accident)** N° ....

STATUS AT __:__	DIAGNOSIS		PROGNOSIS		
Barriers status	**Safety functions status**	**Safety functions control systems**	**Forecast of system avaibality**	**Forecast of safety function**	**Forecast of the barrier status**
CLAD - FUEL No clad failure ☐ Clads failures ☐ ☐ Fuel handling accident Core melt ☐	Reactivity control • Comfortable • Low • Insufficient • Doubtfull	IRWST, Boration : *ECCS*, *CVCS*, RBWMS, ...	IRWST, Boration : *ECCS*, *CVCS*, RBWMS, ...	Reactivity control • Comfortable • Low • Insufficient • Doubtfull	**CLAD - FUEL** No clad failure ☐ Clads failures at __:__ ☐ ☐ Fuel handling accident Core melt at __:__ ☐
	Pool water inventory • Satisfactory • Degraded • Déwatering • Doubtfull	IRWST, FPS, WDS	IRWST, FPS, WDS	Pool water inventory • Satisfactory • Degraded • Déwatering • Doubtfull	
SFP and COOLING SYSTEM Water < 60°C (integrety) ☐ Water > 60°C (subcooling margin low) ☐ Saturated (degraded barrier) ☐ Doubtful ☐ Pool water level .... m ☐ ☐ < cooling pump operation level ☐ Pool rack level Pool break ☐ ☐ Transfer tube open ☐ Circuit break Fuel assembly handling position ☐ ☐ Fuel assembly at hight level ☐ Fuel assembly in tube transfer	Heat removal from the pool Sufficient/Not sufficient Doubtful Controlled/Not controlled	IRWST, FPS, WDS	IRWST, FPS, WDS	Heat removal from the pool Sufficient/Not sufficient Doubtful Controlled/Not controlled	**SFP and COOLING SYSTEM** Water < 60°C (integrety) ☐ Water > 60°C (subcooling margin low) ☐ Saturated (degraded barrier) ☐ Doubtful ☐ Pool water level .... m ☐ ☐ < cooling pump operation level ☐ Pool rack level Pool break ☐ ☐ Transfer tube open ☐ Circuit break Fuel assembly handling position ☐ ☐ Fuel assembly at hight level ☐ Fuel assembly in tube transfer
FUEL BUILDING Normal leak ☐ Direct leak ☐ ☐ Fuel building outsidedoor open Leak to auxiliary building ☐ ☐ penetration ☐ connected system ☐ Fuel building door open Doubtful ☐ Fuel building ventilation operate ☐ ☐ In normal operation ☐ Iiodine trap in operation ☐ Forced air supply Fuel building ventilation out ☐	Building pool containment • Safe • Not assured • Doubtful	Fuel building door open or not FBVS	Fuel building door open or not FBVS	Building pool containment • Safe • Not assured • Doubtful	**FUEL BUILDING** Normal leak ☐ Direct leak ☐ ☐ Fuel building outsidedoor open Leak to auxiliary building ☐ ☐ penetration ☐ connected system ☐ Fuel building door open Doubtful ☐ Fuel building ventilation operate ☐ ☐ In normal operation ☐ Iiodine trap in operation ☐ Forced air supply Fuel building ventilation out ☐

Figure 17: 3D/3P grid for SFP.

DOSE RATE DATA OF MEASURING INSTRUMENTS USED IN NON-GOVERNMENTAL NETWORKS (MINNs) IN THE FRAMEWORK OF PREPAREDNESS EMPIR PROJECT

G. Iurlaro[*]*, L. Sperandio*[*]*, V. Morosh*[**]*, M. Žlivanovic*[***]*, S. Bell*[****]*, F. Mariotti*[*]*, L. Campani*[*]*, P. Ferrari*[*]*, B. Morelli*[*]*, S. Ioannidis*[***]*, G. Pantelic*[***]*, M. De CORT*[*****]

[*]Italian National Agency for New Technologies, Energy and Sustainable Economic Development (ENEA)
[**]Physikalisch-Technische Bundesanstalt (PTB)
[***]Vinca Institute of Nuclear Sciences, University of Belgrade, milosz@vinca.rs
[****]NPL Managment Limited
[*****]Joint Research Centre - European Commission (JRC)

Abstract:

The radiological environmental monitoring using stationary gamma stations is largely used by governmental networks of European Countries and all data are collected by the European Commission which established European Radiological Data Exchange Platform (EURDEP) [1] the central data management system for the automatic exchange of radiological data.

After the Fukushima accident, the new concept of citizen science set up new monitoring stations managed by non-governmental networks and crowd sourced data have rapidly increased.

The radiological measurements by people disseminates in accordance with the expansion of technological developments of cheap devices and of the readiness of the software for the uploading of data. Furthermore, the number of measurements is related with the perception of the risk in nuclear field in different countries and community.

The EMPIR project "16ENV04 Preparedness, Metrology for mobile detection of ionizing radiation following a nuclear or radiological incident" [2] includes the Work Package 3 "Monitoring of ionizing radiation by non-governmental networks [3].

In the first step, a study of the non-governmental networks was conducted, and six web sites were identified and analysed [4]. The partners of Preparedness project PTB, NPL, ENEA and VINCA selected and acquired 16 different type of measuring instruments used in non-governmental networks (MINNs) to investigate the congruity of dose rate data provided in term of ambient dose equivalent H*(10) rate with a metrological approach. Currently, testing of the MINNs is conducting by PTB, NPL, ENEA and VINCA in laboratory condition and the response of all types of MINNs is investigated in the PTB facilities (UDO II, climatic test cabinet, secondary cosmic field and plume simulation sites). A comprehensive study on the possible use of dosimetric data of non-governmental network for dose rate monitoring will be the final task of the project.

1 INTRODUCTION

Nowadays, the nuclear or other radiologically incidents or accidents, including intentionally events caused by malicious acts, could release radioactive materials and cause damage to the workers, the public and the environment. In emergency phase the national competent authorities in nuclear and radiation protection field and other decision makers need quick and credible information on release and contamination because the protection of the of the public against exposition at radiological risk.

The confidence of the public in governmental emergency preparedness and response depends on the availability of reliable radiological data. There is a growing phenomenon of the people or groups, either organised or not, that could use portable instruments to monitor the presence of ionizing radiation with the main purpose to verify or integrate the dose rate data of governmental networks. The main advantage of numerous measurements from non-governmental monitoring networks consists in the reduction of computable statistical uncertainty for mean value of data referred to homogeneous areas, even if used detectors are not optimized for measurements of ambient dose equivalent rates. The synergic work of the two networks could produce a more accurate evaluation of the movement of the radioactive plume and could show small dispersion of radioactive material due for example to a malicious act.

The EMPIR 16 ENV04 "Preparedness" project serve the purpose to establish a metrological basis for mobile detection of ionising radiation to support adequate protective measures in the aftermath of nuclear and radiological emergencies. The project is structured in six work packages and the Preparedness consortium comprises 17 institutions from 12 European countries. In the framework of the Work Package 3 on Monitoring of ionising radiation by non-governmental networks, the objective is to investigate the feasibility to use (quasi) real time dose rate data provided by open-access non-governmental networks for preparedness and response purposes.

2 NON-GOVERNMENTAL RADIATION MONITORING NETWORKS

The non-governmental radiation monitoring networks are created by private company or non-governmental organization (NOG) with the aim of monitoring the radiation level in the environment, collecting data from different location through the world.

Figure 1 Maps on web-pages of non-governmental networks most widespread networks in Europe and example of portable measuring instruments for radiation monitoring.

In the framework of Preparedness project five different organizations were analysed, the study focused on a selection of the available most widespread networks in Europe listed in Table 1.

Table 1 Networks general information [6]

Network and Website	Responsible commercial company (website)
Safecast https://blog.safecast.org/	Non-governmental organization
GMC Map http://www.gmcmap.com/index.asp	GQ Electronics (USA) (http://www.gqelectronicsllc.com)
Radmon http://radmon.org/	Creative Systems Inc. (USA) (http://www.creativesysinc.com)
Radiation network http://radiationnetwork.com/	Mineralab, LLC (USA) (http://www.mineralab.com/)
Radioactive@home http://radioactiveathome.org/en	Non-governmental organization (BOINC Polska Foundation / Poland)
uRadMonitor https://www.uradmonitor.com/	MagnaSCI (Romania) (http://www.magnasci.com/)

The networks allow users to submit data to the network's database in automatic or in manual way. In Table 2 are listed the data submission technique used by the networks considered, the data format required by the network to submit measurements from detectors, the type of data displayed and frequency of data uploading/updating.

In all the site are used fixed stations with the exception of Safecast in which are collected data by mobile devices.

Table 2 Data transmission information [6]

Networks	Data submission technique	Network's database submission format	Network's displayed data	Frequency of data uploading/updating
Safecast	Automatic (in Japan) and manual	CPM[1]	µSv/h	Collection of data as often as possible
GMC Map	Automatic and manual	CPM and ACPM[2]; µSv/h (only in automatic mode)	CPM or µSv/h	Period (in minutes) is the frequency for uploading data and is defined in the activation of the device
Radmon	Automatic and manual	CPM	CPM or µSv/h	Sampling time 1 minute, latest 6 hours readings are specified in the box of the station
Radiation network	Automatic	CPM	CPM	The time and date stamp at the bottom centre of the Map defines how recently the radiation levels have been updated to the map (every minute)
Radioactive@home	Automatic	CPM, µSv/h	µSv/h	Sampling time 1 h, last updated measurement specified in the box of the station
uRadMonitor	Automatic	CPM	µSv/h	Sampling time 1-minute, last updated measurement specified in the box of the station

[1] Count per Minute

[2] Average Count per Minute

Other details useful for completeness of information are present in the sites, i.e. off line stations (out of working) in GMC Map and uRadMonitor, information about the colours of stations points related to the magnitude of ambient equivalent dose rate measurements in Safecast, Radioactive@Home and uRadMonitor or updating time of the data in GMC Map .

3 MEASURING INSTRUMENTS USED IN NON-GOVERNMENTAL NETWORKS (MINNs)

In order to investigate the status of the measurement of ionising radiation (and concentrations of radioactivity) in non-governmental networks, the first step was an overview of electronic devices and the basic methods used for data acquisition and evaluation (see Table 3).

Table 3 Measuring Instruments used in non-governmental Networks in Europe [6]

Example of MINNs	Supplier	Networks
uRAD Monitor Model A	Magna SCI	uRad Monitor
GMC-600	GQ Electronics	GMC map
bGaiger Nano	Safecast	Safecast
Radalert 100	International Medcom	Radiation Network/Safecast
GMC-320 Plus	GQ Electronics	GMC map / Radmon
GMC-500 Plus	GQ Electronics	GMC map / Radmon
uRAD Monitor model KIT1	Magna SCI	uRad Monitor
Monitor 4 Geiger Count KIT	S.E. International Inc.	Radiation Network
GMC-300 Plus	GQ Electronics	GMC map
RADEX 1212	Quarta-RAD Inc.	GMC map/ Radex Read Radiation Mapping
PMR 7000	Mazur	Radiation Network
Monitor 200	S.E. International Inc.	Radiation Network
uRAD Monitor Model D	Magna SCI	uRad Monitor
MyGeiger ver.3 PRO DIY	RH Electronics	Radmon
Inspector Alert	International Medcom	Radiation Network
Rad 100	International Medcom	Radiation Network/Safecast

The operational quantity used for area monitoring in radiation protection is the ambient dose equivalent H*(10) [7] and its unit of measurement is sievert (Sv), so it is recommended to calibrate these instruments in terms of these quantities.

4 TESTING OF THE MINNs IN LABORATORY CONDITION AND PTB FACILITIES

In the framework of Preparedness project, the feasibility study on the use of non-official dosimetry data for preparedness purposes is based on the results of a metrological investigation and comparison of measuring instruments used in non-governmental networks by using reference facilities for dosimetry of PTB, ENEA, NPL, and VINCA.

The linearity and the energy dependence of typical MINNs were tested at 8 radiation qualities in an energy range from about 60 keV to 1250 keV. Each partner used his own X-ray and gamma-ray irradiation facilities. The elaboration of the data is in progress. It is expected that some MINNs show a strong energy dependence of their response to ionising radiation, because simple gamma counters do not have the energy compensation, which is required for dosimeters that are in agreement with appropriate standards.

A measurement campaign was organized in Germany by PTB in June for determining the response of the MINNs types to the terrestrial components as well as to the comic component of the natural radiation and the inherent background of the instrument.

Measurements will be performed in an almost pure secondary cosmic radiation field, realised by a floating platform constructed from material of low radioactivity, on a freshwater lake (see Figure 1).

Figure 2 PTB's floating platform constructed from material of low radioactivity on a lake

The inherent background (reported dose rate in case of no external ionising radiation) of the MINNs was tested by performing measurements in the underground laboratory UDO II of PTB (see Figure 2).

At PTB's reference site for plume simulations (see Figure 3), various MINNs were investigated and the sensitivity to small dose rate changes was been experimentally determined using two different photon fields (^{137}Cs and ^{60}Co). The sensitivity of the MINNs to small variations was tested because it is well known that radioactive plums as well as non-negligible ground contamination levels (some 10 kBq/m^2) cause small increases in the ambient dose equivalent rate; i.e. a few nano sieverts per hour (nSv/h) on top of a natural background radiation level of the order of about 100 nSv/h.

Figure 3 Underground laboratory UDO II of PTB

Figure 4 PTB's reference site for plume simulations

The measurements for testing the dependence of MINNs performance from environmental conditions are in progress at PTB climatic test cabinet.

5 CONCLUSION

The results of the measurement in laboratory condition and of the PTB measurement campaign could summarise advantage and disadvantage in the use of the MINNs in non-governmental networks and explore the possible new use of non-governmental networks for dose rate monitoring.

The promotion of the harmonisation of the measuring methods and online information for emergency preparedness, also in non-governmental radiation monitoring networks, could be considered a big benefit for European authorities and decision makers.

The improvement of the public confidence in the decisions of national governments and the reduction of the risk of socio-economic damages could be strictly related with the promotion of independent measurement of radioactivity and radiation dose by citizens, thus endorsing the transparency, education and acceptance of science.

A training support for operators and users of non-governmental networks web sites is desirable to disseminate an accurate citizen-science on the basis of the results of the metrological investigation defined by WP3 of Preparedness project.

6 ACKNOWLEDGMENTS

The EMPIR initiative is co-funded by the European Union's Horizon 2020 research and innovation programme and the EMPIR Participating States.

7 REFERENCES

[1] EURDEP (EUropean Radiological Data Exchange Platform). Website: https://eurdep.jrc.ec.europa.eu/Entry/Default.aspx, accessed on 22.03.2019

[2] http://www.preparedness-empir.eu/?page_id=1016

[3] 16ENV04 Preparedness, "Publishable Summary for 16ENV04 Preparedness, Metrology for mobile detection of ionizing radiation following a nuclear or radiological incident", February 2018

[4] L. Sperandio, G. Iurlaro, P. Kessler, J. Marganiec, K. Bogucarskis, M. De Cort, "Indagine sulle Reti non governative di monitoraggio delle radiazioni ionizzanti nell'ambito del progetto EMIPR-16ENV04 "Preparedness"", XXXVII Congresso Nazionale di Radioprotezione, 16-19 Ottobre2018, Bergamo

[5] http://www.preparedness-empir.eu/wp-content/uploads/16ENV04_Publishable_Summary-Feb-18.pdf

[6] G. Iurlaro, L. Sperandio, J. Marganiec, P. Kessler, K. Bogucarskis, S. Bell, L. Campani, M. De Cort, H. Dombrowski, A. Helbig, S. Ioannidis, D. Lazarevic, F. Mariotti, B. Morelli, G. Pantelic, A. Röttger, M. Zivanovic, C. Duff "Environmental measurements of radioactivity and radiation protection quantity available in non-governmental networks web sites". Book of abstracts, 3rd European Radiological Protection Research Week", October 2018, Rovinj, 110-111, https://erpw2018.com/wp-content/uploads/2018/09/ERPW-abstracts-book_web_pages.pdf

[7] ICRP 103 - The 2007 Recommendations of the International Commission on Radiological Protection

The software implementation of the method for determining the level of nuclear and radiological events in the INES scale

A. Kirkin, A. Kuryndin*, I. Liashko**

* Scientific and Engineering Centre for Nuclear and Radiation Safety (SEC NRS)

Abstract:

In accordance with the requirements of international standards SF-1 and GSR part 7 the operating organization is responsible for informing the public about accidents in the installations associated with the civil nuclear industry. For example, in accordance with the requirement of the IAEA standard GSR part 7 it is necessary to "Provide instructions, warnings and relevant information to the public for emergency preparedness and response". International Nuclear Events Scale (INES) is supposed to simplify communication with the public on matters of the safety significance of different events associated with nuclear facilities.

However. the INES rating procedure is time-consuming to a significant extent. Therefore. the "INES Classifier" computer program was developed by Scientific and Engineering Centre for Nuclear and Radiation Safety (SEC NRS) in order to carry out an express assessment according to INES methodology. The "INES Classifier" computer program is based on the methodology outlined in the Guidelines for users of the International Nuclear and Radiological Events Scale 2008 edition. The "INES Classifier" computer program was successfully tested at the Federal Environmental, Industrial and Nuclear Supervision Service of Russia (Rostechnadzor) Information and Analytical Center during emergency response drills at nuclear power plants. This article presents an overview of the developed "INES classifier" computer program and examples of its application.

1 REGULATORY FRAMEWORK

Application of INES is established in the IAEA documentary requirements. According to the terms of IAEA Standards SF-1 [1], protection of public and environment against nuclear facilities impact is based on safety principles. One of these principles is emergency preparedness and response for nuclear or radiation incidents.

The given principle is implemented by compliance with the IAEA GSR part 7 [2] terms stating:

- operating organization shall ensure that arrangements are in place to provide the public who are affected or are potentially affected by a nuclear or radiological emergency with information that is necessary for their protection, to warn them promptly and to instruct them on actions to be taken (Requirement 10).
- nuclear or radiological emergency and the emergency response shall be analysed in order to identify actions to be taken to avoid other emergencies and to improve emergency arrangements (Requirement 19).

In order to facilitate the process of providing information about nuclear or radiological emergency to the public the INES was developed. The scale classifies accidents according to levels affecting the safety. Accidents classification stated in INES allows to assess the level of emergency and to make urgent decision about the necessity of organizational and technical measures application directed to emergency response and mitigation of harmful effects. Moreover, INES is a basis for procedure of investigation the causes of radiological emergency and establishment of emergency arrangements.

It should be mentioned that IAEA Standards requirements were implemented in Russian Federation legislative and regulatory framework. In accordance with Application to Ministry of Emergency Situations of Russia Order on 8th of July 2004 No 329, emergency information shall contain the level of accident according to INES. Also, according to Russian federal requirements and regulations in the field of use of nuclear energy NP-004-08 [3], NP-014-16 [4], NP-027-10 [5], NP-047-11 [6] and NP-088-11 [7] in case of radiological accident, the message containing the hazard assessment under INES shall be sent to all the organizations managing emergency response. Besides, in accordance with the federal rules and regulations [3 ÷ 7] commission that is responsible for investigation of nuclear facility incidents shall report the level of emergency according to INES.

However, it should be mentioned that INES is a communication instrument responsible for mutual understanding between nuclear specialists, mass media sources and public on the safety questions. The INES shall not be used as a basis for emergency response actions. The purpose of the INES is to develop understanding of the emergency safety significance while preparing the emergency reports. The emergency reports shall be issued immediately to avoid misinterpretation and wrong emergency assessment in mass media and public. The INES shall not be used for comparing the safety level of different facilities in different organizations and countries.

2 DESCRIPTION OF INES LEVEL OF NUCLEAR AND RADIOLOGICAL ACCIDENTS DEFINITION METHOD

The INES with its full description (published in user manual (manual) [8]), was firstly presented by IAEA and EAEC international expert team in 1990. The scale is mainly used for NPP emergency classification. Later the INES was improved and adjusted for all the types of radiological accidents within civil nuclear industry. Particularly, the INES can be applied to any accident within transportation, storage and utilization of nuclear and radioactive materials and wastes, lost or unauthorized removal of radioactive sources or packing, detection of unclaimed sources and radioactive exposure within other types of practical activities (for example, mining and oil refining industries).

Figure 1 shows generic criteria of INES emergency classification.

Description and INES Level	People and the environment	Radiological barriers and controls at facilities	Defence in depth
Major accident **Level 7**	- Major release of radioactive material with widespread health and environmental effects requiring implementation of planned and extended countermeasures.		
Serious accident **Level 6**	- Significant release of radioactive material likely to require implementation of planned countermeasures.		
Accident with wider consequences **Level 5**	- Limited release of radioactive material likely to require implementation of some planned countermeasures. - Several deaths from radiation.	- Severe damage to reactor core. - Release of large quantities of radioactive material within an installation with a high probability of significant public exposure. This could arise from a major criticality accident or fire.	
Accident with local consequences **Level 4**	- Minor release of radioactive material unlikely to result in implementation of planned countermeasures other than local food controls. - At least one death from radiation.	- Fuel melt or damage to fuel resulting in more than 0.1% release of core inventory. - Release of significant quantities of radioactive material within an installation with a high probability of significant public exposure.	
Serious incident **Level 3**	- Exposure in excess of ten times the statutory annual limit for workers. - Non-lethal deterministic health effect (e.g. burns) from radiation.	- Exposure rates of more than 1 Sv/hr in an operating area. - Severe contamination in an area not expected by design, with a low probability of significant public exposure.	- Near accident at a nuclear power plant with no safety provisions remaining. - Lost or stolen highly radioactive sealed source. - Misdelivered highly radioactive sealed source without adequate radiation procedures in place to handle it.
Incident **Level 2**	- Exposure of a member of the public in excess of 10mSv. - Exposure of a worker in excess of the statutory annual limits.	- Radiation levels in an operating area of more than 50 mSv/h. - Significant contamination within the facility into an area not expected by design.	- Significant failures in safety provisions but with no actual consequences. - Found highly radioactive sealed orphan source, device or transport package with safety provisions intact. - Inadequate packaging of a highly radioactive sealed source.
Anomaly **Level 1**			- Overexposure of a member of the public in excess of statutory limits. - Minor problems with safety components with significant defence in depth remaining. - Low activity lost or stolen radioactive source, device or transport package.
	No safety significance (Below scale/Level 0)		

Figure 1. Generic criteria of INES emergency classification

It is noteworthy that INES is logarithmic i.e. emergency severity ascends by one order of magnitude with the level extension. At the present moment the INES contains seven levels of emergency classification: levels 4÷7 are classified as “accident”, levels 1÷3 are classified as “malfunction” and there are some accidents with level 0 that are classified as “no safety significance incidents". Such situations are not substantial for safety. The given classification is aimed to provide public with information.

The INES emergency level is determined according to the scope of criteria coupled by principles of influence of assessed emergency on "people and environment", "radiological barriers and controls at facilities" and "defence in depth".

Definition of INES emergency level in "people and environment" category is implemened on the basis of radionuclides activity that is released in environment. This activity is calculated with the use of whether conversion factors for different radionuclides or the number of exposed people and values of doses. "Radiological equivalence" concept is applied for determination of INES emergency level from radionuclides activity. In accordance with this approach radionuclides activity in the release is converted into I^{131} with the use of conversion factors.

The INES emergency level related to influence on "people and environment" is determined according to amount of emergency release, which is calculated by means of radionuclides release conversion factor or is based on the number of radiation exposed people and the rate of exposure dose. For determining INES emergency level according to the emergency release the concept of "radiological equivalence" is used. This concept allows to convert emergency release degree, consisting of the different radionuclides, to the value of radiologically equivalent emergency release of I^{131}.

Some criteria based on the number of the exposed people and the rates of exposure doses is stipulated as well. Within the approach to the determination of INES emergency level the criteria relating to the nuclear facility workers and public is applied. It is noteworthy that the rates of exposure doses differ from slightly exceeding year dose threshold exposure to the actual deterministic effect. INES emergency level determination on the basis of emergency release rate differs from the people exposure approach. In the first case the INES level of emergency severity is ranged from 4 to 7 levels and in the second case it is ranged from 1 to 6 levels. It means that the approach to the INES emergency level determination based on the number of radiation exposed people and the degree of their exposure is considered to be more common.

INES criteria related to "radiological barriers and controls at facilities" is associated with the accident classification of two types:

– accidents resulting in severe damage to such physical barriers as fuel matrix, fuel element cladding and primary-system boundary;

– accidents resulting in radioactive release or dose rate increase. Fuel matrix, fuel element cladding and primary-system boundary remain undamaged.

Determination of INES emergency levels depends on the degree of physical barriers degradation, exposure and room contamination levels. INES emergency level depending on room contamination level is determined by means of "radiological equivalence" concept; in this case I^{131}, Cs^{137} and Mo^{99} are used as fiducial radionuclides.

INES criteria referring to the emergency impact on levels of "defence in depth" are distinguished depending on the type of nuclear facility or type of activity in the field of nuclear energy uses. For example, NPP referring criteria are based on emergency frequency and the elements and safety systems abilities to perform safety functions. In this case emergency frequency is determined on the basis of information, provided by nuclear facility project documentation and INES boundary criteria. It is noteworthy that according to manual [8], an element or a safety system failure will not always result in INES emergency level increase, since a large number of elements and systems is responsible for safety.

Finally, the maximum INES emergency assessment is determined on the basis of all the criteria ("radiological barriers and controls at facilities", levels of "defence in depth" and impact on "people and environment") and defines the total INES emergency assessment.

Practically in case of violation of normal nuclear facility operation, accidents or emergency response exercises, the process of INES emergency level determination is quite time consuming. The professional assessing the emergency level shall be experienced qualified and shall have advanced knowledgebase regarding the assessed nuclear facility. It should be mentioned that for more effective assessment of INES emergency level, the professionals shall use the following criteria: radiation consequences, physical barriers and defence in depth levels. As a result, total time taken for the INES emergency level assessment can be reduced, but it takes large human resources. Consequently, time expenditure is reduced. however labor necessity is increased.

Figure 2 shows one part of a flow chart, containing the criteria for the INES emergency level determination relating to radiation consequences. The given flow chart is only a component of a complex flow chart which allows to assess INES emergency level.

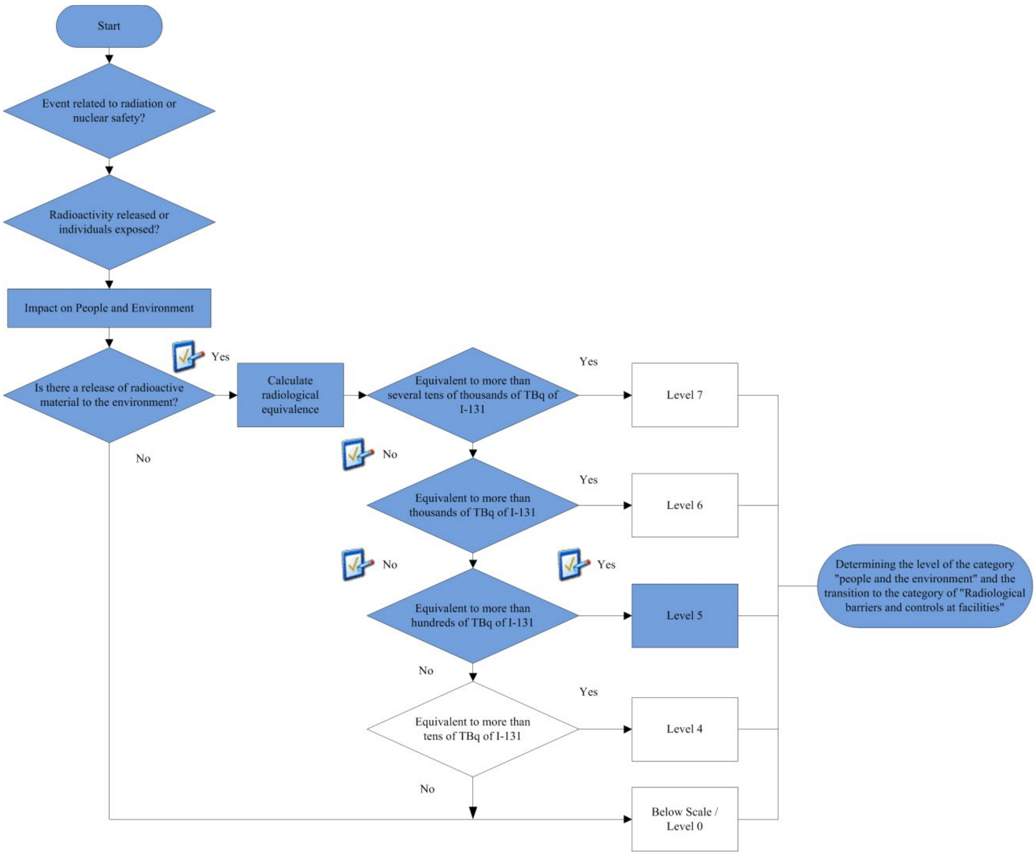

Figure 2. Part of a flow chart, containing the criteria for the INES emergency level determination relating to impact on "people and environment"

For accurate INES emergency level assessment, professionals shall handle large ammount of data on the emergency and make calculations for assessment of emergency release [8] in radiological equivalent of I^{131}. All these actions should be performed immediately. Moreover, human factor, which can affect the assessment result, shall be taken into consideration.

The example of INES use is emergency response exercises of NPP operating organization. Within this procedure NPP operating organization specialists and specialists of Rostechnadzor assess the simulated emergency according to the INES. It is quite time consuming to determine radiation exposure within these emergency response exercises. The reason for that is that additional estimation shall be used for assessment of personnel and public exposure doses by means of specialized software (for example, Nostradamus [9], RECASS [10]). Moreover, some additional emergency information is often required, for instance, the ways of radionuclides diffusion in nuclear facility rooms, qualitative and quantitative characteristics of radionuclides and many other factors required by INES methodology. For another example, physical barriers criteria can be used. For the level of physical barriers damage assessment, neutronic and thermohydraulic calculations shall be performed. To perform the calculations, the specialists shall work with great volume of original data and have ready models for reducing time expenditures connected with INES calculations and assessment. It should also be mentioned that the INES methodology consists of many flow charts that are even more complicated than one mentioned in the Figure 2. Consequently, the INES is much more complicated than it seems to be and it requires great scope of work which influences on the final INES emergency assessment.

3 DESCRIPTION OF THE INES EMERGENCY LEVEL DETERMINATION SOFTWARE

Considering the importance of INES emergency assessments and great time expenditures during the assessments, the necessity for assessment process computerization has appeared. Special software which doesn’t have any analogue was developed for this purpose. The “INES Classifier” computer program was developed at the SEC NRS for this purpose.

The “INES Classifier” computer program is developed on the basis of programming language C# for Windows. It is planned that in the nearest future the software will be presented as a web-application that will avoid the operation system specialities and keep the access to all the software functions.

The “INES Classifier” computer program has user-friendly interface, it is able to promptly perform the INES emergency level assessment and reduce the human error probability.

The “INES Classifier” computer program interface consists of a vertical buttons set, each of the button comprises criterion, execution (or non-performance) of which creates the total INES emergency level assessment. It should be noted that the INES emergency level assessment mechanism is implemented in accordance with the manual [8]. The demonstration of the software interface is presented in figure 3.

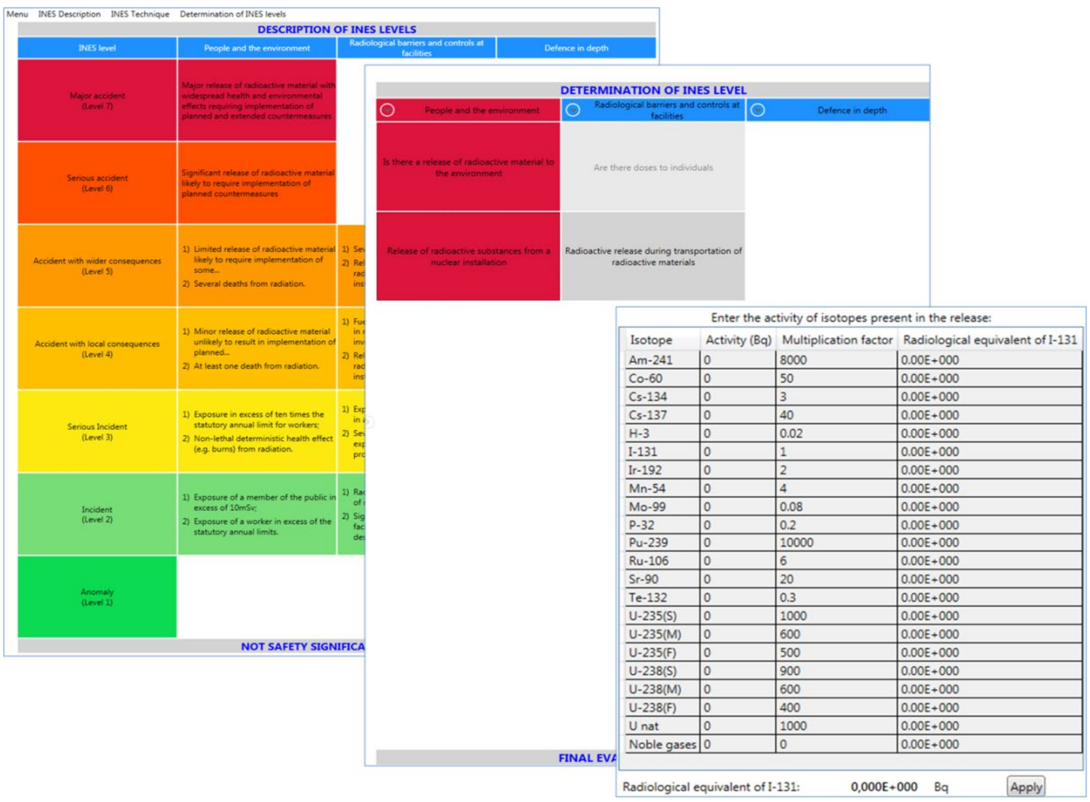

Figure 3. “INES Classifier” computer program interface

During the work with the “INES Classifier” computer program the INES emergency levels or the text of the manual [8] are constantly displayed in left part of the screen, and there are vertical buttons with criteria for determination of INES emergency level in the right part of the screen. By results of performance or non-performance of the criteria “the criteria tree” (which is a visual display of manual block diagrams [8]) is formed. It should be noted that vertical buttons with the criteria do not appear at once, but they are consistent depending on performance or non-performance of the previous criterion, at the same time the total INES emergency level assessment which is displayed in the lower right part of the screen acts as the final result. The built in manual can be used by the specialist performing the INES emergency assessment in case of controversial issues when choosing one or another criterion. Besides, the user-friendly color scheme is implemented in the "INES Classifier" computer program. The program automatically paints elements of "the criteria tree" in the color corresponding to the INES level.

Also the "INES Classifier" computer program forms the reports containing the short description of the emergency scenario and total emergency assessment, at the same time the description of the scenario is formed automatically in process of filling the fields and typing the answers in pop-up windows. The automatically generated report allows to significantly expand the applicability of the given software. Such reports are considered by the group of Rostechnadzor management during decision making on the nuclear facility regulating impacts and on informing mass media.

The "INES Classifier" computer program can be used during work on the analysis of reports on the violations in work of nuclear facility for assessment of correctness of the assesed INES emergency level.

It is noteworthy that the "INES Classifier" computer program went through approbation in Rostechnadzor IAC during the emergency exercises and trainings on NPP. Moreover, due to the interest of operators and regulatory bodies from various countries, the "INES Classifier" computer program, is transferred to the Nuclear Energy Agency Databank in accordance with the Memorandum [11]. On the official website of the OECD, authorized users can submit a request for receiving the "INES Classifier" computer program.

4 THE EXAMPLE OF THE "INES CLASSIFIER" COMPUTER PROGRAM USE

Using the "INES Classifier" computer program the level of the accident at the Fukushima Daiichi NPP on March 11, 2011 was obtained on the INES SCALE.

According to information from the IAEA report [12] and the report by IAEA CEO [13] earthquakes (magnitude 9) and tsunamis caused multiple failures and destruction at the Fukushima Daiichi NPP site on 11.03.2011. The main was the failure of external power supply systems at the NPP site and, therefore, cooling systems of the reactor core in Units 1 ÷ 3 overheated.

To assess the level of event at the Fukushima Daiichi NPP in the category of "defence in depth", the following criteria must be used (taken from the manual [8]):

- the event occurred at the nuclear power plant operating at nominal power;
- the initial event required the action of certain security systems designed to overcome the consequences of the initial event;
- the frequency of the initial event is unlikely, because according to [13] during the design of Fukushima Daiichi NPP an earthquake with a magnitude of 9 points was not considered by developers to be a probable earthquake;
- the performance of safety systems is rated as "insufficient", because according to [12, 13], systems designed to ensure the safety of nuclear power units (for example, the core cooling system and emergency diesel generators) did not do their job.

The results of the event assessment in "defence in depth" category using the "INES Classifier" computer program are presented in Figure 4.

DETERMINATION OF INES LEVEL		
People and the environment	Radiological barriers and controls at facilities	Defence in depth
The impact on defence in depth for transport and radiation source events	The impact on defence in depth specifically for events at power reactors while at power	The impact on defence in depth for events at specified facilities
Initiating event, which requires the operation of some particular safety systems designed to cope with the consequences of this initiator	The degraded operability of one or more safety systems without the occurrence of the initiator for which the safety systems have been provided	
The frequency of the original event is classified as "expected"	The frequency of the original event is classified as "possible"	The frequency of the original event is classified as "unlikely"
Full	Minimum required by operational limits and conditions	Adequate
Inadequate		
FINAL EVALUATION ON SCALE INES (level 3)		

Figure 4. The results of the event assessment in "defence in depth" category using the "INES Classifier" computer program

Thus the "INES Classifier" computer program evaluated the accident at the Fukushima Daiichi NPP in "defence in depth" category as level 3 event.

According to [14] during an accident at the Fukushima Daiichi NPP most of the reactor core in Units 1 ÷ 3 was melted. Therefore, in order to evaluate this accident level with "radiological barriers and controls at facilities" category it is necessary to use the criterion [8]: "An event resulting in the melting of more than the equivalent of a few per cent of the fuel of a power reactor or the release of more than a few per cent of the core inventory of a power reactor from the fuel assemblies" (see Figure 5). Thus, the "INES Classifier" computer program evaluated the accident at the Fukushima Daiichi NPP in "barriers and controls at facilities" category as level 5 event.

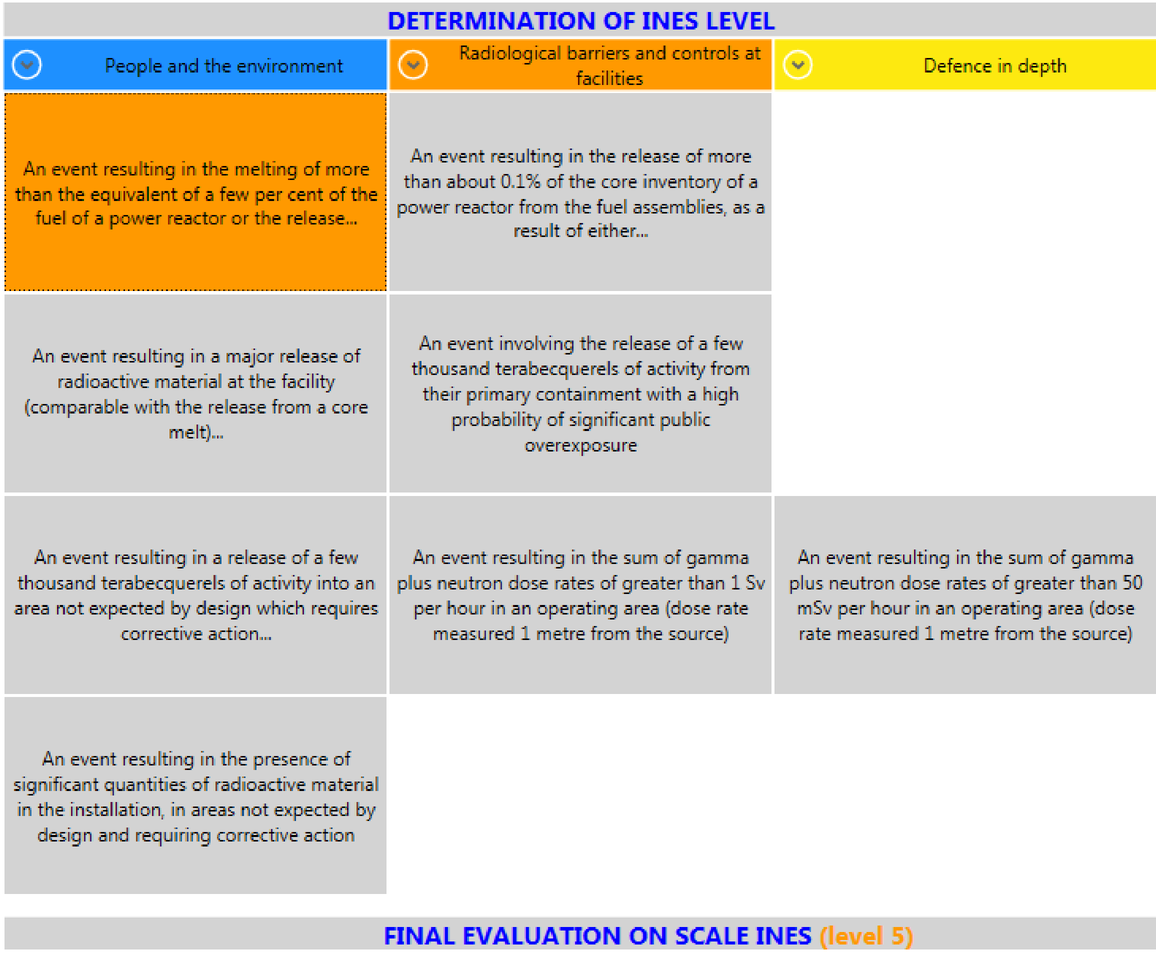

Figure 5. The results of the event assessment in "radiological barriers and controls at facilities" category using the "INES Classifier" computer program

According to [12, 13] during an accident at the Fukushima Daiichi NPP radioactive release was estimated at 400 PBq for the I^{131} and 20 PBq for the Cs^{137}. Therefore, in order to evaluate this accident in "people and environment" category it is necessary to calculate the total activity of the release in units of radiological equivalence of I^{131}. The table 1 shows the values of the release of I^{131} and Cs^{137}, as well as the results of conversion of the release into the radiological equivalent of I^{131}.

Radionuclide	Release by [12], Bq	Multiplication factor (table 2 [8])	Release in units of radiological equivalent I^{131}, Bq
I^{131}	4×10^{17}	1	4×10^{17}
Cs^{137}	2×10^{16}	40	8×10^{17}
Amount			$\mathbf{1{,}2\times10^{18}}$

Table 1. The values of the activities of iodine and cesium that were released during accident at the Fukushima Daiichi NPP

The results of the event assessment in "people and environment" category using the "INES Classifier" computer program are presented in Figure 6.

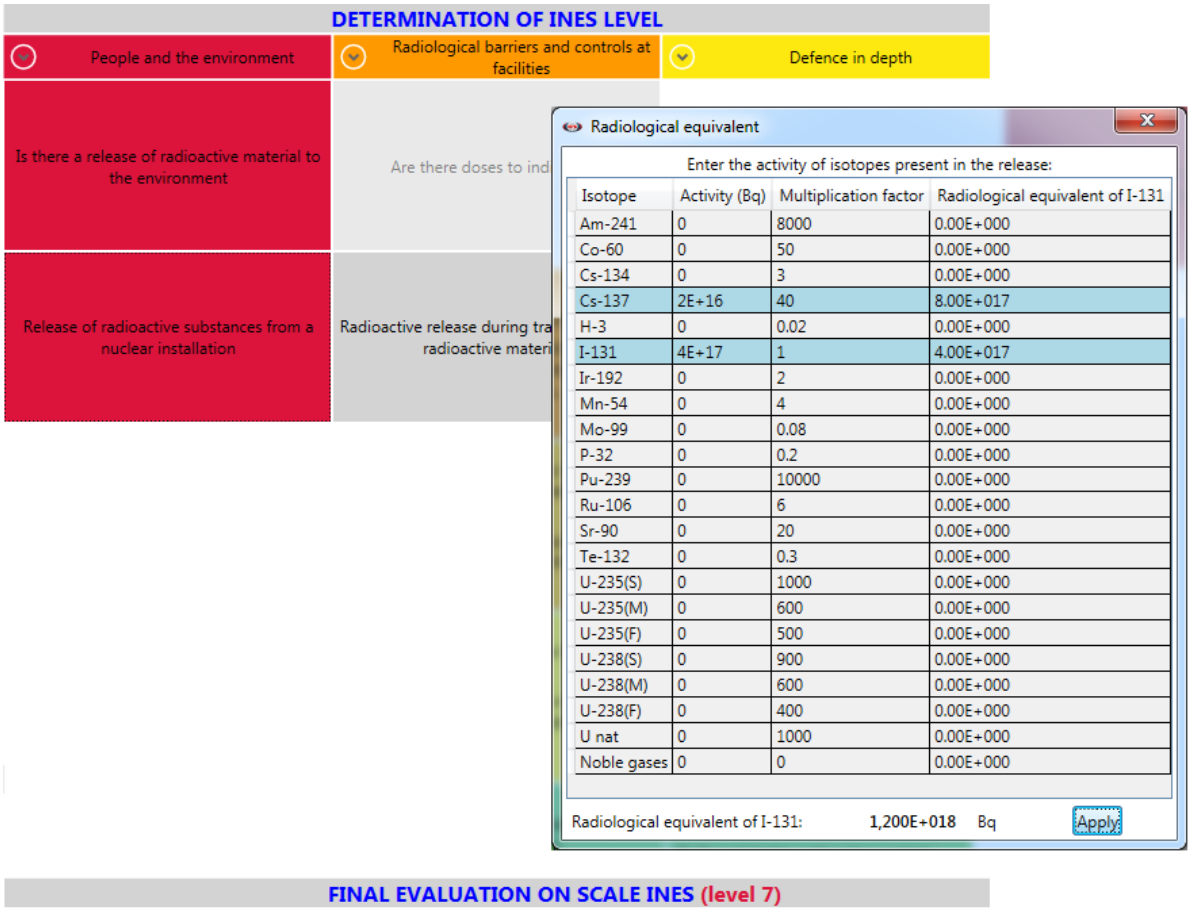

Figure 6. The results of the event assessment in "people and environment" category using the "INES Classifier" computer program

According to Table 1 and Figure 6 total release of radiological equivalent of I^{131} equals $1.2 \cdot 10^{18}$ Bq. Total release value exceeded the value given in paragraph 2.2.2 of the manual [8]. Thus, on the basis of the criteria "people and environment" the given accident is evaluated as 7th INES emergency level.

Total INES emergency level assessment is formed on the basis of the maximum assessment received by the criteria relating to radiation exposure, physical barriers and levels of defence in depth. Fukushima Daiichi NPP accident is treated as the seventh INES level that corresponds to information [8].

5 CONCLUSION

Nuclear facility violation assessment according to INES is an important element of emergency reaction and investigation of violations according to requirements of federal norms and rules of nuclear energy use. The applied software "INES Classifier" computer program is developed for express assessment of nuclear facility emergency classification according to INES; it has a number of advantages:

- minimizes the risk of human errors during determination of the INES emergency level;
- simplifies the process of interaction with INES emergency level assessment method;
- reduces necessary time and human resources during INES emergency level assessment.

The software "INES Classifier" computer program allows forming the reports containing the short description of the emergency development scenario and total emergency assessment. The software can be used by specialists of regulatory bodies and operators for estimation of incidents and preparation of operational messages.

The software “INES Classifier” computer program went through approbation in Rostekhnadzor IAC during the emergency exercises and trainings on the NPP [15].

In accordance with the Memorandum [11] “INES Classifier” computer program is transferred to the OECD/NEA Databank.

6 REFERENCES

1. INTERNATIONAL ATOMIC ENERGY AGENCY. Fundamental safety principles, IAEA Safety Standards Series No SF 1, IAEA, Vienna (2006).
2. Radiation Protection and Safety of Radiation Sources: International Basic Safety Standards, General Safety Requirements Part 7 No GSR Part 7, IAEA, Vienna (2015).
3. Federal Standards and Rules in the Field of Atomic Energy Use. Provision on the Procedure of Investigation and Accounting of Operational Occurrences at Nuclear Power Plants. NP-004-08, 2008.
4. Federal Standards and Rules in the Field of Atomic Energy Use. Rules for Investigation and Accounting of Violations at Operation and Decommissioning of Radiation Sources, Storage Facilities for Radioactive Substances and Radioactive Waste and at Management of Radioactive Substances and Radioactive Waste. NP-014-16, 2016.
5. Federal Standards and Rules in the Field of Atomic Energy Use. Provision on the Procedure of Investigation and Accounting of Operational Occurrences at Nuclear Research Installations. NP-027-10, 2010.
6. Federal Standards and Rules in the Field of Atomic Energy Use. Provisions on the Procedure of Investigation and Accounting of Operational Occurrences at Nuclear Fuel Cycle Facilities. NP-047-11, 2011.
7. Federal Standards and Rules in the Field of Atomic Energy Use. Regulations on Order of Investigation and Accounting of Operational Violations of Ships with Nuclear Installations and Radiation Sources. NP-088-11, 2011.
8. INTERNATIONAL ATOMIC ENERGY AGENCY. The International Nuclear and Radiological Event Scale. User’s Manual 2008 Edition. IAEA, Vienna, 2013.
9. Multipurpose computer programm “NOSTRADAMUS“, http://www.ibrae.ac.ru/contents/950/.
10. Computer program RECASS NT, 2017 http://www.typhoon.obninsk.ru/products/software-hardware/recass.php.
11. The procedure for interaction between Russian organizations and the Nuclear Energy Agency of the Organization for Economic Cooperation and Development and the Nuclear Energy Agency Data Bank. Memorandum of December 30, 2013 No. 1/5198-D.
12. INTERNATIONAL ATOMIC ENERGY AGENCY. The Fukushima Daiichi Accident. Technical Volume 1/5 Description and Context of the Accident. IAEA, Vienna, 2015.
13. The Fukushima Daiichi Accident. Report by the Director General, IAEA, 2015.
14. TOKYO ELECTRIC POWER COMPANY, Evaluation of the Situation of Cores and Containment Vessels of Fukushima Daiichi Nuclear Power Station Units-1 to 3 and Examination into Unsolved Issues in the Accident Progression, TEPCO, Tokyo (2013).
15. Certificate of state registration of the computer program “INES Classifier“, № 2018617337.

Forward and backward analysis of the 2017 release of Ru-106 over Europe using a Lagrangian dispersion model and monitoring station data

Antonio Cervone, Antonio Guglielmelli*, Federico Rocchi**

*ENEA FSN/SICNUC/SIN, via Martiri di Monte Sole 4 40129 Bologna Italy

Abstract:

At the end of September 2017 and in the following weeks many monitoring stations have detected unexplained levels of Ru-106 in the atmosphere over Europe. The concentration of the radioactive cloud was not dangerous for the health, but it could not be connected to any known episode of release in any nuclear power plant or factory that deals with radioactive material over the area that registered the abnormal concentrations.

In this paper we present some analysis of this release using the Lagrangian particle dispersion model implemented in the FLEXPART code. This code is able to model forward atmospheric dispersion of (non-)radioactive material on long distances and predict deposited concentrations in air and deposited to the ground on a Cartesian grid and at relevant sites. The code is also capable of recovering the inverse trajectories of the pollutant particles in order to determine the origin and timing of a release starting from the measured concentrations at different sites. In order to perform these forward and backward simulations, an extensive set of meteorological data, obtained from the ECMWF archive, must be retrieved and manipulated to fed the FLEXPART code.

The paper includes also a comparison between the simulation results and some of the detection data available from different Italian and European sites in order to assess the performance of the code and compare possible emission sites and release dates.

1 INTRODUCTION

The origin of the Ruthenium-106 concentrations measured in the air over Europe is still unknown. Many studies have been devoted to the analysis of this phenomenon, starting from IRSN in the early 2018 [1]. In the following months, other papers have tried to recover the origin of the Ruthenium cloud [2, 3, 4, 5, 6], with a large degree of agreement on the identification of the possible source, time of release and magnitude. Most of the works relay on some kind of backward/inverse modeling of the measured data to identify the source term and its point and time of release.

In this framework, ENEA has tested its capabilities in independently conduct similar analyses and determine the source term retroactively with the use of simulation codes for the dispersion of radioactive pollutant in the atmosphere.

All the simulations shown in this paper have been performed using FLEXPART, that stands for *FLEXible PARTicle dispersion model*. This code is a long-range atmospheric transport code based on the Lagrangian approach. In this type of modeling the evolution of the distribution of a pollutant is simulated through the use of a large number of particles that are dispersed in a fixed grid that describes the atmospheric conditions. A stochastic process is used to simulate the effect of the turbulence and the dispersion in the atmosphere. The code is also capable of modeling wet and dry deposition, together with radioactive decay [7, 8, 9, 10, 11].

Different approaches can be adopted to model this type of releases, such as the Gaussian approach, or the Eulerian model. The main advantage of the Lagrangian approach is the complete absence of numerical diffusion, that is inherently introduced in Eulerian models. FLEXPART can perform forward and backward simulations in time, adding the possibility to recover an emission starting from some receptor values.

Another advantage in the use of Lagrangian codes is the easiness in performing backward simulations, where the measured data become the source term and the simulated cloud represents the probability that connects each point on the computational grid to the measured values [12]. FLEXPART is used in this capability also in the CTBTO for detecting potential radioactive releases in the atmosphere.
FLEXPART requires an extended set of meteorological data as a driver for the simulation of the dispersion of the radioactive cloud. The set of variables include surface quantities, ranging from pressure to cloud cover and convective and large scale precipitation, and model level quantities, such as temperature and wind velocities, defined at several levels above ground.
FLAXPART has been developed to work with different sets of meteorological weather data, such as ECMWF, GFS and WRF. In the following, FLEXPART has been used exclusively with weather data from the European Centre for Medium-range Weather Forecast [13]. In particular, the reanalysis data from the ERA-5 database, at a resolution of 0.25° for the region between longitudes 0°E and 70°E and latitudes 30°N and 70°N and 137 model levels, have been retrieved from the ECMWF servers for the period between the 25th of September 2017 and the 5th of October of the same year.
Each of the upcoming simulations requires about an hour to simulate 10 days of atmospheric transport, when using 10 million particles, on a workstation with high performance consumer-grade processor and fast storage devices.
All the times reported in the following sections are in the Coordinated Universal Time (UTC).

2 BACKWARD SIMULATIONS OF MONITORING DATA

2.1 Monitoring station data

LOCATION	START DATE	END DATE	VALUE [mBq / m3]	UNCERT. [mBq / m3]
Stockholm	2017-09-30 08:43	2017-10-01 08:43	0.032	—
Stockholm	2017-10-01 08:43	2017-10-02 08:43	17	—
Stockholm	2017-10-02 08:43	2017-10-03 08:43	9.8	—
Udine	2017-09-29 00:00	2017-10-02 00:00	12.3	3
Udine	2017-10-02 00:00	2017-10-03 00:00	49.1	12
Udine	2017-10-03 00:00	2017-10-04 00:00	30	9
Udine	2017-10-04 00:00	2017-10-05 00:00	5.2	1.5
Udine	2017-10-05 00:00	2017-10-06 00:00	3.3	1.5
Prague	2017-09-29 06:45	2017-10-02 16:35	15	—
Prague	2017-10-02 16:40	2017-10-02 20:25	1.6	—
Prague	2017-10-02 20:25	2017-10-03 08:10	1.1	—
Prague	2017-10-03 08:10	2017-10-03 15:00	0	0.04
Prague	2017-10-04 07:55	2017-10-05 08:05	0	0.05
Prague	2017-10-05 08:05	2017-10-06 06:40	0	0.012

Table 1: Measured Ru-106 concentrations that have been used in the FLEXPART simulations. the data were extracted from [1, 14, 15].

In the final week of September 2017 and in the first week of the following October many readings of Ruthenium-106 have been reported around Europe [1, 14, 15]. A small selection of them is reported in Table 1. The data reported in the table are the only data that have been used to perform the simulations described below.
The selection has been made based on several principles:

- **Magnitude.** The three sites (Stockholm, Udine and Prague) show relevant values of the Ru concentration, at least for a range of days in the selected period.

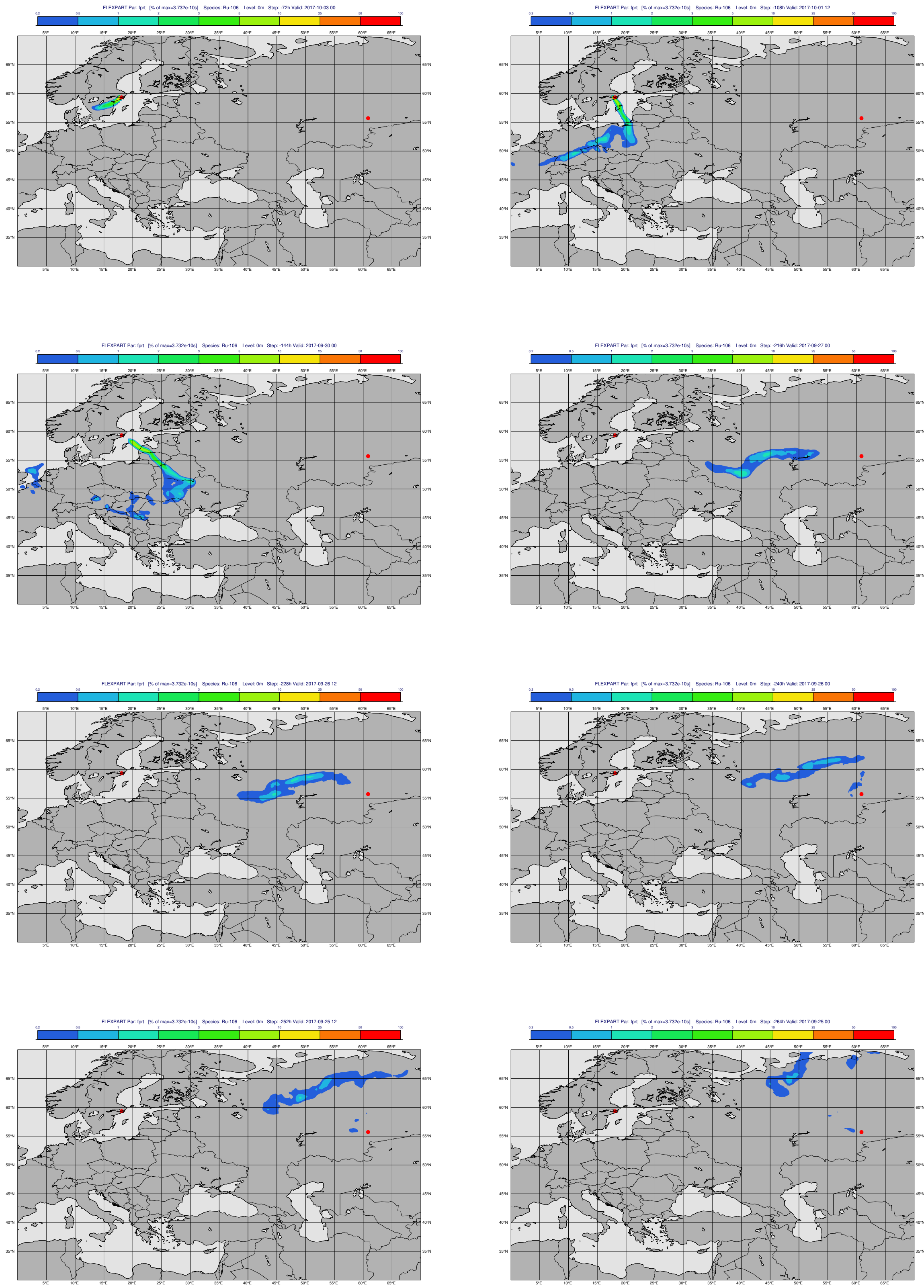

Figure 1: Backward tracking of measured data in Stockholm. The time steps visualized starting from upper left to lower right are: 2017-10-03h00, 2017-10-01h12, 2017-09-30h00, 2017-09-27h00, 2017-09-26h12, 2017-09-26h00, 2017-09-25h12 and 2017-09-25h00.

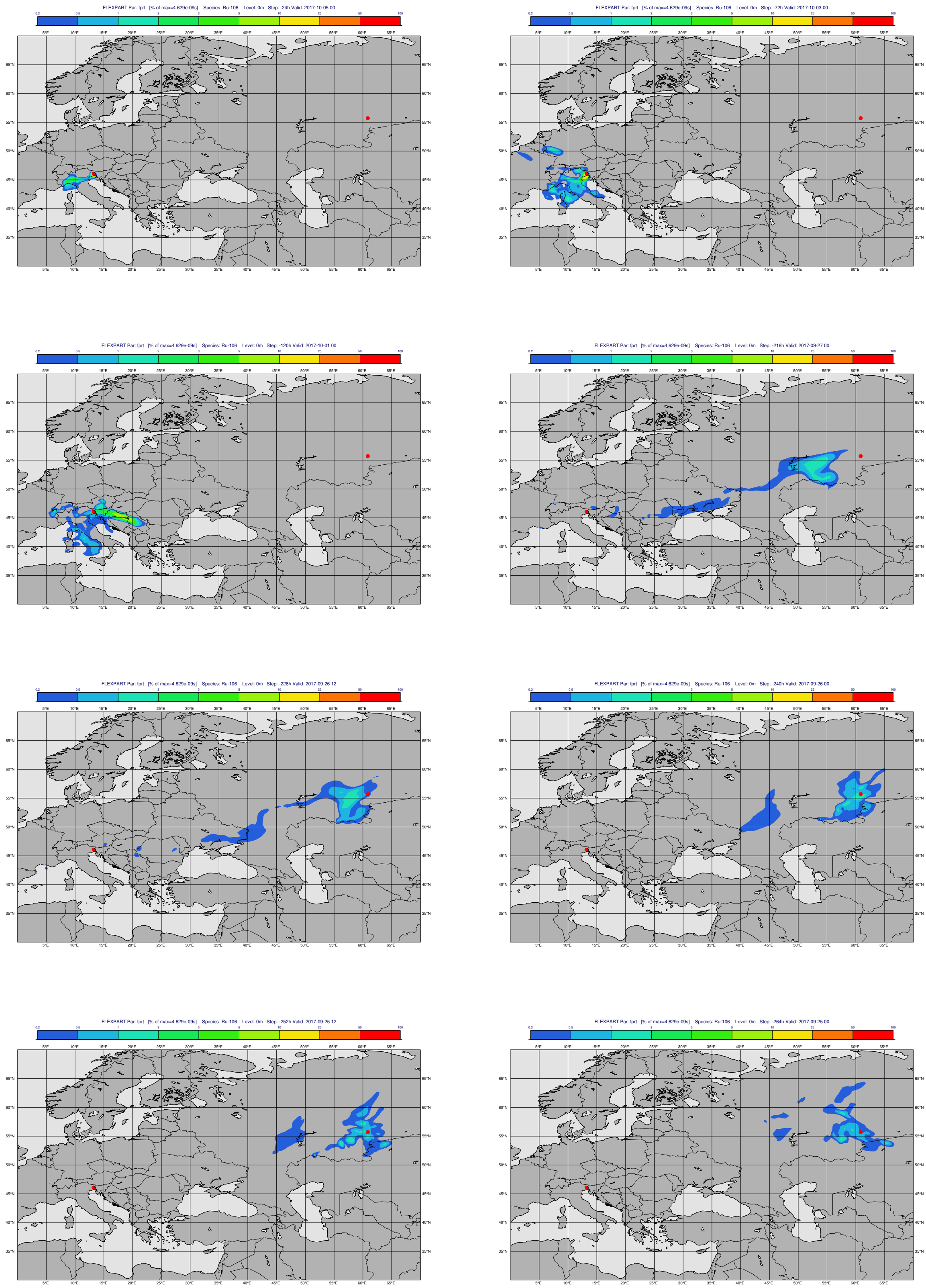

Figure 2: Backward tracking of measured data in Udine. The time steps visualized starting from upper left to lower right are: 2017-10-05h00, 2017-10-03h00, 2017-10-01h00, 2017-09-27h00, 2017-09-26h12, 2017-09-26h00, 2017-09-25h12 and 2017-09-25h00.

- **Duration.** We are interested in measurements that extend for short periods of time, especially when the concentration values are high, in order to capture local maxima of the moving cloud.
- **Consistency.** Differently from the selected above, many of the measurements do not clearly state the start and end time, making it difficult to properly define the value in time.

Among the selected values, the data coming from Stockholm and Udine have been used to perform the backward simulations and determine the original release point, while the data from Prague are only used to assess the forward simulations.

2.2 Backward simulation from a single origin

In order to establish the release location of the Ruthenium cloud FLEXPART can be used in backward mode to trace back the measured concentrations inverting the time and moving the cloud towards its original release point.
The backward simulation using only the data coming from the Stockholm station are shown in Figure 1. The release is split in three constant contributions, corresponding to the three measurements from Table 1, with an amplitude proportional to the measured value.
In the picture, Stockholm is marked with a red dot, together with Mayak, that has been a-posteriori indicated as the region of release. The pictures show the resident time at a given instant, that can be assimilated to the probability that a release at that given time and place will produce the expected concentrations in Stockholm at the measurement intervals. The trajectory of the cloud travels South of Stockholm and splits in different contributions, before heading East towards Mayak, that is reached around the beginning of the 26th of September. In the final part of the backward simulation, the cloud travels North towards the Arctic Sea.
In Figure 2 the equivalent process is demonstrated for Udine, using all the measured data from Table 1. Also in this case, Udine and Mayak are marked with a red dot. The cloud initially moves West, before coming back and enveloping the whole northern part of Italy. Starting from the 1st of October, the cloud starts to travel East before stationing in the Mayak region for more than 2 days. A smaller, separate cloud develops about 200 km West of the main one, with a probability far lower than the other.

2.3 Combined backward simulations

The use of a single source cannot be used to reliably determine the point of release, since the cloud evolves and expands covering a larger and larger part of the map with lower extrema, as can be seen in Figures 1-2.
In order to properly infer the origination point multiple backward simulations should be used. In particular, different types of combination of backward tracking give useful information that help in pinpointing the location of the release and the time interval in which it occurred.
In Figure 3 we can see the sum of the two contributions from Stockholm and Udine. Since all the effects that are simulated in FLEXPART are linear in the concentration, this is completely equivalent to perform a single backward simulation where both the Stockholm and Udine measurement points are taken into account simultaneously for the whole range of days in which those measurements are available. We can see in fact that the clouds are initially separated and resemble the shapes obtained in the single source location cases seen above. The two main clouds starting from the two locations start to merge at about the 29th of September and then travel together towards Mayak. The final state, at the beginning of the 25th of September, shows a large cloud that spans from Mayak up to the Arctic Sea, signaling that the release should have happened later in time. In fact, the maximum across Mayak is reached between the 26th of September at 12 and 24 hours before.
Figure 4 shows instead the *intersection* of the clouds generated by the two single measurement points. This combination of the two single sources gives a measure of the agreement on the point of origin between the two sets of data. In fact, the probability cloud is negligible in the first part of the

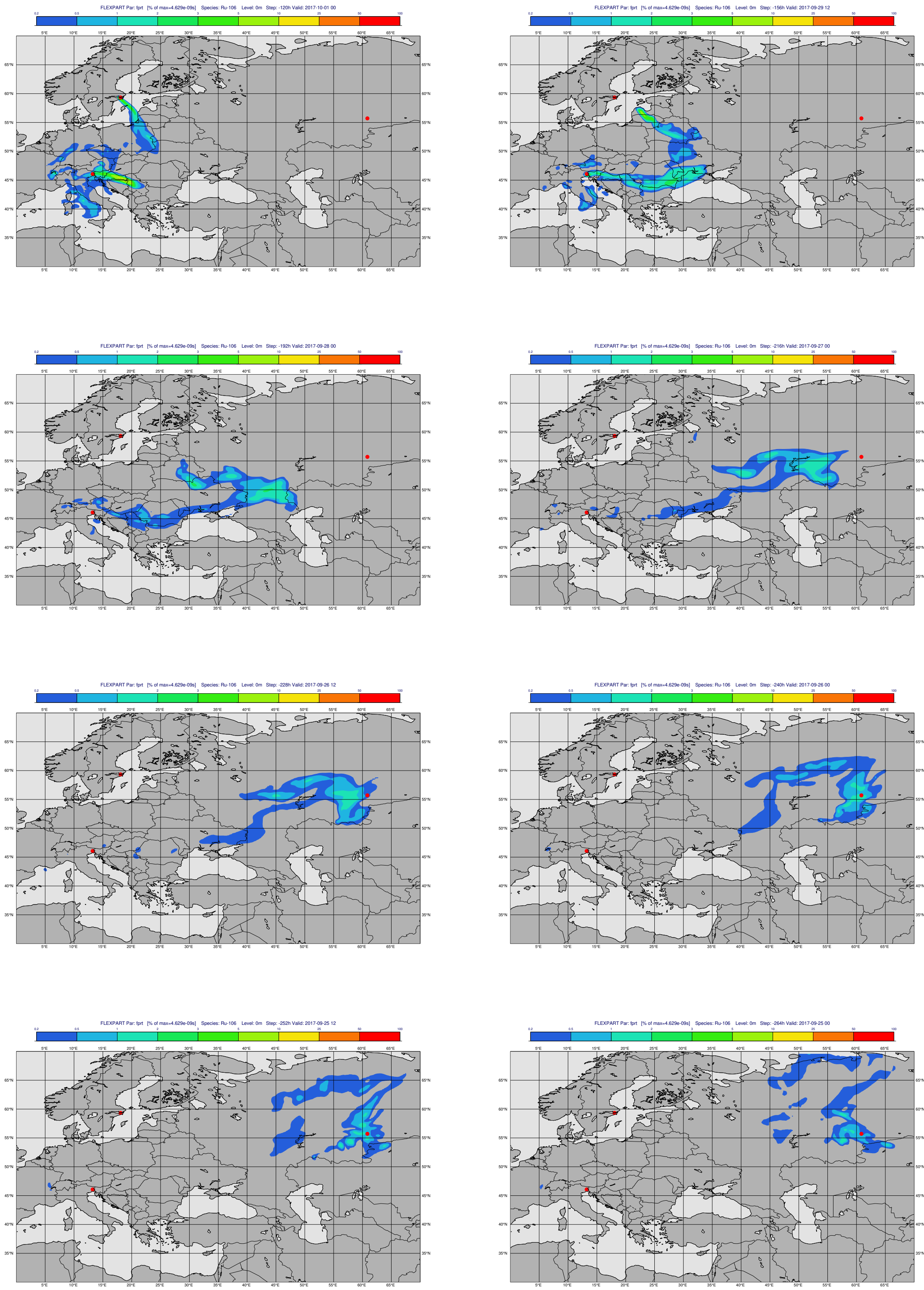

Figure 3: Combination by sum of backward trackings from Stockholm and Udine. The time steps visualized starting from upper left to lower right are: 2017-2017-10-01h00, 2017-09-29h12, 2017-09-28h00, 2017-09-27h00, 2017-09-26h12, 2017-09-26h00, 2017-09-25h12 and 2017-09-25h00.

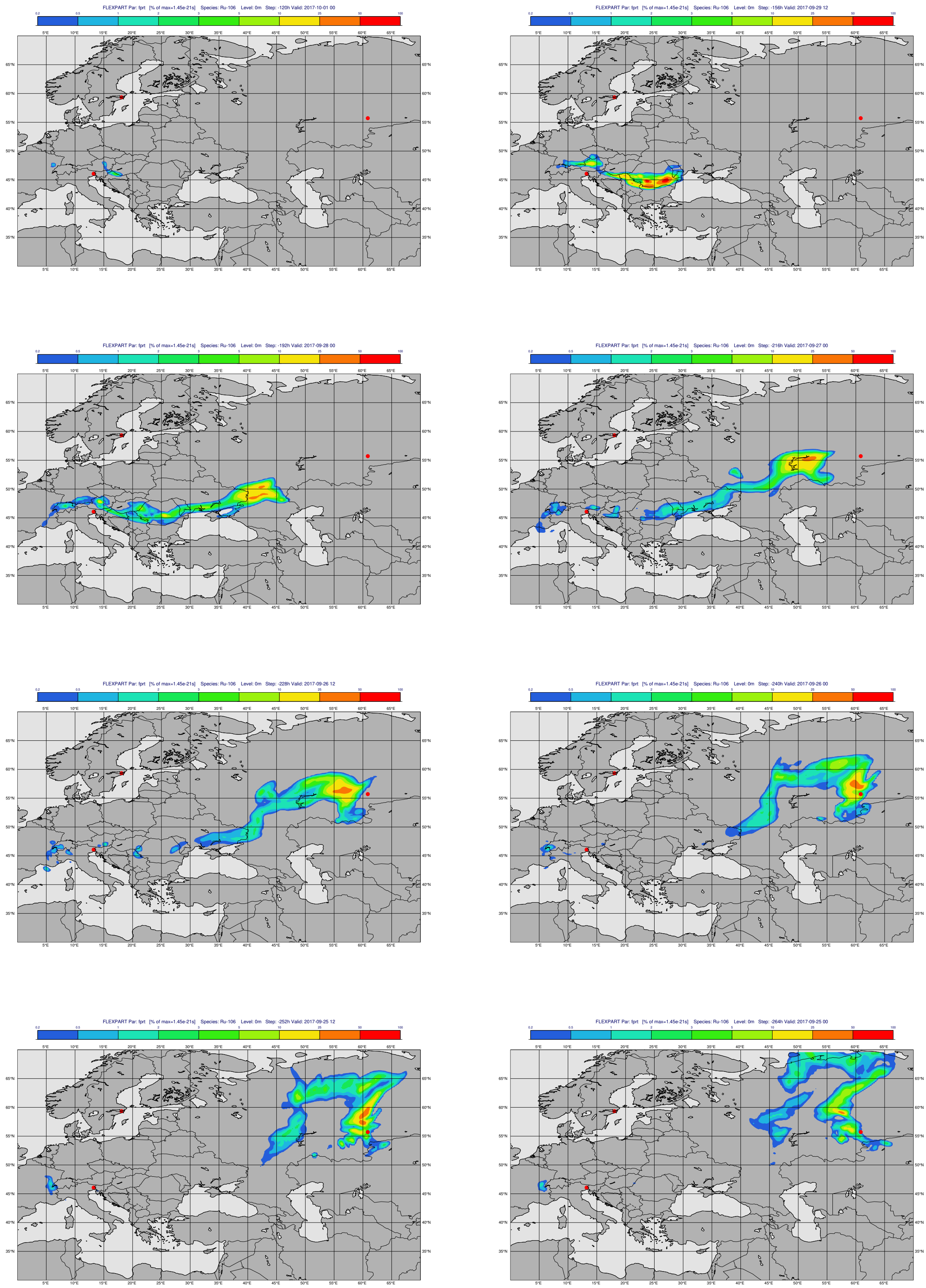

Figure 4: Combination by intersection of backward trackings from Stockholm and Udine. The time steps visualized starting from upper left to lower right are: 2017-10-01h00, 2017-09-29h12, 2017-09-28h00, 2017-09-27h00, 2017-09-26h12, 2017-09-26h00, 2017-09-25h12 and 2017-09-25h00.

simulations, when the two original clouds are away from each other, but starts to develop once the two touch each other, as specified for the previous figure. The combined cloud travels East showing a maximum in its eastern section that reaches Mayak just after 12 on the 26th of September. The maximum is almost stationary in the Mayak region for about 24 hours, and after that time it spreads North and does not show a single maximum, but a distributed cloud. This is a symptom of the fact that the two original clouds are now separating.
The combined use of additive (sum) and multiplicative (intersection) combinations, together with the knowledge of potential release sites, can pinpoint the release zone to the Mayak region with sufficient confidence. In addition, the residence time of the combination clouds can also establish a probable duration of the release.
Finally, the magnitude of the measurement at each location can be used to estimate the magnitude of the release, with what is generally referred to as *poor man's inversion* method. With this approach, the release concentration c_k, estimated from a single measurement k, is connected to the measured value S_{ijt} (where i and j identify the longitude and latitude of the measured value, while t identifies the time step) via the *Source-Receptor-Sensitivity (SRS)* M_{kijt} as

$$c_k = M_{kijt} \cdot S_{ijt}$$

The matrix M_{kijt} is exactly the result of the FLEXPART inverse simulation.
Using this approach, together with findings from other authors in [1, 2, 5], the source term can be estimated to be between 100 and 200 TBq. In the following simulations it is assumed that it is 150 TBq.

3 FORWARD SIMULATIONS BASED ON BACKWARD ANALYSIS

A way to verify the methodology adopted in the backward simulations is to perform a forward simulation of the estimated release source and duration and compare it to the measured data. The results of the previous section can therefore be used to set up a forward simulation with a release point set on Mayak. The source term is fixed at 150 TBq, as estimated in the previous section. The duration of the release is however not completely determined by the backward simulations: the release period can be pinpointed by the crossing of the probability cloud over Mayak, and it is included in the period between the 25th of September at 12 and the 26th at the same time.
In order to assess properly the release period, three possible scenarios are considered:

A) 12 hours release between 2017-09-25h12 and 2017-09-26h00;

B) 6 hours release between 2017-09-25h18 and 2017-09-26h00;

C) 12 hours release between 2017-09-26h00 and 2017-09-26h12;

The three releases are selected in order to establish the duration of the release, by comparing case A and B, and the starting point, by comparing A and C (that share also the duration of the release) together with B (that has a shorter release duration but a starting point in-between the other two).
The air concentration of Ruthenium for case C are shown in Figure 5. The cloud develops in the Mayak region in the early phase and starts to move West while staying compact in the first phase. During the 29th the spreading of the cloud becomes more consistent, with a clear elongation in the east-West direction. On the 2nd of October the cloud reaches the measurement points (marked by a red dot in the figure) of Udine and Prague, in agreement with the measured data. In the following days the cloud spreads North, reaching the third measurement point in Stockholm. The cloud is mainly spread in the North-South direction in the final days, with a tail the develops towards East over the Mediterranean Sea.
The simulation results for case A and B are qualitatively very similar to case C shown in Figure 5 and are not shown in details for the sake of brevity. The overall behavior of the concentration cloud

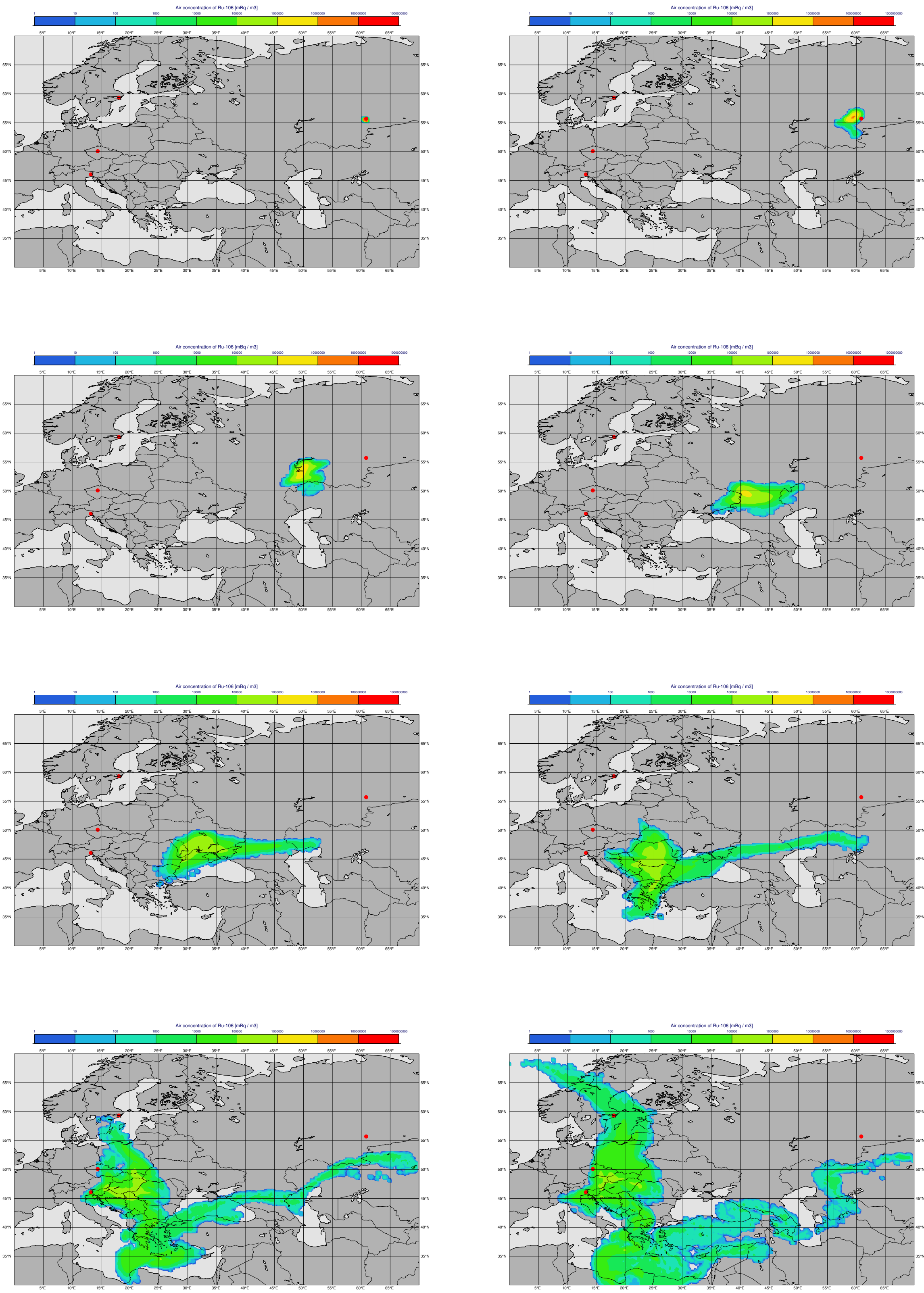

Figure 5: Air concentration of Ru-106 over Europe for case C. The time steps visualized starting from upper left to lower right are: 2017-09-26h12, 2017-09-27h12, 2017-09-28h12, 2017-09-29h12, 2017-09-30h12, 2017-10-01h12, 2017-10-02h12 and 2017-10-03h12.

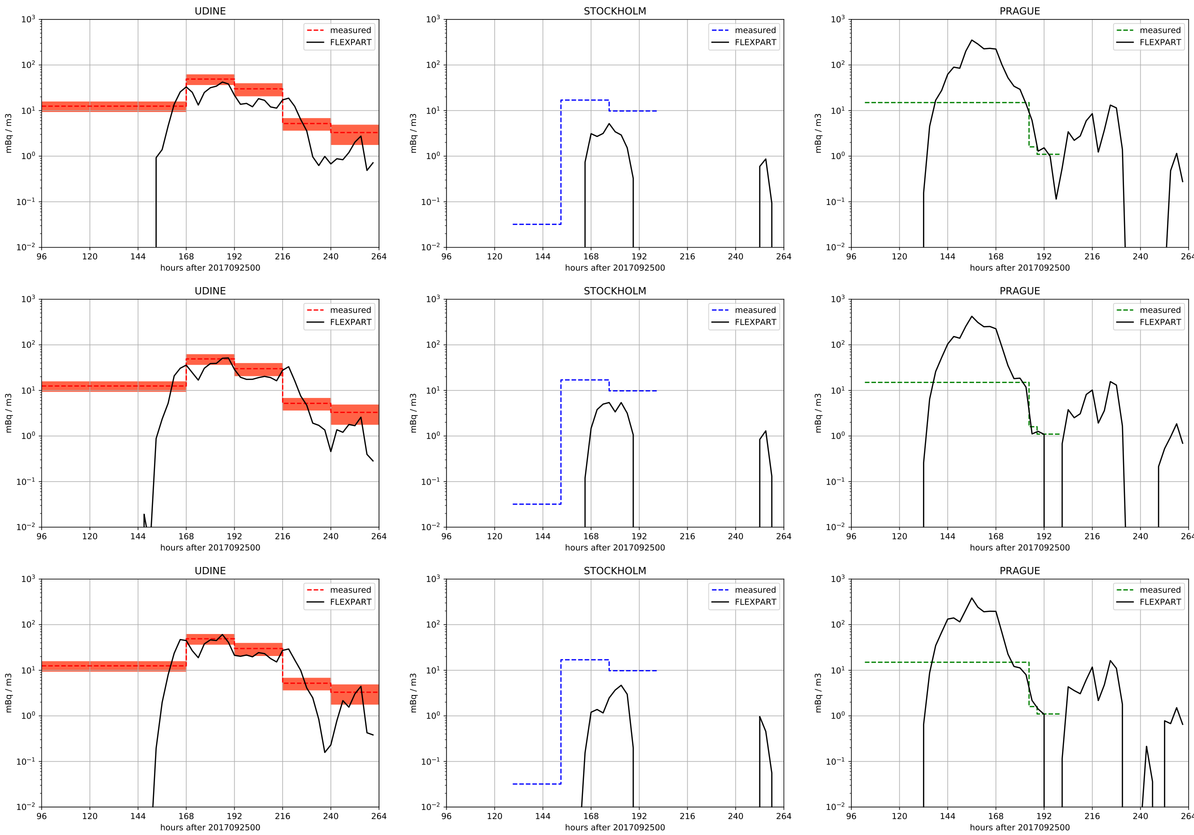

Figure 6: Comparison between measured data (colored) and simulation results (black) for the three cases A, B and C, from top to bottom respectively. When available, measurement uncertainty is reported as a colored stripe.

is not particularly affected by the release duration or initial point, as we will see in the following paragraph.

The forward simulation can be interpolated precisely in the three location marked on the map in order to quantitatively compare the forward simulations with the measured data. The comparison between simulation results and measurements can be seen in Figure 6. First of all, we can see that the three cases A, B, C produce concentration values in the three locations that are very similar. This is a symptom of the fact the meteorological data for the given period lead to a compact cloud near the source that starts moving West at the same time independently (within the given range) of the release starting time and duration. The simulation has in fact a very low sensitivity to this two parameters.

On the other side, we can see that the magnitude of the release, especially for Udine and the first days with measurements in Prague, is quite accurate. The first measurement in Udine spans multiple days and does not catch accurately the arrival time of the cloud, that seems to be in the last half a day of that measurement. The simulation predictions for Stockholm underestimate the measured values in the whole range. This is probably due to the fact the trajectory towards Stockholm is the longest of the ones that have been considered, leading to a larger uncertainty on the result. Prague has not been used in the backward simulations and it is here introduced as an a-posteriori verification of the approach. We can see that the forward simulations correctly predict the arrival time of the cloud, if we take into account the temporal extension of the first measurement. Similarly to Udine, the arrival time was not accurately captured since in normal conditions the measurements are done only once a week. It is worth noting that the FLEXPART simulations predict high value of concentration even after the measured ones. This is also a sign that the uncertainty in the spread of the cloud becomes larger and larger as the day progress, as we have seen for Stockholm.

4 CONCLUSIONS

This paper presented ENEA studies on the Ruthenium-106 unexplained measurements detected over Europe in the fall of 2017. The approach, based on the backward modeling of the Lagrangian atmospheric code FLEXPART, is capable of tracing back the measured concentration from multiple location and recover the point of origin, release interval and magnitude of the source term with a good degree of accuracy when compared with similar methodologies presented by other authors.
Some direct simulations have also been performed in order to quantify the error in the predicted source term when compared to measured data. The result show good performance in particular for the city of Udine, while the results for Stockholm and Prague are not as satisfactory.
These results confirm that the model can be improved, especially in resolution and quality of the meteorological data, that play a fundamental role in the determination of the cloud trajectory and dispersion. The future plan is, in fact, to improve the meteorological data leveraging the newly available ECMWF data with resolutions up to 0.05°.

ACKNOWLEDGEMENTS

The authors would like to acknowledge the ECMWF for providing the meteorological data that have been used in all the simulations in this paper.

REFERENCES

[1] *Detection in October 2017 of Ruthenium 106 in France and in Europe: Results of IRSN's investigations*. 2018. URL: https://www.irsn.fr/EN/newsroom/News/Pages/20180206_Detection-in-October-2017-of-Ruthenium-106-in-France-and-in-Europe-Results-of-IRSN-investigations.aspx.

[2] J. H. Sørensen. "Method for source localization proposed and applied to the October 2017 case of atmospheric dispersion of Ru-106". In: *Journal of Environmental Radioactivity* 189 (2018), pp. 221–226.

[3] V. Shershakov and R. Borodin. "Some results of determining the source and reasons for the appearance of 106Ru in Russia in September-October 2017". In: *IOP Conference Series: Materials Science and Engineering*. Vol. 487. 1. IOP Publishing. 2019, p. 012002.

[4] N. Maffezzoli et al. "The Ruthenium-106 plume over Europe in 2017: a source-receptor model to estimate the source region". In: *Atmospheric Environment* 212 (2019), pp. 239–249.

[5] O. Masson et al. "Airborne concentrations and chemical considerations of radioactive ruthenium from an undeclared major nuclear release in 2017". In: *Proceedings of the National Academy of Sciences* 116.34 (2019), pp. 16750–16759.

[6] I. Penev et al. "106 Ru aerosol activity observation above southeast europe in October 2017". In: *Comptes Rendus de L'Academie Bulgare des Sciences* 71.5 (2018), pp. 613–618. DOI: 10.7546/CRABS.2018.05.04.

[7] A. Stohl et al. *The Lagrangian particle dispersion model FLEXPART version 9.3*. Tech. rep. Tech. rep., Norwegian Institute of Air Research (NILU), Kjeller, Norway, 2010.

[8] A. Stohl, M. Hittenberger, and G. Wotawa. "Validation of the Lagrangian particle dispersion model FLEXPART against large-scale tracer experiment data". In: *Atmospheric Environment* 32.24 (1998), pp. 4245–4264.

[9] A. Stohl and D. J. Thomson. "A density correction for Lagrangian particle dispersion models". In: *Boundary-Layer Meteorology* 90.1 (1999), pp. 155–167.

[10] A. Stohl et al. "The Lagrangian particle dispersion model FLEXPART version 6.2". In: *Atmospheric Chemistry and Physics* 5.9 (2005), pp. 2461–2474.

[11] I. Pisso et al. "The Lagrangian particle dispersion model FLEXPART version 10.3". In: *Geosci. Model Dev. Discuss* (2019), in review.

[12] P. Seibert and A. Frank. "Source-receptor matrix calculation with a Lagrangian particle dispersion model in backward mode". In: *Atmospheric Chemistry and Physics* 4.1 (2004), pp. 51–63.

[13] D. P. Dee et al. "The ERA-Interim reanalysis: Configuration and performance of the data assimilation system". In: *Quarterly Journal of the royal meteorological society* 137.656 (2011), pp. 553–597.

[14] ARPA Friuli Venezia Giulia. *Presenza di Rutenio 106 in aria*. 2017. URL: http://www.arpa.fvg.it/cms/tema/radiazioni/radioattivita/radiazioni-artificiali/dati_ambientali/Rutenio-_06_ottobre_2017.html.

[15] ISIN. *Misure di Rutenio-106 effettuate in Italia nel particolato atmosferico*. 2017.

Specification and Continuation of the Provisions of the Radiation Protection Act Relating to Emergency Protection in Subordinate Regulations

F. Meinerzhagen, M. Sogalla, A. Artmann, S. Holbein, E. Mühr-Ebert, I. Petermann, and T. Stahl

GRS gGmbH, Schwertnergasse 1, 50667 Cologne, Germany

Abstract:

In this contribution, the challenges in the preparation process of the German federal emergency plans for radiological and nuclear emergencies will be presented. The implementation of Directive 2013/59/EURATOM into German law by the Radiation Protection Act (StrlSchG) is accompanied by a reorganization of the structures of emergency preparedness and response. Relevant challenges are taken into account such as the nuclear power phase-out with an associated long-term decline expected in competencies in the field of nuclear technology and radiation protection at *Länder* level due to the abolition of supervisory duties. Furthermore, the state of the art of science and technology as well as lessons learned from the reactor accident in Fukushima are included in the process. During the revision of existing subordinate regulations and newly introduced regulations, various issues must be dealt with. These regulations include in particular the emergency plans to be drawn up at federal and *Länder* level. The federal emergency plans are to be incorporated into German regulation as general administrative provisions. Examples for the preparation process of such plans on the basis of the drafts of the general federal emergency plan and the special federal emergency plan "Waste and Sewage" will be presented.

1 INTRODUCTION

The Council Directive 2013/59/Euratom of 5 December 2013 (EU BSS) [1] laid down basic safety standards for protection against the dangers arising from exposure to ionising radiation. Among the main innovations of the directive requirements for the national emergency management system and increased cooperation between all member states for the purpose of uniform action in the event of an emergency are detailed. This directive had to be transposed into national law by the member states within four years.

The transposition of Directive 2013/59/Euratom into German law and the decision to phase out nuclear power generation in Germany, as a result of which the *Länder* will substantially reduce their powers to assess the radiological situation, necessitated the revision of the legal framework and the organization of the German emergency management system. This led to the enactment announced in June 2017 of the Act on the Reorganisation of the Law on Protection against the Harmful Effects of Ionising Radiation [2]. In the course of this, several ordinances and laws in Germany (including the Radiation Protection Ordinance and the Precautionary Radiation Protection Act) were combined into the Radiation Protection Act (StrlSchG). The Radiation Protection Act reflects international developments in radiation protection and lessons learned from the accident in Fukushima. In particular, recommendations of the Radiation Protection Commission (SSK) were implemented [3]. Part of reorganization of the emergency management system for nuclear and radiological emergencies are the elaboration of federal and *Länder* emergency plans and the establishment of a federal radiological situation centre.

2 EMERGENCY MANAGEMENT SYSTEM IN GERMANY

The German emergency management system is characterised by its federal structure. Emergency preparedness and response function as an interplay of federal, *Länder* and municipal authorities. According to the German Basic Law, the Federal Government has the exclusive legislation for protection against dangers arising from ionising radiation [4]. The execution of the federal laws regarding nuclear safety and radiation protection as part of the emergency preparedness and response in Germany is the responsibility of the *Länder* on behalf of the Federal Government.

In accordance with Directive 2013/59/Euratom, the framework for external emergency preparedness and response is referred to in the Radiation Protection Act as the emergency management system of the Federal Government and the *Länder*. In addition to the Radiation Protection Act and its ordinances, the emergency management system is based on the general legal provisions of the Federal Government and the *Länder*, which serve to avert dangers to human health, the environment or public safety.

A central recommendation of the SSK was to establish a national radiological situation centre. In accordance with the Radiation Protection Act, the Federal Radiological Situation Centre (RLZ) commenced operations in October 2017. The RLZ is managed by the emergency organisation of the Federal Ministry for the Environment, Nature Conservation and Nuclear Safety (BMU) and is supported by the Federal Office for Radiation Protection (BfS), the Federal Office for the Safety of Nuclear Waste Management (BfE), the technical safety organization Gesellschaft für Anlagen- und Reaktorsicherheit gGmbH (GRS) and the Federal Office of Civil Protection and Disaster Assistance (BBK). The tasks of the RLZ include the monitoring, assessment and reporting of the radiological situation, in the area of communication and coordination (protective measures, information of the population, and preparation of recommendations for protective measures). The RLZ coordinates the emergency response within the Federal Government and with the *Länder* as well as internationally, as long as no other responsibility has been specified.

For supra-regional and regional emergencies, the evaluation of the radiological situation by all federal and *Länder* authorities is always based on one common radiological situation report. The report contains information on the appropriateness of measures from a radiological point of view, which should result from the information in the catalogue of measures to be drawn up.

The Radiation Protection Act provides for the preparation of coordinated emergency plans of the Federal Government and the *Länder*, which represent the processes and responsibilities during the emergency response. These emergency plans are currently being prepared and will be reviewed regularly and, if necessary, adjusted to the state of the art in science and technology or a change in the legal situation. In addition to findings from the emergency exercises or the national and international exchange, experiences from real emergencies in Germany or abroad are also taken into account. The general federal emergency plan will contain i.a. a catalogue of reference scenarios including optimised protection strategies to be considered in emergency planning. In addition, special federal emergency plans are being prepared which describe the emergency response in the affected legal areas and in administrative areas outside radiation protection. The emergency plans of the federal government are adopted as general administrative regulations.

The general emergency plan is substantiated by special emergency plans for specific administrative and economic sectors (e.g. agriculture, food and feed, contaminated products, objects and waste, transport). The *Länder* also establish general and specific emergency plans that will put the federal plans in concrete terms and complement them as far as the *Länder* are responsible for planning or implementing protection measures.

According to a transitional provision, the corresponding provisions and descriptions in general administrative regulations, SSK recommendations and other planning documents mentioned in Annex 4 of the Radiation Protection Act are provisionally regarded as federal emergency plans until these new emergency plans of the Federal Government are enacted or until the legal ordinances on emergency precautions provided for in the Radiation Protection Act are passed.

3 FEDERAL EMERGENCY PLANS

3.1 General Federal Emergency Plan

Pursuant to the Radiation Protection Act, the general and special emergency plans of the Federal Government and the *Länder* and the external emergency plans, together with their regulations and presentations already coordinated before the occurrence of the emergency, enable the authorities and organisations involved in the emergency reaction to make coordinated decisions immediately in the event of an emergency and to implement appropriate protective measures. For this purpose, the emergency plan contains binding administrative regulations for federal and *Länder* authorities.

The general federal emergency plan is elaborated by the BMU and coordinated with other federal and *Länder* authorities. The plan will contain a catalogue of reference scenarios including optimised protection strategies to be considered in emergency planning. The plan is based on the principle that the authorities that perform emergency response tasks in everyday business in the implementation of federal laws also retain this responsibility and competence in the case of radiological emergencies (so-called sector interlinking approach).

The BMU commissioned BfS and GRS to prepare suitable reference scenarios, with BfS taking the lead. The reference scenarios serve as a common basis for their planning of appropriate responses to these and other possible emergencies. Ten categories for possible accident scenarios were developed and a risk analysis was carried out [5]. These scenarios will be included in the current draft of the general federal emergency plan. The following scenarios are covered:

- German nuclear power plant,
- Nuclear power plant in neighbouring countries,
- Nuclear power plant in Europe,
- Nuclear power plant outside Europe,
- Nuclear installation or facility other than a nuclear power plant,
- Terrorist or otherwise motivated offence,
- Transport accident,
- Emergency in connection with the handling of radioactive materials,
- Satellite crash, and
- Case of defence or state of tension.

Further content of the emergency plan will be a phase classification. This is based on SSK recommendations on the phase model after a nuclear accident and the phase classification [6], [7].

The coordination processes between the several Federal and *Länder* authorities associated with the preparation of emergency plans provide new insights in connection with the ordering and implementation of protective measures. Furthermore, the emergency plans will contain innovations resulting from the SSK recommendations after the reactor accident in Japan and the associated lessons. This includes among others:

- Specific planning in relevant subject areas such as waste management, in the food and feed sector or in drinking water production outside the previous comprehensive disaster control planning,
- Extension of emergency planning from planning for an accident event in a national nuclear power plant to reference scenarios for various radiological events,
- Extension of the planning by taking into account the probability of occurrence and potential effects of an accident with an associated adjustment of planning radii, and

- Consideration of the transition from an emergency exposure situation to an existing exposure situation.

Part of the planning is to lay down the decision-making process for measures to protect the population and the emergency forces as well as a description of the responsibilities in the federal system.

Optimised strategies for the protection of the population and the emergency forces are described in the general federal emergency plan for each reference scenario. The optimised strategies include in particular the following topics:

- Dose levels, which serve as a radiological criterion for the adequacy of certain protective measures,
- Criteria for alerting and for taking certain protective measures (triggering criteria),
- Limit or guideline values relating to specific, directly measurable consequences of the emergency, e.g. dose rates, contamination levels or activity concentrations.

In addition, the general federal emergency plan includes requirements for reviewing and adapting the protection strategy and measures to the evolving radiological situation and changes in other relevant circumstances of the emergency, including criteria and procedures for the lifting of protective measures.

3.2 Special Federal Emergency Plan „Waste and Sewage"

The Radiation Protection Act contains requirements for the management of waste which is contaminated as a result of emergencies as well as the construction and operation of facilities to be provided for this purpose. Corresponding regulations are to be presented in a special federal emergency plan. The implementation of the special emergency plan "Waste and Sewage" poses complex technical and administrative requirements, some of whose bases for assessment still have to be worked out.

At national level, measures for waste disposal after radiological emergencies are summarised in the "Catalogue of Measures" (SSK recommendation "Overview of measures to reduce radiation exposure after events with not inconsiderable radiological effects" [8]). The focus is on the disposal or recycling of agricultural products that can no longer be marketed. At the European level, the EURANOS Handbook is an analogue to the German catalogue of measures [9]. It contains detailed information on decontamination techniques with regard to achievable decontamination factors and waste produced.

A prototype draft of the plan was prepared by GRS [10]. The following optimisation objectives have been set out in this draft:

(1) The radiation exposure of the population and the emergency response forces in areas affected by the emergency and caused by the handling of waste shall be kept as low as possible by appropriate measures below the relevant reference values taking into account all circumstances of the respective emergency.

(2) The disposal of waste from contaminated areas outside these areas should not contribute significantly to the radiation exposure of the local population.

(3) The uncontrolled spread of contaminated waste from areas affected by emergencies to other areas should be prevented by appropriate measures.

(4) The maintenance or restoration of social and economic life in affected areas should be impaired as little as possible by the measures taken.

These objectives result in balancing principles for the elaboration of the emergency plan. The current draft foresees the following regulations:

- The waste resulting from an emergency exposure situation can be treated and disposed of as normal household or commercial waste if compliance with the 1st optimisation target is ensured. Otherwise, it must be classified as contaminated waste and treated and disposed of separately.

- Waste that is produced in contaminated areas in households and by industry should generally be treated and disposed of as ordinary household or industrial waste.
- The mass and volume of contaminated waste resulting from an emergency exposure situation shall be kept as low as possible by appropriate measures, taking into account all circumstances of the respective emergency.
- Wastes from contaminated areas are generally to be disposed in these areas. They may only be disposed outside these areas if they are either not significantly higher contaminated than waste that does not originate from affected areas or if their safe disposal outside the affected areas is ensured by provisions that prevent a significant contribution to the radiation exposure of the local population. In the latter case, their disposal path and whereabouts are to be documented.

In the framework of the project 3618S62575 “Development of a detailed waste inventory from a radiological point of view for all reference scenarios described in the general federal emergency plan for the preparation of the special emergency plan”, extensive databases for conventional waste with regard to a contamination due to nuclear or radiological emergencies are prepared. The standard classification of waste, such as household, commercial or biodegradable components as well as recyclable fractions, is re-evaluated with regard to the correlation of land utilization and waste accumulation, as well as links between radioactive contamination of land and objects. With an increased spatial resolution, data of land utilization from CORINE (Coordination of Information on the Environment) and test data sets of radiation exposure after nuclear accidents from RODOS (Realtime Online Decision Support System for nuclear emergency management) will be merged and prepared for a comprehensive database for further use in geographic information systems. Additional steps include a re-evaluation of decontamination methods and a possible scheme for an estimation technique to evaluate contamination mechanisms with respect to surface areas and object masses as well as different time factors.

4 CONCLUSION

The implementation of Directive 2013/59/EURATOM into German law is accompanied by a reorganization of the structures of emergency preparedness and response. The Radiation Protection Act provides for the preparation of coordinated emergency response plans for radiological and nuclear emergencies of the Federal Governement and the *Länder*, which represent the processes and responsibilities during the emergency response. The federal emergency plans are to be incorporated into German regulation as general administrative provisions. In drawing up the plans, particular account is taken of the country’s federal structure and the consequences of the imminent nuclear phase-out.

The general federal emergency plan is based on the principle that the authorities performing emergency response tasks in everyday business in the implementation of federal laws also retain this responsibility and competence in the case of radiological emergencies. This so-called sector interlinking approach requires the involvement of several federal and state authorities in the development of optimised protection strategies for each of the reference scenarios. Further challenges in the context of the preparation process of the plan include the consideration of the recently formed federal radiological situation centre and the content and structure of the radiological situation report.

The general emergency plan is substantiated by special emergency plans for specific administrative and economic sectors (e.g. agriculture, food and feed, contaminated products, objects and waste, transport). The estimation of the amount of conventional waste that has been contaminated due to the emergencies represents a specific challenge in the preparation process of the special federal emergency plan “Waste and Sewage”.

5 REFERENCES

[1] Council of the European Union: Council Directive 2013/59/Euratom of 5 December 2013 laying down basic safety standards for protection against the dangers arising from exposure to ionising radiation, and repealing Directives 89/618/Euratom, 90/641/Euratom, 96/29/Euratom, 97/43/Euratom and 2003/122/Euratom (2014).

[2] Deutscher Bundestag: Gesetz zur Neuordnung des Rechts zum Schutz vor der schädlichen Wirkung ionisierender Strahlung (2017).

[3] Strahlenschutzkommission: Weiterentwicklung des Notfallschutzes durch Umsetzen der Erfahrungen aus Fukushima, Empfehlung der Strahlenschutzkommission (2015).

[4] Grundgesetz für die Bundesrepublik Deutschland.

[5] Bundesamt für Strahlenschutz: 4. Zwischenbericht zum BMUB-Erlasses „Szenarien für die Notfallschutzplanung" – Schutzstrategien, (Entwurf, BfS/SW 2.2, Stand 31.07.2017)

[6] Strahlenschutzkommission; Radiologische Grundlagen für Entscheidungen über Maßnahmen zum Schutz der Bevölkerung bei Ereignissen mit Freisetzungen von Radionukliden; Empfehlung der Strahlenschutzkommission (2014).

[7] Sogalla, M.; Büttner, U.; Schnadt, H.: Generalisierte Konzepte für Maßnahmen bei nuklearen und radiologischen Notfällen, Gesellschaft für Anlagen- und Reaktorsicherheit (GRS) gGmbH, GRS-370, 121 S., ISBN 978-3-944161-51-8; Köln (2015).

[8] Strahlenschutzkommission: Übersicht über Maßnahmen zur Verringerung der Strahlenexposition nach Ereignissen mit nicht unerheblichen radiologischen Auswirkungen (Maßnahmenkatalog), Berichte der Strahlenschutzkommission, Heft 60 (2010).

[9] Generic handbook for assisting in the management of contaminated inhabited areas in Europ following a radiological emergency, EURANOS(CAT1)-TN(09)-03 (2010).

[10] Sogalla, M.; Meinerzhagen, F.; Holbein, S.; Stahl T.: Fachliche Unterstützung bei der Umsetzung der Anforderungen an den nuklearen Notfallschutz der Richtlinie 2013/59/Euroatom (EU Basic Safety Standards, EU BSS) im deutschen Regelwerk, Abschlussbericht zum Vorhaben 3615S62544, Gesellschaft für Anlagen- und Reaktorsicherheit (GRS) gGmbH, GRS-A-3943; Köln (2018).

Intercomparison of PERSAN 4 and RASCAL 4.3 Source Term evaluations for a PWR LOCA Scenario

A. Guglielmelli[*], A. Cervone[*], F. Rocchi[*], V. Creach[**], G. Ortega Nicaise[**]

[*]Italian National Agency of New Technologies, Energy and Sustainable Economic Development, FSN-SICNUC-SIN, Via Martiri di Monte Sole 4, 40129 Bologna (BO), Italy
[**]Institut de Radioprotection et de Sûreté Nucléaire, 31 Avenue de la Division Leclerc, 92260 Fontenay-aux-Roses, France

Abstract:

In the last few years, ENEA is improving its skills in the field of Emergency Preparedness and Response (EP&R) with the aim to be able to provide timely and accurate Source Term and radiological consequences (RC) information to national stakeholders. The presence at less than 200 km from Italian national borders of 25 Nuclear Power Plants (NPPs) (i.e. the so call neighboring reactors), highlighted the importance of a reliable estimation of the potential consequences in terms of radiological impact and its geographical distribution of a hypothetical severe accident within a reasonable time (~ 2 ÷ 6 hours). Typical best-estimate SA integral codes are not suitable for this aim during emergencies, because the necessary time and amount of information are definitely too large. The approach currently in use is to apply so-called “fast-running” codes, which can provide answers in the time-frame of a few minutes and with a minimum amount of information, allowing then also parametric analyses and/or improvements of the estimates as soon as new or updated data are available from an NPP. However, the difficulty to have a reliable assessment of the accident progression due to the different methods and options used by different dedicated fast-running codes, significantly affect the ability to provide timely, accurate and coherent information to national stakeholders. Aim of this paper is to perform an intercomparison of the Source Term (ST) results provided by PERSAN 4 and RASCAL 4.3 fast-running codes to evaluate the possible differences between the answers provided by these two tools. The severe accident sequence used for the analysis was proposed in a real-time exercise held in Vienna within the FASTNET Euratom project and is based on a LOCA scenario at a 900 MWe PWR.

After a general description of the accident sequence and the key features of the two codes, three ST requests are defined. The main calculation assumptions introduced in the two codes for these requests are then discussed. The results obtained are then compared for both total and time-dependent STs. The cases of the relevant nuclides I-131 and Cs-137 are also discussed. A rather good agreement between the two codes has been found for this sequence, also taking into due account the differences in initial core inventories and in accidental phenomena modeled by the two fast-running codes. In the Conclusions paragraph, general remarks on the application of the two codes are given.

1 SCENARIO DESCRIPTION

Within the frame of the FASTNET Euratom Project, during the Exercise 2 of the WP4 held in Vienna, IRSN provided information regarding the development of a hypothetical severe accident at the Gravelines NPP to carry out the exercise. The information has been made available in the form of periodic messages (i.e., every 1/4 hours) provided by IRSN and derived from the automatic information acquisition system of SESAME 4.0, the IRSN suite of fast-running codes and tools for ST evaluation. According to the exercise requests, three ST evaluations at different times had to be provided.

1.1 NPP information

The affected plant specified in the exercise was the Gravelines NPP located in the north of France, approximately 20 km from Dunkerque and Calais. The site hosts 6 nuclear reactors of

900 MWe each, of CP1 type. Gravelines is the most important NPP with regard to the overall annual electricity production and reactor number. In 2017, the entire reactors fleets of the plant produced 31.5 billion KWh [1].

1.2 State of the Unit at the beginning of the hypothetical accident

On 22/02/2019 at 07:00 Gravelines Unit 11[1] was in operation at full power (100% NP) since at least the previous 48 hours, with a boron concentration of 14 ppm and a primary activity of 1 GBq/t I131 equivalent. At 07:15, a fire start was confirmed in the electrical building (fire sector #L391). Fire reached and destroyed several train B electrical panels; consequently, the electrical train B was shutdown and all train B safety systems were not available. At this time, the operators applied the Standard Operation Procedures (SOPs). Two further equipments were under repair: the train A Containment Spray System (CSS) pump (EAS001PO), scheduled by the operator to restart at 14:00, and the train A Chemical Volume & Control System (CVCS) charging pump (RCV001PO), which was disassembled and couldn't be restarted. Since 08:27, a pressure increase in the reactor building was observed.

1.3 Core inventory

To evaluate the effect on the ST of the possible differences in the initial core activity between the two fast running codes, an analysis of the different core inventories used by RASCAL 4.3 and PERSAN 4 is here reported. The core inventory used by PERSAN 4 is that of an optimized core with the GARANCE MOX fuel hybrid management, based on Blayais NPP Unit 1, Cycle 23, at EOL. The core inventory adopted in the RASCAL 4.3 is a default one for a PWR reactor, and is obtained through scaling with the thermal power (in this case, 2785 MWth) [2]. Table 1 reports the comparison between the activity of those nuclides included in both PERSAN and RASCAL inventories.

Table 1: Core activity – RASCAL 4.3 vs PERSAN 4

Radionuclide	Activity (PERSAN)	Activity (RASCAL)	Var	Radionuclide	Activity (PERSAN)	Activity (RASCAL)	Var
(-)	(Bq)	(Bq)	(%)	(-)	(Bq)	(Bq)	(%)
Ba-139	4.95E+18	4.87E+18	1.50	Ru-103	4.31E+18	4.47E+18	-3.56
Ba-140	4.76E+18	4.90E+18	-2.90	Ru-105	3.13E+18	3.15E+18	-0.62
Ce-141	4.55E+18	4.52E+18	0.66	Ru-106	1.46E+18	1.60E+18	-8.34
Ce-143	1.77E+17	4.12E+18	-95.71	Sb-127	2.51E+17	2.46E+17	1.91
Ce-144	3.36E+18	3.65E+18	-8.00	Sb-129	8.42E+17	8.94E+17	-5.90
Cm-242	2.33E+17	1.15E+17	101.88	Sr-89	2.53E+18	2.48E+18	1.68
Cs-134	3.42E+17	4.83E+17	-29.14	Sr-90	1.77E+17	2.46E+17	-28.30
Cs-136	1.64E+17	1.54E+17	6.72	Sr-91	3.20E+18	3.10E+18	3.23
Cs-137	2.57E+17	3.35E+17	-23.40	Sr-92	3.62E+18	3.34E+18	8.56
I-131	2.68E+18	2.75E+18	-2.73	Tc-99m	4.52E+18	4.50E+18	0.46
I-132	3.87E+18	4.00E+18	-3.31	Te-127	2.48E+17	2.43E+17	1.99
I-133	5.41E+18	5.59E+18	-3.19	Te-127m	3.33E+16	4.09E+16	-18.70
I-134	6.01E+18	6.15E+18	-2.26	Te-129	8.06E+17	8.50E+17	-5.21
I-135	4.98E+18	5.34E+18	-6.69	Te-129m	2.01E+17	1.73E+17	15.89
Kr83m	3.26E+17	3.14E+17	3.73	Te-131m	4.10E+17	5.57E+17	-26.44
Kr85	2.46E+16	2.86E+16	-14.27	Te-132	4.00E+18	3.93E+18	1.84
Kr-85m	6.97E+17	6.36E+17	9.67	Xe-131m	2.81E+16	3.76E+16	-25.23
Kr-87	1.36E+18	1.27E+18	7.49	Xe-133	5.70E+18	5.60E+18	1.82
Kr-88	1.86E+18	1.75E+18	5.94	Xe-133m	1.84E+17	1.77E+17	3.88
La-140	4.89E+18	5.05E+18	-3.06	Xe-135	1.59E+18	1.46E+18	8.53
La-141	4.59E+18	4.46E+18	2.96	Xe-135m	1.33E+18	1.19E+18	12.06
La-142	4.41E+18	4.34E+18	1.58	Xe-138	4.55E+18	4.70E+18	-3.23

[1] "Unit 11" is a fictitious unit at Gravelines, used for the purposes of the exercise.

Mo-99	5.17E+18	5.08E+18	1.70	Y-90	1.79E+17	2.57E+17	-30.19
Nb-95	4.64E+18	4.64E+18	-0.02	Y-91	3.30E+18	3.27E+18	1.13
Nd-147	1.82E+18	1.80E+18	0.92	Y-92	3.60E+18	3.36E+18	7.04
Np-239	5.59E+19	5.86E+19	-4.59	Y-93	4.09E+18	2.60E+18	57.53
Pr-143	4.23E+18	4.08E+18	3.72	Zr-95	4.90E+18	4.58E+18	7.02
Pu-241	5.46E+17	4.39E+17	24.33	Zr-97	4.65E+18	4.36E+18	6.79
Rb-86	3.59E+15	5.45E+15	-34.22	TOT	1.99E+20	2.04E+20	-2.33
Rh-105	2.97E+18	2.90E+18	2.57				

In Tab. 1, the "Var" columns report the relative percentage difference of the radionuclide activity between RASCAL 4.3 and PERSAN 4 codes with respect to RASCAL 4.3. Table 1 shows that the difference between the total core activity of PERSAN 4 and RASCAL 4.3 – assessed considering the contribution of the only radionuclides that are both included in RASCAL and PERSAN initial core inventories – is negligible (i.e. ~ -2.3 %). With the exception of 2-3 nuclides, whose differences amount to about a factor 2, the single isotopic variations are below about 20-30% and, in the majority of cases, of the order of a few percents. However, it is necessary to emphasize that the total number of radionuclides included in the full PERSAN 4 database core inventory is much greater (i.e., 720) than that contained in the PWR core inventory (i.e., 58) of RASCAL 4.3; PERSAN can in any case resort to different sets of initial inventories with variable number of isotopes. Figures 1 and 2 report a graphical representation of the radionuclides distribution based on the relative difference between RASCAL 4.3 and PERSAN 4 less (Fig. 1) or more (Fig. 2) than 20%.

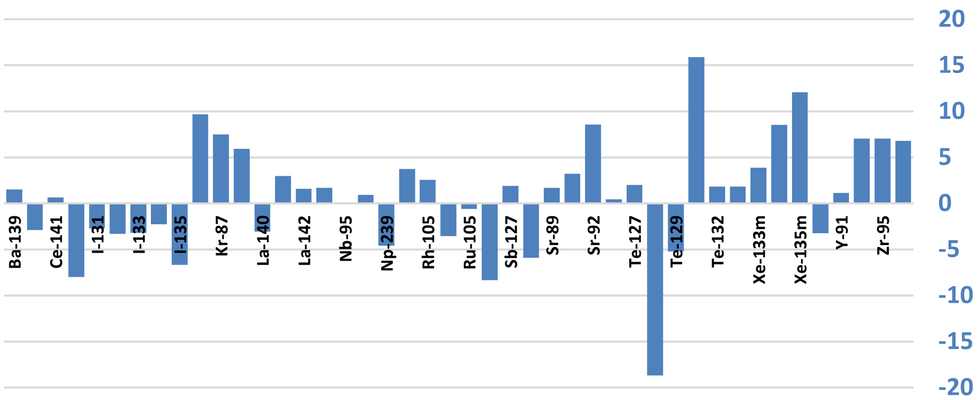

Figure 1: Core inventory radionuclides with a relative difference lower than 20%.

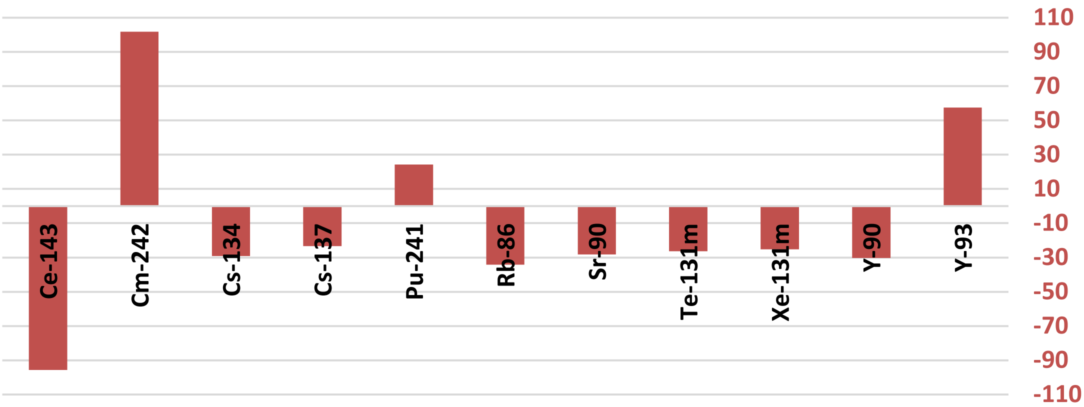

Figure 2: Core inventory radionuclides with a relative difference higher than 20%.

1.4 Severe accident sequence

IRSN made available information in the form of periodic reports and exercise messages during the WP4 Exercise 2 held in Vienna. Based on this information, it was possible to reconstruct the main events characterizing the accident sequence. Table 2 reports the timetable of the main events of the severe accident sequence. The table also indicates three instants of ST evaluation, requested by the real-time Exercise; these are labelled as ST#1, ST#2 and ST#3. ST#1 and ST#2 had to cover 24 hours since the initial release with information available at different times (i.e., 2h30 and 4h30 after reactor trip); ST#3 96 hours since the initial release.

Table 2: Timetable of the Severe Accident scenario – FASTNET Project Excercise 2

Time since SCRAM	Real Time	Event	Source
0	7h32	Reactor Trip (as required by procedures)	State of the Unit at the beginning of the accident (22/02/2019 @ 09:00)
43	8h15	Total shutdown of Train B	Technical Scenario - IRSN
48	8h20	Primary break, cold leg	Technical Scenario - IRSN
55	8h27	Pressure increase in the reactor building	State of the Unit at the beginning of the accident (22/02/2019 @ 09:00)
1h18	8h50	DVN[2] and DVK[2] off, DVW[2] in operation	State of the Containment (Message #1 22/02/2019 @ 08:50)
1h28	9h00	ECP4 – HPSI in operation (On site emergency plan)	SESAME 4.0 Acquisition (Message #1 19/02/2019 @ 09:00)
1h43	9h15	Start of safety injection (train A)	SESAME 4.0 Acquisition (Message #2 19/02/2019 @ 09:15)
1h48	9h20	Containment isolation 1st phase	State of the Containment (Message #2 22/02/2019 @ 09:20)
2h28	10h00	**First ST Evaluation Request: ST#1**	
2h43	10h15	ECP4, Vessel level, top of the hot leg	SESAME 4.0 Acquisition (Message #6 22/02/2019 @ 10:15)
2h48	10h20	DVN in operation, DVK and DVW off	State of the Containment (Message #3 22/02/2019 @ 09:50)
3h43	11h15	Loss of train A LPSI pump	SESAME 4.0 Acquisition (Message #10 22/02/2019 @ 11:15)
4h28	12h00	**Second ST Evaluation Request: ST#2**	
4h28	12h00	Water makeup to PTR tank (planned)	SESAME 4.0 Acquisition (Message #13 22/02/2019 @ 12:00)
4h43	12h15	Loss of train A HPSI pump	SESAME 4.0 Acquisition (Message #14 22/02/2019 @ 12:15)
4h56	12h28	Start of core uncovery (3.1 bar abs)	SESAME 4.0 Acquisition (Message #15 22/02/2019 @ 12:28)
5h14	12h45	Water make up to PTR tank	SESAME 4.0 Acquisition (Message #16 22/02/2019 @ 12:45)
5h28	13h20	SAMG – Core Melt Start	SESAME 4.0 Acquisition (Message #17 22/02/2019 @ 13:20)
5h58	13h50	Restart of RCV	SESAME 4.0 Acquisition (Message #18 22/02/2019 @ 13:50)
6h08	14h00	Level 2 alarm on KRT detection channel, acitivty detected in environment (gamma dose rate)	State of the Containment (Message #9 22/02/2019 @ 14:00)
6h53	14h45	RCV (train A) in operation but low flowrate	SESAME 4.0 Acquisition (Message #20 22/02/2019 @ 14:45)
7h13	15h05	Stop of RCV (train A)	SESAME 4.0 Acquisition (Message #21 22/02/2019 @ 15:05)

[2] DVN is the auxiliaries buildings ventilation system, DVK is the fuel building ventilation system and DVW is the connection building ventilation system.

7h43	15h35	First corium slump into the vessel lower head	Exercise #2 Technical scenario IRSN
8h08	16h00	**Third ST Evaluation Request: ST#3**	
8h38	16h30	Vessel failure – start of MCCI	Exercise #2 Technical scenario IRSN
21h38	05h30	Rupture of lateral walls of the cavity	Exercise #2 Technical scenario IRSN
33h08	17h00	Raft break-through	Exercise #2 Technical scenario IRSN

Figures 3-4 report the graphical representations of the time-dependent values of the main severe accident sequence parameters as reported in the exercise information.

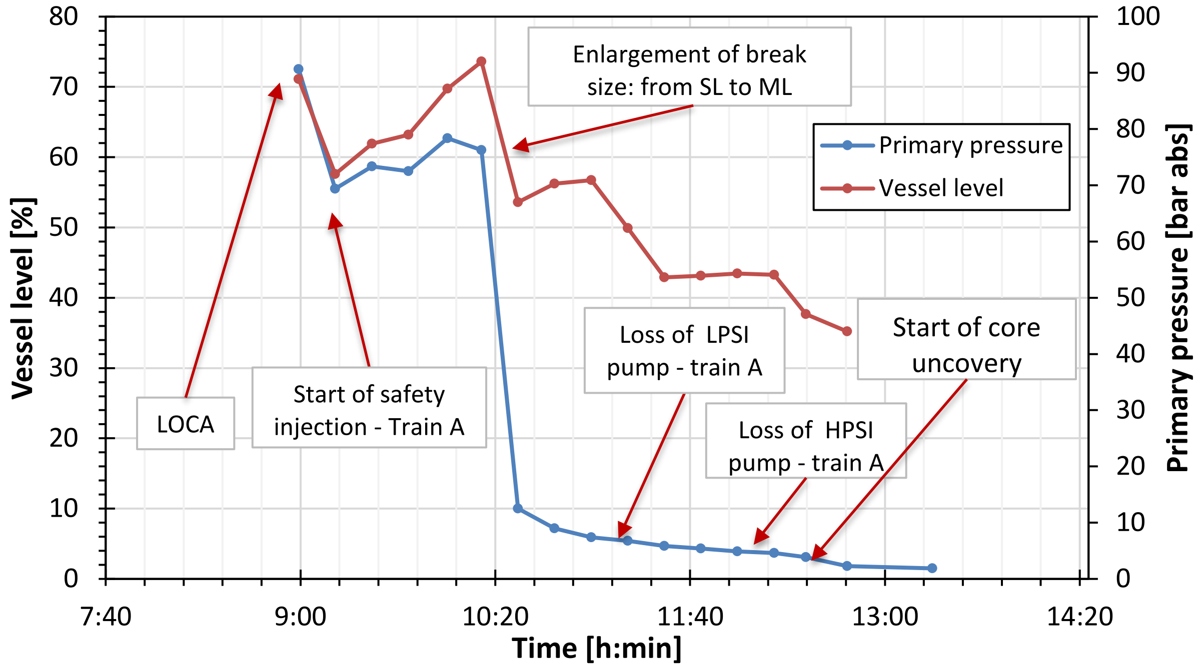

Figure 3: Vessel level and primary pressure time-dependent values.

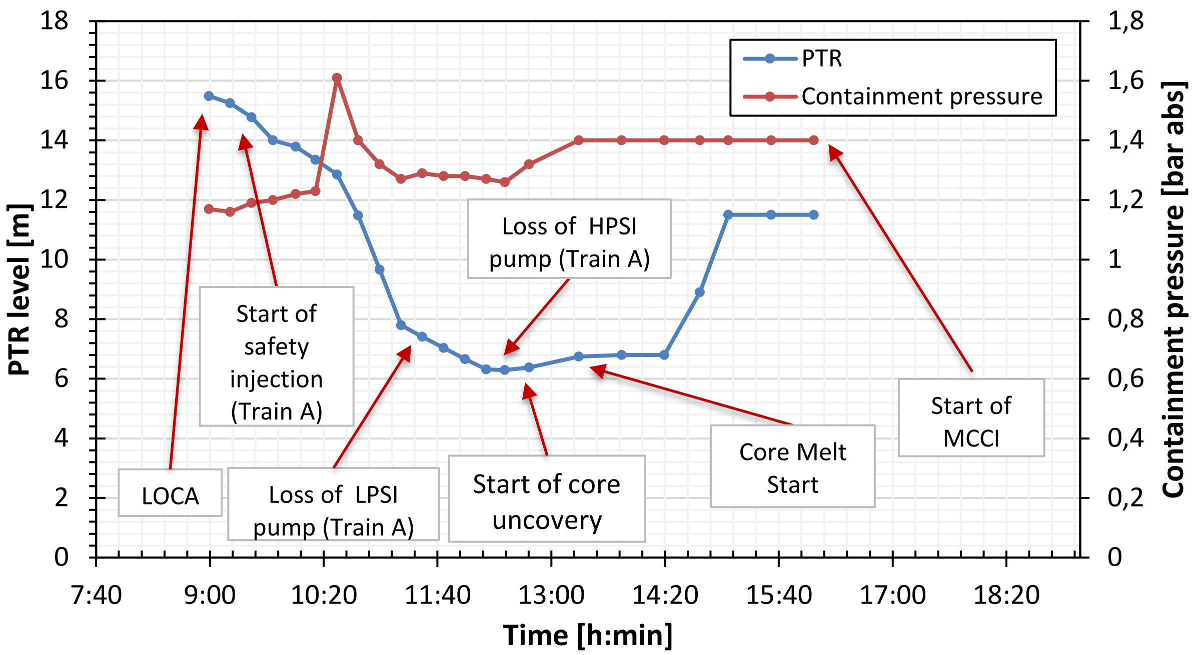

Figure 4: PTR water level and containment pressure time-dependent values.

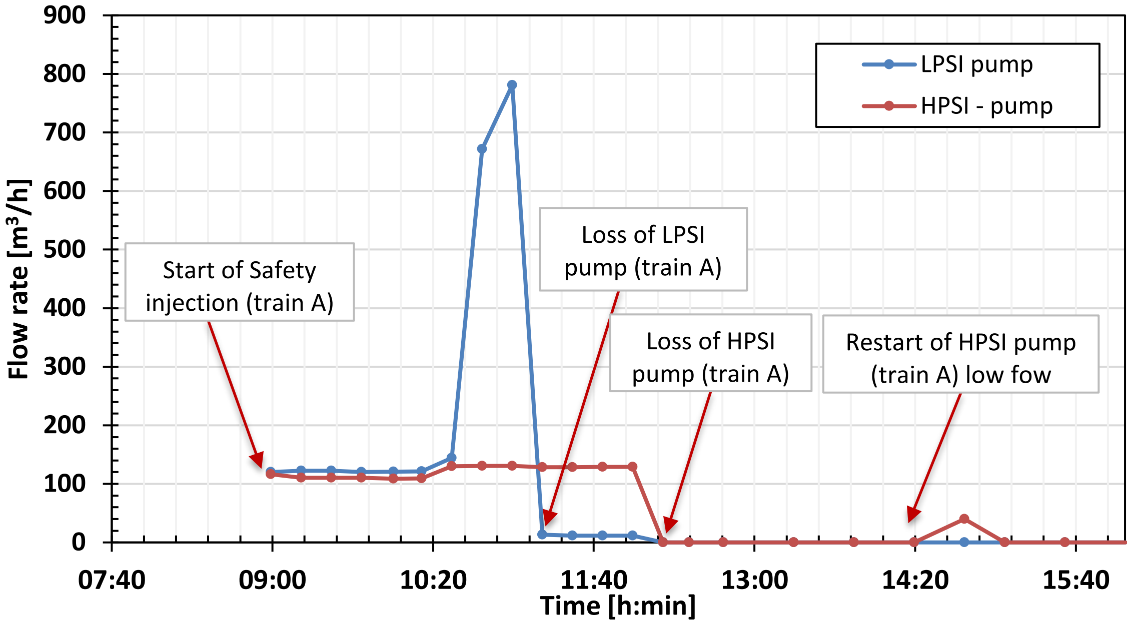

Figure 5: Flow rate of the LPSI and HSPI pumps.

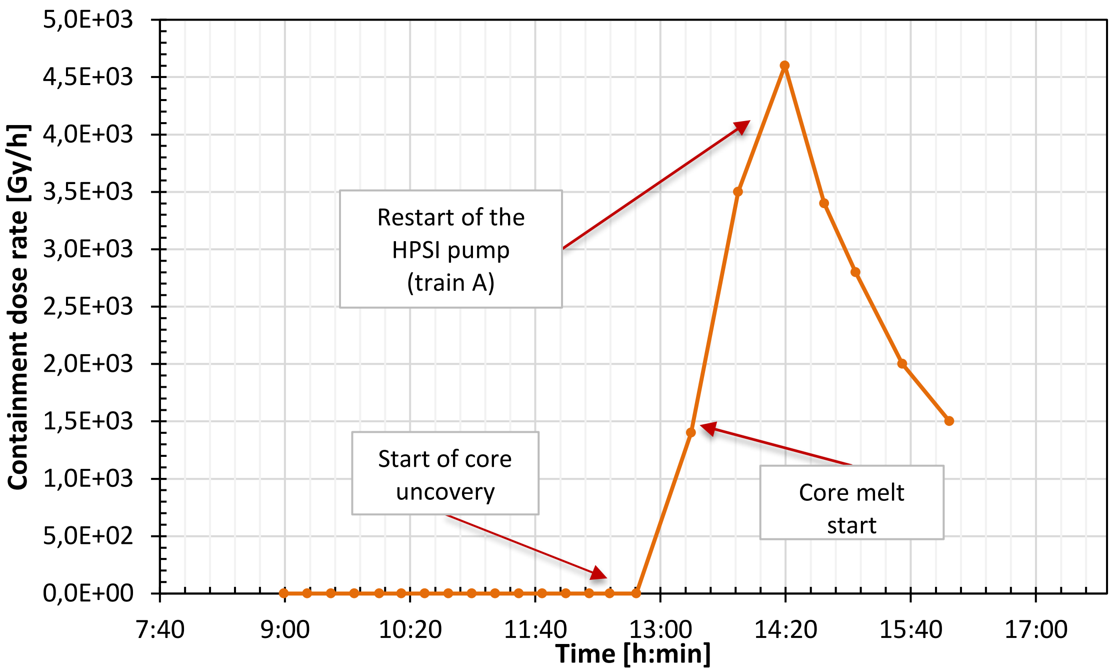

Figure 6: Containment dose rate time-dependent values.

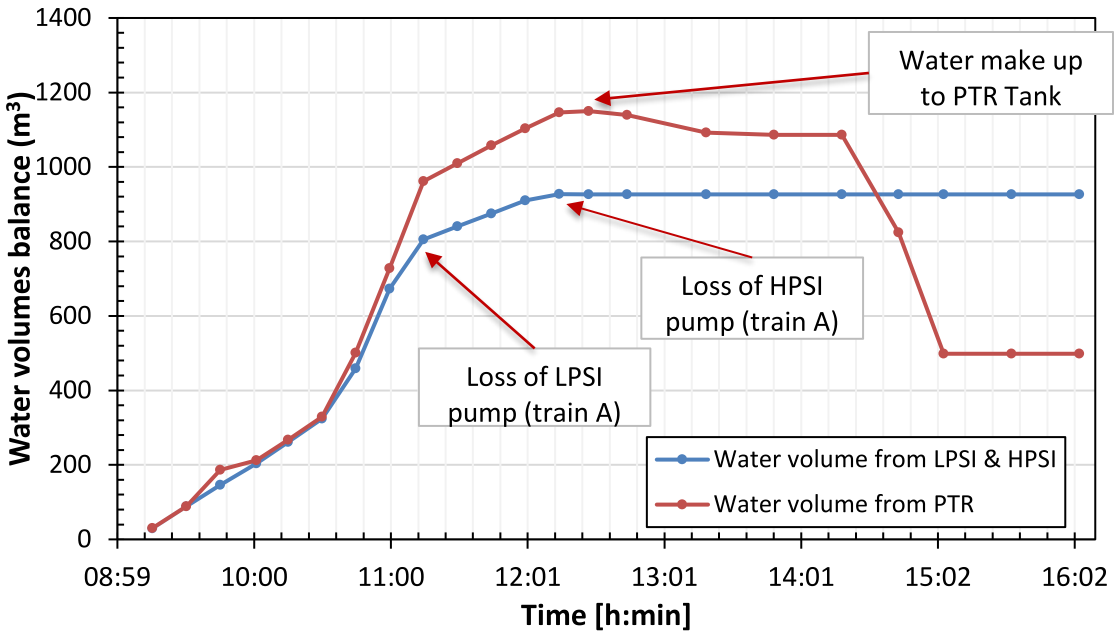

Figure 7: Time-dependent water volumes balance.

The analysis of the information available on the time-dependent water volumes balance from the PTR tank (Fig. 4) revealed that, before water make up, all the water taken from the PTR tank was used to feed the emergency core cooling circuit (ECCS) by means of the LPSI and HPSI pumps (Train A). This is coherent with the fact that CSSs are never used. A discrepancy is observed between the loss of the LPSI pump of train A and the time of start of water make up. It is to be noted that, at a certain time in the sequence, an enlargement of the LOCA break size must be hypothesized in order to explain the sudden and huge change in the time-derivative of the primary system pressure (Fig. 3). In fact, before that instant, the rate of decrease of primary system pressure was indicative of a small-break LOCA; after that, the size should have increased. The solution to Exercise 2 provided by IRSN effectively indicated an enlargement from about 0.7 (SBLOCA) inches to about 5 inches (MBLOCA) [3].

2 CODE DESCRIPTIONS AND SEQUENCE MODELING

This section describes the main technical features of the RASCAL 4.3 and PERSAN 4 codes used in this work to evaluate the Source Term of the severe accident sequences suggested during the exercise 2 proposed by IRSN whitin the WP4 of the FASTNET project.

2.1 RASCAL 4.3

RASCAL 4.3 is a fast-running emergency response consequence assessment tool developed by Athey Consulting for the Protective Measures Team of the U.S. Nuclear Regulatory Commission's (NRC's) Operation Center. RASCAL 4.3 is the U.S. reference tool for the assessment of the radiological consequences of an hypothetical severe accident that could occur to any infrastructure related to civilian uses of nuclear energy (i.e., nuclear power plants, spent fuel storage pools, cask, fuel cycle facilities, and radioactive material handling facilities). The 4.3 version, released on October 31 2011, among the various improvements, extended the RASCAL atmospheric dispersion domain to 100 miles, increased the allowed calculation duration to 96 hours, added the capability to import, merge, and export STs, and included a revision of the pressure-hole size method of calculating the leak rate from the containment [4,5]. RASCAL was developed by NRC over 25 years ago to provide a tool for the rapid assessment of an incident or accident at an NRC-licensed facility and to aid decision-making such as wheter the public should evacuate or shelter itself in place. Its results are not the only criterion used by the authorities during an accident, but certaintly an important one [6]. RASCAL uses a simple algebraic expression in which the several terms are multiplied together to evaluate the time-dependent ST.

$$S_i(t) = I_i \cdot a_i(t) \cdot \prod_{n=1}^{N} RDF(t)_{i,n} \cdot LF_i(t)$$

were I_i is the initial core inventory of ith radionuclide based on the default RASCAL database core invetory for the U.S. reactor plant which can be adjusted depending on the fuel burnup and the power at which reactor was operating; a_i is the core release fraction of radionuclide i that depends on the time progression of the accident through the several accidental phases (i.e., gap release, early in-vessel, ex-vessel, late in vessel) [7]; $RDF_{i,n}$ represents the contribution that the nth reduction mechanism has on the ith radionuclide. It is assumed that 95% of the radioiodine and all fission products besides noble gases are in aerosol form. Therefore, the reduction mechanisms are assumed to affect all fission products equally except for noble gases, which are consequently only affected by radioactive decay [8]; LF_i is the fraction of the ith radionuclide in the containment that is released to the atmosphere. Source Term mechanisms considered by RASCAL for a PWR include: radioactive decay, containment spray, containment natural processes during hold-up, Ice Condenser, plate out for containment bypass pathway, steam generator tube rupture (case: partitioned, non partitioned, condenser off gas release, safety relief valve), filters. The reduction factors for natural deposition and dousing spray are expressed with an exponential decay law (i.e., $e^{-\lambda t}$) where the decay constant changes with the time. The other reduction factors have a constant value with the constraint that the total value of the RDF that includes the overall multiplied reduction factor has to be greater than 0.001. Filters and containment spray have a lower limit on the reduction factor of 0.01 and 0.03, respectively [4].

The evaluation of the ST was carried out with the Primary tool named “Source term to Dose (STDose)” which is based on the U.S. experience on PWRs and BWRs nuclear power plants. The STDose tool requires the specifications of some parameters in order to evaluate the Source Term; these parameters have to be set as input in the following subtools: Event type, Event Location, Source Term, Release Path and Metereology [2].

The Event Type sub-module defines the source (i.e., NPP, Spent Fuel, Fuel Cycle/UF6, Criticality Event, Other type of release) of the radioactive emission; in the case of the scenario of the Exercise 2, the choice has obvioulsy been an NPP.

The Event Location sub-module locates in space the NPP and defines all the necessary plant data in order to evaluate Activity inventory. Two options are available: 1) load an event location from RASCAL database, or 2) define a generic site. The option adopted in this study to simulate a non-U.S. reactor, is the use of a s.c. *surrogate NPP*, already available in RASCAL 4.3 database of U.S. plants, which differs from the real plant (i.e. Gravelines) only as regards actual power and actual core average burnup; this method was effectively tested for the Fukushima accident case [9,10]. In practice, this means to find among the U.S. fleet some PWR Westinghouse 3-loop plants (900 MWe, dry containment) which can be used to mock-up the Gravelines NPP (905 MWe, CP1). The severe accident analysis has been realized using Unit 2 of Beavery Valley, which is a U.S. Westinghouse 3-loop reactor currently in operation. Table 3 gives the BV-U2 main technical specifications.

Table 3: Beavery Valley U2 data – RASCAL 4.3

Parameters	**Data**
Reactor Type	PWR
Thermal Capacity (MWth)	2900
Reference Unit Power (Net Capacity MWe)	905
Reactor vendor	Westinghouse 3-loop
Containment	
Containment type	PWR, Dry Ambient
Containment volume	50970 m3
Design pressure	3.72E+05 Pa
Steam Generator	
SG type	U-Tube
SG water mass	42184 kg
Fuel	
Number of fuel assemblies	157
Number of fuel rods per assembly	264 (17x17)
Gravelines-like parameters	
Power (MWth)	2785
Core average burn-up (MWd/MTU)	30000

The Source Term module allows to characterize the methods for estimating the ST value for a NPP accident. Whitin the ST module it's possible to choose four sub-modules which differ from each other on the basis of the accident sequence or the containment dose-rate levels (Long Term Station Blackout, LOCA, Coolant Release Accidents, Containment Monitor). The method chosen for the RASCAL analysis is LOCA according to the FASTNET Exercise's initiator event. This method is based on reactor conditions and the procedures and results described in NUREG-1228 [11] and its subsequent modifications (NUREG-1465) [12]. Table 4 reports the options adopted whitin the sub-module LOCA for the analysis of the two ST requests ST#2 and ST#3 of the sequence proposed during the FASTNET Exercise. It should be noted that the LOCA module of RASCAL version 4.3 cannot evaluate STs prior to core dewatering, meaning that low releases like that associated to ST#1 request, due mainly to primary water activity into the containment, cannot be dealt with. It must also be noted that, even if this limits the code applicability, such releases are not expected to cause important off-site consequences but only on-site ones.

Table 4: LOCA submodule data – RASCAL 4.3 (ST#2, ST#3)

<table>
<tr><th rowspan="2">Event</th><th rowspan="2">Data</th><th rowspan="2">Time</th><th colspan="2">ΔT since SCRAM</th></tr>
<tr><th>[h]</th><th>[min]</th></tr>
<tr><td>Reactor shutdown</td><td>22/02/2019</td><td>07:32</td><td>0</td><td>00</td></tr>
<tr><td>Core uncovered</td><td>22/02/2019</td><td>13:00</td><td>5</td><td>28</td></tr>
<tr><td colspan="5">Method used for core damage estimate</td></tr>
<tr><td colspan="3">Core recovered (Yes/No)</td><td colspan="2">No</td></tr>
</table>

The "Release path" module defines the release path of the radionuclides inventory from the release point to the environment and the time-dependent emission events. The three options available (i.e., Containment leakage/failure, Steam Generator tube rupture, Containment bypass) differ on the basis of the plant zone (Containment, Auxiliary Building, Turbine Building) in which the release occurs. The Graveline accident has been modeled with the Containment leakage/failure option. Figure 8 shows the release path of the severe accident sequence as modeled by RASCAL 4.3.

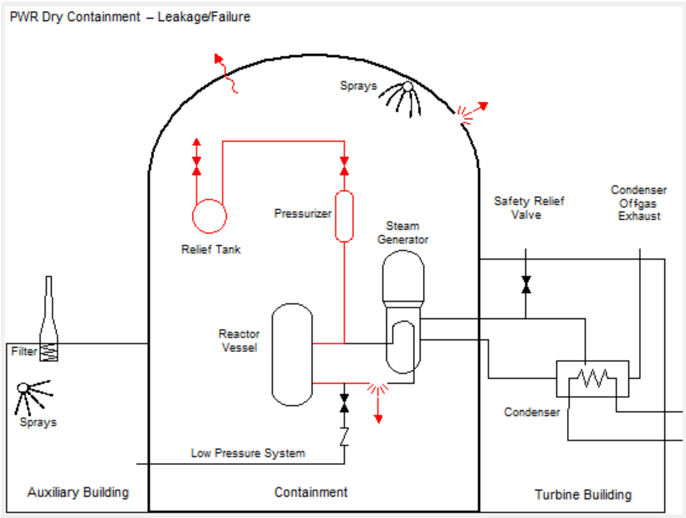

Figure 8. Release path for the severe accident sequence – RASCAL 4.3 (ST#2, ST#3)

Table 5 shows the timetable of the only events that was possible to simulate with RASCAL 4.3 according to the SESAME 4 acquistion system information for ST#2 request.

Table 5: Release path submodule data – RASCAL 4.3 (ST#2)

Event	**Data**	**Time**	**ΔT since SCRAM [h]**	**[min]**	**Value**
Spray	22/02/2019	13:00	5	28	Off
Leak Rate	22/02/2019	13:00	5	28	0.02 %vol /d

In Table 5 the leak rate event defines the leakage of the radionuclides from the containment to the atmosphere expressed as percentage fraction of containment volume per day. The leak rate value of 0.02 %vol /d is the RASCAL nearest settable value to that (namely, 0.01624 % vol /d) adopted by IRSN and EdF for an intact containment of a 900 MWe PWR. Table 6 reports the timetable of the only events that can be implemented in RASCAL according to the information available from IRSN SESAME 4 acquisition system for the third request (ST#3).

Table 6: Release path submodule data – RASCAL 4.3 (ST#3)

Event	**Data**	**Time**	**ΔT since SCRAM [h]**	**[min]**	**Value**
Spray	22/02/2019	13:00	5	28	Off
Leak Rate	22/02/2019	13:00	5	28	0.02
Leak Rate	24/02/2019	17:00	57	28	Total failure (100%vol/h)

In Table 6 an total failure event (100%vol/h) has been chosen in RASCAL to model the effects of a raft breakthrough event reported in the last part of the sequence. RASCAL 4.3, as opposed to PERSAN 4, does not allow to simulate both the status of the ventialtion systems and the Molten Corium Concrete Interaction (MCCI) detailed phenomena and their effects on the ST.

2.2 PERSAN 4

PERSAN 4 is a code developed by IRSN as the reference French fast-running tool to evaluate STs, in particular for LOCA-initiated scenarios to a French NPP. During the FASTNET project, PERSAN was extended to be able to describe accidents at any type of European NPPs (namely, PWRs, BWRs, VVERs and CANDUs) [13]. It allows to examine the behaviour of the 3 typical “defense in depth” barriers, taking into account core damage estimation and release kinetic, retention factor in the primary coolant system, aerosol deposition rates and iodine chemistry modelization, leak rate between the containment, auxiliary building and the atmosphere. The software requires short computation times (i.e., less than one minute to calculate 24 hours of release). The main input parameters in PERSAN are: building leak rates, fuel damage, containment pressure evolution, long term availability of containment spray systems and of ventilation systems in the auxiliary buildings. The measured buildings leak rate obtained during containment building periodic tests are used as default input assumptions. STs calculated by PERSAN are realistic but are believed to be conservative in terms of quantitites released or chemical forms produced in regards with the radiological consequences. The models implemented in PERSAN has been validated with ASTEC using a large representative sample of accident scenarios [14]. PERSAN, to the contrary of RASCAL, keeps distinct the various chemical forms of iodine molecules (like I_2, IOx, ICH_3, etc.) through simplified speciation models. The models used in the PERSAN analysis take into account the CsI, I_2 and ICH_3 species. In detail, the iodine chemistry model considers that: a) the iodine at the break constituted by CsI (95%) and I_2 (5%), b) a fraction of I_2 is adsorbed by Reactor Buildings (RB) walls painting and released in ICH_3 form (ICH_3 creation: 10% wt conversion rate); c) a fraction of ICH_3 reacts to form I_2 again and that, depending on building conditions, the CsI can deposit in reactor building; d) I_2 concentration in the gas phase can be reduced by the Containement Spray System (CSS); e) I_2 can be filtered by Iodine Traps and ICH_3 can not be dropped by CSS nor filtered. The code include several other models such as: aerosol deposition, fission produc release, containment dose rate evaluation, releases calculation. PERSAN can make calculations for more than 3000 isotopes, with real-time filiation decay. The code splits the element in five families according their physical behaviour (Tab. 7).

Table 7: Families of elements – PERSAN 4

Families	Species	Physical state
Noble gas	Xe, Kr, He, Ne, Ar, Rn	Atomic
Volatile aerosol	Cs, Te, Mo, Rb, Se, Rh, Tc,... (21 elements)	Aerosol
Semi-volatile aerosol	Ba, La, Ru, Sr, Sb, U, Np, Pu, Am,… (71 elements)	Aerosol
Halogen species	I, F, Cl, Br, At	Aerosol (CsI)
		Gaseous (molecular, I_2)
		Gaseous (organic, ICH_3)
		Aerosol (oxide, IOx)
Other elements	H, C, N, O, P, S, Se	-

To estimate the time-dependent ST, the code uses a mass balance formula to evaluate, in each reactor building (containment or auxiliaries building), the time dependent amount of each radioisotope:

$$C_i(t+dt) = C_i(t) + [S_i(t) - D_i(t) - L_i(t) - F_i(t)]\, dt$$

were C_i is the mass of ith radionuclide in the building over the time; S_i is the source of release of ith radionuclide over time; D_i is the amount of ith radionuclide that is removed from the building over time due to processes such as natural deposition, spray, adsorption and chemical reactions (e.g. the removal of iodine through the creation of silver iodine in the sump); L_i is the amount of ith radionuclide that leaks out of the building over the time towards two possible paths: directly from the containment to the atmosphere, or through the auxiliary buildings. In the first case the leak rate is evaluated on the bases of flow correlations that depend on the material of the reactor building wall (i.e., linear shielded concrete or simple concrete); in the second case the leak rate is determined by specific flow correlations that take into account the airflows in the auxiliary buildings. Fi(t) is the filiation/decay term, which is calcualted for each isotope at each time step [8]. It is necessary to emphasize that PERSAN 4 was originally not designed as a stand-alone computational code but in connection with additional tools (SESAME 4, 3d/3p, BRECHEMETRE, SCHEHERASADE, etc.) able to predict the evolution of the main plant variables such as containment pressure, containment spray systems, auxiliary building ventilations, which highly impact on the final results. Figure 9 shows a graphical representation of the release routes into atmosphere as modeled by PERSAN 4. It is to be emphasized in fact that PERSAN can take into account all possible parallel release paths during an accident, while RASCAL only the main one.

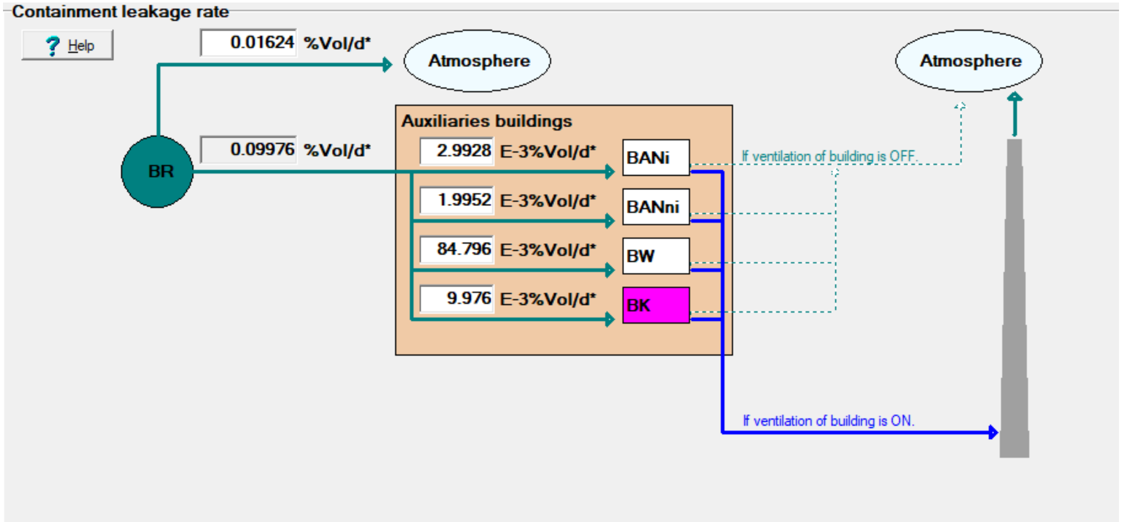

Figure 9: Leakage rate for a pressure up to 5 bar in the Reactor Building – PERSAN 4

Table 8 reports an overall analysis of the leakage rates and flow rates from the reactor plant to the atmosphere according to the values reported in Fig.9 for two situations: with and without (ON/OFF) the activation of the ventilation building systems.

Table 8: Leak and flow rates from containment and reactor buildings – PERSAN 4

Buildings		**Volume**	**leakage rate**	**Note**	**flow rate**
(-)		**m^3**	**%Vol/h**	**(-)**	**m^3/h**
Containment		51400	1.624E-02	to atmosphere	8.770E-01
			2.993E-03	to BANi	1.616E-01
			1.995E-03	to BANni	1.077E-01
			8.480E-02	to BW	4.579E+00
			9.976E-03	to BK	5.387E-01
Auxiliaries buildings	BANi	7500	5.00E+00	to atmosphere (Vent OFF)	3.75E+02
	BANni	67500	5.00E+00	to atmosphere (Vent OFF)	3.38E+03
	BW	3000	5.00E+00	to atmosphere (Vent OFF)	1.50E+02
	BK	26000	5.00E+00	to atmosphere (Vent OFF)	1.30E+03
Stack		-	-	to atmosphere (Normal Conditions - Vent ON)	2.13E+03
		-	-	to atmosphere (Accidental Conditions - Vent ON)	2.39E+03

Table 8 analysis shows that, in normal conditions, the total flow rate from the containment to the atmosphere is 8.770E-1 m^3/h and the total flow rate from the auxiliary buildings to atmosphere is equal to 5.21E+03 m3/h (ventialtion OFF) or 2.13E+03 m^3/h (ventilation ON).

Table 9 reports the calculation assumptions adopted whitin PERSAN 4 to perform the analysis of ST#1, ST#2 and ST#3.

Table 9: Characteristic times of the calculation assumptions – PERSAN 4

Time assumptions	Date	Time	Note
Reactor Trip	22/02/2019	07:32	ST#1, ST#2, ST#3
Core dewatering	22/02/2019	13:00	ST#2, ST#3
Clad failure start	22/02/2019	13:07	ST#2, ST#3
Core melt start	22/02/2019	13:17	ST#2, ST#3
Core melt end (100%)	22/02/2019	14:46	ST#2, ST#3
Calculation end	23/02/2019	13:33	ST#2
MCCI start	22/02/2019	16:30	ST#3
Raft breakthrought	24/02/2019	17:00	ST#3
Calculation end	26/02/2019	08:20	ST#3

The initial primary activity in equivalent of I-131 was set to 4.0E+9 Bq/t. The primary acitivity by family was set to: 8.44E+10 Bq/t for NG, 1.75E+10 Bq/t for Iodine and 8.84E+09 Bq/t for Aerosols.The primary system retention has been set to 0% for all chemical species, chemical groups and solid suspensions (i.e., I_2, IO_x, Noble Gases, ICH_3, aerosols, etc.). The spent fuel of the pit was not considered because no accident occurs in the fuel building. Table 10 reports the main assumptions adopted to perform with PERSAN 4 code the second and third ST requests of the FASTNET exercise.

Table 10: Calculation assumptions – PERSAN 4 (ST#2, ST#3)

Core degradation

Date	Time	% clad failure	% core melt	Requests
22/02/2019	07:31	0	0	ST#2, ST#3
22/0272019	13:07	0	0	ST#2, ST#3
22/02/2019	13:16	100	0	ST#2, ST#3
22/0272019	13:17	100	0	ST#2, ST#3
22/02/2019	14:46	100	100	ST#2, ST#3

Containment pressure

Date	Time	Pressure value (abs bar)	Requests
22/02/2019	07:31	1	ST#2, ST#3
22/02/2019	07:32	Automatic	ST#2, ST#3
22/02/2019	12:28	1.325	ST#2,ST#3
22/02/2019	12:29	1.4	ST#2, ST#3
22/02/2019	16:29	1.4	ST#3
22/02/2019	16:30	1.6	ST#3
23/02/2019	05:29	1.9	ST#3
23/02/2019	05:30	2.3	ST#3
24/02/2019	17:00	4.7	ST#3
25/02/2019	17:00	1.7	ST#3

Containment spray system

Date	Time	Trains number	Sections
22/02/2019	07:31	0	ST#2, ST#3
22/02/2019	07:32	Automatic	ST#2, ST#3
22/02/2019	12:28	0	ST#2, ST#3

Ventilation system

Ventilation: DVN iode (ST#2, ST#3)

Date	Time	Operation	Flow ($E3\ m^3/h$)	Filtering					
				VHE	I_2	ICH_3	IOx	NG	Other
22/02/2019	07:31	Not switched IT	18.8	1000					
22/02/2019	08:00	Switchetd IT	18.8	1000	100	10	1	1	1

Ventilation: DVN non iode (ST#2, ST#3)

Date	Time	Operation	Flow ($E3\ m^3/h$)	Filtering					
				VHE	I_2	ICH_3	IOx	NG	Other
22/02/2019	07:31	ON	178	1000					

Ventilation: DVW (ST#2, ST#3)

Date	Time	Operation	Flow ($E3\ m^3/h$)	Filtering					
				VHE	I_2	ICH_3	IOx	NG	Other
22/02/2019	07:31	Normal	12	1000					
22/02/2019	08:00	Accidental	12	1000	1000	100	1	1	1
22/02/2019	09:30	OFF	0						

Ventilation: DVK (ST#2, ST#3)

Date	Time	Operation	Flow ($E3\ m^3/h$)	Filtering					
				VHE	I_2	ICH_3	IOx	NG	Other
22/02/2019	07:31	Normal	30	1000					
22/02/2019	07:50	OFF	0						

Stack flow (ST#2, ST#3)

Date	Time	Flow (E3 m3/h)
22/02/2019	07:31	213
22/02/2019	07:32	239
22/02/2019	07:50	209
22/02/2019	09:30	197

In Table 10, if Ventilation is set on *"Not switched IT"* the HEPA filters efficiency is set by default to 1000 and the traps efficiencies for other species (I_2, ICH_3, IOx, noble gas and other elemets) fields are empty and unavailable. If the ventilation system is set "*Switched IT*", the HEPA filters efficiency is set by default to 1000, the I_2, ICH_3, IOx, noble gas and other elements efficiency is set to 1000, 100, 10, 1, respectively. If ventilation system is set to "OFF", the ventilations flow rate is forced at 0 and filters and traps efficiency for other species (I_2, ICH_3, IOx, noble gas and other elements) fields are empty and unavailable. If ventilation system is set on "*Accidental*", a ventilation flow rate derived from PERSAN plant data is entered by default and filters and traps for other species (I_2, ICH_3, IOx, noble gas and other elements) efficiencies are also entered by default according to PERSAN plant data. The HEPA filters efficiencies range can be set from 1 to 9999 [15].

3 RESULTS

This section reports the comparison between the time-dependent Source Term evaluated by PERSAN 4 and RASCAL 4.3 for the ST#2 and ST#3 requests of the FASTNET WP4 Exercise 2. The intercomparison of ST#1 has not been made because RASCAL 4.3 does not allow a ST evaluation in a LOCA scenario before any core-dewatering event. The results achieved from the two fat-running tools have been compared both in terms of overall ST time-dependent releases and in terms of radionuclide class contribution to the overall ST.

3.1 ST#1: results

Concerning request ST#1, PERSAN evaluates the fraction of primary water activity due to the LOCA which is released from the containment to the atmosphere, and predicts then the following values: NG 1.54E9 Bq, Iodine 1E9 Bq, Cesium 1.77E8 Bq, Tellurium 0 Bq.

3.2 ST#2: comparison of results

The ST#2 requests an evaluation of the ST 24 hours after the reactor trip with the information available at 12h00 of 22/02/2019 (prognosis mode). IRSN made available some information (i.e. increase of pressure in the reactor building since 08:27) from which it has been hypothesized a LOCA at 08:00. Moreover, IRSN assumed that the flow rate of the Containment Spray System (CSS) is set to OFF; this assumption is in agreement with the fact that the typical nominal values of the CSS rates under severe accident conditions are more than three orders of magnitude greater (i.e., ~ 0.5 m^3/s) than the value reported by the SESAME 4.0 acquisition system (i.e., 0.5 m^3/h). Moreover, a more in depth analysis of the trend of water flow during the accident sequence revealed that before the PTR water make up and the loss of HPSI and LPSI pumps, all the PTR tank water flow feeds the high and low pressure pumps (Fig. 8). The DVN (iode and non iode) system was in operation. Figure 10-13 report an intercomparison of results of the time-dependent releases of Cs-137, I-131, Te and NG for the ST#2 request (PERSAN results include also ST#1 up to core dewatering).

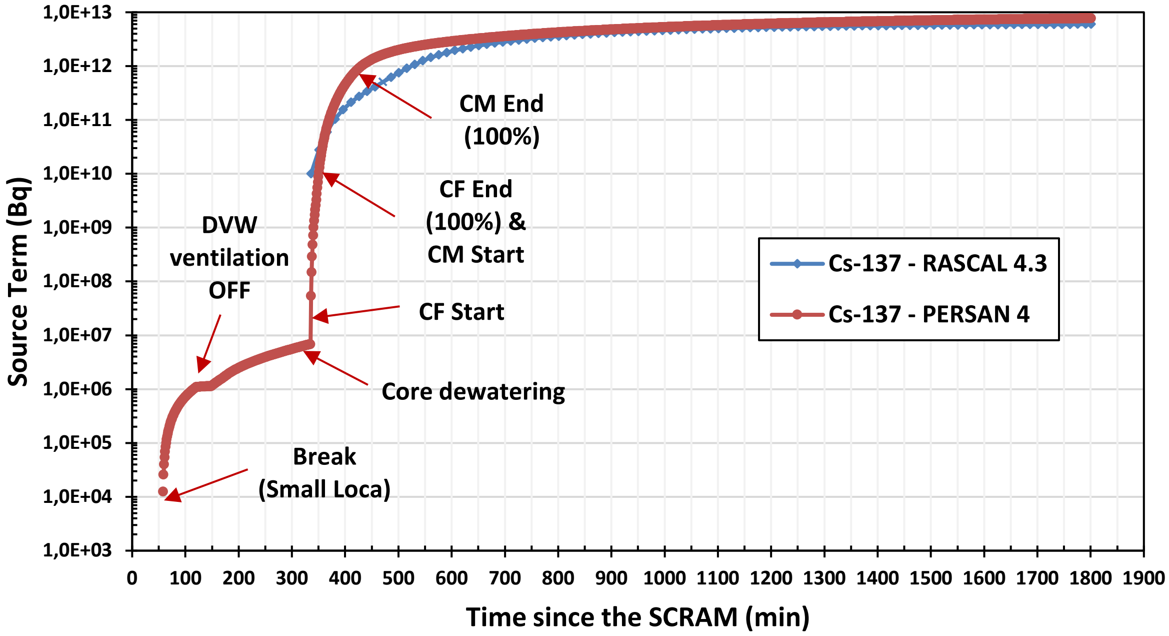

Figure 10: Time-dependent ST (Cs-137) – RASCAL 4.3 vs PERSAN 4 (ST#2)

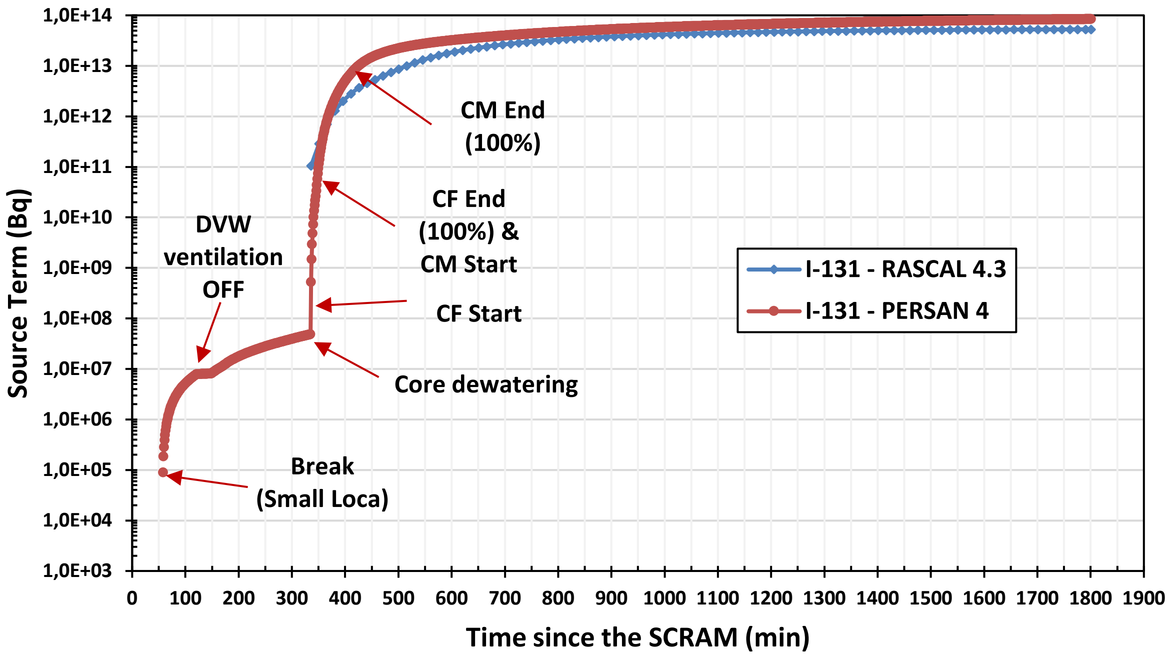

Figure 11: Time-dependent ST (I-131) – RASCAL 4.3 vs PERSAN 4 (ST#2)

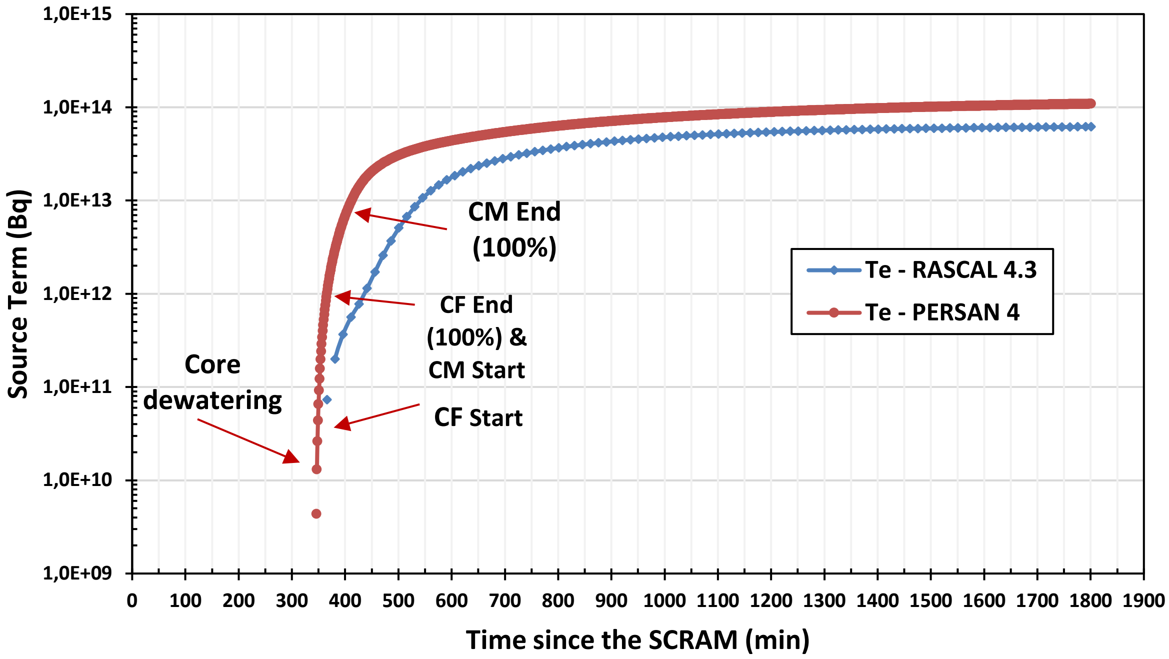

Figure 12:Time-dependent ST (Te) – RASCAL 4.3 vs PERSAN 4 (ST#2)

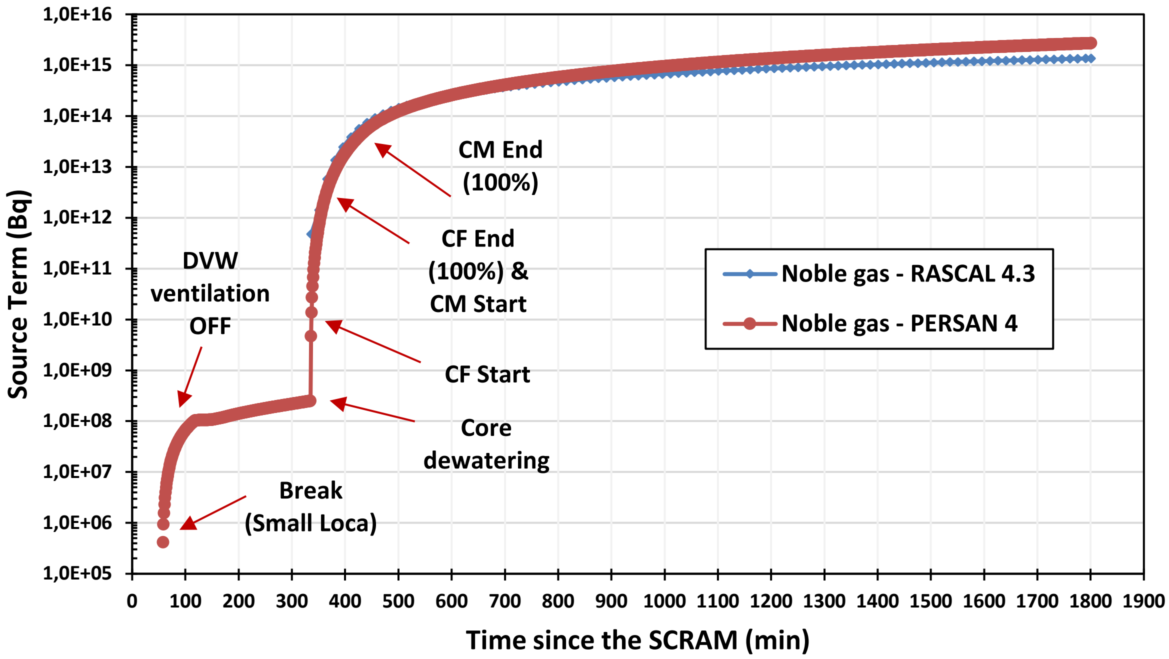

Figure 13: Time-dependent ST (NG) – RASCAL 4.3 vs PERSAN 4 (ST#2)

The outcomes reported in Figures 10-13 reveal that RASCAL 4.3 provides a release into atmosphere of Cs-137, I-131 and NG only after the core dewatering event (i.e., 328 min since the reactor SCRAM). On the contrary, both RASCAL 4.3 and PERSAN 4 provide a release of Tellurium (Te) after the core dewatering event. Table 11 reports a RASCAL 4.3 and PERSAN 4 total release intercomparison for some important chemical classes (Noble gas, Cesium, Iodine, Tellurium).

Table 11: PERSAN 4 vs RASCAL 4.3 Total Release – ST#2

Total Release			
	PERSAN 4	**RASCAL 4.3**	**VAR (%)**
Noble Gas	2.70E+15	1.35E+15	99.26
Cesium	2.27E+13	1.81E+13	25.33
Iodine	3.67E+14	2.20E+14	66.55
Tellurium	1.09E+14	6.17E+13	76.44

In Table 11, VAR is the relative percentage difference of the total release value between PERSAN and RASCAL with respect to RASCAL 4.3 code. The analysis of Table 11 reveals that PERSAN 4 slightly overestimates (i.e. about a factor 1.25 ÷ 2) the ST with respect to RASCAL 4.3 code. Table 12 shows a PERSAN 4 and RASCAL 4.3 radionuclide activity intercomparison for each radionuclide included in RASCAL 4.3 results, except for Kr-83m and Nb-95m that are not present in the PERSAN output.

Table 12: Intercomparison of the Radionuclide activity – ST#2

Nuclide	**RASCAL 4.3**	**PERSAN 4**	**PERSAN /RASCAL ratio**	**Nuclide**	**RASCAL 4.3**	**PERSAN 4**	**PERSAN /RASCAL ratio**
Am-241	2.21E+05	1.28E+08	**580.2**	Pu-241	8.88E+10	6.50E+10	**0.7**
Ba-139	1.28E+11	7.14E+11	**5.6**	Rb-86	1.23E+11	1.04E+11	**0.8**
Ba-140	2.57E+13	7.45E+13	**2.9**	Rb-88	1.09E+13	1.38E+13	**1.3**
Ce-141	1.17E+12	2.91E+12	**2.5**	Rh-103m	7.73E+11	2.63E+13	**34.0**
Ce-143	8.08E+11	2.04E+12	**2.5**	Rh-105	4.41E+11	1.77E+13	**40.1**
Ce-144*	9.48E+11	2.16E+12	**2.3**	Ru-103	7.75E+11	2.58E+13	**33.3**
Cm-242	2.93E+10	2.76E+10	**0.9**	Ru-105	8.84E+10	3.13E+12	**35.4**
Cs-134	8.66E+12	1.02E+13	**1.2**	Ru-106*	2.17E+11	8.87E+12	**40.8**
Cs-136	3.43E+12	4.77E+12	**1.4**	Sb-127	3.00E+12	5.04E+12	**1.7**
Cs-137*	5.99E+12	7.68E+12	**1.3**	Sb-129	1.72E+12	2.85E+12	**1.7**
Cs-138	1.59E+09	1.15E+10	**7.3**	Sr-89	1.33E+13	2.56E+13	**1.9**
I-131	5.30E+13	9.28E+13	**1.8**	Sr-90	1.03E+12	1.81E+12	**1.7**
I-132	6.33E+13	9.64E+13	**1.5**	Sr-91	6.54E+12	1.28E+13	**2.0**
I-133	7.33E+13	1.28E+14	**1.7**	Sr-92	9.37E+11	2.23E+12	**2.4**
I-134	1.00E+11	7.16E+11	**7.1**	Tc-99m	7.29E+11	1.16E+14	**159.4**
I-135	3.06E+13	4.89E+13	**1.6**	Te-127	3.51E+12	5.46E+12	**1.6**
Kr-83m	6.39E+11	-	**-**	Te-127m	5.53E+11	7.81E+11	**1.4**
Kr-85	4.36E+12	2.40E+09	**0.0**	Te-129	1.53E+12	6.31E+12	**4.1**
Kr-85m	1.26E+13	1.83E+13	**1.4**	Te-129m	2.32E+12	4.67E+12	**2.0**
Kr-87	6.32E+11	6.07E+11	**1.0**	Te-131	1.24E+12	1.51E+12	**1.2**
Kr-88	1.27E+13	1.55E+13	**1.2**	Te-131m	5.52E+12	7.10E+12	**1.3**
La-140	3.46E+12	1.82E+13	**5.3**	Te-132	4.70E+13	8.28E+13	**1.8**
La-141	1.33E+11	1.38E+12	**10.4**	Xe-131m	7.07E+12	1.02E+13	**1.4**
La-142	8.07E+09	1.23E+11	**15.2**	Xe-133	9.99E+14	2.00E+15	**2.0**
Mo-99	7.74E+11	1.16E+14	**150.4**	Xe-133m	2.75E+13	6.05E+13	**2.2**
Nb-95	1.18E+12	5.94E+12	**5.0**	Xe-135	2.73E+14	5.60E+14	**2.0**
Nb-95m	8.44E+08	-	**-**	Xe-135m	1.70E+13	2.96E+13	**1.7**
Nb-97	3.64E+10	1.42E+12	**39.1**	Xe-138	2.35E+05	3.03E+06	**12.9**
Nd-147	4.42E+11	3.81E+11	**0.9**	Y-90	1.20E+11	1.80E+11	**1.5**
Np-239	1.29E+13	3.68E+13	**2.9**	Y-91	8.54E+11	8.12E+11	**1.0**
Pm-147	1.87E+08	1.41E+13	**75284.7**	Y-91m	3.13E+12	6.34E+12	**2.0**
Pr-143	1.03E+12	2.71E+12	**2.6**	Y-92	6.72E+11	1.44E+12	**2.1**
Pr-144	9.45E+11	2.13E+12	**2.3**	Y-93	2.70E+11	3.90E+11	**1.4**
Pu-238	3.70E+05	1.50E+09	**4062.5**	Zr-95	1.16E+12	9.93E+11	**0.9**
Pu-239	6.30E+05	1.45E+08	**229.6**	Zr-97*	6.41E+11	5.78E+11	**0.9**

Table 12 reveals that the results are in good agreement; some discrepancies can be found in some actinides (Am-241, Pu-238, Pu-239), probably because PERSAN 4 and RASCAL 4.3 evaluations have been performed starting from a different MOX and UOX core inventory. Other radionuclides (Mo-99, Nb-97, Pm-147, Rh-103m, Rh-105, Ru-106, Tc-99m) also have not negligible differences.

3.3 ST#3: comparison of results

The ST#3 requests an evaluation of the ST four days after the reactor trip with the information available at 16h00 of 22/02/2019 (prognosis mode). For this request it was necessary to extend the progression of the severe accident sequence to lower head vessel failure, MCCI and raft breakthrough. The Containment Spray System (CSS) is set to OFF and the DVN (iode and non iode) is in operation. In RASCAL 4.3 the raft breakthrough event was modeled with a containment total failure (with corresponding leak rate of 100% vol/h) while the chemistry of MCCI cannot be modeled, as stated previously. The leak rate due to raft breakthrough is assumed in PERSAN to be 1000% vol/d, roughly half the value of RASCAL. Figures 14-17 report the intercomparison of time-dependent results for Cs-137, I-131, Te and NG.

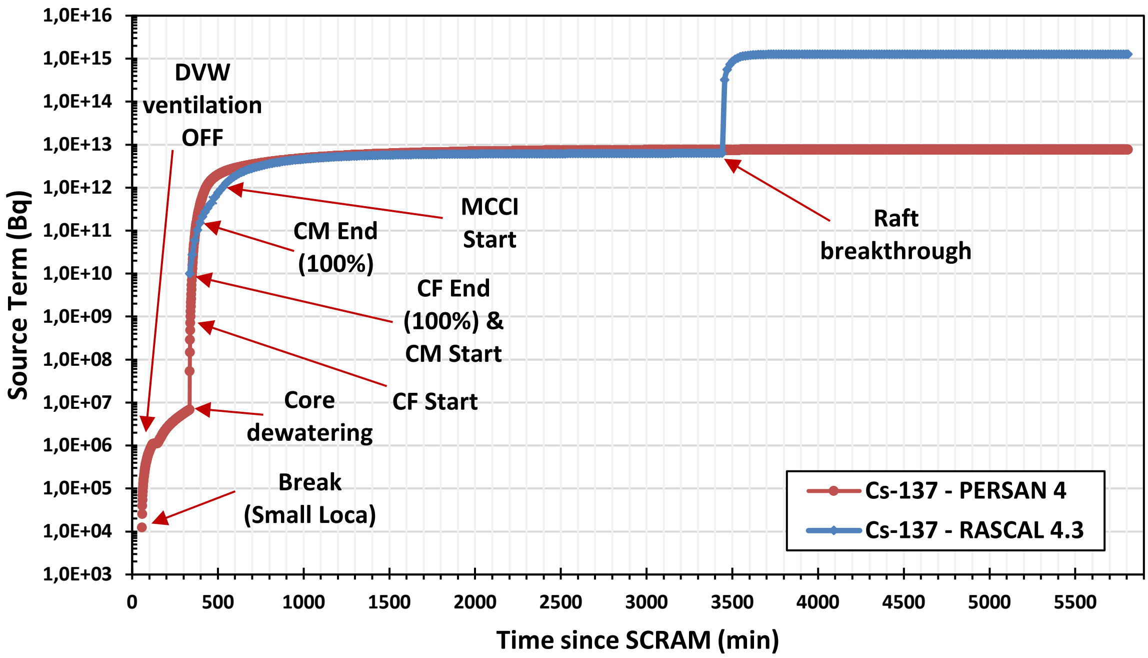

Figure 14: Time-dependent ST (Cs-137) – RASCAL 4.3 vs PERSAN 4 (ST#3)

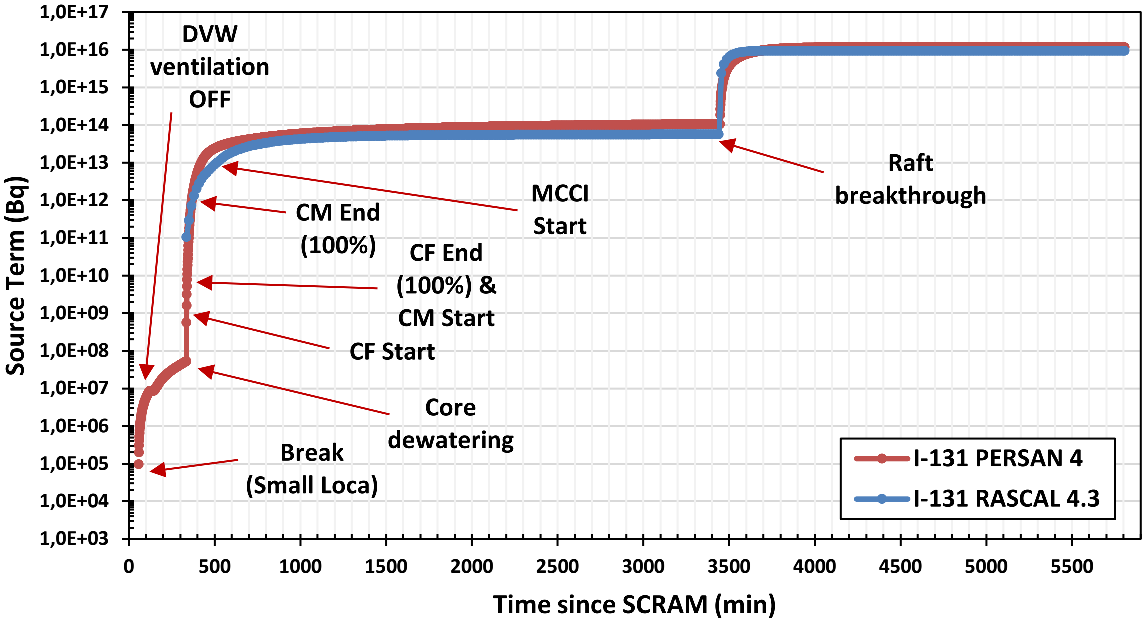

Figure 15: Time-dependent ST (I-131) – RASCAL 4.3 vs PERSAN 4 (ST#3)

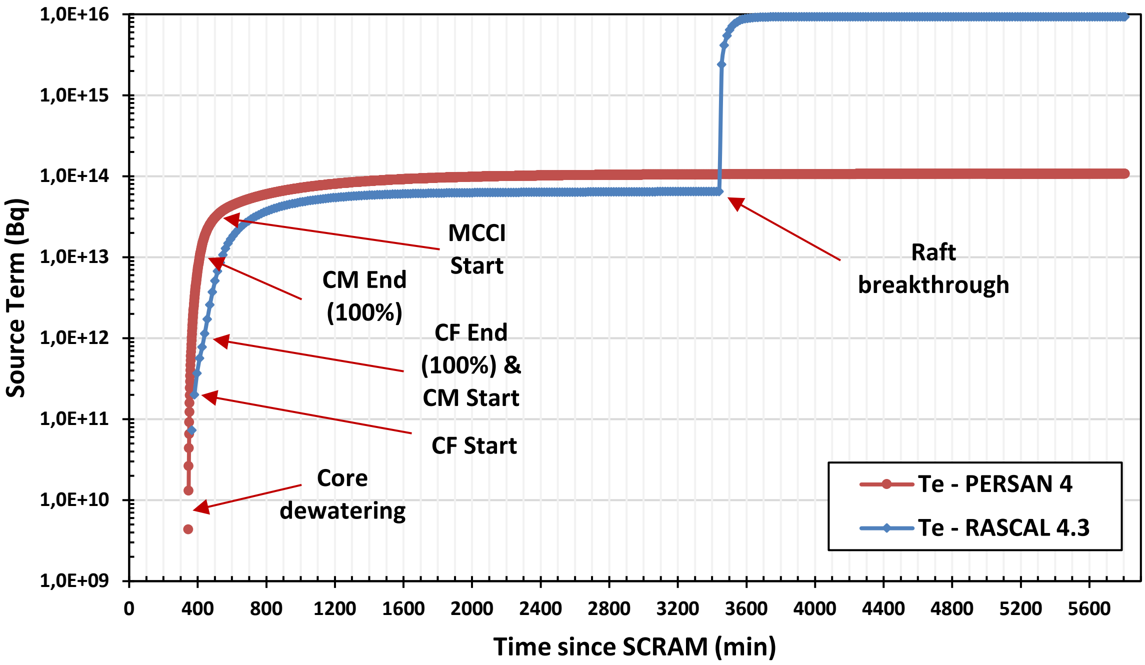

Figure 16: Time-dependent ST (Te) – RASCAL 4.3 vs PERSAN 4 (ST#3)

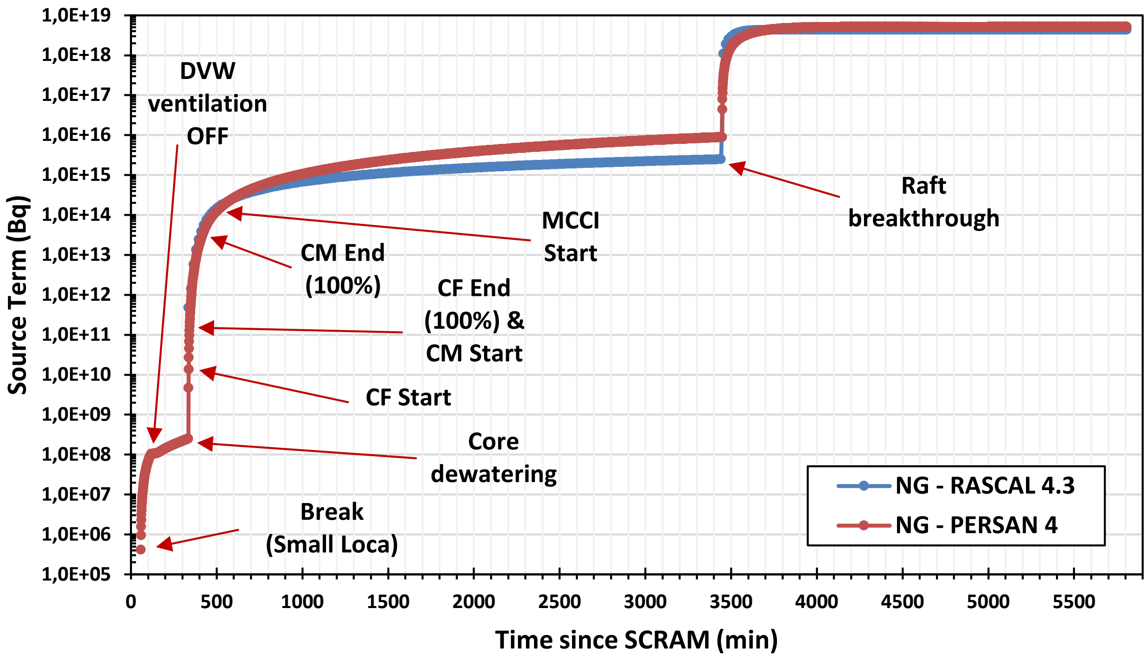

Figure 17: Time-dependent ST (NG) – RASCAL 4.3 vs PERSAN 4 (ST#3)

Figures 15 and 17 show that PERSAN 4 and RASCAL 4.3 tools are in good agreement with respect to the dynamics and the total release of I-131 and Noble Gases (NG). This circumstance confirms that a raft breakthrough event can be modeled in RASCAL 4.3 with a containment total failure (i.e., leak rate of 100% vol/h)to obtain the same PERSAN results for these elements. Figures 14 and 16 highlight that Cs-137 and Te dynamics and total release can not be compared between the two codes, because PERSAN 4 assumptions correctly foresee, at the time of raft breakthrough, a filtering efficiency of 1000 for aerosols (Cs-137, Te) by the surrounding ground. A containment total failure in RASCAL is always of the unfiltered type, and therefore cannot simulate correctly a raft breakthrough release for filtered elements. Since the ground filtering efficiency for aerosols is very high, the results for these elements can however be inferred by simply extrapolating horizontally the results of request ST#2. Table 13 reports a RASCAL 4.3 and PERSAN 4 total release intercomparison.

Table 13: PERSAN 4 vs RASCAL 4.3 Total Release – ST#3

Total Release			
	PERSAN	**RASCAL**	**VAR (%)**
Noble gas	5.19E+18	4.33E+18	19.86
Cesium	2.27E+13	3.76E+15	-99.40
Iodine	1.58E+16	2.00E+16	-21.08
Tellurium	1.06E+14	1.85E+16	-99.43

Table 13 shows that Cesium and Tellurium elements are two orders of magnitude higher in RASCAL 4.3 compared to PERSAN 4, because RASCAL does not include the aerosol filtering option by ground. Table 14 displays a PERSAN 4 and RASCAL 4.3 activity intercomparison for each radionuclide reported in the RASCAL 4.3 outcomes; Kr-83m and Nb-95m are not included in the PERSAN output.

Table 14: Intercomparison of the Radionuclide activity – ST#3

Nuclide	RASCAL 4.3	PERSAN 4	PERSAN /RASCAL ratio	Nuclide	RASCAL 4.3	PERSAN 4	PERSAN /RASCAL ratio
Am-241	2.13E+08	1.26E+08	**0.59**	Pu-241	2.01E+13	6.38E+10	**0.00**
Ba-139	1.28E+11	6.99E+11	**5.46**	Rb-86	2.43E+13	1.04E+11	**0.00**
Ba-140	5.21E+15	7.26E+13	**0.01**	Rb-88	1.22E+13	1.48E+13	**1.21**
Ce-141	2.54E+14	2.85E+12	**0.01**	Rh-103m	1.58E+14	2.63E+13	**0.17**
Ce-143	7.23E+13	1.90E+12	**0.03**	Rh-105	3.96E+13	1.69E+13	**0.43**
Ce-144*	2.14E+14	2.12E+12	**0.01**	Ru-103	1.58E+14	2.58E+13	**0.16**
Cm-242	6.62E+12	2.71E+10	**0.00**	Ru-105	1.02E+11	2.93E+12	**28.85**
Cs-134	1.83E+15	1.02E+13	**0.01**	Ru-106*	4.55E+13	8.89E+12	**0.20**
Cs-136	6.59E+14	4.76E+12	**0.01**	Sb-127	4.83E+14	4.83E+12	**0.01**
Cs-137*	1.27E+15	7.72E+12	**0.01**	Sb-129	1.96E+12	2.63E+12	**1.34**
Cs-138	1.59E+09	1.15E+10	**7.25**	Sr-89	2.91E+15	2.50E+13	**0.01**
I-131	9.28E+15	1.16E+16	**1.25**	Sr-90	2.32E+14	1.78E+12	**0.01**
I-132	7.34E+15	9.42E+13	**0.01**	Sr-91	6.02E+13	1.16E+13	**0.19**
I-133	3.32E+15	4.04E+15	**1.22**	Sr-92	9.39E+11	2.12E+12	**2.25**
I-134	1.00E+11	7.12E+11	**7.11**	Tc-99m	9.81E+13	1.13E+14	**1.15**
I-135	7.86E+13	9.57E+13	**1.22**	Te-127	6.55E+14	5.34E+12	**0.01**
Kr-83m	6.39E+11	-	**-**	Te-127m	1.23E+14	7.84E+11	**0.01**
Kr-85	2.22E+16	7.08E+12	**0.00**	Te-129	3.27E+14	6.07E+12	**0.02**
Kr-85m	9.27E+13	9.04E+13	**0.98**	Te-129m	5.02E+14	4.67E+12	**0.01**
Kr-87	6.32E+11	6.28E+11	**0.99**	Te-131	9.97E+13	1.44E+12	**0.01**
Kr-88	1.39E+13	1.80E+13	**1.29**	Te-131m	4.43E+14	6.76E+12	**0.02**
La-140	3.26E+15	2.01E+13	**0.01**	Te-132	7.11E+15	8.09E+13	**0.01**
La-141	1.42E+11	1.28E+12	**9.05**	Xe-131m	3.27E+16	3.00E+16	**0.92**
La-142	8.07E+09	1.20E+11	**14.83**	Xe-133	4.10E+18	4.88E+18	**1.19**
Mo-99	1.02E+14	1.13E+14	**1.11**	Xe-133m	8.22E+16	1.25E+17	**1.51**
Nb-95	2.68E+14	5.81E+12	**0.02**	Xe-135	9.09E+16	1.45E+17	**1.60**
Nb-95m	6.79E+11	-	**-**	Xe-135m	4.96E+15	6.71E+15	**1.35**
Nb-97	1.36E+12	1.36E+12	**1.00**	Xe-138	2.35E+05	3.03E+06	**12.91**
Nd-147	8.96E+13	3.71E+11	**0.00**	Y-90	1.05E+14	2.25E+11	**0.00**
Np-239	1.70E+15	3.49E+13	**0.02**	Y-91	2.05E+14	8.02E+11	**0.00**
Pm-147	1.69E+11	1.38E+13	**81.80**	Y-91m	3.71E+13	5.57E+12	**0.15**
Pr-143	2.25E+14	2.65E+12	**0.01**	Y-92	7.68E+11	1.25E+12	**1.62**
Pr-144	2.14E+14	2.09E+12	**0.01**	Y-93	3.04E+12	3.53E+11	**0.12**
Pu-238	3.48E+08	1.47E+09	**4.24**	Zr-95	2.58E+14	9.73E+11	**0.00**
Pu-239	4.72E+08	1.42E+08	**0.30**	Zr-97*	2.38E+13	5.28E+11	**0.02**

Table 14 reveals that the RASCAL semi-volatile and volatile aerosol (i.e., Cs, Te, Mo, Rb, Se, Rh, Tc, Ba, La, Ru, Sb, Np,…) results are roughtly two orders of magnitude higher than those of PERSAN, again due to the lack in RASCAL 4.3 of aerosol filtration for raft breakthrough events.

4 CONCLUSIONS

In this study, an intercomparison analysis of the ST results produced by PERSAN 4 and RASCAL 4.3 fast-running codes has been made. The analysis has been performed using the severe accident sequence proposed by IRSN during the WP4 of the Excercise 2 held in Vienna within FASTNET project. The intercomparison with the first ST request (ST#1) of Exercise 2 was not possible, because RASCAL 4.3 does not foresee a release into the atmosphere before a core dewatering event. The results for the second ST request (ST#2) show that PERSAN 4 and RASCAL 4.3 are in rather good agreement; notwithstanding, PERSAN 4 can be considered more accurate because it models the effect on the ST of many more accidental phenomena (containment pressure, ventilation systems, filtering) and because it considers the contribution to the ST of the effect of auxiliary buildings. The ST intercomparison results of the third request (ST#3) revealed that PERSAN 4 and RASCAL 4.3 are in good agreement only for those radionuclides that are not in aerosol form; in fact, although it has been verified by comparison with PERSAN results that RASCAL 4.3 can model a raft breakthrough event with a containment total failure, it does not provide the possibility of ground filtering and then ST reduction. In summary, this code intercomparison analysis reveals that on one side RASCAL 4.3 – through the use of a few accident information (i.e., containment leakage, sprays) and before the late-phase accidental phenomena (i.e., MCCI, raft breakthrough) – produces results that are in good agreement with PERSAN; on the other, PERSAN 4 provides a more precise and comprehensive time-dependent ST prediction using the information of the whole critical parameters (i.e., containment pressure, spray, filter, ventilation of auxiliary system, MCCI, raft breakthrough, clad and fuel melt) of a severe accident event, and is also capable of differentiating between iodine chemical forms for the improvement of the evaluation of radiological consequences.

5 REFERENCES

[1] https://www.edf.fr/groupe-edf/producteur-industriel/carte-des-implantations/centrale-nucleaire-de-gravelines/presentation

[2] J. V. Ramsdell Jr., G. F. Atley, J.P. Rishel, RASCAL 4.3: Descriptions of Models and Methods, May 2015;

[3] R. Nyman, S. Erixon, B. Tomic, H. Wimmer, B. Lydell, Realibility of Piping System Components, Volume 2: PASA LOCA Data base Review of Methods for LOCA Evaluation since the WASH-1400;

[4] NUREG-1940, RASCAL 4: Description of Models and Methods, December 2012;

[5] G. F. Athey, L.K. Brandon, J.V. Ramsdell, RASCAL 4.2 Workbook, NRC March 2012.

[6] https://www.nrc.gov/about-nrc/regulatory/research/ramp.html

[7] J.V. Ramsdell, Jr., G.F. Athey, S.A. McGuire, L.K. Brandon, RASCAL 4: Description of Models and Methods, March, 2012;

[8] Nuclear Energy Agency, Committee on the safety of nuclear installations, Benchmarking of Fast-Running Software Tools Used to Model Release During Nuclear Accidents, NEA/CSNI/R(2015)19, 2016;

[9] A. Guglielmelli, F. Rocchi, "FAST-1: Evaluation of the Accident Source Term through the fast running code RASCAL 4.2: Methods & Results", ENEA Technical Report, UTFISSM-P000-017, 2014;

[10] F. Rocchi, A. Guglielmelli, F. Padoani, P. Meloni, Application of RASCAL 4.2 to estimate the Fukushima Accident Source Term, challenges faced by Technical and Scientific Support Organization (TSOs) in Enhancing Nuclear Safety and Security;

[11] NUREG-1228. Soruce Term Estimation during aIncident Reposnse to Severe Nuclear Power Plant Accidents, october 1988.

[12] L. Soffer, S. B. Burson, C. M. Ferrel, R. Y. Lee, J. N. Ridgely, Accident Source Term for Light-Water Nuclear Power Plants, NUREG-1465, February, 1995;

[13] O. Isnard, PERSAN Source Term calculation tool, FASTNET School, Bologna, 21-25 January 2019.

[14] K. Chevalier-jabet, F. Cousin, L. Bosland, L. Cantrel, V. Créach, S. Fougerolle, J. Denis, E. Veilly, Proceedings of the International OECD-NEA/NUGENIA-SARNET Workshop on the Progress in iodine Behaviour for NPP Accident Analysis and management, March 30, April 1, 2015 – Marseille (France).

[15] G. Ortega Nicaise, B. Quaghebeur, PERSAN user manual, FAST Nuclear Emergency Tools (FASTNET project), November 2018;

Analysis of the Fukushima Source Term: Implications for Source Term Estimation from Radiological Observations during Emergencies

Martin Sogalla, Sebastian Band, Cornelia Richter and Martin Sonnenkalb

Gesellschaft für Anlagen- und Reaktorsicherheit (GRS) gGmbH, Schwertnergasse 1, 50667 Köln, Germany

Abstract:

Our contribution presents a set of conclusions drawn from the analysis of the Fukushima source term (ST) which could be useful for the future development and application of ST backward calculation methods based on radiological measurements. Such a reconstruction has been carried out within the OECD/NEA project "Benchmark Study of the Accident at the Fukushima Daiichi Nuclear Power Plant" (BSAF). Our analysis is based on measured local dose rate (LDR) on-site and nearby and activity measured in soil samples. We employ a deliberately "blind" approach which basically omits the use of plant information on accident progression. Within this approach, nuclide composition of deposits has been reconstructed from soil samples. Unexpectedly, during the first days of the accident, the observed LDR distinctly differs from calculation results based on this composition while the agreement improves later. An in-depth analysis reveals that only contributions by short-lived nuclides which have already decayed in the soil samples can explain observed LDR. The consideration of such short-lived iodine isotopes turns out to be a prerequisite for inclusion of on-site LDR measurements in our reconstruction approach. This inclusion leads to a striking agreement with ST reconstruction results obtained from the Japanese WSPEEDI decision support system and enables at the same time a higher temporal resolution and accuracy. The results provided by both methods have been used for an independent validation of ST calculations by severe accident (SA) analyses within the OECD/BSAF project and allow for a deeper understanding of the accident progression. The results and methodology of our analysis are currently being incorporated into a source term estimation tool based on radiological data which is based on the use of on-site and nearby radiological measurements. The tool is especially designed to deal with situations when information is sparse or even contradictory. It is planned to provide an interface for coupling this tool with fast running ST prediction tools based on plant data.

1 SCOPE AND OBJECTIVES

On behalf of the German Federal Ministry of Economic Affairs and Energy (BMWi), GRS participated in the OECD/NEA project: "Benchmark Study of the Accident at the Fukushima Daiichi Nuclear Power Plant (BSAF)". Within the first phase of this project (2012-2014), deterministic analyses for the severe accident (SA) progression during the first days for the Units 2 and 3 of Fukushima Daiichi nuclear power plant (NPP) have been provided by GRS. The second phase of the project (2015-2018) extended the scope of the SA analyses and added the topic of the comparison of measured local dose rate (LDR) on-site and off-site with calculated releases of radioactive material to the environment, the source term (ST). Forward and backward calculations of radionuclide releases have been performed to assess the appropriateness of the results provided by the SA analyses based on an independent approach. Within this scope, the main objectives of our backward calculations have been to reconstruct radioactive releases from measured LDR on-site Fukushima Daiichi NPP or nearby and to compare our findings with available measured plant parameters as well as with the results of SA analyses performed [1].

2 METHODOLOGY AND DATA

Several studies address the reconstruction of radioactive releases from Units 1 to 3 of the Fukushima Daiichi NPP based on environmental data. Among them, a detailed source term estimation published in [2] is based on the coupling of the WSPEEDI-II (Worldwide version of System for Prediction of Environmental Emergency Dose Information) model to an oceanic dispersion and deposition model. For the reconstruction of atmospheric releases monitoring data around the Fukushima site (distance: 4 km to 81 km) and over the ocean are used together with earlier ST estimations and information on specific events during accident progression in the plant. The focus of our study is on the very local scale, i.e. based on radiological observations on-site and in the near vicinity of the plant (distance: 300 m to 19 km). The data have been made available within the OECD/NEA BSAF project to the partners. A deliberately “blind” approach is followed which omits the use of any plant information for identification of release phases or quantification of releases. As no radiological observations over the Pacific Ocean have been available to the OECD/NEA BSAF project partners, our analysis is confined to phases where radioactive releases are dispersed over land. The results published in [2] are used for comparison (referenced as “WSPEEDI”) as explained later.

2.1 Outline of analysis method

Our reconstruction method aims at the optimized use of available radiological measurements at or nearby the Fukushima site. It thus focuses on the evaluation of the numerous local dose rate measurements, while the nuclide composition must be estimated from a limited number of available soil samples. The reconstruction scheme is based on the following steps:

- *Step 1: Calculation of surface contamination from local dose rate and specific soil activity:* For this purpose, the measured LDR record is first subdivided into cloud phases when a radioactive cloud passes by the monitoring point (MP) and ground phases when ground shine dominates observed LDR. Subdivision is based on characteristic differences in the change rate of LDR. Nuclide-specific surface contamination is estimated during ground phases by relating ground shine to the nuclide composition of deposited nuclides. This composition is determined from soil samples.
- *Step 2: Calculation of air activity concentration from surface contamination and information on precipitation:* During cloud phases, the difference between measured LDR and calculated ground shine is assumed as cloud shine. Air activity concentration is calculated from total increase in surface contamination during the respective cloud phase. Deposition rates are assumed proportional to cloud shine magnitude and are varied according to available precipitation information. This method yields estimates for air concentration of aerosols and gaseous iodine. Noble gas concentration is guessed from the residuum between total cloud shine and calculated contributions by aerosols and gaseous iodine.
- *Step 3: Calculation of radioactive releases from LDR, air concentration and modelled dispersion:* For this step, an inverse calculation is carried out for each MP included. Dispersion parameters are obtained from calculations performed with the Lagrangian dispersion model ARTM (Atmospheric Radionuclide Transport Model) which has been developed by GRS [3]. As dispersion parameters, gamma submersion factors are chosen. These can be directly linked to calculated cloud shine at each MP. The quantity of radionuclides released is then calculated by an appropriate backward calculation method. For this purpose, an optimal solution for radioactive releases to be assumed is sought by minimizing the difference between observed and calculated cloud shine that would result from the release estimate. This minimization problem is solved by the use of the “Non-Negative Least Squares“ (NNLS) algorithm [4].

All dates and times indicated in the remainder of this paper refer to Japan Standard Time (JST). Source term reconstruction has been performed for the period of March 12 00:00 to March 26 00:00. Calculations have been processed with a uniform time step of 10 minutes.

2.2 Observational database

Measurements of LDR on-site Fukushima Daiichi NPP and Fukushima Daini NPP have been published by Tokyo Electric Power Company (TEPCO). They are complemented by a set of LDR observations at 26 MP in the surroundings which have been made available to the OECD/NEA BSAF project. Six MP on-site and eight MP off-site have been employed for ST reconstruction. Details on these MP are summarized in Table 1. Another subset of eight MP in the surroundings of Fukushima Daiichi NPP with shorter data records has been used for validation of the reconstructed ST. Some MP in the surroundings have not been included in the analysis due to either insufficent data or redundancy to neighbouring MP.

Table 1: LDR monitoring posts used for ST reconstruction

Monitoring post	Direction/ distance to Unit 1/2 stack	Measurement period available and used	Temporal resolution used
Kiyohashi	N; 8.2 km	March 12 00:00 - March 14 16:00	1 h
Fukushima I NPP, MP 1	N; 1.7 km	March 12 11:30 - March 13 18:00	10 min
Namie	NNW; 8.6 km	March 12 00:00 - March 25 24:00	1 h
Fukushima I NPP, MP Main Bld N	NNW; 0.35 km	March 17 09:40 - March 21 16:30	10 min
Fukushima I NPP, MP 4	NW; 1.1 km	March 12 15:20 - March 14 11:10	sampled to 10 min
Yamada	WNW, 4.1 km	March 12 00:00 - March 25 24:00	1 h
Fukushima I NPP, MP Main Bld S	WNW; 0.29 km	March 17 09:40 - March 25 24:00	10 min
Oono	WSW, 4.9 km	March 12 00:00 - March 16 16:40	sampled to 10 min
Fukushima I NPP, MP Main Gate	WSW; 0.9 km	March 12 00:00 - March 16 16:20 March 21 16:50 - March 25 24:00	10 min
Yonomori	SSW; 7.3 km	March 12 00:00 - March 15 19:00	1 h
Shoukan	SSW; 14.2 km	March 12 00:00 - March 25 24:00	1 h
Yamadoaka	S 18.7 km	March 12 00:00 - March 25 24:00	1 h
Fukushima II NPP, MP 4	S; 12 km	March 12 00:00 - March 25 24:00	10 min
Fukushima I NPP, MP 8	S; 1.2 km	March 12 03:40 - March 13 07:30	10 min

Samples of specific soil activity for Te-132, I-131, Cs-134, Cs-137, and eight other nuclides are available at eight locations on-site Fukushima Daiichi NPP from March 21, 2011. This data set has been complemented by numerous soil samples of I-131 and Cs-137 in the surroundings of Fukushima Daiichi NPP published by the Ministry of Education, Culture, Sports, Science and Technology (MEXT) in 2011 and digitally archived by GRS at that time.

Measurements of wind direction and velocity as well as precipitation information at Fukushima Daiichi NPP published by TEPCO are used. Until the afternoon of March 16, 2011, additional weather data recorded at Oono MP have been made available to the OECD/NEA BSAF project, which are combined with measurements at Fukushima Daiichi NPP for dispersion calculations.

3 ANALYSIS RESULTS

Nuclide composition of radioactive deposits has been determined using the soil samples described above. All samples are decay-corrected to the date of the first sample (March 21 00:00). By this time, possible releases in the first few days of the accident of short-lived nuclides like I-132 would be no longer detectable in the deposits. Comparison of nuclide ratios relative to Cs-137 shows that the nuclide composition is quite homogeneously distributed over all samples for all nuclides except for Iodine. Ratios of I-131 to Cs-137, however show a systematic dependence on dispersion direction. On average, a higher ratio is found where dry deposition dominates compared to the ratio where deposition is influenced by rainfall. These systematic differences are used to discriminate between dry and wet deposition of Iodine. Contributions of short-lived isotopes I-133 and I-135 are then calculated from the respective reactor core inventory ratios to I-131. I-132, which is continuously produced by decay of Te-132 in the reactor cores after shutdown, is tentatively assumed to be in radioactive equilibrium with Te-132. With these additional assumptions for Iodine and the respective ratios for all other nuclides taken from the average over all soil samples at the NPP site, a basic nuclide composition for the radioactive deposits has been derived.

Calculated ground shine from the basic nuclide composition can thus be directly compared to measured LDR during assumed ground phases. For this purpose, the amount of deposited nuclides on the ground is calculated by a least square fit approach which minimizes the difference between the calculated ground shine and measured LDR. Unexpectedly, this comparison reveals large discrepancies between calculated ground shine and measured LDR during the first days of the accident while the agreement improves later. This disagreement is for example, evident in the mismatch between measured LDR (blue squares) compared to calculated ground shine (orange crosses) in Figure 1 for MP "Main Gate". Like in this example, especially at MPs at or close to the accident site, observed LDR decreases significantly faster than would be expected from radioactive decay in the basic composition. To explain these discrepancies, several possible alternative causes have been investigated, such as slowly passing radioactive clouds, changes in release intensity or reduction of surface contamination by wind-driven resuspension and/or runoff by rainfall. However, an in-depth analysis of the characteristic timescales of these processes shows that only radioactive decay can explain the LDR behavior during the phases in question [5]. Moreover, the distinction between cloud phases and ground phases seems to be consistent with the observed LDR curves.

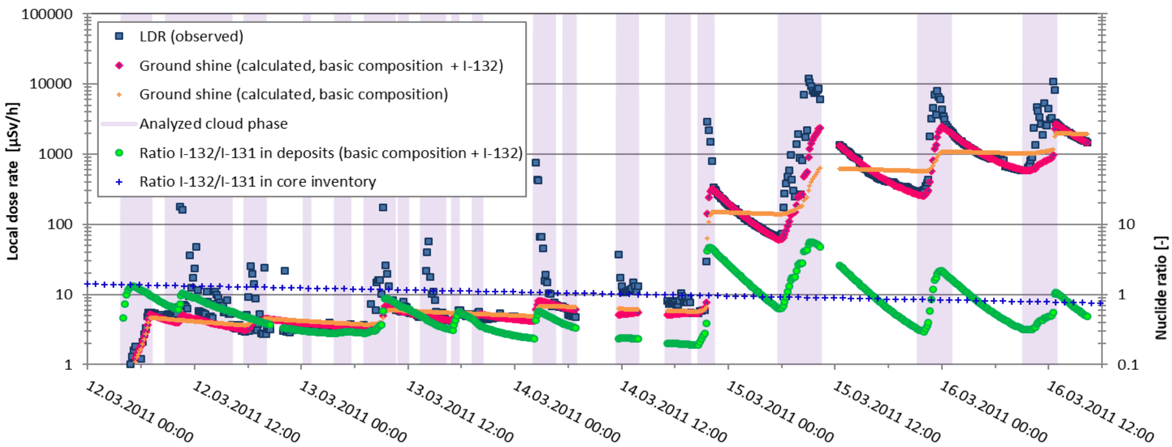

Figure 1: Comparison between observed LDR and calculated ground shine with (purple diamonds) and without (orange crosses) excess release of I-132 for MP "Main Gate". Calculated ratio of I-132 to I-131 in deposits is compared to respective ratio in core.

Hence, it seems reasonable to assume additional contributions by short-lived nuclides to surface contamination. Such nuclides would no longer be detectable in the available soil samples. Faster radioactive decay of these would explain the observed decrease rates in ground shine. Such an effect can be qualitatively attributed to higher release fractions of I-132 (with a half-life of 2.3 hr) compared to those of Te-132. Such excess releases would lead to the deposition of larger amounts of I-132 than of Te-132 and subsequently to a faster decrease in ground shine. I-132 is thus chosen as representative for short-lived nuclides which contribute to surface contamination. Amounts of additional I-132 which are suitable to explain observed LDR are again calculated by a least square fit approach. Results of this calculation for MP "Main Gate" are shown in Figure 1. Agreement between observations (blue squares) and modelled ground shine (purple diamonds) is remarkably improved in contrast to the use of the basic nuclide composition.

In line with theoretical considerations, calculated peak ratios of I-132 to I-131 (green circles in Figure 1) agree with the respective core inventory ratio (blue crosses) for nearly all analyzed cloud phases until March 14, 2011 afternoon. These peak rations seem however unrealistically high especially in the night from March 14 to March 15, 2011. It seems likely that additional short-lived fission products contribute to ground shine during those phases. On the other hand, sensitivity tests show that the actual choice of short-lived nuclides does not significantly affect the calculated amounts of longer-lived nuclides. Therefore, I-132 has been chosen as sole representant of short-lived nuclides.

By the inclusion of I-132, surface contamination can be satisfactorily estimated from local dose rate also at the on-site MP whose employment in our ST reconstruction would otherwise bias the results of analysis step 1. Air activity concentration and radioactive releases are then determined for each MP according to steps 2 and 3 described above. The source term is then reconstructed from the results for the 14 MP included by weighted averaging, considering the magnitude of dispersion coefficients to reduce the effect of errors in the dispersion modelling.

Results are shown for the accumulated release of Cs-137 in Figure 2. The temporal development based on the weighted ensemble average as well as the largest and the smallest ST estimate within the ensemble is illustrated. It is evident that the weighted average provides a reasonable estimate of the Cs-137 release within the ensemble and that minimum and maximum estimate within the ensemble converge with time. As mentioned above, source term reconstruction is confined to time phases when releases are dispersed over land. An observational coverage of about 50% is obtained for the investigation period.

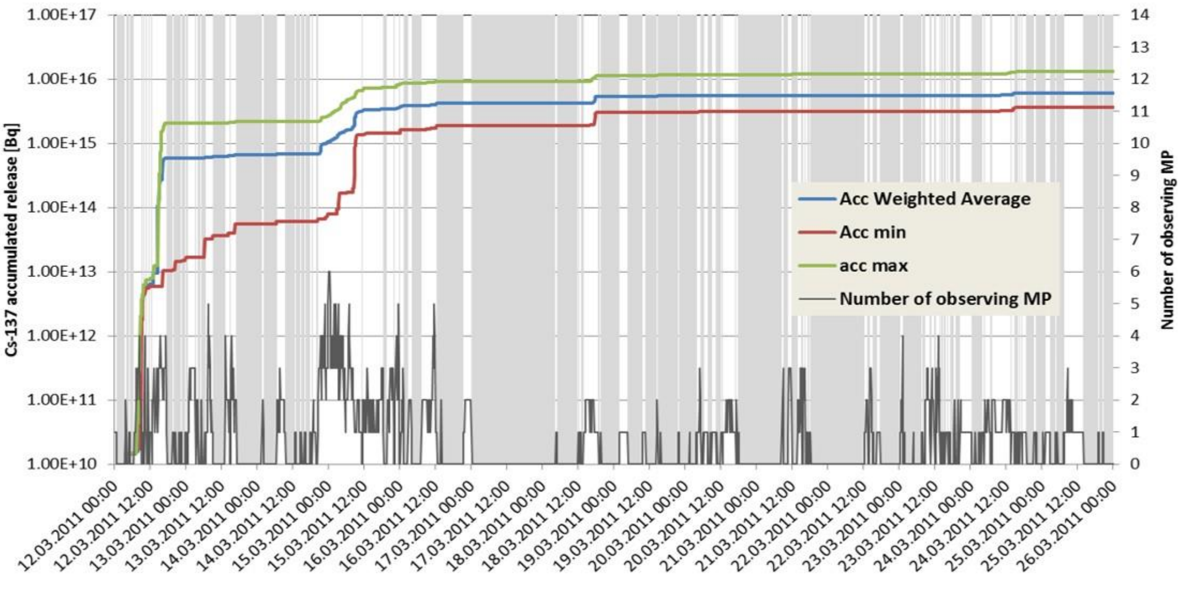

Figure 2: Accumulated release of Cs-137 reconstructed by GRS for the first two weeks of the accident. Blue: weighted ensemble average. Red: minimum estimate within ensemble of MP. Green: Maximum estimate within ensemble. Shaded: no observation by MP ensemble possible. Dark grey: Number of observing MP.

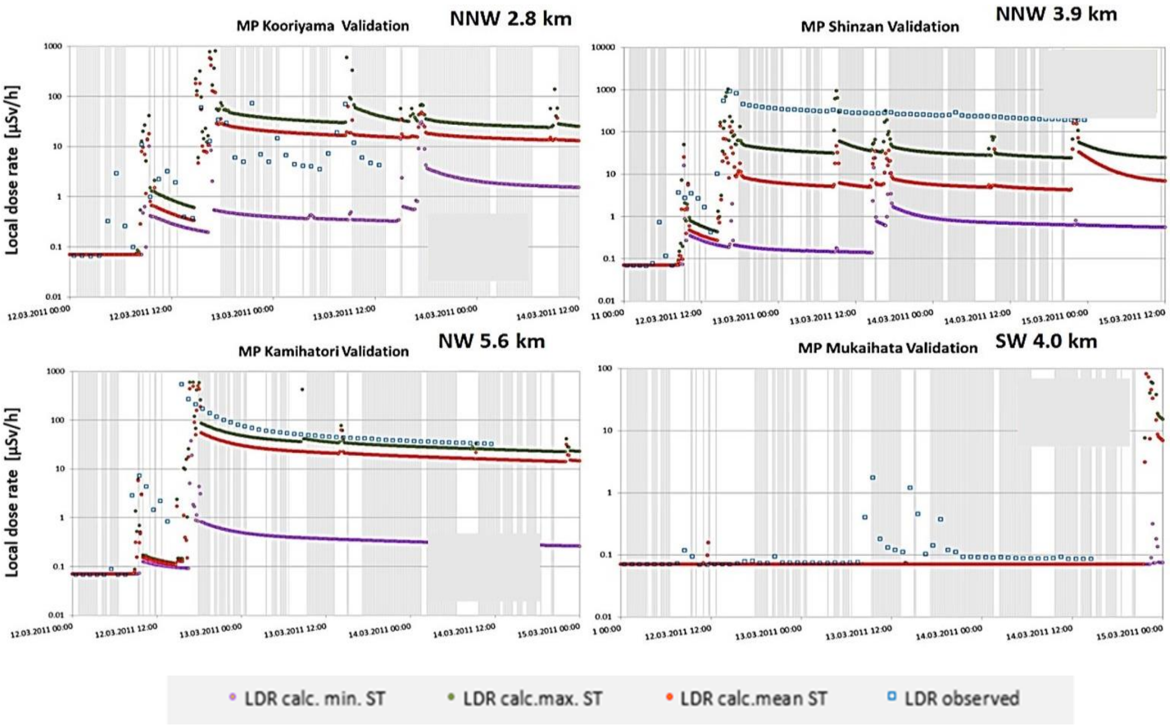

Figure 3: Validation results for four selected MP: Comparison between observed and calculated LDR based on minimum (purple), weighted average (red) and maximum (green) reconstructed source term. Shaded: No observation by MP ensemble possible.

Validation of the ST reconstruction by independent measurements of local dose rate at 8 MP generally shows qualitatively good agreement between calculated and measured local dose rate, too. Pronounced sensitivity to uncertainties in the dispersion calculation at some measuring points is evident. Nevertheless, at most of the monitoring posts, quantitatively good agreement is also achieved within a range substantially less than an order of magnitude. Examples for the correspondence between calculated and measured LDR at four of the MP used for validation are shown in Figure 3.

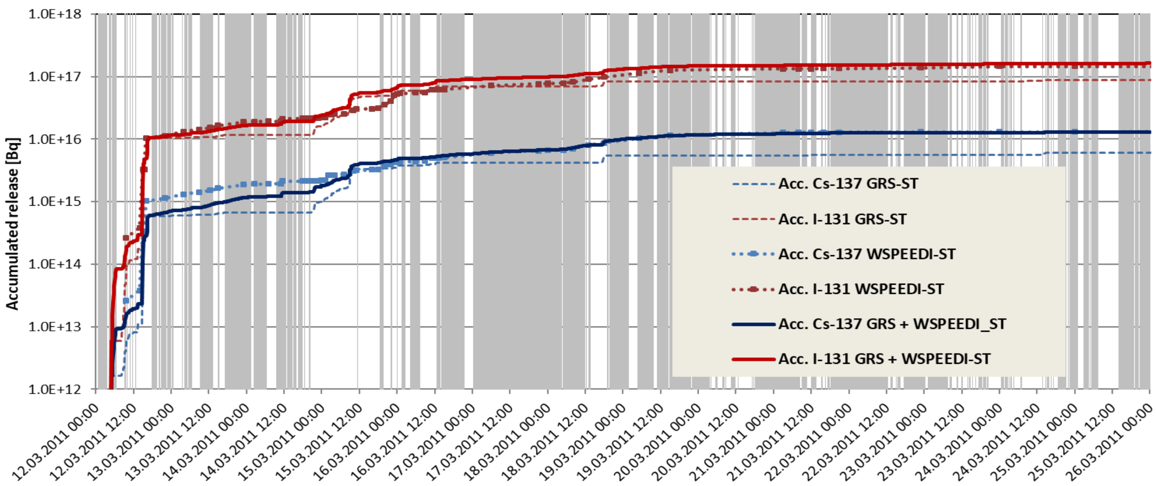

Figure 4: Comparison of accumulated releases of Cs-137 (blue) and I-131 (red) by GRS (dashed) and WSPEEDI (dash-dotted) ST reconstruction methods. Shaded: No observation by MP ensemble used for GRS backwards calculation possible. Solid lines: Accumulated releases for combined GRS + WSPEEDI ST (see text).

The reconstructed source terms obtained from WSPEEDI [2] and GRS backwards calculations are compared in Figure 4. A clear advantage of the WSPEEDI method is the coverage of the whole investigation period, including those periods when the radioactive releases are dispersed over the ocean. On the other hand, the GRS method enables the use of LDR measurements on-site very close to the location of release. By this, the temporal resolution of source term reconstruction is enhanced. The agreement between the results of GRS and WSPEEDI calculations is remarkably evident in the accumulated releases. The calculated accumulated releases are nearly identical by the afternoon of March 16, 2011. Thereafter, the GRS ST estimates are lower, due to reduced observational coverage for the GRS calculations.

Because of the striking agreement between GRS and WSPEEDI source term results during periods covered by both methods, it seems reasonable to combine the source term results. For periods covered by both GRS and WSPEEDI results, the GRS results are taken as source term data because of their higher temporal resolution. For periods not covered by GRS data (wind direction towards the Pacific Ocean) GRS results are completed by WSPEEDI results. This procedure combines the advantages of both datasets.

4 DEVELOPMENT OF A “LOW END” SOURCE TERM ESTIMATION TOOL

The results and methodology of our analysis are currently being incorporated into a source term estimation tool based on radiological data for emergency preparedness and response (EPR). This tool is based on the use of on-site and nearby radiological measurements.

Experience from past accidents clearly shows that, in particular during the early phase of an accident, information may be sparse, ambiguous or error-prone and sometimes even contradictory. The tool which is currently being developed is especially designed to deal with such situations. For this purpose, it is required to operate at the “low end” of information avaliability, i.e. minimum, incomplete and even inconsistent information levels should be interpretable by the tool. At the same time, the limitations and uncertainties of corresponding conclusions should be clearly marked. The level of sophistication in information processing should be able to keep pace with increasing complexity of information when available.

In order to meet these requirements, a two-step approch is chosen for information processing:

- The first step consists of a pre-structured qualitative assessment of information. This step produces one or -if necessary- a set of qualitative interpretations of information and data available, together with an assessment of underlying assumptions, evidence and limitations for each interpretation. A structured interface is foreseen to enable the user to quickly select interpretations, evaluate their plausibility and switch between alternative conclusions.
- Whenever feasible and potentially meaningful, a quantitative source term calculation is carried out in the second step. This step is based on the methodology developed for analysis of the Fukushima source term. Methodology will be extended to a broader range of potentially available radiological data and foresee combination possibilities with information on the plant state.

The working scheme of the tool is illustrated in Figure 5. Necessary assumptions to fill in information gaps will be provided by a knowledge base which will serve as complenentary input to actual information. The results of the tool will be used as feedback to the information base to provide successive evaluation and improvement of information quality by iterative application according to the development of available information during the accident course.

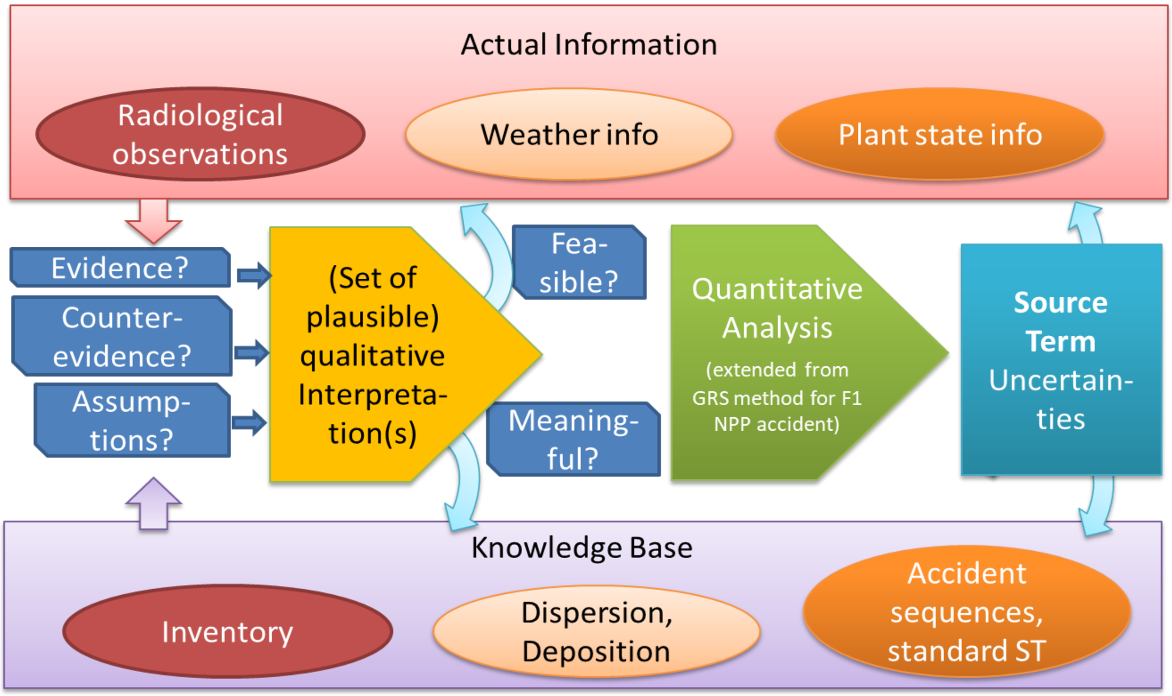

Figure 5: Working scheme of the “low-end” ST estimation tool currently being developed by GRS

The tool is intended to work in a stand-alone version with provisions for manual data input as well as part of a network with interfaces for automatic data transfer. It will include a simple dispersion/deposition scheme which can be driven by point weather data as well as an interface for coupling the backward caculation method to the results of more sophisticted flow and dispersion/deposition modelling. Moreover, an interface to combine information with results of fast running ST prediction tools based on plant data such as FaSTPro [6] will be implemented.

5 CONCLUSIONS

The quality of the results obtained by our source term reconstruction approach crucially depends on the careful analysis of measured LDR and specific soil activity. This analysis reveals that only contributions by short-lived nuclides which have already decayed in the soil samples can explain observed LDR. The consideration of such short-lived nuclides turns out to be a prerequisite for inclusion of on-site LDR measurements in our reconstruction approach.

In comparison to results obtained from the Japanese WSPEEDI decision support system, the employment of on-site LDR measurements by GRS enables a higher temporal resolution during phases covered by both methods. On the other hand, the WSPEEDI results also cover situations when radioactive releases are dispersed over the ocean. The agreement between GRS and WSPEEDI results justifies the combination of the ST calculation results provided by both methods. The blended ST data set combines the advantages of each reconstruction method. It allows for an independent validation of the ST predicted by SA analyses as well as for an improved understanding of the accident progression.

The results and methodology of our analysis are currently being incorporated into a source term estimation tool based on radiological data for emergency situations. This tool is based on the use of on-site and nearby radiological measurements and especially designed to deal with sparse or even contradictory data and information.

6 ACKNOWLEDGEMENTS

This study has been funded by the German Federal Ministry of Economics and Technology under project RS 1534 and by the German Federal Ministry for the Environment, Nature Conservation and Nuclear Safety under project 3616S62550.

7 REFERENCES

[1] Band, S., Richter, C., Sogalla, M., Sonnenkalb, M.: „Unfallablauf- und Quelltermanalysen – Untersuchungen zu den Ereignissen in Fukushima im Rahmen des OECD/NEA BSAF-Projektes, Phase II, Abschlussbericht der GRS zum Vorhaben RS1534.“ GRS-485, https://www.grs.de/sites/default/files/pdf/grs-485.pdf (2018)

[2] Katata, G., Chino, M., Kobayashi, T., Terada, H., Ota, M., Nagai, H., Kajino, M., Draxler, R., Hort, M. C., Malo, A., Torii, T., and Sanada, Y.: “Detailed source term estimation of the atmospheric release for the Fukushima Daiichi Nuclear Power Station accident by coupling simulations of an atmospheric dispersion model with an improved deposition scheme and oceanic dispersion model”, Atmos. Chem. Phys., 15, pp. 1029–1070 (2015)

[3] Richter, C., Thielen, H., Sogalla, M.: „Ergänzende Untersuchungen zur Validierung des Atmosphärischen Radionuklid-Transport-Modells (ARTM).“ GRS-394, https://www.grs.de/sites/default/files/pdf/grs-394.pdf (2015).

[4] Lawson, Charles L. and Richard J. Hanson: Solving Least Squares Problems, Prentice-Hall (1974).

[5] Sogalla, M.; Sonnenkalb, M.; Richter, C.; Klobes, B.: “What the ‘Peaks’ in Local Dose Rate Measured during the Fukushima Accident Tell About Deposition, Air Concentration and Release of Radioactivity.” Eurosafe 2016. https://www.eurosafe forum.org/sites/default/files/Eurosafe2016/Seminar4/4.02_Sogalla_Eurosafe 2016_Seminar RP_161104.pdf. (2016)

[6] Hage, M., et. al.: THE GRS SOURCE TERM PROGNOSIS SOFTWARE FASTPRO FOR PWR AND BWR SPENT FUEL POOLS, Paper 27418, International Topical Meeting on Probabilistic Safety Assessment and Analysis (PSAM14), Charleston, South Carolina, USA. (2019)

Radiological Characterization of Hard to Measure Nuclides Using Accelerator Mass Spectrometry (AMS)

M. Dewald, B.-A. Dittmann-Schnabel*, R. Spanier*, S. Heinze**, M. Schiffer**, C. Müller-Gatermann**, G. Hackenberg**, S. Herb**, A. Stolz**, A. Dewald**, R. Margreiter***, E. Strub***, K. Eberhardt*****

* Gesellschaft für Anlagen- und Reaktorsicherheit (GRS) gGmbH
** Institute for Nuclear Physics, CologneAMS, University of Cologne
*** Department for Nuclear Chemistry, University of Cologne
**** Institute for Nuclear Chemistry, Mainz

Abstract:

In this project irradiated heavy concrete was characterized regarding hard to measure nuclides like Ca-41 using Accelerator Mass Spectrometry (AMS). Concrete samples were irradiated with a known neutron flux and the Ca-41 content was investigated via AMS measurements. The comparison of the results with calculations shows a very good agreement in the Ca-41 content. The project revealed that AMS can be used to characterize irradiated concrete and contributes to improve the methodological basis of the radiological characterization and to extending the validation of nuclide vectors.

1 INTRODUCTION

After planning, construction and operation, the decommissioning is the last phase in the life cycle of a nuclear facility. Many nuclear facilities in Germany as well as in other countries around the world will reach the end of their design operational lifetime soon. Those facilities must be decommissioned on the protection of people and the environment.

In the course of the decommissioning of a nuclear facility the radiological characterization is of vital importance. Beside the radiation protection measures the information of such a characterization are required for the planning and selection of the dismantling order, the planning of decontamination and dismantling strategies as well as the planning of logistic for residual material. In particular for large structures where radionuclides were produced by neutron capture, e. g. the biological shield, the on-side measurement procedures are limited. The amount of so called hard to measure radionuclides is estimated by gamma spectroscopy, where easy to measure reference nuclides, e. g. Eu-152 and nuclide vectors are used. This approach is problematic for example, if the used reference nuclide has a short half-life and becomes unavailable after a longer period of decommissioning, the precise composition of the biological shield is not sufficiently known or if the reference nuclide is populated from nuclides which exists only as seed elements. Since usually parts of the biological shield are supposed for clearance to release them from regulatory control, a precise characterization is of great importance.

Even if the radioactive activity of concrete can be calculated by modern simulations, validating measurements are still required. The measurement methods and techniques are associated with considerable effort for sample preparation and therefore time consuming and expensive.

2 DETECTION OF HARD TO MEASURE RADIONUCLIDES WITH ACCELERATOR MASS SPECTROMETRY

The research project presented is supported by the Federal Ministry for the Environment, Nature Conservation and Nuclear Safety (BMU) and will be investigated by the Gesellschaft für Anlagen- und Reaktorsicherheit (GRS) gGmbH in cooperation with the University of Cologne. The aim is to determine, if Accelerator Mass Spectrometry (AMS) is an efficient and reliable method for the radiological characterization of hard to measure radionuclides in order to obtain a metrological access to these nuclides, which were up to now estimated conservatively.

2.1 Accelerator Mass Spectrometry (AMS)

In the scientific sector AMS is a common and well-established method to determine isotopic ratios and quantity shares in the ultra-trace range. In contrast to other methods, where the radioactive radiation is detected, in the AMS method single atoms are counted. Therefore, radionuclides with long half-life or missing gamma radiation are in principle unproblematic. AMS is, regarding the analysis of long-lived radionuclides in the ultra-trace range and with an ever-growing number of facilities worldwide, state of the art in science and technology. With respect to C-14 the development of compact and dedicated AMS systems was intensified over the last years [1]. The institute for Nuclear Physics at the University of Cologne has a 6 MV AMS system (CologneAMS [2]), where the measurements in the context of the presented research project were performed at. The used system is shown in Fig. 2.1.

Fig. 2.1 6 MV AMS system, as used for the measurements in context to the presented research project (Picture: GRS).

2.2 Measurement procedure for Ca-41 reactor concrete

In the course of this research project the hard to measure radionuclide Ca-41 was chosen, as it is produced in a substantial amount by neutron capture in the biological shield of nuclear reactors and therefore, important for the release of parts of the biological shield.

In a first step heavy concrete (barite concrete) was irradiated at the TRIGA research reactor in Mainz [3] with a well-defined neutron flux. To this end, six unirradiated heavy concrete cylinders (height and diameter 1cm) were cut into six segments each and irradiated for a well-defined time span. These segments were processed into three AMS samples each, in total 108 activated samples could be measured. The aimed isotopic radios of Ca-41 to Ca-40, between 10^{-9} and 10^{-12}, could be achieved by different exposure times. This procedure was chosen, on the one hand to activate the samples with a well-known neutron flux and on the other hand to reduce the administrative effort required to collect samples from a power reactor. An irradiation time of 1000s at the pneumatic post of the TRIGA Mainz is equivalent to the irradiation at a power reactor for one year, at the outer part of the biological shield, see Fig. 2.2.

After the irradiation was finished the samples were investigated, for a common understanding, with a gamma spectrometer at the Institute for Nuclear Physics at the University of Cologne. In the next step, the samples were prepared for the AMS measurements by the Institute of Nuclear Chemistry of the University of Cologne. To this end, a chemical pulping for the preparation of concrete samples for liquid scintillation according to Hou [5] was simplified for the AMS measurements. The AMS measurements were performed at the 6 MV AMS accelerator (CologneAMS [2]), therefore a constant verification of the measurements was ensured.

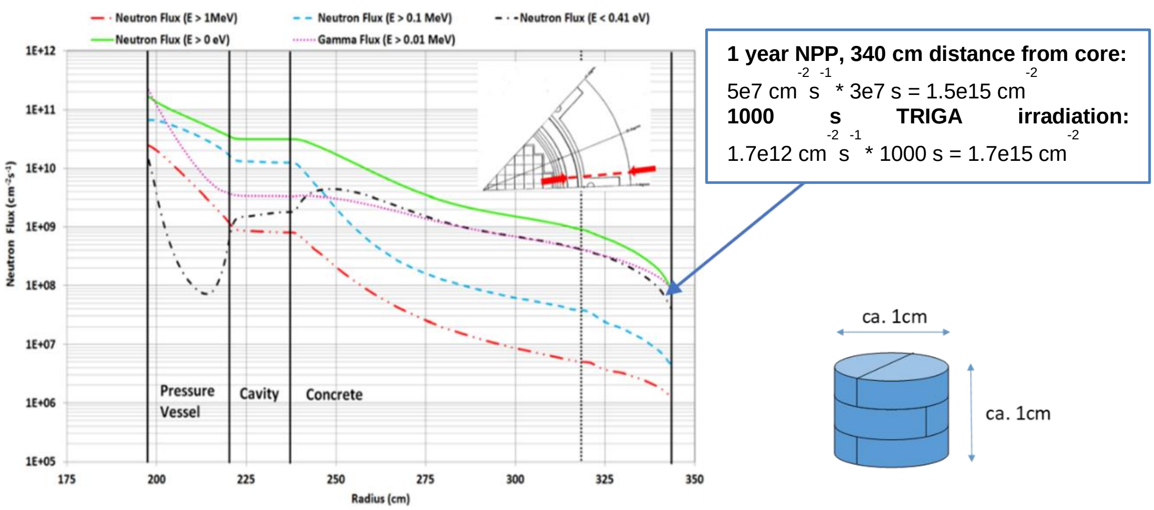

Fig. 2.2 Comparison of the neutron fluxes at the outer parts of a biological shield [4] and the neutron fluxes during irradiations at the TRIGA Mainz. The lower right part shows the segmenting of the heavy concrete cylinders.

3 RESULTS

The results, achieved in this project so far, confirm the suitability of AMS methods for a reliable radiological characterization, even for hard to measure radionuclides. In the following this is set out based on the investigated nuclides Ca-41 and C-14.

In addition to the concrete samples irradiated at the research reactor, also real concrete samples from the biological shields of the prototype reactors KNK-II and MZFR could be investigated. These samples were kindly provided by Kerntechnischen Entsorgung Karlsruhe (KTE) and in parts already investigated in terms of Ca-41 and C-14. The analysis and interpretation of the results is in process.

3.1 Measurement of Ca-41 in reactor concrete

To achieve different isotopic ratios of Ca-41 to Ca-40, the heavy concrete samples were irradiated for different durations. The exposure times were 30s, 300s, 1000s and 3000s. In Tab. 3.1 a comparison is given between the measured and the calculated isotopic ratios (Ca-41 / Ca-40), which are based on the exposure time, the neutron flux, the neutron capture cross section and the composition of the samples. In Fig. 3.1 the good agreement between the measured data and the calculated values is shown. Important for a precise calculation is the exact knowledge of the neutron flux and the neutron capture cross section. The comparison shows the efficient and reliable AMS measurement capabilities of the hard to measure radionuclide Ca-41 in reactor concrete. The requirements for a chemical Ca-41 sample preparation are unproblematic. Therefore, the suitability of AMS methods for the determination of Ca-41 in reactor concrete could be demonstrated.

Tab. 3.1 Comparison of the isotopic ratios (Ca-41 / Ca-40) between the AMS measurement and the calculations for different exposure times [6]. The CaO content of the samples was measured with X-ray fluorescence and determined to 8.68 mass percent.

CaO [$\%_m$]	Irradiation Time [s]	AMS Sample Batch 1	AMS Sample Batch 2	AMS Sample Batch 3	Calculation
8.68	30	2.35(25)E-11	1.64(10)E-11	1.59(13)E-11	1.45(2)E-11
	300	1.53(3)E-10	1.46(3)E-10	1.49(4)E-10	1.45(2)E-10
	1000	4.85(5)E-10	4.69(4)E-10	4.75(6)E-10	4.83(7)E-10
	3000	1.48(1)E-09	1.44(1)E-09	1.45(1)E-09	1.45(2)E-09

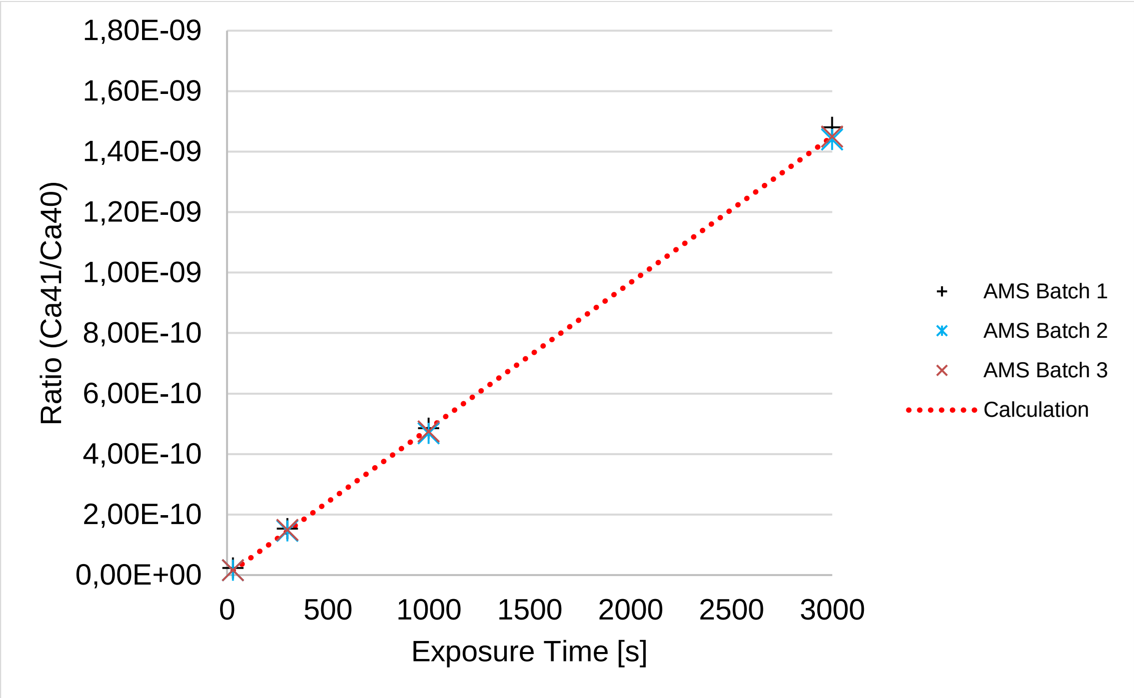

Fig. 3.1 Comparison of the results from the AMS measurements and the calculated isotopic ratios, based on a CaO content of 8.68 mass percent [6].

3.2 Measurement of C-14 in reactor concrete

Beside Ca-41 also the C-14 content of concrete samples was investigated with AMS. The results also confirmed the suitability of AMS for the characterization of the material. Of particular importance in this case is that no chemical sample preparation is required. Inside a gas system, which is linked to the AMS system, the concrete is burned, and the released CO_2 gas is directly fed into to the AMS system [7]. The C-14 concentration could therefore be determined with very limited effort. Furthermore, in the future it will be possible to set defined dilutions, to prevent a contamination of the AMS system for higher activated samples.

4 SUMMARY AND OUTLOOK

The measurements performed within this research project demonstrated that AMS is an efficient and reliable method to measure radionuclides in heavy concrete. In this way, hard to measure radionuclides like Ca-41 become directly accessible, which often could only be estimated conservatively in the past. Therefore, by means of AMS the validation of simulated nuclide vectors could be put on a wider scientific base, which could result in a reduction of uncertainty and therefore in a reduction of conservatism. This would be of great importance concerning the optimization of the amount of released material in the field of nuclear decommissioning. Furthermore, the use of Ca-41 as a reference nuclide is possible since it is a substantial part of concrete, it is reliable measurable over several orders of magnitude, even after many years when other radionuclides already may have decayed to the detection limits.

In further projects other hard to measure radionuclides should be investigated with AMS. This includes e. g. Cl-36 or H-3. During another project, a system for automated content measurements of H-3, C-14 and Cl-36 in reactor graphite should be developed.

5 LITERATURE

[1] Kutschera, W.: Accelerator mass spectrometry, State of the art and perspectives Advances in Physics: X, Bd. 1, Nr. 4, S. 570–595, (2016)

[2] Dewald, A. et al.: CologneAMS, ein neues Zentrum für Beschleuniger- Massenspektrometrie in Deutschland. Verhandlungen der Deutschen Physikalischen Gesellschaft. Frühjahrstagung 2011, Dresden
http://www.cologneams.uni-koeln.de/2669.html

[3] Mainzer Forschungsreaktor TRIGA Mark II mit Pulseinrichtung
https://www.kernchemie.uni-mainz.de/reaktor/

[4] Remec, I. et al.: Characterization of Radiation Fields in Biological Shields of Nuclear Power Plants for Assessing Concrete Degradation, EPJ Web of Conferences 106, 02002 (2016)

[5] Hou, X.: Radiochemical determination of 41Ca in nuclear reactor concrete, Radiochim Acta, 93, 611-617 (2005)

[6] Spanier, R.: PhD Thesis (2019)

[7] Stolz, A. et al.: Radiocarbon measurements of small gaseous samples at CologneAMS, Nucl. Instrum. Methods Phys. Res. A, 406, 283 – 286 (2017)

Comparative Analysis of Modelling Approaches for Safety Assessment of Radioactive Waste Disposal Facilities at Vector Site in Chornobyl Exclusion Zone

S. Tillmann, I. Iarmosh**, T. Weyand**

*Gesellschaft für Anlagen- und Reaktorsicherheit (GRS) gGmbH, Schwertnergasse 1, 50667 Cologne, Germany
**State Enterprise "State Scientific and Technical Center for Nuclear and Radiation Safety" (SSTC NRS), 35-37 V. Stusa St., 03142, P.O. Box 124, Kyiv, Ukraine

Abstract:

The Ukrainian strategy for management of radioactive waste (RW) includes its disposal in near-surface facilities. The long-term safety of such facilities has to be demonstrated by the licensee in the safety case. Mathematical methods for modelling of radionuclide migration and assessment of radiation risks in the long-term period are used to address this issue.

The specific site data of the engineered near-surface RW disposal facility (ENSDF) of the Vector Complex, located in the Chornobyl exclusion zone (ChEZ), were used as an example to set up a conceptual model for a scenario, which describes the potential contamination of drinking water in hypothetical wells located at different distances from the ENSDF.

The aim of this paper is to compare the results of modelling approaches using the different codes SPRING [1] and NORMALYSA [2] and to study their applicability in safety analyses. The modelling by means of both codes was based on using the same underlying assumptions and input data.

Also, a sensitivity analysis regarding selected parameters, which determine the activity concentrations of radionuclides in drinking water in the well, was performed. By considering those parameters and processes with the most significant impact on the modelling results, advantages and disadvantages of both methods were identified and proposals for further improvement of the models and on the selection of input data are given.

Keywords: radioactive waste, near-surface disposal facility, safety analysis, sorption, radionuclide migration, conceptual model, sensitivity analysis, NORMALYSA, SPRING.

1 INTRODUCTION

One of the fundamental safety principles of RW management is to avoid imposing an undue burden on future generations [3]. Therefore, the assessment of the long-term safety of near-surface facilities for the disposal of RW is an important issue that should be addressed by the licensee in the safety case. The licensee shall provide assurance through the safety case that workers, members of the public and the environment are and will remain adequately protected against the hazards associated with the RW envisaged to be disposed [4].

IAEA [5] [6], as well as Ukrainian regulations [7] consider several scenarios to assess the potential exposure arising in the context of long-term safety analyses for near-surface disposal facilities. One of these scenarios considers the consumption of drinking water by residents from a well, located at a certain distance from the disposal facility.

The codes SPRING and NORMALYSA were used to calculate radionuclide concentration in hypothetical wells which serve as monitors for assessing radiation exposures in the long-term safety analyses. This paper presents the comparison of the calculation results of the two codes using the same conceptual model. The ENSDF of the Vector Complex in the ChEZ was selected as an example for modelling.

2 STUDY SITE

Already existing and prospective RW of different origin in Ukraine is intended to be disposed of at the Vector Complex, if they comply with general criteria for placement in near-surface disposal facilities. For this purpose, near-surface disposal facilities for RW in containers, for example ENSDF [8] and SRW-1[1] disposal facilities and for bulk RW, for example SRW-2 disposal facility, were constructed and specific waste acceptance criteria were developed [9].

ENSDF is mainly designed for the disposal of conditioned and solidified RW and has a design capacity of 50,210 m^3 RW. The ENSDF consists of two parallel rows, each having 11 reinforced concrete compartments (modules). The dimensions of the disposal compartments are 18,8 m×24,8 m×7,5 m [9]. The dimensions of the whole ENSDF are 206,8 m×49,6 m×7,5 m. The RW is positioned in the ENSDF mainly in KZ-3.0 containers and in 200 l drums. Containers and drums will be stacked layer by layer. The space between the drums of each layer of drums is filled with concrete and the layer covered by concrete. After filling all compartments with RW and concrete, the disposal facility will be capped with clay and soil layers.

The catchment of the Pripyat and Uzh rivers determines the groundwater flow at the Vector site. Specific geological and hydrogeological information were taken from geological cross sections and laboratory investigations [10], [11], [12], [13]. The uppermost Quaternary aquifer consists of fluvioglacial and alluvial sands of different granulometric composition with layers of sandy loams and loams. The thickness of the saturated zone is approximately 40 m, considering a groundwater level of 120 m a.s.l. at ENSDF. As the groundwater level in the whole modelling area ranges between 115 and 125 m a.s.l., the aquifer thickness varies accordingly. The marly clays of the Paleogene Kiev suite at 80 m a.s.l. serve as aquitard [10].

3 CODES

The NORMALYSA and SPRING software tools were used to model the radionuclide migration.

NORMALYSA (developed by Facilia AB) is a set of models and databases designed to assess radiological impacts from naturally occurring radioactive materials and "legacy" RW

[1] SRW = solid radioactive waste

disposal facilities. These one-dimensional models are relatively simple and were developed for assessments at early stages of designing a RW disposal site in order to identify the most important routes of radionuclide transport and public exposure [2].

SPRING (developed by delta h Ingenieurgesellschaft mbH) sets up mass transport models, combining information of geographical information systems and numerical modelling based on the finite element method to calculate the groundwater flow and the advective-dispersive transport of contaminants [1].

4 CONCEPTUAL MODEL

Previously performed safety assessments of ENSDF [11], [12] showed Am-241 and Np-237 are some of the highest contributors to potential exposure. For this modelling study it was assumed that ENSDF contains only one radionuclide (Am-241). Both codes consider the decay of Am-241 and build-up of Np-237 (daughter radionuclide).

Furthermore, the conceptual model (Fig. 1) considers:

- the failure of all engineered barriers of ENSDF;
- the infiltration of precipitation water into the disposal facility;
- the release of dissolved radionuclides from the disposal facility (seepage) through the unsaturated zone into the saturated aquifer;
- the mixing of seepage water with groundwater;
- the advective-dispersive transport of radionuclides to observation wells at distances of 100 m, 1,500 m and 5,000 m from the disposal site.

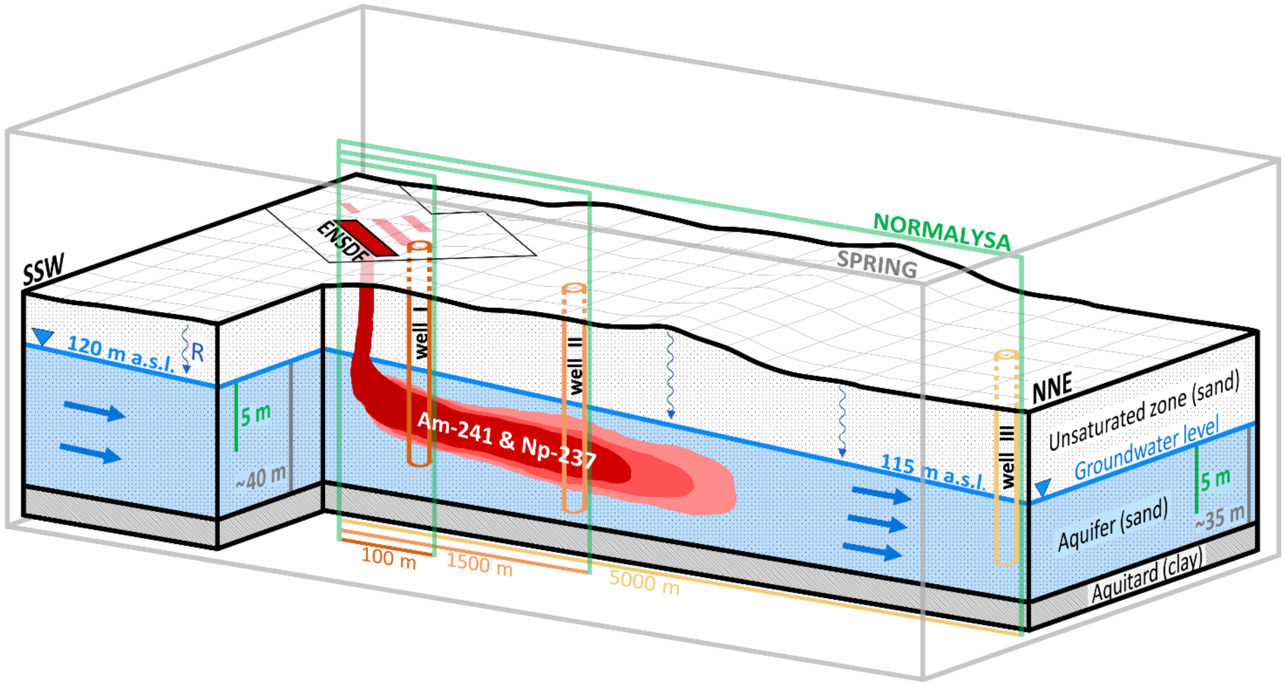

Fig. 1: ***Scheme of the conceptual model using NORMALYSA and SPRING and considering local conditions at the study site.***

Simplifications of the conceptual model were made to allow for the comparison of the results of the codes and consider:

- only the uppermost Quaternary aquifer;
- that RW in ENSDF is set up as a homogeneous waste body with a density similar to the density of cemented waste;

– that sorption of radionuclides at RW is neglected.

Input parameters and assumptions regarding the parameters are listed in Table 1.

Tab. 1: Input parameters for NORMALYSA and SPRING.

No.	Assumptions regarding the input parameters		Value
1.	Bulk densities	RW	2000 kg/m^3 [12]
		soil (unsaturated and saturated zone)	1600 kg/m^3 [12]
2.	Moisture contents	RW (NORMALYSA)	0.34 [12]
		unsaturated zone (SPRING, NORMALYSA)	0.44 [12]
3.	Specific activity of Am-241 in RW; total RW activity based on waste volume and -density		$8.67 \cdot 10^4$ Bq/m^3 [9]; $1.35 \cdot 10^{13}$ Bq
4.	Infiltration recharge rate (R) (infiltration water without additional activity concentration)		0.2 m/a [12]
5.	Matrix porosity (saturated and unsaturated zone)		0.375 [14]
6.	Thickness of the unsaturated zone*		14 m (NORMALYSA); 3-48 m (SPRING)
7.	Aquifer thickness**		5 m (NORMALYSA); 20-50 m (SPRING)
8.	Hydraulic conductivity of the matrix		$2 \cdot 10^{-4}$ m/s [11]

* whole modelling area in SPRING according to groundwater level [11] and surface elevation [15]; average value at ENSDF was used for NORMALYSA.

** 5 m are given as mixing zone in the aquifer according to [16]; for modelling area in SPRING according to groundwater level [11] and lower boundary of the aquifer [10].

The lateral distribution of the Darcy velocity was calculated in SPRING considering the groundwater table, hydraulic conductivity (K-value) and aquifer thickness. The NORMALYSA model used the values of Darcy velocity that comply with the distance of the hypothetical well from the disposal facility which are taken from SPRING. In SPRING, the values ranged from 3.3 up to 17.1 m/a, whereas in NORMALYSA the fixed values were the following: 3.5 m/a (for the distance 100 m), 6.4 m (for the distance 1500 m) and 17.1 m (for the distance 5000 m).

NORMALYSA uses fixed values for dispersivity [2]. The longitudinal dispersivity is 1/10th of the distance from the ENSDF to the well (length of the aquifer) and the transversal dispersivity is 1/10th of thickness of the unsaturated zone. Therefore, the longitudinal dispersivities were 10 m, 150 m and 500 m. The longitudinal dispersivity of NORMALYSA was also employed in SPRING for each well but the transversal dispersivity was 1/10th of the longitudinal dispersivity.

Calculations with different distribution coefficients (K_d) were carried out using SPRING and NORMALYSA. Since reliable site-specific values of K_d were not available, a range of values was used for the investigation of the impact of K_d. The minimum values were assumed to be 0.008 m^3/kg (Am-241) and 0.0005 m^3/kg (Np-237) and the maximum values were assumed to be 300 m^3/kg (Am-241) and 0.39 m^3/kg (Np-237) [12]. The intermediate value for Am-241 was 0.34 m^3/kg [17]. Regarding Np-237, the value 0.015 m^3/kg was used which is different from [16] since [11], [18] stated an overestimation of oxidizing conditions.

5 RESULTS

Selected main results of the calculations for SPRING (cases S1-S6) and NORMALYSA (N1-N6) are presented hereafter. Peaks for Am-241 and Np-237 and the associated periods of time are shown in table 2 and 3.

Tab. 2: Modelled time and peak concentrations of Am-241 using NORMALYSA and SPRING.

Code	N°	K_d [m^3/kg]	Am-241					
			Peak concentration [Bq/m^3]			Time [a]		
		Am-241	100 m (a)	1,500 m (b)	5,000 m (c)	100 m (a)	1,500 m (b)	5,000 m (c)
SPRING	S1	0.008	10,700,000	5,970	106	280	1,580	2,250
	S2	0.34	4	< 0.4*	< 0.4*	4,990	/	/
	S3	300	< 0.4*	< 0.4*	< 0.4*	/	/	/
NORMALYSA	N1	0.008	1,000,000	22,000	5,500	1,200	2,500	2,600
	N2	0.34	< 0.4*	< 0.4*	< 0.4*	/	/	/
	N3	300	< 0.4*	< 0.4*	< 0.4*	/	/	/

(a) longitudinal dispersivity of 10 m; (b) longitudinal dispersivity of 150 m; (c) longitudinal dispersivity of 500 m; * Values below the typical detection limit of measurements for drinking water (0.4 Bq/m^3 [19]) are not shown, as they are considered being negligible.

Tab. 3: Modelled time and peak concentrations of Np-237 using NORMALYSA and SPRING.

Code	N°	K_d [m^3/kg]	Am-241					
			Peak concentration [Bq/m^3]			Time [a]		
		Np-237	100 m (a)	1,500 m (b)	5,000 m (c)	100 m (a)	1,500 m (b)	5,000 m (c)
SPRING	S4	0.0005	1,600	50	6	80	370	560
	S5	0.015	820	11	1	800	4,290	6,600
	S6	0.39	74	0.5	< 0.4*	14,000	94,600	/
NORMALYSA	N4	0.0005	4050	1920	675	300	600	600
	N5	0.015	860	270	88	3,500	7,500	8,000
	N6	0.39	36	11	3	75,000	175,000	190,000

(a) longitudinal dispersivity of 10 m; (b) longitudinal dispersivity of 150 m; (c) longitudinal dispersivity of 500 m; * Values below the typical detection limit of measurements for drinking water (0.4 Bq/m^3 [19]) are not shown, as they are considered being negligible.

For both radionuclides, the modelling results using NORMALYSA and SPRING exhibit decreasing concentrations and increasing times with increasing distance to the disposal facility. At distances of 1,500 and 5,000 m to the disposal facility the time of the peaks is similar for NORMALYSA (N1, N5, N6). The case N4 exhibits an identical time of the Np-237 peak at 1,500 m and 5,000 m.

Compared to Am-241, the peak heights of Np-237 are smaller in case of low K_d-values and appear earlier at each well (S1, S4, N1, N4). The peak height of Np-237 is higher than Am-241 in case of high K_d (S2, S3, S5, S6, N2, N3, N5, N6).

The variation of the K_d shows a high impact on the modelling results. The higher the K_d-value, the lower is the peak. For high and intermediate K_d-values (S2, S3, N2, N3), all Am-

241-concentrations (except one at a distance of 100 m (S2)) are below the detection limit for measurements in water. Furthermore, the maximum of the activity concentrations occurs at later times (Fig. 2).

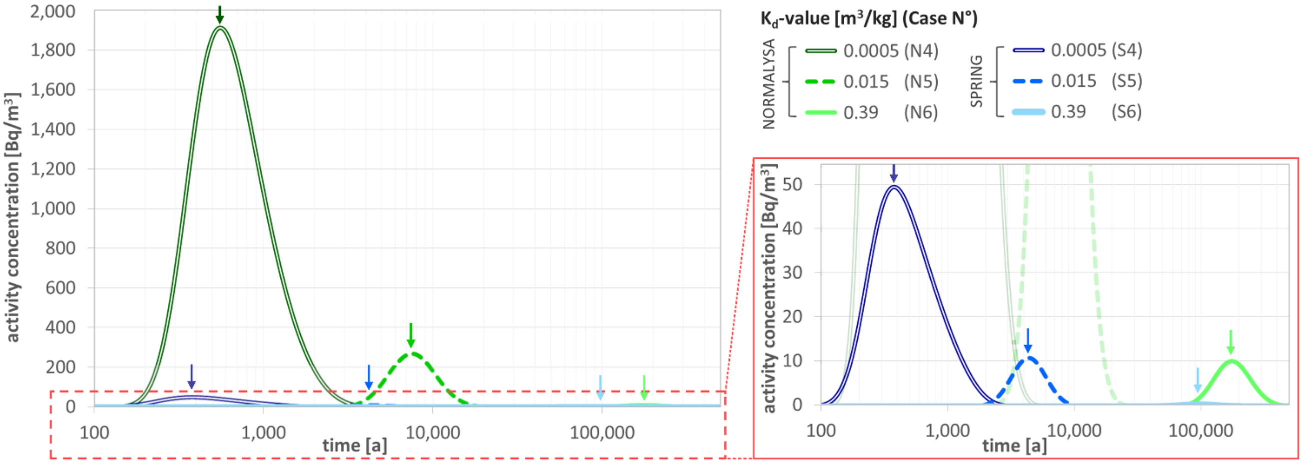

Fig. 2: ***Activity concentration of Np-237 depending on time and K_d at 1,500 m distance to ENSDF; case numbers refer to table 2.***

In all cases, the peak of both radionuclides reaches the well earlier in the SPRING model than in the NORMALYSA model. The most significant difference between the two models is observed in case of using a high K_d value (S6, N6). The difference in time between the two models decreases with increasing distance to the disposal facility (e.g. S4, N4 at 5,000 m).

The Am-241 peak at the 100 m well of the SPRING model (S1) is approximately one order lower than in the NORMALYSA model (N1). Compared to this at the 1,500 m and 5,000 m wells a higher peak is calculated by NORMALYSA (N1) than by SPRING (S1).

All Np-237 peaks show a higher concentration for NORMALYSA (N4, N5, N6) compared to SPRING (S4, S5, S6) except for 100 m distance (N6).

In the frame of this hypothetical study, the radionuclide concentrations of cases S1, N1 and N4 exceed at some distances the limits for Am-241 of 1,000 Bq/m^3 and for Np-237 of 2,000 Bq/m^3, applicable to drinking water according to the radiation protection regulation of Ukraine NRBU-97 [7].

6 DISCUSSION

The results of both models are considered as comparable and no substantial deviations are observed. A larger distance of the well from the disposal facility contributes to a higher sorption in total. Therefore, for both radionuclides a decrease of peak height and an increase of peak time is expected and exhibited by the models. Subsequently, the variation of K_d has a high impact on the modelling results of NORMALYSA and SPRING.

Because of its higher K_d, Am-241 is more readily adsorbed than Np-237. Therefore, the Np-237 peak occurs earlier in the wells than the peak of Am-241. In addition, Np-237 has a lower decay rate and is the daughter nuclide of Am-241. Therefore, it is expected that the peak height of Np-237 is smaller than the peak height of Am-241 in case of low K_d-values. The results for S1, S4, N1 and N4 confirm this expectation.

As the increase of the K_d for Am-241 (S2, S3, N2, N3) is greater than the increase of the K_d for Np-237 (S5, S6, N5, N6), Am-241 is more strongly adsorbed and migrates less far than Np-237. But the daughter nuclide Np-237 has a longer half-life than the strongly adsorbed Am-241 and is accumulated. Since Np-237 is less strongly adsorbed it can more easily migrate than Am-241. In the end, this leads to higher Np-237 peaks compared to Am-241 at more considerable distances.

There are some essential differences in the results of modelling with NORMALYSA and SPRING, respectively. One crucial difference is the approach to address dispersivity. A heterogeneous aquifer is described by high dispersivities, resulting in an enhancement of dispersion [20]. Thus, as SPRING considers finite elements and a horizontal layer the peak is widened and the peak heights at the wells decrease due to the dispersivity more than in NORMALYSA. As there may be more preferential flow paths with higher transport velocities in a heterogeneous matrix than in a homogeneous one [21], the peak reaches the wells earlier. The impact of the preferential flow paths on the transport time is higher in SPRING than in NORMALYSA, as the effect is intensified due to the finite elements in SPRING. Therefore, the peaks in SPRING reach the wells earlier compared to NORMALYSA.

The hydraulic regime has also a significant impact on the modelling results. It is to be noted that Darcy velocities are depending on the groundwater level and hydraulic properties in SPRING. Regarding the distances from the disposal facility to the wells, the velocity ranges from 3 m/a near the ENSDF to 17 m/a at 5,000 m distance. In NORMALYSA, the Darcy velocity is fixed at each distance of the well (cf. p. 3), which leads to an overestimation of flow velocity at greater distances compared to SPRING. The peak time of NORMALYSA is delayed compared to SPRING, since the effect of the dispersivity overcompensates the effect of the Darcy velocity. But, in NORMALYSA the peak times are levelled in greater distances to ENSDF due to the Darcy velocities.

Furthermore, the difference in aquifer thickness of the two models, namely a defined thickness of 5 m in NORMALYSA and a variation of thickness with an average value of 40 m at ENSDF in SPRING has an impact on the hydraulic regime. Comparing both models, the increase of dilution processes in the thicker aquifer of the SPRING model results in overall smaller peak heights than in NORMALYSA.

At 100 m distance, slightly smaller peaks of Am-241 are calculated in NORMALYSA compared to SPRING. We assume that this is due to the retardation of advective-dispersive radionuclide transport in the capillary water of the disposal facility itself **Fehler! Verweisquelle konnte nicht gefunden werden.**. Therefore, as the moisture content in the disposal facility is not considered in SPRING, a more significant peak at 100 m distance from the disposal facility is calculated. At more considerable distances, the difference in aquifer thickness is considered to have a more significant impact on the results.

It is to be mentioned here that time required and other efforts for modelling are of high importance in the course of safety analysis. NORMALYSA provides results in a shorter period of time compared to SPRING, which needs a set-up of a model grid and computation time (days) due to the finite elements. However, SPRING can provide more detailed results, e.g. the lateral spreading of the concentration plume. NORMALYSA offers a one-dimensional insight in radionuclide transport within minutes of modelling set-up and calculation.

7 CONCLUSIONS AND OUTLOOK

It is concluded that similar calculation results were obtained by modelling with the same basic assumptions and input data of the two codes NORMALYSA and SPRING. The identified differences between the results can be related to the use of input parameters and the inherent assumptions in both codes.

Advantages and disadvantages can be determined in both modelling with NORMALYSA and SPRING. Therefore, the choice of code should depend on the aim of modelling and its specific application. If results are needed in a short period of time and a one-dimensional model is considered suitable, NORMALYSA could be a good choice. The higher peaks and times can be considered as conservative for the conceptual model compared to SPRING. If more detailed results including consideration of lateral information and of the impact of other disposal facilities is requested, SPRING should be selected.

The shown activity concentrations obtained as results of modelling represent only the initial steps of a safety analysis based on a simplified conceptual model to compare codes and the impact of K_d-value on the results for two radionuclides. A future safety assessment should include the analysis of the potential radiation exposure based upon dedicated modelling approaches for disposal facilities.

Further safety analyses focussing on the relationship of K_d and activity concentrations should include a sampling campaign to obtain precise and site-specific data on K_d values by laboratory investigations. A future safety analysis should also consider the total anticipated activity of all radionuclides of ENSDF and other disposal facilities of the Vector Complex.

Further studies could also include a sensitivity analysis of other parameters (hydraulic conductivity, porosity, recharge, solubility, inventory, etc.) using NORMALYSA and SPRING to obtain more detailed and sound results for safety assessments.

8 ACKNOWLEDGEMENTS

We would like to give special thanks to Lutz Küchler, Oleksii Tokarevskyi and Guido Bracke.

9 REFERENCES

[1] König, C., Becker, M., Diehl, A., Seidel, T., Rosen, B., Rüber, O.& Zimmermann, C. (2019): Simulation of Processes in Groundwater (SPRING), Manual for Version 5, 465 p., delta h Ingenieursgesellschaft mbH: Witten. https://www.delta-h.de/index.php/de/software?

[2] Avila, R., Johansson, E., Bugai, D. & Koliabina, D. (2018): User's manual for NORMALYSA v.2.1. Description of Program Module Libraries, Mathematical Models and Parameters, 189 p., Facilia AB: Bromma. http://project.facilia.se/normalysa/software.html

[3] IAEA (2006): Fundamental Safety Principles. IAEA Safety Standards Series: Safety Fundamentals, No. SF-1, 37 p., IAEA: Vienna.

[4] WENRA WGWD (2014): Report. Radioactive Waste Disposal Facilities Safety Reference Levels. WENRA WGWD Report, 22 December 2014, 81 p.

[5] IAEA (2012): The Safety Case and Safety Assessment for the Disposal of Radioactive Waste. IAEA Safety Standards Series: Specific Safety Guide, No. SSG-23, 140 p., IAEA: Vienna.

[6] IAEA (2014): Near Surface Disposal Facilities for Radioactive Waste. IAEA Safety Standards Series: Specific Safety Guide, No. SSG-29, 124 p., IAEA: Vienna.

[7] Ukrainian Center for Health and Safety Control (1997): NRBU-97. Radiation Safety Standards of Ukraine. State Health and Safety Regulations, Ministry of Health of Ukraine: Kyiv, 125 p. (Ukr).

[8] Tekhnocenter (2009): Safety Analysis Report for ENSDF, Revision 2, Addition and Changes, Chapters 1-6, Tekhnocenter: Chornobyl, 228 p. (Rus).

[9] UkrDO Radon & Tekhnocenter (2009): Radioactive Waste Management. Criteria for Radioactive Waste Acceptance for Disposal in the Engineered Near-Surface Disposal Facility (ENSDF). ENSDF First Stage of Operation. Radioactive Waste Acceptance from ChNPP LRTP and SRTP to be Disposed in Two Symmetrical Sections of ENSDF, Rev. 5, Tekhnocenter: Chornobyl, 33 p. (Ukr).

[10] Shekhtman, L. M., Baranov, V. T., Nesterenko, H. F., Kishinskaia, Y. A., Chiornaia, V. M. & Yakovlev, V.A. (1996): Assessment of protective Abilities of Vector Complex Geology against Radioactive Contamination in 30-km ChNPP Area. In: Ministry of Ukraine on Affairs of Protection of the Population (Ed.): Problems of Chernobyl Exclusion Zone, Vol. 3, pp. 134-145, Naukova Dumka: Kyiv.

[11] Empresarios Agrupados & KIEP (2018): Task B3 Safety Re-Assessment of ENSDF Disposal Facility Safety Analysis Report, Chapter 6 Safety Analysis, Support on

radioactive waste management at the Vector Industrial Complex in Ukraine (PROJECT U4.01/11AB), No. 6, 249 p., 26 March 2018.

[12] PLEJADES GmBH, Brenk Systemplanung GmbH & Westinghouse Electric Sweden AB (2017): Technical Report Task F4. Safety Assessment of RAW Management Facilities at the Vector Complex, Version 2.0, Support to radioactive waste management in Ukraine (U4.01/10 C+D+F), May 2017, 234 p.

[13] Bugai, D., Skalskyy, A., Haneke, K., Thierfeldt, S., Nitzsche, O., Tretyak, A.& Kubko, Y. (2017): Groundwater Monitoring and Modelling of the “Vector” Site for near-surface radioactive Waste Disposal in the Chornobyl Exclusion Zone. Nuclear Physics and Atomic Energy, Vol. 18, No. 4, pp. 382-389.

[14] KIEP (1992): Proceedings of Engineering and Geological Studies of Vector Complex, Severnaya Site Design (Buryakovka point), 150p (Rus).

[15] Data from Google Maps, available at: https://www.google.de/maps (accessed 26 April 2018).

[16] Iarmosh, I. & Olkhovyk, Yu. (2016): Conceptual Model to Determine Maximum Activity of Radioactive Waste in Near-Surface Disposal Facilities. Nuclear and Radiation Safety, No. 3 (71), pp. 61–64.

[17] IAEA (2003): Derivation of Activity Limits for the Disposal of Radioactive Waste in Near Surface Disposal Facilities. IAEA-TECDOC-1380, 150 p., IAEA: Vienna.

[18] Chantaraprachoom, N., Tanaka, T. & Nakayama, S. (2003): Sorption and Migration Mechanisms of Neptunium-237 through Sandy Soil. The 6th NUCEF Seminar Working Group, 20 February 2003, pp. 118-122, Japan Atomic Energy Research Institute: Tokai.

[19] Website of the Radioanalytical Laboratory of Forschungszentrum Jülich, available at: https://www.fz-juelich.de /gs/DE/UeberUns/Organisation/S-B/S-BA/PreislisteUmweltanalytik.html?nn=1308294 (accessed 31 July 2019).

[20] Gelhar, L. W., Welty, C. & Rehfeldt, K. R. (1992): A Critical Review of Data on Field-Scale Dispersion in Aquifers. Water Resources Research, Vol. 28, No. 7, pp. 1955-1974.

[21] Berger, W., Engeser, B., Fickus, M., Hahn, R., Lichtfuss, R., Mies, B., Sohr, A., Stoepker, K., Werner, K., Wünsch, A. & Zeisberger, V. (10/2006): LABO-Arbeitshilfe: Sickerwasserprognose bei Detailuntersuchungen. 111 p., Bund-/ Länderarbeitsgemeinschaft Bodenschutz (LABO).

[22] Bedinger, M. S. (1989): Geohydrologic Aspects for Siting and Design of Low-Level Radioactive-Waste Disposal. U.S. Geological Survey Circular, Vol. 1034, 44 p., U.S Govern

www.eurosafe-forum.org ISBN 978-3-947685-51-6